

**UCLA**

**UCLA Electronic Theses and Dissertations**

**Title**

Symmetry-Based Access to Polycyclic Bis-guanidines: Total Synthesis of ( $\pm$ )-Ageliferin and the Complete Axinellamine Ring System

**Permalink**

<https://escholarship.org/uc/item/7d94j8wz>

**Author**

Roberts, Andrew George

**Publication Date**

2013

Peer reviewed|Thesis/dissertation

UNIVERSITY OF CALIFORNIA  
Los Angeles

Symmetry-Based Access to Polycyclic Bis-guanidines:  
Total Synthesis of ( $\pm$ )-Ageliferin and the Complete Axinellamine Ring System

A dissertation submitted in partial satisfaction of the  
requirements for the degree Doctor of Philosophy  
in Chemistry

by

Andrew George Roberts

2013

© Copyright by

Andrew George Roberts

2013

## ABSTRACT OF THE DISSERTATION

Symmetry-Based Access to Polycyclic Bis-guanidines:  
Total Synthesis of ( $\pm$ )-Ageliferin and the Complete Axinellamine Ring System

by

Andrew George Roberts

Doctor of Philosophy in Chemistry

University of California, Los Angeles, 2013

Professor Patrick G. Harran, Chair

Chapter One provides an overview of the complex pyrrole–imidazole dimers; palau’amine, axinellamines, massadines and ageliferin. This includes a brief discussion of their isolation, structural features, and biochemical properties. Pertinent biosynthetic proposals are discussed, followed by an introduction to our symmetry-based synthetic strategy. Previous research efforts from our laboratory are discussed to highlight key reactivity observed and the development of a unique strategy for the synthesis of complex pyrrole–imidazole dimers. Standing challenges are addressed in a refined synthetic proposal (this thesis). A discussion of completed efforts and total syntheses of the complex pyrrole–imidazole dimers is provided. The chapter concludes with a summary of advanced intermediates obtained by other research groups en route to targeted total syntheses of these alkaloids.

We have charted a symmetry-based approach to the most complex dimeric members of the group. New methods to prepare and manipulate bis-guanidine containing intermediates in this context are discussed in Chapter Two. These efforts culminated in the synthesis of a partially halogenated variant of the complete ( $\pm$ )-axinellamine A ring system. The route features a host of unusual reactions and developed methods including the use of lithium amidotrihydroborate and samarium iodide for the controlled reductive transformation of glycoyamidine carbonyl functionality.

Chapter Three describes the total synthesis of ( $\pm$ )-ageliferin from a common spirocyclopentane intermediate. A novel *N*-amidinylium ion rearrangement was examined for the requisite ring-expansion to provide the 2-aminotetrahydrobenzimidazole core of ageliferin directly. This method was applied to epimeric intermediates to obtain structurally novel tetracycles coined ‘iso’axinellamines.

Chapter Four describes proposed access to ( $\pm$ )-axinellamine A via controlled oxidation and subsequent ring-contraction of ( $\pm$ )-ageliferin. This led us to examine oxidative methods for the transformation of 2-aminotetrahydrobenzimidazoles. The discovery of 4-phenyl-1,2,4-triazole-3,5-dione (PTAD) as a reagent for the controlled oxidation of 2-aminoimidazoles inspired a novel proposal for an alternative total synthesis of (–)-ageliferin. Progress toward the synthesis of (–)-ageliferin via the oxidative desymmetrization of symmetric 2-aminotetrahydrobenzimidazole intermediates is discussed.

Chapter Five entails synthetic access to functionalized 3,3'-bipyrrolidines, coined ‘dispacamide dimer precursors’, for the synthesis of complex pyrrole–imidazole dimers. The dimeric framework was obtained by a diastereoselective, nickel-catalyzed reductive homocoupling of an unactivated secondary bromide derived from *trans*-4-hydroxy-*L*-proline.

Dimeric precursors were desymmetrized by an auto-oxidative process. The method involves a cascading sequence of indiscrete oxidation and guanidine incorporation events followed by desymmetrization. The desymmetrization process parallels spirocycloisomerization reactivity described in Chapter Two. Desymmetrized compounds were elaborated to intercept a common spirocyclopentane core containing intermediate described in Chapter Two. Notably, intermediates obtained from this sequence are optically active as they derive from *trans*-4-hydroxy-*L*-proline. *Results from this novel route are preliminary. Efforts to render this unique synthetic strategy scalable are ongoing.*

Neil K. Garg

Paula Diaconescu

Hsian-Rong Tseng

Patrick G. Harran, Committee Chair

University of California, Los Angeles

2013

*For my parents, Vicki and Charles Roberts.*



## TABLE OF CONTENTS

Abstract.....	ii
Committee Page.....	v
Dedication Page.....	vi
Table of Contents.....	vii
CHAPTER ONE.....	viii
CHAPTER TWO.....	viii
CHAPTER THREE.....	x
CHAPTER FOUR.....	xi
CHAPTER FIVE.....	xii
List of Figures.....	xiv
List of Schemes.....	xxv
List of Tables.....	xxix
List of Abbreviations.....	xxx
Acknowledgements.....	xxxiv
Curriculum Vitae.....	xxxvi

## TABLE OF CONTENTS

### CHAPTER ONE:

#### **Dimeric Pyrrole–Imidazole Alkaloids: A Unique Challenge for Synthesis**

1.1 Abstract.....	001
1.2 Introduction	
1.2.1 Introduction: Dimeric Pyrrole–Imidazole Alkaloids.....	001
1.2.2 Complex Dimeric Pyrrole–Imidazole Alkaloids: Isolation, Structure and Biochemical Properties.....	003
1.2.3 Complex Dimeric Pyrrole–Imidazoles: Biosynthetic Pathways.....	006
1.3 Symmetry-Based Access to Complex Dimeric Pyrrole–Imidazoles	
1.3.1 Retrosynthetic Analysis .....	010
1.3.2 Initial Model Systems and Reactivity Studies.....	014
1.4 Thesis Research – Refinements for Future Reaction Discovery	
1.4.1 Controlled Preparation of Bis-Guanidine Intermediates en Route to Palau’amine and Axinellamines.....	019
1.5 Complex Dimeric Pyrrole–Imidazole Alkaloids Synthesis	
1.5.1 Completed Efforts and Total Syntheses.....	022
1.5.2 Progress Toward Palau’amine and Related Dimers.....	025
1.6 References and Notes.....	028

### CHAPTER TWO:

#### **Symmetry-Based Logic for the Total Synthesis of Axinellamines and Palau’amine**

2.1 Introduction	
------------------	--

2.1.1 Introduction and General Strategy.....	034
2.1.2 General Access to Dispacamide Dimers – Proposed Preparation of Target Bis-Alkylidene.....	036
2.2 Results and Discussion	
2.2.1 Synthesis of a Alkyl Isothiuron, Dispacamide Surrogate and Initial Dimerization Studies.....	038
2.2.2 Demonstration of Essential Transformations for the Reduction and Unveiling of Glycocyamidine Derivatives.....	042
2.2.3 Refined Synthesis – Preparation of a Non-Halogenated Monomer: A Scalable Procedure with Fewer Purification Events.....	044
2.2.4 Synthesis of Carbonyl Congeners of Dispacamide Monomer.....	049
2.2.5 Dimerization of Dispacamide Monomer and Late-Stage Manipulation of Functionality .....	050
2.2.6 Equilibration of Dispacamide Dimers, Bis-spiroaminals.....	059
2.2.7 Oxadiazine Ring Degradations and Glycocyamidine Reductions.....	061
2.2.8 Controlled, Chemoselective Reduction of Glycocyamidines.....	063
2.2.9 Synthesis of Halogen-Deficient (±)-Axinellamine A.....	066
2.2.10 Additional Reactivity of Bis-Spirocycles: Access to Chlorinated Intermediates.....	068
2.3 Conclusion.....	072
2.4 References and Notes.....	073
2.5 Experimental	
2.5.1 Materials and Methods.....	080

2.5.2 Experimental Procedures and Characterization Data.....	081
2.5.3 Experimental References.....	121
APPENDIX ONE (A1, Chapter Two):	
2.6.1 Spectra Relevant to Chapter Two.....	122
2.6.2 X-ray crystallographic data for Compound <b>2-46b</b> .....	195
 <b>CHAPTER THREE:</b>	
<b>Total Synthesis of (±)-Ageliferin via N-amidinyliminium Ion Rearrangement</b>	
3.1 Introduction.....	223
3.2 Results and Discussion	
3.2.1 Synthesis and Equilibrium of Spirocyclopentane Aminoimidazoles.....	225
3.2.2 Synthesis of (±)-Ageliferin and <i>l</i> -Iso'axinellamines.....	228
3.2.3 Related Rearrangement Transformations in Hydantoin and Model Glycocyamidine Systems.....	232
3.2.4 Deuterium Exchange Reactions in a Model 2-aminoimidazoles.....	234
3.3 Conclusion.....	237
3.4 References and Notes.....	238
3.5 Experimental	
3.5.1 Materials and Methods.....	240
3.5.2 Experimental Procedures and Characterization Data.....	241
3.5.3 Experimental References.....	255
APPENDIX TWO (A2, Chapter Three)	
3.6.1 Spectra Relevant to Chapter Three.....	256

## CHAPTER FOUR:

### Regarding an Alternative Route to (±)-Axinellamine A from (±)-Ageliferin

#### *Controlled, oxidative transformations of 2-aminoimidazoles (Part I)*

4.1 Introduction (Part I)	
4.1.1 Proposed Synthesis of (±)-Axinellamine A from (±)-Ageliferin.....	286
4.1.2 Related Synthetic Efforts.....	289
4.2 Results and Discussion (Part I)	
4.2.1 Synthesis of the Ageliferin Core.....	290
4.2.2 Reactivity of 2-Aminoimidazoles with 1,2,4-Triazolidene-3,5-diones and Singlet Oxygen.....	292

#### *Progress Toward the Total Synthesis of (–)-Ageliferin (Part II)*

4.3 Introduction (Part II)	
4.3.1 Proposed Synthesis of (–)-Ageliferin.....	296
4.3.2 Related Synthetic Approaches to (±)-Ageliferin.....	298
4.3.3 Precedent in Related Systems, 2-Aminoimidazole Oxidations.....	299
4.4 Results and Discussion (Part II)	
4.4.1 Synthesis of <i>Trans</i> -substituted 2-aminoimidazole.....	301
4.4.2 Attempted Oxidative Activation–Alkylations to Access (–)-Ageliferin...	303
4.4.3 Alternative Synthesis of Bis-Phthalimide Derivative.....	307
4.5 Conclusion (Part I & II) .....	309
4.6 References and Notes (Part I & II) .....	310
4.7 Experimental (Part I & II)	
4.7.1 Materials and Methods .....	314

4.7.2 Experimental Procedures and Characterization Data.....	315
4.7.3 Experimental References.....	337
APPENDIX THREE (A3, Chapter Four)	
4.8.1 Spectra Relevant to Chapter Four.....	338
 <b>CHAPTER FIVE:</b>	
<b>Alternative Access to Dispacamide Dimers: <i>Auto-oxidation of 3,3'-Bipyrrolidines for the Synthesis of Dimeric Pyrrole–Imidazole Alkaloids</i></b>	
5.1 Introduction	
5.1.1 Introduction and General Strategy.....	388
5.1.2 Auto-oxidative Incorporation of Guanidine into Partially Oxidized Proline Dimers.....	389
5.1.3 Literature Precedent for the Reductive Dimerization of Unactivated Alkyl Halides.....	392
5.2 Results and Discussion	
5.2.1 Initial Preparation of 4-bromopyrrolidine Monomer, Dimerization and Characterization.....	394
5.2.2 Development of New Methods for Homodimerization, Elaboration of Dimers to Target <i>N</i> -acylated Dimers.....	398
5.2.3 Auto-oxidative Guanidine Incorporation into <i>N</i> -acylated Dimers.....	401
5.2.4 Future Research: Endgame Strategies for the Synthesis of (–)-Ageliferin and Intact Konbu'acidin and Carteramine Core Structures from a Common, Optically Active Intermediate.....	405

5.3 Conclusion.....	407
5.4 References and Notes.....	408
5.5 Experimental	
5.5.1 Materials and Methods .....	411
5.5.2 Experimental Procedures and Characterization Data.....	412
APPENDIX FOUR (A4, Chapter Five)	
5.6.1 Spectra Relevant to Chapter Five.....	422

## LIST OF FIGURES

### CHAPTER ONE

Figure 1.1 Postulated Oroidin-Based Origins of Dimeric Pyrrole–Imidazole Alkaloids.....	001
Figure 1.2 Biosynthesis of Primary Metabolites, Oroidin <b>1-1a</b> , Hymendin <b>1-1b</b> and Dispacamide <b>1-6</b> .....	002
Figure 1.3 Structural and Stereochemical Reassignment of Palau'amine.....	004
Figure 1.4 Related Dimers and Numerical Reference.....	005
Figure 1.5 Scheurer & Kinnel's Proposed Biosynthesis of Palau'amine <b>1-2a</b> .....	006
Figure 1.6 Proposed Pathways to Axinellamine A <b>1-3a</b> and Related Dimers.....	008
Figure 1.7 Retrosynthetic Analysis: A Symmetry-Based Synthesis of Palau'amine.....	010
Figure 1.8 Regio- and Stereocontrolled Dimerization of Dispacamide <b>1-6</b> .....	011
Figure 1.9 Early Proposals: Is palau'amine <b>1-2a</b> an outlier?.....	012
Figure 1.10 Proposed Access to Axinellamines <b>1-3</b> and Related Dimeric Pyrrole–Imidazoles from a Dispacamide Monomer <b>1-36</b> .....	020
Figure 1.11 Completed Synthetic Efforts.....	022
Figure 1.12 Summary of Synthetic Approaches Toward Palau'amine <b>1-2a</b> and <b>1-2b</b> , Axinellamines <b>1-3</b> , Massadines <b>1-5</b> and Ageliferin <b>1-4a</b> .....	026

### CHAPTER TWO

Figure 2.1 Monomer, Dimer, Remolded – Hypothesis.....	035
Figure 2.2 Alternative Masked Guanidine Synthons.....	036
Figure 2.3 Modified Strategy to Access Monomer <b>2-26</b> .....	045



Figure 2.4 Optimized cyclization conditions for intramolecular guanidine synthesis....	047
Figure 2.5 X-ray crystal structure of <i>meso</i> dimer <b>2-38b</b> .....	052
Figure 2.6 Optimization of Oxidative Dimerization.....	054
APPENDIX ONE	
Figure A1.1 <sup>1</sup> H NMR (500 MHz, DMSO- <i>d</i> <sub>6</sub> ) spectrum of compound <b>2-10</b> .....	123
Figure A1.2 <sup>13</sup> C NMR (125 MHz, DMSO- <i>d</i> <sub>6</sub> ) spectrum of compound <b>2-10</b> .....	124
Figure A1.3 <sup>1</sup> H NMR (600 MHz, H <sub>2</sub> O- <i>d</i> <sub>2</sub> ) spectrum of compound <b>2-10</b> .....	125
Figure A1.4 <sup>13</sup> C NMR (125 MHz, H <sub>2</sub> O- <i>d</i> <sub>2</sub> ) spectrum of compound <b>2-10</b> .....	126
Figure A1.5 <sup>1</sup> H NMR (500 MHz, CH <sub>3</sub> CN- <i>d</i> <sub>3</sub> ) spectrum of compound <b>2-17</b> .....	127
Figure A1.6 <sup>1</sup> H NMR (500 MHz, CH <sub>3</sub> CN- <i>d</i> <sub>3</sub> ) spectrum of compound <b>2-8</b> .....	128
Figure A1.7 <sup>1</sup> H NMR (500 MHz, CHCl <sub>3</sub> - <i>d</i> <sub>1</sub> ) spectrum of compound <b>2-21</b> .....	129
Figure A1.8 <sup>1</sup> H NMR (500 MHz, CH <sub>3</sub> CN- <i>d</i> <sub>3</sub> ) spectrum of compound <b>2-23</b> .....	130
Figure A1.9 <sup>13</sup> C NMR (125 MHz, CH <sub>3</sub> CN- <i>d</i> <sub>3</sub> , 343 K) spectrum of compound <b>2-23</b> .....	131
Figure A1.10 <sup>1</sup> H NMR (500 MHz, CH <sub>3</sub> CN- <i>d</i> <sub>3</sub> ) spectrum of compound <b>2-24a</b> .....	132
Figure A1.11 <sup>1</sup> H NMR (500 MHz, DMSO- <i>d</i> <sub>6</sub> ) spectrum of compound <b>2-28</b> .....	133
Figure A1.12 <sup>13</sup> C NMR (125 MHz, DMSO- <i>d</i> <sub>6</sub> ) spectrum of compound <b>2-28</b> .....	134
Figure A1.13 <sup>1</sup> H NMR (500 MHz, CH <sub>3</sub> CN- <i>d</i> <sub>3</sub> ) spectrum of compound <b>2-29a</b> .....	135
Figure A1.14 <sup>13</sup> C NMR (125 MHz, CH <sub>3</sub> CN- <i>d</i> <sub>3</sub> ) spectrum of compound <b>2-29a</b> .....	136
Figure A1.15 <sup>1</sup> H NMR (500 MHz, DMSO- <i>d</i> <sub>6</sub> ) spectrum of compound <b>2-29b</b> .....	137
Figure A1.16 <sup>13</sup> C NMR (125 MHz, DMSO- <i>d</i> <sub>6</sub> ) spectrum of compound <b>2-29b</b> .....	138
Figure A1.17 <sup>1</sup> H NMR (600 MHz, benzene- <i>d</i> <sub>6</sub> ) spectrum of compound <b>2-30</b> .....	139
Figure A1.18 <sup>13</sup> C NMR (125 MHz, CH <sub>3</sub> CN- <i>d</i> <sub>3</sub> ) spectrum of compound <b>2-30</b> .....	140
Figure A1.19 <sup>1</sup> H NMR (600 MHz, DMSO- <i>d</i> <sub>6</sub> ) spectrum of compound <b>2-26</b> .....	141

Figure A1.20 $^{13}\text{C}$ NMR (125 MHz, $\text{DMSO-}d_6$ ) spectrum of compound <b>2-26</b> .....	142
Figure A1.21 $^1\text{H}$ NMR (500 MHz, $\text{CH}_3\text{CN-}d_3$ ) spectrum of compound <b>2-31</b> .....	143
Figure A1.22 $^1\text{H}$ NMR (600 MHz, $\text{CH}_3\text{CN-}d_3$ , 343 K) spectrum of compound <b>2-31</b> .....	144
Figure A1.23 $^{13}\text{C}$ NMR (125 MHz, $\text{CH}_3\text{CN-}d_3$ ) spectrum of compound <b>2-31</b> .....	145
Figure A1.24 $^1\text{H}$ NMR (500 MHz, $\text{CH}_3\text{CN-}d_3$ ) spectrum of compound <b>2-40</b> .....	146
Figure A1.25 $^{13}\text{C}$ NMR (125 MHz, $\text{CH}_3\text{CN-}d_3$ ) spectrum of compound <b>2-40</b> .....	147
Figure A1.26 $^1\text{H}$ NMR (600 MHz, $\text{DMSO-}d_6$ , 343 K) spectrum of compound <b>2-38a</b> .....	148
Figure A1.27 $^{13}\text{C}$ NMR (125 MHz, $\text{CH}_3\text{CN-}d_3$ , 343 K) spectrum of compound <b>2-38a</b> .....	149
Figure A1.28 $^1\text{H}$ NMR (600 MHz, $\text{DMSO-}d_6$ , 373 K) spectrum of compound <b>2-38b</b> .....	150
Figure A1.29 $^{13}\text{C}$ NMR (150 MHz, $\text{DMSO-}d_6$ , 373 K) spectrum of compound <b>2-38b</b> .....	151
Figure A1.30 $^1\text{H}$ NMR (600 MHz, $\text{DMSO-}d_6$ , 373 K) spectrum of compound <b>2-39</b> .....	152
Figure A1.31 $^1\text{H}$ NMR (500 MHz, $\text{CH}_3\text{CN-}d_3$ ) spectrum of compound <b>2-41</b> .....	153
Figure A1.32 $^{13}\text{C}$ NMR (125 MHz, $\text{CH}_3\text{CN-}d_3$ ) spectrum of compound <b>2-41</b> .....	154
Figure A1.33 $^1\text{H}$ NMR (500 MHz, $\text{CHCl}_3\text{-}d_1$ ) spectrum of compound <b>2-42a</b> .....	155
Figure A1.34 $^{13}\text{C}$ NMR (125 MHz, $\text{CHCl}_3\text{-}d_1$ ) spectrum of compound <b>2-42a</b> .....	156
Figure A1.35 $^1\text{H}$ NMR (500 MHz, $\text{CH}_3\text{CN-}d_3$ ) spectrum of compound <b>2-44a</b> .....	157
Figure A1.36 $^{13}\text{C}$ NMR (125 MHz, $\text{CH}_3\text{CN-}d_3$ ) spectrum of compound <b>2-44a</b> .....	158
Figure A1.37 $^1\text{H}$ NMR (600 MHz, $\text{CH}_3\text{CN-}d_3$ ) spectrum of compound <b>2-44b</b> .....	159
Figure A1.38 $^{13}\text{C}$ NMR (150 MHz, $\text{CH}_3\text{CN-}d_3$ ) spectrum of compound <b>2-44b</b> .....	160
Figure A1.39 $^1\text{H}$ NMR (500 MHz, acetic acid- $d_4$ ) spectrum of compound <b>2-44b-1</b> .....	161
Figure A1.40 $^{13}\text{C}$ NMR (125 MHz, acetic acid- $d_4$ ) spectrum of compound <b>2-44b-1</b> .....	162
Figure A1.41 $^1\text{H}$ NMR (500 MHz, $\text{CH}_3\text{CN-}d_3$ ) spectrum of compound <b>2-47a</b> .....	163
Figure A1.42 $^{13}\text{C}$ NMR (125 MHz, $\text{CH}_3\text{CN-}d_3$ ) spectrum of compound <b>2-47a</b> .....	164

Figure A1.43 $^1\text{H}$ NMR (500 MHz, $\text{CH}_3\text{CN-}d_3$ ) spectrum of compound <b>2-47b</b> .....	165
Figure A1.44 $^{13}\text{C}$ NMR (125 MHz, $\text{CH}_3\text{CN-}d_3$ ) spectrum of compound <b>2-47b</b> .....	166
Figure A1.45 $^1\text{H}$ NMR (500 MHz, $\text{CH}_3\text{CN-}d_3$ ) spectrum of compound <b>2-49</b> .....	167
Figure A1.46 $^1\text{H}$ NMR (500 MHz, $\text{MeOH-}d_4$ ) spectrum of compound <b>2-50a (2·CF<sub>3</sub>CO<sub>2</sub>H)</b> <b>(major)</b> .....	168
Figure A1.47 $^{13}\text{C}$ NMR (125 MHz, $\text{MeOH-}d_4$ ) spectrum of compound <b>2-50a (2·CF<sub>3</sub>CO<sub>2</sub>H)</b> <b>(major)</b> .....	169
Figure A1.48 $^1\text{H}$ NMR (500 MHz, $\text{MeOH-}d_4$ ) spectrum of compound <b>2-50a (2·CF<sub>3</sub>CO<sub>2</sub>H)</b> <b>(minor)</b> .....	170
Figure A1.49 $^{13}\text{C}$ NMR (125 MHz, $\text{MeOH-}d_4$ ) spectrum of compound <b>2-50a (2·CF<sub>3</sub>CO<sub>2</sub>H)</b> <b>(minor)</b> .....	171
Figure A1.50 $^1\text{H}$ NMR (500 MHz, $\text{MeOH-}d_4$ ) spectrum of compound <b>2-50b (2·CF<sub>3</sub>CO<sub>2</sub>H)</b> <b>(minor)</b> .....	172
Figure A1.51 $^{13}\text{C}$ NMR (125 MHz, $\text{MeOH-}d_4$ ) spectrum of compound <b>2-50b (2·CF<sub>3</sub>CO<sub>2</sub>H)</b> <b>(minor)</b> .....	173
Figure A1.52 $^1\text{H}$ NMR (500 MHz, $\text{H}_2\text{O-}d_2$ ) spectrum of compound <b>2-51b (2·CF<sub>3</sub>CO<sub>2</sub>H)</b> .....	174
Figure A1.53 $^{13}\text{C}$ NMR (125 MHz, $\text{H}_2\text{O-}d_2$ ) spectrum of compound <b>2-51b (2·CF<sub>3</sub>CO<sub>2</sub>H)</b> .....	175
Figure A1.54 $^1\text{H}$ NMR (500 MHz, $\text{MeOH-}d_4$ ) spectrum of compound <b>2-51a (2·CF<sub>3</sub>CO<sub>2</sub>H)</b> ...	176
Figure A1.55 $^{13}\text{C}$ NMR (125 MHz, $\text{MeOH-}d_4$ ) spectrum of compound <b>2-51a (2·CF<sub>3</sub>CO<sub>2</sub>H)</b> ...	177
Figure A1.56 $^1\text{H}$ NMR (600 MHz, $\text{MeOH-}d_4$ ) spectrum of compound <b>2-57a (2·CF<sub>3</sub>CO<sub>2</sub>H)</b> ...	178
Figure A1.57 $^{13}\text{C}$ NMR (125 MHz, $\text{MeOH-}d_4$ ) spectrum of compound <b>2-57a (2·CF<sub>3</sub>CO<sub>2</sub>H)</b> ...	179
Figure A1.58 $^1\text{H}$ NMR (600 MHz, $\text{MeOH-}d_4$ ) spectrum of compound <b>2-57b (2·CF<sub>3</sub>CO<sub>2</sub>H)</b> ...	180
Figure A1.59 $^{13}\text{C}$ NMR (125 MHz, $\text{MeOH-}d_4$ ) spectrum of compound <b>2-57b (2·CF<sub>3</sub>CO<sub>2</sub>H)</b> ...	181

Figure A1.60 $^1\text{H}$ NMR (500 MHz, $\text{MeOH-}d_4$ ) spectrum of compound <b>2-58a</b> ( <b>2·CF<sub>3</sub>CO<sub>2</sub>H</b> )...182	182
Figure A1.61 $^1\text{H}$ NMR (500 MHz, $\text{DMSO-}d_6$ ) spectrum of compound <b>2-58a</b> ( <b>2·CF<sub>3</sub>CO<sub>2</sub>H</b> )...183	183
Figure A1.62 ROESY (600 MHz, $\text{DMSO-}d_6$ ) spectrum of compound <b>2-58a</b> ( <b>2·CF<sub>3</sub>CO<sub>2</sub>H</b> )....184	184
Figure A1.63 HMBC (600 MHz, $\text{MeOH-}d_4$ ) spectrum of compound <b>2-58a</b> ( <b>2·CF<sub>3</sub>CO<sub>2</sub>H</b> ).....185	185
Figure A1.64 Comparison of $^1\text{H}$ NMR ( $\text{DMSO-}d_6$ ) spectra (Top: synthetic <b>2-58a</b> , Bottom: natural axinellamine A <b>2-5a</b> ).....186	186
Figure A1.65 $^1\text{H}$ NMR (600 MHz, $\text{CH}_3\text{CN-}d_3$ ) spectrum of compound <b>2-59</b> ( <b>HCO<sub>2</sub>H</b> ) ( <b>major</b> ).....187	187
Figure A1.66 COSY (600 MHz, $\text{CH}_3\text{CN-}d_3$ ) spectrum of compound <b>2-59</b> ( <b>HCO<sub>2</sub>H</b> ) ( <b>major</b> ) .....188	188
Figure A1.67 $^1\text{H}$ NMR (600 MHz, $\text{CH}_3\text{CN-}d_3$ ) spectrum of compound <b>2-59</b> ( <b>HCO<sub>2</sub>H</b> ) ( <b>minor</b> ).....189	189
Figure A1.68 COSY (600 MHz, $\text{CH}_3\text{CN-}d_3$ ) spectrum of compound <b>2-59</b> ( <b>HCO<sub>2</sub>H</b> ) ( <b>minor</b> ).....190	190
Figure A1.69 $^1\text{H}$ NMR (600 MHz, $\text{CH}_3\text{CN-}d_3$ ) spectrum of compound <b>2-60</b> ( <b>HCO<sub>2</sub>H</b> ) ( <b>major</b> ).....191	191
Figure A1.70 $^1\text{H}$ NMR (600 MHz, $\text{CH}_3\text{CN-}d_3$ ) spectrum of compound <b>2-60</b> ( <b>HCO<sub>2</sub>H</b> ) ( <b>minor</b> ).....192	192
Figure A1.71 $^1\text{H}$ NMR (600 MHz, $\text{CH}_3\text{CN-}d_3$ ) spectrum of compound <b>2-61</b> ( <b>2·HCO<sub>2</sub>H</b> ).....193	193
Figure A1.72 COSY (600 MHz, $\text{CH}_3\text{CN-}d_3$ ) spectrum of compound <b>2-61</b> ( <b>2·HCO<sub>2</sub>H</b> ).....194	194

## CHAPTER THREE

Figure 3.1 Pyrrole–Imidazole Alkaloids: Monomer Oxidation State ( <b>3-1</b> , <b>3-3</b> ) and the Interrelatedness of Derived Dimers.....	223
Figure 3.2 Spirocycles <b>3-12</b> Synthesis.....	225
Figure 3.3 Reactivity and Characterization of Pentacycle <b>3-21</b> .....	230
Figure 3.4 Model Studies.....	232
Figure 3.5 Precedent for Reductive Ring Expansions in Hydantoin Systems.....	233
Figure 3.6 Deuterium Exchange Studies, 2-Aminoimidazole Model System <b>3-38</b> for Mechanistic Speculation Relevant to Thermolysis Experiments.....	235
Figure 3.7 Mechanistic Proposals for the Equilibration of C10,C14 in Isomer <b>3-12</b> .....	236

## APPENDIX TWO

Figure A2.1 <sup>1</sup> H NMR (500 MHz, MeOH- <i>d</i> <sub>4</sub> ) spectrum of compound <b>3-12d</b> ( <b>2·CF<sub>3</sub>CO<sub>2</sub>H</b> ).....	257
Figure A2.2 <sup>13</sup> C NMR (125 MHz, MeOH- <i>d</i> <sub>4</sub> ) spectrum of compound <b>3-12d</b> ( <b>2·CF<sub>3</sub>CO<sub>2</sub>H</b> ).....	258
Figure A2.3 <sup>1</sup> H NMR (500 MHz, MeOH- <i>d</i> <sub>4</sub> ) spectrum of compound <b>3-12b</b> ( <b>2·CF<sub>3</sub>CO<sub>2</sub>H</b> ).....	259
Figure A2.4 <sup>13</sup> C NMR (125 MHz, MeOH- <i>d</i> <sub>4</sub> ) spectrum of compound <b>3-12b</b> ( <b>2·CF<sub>3</sub>CO<sub>2</sub>H</b> ).....	260
Figure A2.5 <sup>1</sup> H NMR (500 MHz, MeOH- <i>d</i> <sub>4</sub> ) spectrum of compound <b>3-2</b> ( <b>2·CF<sub>3</sub>CO<sub>2</sub>H</b> ).....	261
Figure A2.6 <sup>13</sup> C NMR (125 MHz, MeOH- <i>d</i> <sub>4</sub> ) spectrum of compound <b>3-2</b> ( <b>2·CF<sub>3</sub>CO<sub>2</sub>H</b> ).....	262
Figure A2.7 <sup>1</sup> H NMR (500 MHz, MeOH- <i>d</i> <sub>4</sub> ) spectrum of compound <b>3-16</b> ( <b>2·CF<sub>3</sub>CO<sub>2</sub>H</b> ).....	263
Figure A2.8 <sup>13</sup> C NMR (125 MHz, MeOH- <i>d</i> <sub>4</sub> ) spectrum of compound <b>3-16</b> ( <b>2·CF<sub>3</sub>CO<sub>2</sub>H</b> ).....	264
Figure A2.9 <sup>1</sup> H NMR (500 MHz, MeOH- <i>d</i> <sub>4</sub> ) spectrum of compound <b>3-17</b> ( <b>2·CF<sub>3</sub>CO<sub>2</sub>H</b> ).....	265
Figure A2.10 <sup>13</sup> C NMR (125 MHz, MeOH- <i>d</i> <sub>4</sub> ) spectrum of compound <b>3-17</b> ( <b>2·CF<sub>3</sub>CO<sub>2</sub>H</b> ).....	266
Figure A2.11 <sup>1</sup> H NMR (500 MHz, MeOH- <i>d</i> <sub>4</sub> ) spectrum of compound <b>3-21a</b> ( <b>2·CF<sub>3</sub>CO<sub>2</sub>H</b> ).....	267

Figure A2.12	$^1\text{H}$ NMR (500 MHz, $\text{DMSO-}d_6$ ) spectrum of compound <b>3-21a</b> ( $2\cdot\text{CF}_3\text{CO}_2\text{H}$ )	268
Figure A2.13	$^{13}\text{C}$ NMR (125 MHz, $\text{MeOH-}d_4$ ) spectrum of compound <b>3-21a</b> ( $2\cdot\text{CF}_3\text{CO}_2\text{H}$ )	269
Figure A2.14	$^1\text{H}$ NMR (500 MHz, $\text{MeOH-}d_4$ ) spectrum of compound <b>3-21b</b> ( $2\cdot\text{CF}_3\text{CO}_2\text{H}$ )	270
Figure A2.15	$^1\text{H}$ NMR (500 MHz, $\text{DMSO-}d_6$ ) spectrum of compound <b>3-21b</b> ( $2\cdot\text{CF}_3\text{CO}_2\text{H}$ )	271
Figure A2.16	$^{13}\text{C}$ NMR (125 MHz, $\text{MeOH-}d_4$ ) spectrum of compound <b>3-21b</b> ( $2\cdot\text{CF}_3\text{CO}_2\text{H}$ )	272
Figure A2.17	$^1\text{H}$ NMR (500 MHz, $\text{MeOH-}d_4$ ) spectrum of compound <b>3-23</b> (freebase)	273
Figure A2.18	$^{13}\text{C}$ NMR (125 MHz, $\text{MeOH-}d_4$ ) spectrum of compound <b>3-23</b> (freebase)	274
Figure A2.19	$^1\text{H}$ NMR (500 MHz, $\text{MeOH-}d_4$ ) spectrum of compound <b>3-23</b> ( $\text{CF}_3\text{CO}_2\text{H}$ )	275
Figure A2.20	$^{13}\text{C}$ NMR (125 MHz, $\text{MeOH-}d_4$ ) spectrum of compound <b>3-23</b> ( $\text{CF}_3\text{CO}_2\text{H}$ )	276
Figure A2.21	$^1\text{H}$ NMR (500 MHz, $\text{MeOH-}d_4$ ) spectrum of compound <b>3-25</b> ( $\text{CF}_3\text{CO}_2\text{H}$ )	277
Figure A2.22	$^{13}\text{C}$ NMR (125 MHz, $\text{MeOH-}d_4$ ) spectrum of compound <b>3-25</b> ( $\text{CF}_3\text{CO}_2\text{H}$ )	278
Figure A2.23	$^1\text{H}$ NMR (500 MHz, $\text{CHCl}_3\text{-}d_1$ ) spectrum of compound <b>3-37a</b>	279
Figure A2.24	$^{13}\text{C}$ NMR (150 MHz, $\text{CHCl}_3\text{-}d_1$ ) spectrum of compound <b>3-37a</b>	280
Figure A2.25	$^1\text{H}$ NMR (500 MHz, $\text{MeOH-}d_4$ ) spectrum of compound <b>3-37b</b> (crude)	281
Figure A2.26	$^{13}\text{C}$ NMR (125 MHz, $\text{MeOH-}d_4$ ) spectrum of compound <b>3-37b</b> (crude)	282
Figure A2.27	$^1\text{H}$ NMR (600 MHz, $\text{H}_2\text{O-}d_2$ ) spectrum of compound <b>3-38</b> ( $\text{CF}_3\text{CO}_2\text{H}$ )	283
Figure A2.28	$^{13}\text{C}$ NMR (125 MHz, $\text{H}_2\text{O-}d_2$ ) spectrum of compound <b>3-38</b> ( $\text{CF}_3\text{CO}_2\text{H}$ )	284
Figure A2.29	$^1\text{H}$ NMR (600 MHz, $\text{H}_2\text{O-}d_2$ ) spectrum of compound <b>3-40</b> ( $\text{CF}_3\text{CO}_2\text{H}$ )	285

## CHAPTER FOUR

Figure 4.1	Proposed Access to Chlorospirocyclopentane ( <b>4-3</b> ) via oxidative ring contraction of ( $\pm$ )-ageliferin	286
Figure 4.2	Proposed Study to understand reactivity towards oxidations	288

Figure 4.3 Key Characterization Data.....	295
Figure 4.4 Proposed Synthesis of (-)-Ageliferin ( <b>4-1a</b> ).....	296
APPENDIX THREE	
Figure A3.1 <sup>1</sup> H NMR (500 MHz, MeOH- <i>d</i> <sub>4</sub> ) spectrum of compound <b>4-7 (freebase)</b> .....	339
Figure A3.2 <sup>13</sup> C NMR (125 MHz, MeOH- <i>d</i> <sub>4</sub> ) of compound <b>4-7 (freebase)</b> .....	340
Figure A3.3 <sup>1</sup> H NMR (500 MHz, MeOH- <i>d</i> <sub>4</sub> ) spectrum of compound <b>4-7b (CF<sub>3</sub>CO<sub>2</sub>H)</b> .....	341
Figure A3.4 <sup>13</sup> C NMR (125 MHz, MeOH- <i>d</i> <sub>4</sub> ) spectrum of compound <b>4-7b (CF<sub>3</sub>CO<sub>2</sub>H)</b> .....	342
Figure A3.5 <sup>1</sup> H NMR (500 MHz, MeOH- <i>d</i> <sub>4</sub> ) spectrum of compound <b>4-13</b> .....	343
Figure A3.6 <sup>1</sup> H NMR (500 MHz, H <sub>2</sub> O- <i>d</i> <sub>2</sub> ) spectrum of compound <b>4-8 (HCl)</b> .....	344
Figure A3.7 <sup>13</sup> C NMR (125 MHz, MeOH- <i>d</i> <sub>4</sub> ) spectrum of compound <b>4-8 (HCl)</b> .....	345
Figure A3.8 <sup>1</sup> H NMR (500 MHz, MeOH- <i>d</i> <sub>4</sub> ) spectrum of compound <b>4-10 (freebase)</b> .....	346
Figure A3.9 <sup>1</sup> H NMR (500 MHz, H <sub>2</sub> O- <i>d</i> <sub>2</sub> ) spectrum of compound <b>4-11 (CF<sub>3</sub>CO<sub>2</sub>H)</b> .....	347
Figure A3.10 <sup>1</sup> H NMR (500 MHz, H <sub>2</sub> O- <i>d</i> <sub>2</sub> ) spectrum of compound <b>4-5 (2·CF<sub>3</sub>CO<sub>2</sub>H)</b> .....	348
Figure A3.11 <sup>1</sup> H NMR (500 MHz, MeOH- <i>d</i> <sub>4</sub> ) spectrum of compound <b>4-5 (2·CF<sub>3</sub>CO<sub>2</sub>H)</b> .....	349
Figure A3.12 <sup>13</sup> C NMR (125 MHz, H <sub>2</sub> O- <i>d</i> <sub>2</sub> ) spectrum of compound <b>4-5 (2·CF<sub>3</sub>CO<sub>2</sub>H)</b> .....	350
Figure A3.13 <sup>13</sup> C NMR (125 MHz, MeOH- <i>d</i> <sub>4</sub> ) spectrum of compound <b>4-5 (2·CF<sub>3</sub>CO<sub>2</sub>H)</b> .....	351
Figure A3.14 <sup>1</sup> H NMR (500 MHz, MeOH- <i>d</i> <sub>4</sub> ) spectrum of compound <b>4-12 (2·CF<sub>3</sub>CO<sub>2</sub>H)</b> .....	352
Figure A3.15 <sup>1</sup> H NMR (500 MHz, CH <sub>3</sub> CN- <i>d</i> <sub>3</sub> ) spectrum of compound <b>4-15</b> .....	353
Figure A3.16 <sup>1</sup> H NMR (500 MHz, DMSO- <i>d</i> <sub>6</sub> ) spectrum of compound <b>4-15</b> .....	354
Figure A3.17 <sup>13</sup> C NMR (125 MHz, DMSO- <i>d</i> <sub>6</sub> ) spectrum of compound <b>4-15</b> .....	355
Figure A3.18 <sup>1</sup> H NMR (500 MHz, CH <sub>3</sub> CN- <i>d</i> <sub>3</sub> ) spectrum of compound <b>4-16</b> .....	356
Figure A3.19 <sup>13</sup> C NMR (125 MHz, CH <sub>3</sub> CN- <i>d</i> <sub>3</sub> ) spectrum of compound <b>4-16</b> .....	357
Figure A3.20 <sup>1</sup> H NMR (500 MHz, MeOH- <i>d</i> <sub>4</sub> ) spectrum of compound <b>4-18 (HCl)</b> .....	358

Figure A3.21 $^{13}\text{C}$ NMR (125 MHz, $\text{MeOH-}d_4$ ) spectrum of compound <b>4-18 (HCl)</b> .....	359
Figure A3.22 $^1\text{H}$ NMR (500 MHz, $\text{CHCl}_3-d_1$ ) spectrum of compound <b>4-42a</b> .....	360
Figure A3.23 $^{13}\text{C}$ NMR (125 MHz, $\text{CHCl}_3-d_1$ ) spectrum of compound <b>4-42a</b> .....	361
Figure A3.24 $^1\text{H}$ NMR (500 MHz, $\text{CHCl}_3-d_1$ ) spectrum of compound <b>4-42b</b> .....	362
Figure A3.25 $^{13}\text{C}$ NMR (125 MHz, $\text{CHCl}_3-d_1$ ) spectrum of compound <b>4-42b</b> .....	363
Figure A3.26 $^1\text{H}$ NMR (500 MHz, $\text{CHCl}_3-d_1$ ) spectrum of compound <b>4-43a</b> .....	364
Figure A3.27 $^{13}\text{C}$ NMR (125 MHz, $\text{CHCl}_3-d_1$ ) spectrum of compound <b>4-43a</b> .....	365
Figure A3.28 $^1\text{H}$ NMR (500 MHz, $\text{CHCl}_3-d_1$ ) spectrum of compound <b>4-43b</b> .....	366
Figure A3.29 $^{13}\text{C}$ NMR (125 MHz, $\text{CHCl}_3-d_1$ ) spectrum of compound <b>4-43b</b> .....	367
Figure A3.30 $^1\text{H}$ NMR (500 MHz, $\text{H}_2\text{O-}d_2$ ) spectrum of compound <b>4-24 (<math>3\cdot\text{CF}_3\text{CO}_2\text{H}</math>)</b> .....	368
Figure A3.31 $^1\text{H}$ NMR (500 MHz, $\text{MeOH-}d_4$ ) spectrum of compound <b>4-24 (<math>3\cdot\text{CF}_3\text{CO}_2\text{H}</math>)</b> .....	369
Figure A3.32 $^{13}\text{C}$ NMR (125 MHz, $\text{MeOH-}d_4$ ) spectrum of compound <b>4-24 (<math>3\cdot\text{CF}_3\text{CO}_2\text{H}</math>)</b> .....	370
Figure A3.33 $^1\text{H}$ NMR (500 MHz, $\text{CHCl}_3-d_1$ ) spectrum of compound <b>4-47</b> .....	371
Figure A3.34 $^1\text{H}$ NMR (500 MHz, $\text{MeOH-}d_4$ ) spectrum of compound <b>4-48</b> .....	372
Figure A3.35 $^{13}\text{C}$ NMR (125 MHz, $\text{MeOH-}d_4$ ) spectrum of compound <b>4-48</b> .....	373
Figure A3.36 $^1\text{H}$ NMR (500 MHz, $\text{MeOH-}d_4$ ) spectrum of compound <b>4-45</b> .....	374
Figure A3.37 $^1\text{H}$ NMR (500 MHz, $\text{CH}_3\text{CN-}d_3$ ) spectrum of compound <b>4-45</b> .....	375
Figure A3.38 $^{13}\text{C}$ NMR (125 MHz, $\text{MeOH-}d_4$ ) spectrum of compound <b>4-45</b> .....	376
Figure A3.39 $^{13}\text{C}$ NMR (125 MHz, $\text{CH}_3\text{CN-}d_3$ ) spectrum of compound <b>4-45</b> .....	377
Figure A3.40 $^1\text{H}$ NMR (500 MHz, $\text{MeOH-}d_4$ ) spectrum of compound <b>4-26 (<math>\text{CF}_3\text{CO}_2\text{H}</math>)</b> .....	378
Figure A3.41 $^{13}\text{C}$ NMR (125 MHz, $\text{MeOH-}d_4$ ) spectrum of compound <b>4-26 (<math>\text{CF}_3\text{CO}_2\text{H}</math>)</b> .....	379
Figure A3.42 $^1\text{H}$ NMR (500 MHz, $\text{CH}_3\text{CN-}d_3$ ) spectrum of compound <b>4-46 (<math>\text{CF}_3\text{CO}_2\text{H}</math>)</b> .....	380
Figure A3.43 $^{13}\text{C}$ NMR (125 MHz, $\text{CH}_3\text{CN-}d_3$ ) spectrum of compound <b>4-46 (<math>\text{CF}_3\text{CO}_2\text{H}</math>)</b> .....	381



Figure A3.44 $^1\text{H}$ NMR (500 MHz, $\text{MeOH-}d_4$ ) spectrum of compound <b>4-53</b> ( $2\cdot\text{CF}_3\text{CO}_2\text{H}$ ).....	382
Figure A3.45 $^1\text{H}$ NMR (500 MHz, $\text{MeOH-}d_4$ ) spectrum of compound <b>4-54</b> ( $\text{CF}_3\text{CO}_2\text{H}$ ).....	383
Figure A3.46 $^1\text{H}$ NMR (500 MHz, $\text{DMSO-}d_6$ ) spectrum of compound <b>4-56</b> .....	384
Figure A3.47 $^{13}\text{C}$ NMR (125 MHz, $\text{DMSO-}d_6$ ) spectrum of compound <b>4-56</b> .....	385
Figure A3.48 $^1\text{H}$ NMR (500 MHz, $\text{MeOH-}d_4$ ) spectrum of compound <b>4-62</b> .....	386
Figure A3.49 $^{13}\text{C}$ NMR (125 MHz, $\text{MeOH-}d_4$ ) spectrum of compound <b>4-62</b> .....	387

## CHAPTER FIVE

Figure 5.1 Prospect and Current Understanding of Dispacamide Dimer Equilibrium...	388
Figure 5.2 Alternative Access to Dispacamide Dimers.....	389
Figure 5.3 Targeted 3,3'-bipyrrolidine Homodimer <b>5-9</b> .....	391
Figure 5.4 Nickel-catalyzed Reductive Cross-Coupling of Unactivated Alkyl Halides.	392
Figure 5.5 Analysis of Diastereomers <b>5-25</b> .....	396
Figure 5.6 Characterization of Minor $C_2$ -diastereomer <b>5-25-1</b> .....	397
Figure 5.7 Nickel-catalyzed Reductive Homodimerization.....	399

## APPENDIX FOUR

Figure A4.1 $^1\text{H}$ NMR (500 MHz, $\text{CHCl}_3-d_1$ ) spectrum of compound <b>5-22</b> .....	423
Figure A4.2 $^{13}\text{C}$ NMR (125 MHz, $\text{CHCl}_3-d_1$ ) spectrum of compound <b>5-22</b> .....	424
Figure A4.3 $^1\text{H}$ NMR (500 MHz, $\text{CHCl}_3-d_1$ ) spectrum of compound <b>5-23</b> (mixture).....	425
Figure A4.4 $^1\text{H}$ NMR (500 MHz, $\text{CHCl}_3-d_1$ ) spectrum of compound <b>5-23</b> (mixture).....	426
Figure A4.5 $^{13}\text{C}$ NMR (125 MHz, $\text{CHCl}_3-d_1$ ) spectrum of compound <b>5-23</b> (mixture).....	427
Figure A4.6 $^1\text{H}$ NMR (500 MHz, $\text{DMSO-}d_6$ ) spectrum of diamine derived from <b>5-23</b> .....	428
Figure A4.7 $^{13}\text{C}$ NMR (125 MHz, $\text{DMSO-}d_6$ ) spectrum of diamine derived from <b>5-23</b> .....	429
Figure A4.8 $^1\text{H}$ NMR (500 MHz, $\text{MeOH-}d_4$ ) spectrum of compound <b>5-18</b> .....	430

Figure A4.9 $^{13}\text{C}$ NMR (125 MHz, $\text{MeOH-}d_4$ ) spectrum of compound <b>5-18</b> .....	431
Figure A4.10 $^1\text{H}$ NMR (500 MHz, $\text{MeOH-}d_4$ ) spectrum of compound <b>5-26</b> .....	432
Figure A4.11 $^{13}\text{C}$ NMR (125 MHz, $\text{MeOH-}d_4$ ) spectrum of compound <b>5-26</b> .....	433
Figure A4.12 $^1\text{H}$ NMR (500 MHz, $\text{CHCl}_3\text{-}d_1$ ) spectrum of compound <b>5-27</b> .....	434
Figure A4.13 $^{13}\text{C}$ NMR (125 MHz, $\text{CHCl}_3\text{-}d_1$ ) spectrum of compound <b>5-27</b> .....	435
Figure A4.14 Analytical LC-MS UV trace (254-nm) of crude derivative mixture <b>5-25</b> .....	436
Figure A4.15 $^1\text{H}$ NMR (500 MHz, $\text{DMSO-}d_6$ ) spectrum of compound <b>5-25-1</b> .....	437
Figure A4.16 $^{13}\text{C}$ NMR (125 MHz, $\text{DMSO-}d_6$ ) spectrum of compound <b>5-25-1</b> .....	438
Figure A4.17 $^1\text{H}$ NMR (500 MHz, $\text{DMSO-}d_6$ ) spectrum of compound <b>5-25-2</b> .....	439
Figure A4.18 $^{13}\text{C}$ NMR (125 MHz, $\text{DMSO-}d_6$ ) spectrum of compound <b>5-25-2</b> .....	440
Figure A4.19 $^1\text{H}$ NMR (500 MHz, $\text{DMSO-}d_6$ ) spectrum of compound <b>5-25-3</b> .....	441
Figure A4.20 $^{13}\text{C}$ NMR (125 MHz, $\text{DMSO-}d_6$ ) spectrum of compound <b>5-25-3</b> .....	442

## LIST OF SCHEMES

### CHAPTER ONE

Scheme 1.1 Demonstrated Oxidative ‘Enamine’ Reactivity in Model Glycocyamidine.....	014
Scheme 1.2 Tethered Bis-alkylidenes are Prone to Spirocyclization.....	015
Scheme 1.3 A Symmetry-Based Approach.....	016
Scheme 1.4 Key Reactivity, Oxidative Spirocyclization of Bis-alkylidene <b>1-34</b> .....	018

### CHAPTER TWO

Scheme 2.1 Synthesis of Novel 4-(methylthio)-3,6-dihydro-2 <i>H</i> -1,3,5-oxadiazine <b>2-10</b> for Guanidine Synthesis.....	038
Scheme 2.2 Initial Synthesis of Reduced Dimers <b>2-20a</b> from Monomer <b>2-8</b> .....	040
Scheme 2.3 Model Studies Using Dispacamide Synthon <b>2-8</b> to Demonstrate Key Transformations.....	042
Scheme 2.4 Synthesis of Monomer <b>2-26</b> Using Discovered (COCl) <sub>2</sub> Activation.....	046
Scheme 2.5 Optimized 3-pot Procedure for a Scalable Synthesis of Monomer <b>2-31</b> .....	048
Scheme 2.6 General Synthesis of Dispacamide Monomers ( <b>2-36b</b> , <b>2-37b</b> ).....	049
Scheme 2.7 Regioselective Oxidative Dimerization of Titanocene Dienolates.....	051
Scheme 2.8 Elaboration of C <sub>2</sub> Dimer <b>2-38a</b> to Key Tetrabrominated C <sub>2</sub> -dimer <b>2-42</b> .....	056
Scheme 2.9 Base Induced Hydrazide Fragmentations in <b>2-42a</b> Does Not Provide Bis- alkylidene <b>2-43</b> .....	057

Scheme 2.10 Hydrazide Fragmentations with <b>2-42</b> provide solely bis-spirocyclic aminals.....	058
Scheme 2.11 Reactivity in the <i>Meso</i> series (from <b>2-19b</b> ) parallels observations in the $C_2$ Series.....	059
Scheme 2.12 Spirocycloisomerization of Bis-Spirocyclic Aminals <b>2-44</b> - Projected Access to Des-chloro (C13) Axinellamine A <b>2-48</b> .....	060
Scheme 2.13 Establishment of Spirocyclopentane <b>2-47a</b> Relative Stereochemistry.....	061
Scheme 2.14 Oxadiazine Ring Degradations and Chemoselective Glycoamidine Reduction Provides Aminoimidazoles <b>2-51</b> .....	062
Scheme 2.15 Access to Des-chloro (C13) Axinellamine A.....	063
Scheme 2.16 Access to Fully Synthetic, Partially Halogenated ( $\pm$ )-Axinellamine A <b>2-58a</b> from Aminoimidazole <b>2-51b</b> .....	066
Scheme 2.17 Unique Equilibrium of $C_2$ Dispacamide Dimers <b>2-44</b> - Access to Chlorinated (C13) Intermediates.....	068
Scheme 2.18 Access to Chlorinated ‘Bis-alkylidene’ <b>2-61</b> – Potential Access to Chlorinated Spirocyclopentane <b>2-45</b> .....	070

### CHAPTER THREE

Scheme 3.1 Thermolysis of Diastereomers <b>3-12</b> in $H_2O$ .....	226
Scheme 3.2 Thermolysis of Diastereomers <b>3-12</b> in $D_2O$ .....	227
Scheme 3.3 Total Synthesis of ( $\pm$ )-Ageliferin <b>3-2</b> .....	228
Scheme 3.4 Synthesis of <i>'Iso'</i> axinellamines ( <b>3-16</b> , <b>3-17</b> ).....	229

## CHAPTER FOUR

Scheme 4.1 Synthesis of Bis-Guanidine <b>4-5</b> .....	290
Scheme 4.2 Reactions of aminoimidazoles ( <b>4-7</b> , <b>4-13</b> ) with PTAD.....	292
Scheme 4.3 Aminoimidazole Oxidations with Singlet Oxygen.....	294
Scheme 4.4 Huigens <i>et al.</i> Attempted Synthesis of ( $\pm$ )-Ageliferin.....	298
Scheme 4.5 Horne's 'Biomimetic' Synthesis of Oroidin Derived Alkaloid Stevensine <b>4-39</b> .....	300
Scheme 4.6 Synthesis of Substituted 2-aminotetrahydrobenzimidazole ( <b>4-24</b> ).....	301
Scheme 4.7 Derivatization of 2-aminotetrahydrobenzimidazole ( <b>4-24</b> ).....	303
Scheme 4.8 Uncontrolled Oxidation of Ageliferin Core Substrates ( <b>4-24</b> , <b>4-26</b> , <b>4-45</b> )..	304
Scheme 4.9 Controlled Oxidation of Phthalimide Protected 2- aminotetrahydrobenzimidazole ( <b>4-46</b> ).....	306
Scheme 4.10 Proposed Alternative Synthesis of aminoimidazole ( <b>4-46</b> ).....	307

## CHAPTER FIVE

Scheme 5.1 Synthesis and Dimerization of (2 <i>S</i> ,4 <i>S</i> )-1-benzyl 2-ethyl 4-bromopyrrolidine- 1,2-dicarboxylate <b>5-22</b> to Access 3,3'-bipyrrolidine Homodimers <b>5-23</b> .....	394
Scheme 5.2 Initial Synthetic Route to Access N-acylated Homodimers <b>5-25</b> from 3,3'- bipyrrolidines <b>5-23</b> .....	395
Scheme 5.3 Initial Auto-Oxidative Guanidine Incorporation Attempts.....	402
Scheme 5.4 Optimized Conditions for the Auto-Oxidative Incorporation of Guanidine into <i>N</i> -acylated Homodimers <b>5-25</b> .....	403
Scheme 5.5 Elaboration of Spirocycloalkylidenes <b>5-12</b> .....	404

Scheme 5.6 Future Research.....405

## LIST OF TABLES

### CHAPTER TWO

Table 2.1 Optimization of Conditions to generate <b>2-26</b> & <b>2-8</b> from precursors <b>2-30</b> & <b>2-17</b> .....	047
Table 2.2 Optimization of Titanocene Dienolate based Oxidative Dimerization of <b>2-31</b> .....	054

### CHAPTER FIVE

Table 5.1 Optimization of Metal Catalyzed Reductive Dimerization of bromide <b>5-22</b> ..	400
--	-----

## LIST OF ABBREVIATIONS

18-C-6	18-Crown-6, 1,4,7,10,13,16-hexaoxacyclooctadecane
Bn	benzyl
Boc	<i>tert</i> -Butoxycarbonyl
Cbz	benzyloxycarbonyl
CCDC	Cambridge Crystallographic Data Centre
COSY	Correlation Spectroscopy
DBU	1,8-Diazobicyclo[5.4.0]undec-7-ene
DDQ	2,3-Dichloro-5,6-dicyano-1,4-benzoquinone
DEAD	N,N'-Diethyl azodicarboxylate
DIAD	N,N'-Diisopropyl azodicarboxylate
diglyme	1-Methoxy-2-(2-methoxyethoxy)ethane
DMA	N,N-Dimethylacetamide
DMAP	4-Dimethylaminopyridine
DMB	3,4-Dimethoxybenzyl
DMDO	Dimethyldioxirane
DME	1,2-Dimethoxyethane
DMF	Dimethylformamide
DMSO	Dimethylsulfoxide
<i>dr</i>	Diastereomeric ratio
<i>ee</i>	Enantiomeric excess
equiv	Equivalents
ESI	Electrospray ionization



glyme	1,2-Dimethoxyethane
HMBC	Heteronuclear Multiple Bond Correlation
HMQC	Heteronuclear Multiple Quantum Coherence
HPLC	High performance liquid chromatography
HRMS	High resolution mass spectrometry
HSQC	Heteronuclear Single Quantum Coherence
Hz	Hertz
IMDA	Intramolecular Diels-Alder Reaction
IR	Infrared
KHMDS	Potassium Hexamethyldisilazide, Potassium bis(trimethylsilyl)amide
LAB	Lithium amidotrihydroborate
LCMS	Liquid chromatography – mass spectrometry
m	meter
<i>m</i> CPBA	3-Chloroperbenzoic acid
mesyl	Methanesulfonyl
MMPP	Magnesium monoperoxyphthalate
mol	mole
MOM	Methoxymethyl
Ms	Methanesulfonyl
NBS	N-bromosuccinimide
NCS	N-chlorosuccinimide
NMR	Nuclear magnetic resonance
NOE	Nuclear Overhauser Effect

PDC	Pyridinium dichromate
PCC	Pyridinium chlorochromate
pHPLC	Preparative High performance liquid chromatography
Phth	Phthaloyl
PMB	4-Methoxybenzyl
PTAD	4-Phenyl-1,2,4-triazoline-3,5-dione
pyr	Pyridine
quant.	Quantitative
ROESY	Rotating frame Nuclear Overhauser Effect Spectroscopy
SEM	2-(Trimethylsilyl)ethoxymethyl
TBAF	Tetrabutylammonium fluoride
TBD	1,5,7-Triazabicyclo[4.4.0]dec-5-ene
TBDPS	tert-Butyldiphenylsilyl
TBHP	tert-Butyl hydroperoxide
TBS	tert-Butyldimethylsilyl
TBTU	O-(Benzotriazol-1-yl)-N,N,N',N'-tetramethyluronium tetrafluoroborate
Tf	Trifluoromethanesulfonyl
TFA	Trifluoroacetic acid
TFAA	Trifluoroacetic anhydride
TFE	2,2,2-Trifluoroethanol
THF	Tetrahydrofuran
TIPS	Tri- <i>iso</i> -propylsilyl
TLC	Thin-layer chromatography

TMG	tetramethylguanidine
TMS	Trimethylsilyl
tosyl	4-Toluenesulfonyl
TPAP	Tetrapropylammonium perruthenate
Ts	4-Toluenesulfonyl
UV	Ultraviolet

## ACKNOWLEDGEMENTS

I would like to thank my advisor, Professor Patrick G. Harran, for his continued support, mentorship and guidance. His creativity is contagious. The success of several methods developed during this project can be attributed to his persistence and motivation. *Never hesitate to revisit a failed result.* I would also like to thank Professor Neil K. Garg for his excellent mentorship as my organic faculty committee member. In addition, I am grateful for my committee members, Professor Paula Diaconescu and Professor Hsian-Rong Tseng. I appreciate their time and helpful suggestions during my qualification exam. I am indebted to Dr. Saeed I. Khan. His ability to solve X-ray crystal structures of synthetic intermediates obtained during my research was instrumental to the success of this project.

I am thankful for all past and present members of the Harran laboratory. I am grateful for the mentorship of Dr. Hui Ding. He is a great friend and an invaluable research partner. His work ethic and productivity are inspiring. I will always value the friendship of my peers at the University of California, Los Angeles. My talented colleagues Ken Lawson, Tristan Rose, Ryan Hollibaugh, Robert Jordan, Jack Bracken, Dr. James Frederich and Brice Curtin have become great friends over the years.

I appreciate the early support and guidance of my undergraduate research advisors, Professor Yitzhak Tor and Dr. Haim Weizman at the University of California, San Diego. In addition, the mentorship of Dr. Allen Seligson and Dr. Sheldon Saul-Hendler during my time in San Diego was invaluable. I am thankful for Professor Tom J. Maricich and my grandfather, Professor Charles Alfred Roberts. They are independently responsible for my general interest in chemistry. Some of my first organic chemistry experiments were conducted with Professor Maricich. The dedication of these scientific mentors is inspiring.

Lastly, I wish to thank my family. My parents, Charles and Vicki Roberts, are tremendously supportive of my academic career in science. Equally appreciated are my siblings, Laura, Nicholas, Daniel and my brother-in-law Beck Roghaar. Their general interest in my studies and research is motivational. I am grateful for my wife, Tiffany Yu Roberts. Her continued love and support gives me confidence in my career choices.

## CURRICULUM VITAE

*Andrew George Roberts*

### Education

B.S. Chemistry      University of California, San Diego      June 2008  
*September 2004 to June 2008*

HS Diploma      Wilson Classical High School, Long Beach, CA      June 2004  
*September 2000 to June 2004*

*4.0 GPA High School Valedictorian*

### Professional and Academic Experience

**Graduate Student Researcher**      University of California, Los Angeles  
*August 2008 to June 2013*

Advisor: Dr. Patrick Harran  
Advanced to Ph.D. Candidacy      December 2010

Total Synthesis of Pyrrole–Imidazole Alkaloids: (±)-Ageliferin and the Complete Axinellamine Ring System  
Developed several methods for the synthesis of polycyclic bis-guanidines

**Undergraduate Researcher**      University of California, San Diego  
*January 2008 to July 2008*

Advisors: Dr. Yitzhak Tor, Dr. Haim Weizman

Synthesis of fluorescent nucleosides: Novel preparation of 5-meso-borondipyrromethene-2'-deoxyuridine for incorporation into a DNA oligomer to study physical and fluorescent properties

**Synthetic Chemist**      Biophysica Inc., San Diego, CA  
*March 2007 to July 2008*

Synthesis and testing of novel antiandrogens designed as SERMs (Selective Estrogen Receptor Modulators) under the direction of Dr. Allen Seligson

**Research Assistant**      IriSys Inc., San Diego, CA  
*September 2006 to March 2007*

GMP Pharmaceutical Production  
QC laboratory technician – HPLC analysis, stability studies of novel pharmaceuticals

**Undergraduate Researcher**  
*June 2006 to September 2006*

California State University Long Beach

Advisor: Dr. Tom Maricich  
Synthesis of sulfonamides and sulfonimidates; studies on the use of *O*-ethyl sulfonimidates for acid catalyzed *O*-alkylations

## **Publications**

1. Ding, H.; **Roberts, A. G.**; Harran, P. G. *Total Synthesis of Ageliferin via Acyl N-amidinyliminium Ion Rearrangement*, *Chem. Sci.* **2013**, *4*, 303 – 306.
2. Ding, H.; **Roberts, A. G.**; Harran, P. G. *Synthetic (±)-Axinellamines Deficient in Halogen*, *Angew. Chem. Int. Ed.* **2012**, *51*, 4340 – 4343.
3. Li, Q.; Hurley, P.; Ding, H.; **Roberts, A. G.**; Akella, R.; Harran, P. G. *Exploring Symmetry-Based Logic for a Synthesis of Palau'amine*, *J. Org. Chem.* **2009**, *74*, 5909 – 5919.

## **Presentations**

1. **Roberts, A. G.**; Harran, P. G. *Total Synthesis of Pyrrole–Imidazole Alkaloids: Symmetry Based Access to Complex Polycyclic Bis-Guanidines*, Division of Organic Chemistry, ACS Graduate Research Symposium, University of Colorado, Boulder, CO. July 2012. (oral presentation)
2. **Roberts, A. G.**; Ding, H.; Harran, P. G. *Navigating dispacamide dimer ensembles to access complex pyrrole–imidazole alkaloids*, 243rd ACS National Meeting, San Diego, CA. March 2012. (poster presentation – ORGN 253)
3. **Roberts, A. G.**; Ding, H.; Harran, P. G. *Navigating Dispacamide Dimer Ensembles to Access Complex Pyrrole–Imidazole Alkaloids*, 243rd ACS National Meeting, UCLA Cram, Kavli, Foote, Stone and Winstein Chair Poster Session, San Diego, CA. March 2012. (poster presentation)
4. **Roberts, A. G.**; Ding, H.; Harran, P. G. *Synthesis of (±)-Axinellamine A Deficient in Halogen and (±)-Ageliferin*, UCLA Donald J. and Jane M. Cram Chair Poster Session, Los Angeles, CA. March 2012. (poster presentation)
5. **Roberts, A. G.**; Ding, H.; Harran, P. G. *Palau'amine: A unique challenge for synthesis*, 239th ACS National Meeting, San Francisco, CA. March 2010. (poster presentation – ORGN 642)

6. **Roberts, A. G.;** Ding, H.; Harran, P. G. *Palau'amine: A unique challenge for synthesis*, 239th ACS National Meeting, *UCLA Cram and Winstein Chair Poster Session*, San Francisco, CA. March 2010. (poster presentation)

## **Awards**

UCLA Dissertation Year Fellowship, 2012 – 2013.

Senior Foote Fellow, Christopher S. Foote Graduate Fellowship in Organic Chemistry, 2011 – 2013.

UCLA Travel Award for 243<sup>rd</sup> ACS National Meeting, San Diego, CA, March 2012.

UCLA Travel Award for 239<sup>th</sup> ACS National Meeting, San Francisco, CA, March 2010.

*Honors*, B.S. Chemistry, University of California, San Diego (award for excellence in undergraduate research), June 2008.



## Chapter One – Dimeric Pyrrole–Imidazole Alkaloids: A Unique Challenge for Synthesis

### 1.1 Abstract.

Polycyclic ‘pyrrole–imidazole’ alkaloids isolated from marine organisms are structurally intriguing molecules. Their densely functionalized ring systems pose a unique challenge to existing synthetic methods. Moreover, the range of compelling, but poorly defined biological activities exhibited by members of this class continues to pique the interest of chemists and biochemists alike. Natural isolates in this family are scarce, causing many to pursue their synthesis in the laboratory.

### 1.2.1 Introduction: Dimeric Pyrrole–Imidazole Alkaloids.

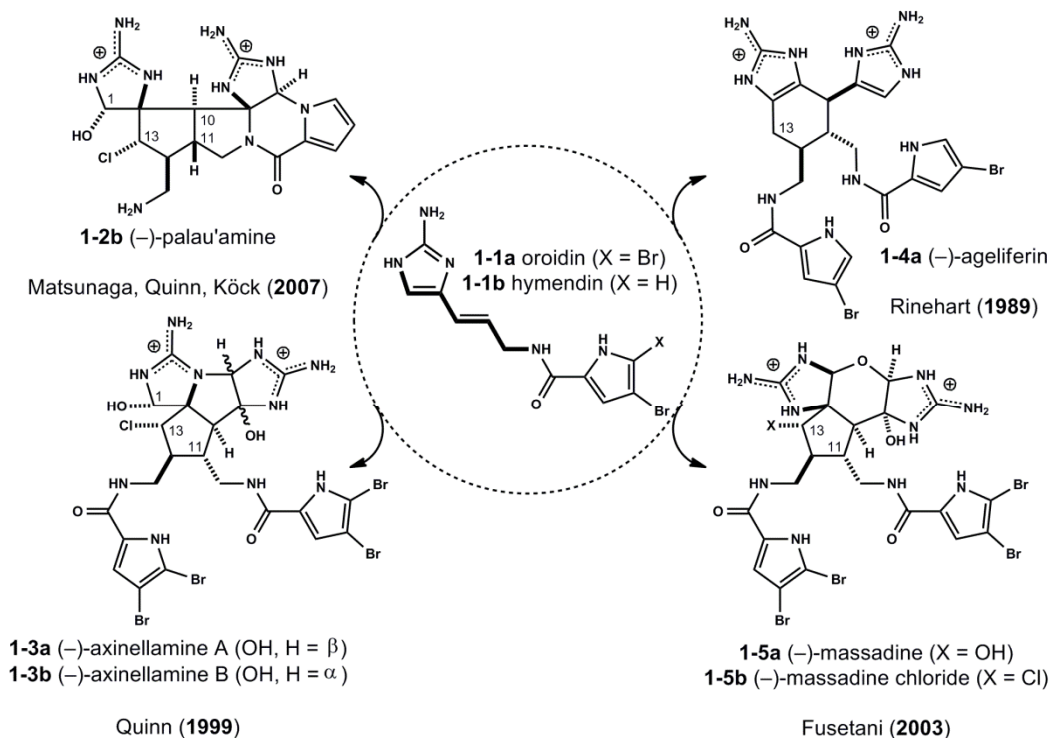


Figure 1.1. Postulated Oroidin-based Origins of Dimeric Pyrrole–Imidazole Alkaloids.

The dimeric pyrrole–imidazoles comprise a distinctive and growing list of alkaloids discovered in extracts of marine sponges of varying genera, these include: *Agelas*, *Axinella*, *Cymbastella*, *Hymeniacidon*, *Phakellia* and *Stylissa*.<sup>[1,2]</sup> The subset of dimeric and tetrameric pyrrole–imidazoles can be traced to simpler, monomeric units, oroidin **1-1a**<sup>[3]</sup> and its monobrominated congener, hymendin **1-1b** (Figure 1.1). The genesis of common, ‘imidazole intact’ congeners, sceptrin (not shown)<sup>[4]</sup> and ageliferin **1-4a**<sup>[5]</sup> are viewed as dimers of hymendin **1-1b**. The biosynthetic origins of dimeric pyrrole–imidazoles are largely speculative.<sup>[2d,6]</sup> However, studies link 3-amino-1-(2-aminoimidazolyl)prop-1-ene **1-7**<sup>[7]</sup> and 4,5-dibromopyrrole-2-carboxylic acid to oroidin **1-1a** and related metabolites (Figure 1.2).<sup>[8]</sup> Recent studies support such primary constituents may derive from *L*-lysine and *L*-proline.<sup>[9]</sup> Interestingly, other alternative reports demonstrate that partially oxidized proline dimers are susceptible to oxidation to form reactive intermediates such as dioxetanone **1-8** (Figure 1.2). In situ reaction with guanidine and oxidation provides dispacamide **1-6**, itself an oxidized metabolite of oroidin **1-1a**.<sup>[10]</sup>

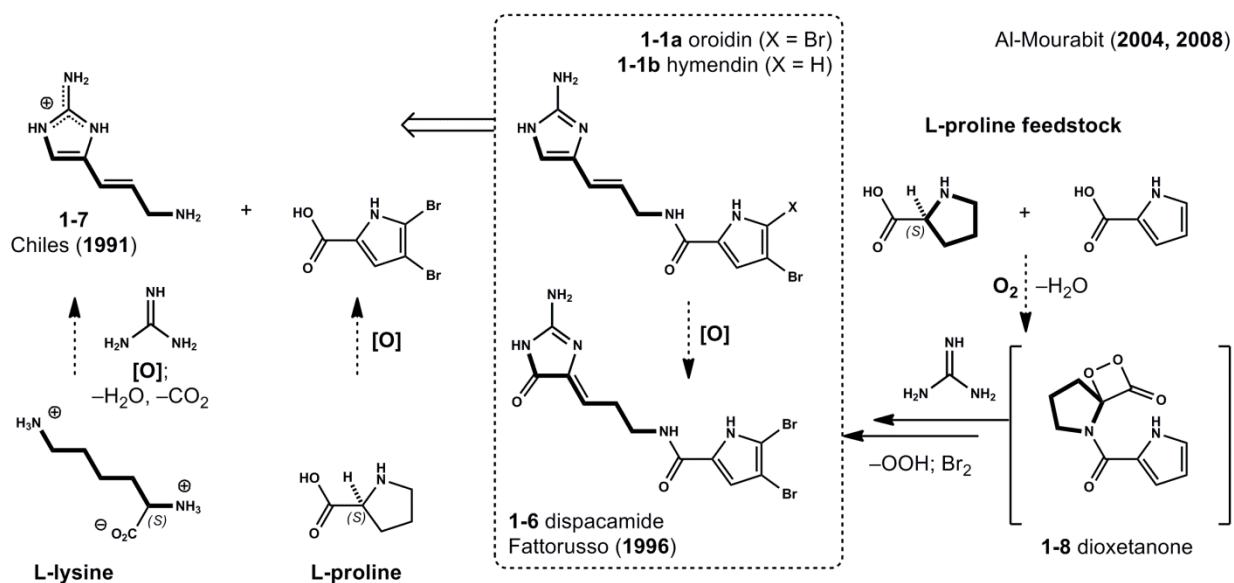


Figure 1.2. Biosynthesis of Primary Metabolites, Oroidin **1-1a**, Hymendin **1-1b** and Dispacamide **1-6**.

Early speculations on the diverse reactivity and cyclization modes available to monomeric metabolites such as oroidin **1-1a** are insightful.<sup>[6]</sup> However, the precise genesis of dimeric pyrrole–imidazoles is unknown and continues to be an intriguing topic of research. Recent interest in preparing pyrrole–imidazole dimers *de novo* using cell-free enzyme preparations from relevant marine sponge species holds considerable promise for the resolution of this issue.<sup>[11]</sup> Presumably, oxidative enzyme-mediated single-electron transfer mechanisms differentiate two units of oroidin **1-1a** to controllably access dimeric intermediates. Additionally, recent biomimetic studies with oroidin **1-1a** suggest the formation of non-oxidized, dimeric pyrrole–imidazoles can be achieved in the laboratory.<sup>[12]</sup> Future research in this area may provide insight into the precise origin of complex dimers (*e.g.* **1-2b**, **1-3**, **1-5**).

### **1.2.2 Complex Dimeric Pyrrole–Imidazole Alkaloids: Isolation, Structure and Biochemical Properties.**

Palau'amine **1-2b**, axinellamines **1-3**, ageliferin **1-4a** and massadines **1-5** are four exemplary members of a growing family of oroidin **1-1a** derived, dimeric derivatives (Figure 1.1).<sup>[1,2]</sup> Their complex structures and various biochemical properties are compelling.

Palau'amine **1-2b** was isolated in 1993 by Scheurer and Kinnel from extracts of marine sponge *Stylotella aurantium*.<sup>[13]</sup> Its originally proposed stereochemistry **1-2a** (Figure 1.3) has since been reassigned (*vide infra*).<sup>[14]</sup> The molecule is water soluble and stable under acidic conditions, however it reportedly decomposes above pH = 6.5.<sup>[13]</sup> Initial reports detail palau'amine **1-2b** exhibits both anti-bacterial (*S. aureus*, *B. subtilis*) and anti-fungal (*Penicillium notatum*) properties.<sup>[13]</sup> Additionally, the compound is cytotoxic against select tumor cell lines and possesses potent immunosuppressive activity in vitro (IC<sub>50</sub> < 35 nm, mixed lymphocyte

reaction).<sup>[13]</sup> Early biochemical experiments distinguished palau'amine **1-2b** from monomeric phakellin-type compounds, suggesting its hexacyclic composition was important for activity.<sup>[1,15]</sup> Recently, the immunosuppressive properties of **1-2b** have been revisited with synthetically prepared materials.<sup>[16]</sup> The report suggests palau'amine **1-2b** cytotoxicity may be due to inhibition of proteolytic activity via irreversible binding to the human 20S proteasome, preventing the degradation of ubiquitin proteins.<sup>[16]</sup> Further examination of these cellular functions will undoubtedly help elucidate the molecular mode of action exhibited by palau'amine **1-2b**.

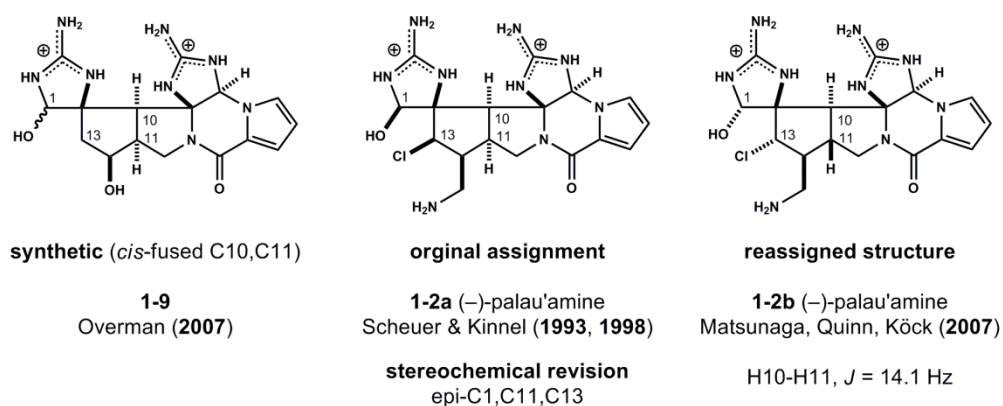


**Figure 1.3.** Structural and Stereochemical Reassignment of Palau'amine.

In 2007, a series of reports from Matsunaga<sup>[14a]</sup>, Quinn<sup>[14bc]</sup> and Köck<sup>[14d]</sup> established that the relative stereochemical assignment (C11, C13) of palau'amine **1-2a** was incorrect (Figure 1.3).<sup>[17]</sup> The revision of palau'amine received further attention in a thorough study published by the Overman group that corroborated these concerns.<sup>[18]</sup> This seminal report provided spectroscopic data for *cis*-fused (H10-H11) synthetic hexacyclic congeners **1-9**, as equilibrating C1 epimers, and allowed for direct comparison of relevant spectroscopic data. Specifically, the large observed coupling constant ( $J = 14.1$  Hz) for protons H10-H11 suggested the originally assigned *cis*-fused 3-azabicyclo[3.3.0]octane core **1-2a** was inconsistent with the smaller values observed for **1-9** (H10-H11, <sup>1</sup>H NMR data for both C1 epimers,  $J = 12.0$  Hz and 10.7 Hz). This

conclusion required many groups to adapt or reevaluate their synthetic strategy to access the *trans*-fused 3-azabicyclo[3.3.0]octane core of palau'amine **1-2b**.<sup>[1,2d]</sup> Additional details of this revision and its impact on ring strain and structure in **1-2b** have been reviewed.<sup>[2d,19]</sup>

With regard to structure **1-2b**, the high nitrogen content within its densely functionalized hexacyclic core presents a challenge for synthesis.<sup>[20]</sup> The strained *trans*-fused 3-azabicyclo[3.3.0]octane core **1-2b** scaffolds spirocyclic guanidine moieties and harbors a secondary alkyl chloride at C13. Notably, the chlorinated spirocyclopentane core is a shared feature of related dimer, donnazole B (Figure 1.4)<sup>[21]</sup>, axinellamines **1-3**<sup>[22]</sup>, and massadine chloride **1-5b**<sup>[23]</sup>. Moreover, overall oxidation state in dimers **1-3** and **1-5** is conserved. As reassigned, palau'amine **1-2b** shares a uniform relative (C11,C13) stereochemistry with the set (**1-3**, **1-5**).<sup>[14,17]</sup> Completed total syntheses of (–)-palau'amine **1-2b**, (–)-axinellamines **1-3** and (–)-massadines **1-5** confirm unified stereochemical relationships (both relative and absolute) within the group (*vide infra*).<sup>[24]</sup>

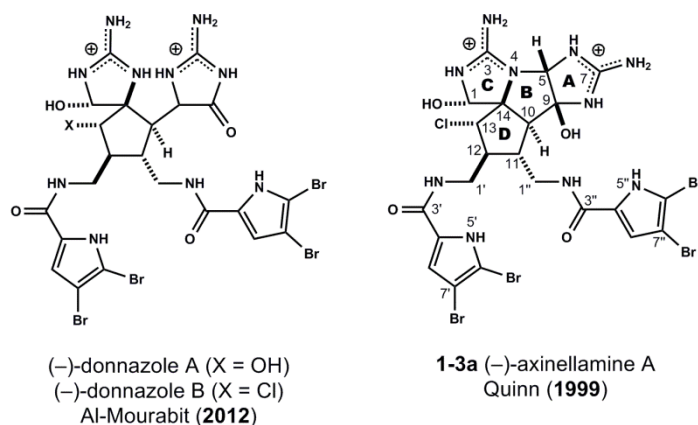


**Figure 1.4.** Related Dimers and Numerical Reference. Donnazoles A and B. For reference, numeration of (–)-axinellamine A **1-3a** according to isolation data (Urban *et al. J. Org. Chem.* **1999**, 64, 731.)

The axinellamines (**1-3**) were isolated in 1999 by Quinn and co-workers from polar solvent extracts of *Axinella sp.*<sup>[22]</sup> Their tetracyclic frameworks are defined by an internal aminal linkage connecting the C and A guanidine rings (Figure 1.4). Moderate antibacterial activity was

observed for **1-3** and related isolates against *Helicobacter pylori*.<sup>[22]</sup> Massadine **1-5a** was isolated from marine sponge *Stylissa aff. massa* in 2003 as an inhibitor of geranylgeranyltransferase type I.<sup>[23]</sup> The hydroxyl functionality at C13 was unique among known dimers. Intriguingly, the existence of massadine chloride **1-5b** was posited and isolated from extracts of *Stylissa caribica* shortly thereafter.<sup>[25]</sup> Massadine-aziridinium intermediates (not shown) are proposed wherein massadine chloride **1-9b** is hydrolyzed en route to massadine hydroxide **1-5a**.<sup>[25,26]</sup> Massadine chloride **1-5b** is also thought a biosynthetic precursor to tetrameric oroidin **1-1a** conjugates, stylissadines. These interconversions are among several interesting transformations proposed to interrelate the complex, dimeric pyrrole–imidazole alkaloids. A summary of putative biosynthetic pathways are described below.

### 1.2.3 Complex Dimeric Pyrrole–Imidazole Alkaloids: Biosynthetic Pathways

Scheurer & Kinnel (1993)

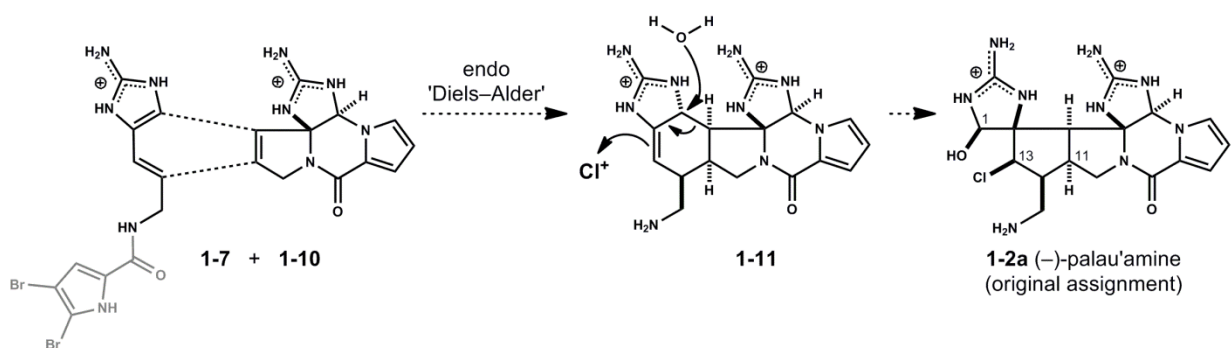
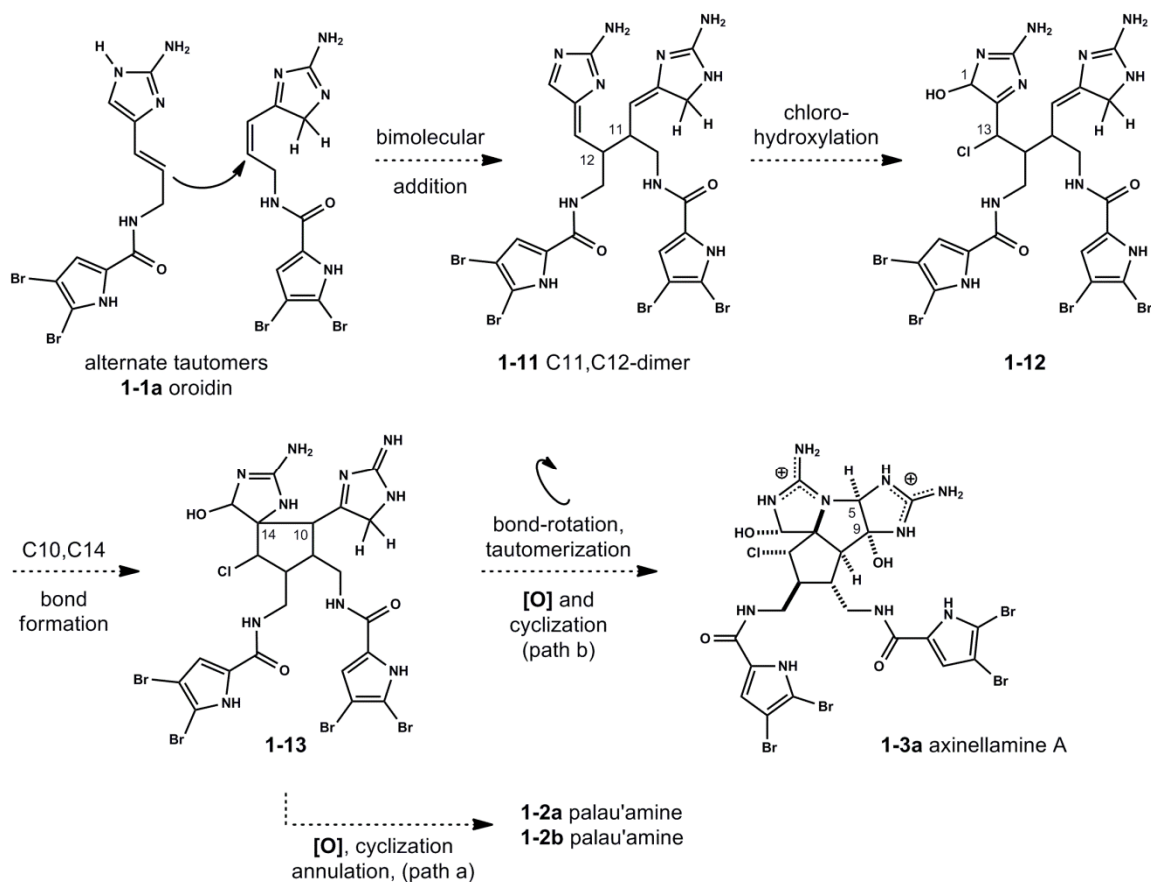


Figure 1.5. Scheurer & Kinnel's Proposed Biosynthesis of Palau'amine **1-2a**.

Several biosynthetic proposals suggest varying pathways to higher pyrrole–imidazoles from the appropriately halogenated monomer (e.g. **1-1**, Figure 1.1).<sup>[1,2,6]</sup> Early proposals for palau'amine **1-2a** biosynthesis were influential to synthetic chemists (Figure 1.5).<sup>[13c]</sup> A speculative *endo* selective Diels–Alder between 3-amino-1-(2-aminoimidazolyl)prop-1-ene **1-7**<sup>[7]</sup> and dehydrophakellin **1-10** (an unknown and likely unstable compound) would intercept a *cis*-

fused azabicyclo[4.3.0]nonane cycloadduct **1-11** poised for reaction with hypochlorite. The resultant chlorinated iminium species (not shown) could undergo hydration and ring contraction via net 1,2-shift to provide palau'amine **1-2a** directly. In line with these proposals, albeit with minor refinement, the Romo and Lovely groups considered expedited access to axinellamines **1-3** and palau'amine (**1-2a** and **1-2b**) via the oxidative ring contraction of prototype ageliferin **1-4a** intermediates.<sup>[26a]</sup> Methods for the oxidation, chlorination and ring-contraction of substituted tetrahydrobenzimidazoles prepared *via* Diels–Alder reactions have been reported.<sup>[26a,27,28]</sup> The brevity of Scheuer and Kinnel's Diels–Alder proposal to access palau'amine **1-2a** was attractive (Figure 1.5).<sup>[13c]</sup> However, the proposal limits access to **1-2a**. The proposed Diels–Alder cycloaddition could not account for the direct formation of related dimers axinellamines **1-3** and massadines **1-5**. Alternative biosynthetic proposals sought to address this issue.



**Figure 1.6.** Proposed Pathways to Axinellamine A **1-3a** and Related Dimers, see Al-Mourabit & Potier (2001).

The head-to-head oroidin dimer **1-11** is prominent in proposals for palau'amine **1-2**, axinellamine **1-3** and massadine **1-5** biosyntheses (Figure 1.6).<sup>[1,2,6]</sup> Various cyclization modes are reliant on the differential prototropic tautomerism of oroidin **1-1a**.<sup>[6]</sup> In the instance where two units of oroidin **1-1a** exist simultaneously in alternate tautomeric forms (imine/enamine tautomers), a bimolecular C–C bond forming event would provide C11,C12-dimer **1-11**. The diazafulvene motif in **1-11** would be susceptible to oxidative chlorohydroxylation (net) to form dissymmetric imine-enamine dimer **1-12**. The subsequent 5-*exo*-trig cyclization of **1-12** would provide access to a common intermediate chlorinated spirocyclopentane core **1-13**. Divergent cyclization pathways from **1-13**, presumably dictated by controlled oxidative events could provide palau'amine **1-2a** (path a) and axinellamine A **1-3a** (path b). The oxidative



desymmetrization of  $\gamma,\gamma$ -homodimers (confer dimer **1-11**) derived from oroidin **1-1a** is intriguing (Figure 1.6).<sup>[6]</sup> However, attempts to emulate this oxidative desymmetrization in the lab were reportedly unsuccessful.<sup>[24]</sup> The simpler dimers, sceptrin (not shown) and ageliferin **1-4a** have been proposed as reduced progenitors of complex, oxidized dimers such as axinellamines **1-3** and massadines **1-5**.<sup>[29]</sup> The tetrahydrobenzimidazole core present in ageliferin **1-4a** is envisioned to arise from a net [4+2] cycloaddition to differentially incorporate two units of hymendin **1-1b** (Figure 1.1).<sup>[5d]</sup> Such Diels–Alder type events have been emulated by Ohta and co-workers in their synthesis of 12,12'-dimethylageliferin **1-40** (*vide infra*, Figure 1.11).<sup>[30]</sup> These biosynthetic postulates continue to inspire chemists. Synthetic efforts toward pyrrole–imidazole dimers are influenced by these biomimetic bond disconnections. However, many strategies are primarily focused on abiotic constructions of a functionalized cyclopentane core.<sup>[31]</sup>

Our own symmetry-based strategy was related to the proposed intermediacy of dimers **1-11**.<sup>[6]</sup> However, to avoid tenuous and uncontrollable imine/enamine equilibria, we chose to work at an oxidation state where the tautomeric preference of synthetic intermediates could be predicted with confidence.

### 1.3.1 Symmetry-Based Access to Complex Pyrrole–Imidazoles: Retrosynthetic Analysis

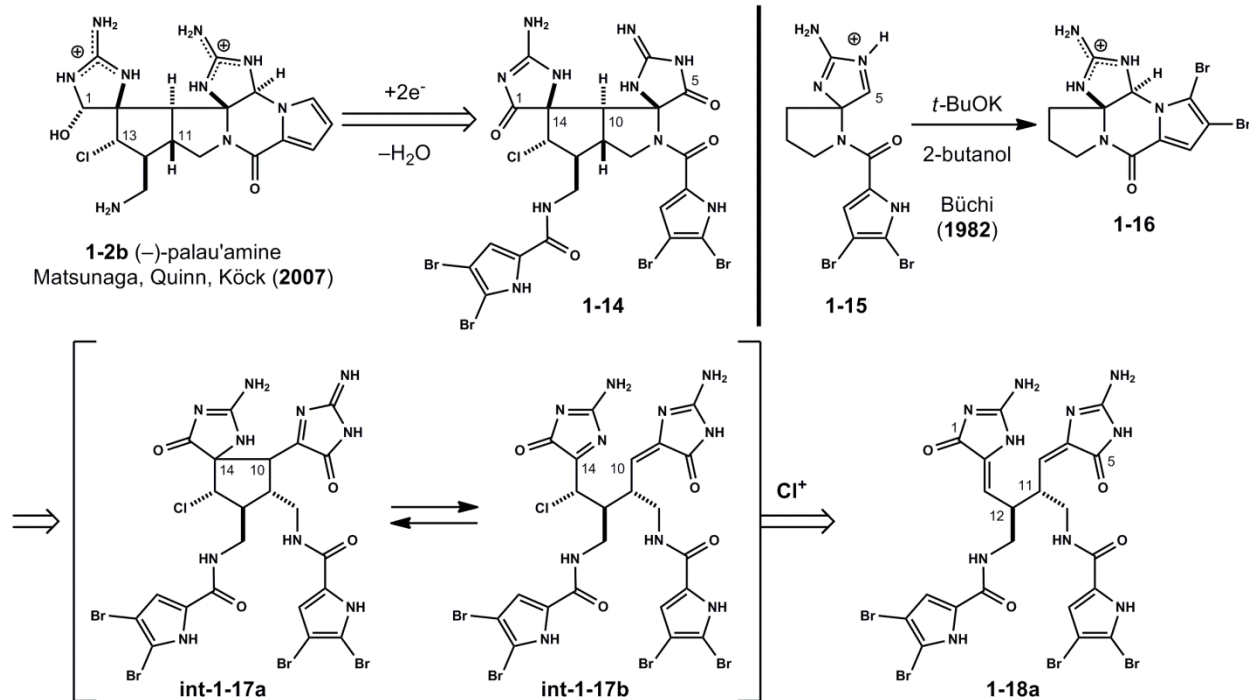
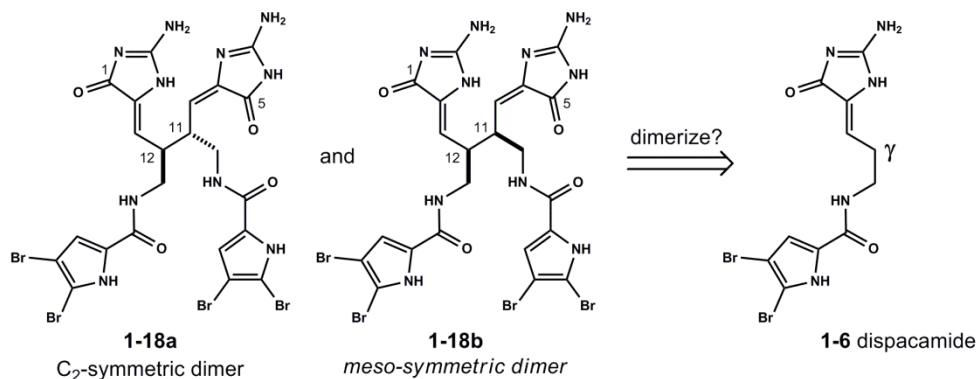


Figure 1.7. Retrosynthetic Analysis: A Symmetry-Based Synthesis of Palau'amine **1-2b**.

We view palau'amine **1-2b** (Figure 1.7) and related complex pyrrole–imidazoles (*e.g.* **1-3**, **1-5**, Figure 1.1) as oxidized, dimeric conjugates of oroidin **1-1a**. Our original synthetic strategy is reminiscent of early biosynthetic proposals.<sup>[6]</sup> However, we reasoned control of tautomeric preference in dimeric intermediates such as **1-11** could present a challenge (Figure 1.6). Retrosynthetic analysis of palau'amine **1-2b** provided further insight for our targeted symmetric intermediates. The right hand, ‘phakellin’ portion of **1-2b** was envisioned to arise from a Büchi-type annulation of a  $C_5$ -reduced, intermediate tetracycle **1-14**.<sup>[32]</sup> This pyrrole N– $C_5$  bond disconnection parallels the known transformation of spirocyclic intermediate **1-15** to dibromophakellin **1-16** (Figure 1.7). Tetracycle **1-14** could derive from the oxidative spirocyclization of  $C_2$ -symmetric dimer **1-18a**. We posited the adjusted  $C_1, C_5$ -oxidation state in **1-18a** as compared to dimer **1-11** (Figure 1.6) would permit desired ‘enamine’ tautomers to exist exclusively. In the forward sense, chlorination of this reactive dimeric intermediate **1-18a** could

intercept dissymmetric **int-1-17b** and undergo subsequent cyclization forming the C10–C14 bond of chlorinated cyclopentane **int-1-17a**. Additionally, controlled reduction and cyclizations of **int-1-17a** could provide access to axinellamines **1-3** and massadines **1-5** along putatively biosynthetic lines.

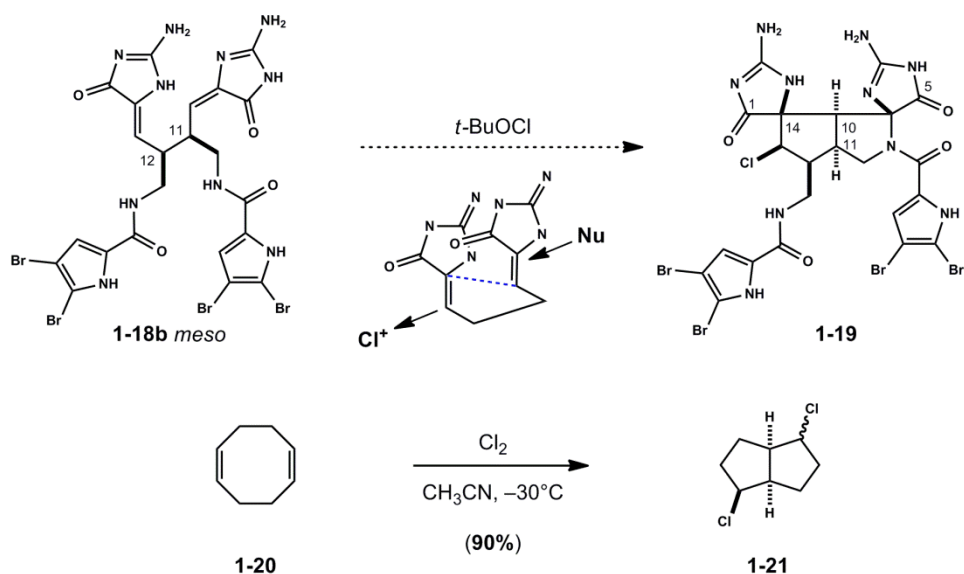


**Figure 1.8.** Regio- and Stereocontrolled Dimerization of Dispacamide **1-6**.

A symmetry-based strategy was proposed (Figure 1.8).<sup>[33,34]</sup> To control reactivity, we sought to work at a higher oxidation state and targeted a monomeric synthon for the natural product dispacamide **1-6**.<sup>[35]</sup> Dispacamide **1-6** is formally viewed as an oxidation product of oroidin **1-1a**. We posited the alkylidene glycoyamidine<sup>[36]</sup> present in **1-6** would provide for reactivity at the indicated  $\gamma$  position. It became apparent that methods to control  $\gamma$  regioselectivity and diastereoselectivity in homodimerization events would require new discoveries. The dimerization of monomer intermediate, dispacamide **1-6** would provide  $C_2$ -symmetric **1-18a** and *meso*-symmetric **1-18b** dimers (Figure 1.8).

At the outset of this project, the later dimer **1-18b** contained the desired *syn*-C11,C12 stereochemistry required to complete a synthesis of palau'amine **1-2a** as originally assigned (*vide infra*, Figure 1.9). However,  $C_2$ -symmetric dimers **1-18a** containing *anti*-C11,C12 stereochemistry, could be simultaneously pursued for syntheses of axinellamines **1-3** and massadines **1-5**. Moreover, the relative stereochemical outcome in products derived from the

oxidative spirocyclization of either bis-alkylidene dimer (**1-18**) was an interesting topic for study.



Uemura *et al.* *J. Org. Chem.* **1983**, *48*, 270.

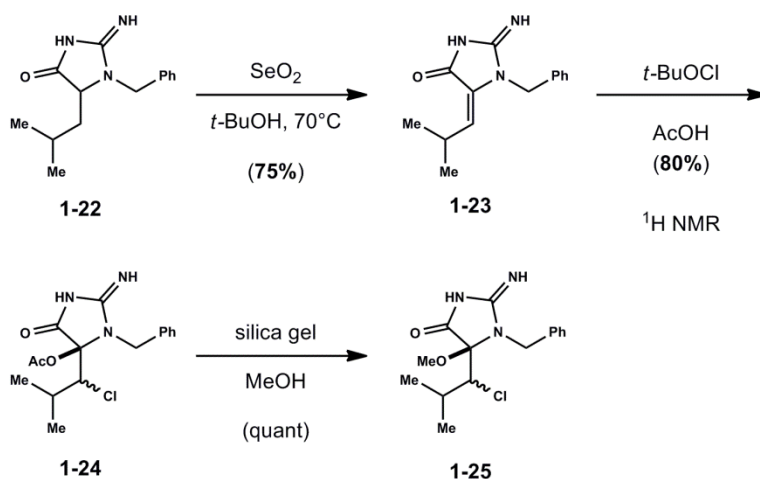
**Figure 1.9.** Early Proposals: Is palau'amine **1-2a** (C11, C13) an outlier?

With regard to stereochemical concerns, the ponderance of palau'amine **1-2a** as an outlier among related dimers axinellamines **1-3** and massadines **1-5** was intriguing. Control of relative stereochemical outcome in products derived from the oxidative spirocyclization of *meso*-symmetric dimer **1-18b** was a foreseeable issue. The desired reactivity is similar to the oxidation of 1,5-cyclooctadiene **1-20** with chlorine to give halogenated bicyclo[3.3.0]octanes **1-21**.<sup>[37]</sup> The net result can be described as a homologated vicinal functionalization of tethered alkenes. In the ideal case, hypohalite oxidations of **1-18b** could initiate spirocyclization with the formation of two rings and four stereocenters as drawn in tetracycle **1-19**. Oxidative spirocyclization induced in intermediate **1-18b** would require tethered heterocycles to stack in parallel. These presumed cyclization modes have been discussed in detail.<sup>[33,34]</sup> Early efforts in our lab addressed these issues within constrained, *meso*-derived dimers.<sup>[34]</sup> The reactivity of glycoyamidine alkylidenes

toward oxidation with hypohalite and the spirocyclization of tethered alkylidenes required examination in model systems.

### 1.3.2 Symmetry-Based Access to Complex Dimeric Pyrrole–Imidazoles: Initial Model

#### Systems and Reactivity Studies

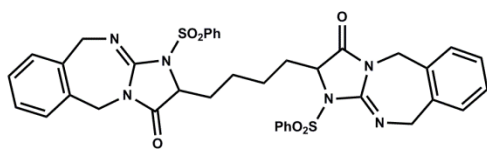


**Scheme 1.1.** Demonstrated Oxidative 'Enamine' Reactivity in Model Glycocyamidine **1-22**.

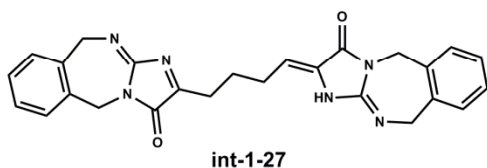
Several model systems validated the key tenets and demonstrated desirable reactivity consistent with our proposal. Monomeric alkylidenes **1-23** derived from the oxidation of glycocyamidine **1-22** possessed desired reactivity towards hypohalite (Scheme 1.1).<sup>[33]</sup> Interestingly, angular acetates **1-24** were the unstable adducts derived from presumed 'trapping' of  $\alpha$ -chloro iminium intermediates in acetic acid. Adduct exchange following dissolution of **1-24** in methanol containing silica gel provided hemiaminals **1-25**. These monomeric model systems confirmed desired 'enamine' type reactivity.

In 2005 our lab reported that tethered bis-alkylidenes were indeed prone to undergo spirocyclization.<sup>[33]</sup> Initially, a dimeric model **1-26** was prepared to study the proposed oxidative spirocyclization reaction (Scheme 1.2). However, the insolubility of bis-alkylidene **1-26** hindered further experimentation. Favorable solubility properties were observed when polar glycocyamidine functionality was assembled as part of a 1,3-benzodiazepine heterocycle.

**Prone to Spirocyclization**

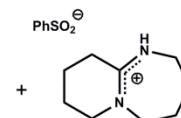
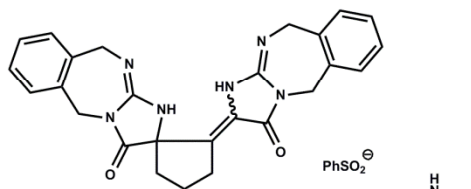


2.4 equiv DBU  
DMF, 35°C



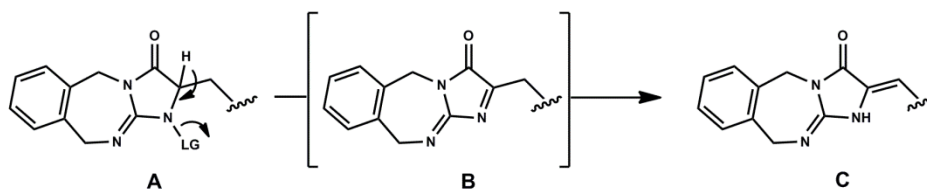
DMF, 35°C

(90%)



1-26  
Extreme insolubility due to H-bonding  
induced aggregation (from X-ray)

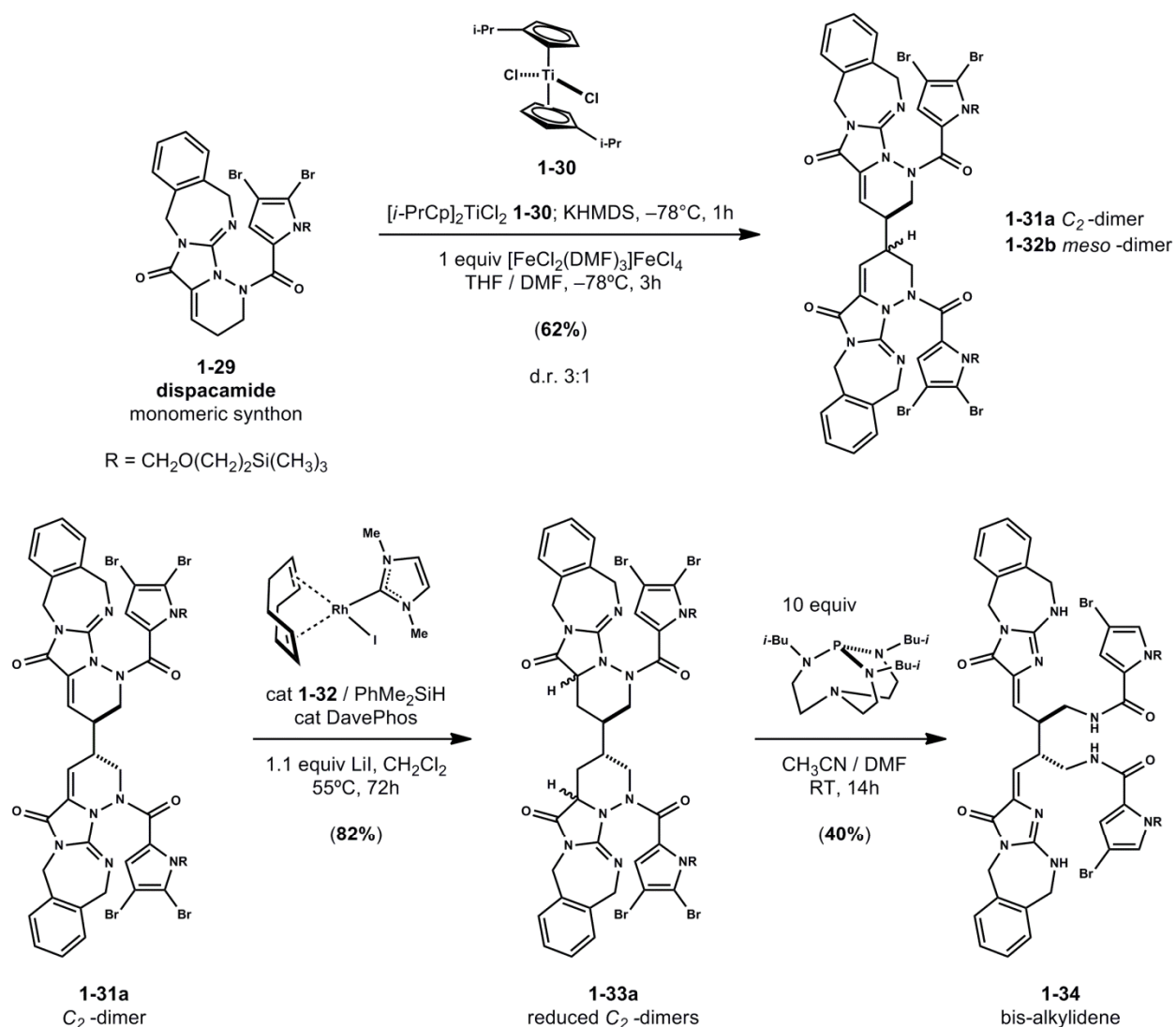
**Mechanism:** Fragmentation, Tautomerization, Cyclization



**Scheme 1.2.** Tethered Bis-alkylidenes are Prone to Spirocyclization – Desymmetrization provides spirocyclopentane **1-28**.

Following these observations, dimeric glycoyamidines **1-27** were designed as precursors to desired bis-alkylidene intermediates (Scheme 1.2). The intention was to isolate bis-alkylidene intermediates and explore their oxidative desymmetrization with hypohalite. However, it was observed that tethered glycoyamidines **1-27** proceed through transient alkylidene species **int-1-27** under basic conditions. Presumably, the reaction occurs via base-induced fragmentation with loss of phenyl sulfinate (LG) in **A** to form an intermediate imine species **B**. Intermediate **B** can tautomerize to form glycoyamidine alkylidene **C**. These experiments suggest intramolecular cyclization of **int-1-27** as the predominate pathway to provide spirocyclopentane isomers **1-28**. Interestingly, this reactivity parallels that anticipated for spirocyclization events induced by oxidation (Figure 1.7, confer conversion of **1-18** to **1-14**). This spirocyclization method

demonstrated viability of the proposed reactivity of advanced intermediates such as bis-alkylidene **1-18** (Figure 1.7).



**Scheme 1.3.** A Symmetry-Based Approach – Elaboration of Dispacamide Derived Monomer **1-29** to Target Bis-alkylidene **1-34**  
Regio- and diastereocontrolled oxidative dimerization of titanocene dienolates derived from **1-29** provide access to C<sub>2</sub> and *meso* symmetric-dimers (**1-31a**, **1-31b**). The desired C<sub>2</sub> symmetric-dimer **1-31a** is elaborated *via* Rh<sup>I</sup> **1-32** catalyzed hydro-silylation and subsequent base-induced hydrazide fragmentation of **1-33a** utilizing Verkade's base (10 equiv) providing bis-alkylidene **1-34a**. KHMDS = potassium hexamethyldisilazide, DavePhos = 2-(dicyclohexylphosphino)-2'-(*N,N*-dimethylamino) biphenyl, Verkade's base = 2,8,9-triisobutyl-2,5,8,9-tetraaza-1-phosphabicyclo[3.3.3]undecane

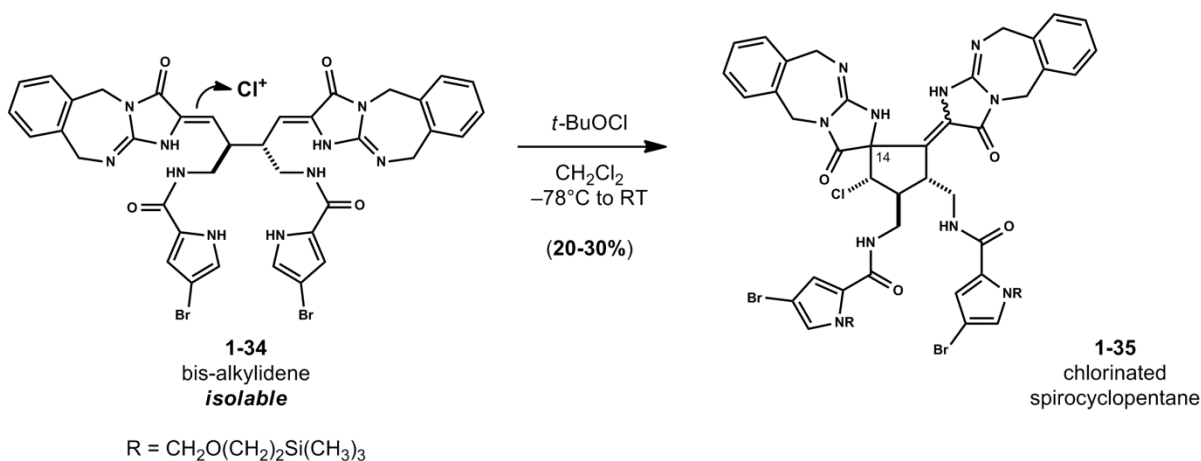
In 2009 our lab reported the development of several novel strategies for the preparation and elaboration of bis-guanidine containing intermediates en route to the total synthesis of palau'amine **1-2b**.<sup>[34]</sup> Methods for the scalable synthesis of a novel dispacamide derived



monomeric synthon **1-29** were addressed (Scheme 1.3). Subsequently, Harran and co-workers developed a method for the homodimerization of titanocene dienolates derived from monomer **1-29**. This oxidative enolate homocoupling is a regio- and diastereoselective process. Stereochemical outcome is dependent on oxidant (*vide infra*, Chapter 2). Under optimized conditions titanocene dienolates derived from treatment of **1-29** and diisopropyl titanocene dichloride **1-30** with potassium hexamethyldisilazide provided a favorable mixture of  $\gamma,\gamma$ -linked homodimers **1-31a** and **1-32b** following oxidation with  $[\text{FeCl}_2(\text{DMF})_3]\text{FeCl}_4$ . The  $C_2$ -symmetric dimer **1-31a** was elaborated in two steps to provide targeted bis-alkylidene **1-34**. The desired conversion of **1-31a** to reduced  $C_2$ -dimers **1-33a** led to the development of a  $\text{Rh}^{\text{I}}$  **1-32** catalyzed hydrosilylation method. Subsequent base-induced hydrazide fragmentation of **1-33a** using Verkade's base provided targeted bis-alkylidene **1-34** albeit with an intriguing concomitant debromination. The net transformation can be explained by analogy to the conversion of intermediate **A** to **C** in Scheme 1.2. Interestingly, under these conditions, tautomerization occurs to provide a bis-alkylidene **1-34** that does not immediately undergo spirocycloisomerization.

The reactivity of bis-alkylidene **1-34** towards oxidation was explored (Scheme 1.4). Notably, under neutral and basic conditions, bis-alkylidene **1-34** is a stable, isolable intermediate.<sup>[34]</sup> As anticipated,  $C_2$ -symmetric bis-alkylidene **1-34** was effectively desymmetrized upon treatment with *tert*-butyl hypochlorite. The resultant chlorinated (C13) spirocycloalkylidene **1-35** validated our proposed hypothesis.

### Isolable Bis-Alkylidenes are Prone to Oxidative Spirocyclization



**Scheme 1.4.** Key Reactivity, Oxidative Spirocyclization of Bis-alkylidene **1-34** – Oxidative desymmetrization provided a fully substituted chlorinated spirocyclopentane intermediate **1-35**.

Tethered bis-alkylidenes **1-34** were prone to undergo oxidative spirocyclization (Scheme 1.4).<sup>[34]</sup> However, three key issues remained to be addressed. Specifically: 1) develop methods to efficiently degrade benzodiazepine heterocycles in **1-35**, 2) establish relative stereochemistry at the C14 spirocenter in **1-35** and 3) elaborate intermediate **1-35** by controlled glycoyamidine reductions to access **1-2b** and **1-3**. Unfortunately, attempts to cleave benzylic C–N bonds present in **1-35** under hydrogenolysis conditions were not effective. Presumably, the C–N bonds as incorporated in 1,3-benzodiazepine heterocycles are orthogonal to the aromatic ring and exhibit diminished benzylic character required for reductive cleavage. Various oxidative methods for benzylic cleavage were potentially useful but required multiple events to occur with control and efficiency. This inability to obtain free glycoyamidine functionality in advanced intermediates was unacceptable. However, the general strategy proved an efficient means to quickly prepare advanced intermediates. We proposed minor refinements in an alternative series to address these issues.

### 1.4.1 Thesis Research – Refinements for Future Reaction Discovery: Controlled Preparation of Bis-Guanidine Intermediates en Route to Palau’amine 1-2b and Axinellamines 1-3.

Our symmetry-based strategy is dependent on the development of efficient methods to prepare bis-guanidine containing intermediates derived from monomeric diisocyanide synthons such as **1-29** (Scheme 1.3).<sup>[34]</sup> The challenging prospect of carrying two basic guanidine units intact through the synthesis is intuitive and direct. Access to advanced intermediate **1-35** (Scheme 1.4) obtained in the previous series validated our key hypotheses pertaining to the reactivity of tethered alkylidenes towards oxidative spirocyclization. However, the inability to cleave the benzylic N–C bonds by hydrogenolysis thwarted efforts to elaborate advanced intermediate **1-35** to the targeted natural products (*e.g.* **1-2b**, **1-3**). We posited that important refinements to this strategy could enable future reaction discovery and permit complete syntheses of palau’amine **1-2b** and the axinellamines **1-3**.

Central to the design of targeted diisocyanide monomers (*e.g.* **1-29**) was the development of methods to controllably ‘mask’ the inherent polarity and reactivity of their guanidine functionality.<sup>[38]</sup> The appropriate guanidine ‘mask’ would reduce polarity, facilitating purification and handling of intermediates, while maintaining a certain lability to permit ‘unveiling’ of requisite glycoamidine<sup>[36]</sup> motifs in a late-stage setting. For these purposes, a new monomer **1-36** was proposed (Figure 1.10). We anticipated that guanidine functionality as incorporated within this novel oxadiazine heterocycle would have favorable properties.<sup>[39]</sup> This would allow for the preparation and elaboration of bis-guanidine containing intermediates. Moreover, we anticipated hydrolytic degradation of this heterocycle could permit access to requisite free glycoamidine functionality of late-stage intermediates.<sup>[39]</sup>

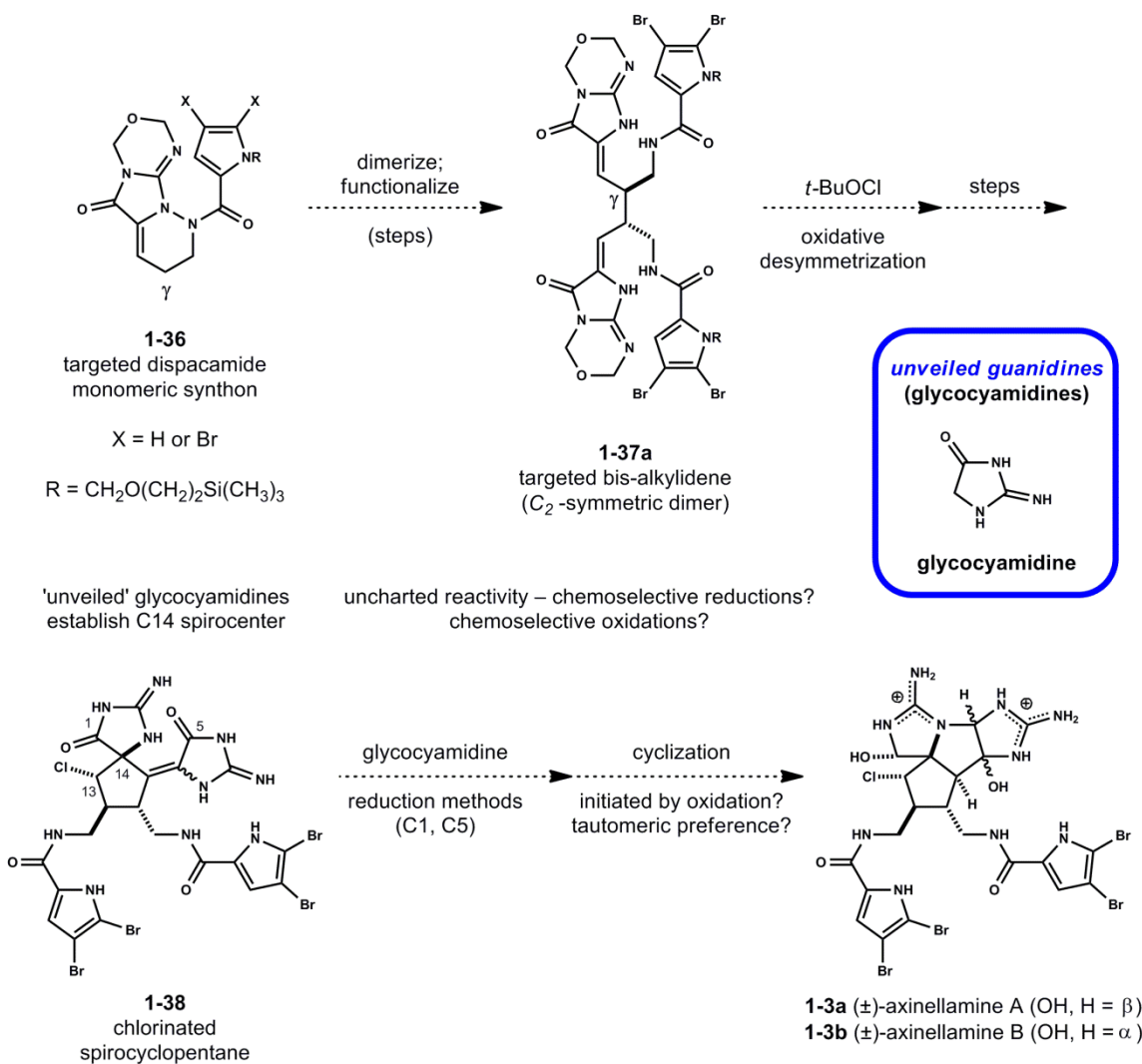


**Figure 1.10.** Proposed Access to Axinellamines **1-3** and Related Dimeric Pyrrole–Imidazoles from a Dispacamide Monomer **1-36**.

Targeted dispacamide monomer **1-36** (X = H or Br) could be prepared by analogy to previous methods developed for the synthesis of benzodiazepine monomer **1-29** (Figure 1.10).<sup>[34]</sup> Efficient methods for the synthesis and handling of target glycoyamidine **1-36** would be developed. Regiocontrolled dimerization of **1-36** and subsequent functionalization of C<sub>2</sub>-symmetric intermediate dimers could provide target bis-alkylidene **1-37**. Key intermediate **1-37** was envisioned to undergo oxidative spirocyclization induced by hypochlorite to access desired chlorinated (C13) spirocyclopentane intermediates. Subsequent elaboration would entail the

development of methods to degrade oxadiazine heterocycles with net loss of two equivalents of formaldehyde and unveil free glycoyamidine functionality.

Access to key chlorinated spirocycloalkylidene intermediate **1-38** (Figure 1.10) would represent substantial progress relative to previously obtained advanced intermediate **1-35** (Scheme 1.4). From **1-38**, a series of controlled glycoyamidine carbonyl (C1, C5) reductions are required. Reductive transformations of glycoyamidines were unexplored at the time of proposal (*vide infra*, Chapter 2).<sup>[40]</sup> Subsequent controlled cyclization(s) were envisioned to complete total syntheses of the axinellamines **1-3** and palau'amine **1-2b**. The preference of these variable cyclization modes would be dependent on product outcome from selective glycoyamidine reductions of **1-38**. These challenges presented a unique opportunity to develop methods for the preparation and manipulation of bis-guanidine intermediates.

## 1.5.1 Complex Dimeric Pyrrole–Imidazole Alkaloids Synthesis: Completed Efforts and Total Syntheses

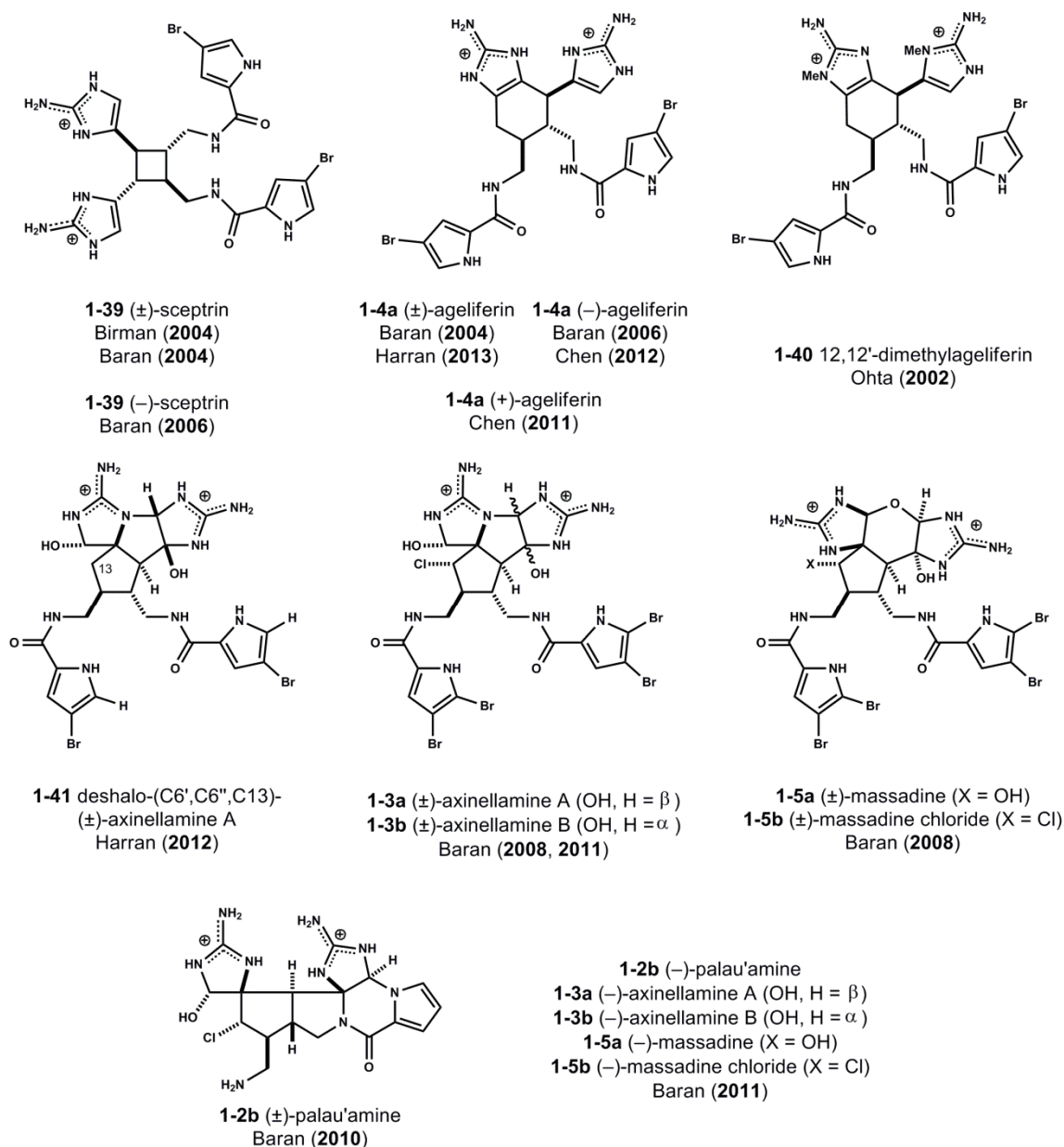


**Figure 1.11.** Completed Synthetic Efforts. Total synthesis of ( $-$ )-palau'amine **1-2b** and related dimeric pyrrole–imidazoles.

The simpler ‘imidazole intact’ dimers, sceptrin **1-39** and ageliferin **1-4a** have garnered significant interest from the synthetic community (Figure 1.11).<sup>[1,2]</sup> Both dimers have been viewed as reduced progenitors of the complex pyrrole–imidazoles.<sup>[24,27,28,29]</sup> Initial efforts to

prepare the all *trans*-substituted cyclobutane core pertinent to scep trin **1-39** via photochemically induced [2+2] cycloaddition strategies were reportedly unsuccessful.<sup>[4]</sup> Utilizing similar logic, Birman and Jiang prepared **1-39** in 10 steps from known [2+2] cycloadduct derived from maleic anhydride and *trans*-1,4-dichloro-2-butene.<sup>[41a]</sup> The Baran laboratory completed a short total synthesis of (±)-scep trin **1-39** via rearrangement of a 3-oxaquadracyclane intermediate.<sup>[41b]</sup> The group subsequently demonstrated compelling access to ageliferin **1-4a** and its epimer, nagelamide E (not shown) via a thermally-induced vinyl cyclobutane rearrangement of (±)-scep trin **1-39**.<sup>[26b,29,42]</sup> The analogous asymmetric preparation of (-)-scep trin **1-34** provided (-)-ageliferin **1-4a**.<sup>[42b]</sup> Inspired by speculative biogenesis pathways, the group intended to access axinellamines **1-3** from ageliferin **1-4a**.<sup>[29]</sup> Controlled oxidation and induced ring-contraction of the substituted tetrahydrobenzimidazole core **1-4a** was an ambitious undertaking.<sup>[43]</sup> These efforts were rewarded with the first reported access to a des-chlorinated (C13) pre-axinellamine by oxidation with a subsequent thermally induced ring-contraction.<sup>[29,43]</sup> Unfortunately, incorrect stereochemistry at the C14-spirocenter and the inability to directly incorporate chlorine at the C13 position thwarted efforts to pursue axinellamine **1-3** synthesis from this novel intermediate.

Chen and co-workers have described Mn<sup>III</sup> mediated annulations to construct six membered carbocycles relevant to syntheses of ageliferin **1-4a** and complex dimeric pyrrole–imidazoles (Figure 1.10).<sup>[44]</sup> Their routes have culminated with the controlled total synthesis of (+)-ageliferin **1-4a** from a linear synthetic precursor.<sup>[45a]</sup> These strategies have been recently adapted to obtain access to (-)-ageliferin **1-4a** and congeners.<sup>[45b]</sup>

Our own interests in preparing complex pyrrole–imidazole dimers (*e.g.* **1-2b**, **1-3**, **1-5**) have resulted in the construction of a partially halogenated variant of the complete (±)-axinellamine A ring system **1-41** (Figure 1.6).<sup>[46a]</sup> This completed effort (*vide infra*, Chapter 2) was inspirational.

Access to a common intermediate permitted total synthesis of (±)-ageliferin **1-4a** via a novel *N*-amidinyliiminium ion ring-expansion rearrangement (*vide infra*, Chapter 3).<sup>[46b]</sup>

Continued effort from the Baran laboratory has culminated in total syntheses of axinellamines **1-3**, massadines **1-5** and palau'amine **1-2b**.<sup>[24]</sup> A re-evaluated synthetic strategy permitted the synthesis of a platform molecule, (±)-1,9-dideoxy-pre-axinellamine (not shown) derived from the intramolecular Aldol-cyclization of a linear precursor.<sup>[47]</sup> Total syntheses of (±)-axinellamines **1-3**<sup>[48a]</sup>, (±)-massadines **1-5**<sup>[48b]</sup> and (±)-palau'amine **1-2b**<sup>[48c]</sup> shortly followed and have been reviewed.<sup>[1,2]</sup> Notably, these completed efforts derive from the development of a silver (II) picolinate promoted oxidative method to install requisite hemiaminal functionality at C1.<sup>[24]</sup> The development of an asymmetric Diels–Alder reaction permitted enantioselective syntheses of these complex dimers along similar lines.<sup>[24]</sup> A refined, diastereoselective and scalable total synthesis of (±)-axinellamines **1-3** that exploits hidden symmetry elements has also been reported.<sup>[49]</sup>



## 1.5.2 Complex Dimeric Pyrrole–Imidazole Alkaloid Synthesis: Progress Toward Palau'amine and Related Dimers

Synthetic efforts toward palau'amine structures (both **1-2a** and **1-2b**) and related dimeric pyrrole–imidazoles (**1-3**, **1-5**) are strategically distinct from our original proposal. Specifically, these strategies address primary concerns of functionalized cyclopentane synthesis.<sup>[31]</sup> These efforts have been reviewed and will therefore, only be covered briefly.<sup>[1,2]</sup>

As previously noted, Büchi's biomimetic synthesis of dibromophakellin **1-16** is seminal.<sup>[32]</sup> Many proposals were reliant on such a late-stage oxidative annulation strategy to form the right-hand portion of the hexacyclic core pertinent to palau'amine syntheses (**1-2a** or **1-2b**). As a result, efforts targeting complex dimers (**1-2**, **1-3**, **1-5**) largely focused on the construction of an appropriately functionalized cyclopentane core.<sup>[31]</sup> Figure 1.12 summarizes these reports by depicting selected late-stage intermediates obtained by the research groups of: Romo **1-44**<sup>[50a]</sup> and **1-45**<sup>[50b]</sup>, Lovely **1-46**<sup>[51]</sup>, Gin **1-47**<sup>[52]</sup>, Gleason **1-48**<sup>[53]</sup>, Carreira **1-49**<sup>[54]</sup>, Williams & Nishizawa **1-51**<sup>[55]</sup>, Shair **1-52**<sup>[56]</sup>, Austin **1-53**<sup>[57]</sup>, Williams **1-54**<sup>[58]</sup>, and Nagasawa **1-54**<sup>[59]</sup>. Recently, Carreira and co-workers have extended similar logic to prepare a protected bis-guanidine **1-50** en route to massadine **1-5a**.<sup>[60]</sup>

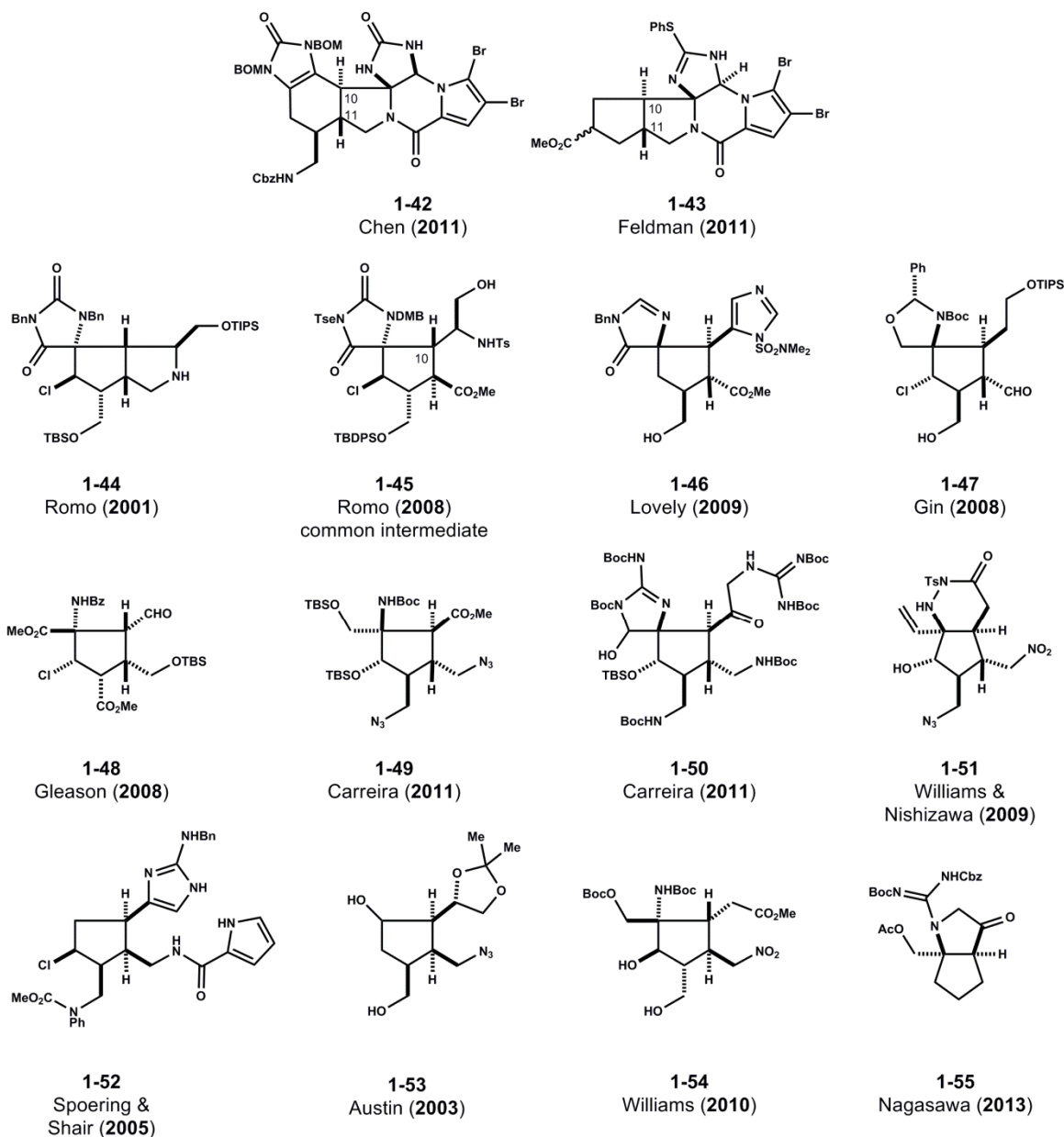


**Figure 1.12.** Summary of Synthetic Approaches Toward Palau'amine **1-2a** and **1-2b**, Axinellamines **1-3**, Massadines **1-5** and Ageliferin **1-4a**. Structures represent advanced published intermediates by various groups that focus primarily on the construction of an appropriately configured cyclopentane core.

Furthermore, significant progress has been made toward preparing *trans*-fused 3-azabicyclo[3.3.0]octane core containing intermediates relevant to completing syntheses of **1-2b**. The development of a C10 epimerization strategy provided the Romo lab with efficient access to key fully substituted cyclopentane core **1-45** (Figure 1.12).<sup>[50b]</sup> The group subsequently

demonstrated **1-45** as a useful common intermediate to access the tricycle core of axinellamines **1-3** (Figure 1.4, **B**, **C**, **D** rings) as well as a functionalized *trans*-fused 3-azabicyclo[3.3.0]octane core (not shown) relevant to palau'amine **1-2b** synthesis. The groups of Chen and Feldman have reported similar findings with regard to the right-hand 'phakellin' portion of palau'amine **1-2b**. With a minor revision of Scheurer and Kinnel's original proposal, Chen and co-workers reported access to an interesting 'ageliferin-palau'amine' hybrid structure **1-42**.<sup>[61]</sup> Feldman and co-workers have advanced a novel Pummerer-type oxidative method<sup>[62a]</sup> with a subsequent ring contraction sequence to prepare an intermediate *trans*-fused 3-azabicyclo[3.3.0]octane core **1-43**.<sup>[62b]</sup> Notably, these revised solutions proceed through presumably less-strained *trans*-fused azabicyclo[4.3.0]nonane intermediates.

The synthetic contributions in this arena are fascinating.<sup>[1,2]</sup> Notably, alternative strategies employed to prepare the *trans*-fused 3-azabicyclo[3.3.0]octane core of palau'amine **1-2b** are intriguing.<sup>[24,50b,61,62]</sup> While impressive in their own right, the majority of advanced substituted cyclopentane intermediates (Figure 1.12) require late-stage guanidine or amino functionality to be differentially incorporated – a formidable challenge. Our efforts to prepare and desymmetrize dimeric bis-guanidine containing intermediates en route to syntheses of palau'amine **1-2b** and related dimeric congeners (**1-3**, **1-5**) aims to circumvent such issues entirely (Chapter 2).

## 1.6 References and Notes

- [1] For recent reviews: (a) Ebada, S. S.; Proksch, P. in *Handbook of Marine Natural Products* (Eds: Fattorusso, E.; Gerwick, W. H.; Tagliatela-Scafati, T.), Springer, **2012**, 191–294; (b) Al-Mourabit, A.; Zancanella, A.; Tilvi, S.; Romo, D. *Nat. Prod. Rep.* **2011**, *28*, 1229; (c) J. Wang, Y. Zhan, B. Jiang, *Progress in Chemistry* **2011**, *23*, 2065; (d) Appenzeller, J.; Al-Mourabit, A. in *Biomimetic Organic Synthesis*, 1<sup>st</sup> Ed. (Eds: Poupon, E.; Nay, B.), WILEY-VCH, Weinheim, **2011**, 225.
- [2] For reviews, see: (a) Hoffmann, H.; Lindel, T. *Synthesis* **2003**, 1753; (b) Jacquot, D. E. N.; Mayer, P.; Lindel, T. *Chem. Eur. J.* **2004**, *10*, 1141; (c) Weinreb, S. M. *Nat. Prod. Rep.* **2007**, *24*, 931; (d) Köck, M.; Grube, A.; Seiple, I. B.; Baran, P. S. *Angew. Chem. Int. Ed.* **2007**, *46*, 6586; (e) Arndt, H. D.; Riedrich, M. *Angew. Chem. Int. Ed.* **2008**, *47*, 4785; (f) K. Takao, K. Tadano, *Kagaku* **2009**, *64*, 70; (g) Forte, B.; Malgesini, B.; Piutti, C.; Quartieri, F.; Scolaro, A.; Papeo, G. *Mar. Drugs* **2009**, *7*, 705.
- [3] For the original isolation of oroidin **1-1a**: Forenza, S.; Minale, L.; Riccio, R. *Chem. Commun.* **1971**, 1129; (b) For the isolation and reassignment of oroidin **1-1a**: Garcia, E. E.; Benjamin, L. E.; Fryer, R. I. *J. Chem. Soc., Chem. Commun.* **1973**, 78.
- [4] Scepterin isolation: Walker, R. P.; Faulkner, D. J.; van Engen, D.; Clardy, J. *J. Am. Chem. Soc.* **1981**, *103*, 5772.
- [5] Ageliferin **1-4a** isolation: (a) Rinehart, K. L. U.S. Patent 4737510, Apr. 12, 1988; (b) Rinehart, K. L. *Pure Appl. Chem.* **1989**, *61*, 525; (c) Reisolation and assignment of stereochemistry: Kobayashi, J.; Tsuda, H.; Murayama, T.; Nakamura, H., Ohizumi, Y., Ishibashi, M.; Iwamura, M. *Tetrahedron* **1990**, *46*, 5579; (d) Keifer, P. A.; Schwartz, R. E.; Koker, M. E. S.; Hughes, Jr., R. G.; Rittschof, D.; Rinehart, K. L. *J. Org. Chem.* **1991**, *56*, 2965.
- [6] Al-Mourabit, A.; Potier, P. *Eur. J. Org. Chem.* **2001**, 237.
- [7] For the isolation of 3-amino-1-(2-aminoimidazolyl)prop-1-ene **1-7**: Wright, A. E.; Chiles, S. A.; Cross, S. S. *J. Nat. Prod.* **1991**, *54*, 1684.
- [8] (a) Andrade, P.; Willoughby, R.; Pomponi, S. A.; Kerr, R. G. *Tetrahedron Lett.* **1999**, *40*, 4775; (b) For commentary on biosynthetic origins: Gautschi, J. T.; Whitman, S.; Holman, T. R.; Crews, P. *J. Nat. Prod.* **2004**, *67*, 1256.
- [9] Revisiting oroidin **1-1a** biosynthesis: Genta-Jouve, G.; Cachet, N.; Holderith, S.; Oberhänsli, F.; Teyssié, J.-L.; Jeffree, R.; Al Mourabit, A.; Thomas, O. P. *ChemBioChem* **2013**, *12*, 2298.
- [10] (a) Travert, N.; Al-Mourabit, A. *J. Am. Chem. Soc.* **2004**, *126*, 10252; (b) Vergne, C.; Boury-Esnault, N.; Perez, T.; Martin, M.-T.; Adeline, M.-T.; Du, E. T. H.; Al-Mourabit, A. *Org. Lett.* **2006**, *8*, 2421; (c) Vergne, C.; Appenzeller, J.; Ratinaud, C.; Martin, M.-T.; Debitus, C.; Zaparucha, A.; Mourabit, A. *Org. Lett.* **2008**, *10*, 493.

[11] De novo benzoscaptopin C and nagelamide H synthesis from 7-<sup>15</sup>N-oroidin **1-1a**: Stout, E. P.; Morinaka, B. I.; Wang, Y.-G.; Romo, D.; Molinski, T. F. *J. Nat. Prod.* **2012**, *75*, 527; (b) Pyrrole–imidazole metabiosynthesis: Stout, E. P.; Wang, Y.-G.; Romo, D.; Molinski, T. F. *Angew. Chem. Int. Ed.* **2012**, *51*, 4877 and references cited therein.

[12] For a recent biomimetic homodimerization of oroidin **1-1a**: Lejeune, C.; Appenzeller, J.; Ermolenko, L.; Martin, M.-T.; Al-Mourabit, A. *J. Nat. Prod.* **2013**, *76*, 903.

[13] Palau'amine **1-2b** isolation: (a) Kinnel, R. B.; Gehrken, H.-P.; Scheuer, P. J. *J. Am. Chem. Soc.* **1993**, *115*, 3376; (b) Kinnel, R. B.; Gehrken, H.-P.; Scheuer, P. J.; Bravalos, D. G.; Faircloth, G. T. *Eur. Pat. Appl.* **1994**, 94302770; (c) Kinnel, R. B., Gehrken H.-P.; Swali, R.; Skoropowski, G.; Scheuer, P. J. *J. Org. Chem.* **1998**, *63*, 3281.

[14] For the reassignment of palau'amine (**1-2a** to **1-2b**): (a) Kobayashi, H.; Kitamura, K.; Nagai, K.; Nakao, Y.; Fusetani, N.; van Soest, R. W. M.; Matsunaga, S. *Tetrahedron Lett.* **2007**, *48*, 2127; (b) Buchanan, M. S.; Carroll, A. R.; Addepalli, R.; Avery V. M.; Hooper, J. N. A.; Quinn R. J. *J. Org. Chem.* **2007**, *72*, 2309; (c) Buchanan, M. S.; Carroll, A. R.; Quinn, R. J. *Tetrahedron Lett.* **2007**, *48*, 4573; (d) Grube, A.; Köck, M.; *Angew. Chem. Int. Ed.* **2007**, *46*, 2320.

[15] Nakadai, M.; Harran, P. G. *Tetrahedron Lett.* **2006**, *47*, 3933.

[16] Lansdell, T. A.; Hewlett, N. M.; Skoumbourdis, A. P.; Fodor, M. D.; Seiple, I. B.; Su, S.; Baran, P. S.; Feldman, K. S.; Tepe, J. J. *J. Nat. Prod.*, **2012**, *75*, 980.

[17] As depicted in Figure 1.3, the reassignment of palau'amine (**1-2a** to **1-2b**) constitutes stereochemical revision at positions indicated C1,C11,C13. For atom numeration see Figure 1.4. For further commentary, see reference 2d.

[18] For the preparation and analysis of hexacyclic core **1-9**: (a) Lanman, B. A.; Overman, L. E.; Paulini, R.; White, N. S. *J. Am. Chem. Soc.* **2007**, *129*, 12896; For the development of related methods, see: (b) Katz, J. D.; Overman, L. E.; *Tetrahedron* **2004**, *60*, 9559; (c) Overman, L. E.; Rogers, B. N.; Tellew, J. E.; Trenkle, W. C. *J. Am. Chem. Soc.* **1997**, *119*, 7159.

[19] Seiple, I. B. Ph.D. Dissertation, the Scripps Research Institute, **2011**, UMI # 3464265.

[20] Jacquot, D. E. N.; Lindel, T. *Curr. Org. Chem.* **2005**, *15*, 1551.

[21] Donnazoles A and B isolation: Muñoz, J.; Moriou, C.; Gallard, J.-F.; Marie, P. D.; Al-Mourabit, A. *Tetrahedron Lett.* **2012**, *53*, 5828.

[22] Axinellamines **1-3** isolation: Urban, S.; de Almeida Leone, P.; Carroll, A. R.; Fechner, G. A.; Smith, J.; Hooper, J. N. A.; Quinn, R. J. *J. Org. Chem.* **1999**, *64*, 731.

[23] Massadine **1-5a** isolation: Nishimura, S.; Matsunaga, S.; Shibazaki, M.; Suzuki, K.; Furihata, K.; van Soest, R. W.; Fusetani, N. *Org. Lett.* **2003**, *5*, 2255.

- [24] Enantioselective total synthesis of (–)-palau’amine **1-2b**, (–)-axinellamines **1-3** and (–)-massadines **1-5**: Seiple, I. B.; Su, S.; Young, I. S.; Nakamura, A.; Yamaguchi, J.; Jørgensen, L.; Rodriguez, R. A.; O’Malley, D. P.; Gaich, T.; Köck, M.; Baran, P. S. *J. Am. Chem. Soc.* **2011**, *133*, 14710.
- [25] Massadine chloride **1-5b** isolation: Grube, A.; Immel, S.; Baran, P. S.; Köck, M. *Angew. Chem. Int. Ed.* **2007**, *46*, 6721.
- [26] Massadine aziridine intermediate proposals: (a) Wang, S.; Dilley, A. S.; Poullennec, K. G.; Romo, D. *Tetrahedron* **2006**, *62*, 7155; (b) Northrup, B. H.; O’Malley, D. P.; Zografos, A. L.; Baran, P. S.; Houk, K. N. *Angew. Chem. Int. Ed.* **2006**, *45*, 4126.
- [27] (a) Dransfield, P. J.; Dilley, A. S.; Wang, S.; Romo, D. *Tetrahedron* **2006**, *62*, 5223; (b) Dransfield, P. J.; Wang, S.; Dilley, A.; Romo, D. *Org. Lett.* **2005**, *7*, 1679; (c) Poullennec, K. G.; Romo, D. *J. Am. Chem. Soc.* **2003**, *125*, 6344; (d) Poullennec, K. G.; Kelly, A. T.; Romo, D. *Org. Lett.* **2002**, *4*, 2645.
- [28] Diels–Alder chemistry of 4-vinyl imidazoles: (a) He, Y.; Krishnamoorthy, P.; Lima, H.; Chen, Y.; Wu, H.; Sivappa, R.; Dias, H. V. R.; Lovely, C. J. *Org. Biomol. Chem.* **2011**, *9*, 2685; (b) Lovely, C. J.; Du, H.; Sivappa, R.; Bhandari, M. K.; He, Y.; Dias, H. V. R. *J. Org. Chem.* **2007**, *72*, 3741. (c) Du, H.; He, Y.; Lovely, C. J. *Synlett* **2006**, 965.
- [29] Total synthesis of dimeric pyrrole–imidazole alkaloids: O’Malley, D. P.; Li, K.; Maue, M.; Zografos, A. L.; Baran, P. S. *J. Am. Chem. Soc.* **2007**, *129*, 4762.
- [30] Synthesis of 12,12’-dimethylageliferin and related substituted tetrahydrobenzimidazole cores via Diels–Alder reaction of vinyl imidazoles: (a) Kawasaki, I.; Sakaguchi, N.; Khadeer, A.; Yamashita, M.; Ohta, S. *Tetrahedron* **2006**, *62*, 10182; (b) Kawasaki, I.; Sakaguchi, N.; Fukushima, N.; Fujioka, N.; Nikaido, F.; Yamashita, M.; Ohta, S. *Tetrahedron Lett.*, **2002**, *43*, 4377.
- [31] Fully substituted cyclopentane synthesis: Heasley, B. *Eur. J. Org. Chem.* **2009**, 1477.
- [32] For a biomimetic synthesis of dibromophakellin **1-16** see: Foley, L. H.; Büchi, G. *J. Am. Chem. Soc.* **1982**, *104*, 1776.
- [33] Spirocycloisomerization of Tethered Alkylidene Glycoamidines: Synthesis of a Base Template Common to Palau’amine Family Alkaloids: Garrido-Hernandez, H.; Nakadai, M.; Vimolratana, M.; Li, Q.; Doundoulakis, T.; Harran, P. G. *Angew. Chem. Int. Ed.* **2005**, *44*, 765
- [34] (a) Exploring Symmetry-Based Logic for a Synthesis of Palau’amine: Li, Q.; Hurley, P.; Ding, H.; Roberts, A. G.; Akella, R.; Harran, P. G. *J. Org. Chem.* **2009**, *74*, 5909; (b) Li, Q. Ph.D. Dissertation, the University of Texas Southwestern Medical Center, **2008**.

[35] For the isolation of dispacamide **1-6**: Cafieri, F.; Fattorusso, E.; Mangoni, A.; Tagliatela-Scafati, O. *Tetrahedron Lett.* **1996**, *37*, 3587.

[36] The term **glycocyamidine** refers to heterocyclic structures (of the type present in **1-6**) which are often incorrectly described as 2-imino analogs of the commonly known hydantoin heterocycle. The systematic name for glycocyamidine is 2-imino-4-imidazolidinone. For a review of glycocyamidine chemistry: Lempert, C. *Chem. Rev.* **1959**, *59*, 667.

[37] Uemura, S.; Fukuzawa, A.; Toshimitsu, M.; Okano, M. *J. Org. Chem.* **1983**, *48*, 270.

[38] For alternative strategies used to mask guanidine functionality of 2-aminoimidazoles: Sivappa, R.; Kumbam, V.; Dhawane, Golen, J. A.; Lovely, C. J.; Rheingold, A. L. *Org. Biomol. Chem.* **2013**, *11*, 4133 and references cited therein.

[39] For preparation, properties and stability of related 1,3,5-oxadiazinane heterocycles, see: (a) Kadowaki, H. *Bull. Chem. Soc. Japan.* **1936**, *11*, 248; (b) Beachem, M. T.; Oppelt, J. C.; Cowen, F. M.; Schickedantz, P. D.; Maier, D. V. *J. Org. Chem.* **1963**, *28*, 1876; (c) Egginton, C. D.; Vale, C. P. *Text. Res. J.* **1969**, *39*, 140.

[40] For related strategies to prepare the spirocyclic guanidine hemiaminal motif by reduction: (a) McAlpine, I. J.; Armstrong, R. W. *J. Org. Chem.* **1996**, *61*, 5674; (b) Lanman, B. A.; Overman, L. E. *Heterocycles* **2006**, *70*, 557; (c) Tang, L.; Romo, D. *Heterocycles* **2007**, *74*, 999.

[41] Total syntheses of (±)-sceptrin **1-39**: (a) Birman, V. B.; Jiang, X.-T. *Org. Lett.* **2004**, *6*, 2369; (b) Baran, P. S.; Zografos, A. L.; O'Malley, D. P. *J. Am. Chem. Soc.* **2004**, *126*, 3726.

[42] (a) Total synthesis of (±)-ageliferin **1-4a** and nagelamide E: Baran, P. S.; O'Malley, D. P.; Zografos, A. L. *Angew. Chem. Int. Ed.* **2004**, *43*, 2674; (b) Total synthesis of (–)-sceptrin **1-39** and (–)-ageliferin **1-4a**: Baran, P. S.; Li, L.; O'Malley, D. P.; Mitsos, C. *Angew. Chem. Int. Ed.* **2006**, *45*, 249.

[43] O'Malley, D. P. Ph.D. Dissertation, the Scripps Research Institute, **2008**, UMI #3313886.

[44] For the development of this method: Tan, X.; Chen, C. *Angew. Chem. Int. Ed.* **2006**, *45*, 4345.

[45] (a) For the total synthesis of (+)-ageliferin **1-4a**: Wang, X.; Ma, Z.; Lu, J.; Tan, X.; Chen, C. *J. Am. Chem. Soc.* **2011**, *133*, 15350; (b) For the total synthesis of (–)-ageliferin **1-4a** and congeners: Wang, X.; Wang, X.; Tan, X.; Lu, J.; Cormier, K. W.; Ma, Z.; Chen, C. *J. Am. Chem. Soc.* **2012**, *134*, 18834.

[46] (a) Synthetic (±)-Axinellamines Deficient in Halogen: Ding, H.; Roberts, A. G.; Harran, P. G. *Angew. Chem. Int. Ed.* **2012**, *51*, 4416; (b) Total synthesis of (±)-Ageliferin **1-4a** via N-amidinylium Ion Rearrangement: Ding, H.; Roberts, A. G.; Harran, P. G. *Chem. Sci.* **2013**, *4*, 303.

- [47] Synthesis of (±)-1,9-Dideoxy-pre-axinellamine: Yamaguchi, J.; Seiple, I. B.; Young, I. S.; O'Malley, D. P.; Maue, M.; Baran, P. S. *Angew. Chem. Int. Ed.* **2008**, *47*, 3578
- [48] (a) Total synthesis of (±)-axinellamines **1-3**: O'Malley, D. P.; Yamaguchi, J.; Young, I. S.; Seiple, I. B.; Baran, P. S. *Angew. Chem. Int. Ed.* **2008**, *47*, 3581; (b) Total synthesis of (±)-massadines **1-5**: Su, S.; Seiple, I. B.; Young, I. S.; Baran, P. S. *J. Am. Chem. Soc.* **2008**, *130*, 16490; (c) Total synthesis of (±)-palau'amine **1-2b**: Seiple, I. B.; Su, S.; Young, I. S.; Lewis, C. A.; Yamaguchi, J.; Baran, P. S. *Angew. Chem. Int. Ed.* **2010**, *122*, 1113.
- [49] Refined, total synthesis of (±)-axinellamines **1-3**: Su, S.; Rodriguez, R. A.; Baran, P. S. *J. Am. Chem. Soc.* **2011**, *133*, 13922.
- [50] (a) Dilley, A. S.; Romo, D. *Org. Lett.* **2001**, *3*, 1535; (b) Zancanella, M. A.; Romo, D. *Org. Lett.* **2008**, *10*, 3685.
- [51] (a) For the preparation of **1-46**: Sivappa, R.; Mukherjee, S.; Lovely, C. J. *Org. Biomol. Chem.* **2009**, *7*, 3215; (b) For a related strategy: Sivappa, R.; Hernandez, N. M.; He, Y.; Lovely, C. J. *Org. Lett.* **2007**, *9*, 3861.
- [52] Bultman, M. S.; Ma, J.; Gin, D. Y. *Angew. Chem. Int. Ed.* **2008**, *47*, 6821
- [53] (a) Hudon, J.; Cernak, T. A.; Ashenurst, J. A.; Gleason, J. L. *Angew. Chem. Int. Ed.* **2008**, *47*, 8885; (b) Cernak, T. A.; Gleason, J. L. *J. Org. Chem.* **2008**, *73*, 102.
- [54] (a) Toward the synthesis of massadine **1-5a**: Chinigo, G. M.; Breder, A.; Carreira, E. M. *Org. Lett.* **2011**, *13*, 78; (b) Related core **1-25** synthesis: Breder, A.; Chinigo, G. M.; Waltman, A. W.; Carreira, E. M. *Angew. Chem. Int. Ed.* **2008**, *47*, 8514; (c) Toward the synthesis of axinellamines **1-8**: Starr, J. T.; Koch, G.; Carreira, E. M. *J. Am. Chem. Soc.* **2000**, *122*, 8793.
- [55] Namba, K.; Kaihara, Y.; Yamamoto, H.; Imagawa, H.; Tanino, K.; Williams, R. M.; Nishizawa, M. *Chem.–Eur. J.* **2009**, *15*, 6560.
- [56] Spoering, R. M. Studies Toward a Synthesis of Palau'amine. Ph.D. Dissertation, Harvard University, **2005**.
- [57] Koenig, S. G.; Miller, S. M.; Leonard, K. A.; Löwe, R. S.; Chen, B. C.; Austin, D. J. *Org. Lett.* **2003**, *5*, 2203.
- [58] Namba, K.; Inai, M.; Sundermeier, U.; Greshock, T. J.; Williams, R. M. *Tetrahedron Lett.* **2010**, *51*, 6557.
- [59] Fukahori, Y.; Takayuma, Y.; Imaoka, T.; Iwamoto, O.; Nagasawa, K. *Chem. Asian J.* **2013**, *8*, 244.
- [60] Toward the synthesis of massadine **1-5a**: Breder, A.; Chinigo, G. M.; Waltman, A. W.; Carreira, E. M. *Chem. Eur. J.* **2011**, *17*, 12405



[61] Ma, Z.; Lu, J.; Wang, X.; Chen, C. *Chem. Commun.* **2011**, 47, 427.

[62] (a) For the development of these methods: Feldman, K. S.; Fodor, M. D.; Skoumbourdis, A. P. *Synthesis* **2009**, 3162; (b) For an interesting discussion related to the preparation of **1-43**: Feldman, K. S.; Nuriye, A. Y.; Li, J. *J. Org. Chem.* **2011**, 76, 5042.

## Chapter 2 – Symmetry–Based Logic for the Synthesis of Axinellamines and Palau’amine

adapted in part from

### Synthetic ( $\pm$ )-Axinellamines Deficient in Halogen

*Hui Ding, Andrew G. Roberts and Patrick G. Harran*

*Angew. Chem. Int. Ed.* **2012**, *51*, 4416 – 4419.

## 2.1 Introduction.

### 2.1.1 Introduction and General Strategy.

Marine organism derived pyrrole–imidazole alkaloids have drawn attention from laboratories worldwide. Their structures, biosynthetic origins, preliminary biochemical activities and chemical syntheses form an extensive literature.<sup>[1]</sup> The family contains hundreds of members, often grouped based upon their oroidin content.<sup>[2]</sup> So-called monomers, dimers and dimers of dimers are known. Further diversity derives from oxidative transformations of the monomeric and/or dimeric units. The most intricate polycyclic ‘dimers’ are uniquely challenging synthetic targets and, despite numerous efforts, have been prepared by one group. Baran and coworkers synthesized axinellamines<sup>[3]</sup> (**2-5**, Figure 2.1), massadines<sup>[4]</sup> (not shown) and palau’amine<sup>[5]</sup> (**2-6**) from a common intermediate.<sup>[6]</sup> This work evolved in stages, and beautifully leveraged collaborative re-interpretation of data on natural samples to confirm a uniform stereochemistry for the set.<sup>[7]</sup> A refined synthesis of ( $\pm$ )-axinellamines A and B has also been reported by the Baran lab.<sup>[8]</sup>

Among the creative ways envisioned to prepare structures **2-5**<sup>[9]</sup>, a strategy reminiscent of early biosynthetic proposals<sup>[10]</sup> was attractive to us. The core of the molecules would derive from a homodimeric precursor (of type **2-1**, Figure 2.1), whose oxidative desymmetrization (of type **2-**

2) with hypochlorite (X–Y, e.g. *t*-BuOCl) would install the halogenated spirocycle (2-3).<sup>[11abc]</sup>

Notwithstanding the tenuous and challenging prospect of carrying two basic guanidine units intact through the synthesis, this approach was intuitive and direct.

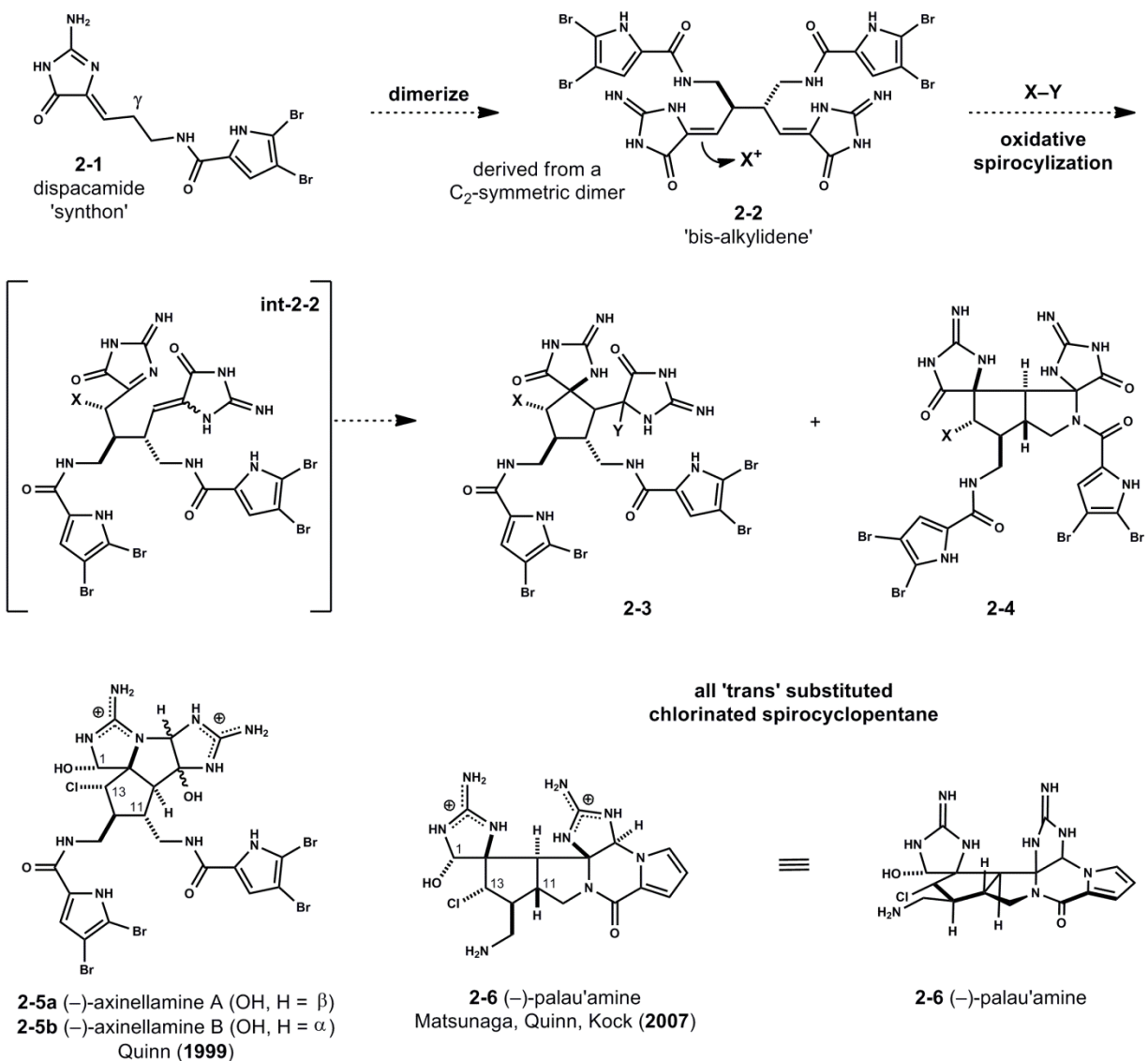


**Figure 2.1.** Monomer, Dimer, Remolded - Hypothesis: Access to 2-5 and 2-6 via the oxidative desymmetrization of dispacamide dimer 'bis-alkylidene' 2-2.

We chose to work with an oroidin synthon at higher oxidation state (2-1) and targeted a dispacamide dimer (e.g. 2-2) as our key intermediate.<sup>[11]</sup> The intention was to initiate oxidative spirocyclization at this stage and subsequently diverge to chlorinated spirocyclopentane 2-3 or azabicyclo[3.3.0]octane 2-4. Here we report a unique system wherein alkylidenes of type 2-2

actually exist as an alternate set of equilibrating structural isomers.<sup>[11d]</sup> The full ensemble spirocycloisomerizes with ease under non-oxidative conditions. This has allowed us to synthesize axinellamines **2-5** in partially halogenated forms – providing new synthetic variants of the natural products.

### 2.1.2 General Access to Dispacamide Dimers – Proposed Preparation of Bis-alkylidene **2-2**.

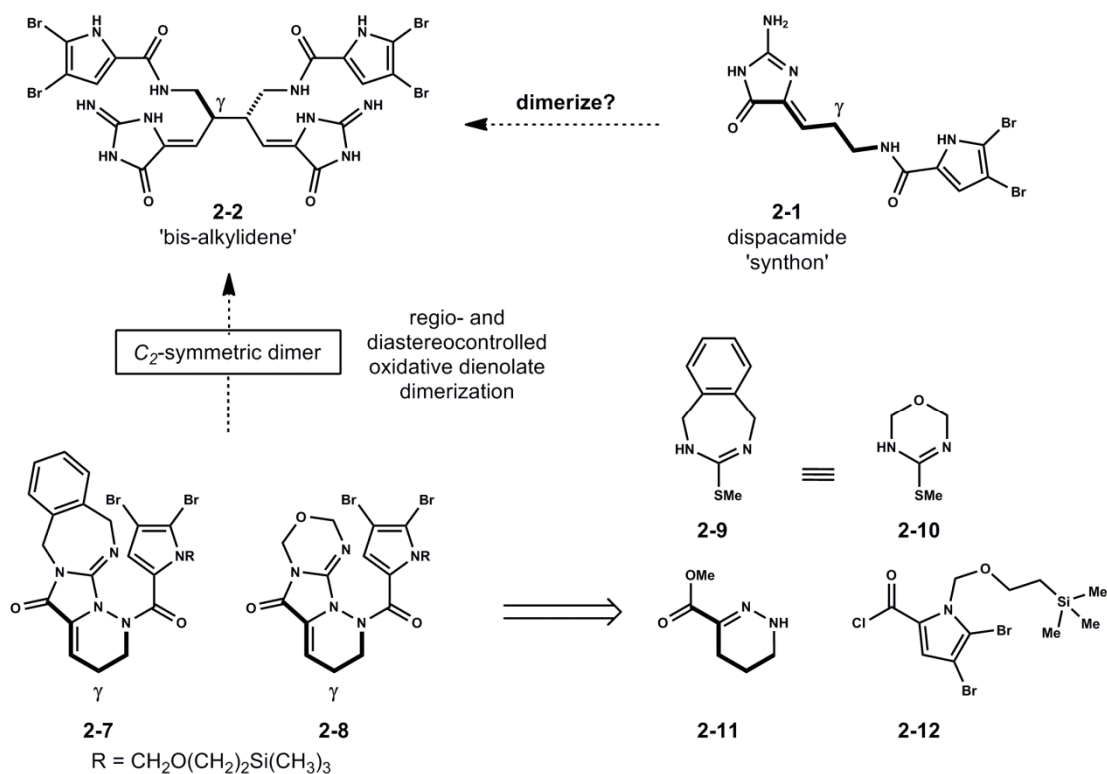


**Figure 2.2.** Alternative Masked Guanine Synthons - retrosynthesis parallels previous strategy

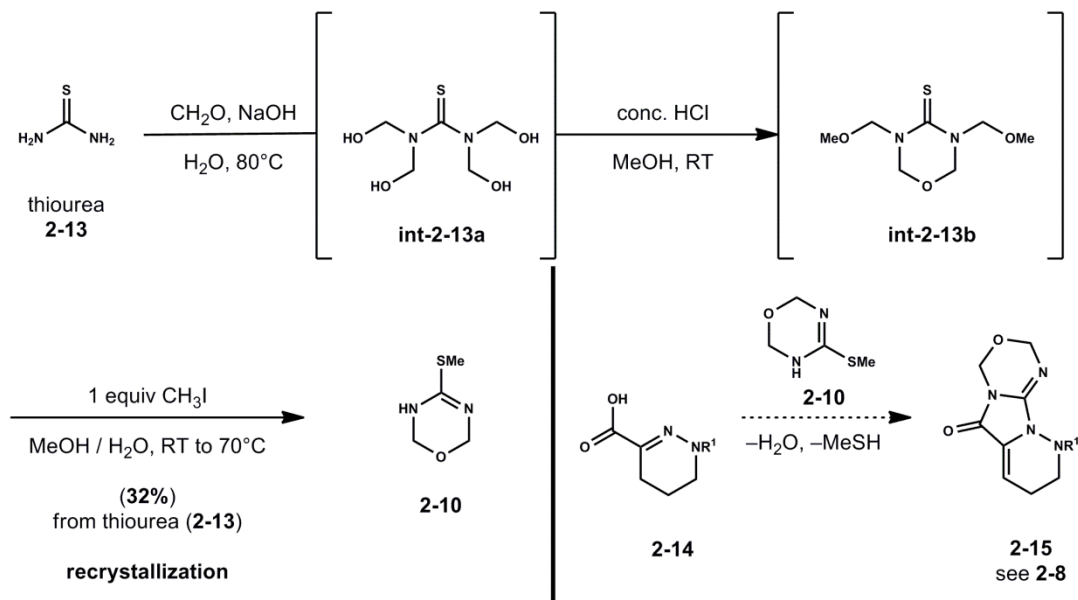
Initially we targeted dispacamide monomer **2-8** (Figure 2.2) and proposed a synthesis that paralleled our previous strategy to access familiar heterocycles such as 2,5-dihydrobenzo[*e*][1,3]diazepine monomer **2-7**.<sup>[11bc]</sup> Along these lines, monomer **2-8** would derive from novel heterocycle **2-10** (confer 1,3-benzodiazepine **2-9**), methyl 1,4,5,6-tetrahydropyridazine-3-carboxylate **2-11** and acid chloride **2-12**. Central to the design of these dispacamide monomers (**2-7**, **2-8**) was the development of strategies to controllably ‘mask’ the inherent polarity and

reactivity of their guanidine functionality.<sup>[12]</sup> The appropriate guanidine ‘mask’ would reduce polarity – facilitating purification and handling of intermediates, while maintaining a certain lability to permit ‘unveiling’ of requisite glycoyamidine<sup>[13]</sup> motifs in a late-stage setting. In the first iteration of this strategy, masked guanidine benzodiazepine monomers (of type **2-7**) proved to be highly robust for multiple chemical manipulations and purifications. Titanocene dienolates (not shown) derived from benzodiazepine monomer **2-7** were effectively dimerized oxidatively with high  $\gamma$  regio- and diastereoselectivity.<sup>[11bc]</sup> In this series, the obtained  $C_2$  symmetric dimer (not shown) was efficiently elaborated to the first fully functionalized bis-alkylidene (of type **2-2**) and provided access to chlorinated (C13) spirocycloalkylidenes (of type **2-3**, Figure 2.1, and see Chapter 1). Although enabling, the 1,3-benzodiazepine ring systems were originally designed to facilitate oxidative spirocyclization and ultimately proved to be too robust.<sup>[14]</sup> Therefore, we sought alternative means to effectively ‘mask’ and ‘unveil’ requisite glycoyamidine functionality.

For this exact purpose, the oxymethylene motif ( $-\text{CH}_2\text{O}-$ ) was attractive to us.<sup>[15]</sup> As an extension of previous logic, we envisioned the incorporation of this heterocycle could bestow properties of diminished polarity and tame the reactivity of guanidine-containing intermediates.<sup>[11d]</sup> The preparation of dispacamide monomer **2-8** required the efficient preparation of precursor 4-(methylthio)-3,6-dihydro-2H-1,3,5-oxadiazine **2-10**.

## 2.2 Results and Discussion

### 2.2.1 Synthesis of Alkyl Isothiuron 2-10, Dispacamide Surrogate 2-8 and Initial Dimerization Studies.



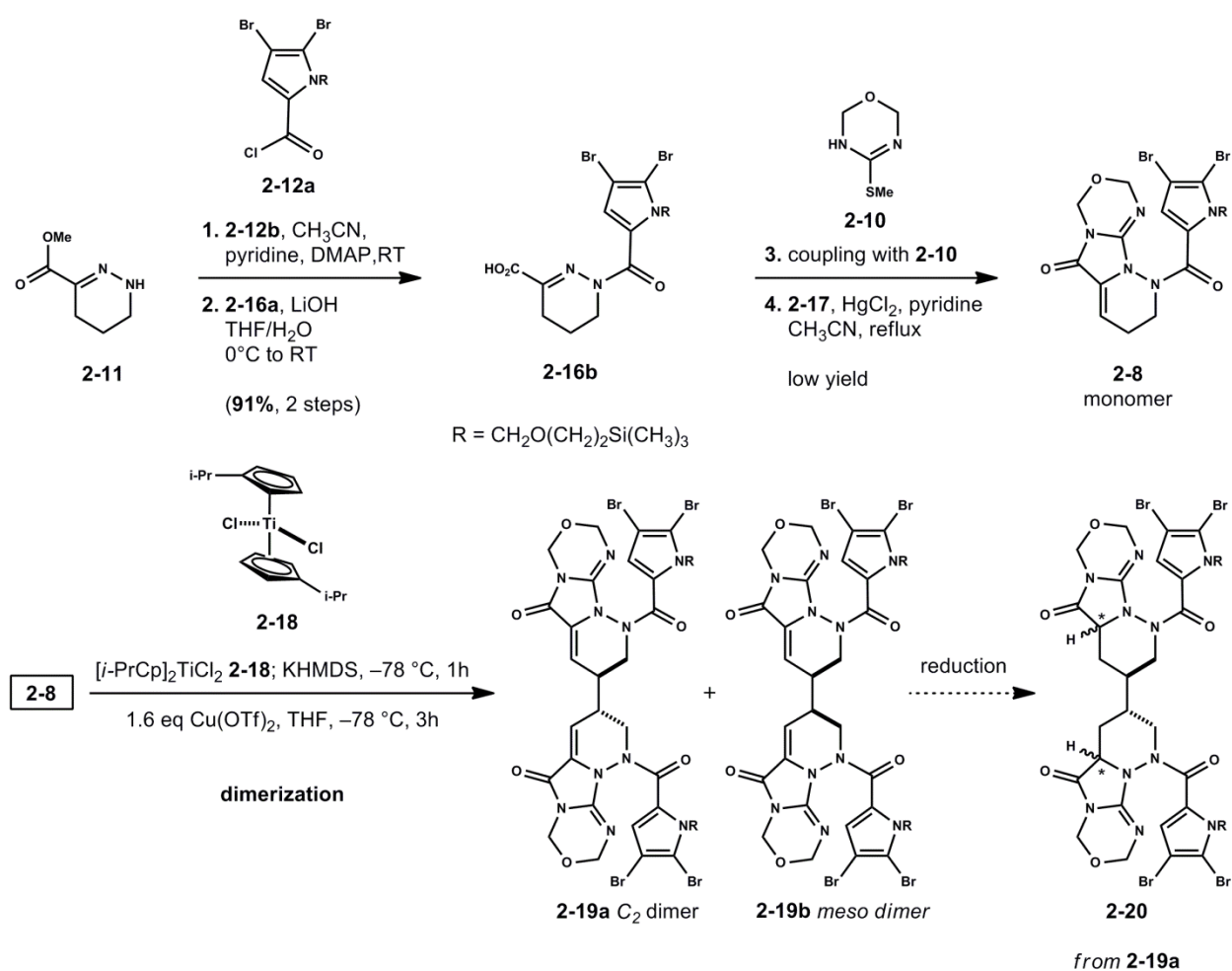
**Scheme 2.1.** Synthesis of novel 4-(methylthio)-3,6-dihydro-2H-1,3,5-oxadiazine **2-10** for guanidine synthesis. Urea Synthesis (**int-2-13b**): Egginton, C. D.; Vale, C. P. *Text. Res. J.* **1969**, 39, 140–147.

A scalable, one-pot procedure was developed for the synthesis of 4-(methylthio)-3,6-dihydro-2H-1,3,5-oxadiazine **2-10** based on useful precedent from Egginton and Vale.<sup>[16]</sup> Under basic conditions, thiourea **2-13** was reacted with excess formaldehyde to provide tetrahydroxymethylated thiourea **int-2-13a** as a viscous oil. Treatment of this material with HCl in methanol yields cyclic bis-*N*-methoxymethylated thiourea **int-2-13b** that was subsequently alkylated with methyl iodide. This material was controllably degraded under the resultant acidic conditions (formation of HI salt,  $\text{pH} = 2\text{--}3$ ) to form *S*-methyl isothiurea **2-10** as its hydroiodide salt. The aqueous soluble hydroiodide salt of heterocycle **2-10** was routinely separated from organic soluble by-products by successive organic solvent washes ( $\text{EtOAc}$ ,  $\text{CH}_2\text{Cl}_2$ ). Subsequent neutralization with aqueous sodium hydroxide provided crude freebase **2-10**. Following lyophilization,  $^1\text{H}$  NMR (500 MHz,  $\text{DMSO}-d_6$ ) analysis of the crude aqueous layer containing **2-**

**10** indicated that the sequence occurred with high efficiency over three steps from thiourea **2-13**. However, it was discovered that treatment of crude **int-2-13b** after methylation, slowly degraded both N-methoxymethylated units to form S-methyl isothiurea **2-10**. Prolonged reaction times further degraded this heterocycle resulting in diminished overall yield for the sequence. Insight to this yield erosion was obtained by identifying ammonium iodide, a putative degradant, as the major impurity present in crude reaction mixtures. Ultimately, this issue was resolved by reduced reaction time and the development of optimal conditions for the recrystallization of **2-10** (2-propanol / hexanes (4:1)).<sup>[16]</sup> With efficient access to **2-10** we explored its application for the synthesis of ‘dispacamide’ monomers (of type **2-15**) via amide bond formation with 1,4,5,6-tetrahydropyridazine-3-carboxylic acid derivative **2-14**. The resultant adduct would undergo intramolecular cyclization and tautomerization with net extrusion of methylmercaptan (–MeSH) to form prototype dispacamide monomer **2-15**.<sup>[11b]</sup> We targeted monomer **2-8** with the acylpyrrole component installed early for convergence and to provide dimeric intermediates with requisite bis-pyrrole functionality common to the axinellamines **2-5** and related dimeric pyrrole–imidazoles.<sup>[11d]</sup>

Previous research in our lab<sup>[11bc]</sup> suggested monomer **2-8** could be readily prepared beginning with the *N*-acylation of methyl tetrahydropyridazine-3-carboxylate **2-11** with acyl pyrrole derivative **2-12b**. The acylation proceeded in high crude yield with subsequent ester hydrolysis (Step 2, Scheme 2.2) to provide piperazic acid **2-16**. Condensation of **2-16** with S-methyl isothiurea **2-10** proceeded smoothly to provide amide **2-17** (not shown) under standard coupling conditions with TBTU. The target monomer **2-8** was obtained following mild thermolysis of S-methylisothiurea adduct **2-17** in the presence of excess HgCl<sub>2</sub> and pyridine. The net transformation proceeds via putative Lewis acid activation of the thiomethyl group and

subsequent 5-*exo*-trig cyclization of the pendant hydrazone. Unfortunately, the transformation was sluggish and additional mercuric chloride or prolonged reaction times resulted in low yields (<20%). In addition to undesirable conditions, purification and recovery of **2-8** was challenged by requisite harsh decomplexation methods to remove excess mercuric salts.<sup>[17]</sup> Eager to obtain dimeric intermediates and pursue their reactivity, we proceeded with sufficient access to monomer **2-8** in hopes of optimizing the guanidine synthesis (conversion of **2-17** to **2-8**, *vide infra*, Scheme 2.4) after establishing the overall route.



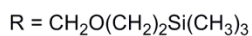
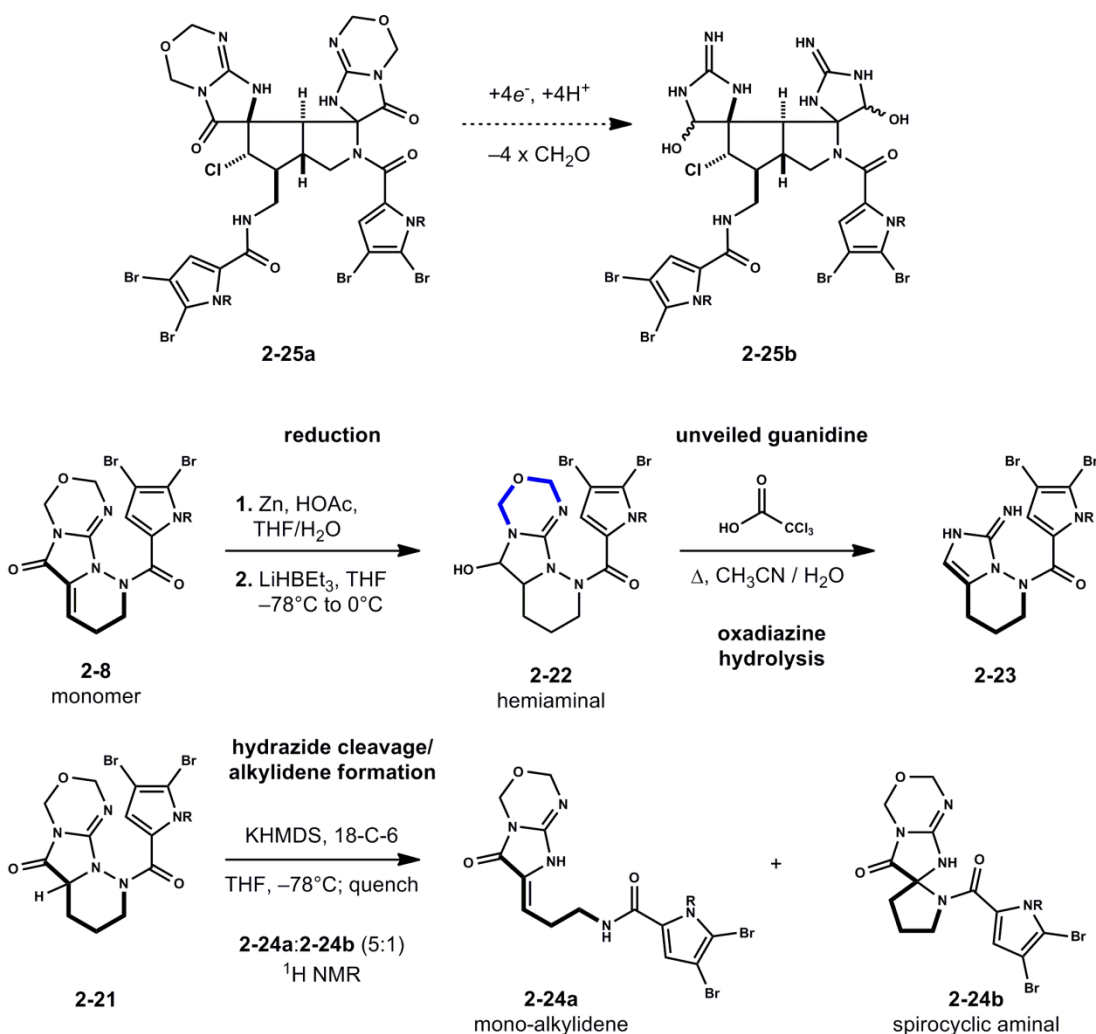
Scheme 2.2 Initial Synthesis of Reduced Dimers **2-20** From Monomer **2-8**.

The titanocene dienolate (not shown, *vide infra*) derived from enolization of diisopropylamide monomer **2-8** (KHMDS, THF,  $-78^\circ\text{C}$ , 1h) in the presence of titanocene **2-18**<sup>[18]</sup> was



regioselectively dimerized upon addition of cupric triflate in deoxygenated THF at  $-78^{\circ}\text{C}$ . This procedure routinely afforded  $\gamma,\gamma$ -dimers **2-19** albeit in poor yield and diastereoselectivity (20%, d.r. 1:1, Scheme 2.2).<sup>[11bc]</sup> Following arduous chromatographic separation of dimers **2-19** to obtain  $C_2$  symmetric isomer **2-19a**, we explored reduction conditions for the preparation of reduced  $C_2$  dimer **2-20**. Our previous method relied upon rhodium catalyzed hydrosilylation of the  $\alpha,\beta$ -unsaturated amides in **2-19a**.<sup>[11bc]</sup> Unfortunately these conditions provided reduced dimers **2-20** in low yield and as a mixture of diastereomers. Although the stereochemistry at  $C^*$  is ultimately cleared, the preparation of **2-20** (3 steps from **2-17**) was laborious and proceeded with low overall yield. Ultimately, this challenging sequence was reevaluated and led to the preparation of reduced dimeric intermediates (of type **2-20**) by a modified route. We targeted a new monomer **2-26** (Figure 2.3) for this purpose. Additional methods required for the transformation of late-stage dimeric intermediates were simultaneously developed using diisopropylamide surrogate **2-8** as a model system (Scheme 2.3).

## 2.2.2 Demonstration of Essential Transformations for the Reduction and Unveiling of Glycocyamidine Derivatives (from dispacamide monomer 2-8).



**Scheme 2.3.** Model Studies Using Dispacamide Synthon **2-8** to Demonstrate Key Transformations.

With sufficient access to dispacamide monomer **2-8** we were able to demonstrate several essential transformations. These methods were necessary to advance dimeric intermediates to a functionalized bis-alkylidene (of type **2-2**, Figure 2.1). We sought methods to effect the requisite reduction of intermediates (confer **2-25a**) to access the proper oxidation state (confer **2-25b**) for the preparation of axinellamines **2-5**, palau'amine **2-6** and related dimeric pyrrole-imidazoles. In addition, we desired access to free guanidine functionality from masked dimeric intermediates.

As discussed previously, our masked guanidine strategy has several benefits. These include properties of reduced polarity and high-crystallinity in intermediates, aiding purification. While important for handling, degradation of the heterocyclic mask (of type **2-8**) was necessary for the proposed late-stage isolation of bis-guanidine intermediates (e.g. **2-25b**). Monomer **2-8** was an excellent model for these important transformations.

Following reduction of **2-8** with Zn in HOAc / THF<sup>[19]</sup>, we explored controlled reduction of the glycoyamidine<sup>[13]</sup> (C1) heterocycle (Scheme 2.3). The  $2e^-$  reduction of glycoyamidine **2-21** with lithium triethylborohydride (LiHBEt<sub>3</sub>) provided hemiaminal **2-22** in good yield. The chemoselectivity observed in the reduction of this carbonyl (C1) can be explained by resonance delocalization within the glycoyamidine ring making the carbonyl (C1) more electrophilic.<sup>[20]</sup>

We subsequently examined hydrolytic degradation of the oxadiazine ring in **2-22** (Scheme 2.3). We were cognizant of the substantial difficulty associated with handling highly-polar bis-guanidines, which are typically purified as their corresponding bis-trifluoroacetate salts by preparative HPLC using acidic eluent (0.1-1% CF<sub>3</sub>CO<sub>2</sub>H). Therefore, such transformations were desirable in a late-stage setting. It was discovered that hemiaminal **2-22** was efficiently degraded under hydrolytic conditions using trichloroacetic acid in aqueous CH<sub>3</sub>CN at elevated temperatures to provide aminoimidazole **2-23**. Compound **2-23** was converted to its free-base and purified by preparative TLC (SiO<sub>2</sub>, eluent CH<sub>2</sub>Cl<sub>2</sub> / MeOH (12:1)). Under these conditions, hydrolysis occurs with net loss of two formaldehyde equivalents and concomitant dehydration. We next examined the propensity of reduced monomer **2-21** to undergo base-induced hydrazide fragmentation to provide access to mono-alkylidene **2-24a**.

Previous methods developed in our lab involved the use of excess 2,8,9-triisobutyl-2,5,8,9-tetraaza-1-phospha-bicyclo[3.3.3]undecane (see Chapter 1), however this reagent is strongly basic

and was found incompatible with compound **2-21**.<sup>[11b]</sup> Therefore, we developed new conditions for this transformation. We were influenced by successful conditions (KHMDS, Cy<sub>2</sub>BOTf, THF) developed previously by Li for hydrazide fragmentations in *meso*- derived dimers (not shown).<sup>[11bc]</sup> When reduced monomer **2-21** was added dropwise to a solution of KHMDS containing 1 equiv. 18-*crown*-6 (RT, THF) the major product isolated following work-up was mono-alkylidene **2-24a** (Scheme 2.3). Interestingly, **2-24a** was isolated alongside minor amounts of impure spirocyclic amination **2-24b**.<sup>[21]</sup> The use of 18-*crown*-6 was essential to observe rapid conversion (0.15 M THF, RT, 10-15 min) of **2-21** to **2-24b** in good yields.<sup>[22]</sup> It was also discovered that spirocyclic amination **2-24b** could be equilibrated to its open-form mono-alkylidene **2-24a** with catalytic DBU in MeOH. With these methods in hand, we were prepared to revisit the synthesis of reduced dimers **2-20** (Scheme 2.2). We proposed access to reduced dimers **2-20** from the oxidative dimerization of modified monomer **2-26** en route to targeted bis-alkylidene of type **2-2** (Figure 2.1).

### **2.2.3 Refined Synthesis – Preparation of Non-halogenated Monomer 2-26: A Scalable Procedure with Fewer Purification Events.**

Based on precedent for the preparation of related diisocyanide monomers (*e.g.* **2-7**, **2-8**), we targeted non-halogenated monomer **2-26** (Figure 2.3). We anticipated later intermediates could be effectively derivatized (*N*-trimethylsilyloxyethylation of pyrrole unit) and halogenated (*e.g.* NBS, THF). In addition, we proposed a more convergent synthesis of monomer **2-26** derived from the condensation of methyl-5-bromo-2-oxopentanoate **2-27**<sup>[23]</sup>, pyrrole-2-carboxylic acid hydrazide **2-28** and S-alkyl isothiuron **2-10**. Initially, carboxylic acid **2-29b**

was prepared from the *N*-acylation of methyl tetrahydropyridazine 3-carboxylate **2-11** (not shown) and subsequent saponification (Scheme 2.4).

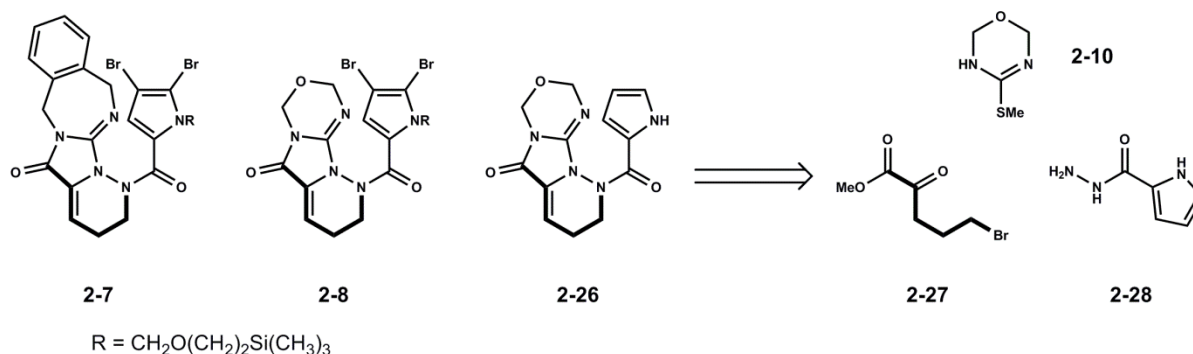
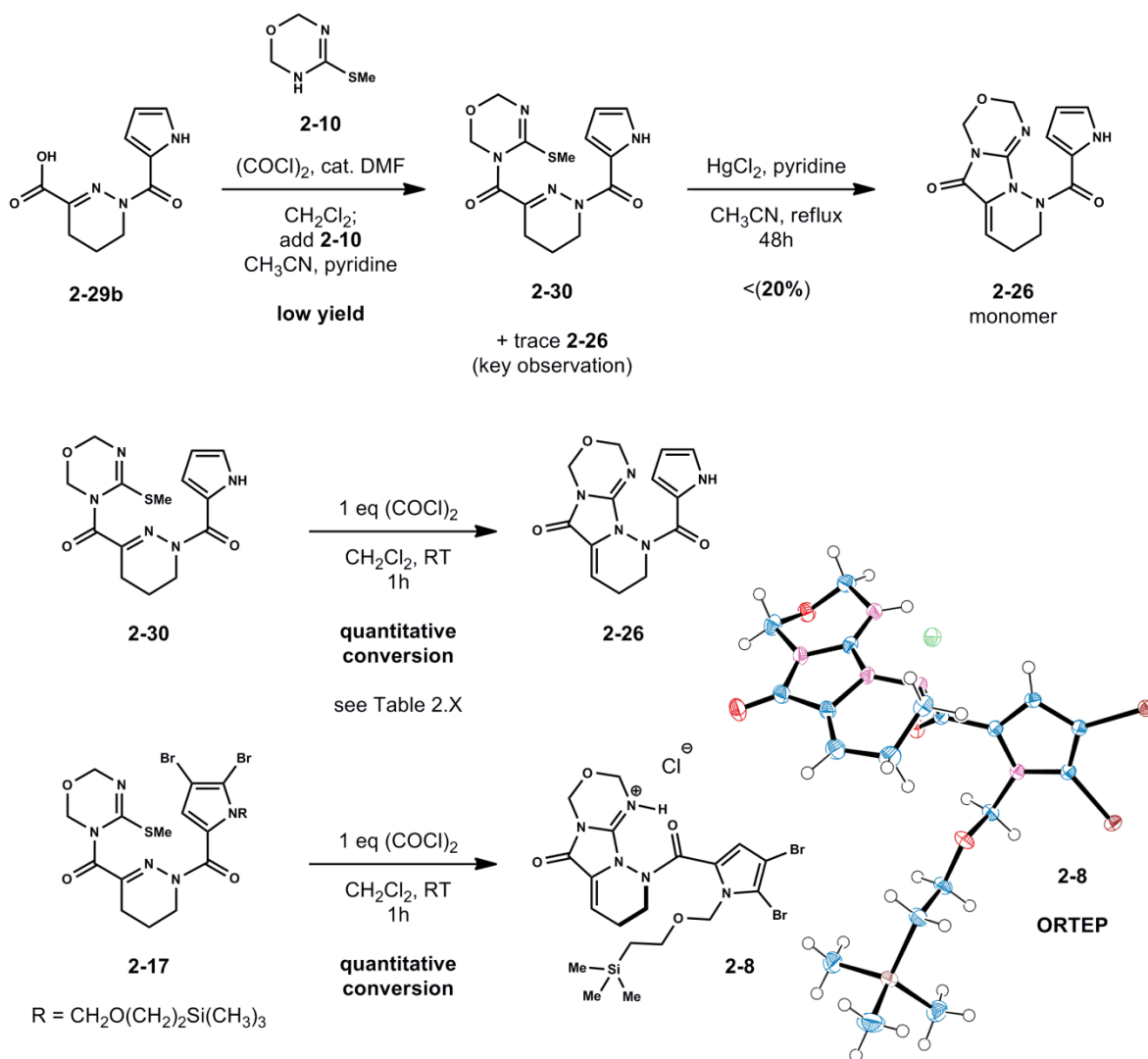


**Figure 2.3.** Modified Strategy to Access Monomer **2-26** - targeted dispacamide **2-1** monomers derived from key fragments (**2-10**, **2-27**, **2-28**).

The acid chloride derived from **2-29b** was then used to *N*-acylate thiourea derived methylisothiourea **2-10**. In developing this procedure, we observed that crude amide **2-30** was often contaminated with small amounts of **2-26** – the desired product from what was to be the next step in our sequence. Control experiments established that pure **2-30** was cleanly converted to **2-26** when treated with oxalyl chloride alone. Ultimately, we demonstrated the utility of oxalyl chloride as an effective reagent for the activation of S-methyl isothioureia adducts (**2-30** and **2-17**) to form their corresponding guanidines (**2-26** and **2-8**).<sup>[24]</sup> Notably, the method forgoes use of stoichiometric mercuric chloride. Treatment of S-methyl isothioureia adduct **2-30** under mild thermolysis conditions with mercuric chloride did provide target monomer **2-26**, but in low isolated yields.<sup>[25]</sup> A crystal of suitable quality for X-ray diffraction was obtained for monomer **2-8** (**2-8** HCl, CCDC 942601, CH<sub>3</sub>CN, solvent removed for clarity).<sup>[26]</sup>



**Scheme 2.4.** Synthesis of Monomer **2-26** Using Discovered  $(\text{COCl})_2$  Activation.

Admittedly, control reactions were not conducted first. The observation of trace **2-26** present in crude mixtures of **2-30** suggested an alternate activation of **2-30** had occurred in situ. We speculated this involved reaction of **2-30** with excess  $(\text{COCl})_2$  and/or the acid chloride from **2-29b** indeterminate acylation (*on sulfur or nitrogen*) to afford **int-2-30** (e.g.  $\text{Y} = [-\text{SMeAc}]^+$ ). This suggested other acid halides (e.g.  $\text{AcCl}$ ,  $\text{PivCl}$ ) may also provide access to monomers (**2-26**, **2-8**). Several conditions examined for the conversion of **2-30**  $\rightarrow$  **2-26** (Entry 1-3) and **2-17**  $\rightarrow$  **2-8** (Entry 4-9) are summarized in Table 2.1. Interestingly, acetyl chloride ( $\text{AcCl}$ , Entries 2 & 5)

was also effective for this transformation albeit with lower, variable yields. Control experiments with oxalyl chloride (Entry 3, 8) were most efficient. Mechanistic aspects of this transformation were not explored in detail. Although not directly observed, one cannot exclude the possibility **int-2-30** (Y = Cl) as an intermediate en route to monomers (**2-26**, **2-8**).<sup>[27]</sup> With a novel method in hand, we targeted the synthesis of non-brominated monomer **2-26**. We also sought convergent access to the system beginning with methyl-5-bromo-2-oxopentanoate **2-27** and pyrrole-2-carboxylic acid hydrazide **2-28** (Scheme 2.5).

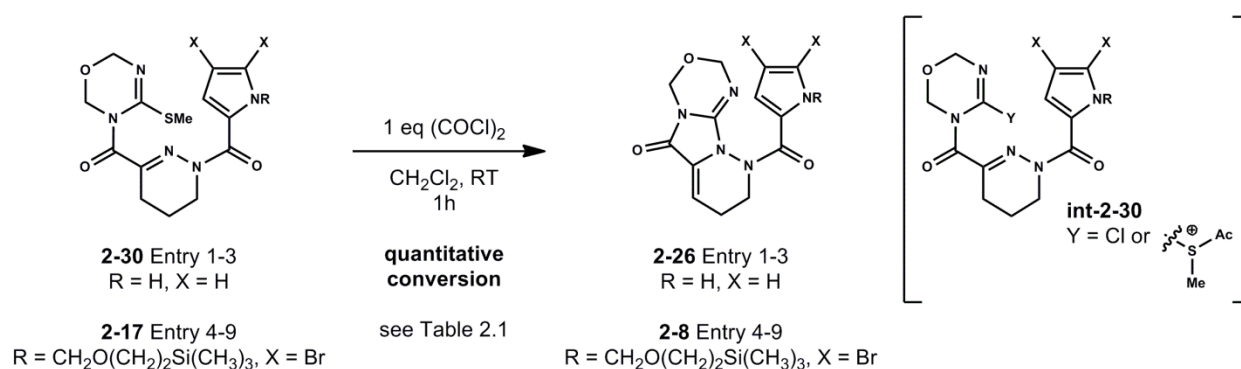
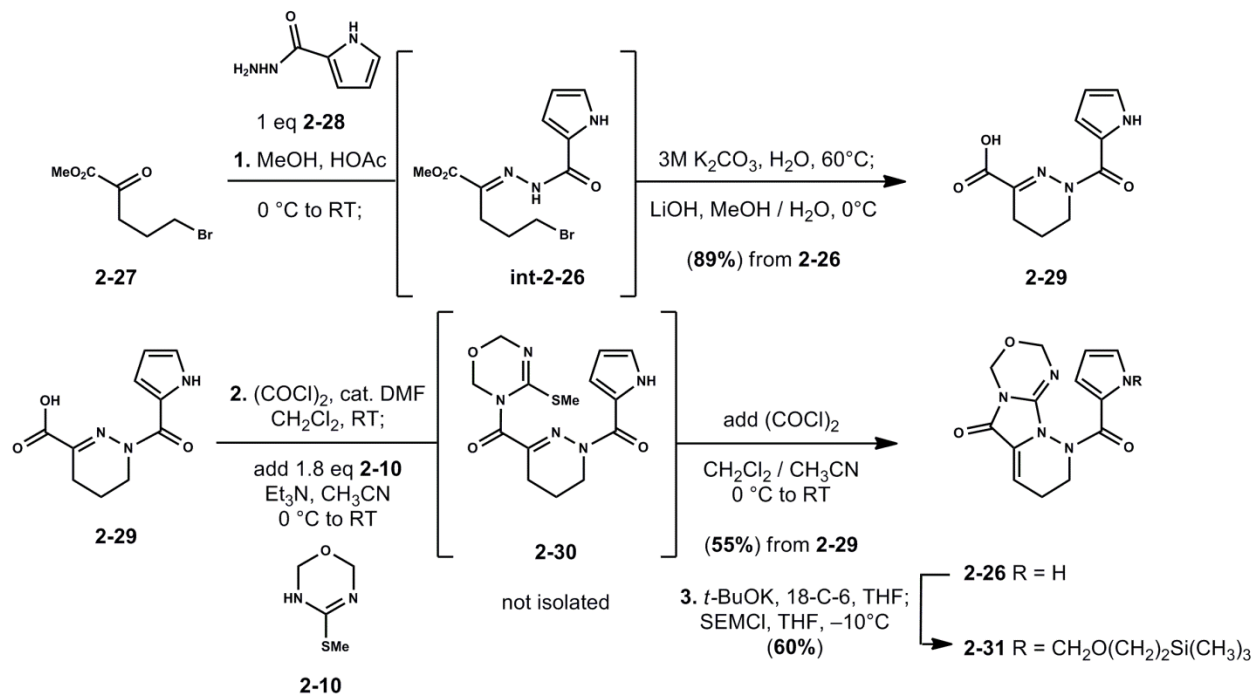


**Figure 2.4.** Optimized cyclization conditions for intramolecular guanidine synthesis.

**Table 2.1** Optimization of conditions to generate **2-26** & **2-8** from precursors **2-30** & **2-17**.

Entry	Reagent	Base / Equiv.	Solvent	Additive / Notes	Yield (%)
1	HgCl <sub>2</sub> / 1.7	pyridine / 3.0	CH <sub>3</sub> CN (0.2 M)	100°C, 48h, 5.3 mmol	(13–20%)
2	AcCl / 1.1	pyridine / 2.0	CH <sub>3</sub> CN (0.2 M)	70°C, 0.1 mmol, <10% <b>2-26</b> , <b>2-30</b> major	ND
3	(COCl) <sub>2</sub> / 1.1	none	CH <sub>2</sub> Cl <sub>2</sub> (0.15 M)	RT, 1h, crude <b>2-30</b> used	(47%)
4	HgCl <sub>2</sub> / 1.7	pyridine / 3.0	CH <sub>3</sub> CN (0.2 M)	100°C, 48h	(20%)
5	AcCl / 2.5	pyridine / 3.0	CH <sub>3</sub> CN (0.2 M)	70°C, 12–20h	(12%), (18%), (35%)
6	PivCl / 2.5	pyridine / 3.0	CH <sub>3</sub> CN (0.2 M)	70°C, 20h, trace <b>2-26</b>	ND
7	(COCl) <sub>2</sub> / 1.1	none	CH <sub>2</sub> Cl <sub>2</sub> (0.1 M)	RT, 20 min, 6.8 mmol	(51%)
8	(COCl) <sub>2</sub> / 1.1	none	CH <sub>2</sub> Cl <sub>2</sub> (0.1 M)	RT, 1.5h, 8.8 mmol,	(80%)

Upon refining this route, we were able to generate 50 grams of monomer **2-26** in one pass.<sup>[11d]</sup> Methyl-5-bromo-2-oxopentanoate **2-27** (Scheme 2.5) is available on mole scale by degrading carboethoxylated  $\gamma$ -butyrolactone with HBr/AcOH and Fischer esterification of the resultant  $\alpha$ -ketoacid.<sup>[23]</sup> When **2-27** was condensed with pyrrole-2-carboxylic acid hydrazide **2-28** an intermediate hydrazone (**int-2-26**) formed.



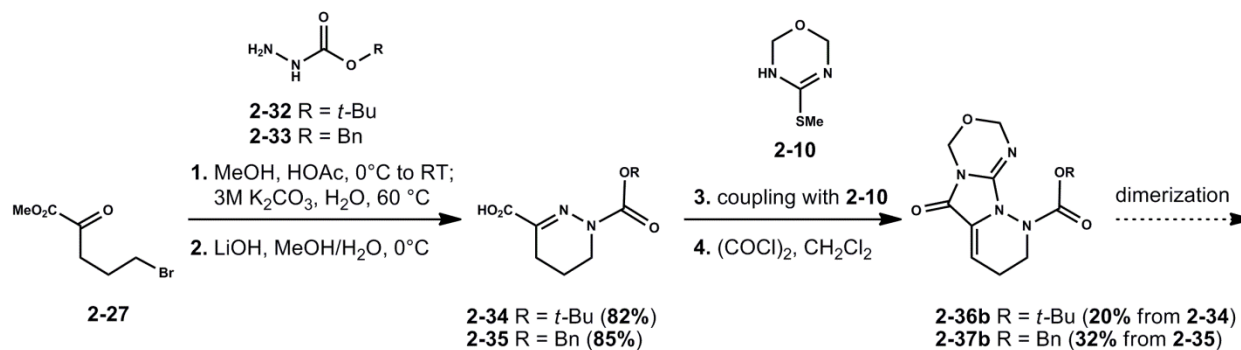
**Scheme 2.5.** Optimized 3-pot procedure for a scalable synthesis of monomer **2-31**.

The intermediate did not require isolation and could be cyclized and saponified in situ to obtain tetrahydropyridazinecarboxylic acid **2-29** in high yield. The modified procedures outlined above then allowed for the development of a one-pot procedure wherein **2-29** is transformed to monomer **2-26** via the intermediacy of **2-30** (Scheme 2.5). *S*-methyl isothiouraea **2-10** was *N*-acylated with the corresponding acyl chloride of **2-29** to afford intermediate amide **2-30**. Without isolation, intermediate **2-30** was treated with oxalyl chloride to induce ring closure in situ via net expulsion of methylmercaptan<sup>[24]</sup> to afford tricyclic glycoxyamidine **2-26** in good overall



yield.<sup>[28]</sup> For solubility purposes, monomer **2-26** was silylethoxymethylated to provide derivative **2-31** in 60% yield under optimized conditions.<sup>[29]</sup>

## 2.2.4 Synthesis of Carbonyl Congeners of Dispacamide Monomer 2-26.

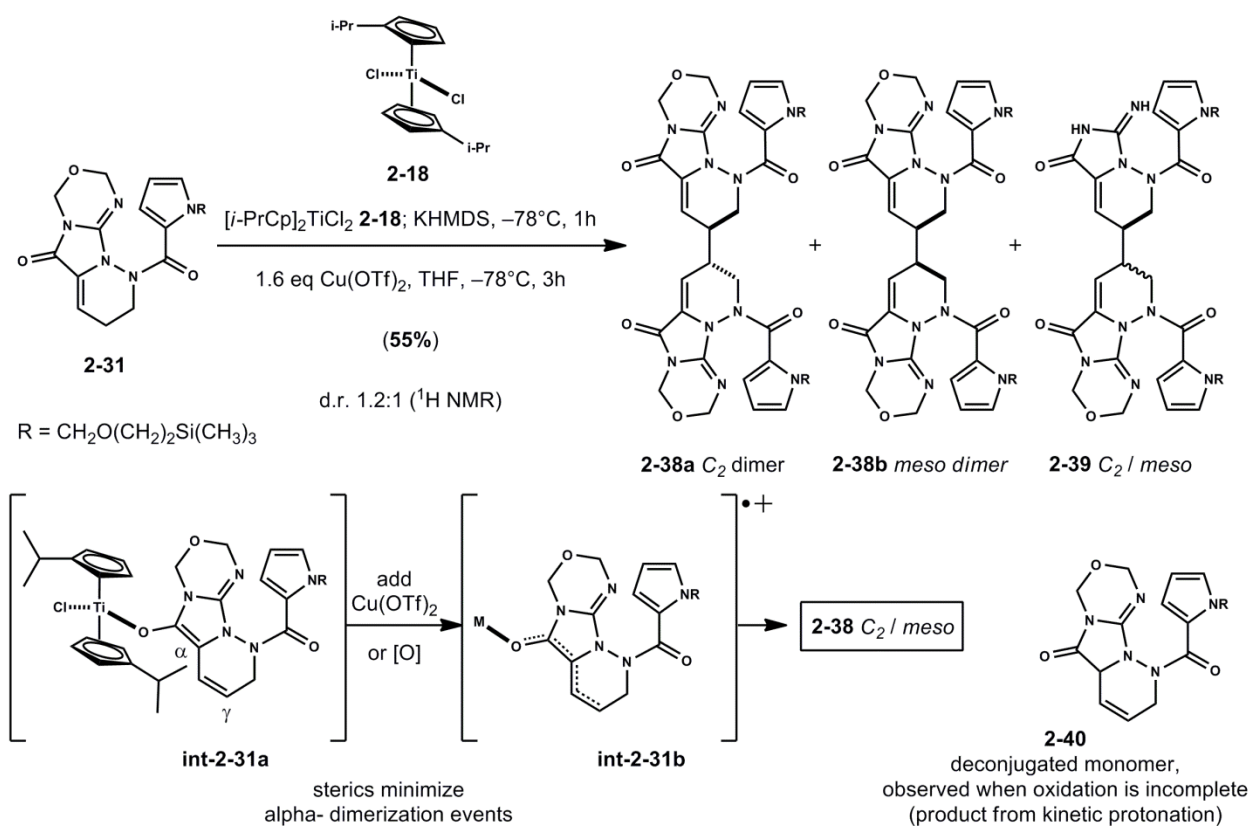


**Scheme 2.6.** General synthesis of dispacamide monomers (**2-36b**, R = *t*-Bu and **2-37b**, R = Bn)

We briefly examined the generality of our synthetic route to prepare related dispacamide monomers (**2-36b** R = *t*-Bu, **2-37b** R = Bn). Condensation of the methyl 5-bromo-2-oxopentanoate **2-11** with either hydrazine carboxylate (**2-32**, **2-33**) and subsequent saponification of the resultant ester provided the corresponding tetrahydropyridazinecarboxylic acids (**2-34b** and **2-35b**, respectively) in good yield. Their coupling with **2-10** (Step 3) and intramolecular cyclization with oxalyl chloride (Step 4) provided monomers (**2-36b** and **2-37b**, respectively) without event. Coupling yields with **2-10** were not optimized and were generally low when TBTU was employed.<sup>[30]</sup> These monomers (**2-36b**, **2-37b**) were also suitable substrates for dimerization but yield and diastereomeric ratios were not examined in detail. These derivative monomers (**2-36b**, **2-37b**) may prove useful in alternative syntheses of dispacamide monomers or dimers where the acyl pyrrole subunit is not immediately required.

### 2.2.5 Dimerization of Dispacamide Monomer 2-31 and Late-Stage Manipulation of Functionality.

Although various methods exist for the oxidative heterocoupling and dimerization of enolates<sup>[31]</sup> there is limited precedent for control of regioselectivity in dienolate oxidations. Notable studies on the dimerization of dienolates include the work of Saegusa<sup>[32]</sup>, Mestres<sup>[33]</sup> and Paquette<sup>[34]</sup>. The Paquette group observed moderate  $\gamma,\gamma$  regioselectivity when cupric chloride was used as the oxidant for the dimerization of (*IR*)-(+)-verbenone (not shown) derived dienolates. Earlier work in our group by Li *et al.* established a general solution to afford  $\gamma,\gamma$ -dimers with high regiocontrol and moderate diastereoselectivity.<sup>[11bc]</sup> Li developed a method that involved the formation of extended titanocene dienolates under optimized enolization conditions followed by the addition of a single-electron oxidant (*e.g.*  $[\text{Fe}^{\text{III}}\text{Cl}_2(\text{DMF})_3]\text{FeCl}_4$  or  $\text{Cu}(\text{OTf})_2$ ). Although details of mechanism are unclear, observed regiocontrol can be explained by analogy to the research of Schmittel and co-workers which suggests that the dienolate Ti–O (*e.g.* **int-2-31b**, Scheme 2.7) bond is intact during C–C bond formation.<sup>[35]</sup> Control experiments demonstrated that the isopropyl substitution on derivative titanocene **2-18** (Scheme 2.7) was important for high  $\gamma$ -regiocontrol. The isopropyl substitution (**int-2-31a**) serves as a steric shield to occlude  $\alpha$ -dimerization events.<sup>[11bc]</sup> Although developed and optimized for the dimerization of benzodiazepine monomer **2-7**, this method was found effective for the oxidative dimerization of monomer **2-31**.<sup>[11d]</sup>



**Scheme 2.7.** Regioselective oxidative dimerization of titanocene dienolates **int-2-31a**.

The pyrrole nitrogen in **2-26** was silylethoxymethylated to increase solubility in THF at  $-78^\circ\text{C}$ .<sup>[36]</sup> Derivative **2-31** was then mixed with diisopropyltitanocene dichloride **2-18** in THF and cooled to  $-78^\circ\text{C}$  prior to treatment with potassium hexamethyldisilazide (KHMDS). The putative titanocene dienolate (**int-2-31a**) formed was oxidized *in situ* with cupric triflate ( $\text{Cu}(\text{OTf})_2$ ) to initiate regioselective homodimerization at the enolate  $\gamma$  position. The  $C_2$  symmetric product **2-38a** could be separated by precipitation of **2-38b** in  $\text{CH}_3\text{CN}$  from its *meso* counterpart **2-38b** in moderate yield (d.r. 1.2:1,  $^1\text{H NMR}$  analysis). Fortunately, the diastereomeric outcome was readily assigned by X-ray diffraction analysis of *meso* dimer **2-38b** (Figure 2.4, CCDC 859079).<sup>[26]</sup>

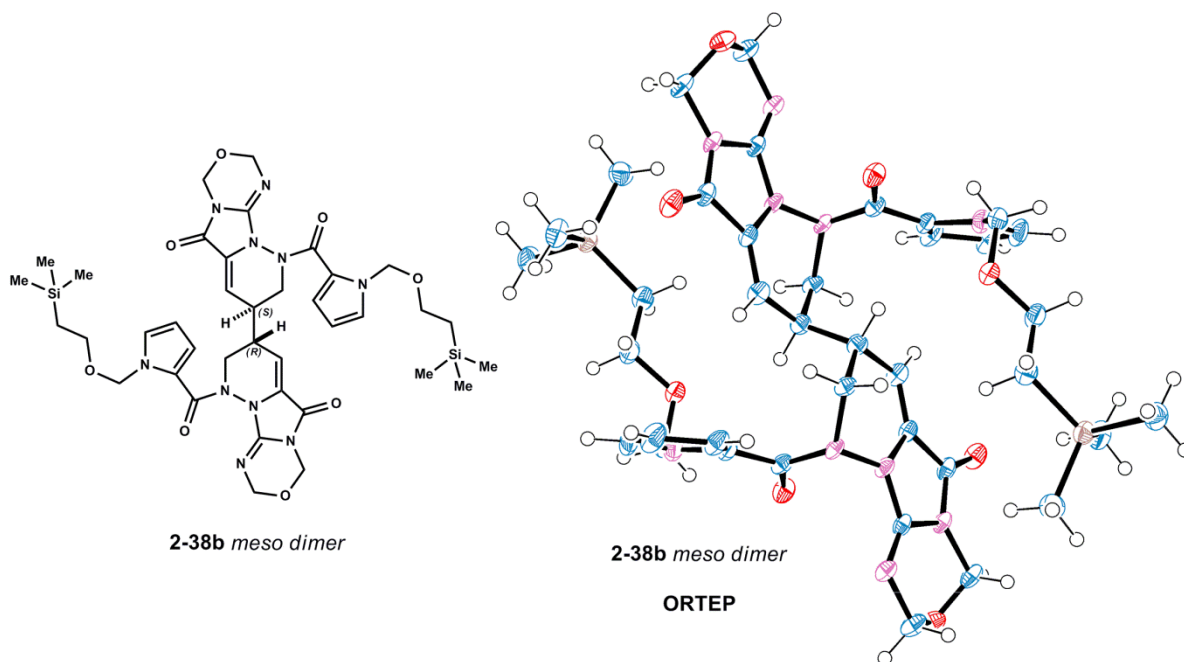


Figure 2.5. X-ray crystal structure of *meso* dimer **2-38b**.

This dimerization procedure initially developed by Li *et al.* was robust and reproducible.<sup>[11bc]</sup> However, several minor modifications greatly simplified this general protocol. Solvent deoxygenation via freeze-pump-thaw cycles was found unnecessary. Prolonged sparging with Ar was sufficient. Dimerization conditions were optimized with cupric triflate. High regiocontrol was obtained, but we did not observe substantial diastereocontrol in dimerizations of **int-2-31a**. This result contrasts previous observations in the dimerization of benzodiazepine monomer **2-7**.<sup>[11bc]</sup> Interestingly, careful analysis of crude reaction mixtures identified that partial heterocycle degradation occurred to provide mono-glycocyamidines **2-39** (20-30%, crude yield). This result supported high efficiency in overall dimerization events (est. 80% productive conversion of **2-31**).<sup>[37]</sup> Equally noteworthy, deconjugated monomer **2-40** was observed when oxidations were incomplete. Control experiments demonstrated that **2-40** was the product of kinetic protonation of putative **int-2-31a** (Table 2.3, Entry 4). Resubjection of the deconjugated monomer **2-40** to dimerization conditions (deprotonation, oxidation) was consistent with the putative formation of

titanocene dienolate **int-2-31a**. Substantial effort was made to render moderate diastereocontrol and improve yield with minor procedural modifications. The results are summarized in Table 2.2.

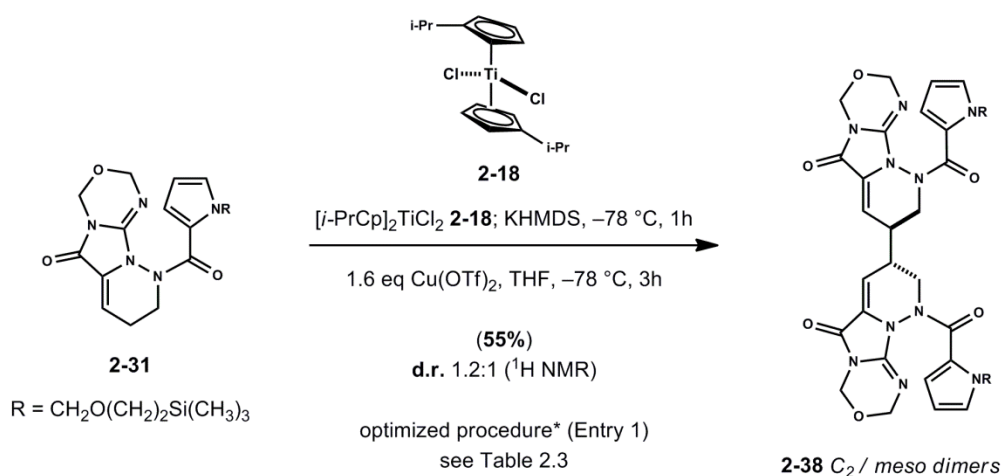
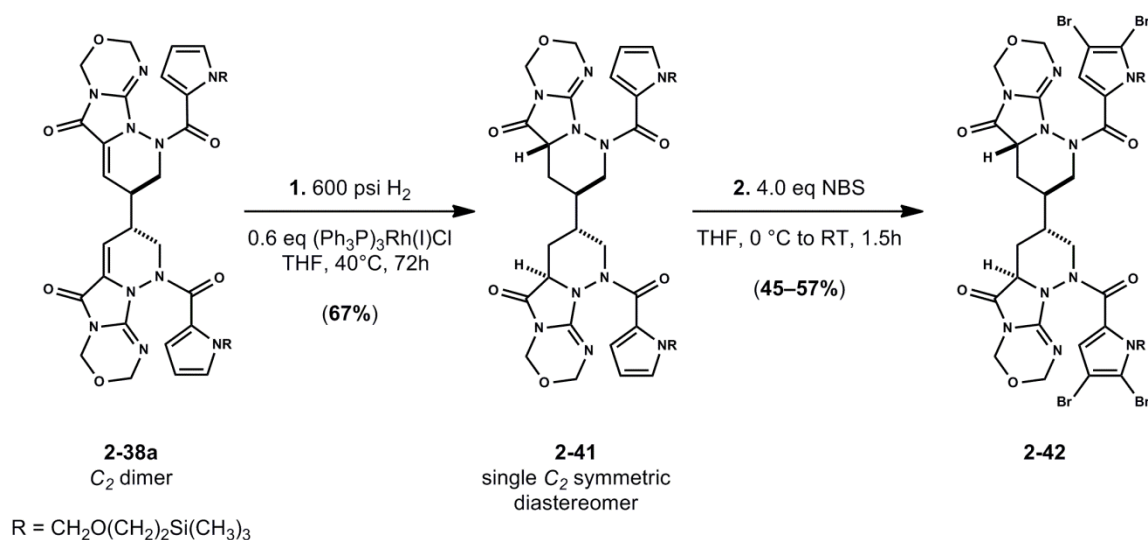


Figure 2.6. Optimization of oxidative dimerization.

Table 2.2 Optimization of titanocene dienolate based oxidative dimerization of 2-31.

Entry	Oxidant / Equiv.	Solvent	Additive / Notes	Combined Yield (%)	Ratio (38a:38b)
1	Cu(OTf) <sub>2</sub> / 1.6	THF	standard condition (quench, EDTA, pH = 8.5)	(55%)*	1.2 : 1
2	Cu(OTf) <sub>2</sub> / 1.6	THF	purification (neutral Al <sub>2</sub> O <sub>3</sub> )	(42%)	1.2 : 1
3	Cu(OTf) <sub>2</sub> / 1.6	THF	basic quench (EDTA, pH = 9)	(57%)	1.2 : 1
4	none	THF	quench dienolate <b>int-2-31a</b> (after 20 min) with EDTA	(86%) of <b>2-40</b>	NA
5	Cu(OTf) <sub>2</sub> / 1.6	CH <sub>3</sub> CN	Cu(OTf) <sub>2</sub> soluble in CH <sub>3</sub> CN	(42%)	1.1 : 1
6	Cu(OTf) <sub>2</sub> / 1.6	DME	reaction run in DME	(35%)	1.1 : 1
7	Cu(OTf) <sub>2</sub> / 1.6	THF	large scale (mechanical stirring) oxidant added in 3 portions	(34%)	1.2:1
8a	Cu(OTf) <sub>2</sub> / 1.6	THF	none (control for <b>8b</b> )	(46%)	1 : 1
8b	Cu(OTf) <sub>2</sub> / 1.6	THF	18-C-6 (1.2 equiv)	(42%)	1 : 1
9a	V(O)Cl <sub>2</sub> (OCH <sub>2</sub> CF <sub>3</sub> ) / 1.0	THF	oxidant added neat	(26%)	1.1 : 1
9b	V(O)Cl <sub>2</sub> (OCH <sub>2</sub> CF <sub>3</sub> ) / 1.3	THF	oxidant added neat	(26%)	1.1 : 1
9c	V(O)Cl <sub>2</sub> (OCH <sub>2</sub> CF <sub>3</sub> ) / 1.5	THF	oxidant added neat	(30%)	1.1 : 1
10	Ag <sup>II</sup> (picolinate) <sub>2</sub> / 2.0	THF	slow oxidation, warm to RT (23 °C), 12h	(25%)	1 : 1
11	[Fe <sup>III</sup> Cl <sub>2</sub> (DMF) <sub>3</sub> ]FeCl <sub>4</sub> / 2.0	DMF	dimer observed, complex mix	ND	ND
12	Co <sup>III</sup> (acac) <sub>3</sub> / 2.0	THF	dimer observed, complex mix	ND	ND
13	Cu <sup>II</sup> (hfacac) <sub>2</sub> / 1.6	THF	dimer observed, complex mix	ND	ND

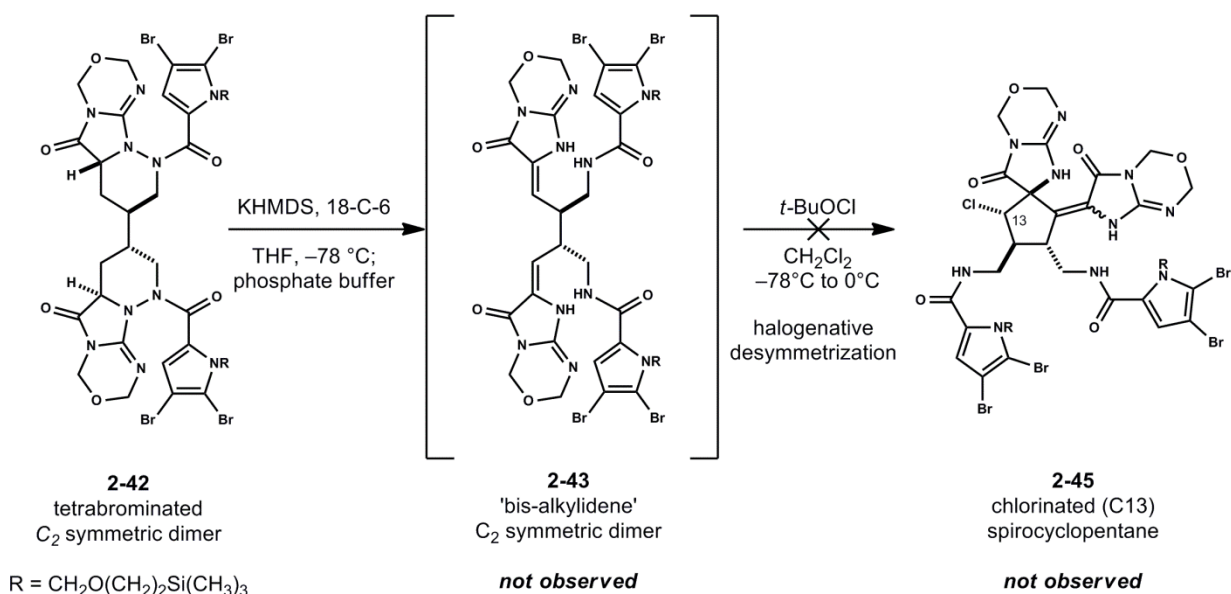
Considerable effort was made to improve diastereocontrol in dimerization reactions (Figure 2.5, Table 2.3). In all experiments, the putative dienolate **int-2-31a** was formed under ‘standard’ conditions by the addition of KHMDS to a premixed solution of monomer **2-31** and titanocene **2-18** in degassed THF (Ar sparged) at  $-78^{\circ}\text{C}$ . Unfortunately, improved conditions/procedures were not forthcoming for the dimerization of monomer **2-31** (**2-38a:2-38b**, d.r. 1.2:1, 55% yield, Entry 1, optimal conditions). Several oxidants acted upon putative dienolate **int-2-31a** to generate dimers **2-38** with low d.r. 1:1 and with variable yields (Entries 8–10), while other oxidants employed failed to induce dimerization with comparable regiocontrol (Entries 11–13). The use of  $\text{V}(\text{O})\text{Cl}_2(\text{OCH}_2\text{CF}_3)$  reproducibly provided regiocontrolled dimers **2-38** (Entry 9).<sup>[38]</sup> Although yield (Entry 9) was not improved with increased oxidant, the ability to add this reagent neat (orange liquid) was procedurally convenient.<sup>[39]</sup> With high regiocontrol established using cupric triflate, we studied minor procedural changes. These included the following reaction/purification modifications: purification of crude mixture (Entry 2, neutral  $\text{Al}_2\text{O}_3$  vs.  $\text{SiO}_2$ ), quench modification (Entry 3, EDTA, pH = 9 vs. pH = 8.5) and the addition of additives (Entry 8b, 18-C-6). Procedural modifications included: changing the solvent used to dissolve  $\text{Cu}(\text{OTf})_2$  to  $\text{CH}_3\text{CN}$  (Entry 5, contrasts slurry observed when THF was employed), alternative solvent DME (Entry 6) and the ability to scale reactions (above 12 mmol, 5g of **2-31**) assisted by mechanical stirring (Entry 7, 36 mmol of **2-31**).<sup>[39]</sup> None of the modifications resulted in improved yield. We proceeded with sufficient access to  $\text{C}_2$  dimer **2-38a** (Entry 1). Dimerizations were routinely and reproducibly conducted with **2-31** (up to 12 mmol, 5g of **2-31**) to provide gram quantities (multiple 12 mmol dimerizations combined) of pure  $\text{C}_2$  dimer **2-38a**.<sup>[40]</sup>



**Scheme 2.8.** Elaboration of C<sub>2</sub> dimer **2-38a** to key tetrabrominated C<sub>2</sub> dimer **2-42**.

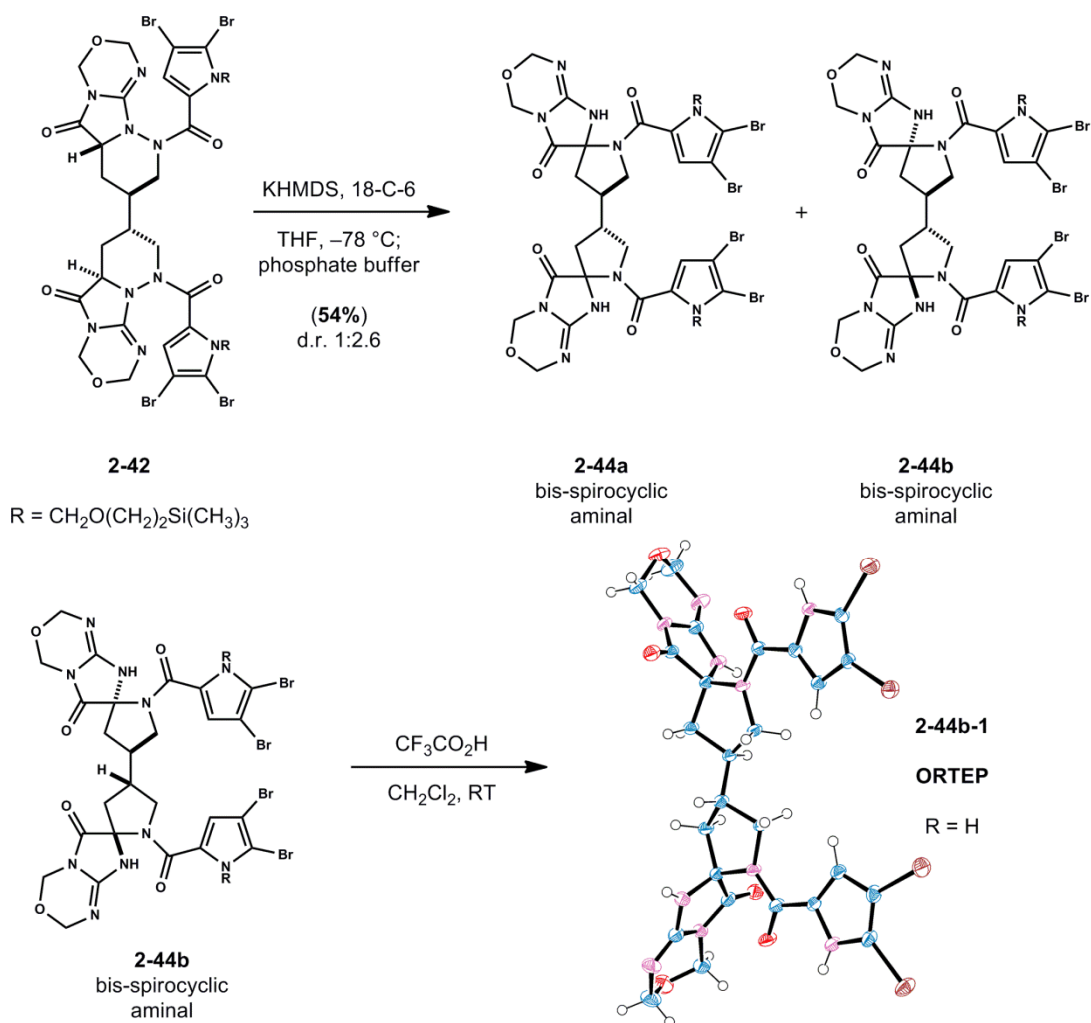
The C<sub>2</sub> symmetric dimer **2-38a** was hydrogenated in the presence of Wilkinson's complex to afford a four-electron reduction product in high diastereomeric excess.<sup>[41]</sup> The reaction required high catalyst loading to proceed efficiently.<sup>[41b,41c]</sup> Heterogeneous hydrogenation conditions (*e.g.* H<sub>2</sub>, Pd/C) were equally sluggish and proceeded with lower yield and moderate diastereocontrol. It was discovered that the addition of 2 equiv. anhydrous HCl in methanol or acetic acid accelerated heterogeneous reduction, albeit with reduced yields presumably due to acidolysis of the oxadiazine rings. The reduced C<sub>2</sub> symmetric dimer **2-41** obtained was smoothly tetrabrominated using NBS in THF to afford **2-42a**. Small amounts of tri- and pentahalogenated dimers (confer **2-42a**) are formed in this reaction. This outcome was highly dependent on the purity of **2-41** and control of reagent stoichiometry.<sup>[42]</sup> This sequence was routinely conducted on gram-scale to provide sufficient quantities (several grams) of desired tetrabrominated dimer **2-42a**.





**Scheme 2.9.** Base induced hydrazide fragmentations in **2-42** does not provide bis-alkylidene **2-43**.

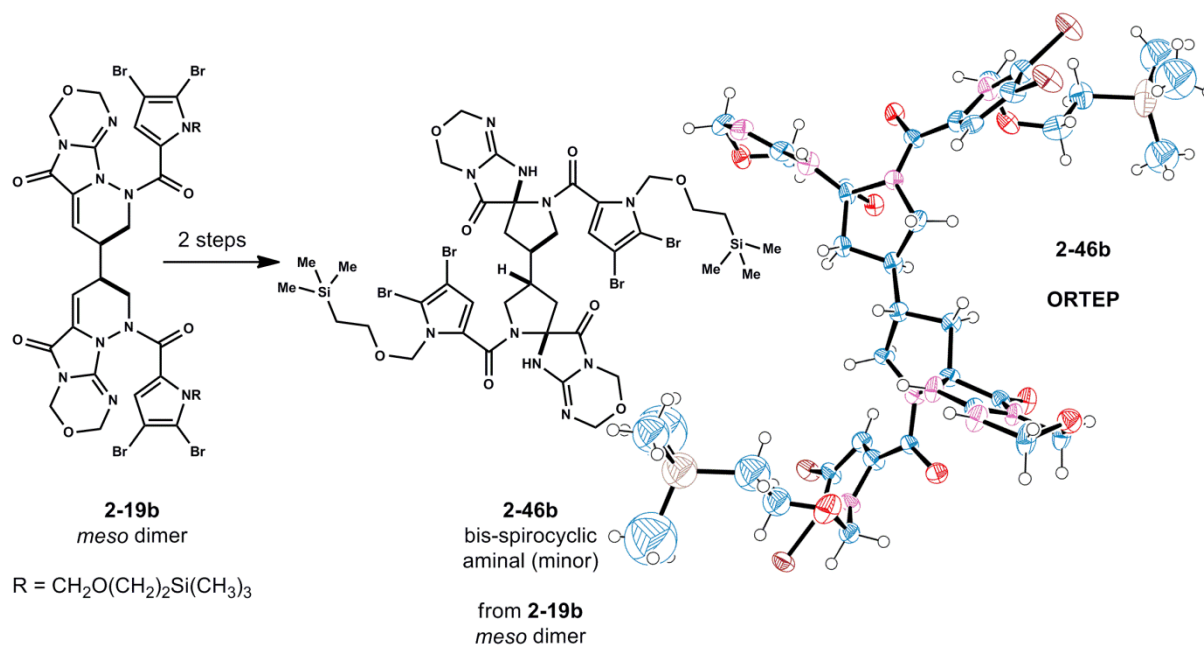
With sufficient quantities of tetrabrominated dimer **2-42a** in hand, we applied previously developed conditions to access targeted bis-alkylidene **2-43** (Scheme 2.9). When tetrabrominated dimer **2-42a** was added to a solution of 18-crown-6 containing a two-fold excess of potassium hexamethyldisilazide (KHMDS) at -78 °C, both hydrazide N-N bonds undergo cleavage.<sup>[11b]</sup> Presumably this occurred via sequential or cascading enolate formation /  $\beta$ -elimination pathways. Based on our own precedent as well as results found using a monomeric model **2-21** (Scheme 2.3), we anticipated bis-alkylidene **2-43** would be formed in this reaction.<sup>[43]</sup> Inexplicably, no such material was detected, however the increased polarity of unknown products **2-44** suggested N-N bond cleavage had occurred. Anticipated bis-alkylidene **2-43** was required to obtain direct access to a chlorinated (C13) spirocyclopentane **2-45** in this series. Therefore, a substantial effort was devoted to determining the structure and reactivity of the unknown products.



**Scheme 2.10.** Hydrazide Fragmentations with **2-42** provide solely bis-spirocyclic aminals **2-44a** and **2-44b**

Intriguingly, we isolated two separable fractions of bis-spiroaminal isomers **2-44**, wherein the tethered amides have 5-*exo* cyclized onto imino tautomers of the target alkylidenes. Analyses of crude reaction mixtures showed one diastereomer (**2-44b**) of **2-44** predominated; yet several isomeric variants are present in lesser amounts. Treatment of purified isomer **2-44b** with  $\text{CF}_3\text{CO}_2\text{H}$  followed by workup with aqueous  $\text{NaHCO}_3$ <sup>[44]</sup> afforded product **2-44b-1**. X-ray crystallographic analysis of product **2-44b-1** showed it to possess the relative stereochemistry we tentatively assign to **2-44b-1** (CCDC 859080).<sup>[26]</sup> For record, brief studies conducted with intermediates derived from *meso* symmetric dimer **2-19b** (Scheme 2.11) suggest the analogous

bis-spirocyclic aminals (such as **2-46b**) are also formed as major components. X-ray crystallographic analysis of product **2-46b** confirmed bis-spirocyclic aminal structural assignment in the *meso* series.<sup>[26]</sup>

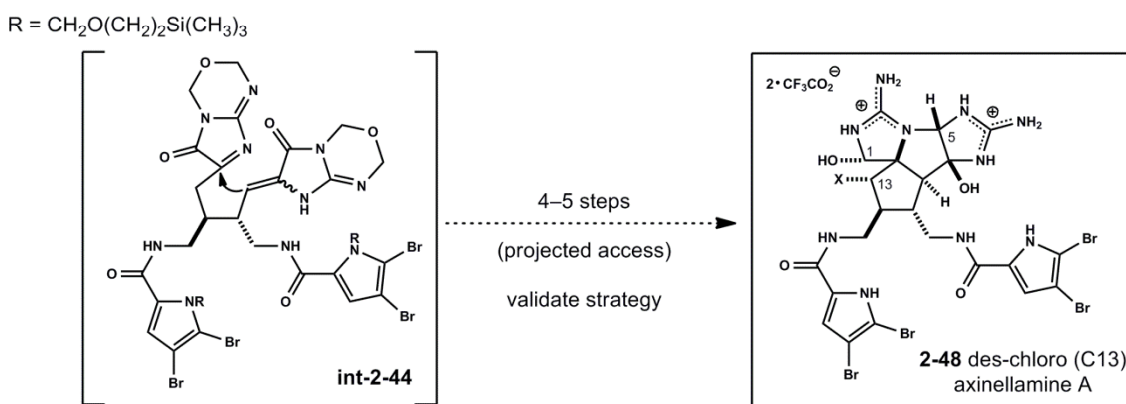
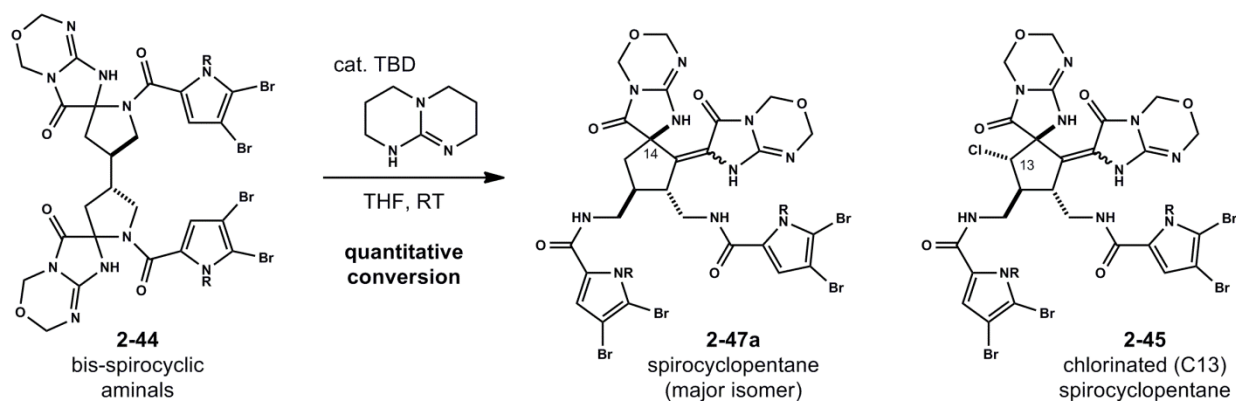


**Scheme 2.11.** Reactivity in the *meso* series (from **2-19b**) parallels observations in the C<sub>2</sub> series (see Scheme 2.10)

## 2.2.6 Equilibration of Dispacamide Dimers, Bis-spiroaminals.

Structural dynamics in this dimeric system are fascinating and can be channeled. Stirring **2-44a** or **2-44b** with 1,5,7-triazabicyclo[4.4.0]dec-5-ene (TBD) at RT, either individually or as a mixture, initiated isomerization to common monoalkylidene-containing spirocycles **2-47** (Scheme 2.12) (diagnostically fluorescent upon UV irradiation)<sup>[11a]</sup>. Initially, we hoped such equilibration conditions would provide the targeted ring-open form isomer bis-alkylidene **2-43**. We examined several basic conditions (*e.g.* TBD, 1,8-Diazabicyclo[5.4.0]undec-7-ene (DBU), tetramethyl guanidine (TMG)) for the spirocycloisomerization of bis-spiroaminals **2-44** to provide spirocycloalkylidenes **2-47** although bis-alkylidene **2-43** was never observed. However,

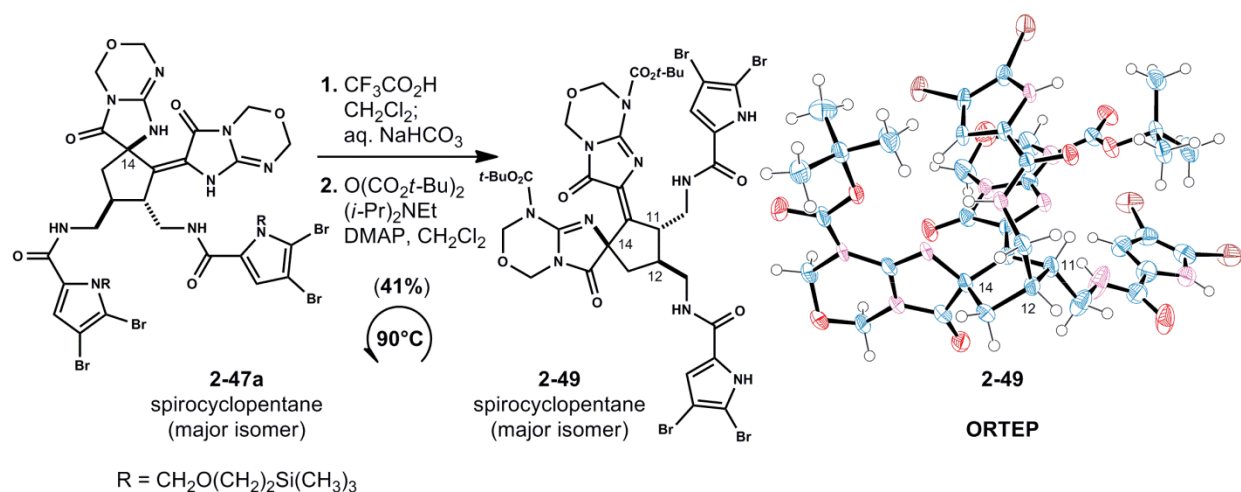
when mixtures of **2-44** are treated under basic conditions<sup>[45]</sup> with catalytic TMG in THF one can obtain moderate yields of isolated mono-alkylidene containing dimers (*vide infra*, Scheme 2.17).



**Scheme 2.12.** Spirocycloisomerization of bis-spirocyclic aminals **2-44** - projected access to des-chloro (C13) axinellamine A **2-48**.

Interestingly, desymmetrization of these dispacamide dimers proceeded without oxidative initiation via putative 5-*exo*-cyclization of **int-2-44** (Scheme 2.12). Catalytic TBD effectively induced spirocycloisomerization to provide major diastereomer **2-47a** alongside its *epi*-C14 isomer **2-47b** (not shown). Optimal conditions employed stoichiometric TBD (1 equiv) in THF at RT to afford moderate diastereoselectivity (d.r. ~2:1, **2-47a** (major olefin isomer): **2-47b** (major olefin isomer)). Reactions conducted in acetonitrile, DME, DMF were also effective, although side products were observed. We immediately recognized the potential to convert spirocycloalkylidene **2-47a** to des-chloro (C13) axinellamine A **2-48** to validate our overall strategy. We projected that des-chloro (C13) **2-48** could be prepared in 4 to 5 steps. Fortunately,

derivatization of spirocycloalkylidene **2-47a** following acid catalyzed degradation of trimethylsilylethoxymethyl units (Scheme 2.13) and treatment with di-*tert*-butyl dicarbonate provided major isomer spirocyclopentane **2-49**. X-ray crystallographic analysis of product **2-49** showed it to possess the desired relative C14 stereochemistry (CCDC 859078).<sup>[26]</sup>

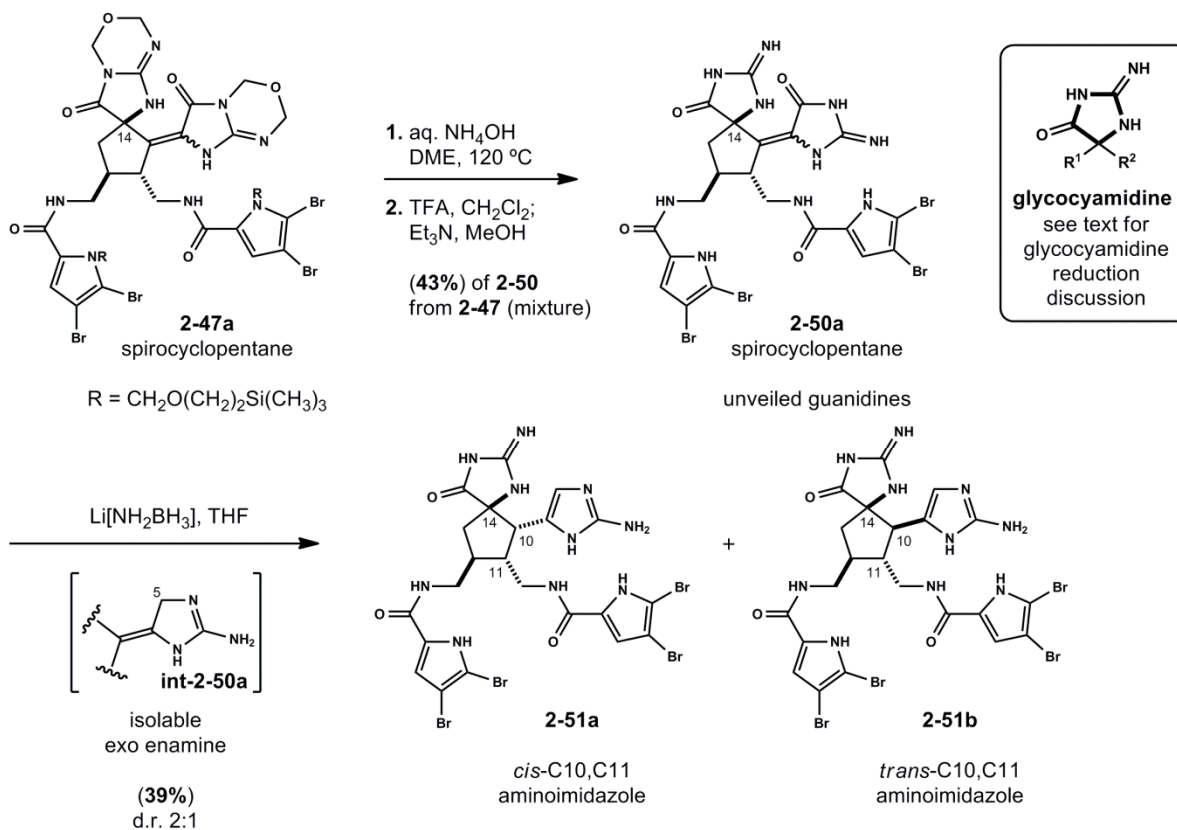


**Scheme 2.13.** Establishment of spirocyclopentane **2-47a** relative stereochemistry (C14 spiro).

## 2.2.7 Oxadiazine Ring Degradations and Glycoamidine Reductions.

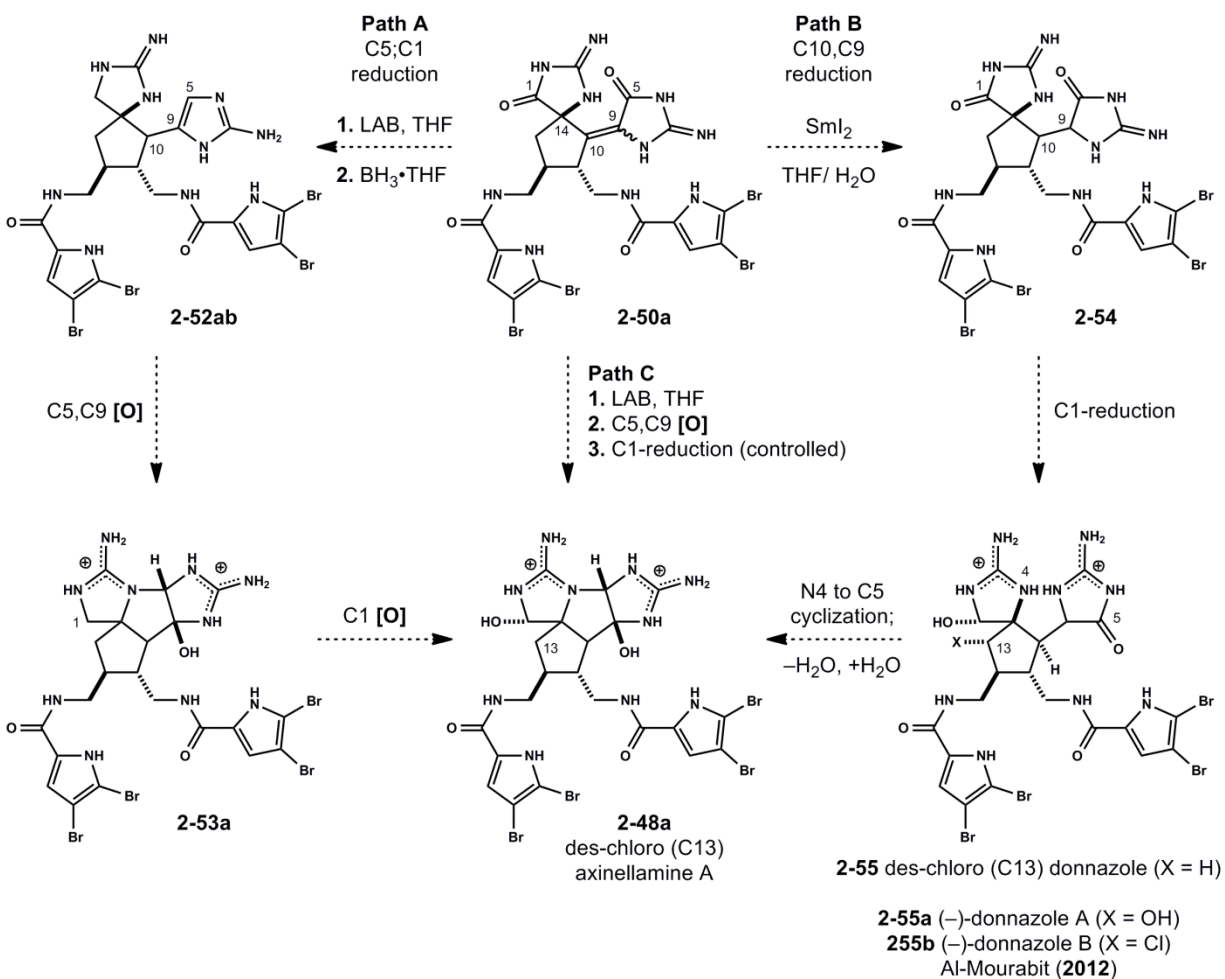
When a mixture of spirocycloalkylidenes (**2-47**) were treated with aqueous  $\text{NH}_4\text{OH}$ <sup>[46]</sup> followed by  $\text{CF}_3\text{CO}_2\text{H}$ ;  $\text{Et}_3\text{N}/\text{MeOH}$ <sup>[47]</sup>, we obtained fully unmasked spirocyclic bis-guanidines (**2-50**) as a favorable mixture of C14 epimers.<sup>[48]</sup> After extensive screening of reduction conditions (*vide infra*), it was found that warming a THF solution of **2-50** with Myers' lithium amidotrihydroborate (LAB)<sup>[49]</sup> chemoselectively reduced the C5 carbonyl. These conditions gradually deoxygenate C5 to give an intermediate having  $^1\text{H}$  NMR data consistent with an alkylidene aminoimidazoline (namely, **int-2-50a**).<sup>[50]</sup> This substance could be isolated (impure), but was typically not. Rather, the reaction was quenched and stirred with 10% aqueous  $\text{CF}_3\text{CO}_2\text{H}$

at 60°C for several hours. This sequestered residual boron away from reaction products while migrating the alkene to afford a separable mixture of aminoimidazoles **2-51**.



**Scheme 2.14.** Oxadiazine Ring Degradations and Chemoselective Glycocyamidine Reduction Provides Aminoimidazoles **2-51**.

## 2.2.8 Controlled, Chemoselective Reduction of Glycoyamidines.



**Scheme 2.15.** Access to des-chloro (C13) axinellamine A **2-48a**, chemoselective glycoyamidine reduction dictates alternative pathways.

Efficient preparation of glycoyamidines **2-50** allowed us to consider several possible routes to access des-chloro (C13) axinellamine A **2-48a** (Scheme 2.15). It should be noted that prior to developing heterocycle degradation conditions (**2-50**, aqueous NH<sub>4</sub>OH, DME, Scheme 2.14) we envisioned similar strategies to convert masked bis-guanidines (such as **2-47a**) to corresponding masked des-chloro (C13) axinellamine A. These routes were ultimately unsuccessful.

In the glycoyamidine series (**2-50**), we considered several pathways. These proposed pathways were dependent on our ability to effect chemoselective reductions on highly polar intermediates (Scheme 2.15). We reasoned that sequential 4e<sup>-</sup> glycoyamidine reduction (Path A,

*e.g.* LAB; BH<sub>3</sub>·THF) could provide spirocyclic guanidine intermediates (**2-52**). With access to **2-52** we could examine C5,C9 oxidation under aqueous conditions to provide didehydro (C1) des-chloro (C13) axinellamine A **2-53a** requiring subsequent 2e<sup>-</sup> oxidation (C1) to obtain target **2-48a**.<sup>[7a]</sup> Pathway A appeared feasible although the strategy is indirect and deviates from our original goal of accessing target natural products via controlled reduction of C1 and C5 glycoyamidine functionality.

We simultaneously considered Path B which relied on a controlled C10,C9 reduction to access glycoyamidines **2-54**. Interestingly, the use of aqueous SmI<sub>2</sub> chemoselectively provided reduced variants **2-54** in moderate yield. Although these conditions suggest intriguing reactivity in the series, reduction of the C10,C9 olefin provided a mixture of several diastereomers (**2-54**). The route was not further pursued, though one can envision a controlled (2e<sup>-</sup>) C1 reduction to access des-chloro (C13) donnazole **2-55** analogous to the donnazoles (**2-55ab**) recently isolated by Al-Mourabit and co-workers.<sup>[51]</sup> Interestingly, donnazole B (**2-55b**, X = Cl) is an isomer of axinellamine A **2-5a** which could arise from a net N4 to C5 cyclization with re-hydration.

Ultimately, Path C prevailed due to the discovery of successful LAB reduction conditions. From desired aminoimidazole **2-51b** (Scheme 2.14), we proposed access to **2-48a** following C5,C9 oxidation and controlled (2e<sup>-</sup>) C1 glycoyamidine reduction. With regard to the developed lithium amidotrihydroborate (LAB) reduction<sup>[49]</sup>, many other glycoyamidine (**2-50**) reduction conditions were explored. There is a paucity of literature pertaining to the controlled reduction of free glycoyamidines.<sup>[13]</sup> It is of note that strategies developed independently by the Armstrong<sup>[52]</sup>, Overman<sup>[53]</sup> and Romo<sup>[54]</sup> labs address this issue albeit effective in derivatized systems. Certainly, one can also seek insight by drawing analogy to the early literature of hydantoin reduction methods.<sup>[55]</sup> We were initially influenced by the pioneering work of

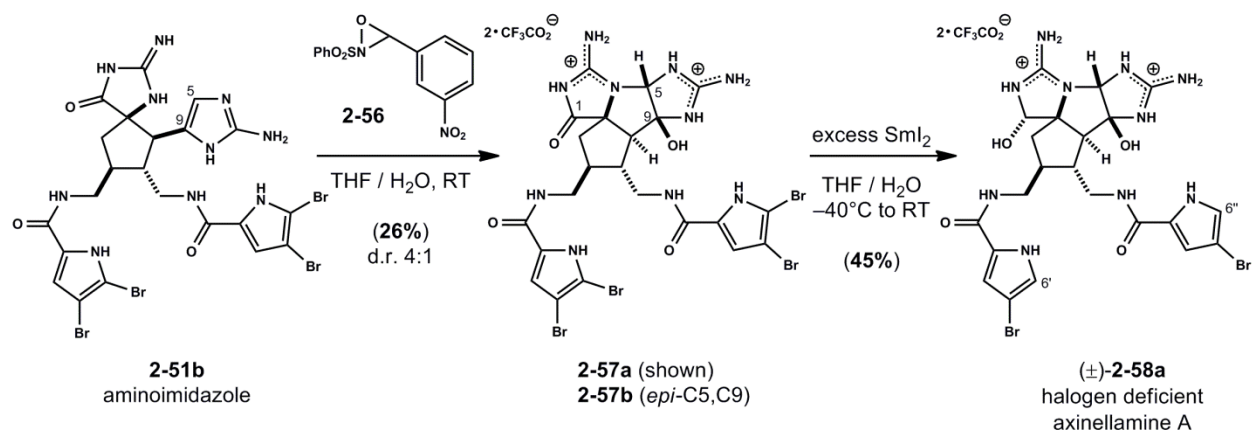


Speckamp and co-workers which demonstrates the ability to effect selective mono reduction of cyclic imides (*e.g.* glutarimide) with NaBH<sub>4</sub>, HCl in alcoholic solvents.<sup>[56]</sup> The study suggests a predominate resonance contributor present in cyclic imides can serve to explain control in their mono-reduction. An analogous resonance-based argument can be made for glycoamidines **2-50**.<sup>[20]</sup>

Initially, we examined reductive conditions using a purified mixture of spirocyclic alkylidenes **2-50** as their bis-trifluoroacetate salt forms. We sought reduction methods compatible with the highly-polar functionality of glycoamidines **2-50**. With regard to solubility, aqueous or alcoholic solvents were attractive, but limited the range of compatible reductants (*e.g.* LiAlH<sub>4</sub>).<sup>[55]</sup> Glycoamidines **2-50** in their salt forms (bis-trifluoroacetates, 2-CF<sub>3</sub>CO<sub>2</sub>H) were sparingly soluble in ethereal solvents (*e.g.* THF, DME). Various reductive methods including Et<sub>3</sub>SiH, H<sub>2</sub>SO<sub>4</sub>, CH<sub>3</sub>CN<sup>[57]</sup> / PhSiH<sub>3</sub>, H<sub>2</sub>SO<sub>4</sub><sup>[57]</sup> / Cp<sub>2</sub>TiF<sub>2</sub>, PhSiH<sub>3</sub>, THF or toluene<sup>[58]</sup> / ZnCl<sub>2</sub>, NaBH<sub>4</sub>, THF<sup>[59]</sup> / NaBH<sub>4</sub>, CF<sub>3</sub>CO<sub>2</sub>H, RT / NaBH<sub>4</sub>, pyridine (as solvent), 120°C<sup>[60]</sup> / Schwartz reagent, Cp<sub>2</sub>Zr(H)Cl, THF, RT to 50°C<sup>[61]</sup> / BH<sub>3</sub>·NH<sub>2</sub>*t*-Bu, THF, RT to 60°C<sup>[62]</sup> / Tf<sub>2</sub>O, CH<sub>2</sub>Cl<sub>2</sub>; NaBH<sub>4</sub>, THF, CH<sub>2</sub>Cl<sub>2</sub><sup>[60]</sup> / LiHBEt<sub>3</sub>, THF, -78°C to RT (see Scheme 2.3) and others provided complex reaction mixtures. Admittedly, monitoring the reduction of a diastereomeric mixture was non-ideal. Under the listed conditions (*vide supra*), we primarily observed 2e<sup>-</sup> reduction products (LC/MS analysis) with various concomitant reductive dehalogenation events. Brief attempts to effect Fukuyama-type reductions via intermediate formation of ethyl thioester adducts with NaSEt, DMF, 60°C or KSPH, DMF, RT followed by hydrogenolysis with Pd/C, Et<sub>3</sub>SiH were not productive and resulted in complex mixtures.<sup>[64]</sup> The use of aqueous hydrazine followed by oxidation of the anticipated acyl hydrazide (from glycoamidine opening) with IBX to effect a net McFayden–Stevens reduction under modified

conditions was not fruitful.<sup>[65]</sup> Attempts to temporarily mask guanidine polarity by global silylation with N,O-bis(trimethylsilyl)acetamide (BSA) followed by reduction with excess lithium triethylborohydride in THF ( $-78^{\circ}\text{C}$  to RT) were equally unsuccessful.<sup>[66]</sup> Interestingly, the use of aqueous  $\text{SmI}_2$  in THF was found to selectively reduce the *exo*-cyclic alkylidene to provide **2-54** as a mixture of currently unassigned diastereomers. These conditions, monitored carefully by LC/MS, provided insight for the discovery that aqueous  $\text{SmI}_2$  could effect a  $2e^-$  reduction of the spirocyclic glycoamidinium without overreduction (*vide infra*).<sup>[67]</sup> Ultimately, for the desired reductive transformation,  $\text{BH}_3\cdot\text{THF}$ , aminoborane (*e.g.* LAB) type reductions (in THF), and  $\text{SmI}_2$  (in THF/ $\text{H}_2\text{O}$ ) prevailed as promising reagents for the reduction of free glycoamidines.

### 2.2.9 Synthesis of Halogen Deficient ( $\pm$ )-Axinellamine A (2-58).

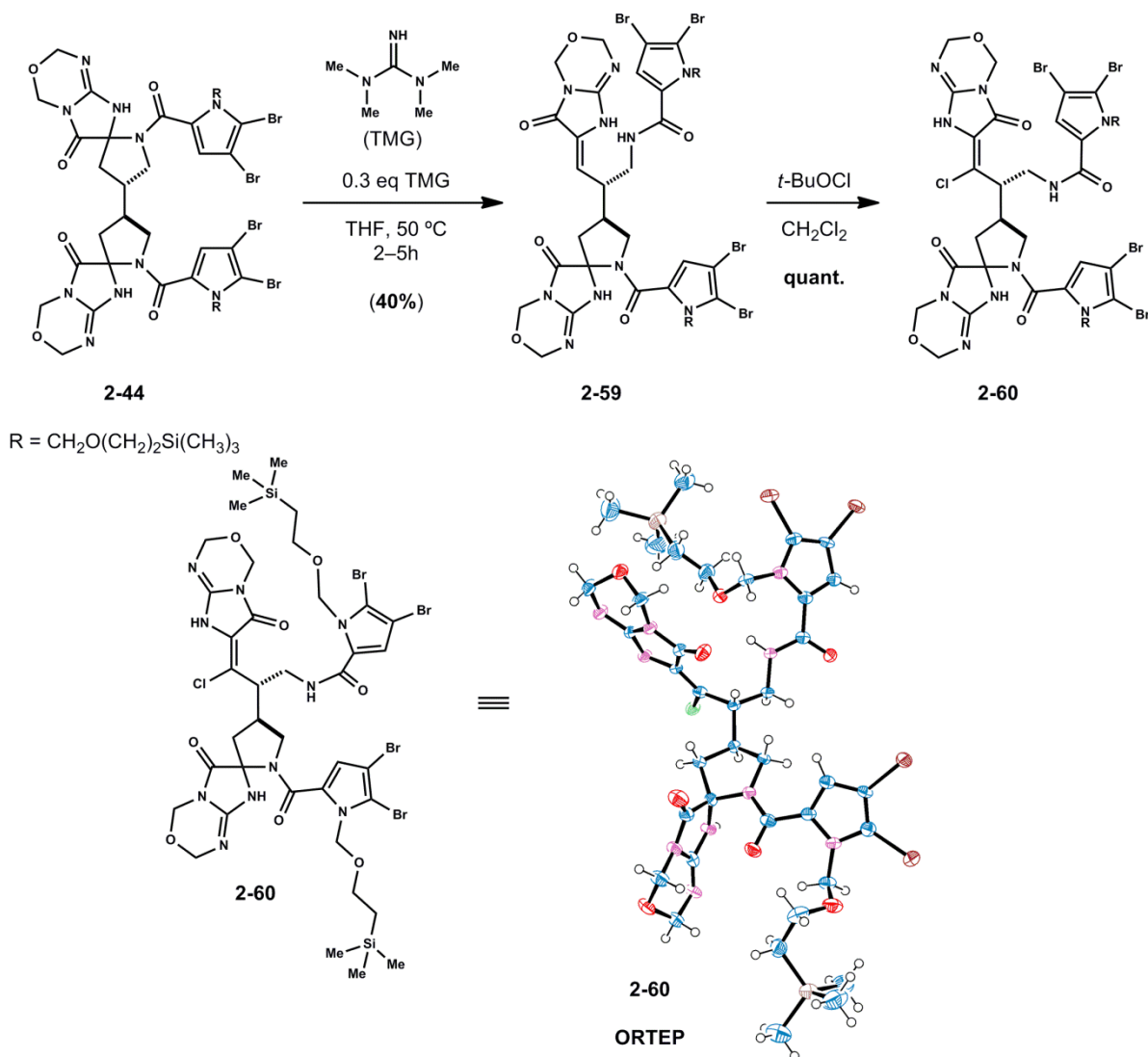


**Scheme 2.16** Access to fully synthetic, partially halogenated ( $\pm$ )-axinellamine A **2-58a** from aminoimidazole **2-51b**

With aminoimidazole **2-51b** in hand, advancement to the axinellamine ring system occurred in two carefully orchestrated steps. The bis-trifluoroacetate salt of C10,C11 anti diastereomer **2-51b**<sup>[68]</sup> was isolated by preparative HPLC and oxidized with 3-(3-nitrophenyl)-2-(phenylsulfonyl) oxaziridine **2-56** (Scheme 2.16) in aqueous THF.<sup>[69,70]</sup> This initiated a net

aminohydroxylation of the imidazole to provide a C9 angularly hydroxylated C5 aminal **2-57a** and its *epi*-C5,C9 diastereomer (confer **2-5a** vs **2-5b**) in roughly a 4:1 ratio following preparative HPLC purification on a fluorinated stationary phase. Attempts at similarly 'biomimetic' oxidations of related substrates reduced at C1 were reported unsuccessful.<sup>[7a]</sup> Here, the oxidation proceeded smoothly under aqueous conditions although low isolated yields reflect the difficulty in purifying individual diastereomers by HPLC. The major isomer **2-57a** was exposed to an excess of aqueous SmI<sub>2</sub>. This effected rapid and selectively debromination at C6' and C6'' with slow C1 carbonyl reduction to the corresponding hemiaminal **2-58a**.<sup>[71]</sup> Product **2-58a**<sup>[72]</sup> uniquely combines a non-chlorinated (C13) axinellamine A core structure with the monobrominated pyrrole units common to sceptrins<sup>[73]</sup> (not shown) and agelifेरins<sup>[74]</sup> (not shown).

## 2.2.10 Additional Reactivity of Bis-spirocycles 2-44: Access to Chlorinated Intermediates.



**Scheme 2.17.** Unique equilibrium of bis-spirocyclic aminals **2-44** - access to chlorinated intermediates.

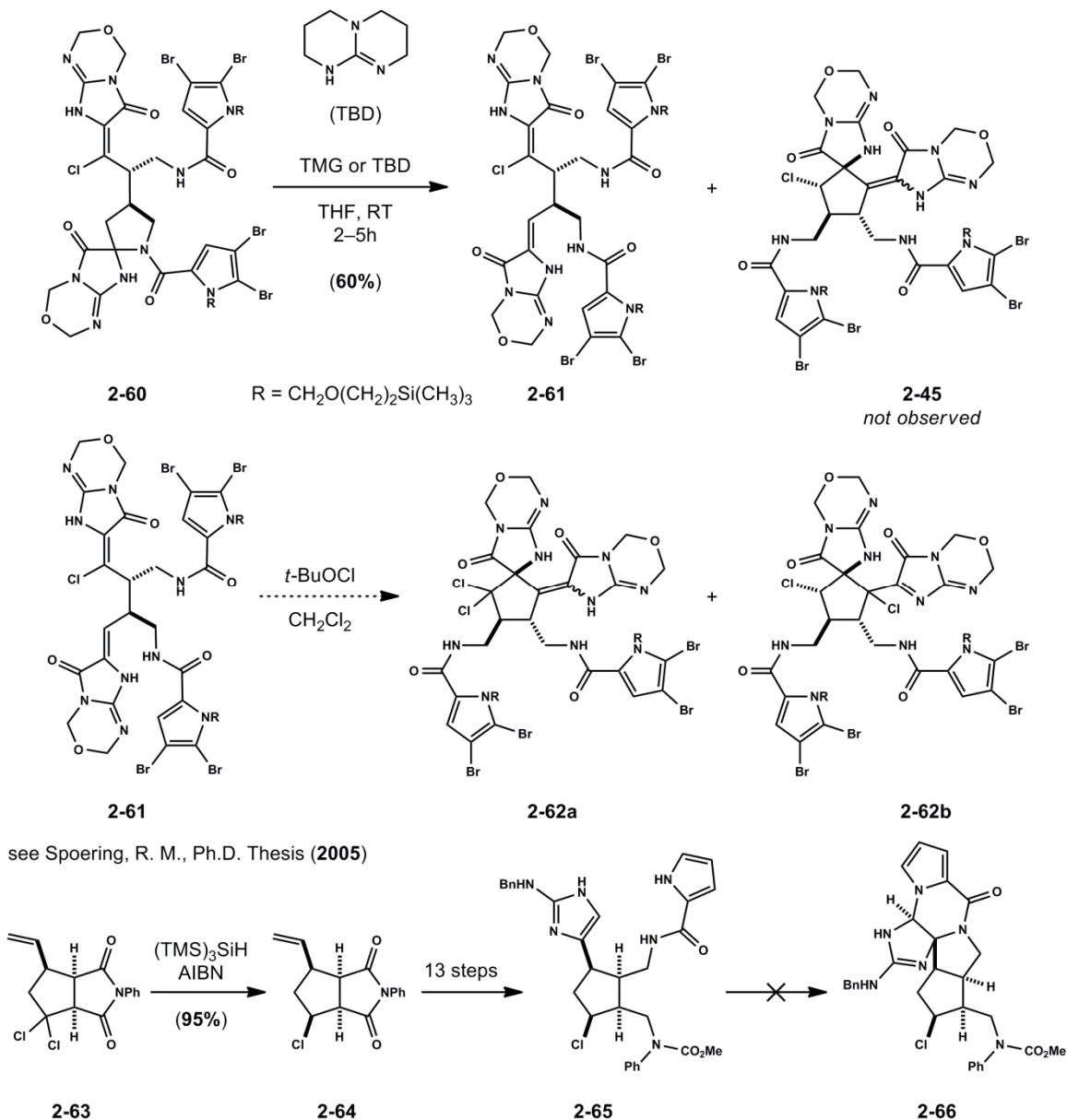
Having established access to des-chloro (C13) spirocycloalkylidenes (**2-47**, Scheme 2.12) we became intrigued to further understand the equilibrium of the bis-spirocyclic diisacamide dimers (**2-44**). Although bis-alkylidenes **2-43** in this series were not observed, we noticed the development of minor, transient intermediates that proceed to spirocycloalkylidenes (**2-47**) when bis-spirocycles **2-44** are treated with catalytic TBD in THF or  $\text{CH}_3\text{CN}$  at RT. A reasonable mechanism for this transformation involves base induced spirocycloisomerization of bis-spirocycles **2-44** via stepwise aminal ring opening with subsequent 5-*exo*-trig enamine-imine

cyclization (Scheme 2.14, **int-2-44**). If one could control amination ring opening, with subsequent tautomerization on both amination spirocycles, a bis-alkylidene **2-43** could be obtained. Ultimately, we discovered that catalytic spiroamination opening with slightly less basic guanidines, such as tetramethyl guanidine (TMG) effected transformation to intermediate mono-alkylidene containing dimers (**2-59**).<sup>[45]</sup> This feat was certainly credited to stoichiometry control as mono-alkylidenes (**2-59**) were proven intermediates en route to spirocycloalkylidenes **2-47**. Under controlled conditions, treatment of purified **2-44b** with 0.3 equivalents of TMG in warm CH<sub>3</sub>CN provided a single mono-alkylidene diastereomer **2-59** (unassigned *E/Z* stereochemistry). As anticipated, treatment of isolated **2-59** with *tert*-butyl hypochlorite proceeded with quantitative conversion to a mixture of chlorinated isomers. Analysis (<sup>1</sup>H NMR, 600 MHz, acetic acid-*d*<sub>4</sub>) of crude chlorination mixtures suggest primary oxidation occurs at the enamine moiety to provide an iminium ion intermediate. The resultant  $\alpha$ -chloro iminium may diverge to multiple isomeric products as suggested by <sup>1</sup>H NMR analysis of crude reaction mixtures. Fortunately, an X-ray quality crystal for the major component of crude reaction mixtures was obtained and determined to be vinyl chloride **2-60** (CCDC 942603, solvents removed for clarity).<sup>[26]</sup> Apparently, the putative  $\alpha$ -chloro iminium underwent tautomerization to vinyl chloride **2-60**. The exact nature of this tautomerization event requires further attention.

Rather than determine the structure and reactivity all chlorinated isomers obtained in oxidations with isolated **2-59** (from **2-44b**, TMG, THF) or mixtures of **2-59** (from mixtures of **2-44**, TMG, THF) we sought equilibration conditions for their uniform conversion to a presumably stable chlorinated (C13) spirocycloalkylidene (**2-45**, Scheme 2.18). Interestingly, when crude chlorinated isomers (*e.g.* **2-60**) were treated with stoichiometric TBD or TMG, anticipated product **2-45** was not observed. In monitoring reaction mixtures (LC/MS, UV detection 254-nm,

MS analysis - LRMS-ESI ( $m/z$ ) calcd for  $[C_{38}H_{51}Br_4ClN_{10}O_8Si_2+H]^+$ : 1187.0 ; found: 1186.9) it became apparent that all chlorinated isomers (e.g. **2-60**) converge to a single isomer (LRMS-ESI ( $m/z$ ) calcd for  $[C_{38}H_{51}Br_4ClN_{10}O_8Si_2+H]^+$ : 1187.0 ; found: 1186.9) tentatively characterized chlorinated bis-alkylidene **2-61** ( $^1H$  NMR, 600 MHz,  $CH_3CN-d_3$ , (ppm) 5.50,  $J = 9.9$  Hz, 1H).<sup>[76]</sup>

*Experimentation in this realm requires further attention.*



**Scheme 2.18.** Access to chlorinated 'bis-alkylidene' **2-61** - potential access to chlorinated spirocyclopentane **2-45**.

Preliminary studies suggest tentatively assigned chlorinated bis-alkylidene **2-61** is stable to treatment in acetic acid at RT and is non-reactive when resubjected to initial equilibration conditions (TBD or TMG, THF). Heating isolated **2-61** (40-60°C, THF) proceeds with apparent loss of HCl (LC/MS, MS analysis) presumably via an elimination mechanism, although these and related experiments should be revisited. Lastly, we proposed that chloro bis-alkylidene **2-61** may undergo further oxidation with a second exposure to *tert*-butyl hypochlorite.

These intriguing experiments would provide chemical reactivity information to support the tentative assignment of chloro ‘bis-alkylidene’ **2-61**. It was envisioned that treatment of **2-61** with *tert*-butyl hypochlorite could provide dichlorinated isomers **2-62a** or **2-62b**. A preliminary oxidation experiment suggests that **2-61** can indeed be chlorinated to afford several uncharacterized dichlorinated and trichlorinated isomers (LC/MS, MS analysis). Unfortunately, low material supply at the time of investigation prohibited further examination of this route. Provided access to desired dichloro **2-62a**, one could envision conditions that parallel the work of Spoering for the reduction of dichloro cycloadduct **2-63** to **2-64** with tris(trimethylsilyl)silane and azobisisobutyronitrile (AIBN).<sup>[77]</sup> Admittedly, general interest in **2-61** or related chlorinated isomers (**2-60**) derived from bis-spirocycles **2-44** (2 steps) was diminished. Although fascinating, we had strayed (several transformations) from the original tenets of our ‘bis-alkylidene’ hypothesis. *Managing equilibria of related isomers at each step is an apparent challenge that requires attention.*

### 2.3 Conclusion

The total synthesis of non-chlorinated ( $\pm$ )-axinellamine A congener **2-58a** occurs in 13 operations. The route is concise and features a host of unusual and unexpected reactions. The use of formaldehyde/thiourea composite heterocycle **2-10** as both a guanidine precursor and reactivity mask is new, and represents a novel strategy. The work also saw the use of LAB and  $\text{SmI}_2$  for controlled glycoamidine reductions. Notably, final oxidation state at both C1 and C5 in **2-58a** is derived from reductive events, rather than oxidation.<sup>[4]</sup> The structural plasticity of dimers **2-58a**, including the ease and fidelity with which they isomerize, holds considerable promise. As we learn to further manipulate these complex spiroaminals, there is potential to synthesize numerous additional members of this alkaloid family. Preliminary experiments suggest mono-alkylidenes may provide access to desired chlorinated (C13) spirocyclopentanes **2-45** en route to ( $\pm$ )-axinellamines **2-5**.



## 2.4 References and Notes

[1] Recent reviews: (a) Forte, B.; Malgesini, B.; Piutti, C.; Quartieri, F.; Scolaro, A.; Papeo, G. *Mar. Drugs* **2009**, *7*, 705; (b) Al-Mourabit, A.; Zancanella, A.; Tilvi, S.; Romo, D. *Nat. Prod. Rep.* **2011**, *28*, 1229; (c) J. Wang, Y. Zhan, B. Jiang, *Progress in Chemistry* **2011**, *23*, 2065.

[2] (a) Hoffmann, H.; Lindel, T. *Synthesis* **2003**, 1753; (b) Appenzeller, J.; Al-Mourabit, A. in *Biomimetic Organic Synthesis*, 1<sup>st</sup> Ed. (Eds: Poupon, E.; Nay, B.), WILEY-VCH, Weinheim, **2011**, 225.

[3] Axinellamines isolation: Urban, S.; de Almeida Leone, P.; Carroll, A. R.; Fechner, G. A.; Smith, J.; Hooper, J. N. A.; Quinn, R. J. *J. Org. Chem.* **1999**, *64*, 731.

[4] Massadines isolation: Nishimura, S.; Matsunaga, S.; Shibazaki, M.; Suzuki, K.; Furihata, K.; van Soest, R. W.; Fusetani, N. *Org. Lett.* **2003**, *5*, 2255.

[5] Palau'amine isolation: (a) Kinnel, R. B.; Gehrken, H-P.; Scheuer, P. J. *J. Am. Chem. Soc.* **1993**, *115*, 3376; (b) Kinnel, R. B., Gehrken H-P.; Swali, R.; Skoropowski, G.; Scheuer, P. J. *J. Org. Chem.* **1998**, *63*, 3281; For the reassignment of palau'amine: (c) Kobayashi, H.; Kitamura, K.; Nagai, K.; Nakao, Y.; Fusetani, N.; van Soest, R. W. M.; Matsunaga, S. *Tetrahedron Lett.* **2007**, *48*, 2127; (d) Buchanan, M. S.; Carroll, A. R.; Addepalli, R.; Avery V. M.; Hooper, J. N. A.; Quinn R. J. *J. Org. Chem.* **2007**, *72*, 2309; (e) Buchanan, M. S.; Carroll, A. R.; Quinn, R. J. *Tetrahedron Lett.* **2007**, *48*, 4573; (f) Grube, A.; Köck, M.; *Angew. Chem. Int. Ed.* **2007**, *46*, 2320.

[6] (a) Yamaguchi, J.; Seiple, I. B.; Young, I. S.; O'Malley, D. P.; Maue, M.; Baran, P. S. *Angew. Chem. Int. Ed.* **2008**, *47*, 3578; (b) O'Malley, D. P.; Yamaguchi, J.; Young, I. S.; Seiple, I. B.; Baran, P. S. *Angew. Chem. Int. Ed.* **2008**, *47*, 3581; (c) Su, S.; Seiple, I. B.; Young, I. S.; Baran, P. S. *J. Am. Chem. Soc.* **2008**, *130*, 16490; (d) Seiple, I. B.; Su, S.; Young, I. S.; Lewis, C. A.; Yamaguchi, J.; Baran, P. S. *Angew. Chem. Int. Ed.* **2010**, *122*, 1113;

[7] (a) Seiple, I. B.; Su, S.; Young, I. S.; Nakamura, A.; Yamaguchi, J.; Jørgensen, L.; Rodriguez, R. A.; O'Malley, D. P.; Gaich, T.; Köck, M.; Baran, P. S. *J. Am. Chem. Soc.* **2011**, *133*, 14710 and references cited therein; (b) Grube, A.; Köck, M. *Angew. Chem. Int. Ed.* **2007**, *46*, 2320.

[8] Su, S.; Rodriguez, R. A.; Baran, P. S. *J. Am. Chem. Soc.* **2011**, *133*, 13922.

[9] (a) Starr, J. T.; Koch, G.; Carreira, E. M. *J. Am. Chem. Soc.* **2000**, *122*, 8793; (b) Dilley, A. S.; Romo, D. *Org. Lett.* **2001**, *3*, 1535; (c) Tan, X.; Chen, C. *Angew. Chem. Int. Ed.* **2006**, *45*, 4345; (d) Lanman, B. A.; Overman, L. E. *Heterocycles* **2006**, *70*, 557; (e) Sivappa, R.; Hernandez, N. M.; He, Y.; Lovely, C. J. *Org. Lett.* **2007**, *9*, 3861; (f) Lovely, C. J.; Du, H.; Sivappa, R.; Bhandari, M. K.; He, Y.; Dias, H. V. R. *J. Org. Chem.* **2007**, *72*, 3741; (g) Bultman, M. S.; Ma, J.; Gin, D. Y. *Angew. Chem. Int. Ed.* **2008**, *47*, 6821; (h) Breder, A.; Chinigo, G. M.; Waltman, A. W.; Carreira, E. M. *Angew. Chem. Int. Ed.* **2008**, *47*, 8514; (i) Hudon, J.; Cernak, T. A.; Ashenhurst, J. A.; Gleason, J. L. *Angew. Chem. Int. Ed.* **2008**, *47*, 8885; (j) Zancanella, M.

A.; Romo, D. *Org. Lett.* **2008**, *10*, 3685; (k) Namba, K.; Kaihara, Y.; Yamamoto, H.; Imagawa, H.; Tanino, K.; Williams, R. M.; Nishizawa, M. *Chem. Eur. J.* **2009**, *15*, 6560; (l) Chinigo, G. M.; Breder, A.; Carreira, E. M. *Org. Lett.* **2011**, *13*, 78.

[10] Al-Mourabit, A. ; Potier, P. *Eur. J. Org. Chem.* **2001**, 237. For commentary on the origin of these proposals see Ref. 7a.

[11] (a) Garrido-Hernandez, H.; Nakadai, M.; Vimolratana, M.; Li, Q.; Doundoulakis, T.; Harran, P. G. *Angew. Chem. Int. Ed.* **2005**, *44*, 765; (b) Li, Q.; Hurley, P.; Ding, H.; Roberts, A. G.; Akella, R.; Harran, P. G. *J. Org. Chem.* **2009**, *74*, 5909; (c) Li, Q. Ph.D. Dissertation, the University of Texas Southwestern Medical Center, **2008**; (d) Ding, H.; Roberts, A. G.; Harran, P. G. *Angew. Chem. Int. Ed.* **2012**, *51*, 4416; (e) Ding, H.; Roberts, A. G.; Harran, P. G. *Chem. Sci.* **2013**, *4*, 303.

[12] For alternative strategies used to mask guanidine functionality of 2-aminoimidazoles: Sivappa, R.; Kumbam, V.; Dhawane, Golen, J. A.; Lovely, C. J.; Rheingold, A. L. *Org. Biomol. Chem.* **2013**, *11*, 4133 and references cited therein.

[13] The term **glycoyamidine** refers to heterocyclic structures of type **2-1** which are often described as a 2-imino analog of the commonly known hydantoin heterocycle. The systematic name for glycoyamidine is 2-imino-4-imidazolidinone. For a review of glycoyamidine chemistry: Lempert, C. *Chem. Rev.* **1959**, *59*, 667.

[14] To date we have not succeeded in the efficient degradation of benzodiazepine units in late intermediates to provide the corresponding free glycoyamidines.

[15] (a) For the corresponding azamethylene subunit ( $-\text{CH}_2\text{NR}-$ ) in tetrahydro-5-substituted-2(1)-s-triazones: Burke, Wm. J. *J. Am. Chem. Soc.* **1947**, *69*, 2136; (b) For the use of metallated triazones for imidazolone synthesis: Movassaghi, M.; Siegal, D.; Han, S. *Chem. Sci.* **2010**, *1*, 561; (c) For the synthesis of conformationally modified (cyclic hemiaminal ethers) peptides: Wu, X.; Park, P. K.; Danishefsky, S. J. *J. Am. Chem. Soc.* **2011**, *133*, 7700.

[16] Isothiourea **2-10** (m.p. 124–126°C, 2-propanol / hexanes (4:1)) is prepared directly from thiourea, formalin and methyl iodide using a modified protocol: Egginton, C. D.; Vale, C. P. *Text. Res. J.* **1969**, *39*, 140. See Appendix of this chapter.

[17] Decomplexation of  $\text{HgCl}_2$  from polar guanidines (such as **2-8**) requires washing with dilute aqueous sodium hydroxide or thiourea solutions. Low yields are attributed to poor recovery and degradation of **2-8**.

[18] For the preparation of *i*-PrCp<sub>2</sub>TiCl<sub>2</sub> (**2-18**) refer to: Giolando, D. M.; Rauchfuss, T. B.; Rheingold, A. L.; Wilson, S. R. *Organometallics* **1987**, *6*, 667.

[19] In a related series, we discovered Zn, HOAc, THF conditions during attempts to debrominate acyl pyrroles. Interestingly, this reduction can be controlled for olefin reduction in monomeric systems (such as **2-8**). Also, see Ref. 11b

[20] (a) Tautomeric preferences among glycoamidines: Kenyon, G. L.; Rowley, G. L. *J. Am. Chem. Soc.* **1971**, *93*, 5552; (b) <sup>13</sup>C NMR chemical shift differences in glycoamidines: Olofson, A.; Yakushijin, K.; Horne, D. A. *J. Org. Chem.* **1998**, *63*, 5787

[21] For examples of related spirocyclic amins in monomeric systems see: (a) Travert, N.; Al-Mourabit, A. *J. Am. Chem. Soc.* **2004**, *126*, 10252; (b) Jacquot, D. E. N.; Zollinger, M.; Lindel, T. *Angew. Chem. Int. Ed.* **2005**, *44*, 2295; (c) An iminophosphorane-based approach for the synthesis of spiropyrrolidine-imidazoles: Fresneda, P. M.; Casteñada, M.; Sanz, M. A.; Bautista, D.; Molina, P. *Tetrahedron* **2007**, *63*, 1849.

[22] Potassium hydride (KH) suspended in THF with added crown ether (18-C-6) was equally effective although the use of KHMDS is procedurally more convenient.

[23] Cushman, M.; Gerhardt, S.; Huber, R.; Fischer, M.; Kis, K.; Bacher, A. *J. Org. Chem.* **2002**, *67*, 5807 and see Ref. 11b.

[24] The reaction proceeds in benzene, CHCl<sub>3</sub> and CH<sub>3</sub>CN as well, although these solvents were not examined in detail.

[25] Stoichiometric HgCl<sub>2</sub> was required to achieve a related ring closure in previous series (Ref. 11bc)

[26] CCDC 942601 (Compound **2-8**), CCDC 859078 (Compound **2-49**), 859079 (Compound **2-39b**), 859080 (Compound **2-44b-1**), CCDC 942603 (Compound **2-60**) contain the supplementary crystallographic data for this chapter. These data can be obtained free of charge from The Cambridge Crystallographic Data Centre via [www.ccdc.cam.ac.uk/data\\_request/cif](http://www.ccdc.cam.ac.uk/data_request/cif). Crystallographic data obtained for compound **2-46b** is tabulated in Appendix One.

[27] (a) For 2-chloro- intermediates en route to 2-aminated benzoxazoles and benzothiazoles: Stewart, G. W.; Baxter, C. A.; Cleator, E.; Sheen, F. J. *J. Org. Chem.* **2009**, *74*, 3229; (b) For curious reactivity of (COCl)<sub>2</sub> in related systems: Lee, V. J.; Woodward, R. B. *J. Org. Chem.* **1979**, *44*, 2487.

[28] We are not aware of the ring systems in **2-30** and **2-26** being reported previously.

[29] Numerous conditions were examined for the trimethylsilylethoxymethylation of **2-26**. (See Appendix of this chapter).

[30] These couplings were conducted with **2-10**, TBTU, *i*-Pr<sub>2</sub>NEt, CH<sub>3</sub>CN, RT conditions that have since been optimized. (low yield is attributed to the degradation of **2-10** under these conditions)

[31] For selected comprehensive articles on the oxidative coupling of enolates: (a) Demartino, M. P.; Chen, K.; Baran, P. S. *J. Am. Chem. Soc.* **2008**, *130*, 11546; (b) Guo, F.; Clift, M. D.; Thomson, R. J. *Eur. J. Org. Chem.* **2012**, *26*, 4881; (c) For a recent example in the total synthesis

of actinophyllic acid: Martin, C. L.; Overman, L. E.; Rohde, J. A. *J. Am. Chem. Soc.* **2010**, *132*, 4894; (d) Oxidative enolate dimerization in the synthesis of lomaiviticin aglycon: Lee, H. G.; Ahn, J. Y.; Lee, A. S.; Shair, M. D. *Chem. Eur. J.* **2010**, *16*, 13058.

[32] Ito, Y.; Konoike, T.; Harada, T.; Saegusa, Y. *J. Am. Chem. Soc.* **1977**, *99*, 1487.

[33] Silver ion oxidative coupling of dien- and trienolates: Aurell, M. J.; Gil, S.; Tortajada, A.; Mestres, R.; García-Raso, A. *Tetrahedron Lett.* **1988**, *29*, 6181.

[34] Paquette, L. A.; Bzowej, E. I.; Branan, B. M.; Stanton, K. J. *J. Org. Chem.* **1995**, *60*, 7277.

[35] (a) Schmittel, M.; Söllner, R. *Chem. Ber.* **1997**, 771; (b) Schmittel, M.; Burghart, A.; Malisch, W.; Reising, J.; Söllner, R. *J. Org. Chem.* **1998**, *63*, 396.

[36] While not examined in detail, preliminary experiments suggest monomer **2-26** can be dimerized oxidatively under similar conditions although the solubility of **2-26** in THF at  $-78^{\circ}\text{C}$  is procedurally limiting.

[37] Several control experiments including the exposure of monomer **2-31** or dimers **2-38** to  $\text{Cu}(\text{OTf})_2$  in THF or titanocene **2-18** in THF did not effect heterocycle degradation. In addition, when **2-31** is deprotonated (KHMDS, THF,  $-78^{\circ}\text{C}$ , 30 min) and quenched with EDTA buffer (pH = 8.5) deconjugated **2-40** (86% yield) is obtained with good recovery suggesting the heterocycle in **2-31** is stable to strongly basic conditions. It is possible that partial heterocycle degradation occurs on  $\text{SiO}_2$  during the purification of crude reaction mixtures.

[38] Of many oxidants examined, only the Livinghouse reagent  $[(\text{CF}_3\text{CH}_2\text{O})\text{V}(\text{O})\text{Cl}_2]$  provides **2-38** in yield and regioselectivity comparable to  $\text{Cu}(\text{OTf})_2$ : Ryter, K.; Livinghouse, T. *J. Am. Chem. Soc.* **1998**, *120*, 2658.

[39] The addition of 1.6 equiv.  $\text{Cu}(\text{OTf})_2$  in THF is typically transferred via 14 gauge syringe as it quickly forms a gelatinous slurry. Reactions scaled above 12 mmol of **2-31** require multiple transfers of 1.6 equiv  $\text{Cu}(\text{OTf})_2$  in THF.

[40] Lower yields observed when the reaction is scaled above 12 mmol are attributed to stirring difficulties and error during transfer of oxidant solutions (e.g.  $\text{Cu}(\text{OTf})_2$  in THF). See Ref. 39.

[41] (a) Osborn, J. A.; Jardine, F. H.; Young, J. F.; Wilkinson, G. *J. Chem. Soc. A.* **1966**, 1711; (b) High catalyst loadings were required for complete hydrogenation. Wilkinson's catalyst was freshly prepared prior to use according to Crane, S. N.; Bateman, K. Gagne, S.; Levesque, J.-F. *J. Label. Compd. Radiopharm.* **2006**, *49*, 1273; (c) For a thorough evaluation of Wilkinson catalyst quality, see: Evans, D. A.; Fu, G. C.; Anderson, B. A. *J. Am. Chem. Soc.* **1992**, *114*, 6679.

[42] Typical yields for **2-42a** ranged from (45–57%). Lower yields are due to incomplete bromination, in which case tribrominated **2-42b** (not shown) was isolated as a minor product. **2-**

**42b** can be resubjected to NBS bromination conditions although this process has not been optimized.

[43] Under identical reaction and work-up conditions, treatment of **2-21** with KHMDS affords mono-alkylidene **2-24a** (Scheme 2.3). It is not yet clear why corresponding dimers **2-44** exist in spiroaminal forms.

[44] Evans, D. A.; Borg, G.; Scheidt, K. A. *Angew. Chem. Int. Ed.* **2002**, *41*, 3188.

[45] Basicity of substituted 2-phenyl-1,1,3,3,-tetramethylguanidines and other bases in acetonitrile solvent: Leffek, K. T.; Pruszyński, P.; Thanapaalasingham, K. *Can. J. Chem.* **1989**, *67*, 590.

[46] Initially we observed isomers **12** would convert to **21** upon prolonged heating in DMF (110°C). We speculated that trace Me<sub>2</sub>NH was responsible for the oxadiazine degradation observed. Aqueous NH<sub>4</sub>OH was subsequently found to promote full deprotection. This contrasts acidic hydrolyses in these systems which afford largely hydantoin products.

[47] (a) Transformation of methoxyethoxymethyl (MEM) or methoxymethyl (MOM) groups: Corey, E. J.; Hua, D. H.; Seitz, S. P. *Tetrahedron Lett.* **1984**, *25*, 3; (b) Hydrolysis (1,3-propanedithiol, 2% HCl in CF<sub>3</sub>CH<sub>2</sub>OH) of a cyclic oxymethylene hemiaminal in the synthesis of lactacystin: Corey, E. J.; Reichard, G. A. *Tetrahedron Lett.* **1993**, *34*, 6973; (c) Deprotection of methoxymethyl (MOM) ethers with catechol boron bromide and acetic acid: Yu, C.; Liu, B.; Hu, L. *Tetrahedron Lett.* **2000**, *41*, 819.

[48] Treatment of amins **2-44** with TBD provides two spirocyclic products (**2-47a**, **2-47b**). We have discussed mechanistic possibilities for related transformations previously (Ref. 11ab). When the major isomer (**2-47a**) is exposed to CF<sub>3</sub>CO<sub>2</sub>H followed by aqueous base work-up and the resultant material acylated with O(CO<sub>2</sub>*t*-Bu)<sub>2</sub>, X-ray crystallographic analysis (Ref. 26) shows the product to be **2-49**. Fully deprotecting **2-47a** in the manner shown in Scheme 2.14, affords two geometric isomers of **2-50a**, but no **2-50b**. Both isomers of **2-50a** convert to products **2-51** upon LAB reduction. Consistent with their stereochemical assignments, **2-47b** (*epi*-C14, not shown) is likewise converted to two isomers of **2-50b** (not shown), neither of which give **2-51a** or **2-51b** after LAB reduction.

[49] Lithium amidotrihydroborate (LAB) reagent: Myers, A. G.; Yang, B. H.; Kopecky, D. J. *Tetrahedron Lett.* **1996**, *37*, 3623.

[50] Diastereotopic C5 methylene protons in **int-2-50a** appear as a signature spectral pattern: (**int-2-50a**, 2·CF<sub>3</sub>CO<sub>2</sub>H salt) <sup>1</sup>H NMR (600 MHz, MeOH-*d*<sub>4</sub>) δ (ppm) 4.40, 4.12 (ppm) (AB, *J*<sub>AB</sub> = 16.2 Hz, 2H).

[51] Donnazoles A and B, isolation: Muñoz, J.; Moriou, C.; Gallard, J.-F.; Marie, P. D.; Al-Mourabit, A. *Tetrahedron Lett.* **2012**, *53*, 5828.

[52] McAlpine, I. J.; Armstrong, R. W. *J. Org. Chem.* **1996**, *61*, 5674.

- [53] Lanman, B. A.; Overman, L. E. *Heterocycles* **2006**, *70*, 557.
- [54] Tang, L.; Romo, D. *Heterocycles* **2007**, *74*, 999.
- [55] For selected reduction conditions of hydantoins: (a) LiAlH<sub>4</sub> reduction of hydantoins: Marshall, F. J. *J. Am. Chem. Soc.* **1956**, *78*, 3696; (b) N-substituted hydantoin reduction with LiAlH<sub>4</sub>: Cortes, S.; Kohn, H. *J. Org. Chem.* **1983**, *48*, 2246; (c) de la Cuesta, E.; Ballesteros, F.; Trigo, G. G. *Heterocycles* **1981**, *16*, 1647; (d) LiAlH<sub>4</sub> reduction of acyl guanidines (including glycoyamidines): Stearns, J. F.; Rapoport, H. *J. Org. Chem.* **1977**, *42*, 3608.
- [56] NaBH<sub>4</sub> reduction of cyclic imides: Hubert, J. C.; Wijnberg, J. B. P. A.; Speckamp, W. N. *Tetrahedron* **1975**, *31*, 1437.
- [57] Silane reductions in acidic media: Doyle, M. P.; DeBruyn, D. J.; Donnelly, S. J.; Kooistra, D. A.; Odubela, A. A.; West, C. T.; Zonnebelt, S. M. *J. Org. Chem.* **1974**, *39*, 2740.
- [58] (a) Preparation of Cp<sub>2</sub>TiF<sub>2</sub>: Druce, P. M.; Kingston, B. M.; Lappert, M. F.; Spalding, T. R.; Srivastava, R. C. *J. Chem. Soc. A* **1969**, 2106; (b) Titanocene-catalyzed reduction of lactones to lactols: Verdaguer, X.; Hansen, M. C.; Berk, S. C.; Buchwald, S. L. *J. Org. Chem.* **1997**, *62*, 8522; (c) Ti(Oi-Pr)<sub>4</sub>, Ph<sub>2</sub>SiH<sub>2</sub>, amide reductions: Bower, S.; Kreutzer, K. A.; Buchwald, S. L. *Angew. Chem. Int. Ed.* **1996**, *35*, 1515; (d) Titanocene-catalyzed tertiary amine reduction with PhMeSiH<sub>2</sub>: Selvakumar, K.; Rangareddy, K.; Harrod, J. F. *Can. J. Chem.* **2004**, *82*, 1244.
- [59] (a) Brown, H. C.; Rao, B. C. S. *J. Am. Chem. Soc.* **1956**, *78*, 2582; (b) Zn(OAc)<sub>2</sub>, silane reduction of amides: Das, S.; Addis, D.; Zhou, S.; Junge, K.; Beller, M. *J. Am. Chem. Soc.* **2010**, *132*, 1770; (c) ZnBH<sub>4</sub> reduction of amides to amines: Narasimhan, S.; Balakumar, M. R.; Swarnalakshimi, S. *Syn. Comm.* **1997**, *27*, 391.
- [60] (a) NaBH<sub>4</sub> in pyridine: Yamada, S.; Kikugawa, Y.; Ikegami, S. *Chem. Pharm. Bull.* **1965**, *13*, 394; (b) Reduction of ureas to amidines: Kikugawa, Y.; Yamada, S.; Nagashima, H.; Kaji, K. *Tetrahedron Lett.* **1969**, *9*, 699; (c) LiBH<sub>4</sub> in pyridine: Giles, R. G.; Lewis, N. J.; Quick, J. K.; Sasse, M. J.; Urquhart, M. W.; Youssef, L. *Tetrahedron* **2000**, *56*, 4531.
- [61] (a) Schwartz's reagent for the reductive deoxygenation of amides: Schedler, D. J. A.; Godfrey, A. G.; Ganem, B. *Tetrahedron Lett.* **1993**, *34*, 5035; (b) Schwartz's reagent for the hydrozirconation of amides to aldehydes: Spletstoser, J. T.; White, J. A.; Tunoori, A. R.; Georg, G. I. *J. Am. Chem. Soc.* **2007**, *129*, 3408.
- [62] BH<sub>3</sub>·NH<sub>2</sub>*t*-Bu as a reducing agent: Hutchins, R. O.; Learn, K.; El-Telbany, F.; Stercho, Y. P. *J. Org. Chem.* **1984**, *49*, 2438.
- [63] (a) Amide activation, reduction with NaBH<sub>4</sub>: Xiang, S.-H.; Xu, J.; Yuan, H.-Q.; Huang, P.-Q. *Synlett* **2010**, 1829; (b) Amide activation, reduction with Et<sub>3</sub>SiH: Pelletier, G.; Bechara, W. S.; Charette, A. B. *J. Am. Chem. Soc.* **2010**, *132*, 12817.

- [64] (a) Fukuyama, T.; Lin, S.-C.; Li, L. *J. Am. Chem. Soc.* **1990**, *112*, 7050-7051; (b) Han, Y.; Chorev, M. *J. Org. Chem.* **1999**, *64*, 1972.
- [65] Modified McFayden–Stevens reduction: Takale, B. S.; Telvekar, V. N. *Chem. Lett.* **2010**, *39*, 546.
- [66] N,O-bis(trimethylsilyl)acetamide (BSA): Claraz, A. *Synlett* **2013**, *24*, 657.
- [67] The observation of further reduction products along Scheme 2.15, Path B suggested the C1 glycoyamidine could be controllably reduced at a later time with aqueous SmI<sub>2</sub>.
- [68] *anti*-C10,C11 stereochemistry in **2-51b** is assigned based upon <sup>1</sup>H NMR chemical shift and coupling constant data (C10H, δ (ppm) 3.28, d, *J* = 11.6 Hz) as well as ROESY correlations relative to its *syn*-C10,C11 counterpart **2-51a**.
- [69] Brief KMnO<sub>4</sub> treatment (1 eq, acetone / H<sub>2</sub>O, –30°C, < 1 min) also generates the axinellamine ring system from **2-51b**, albeit in lower yield. For the development of these conditions: Li, Y.; Cooksey, J. P.; Gao, Z.; Kociński, P. J.; McAteer, S. M.; Snaddon, T. N. *Synthesis* **2011**, 104.
- [70] Oxaziridines are known to oxidize imidazoles and 2-aminoimidazoles: Koswatta, P. B.; Sivappa, R.; Dias, H. V. R.; Lovely, C. J. *Synthesis* **2009**, 2970.
- [71] Dehalogenation with Sm<sup>II</sup> and related single-electron reductants: (a) For a selective monodebromination with concomitant deprotection using Zn, HOAc, MeOH, 40°C: Wang, S.; Romo, D. *Angew Chem. Int. Ed.* **2008**, *47*, 1284; (b) For a related monodebromination using SmI<sub>2</sub>, THF; MeOH (see Ref. 21b).
- [72] Spectra of **2-58a** closely resemble those of natural axinellamine A (Ref. 3, see Appendix of this chapter). Characteristic <sup>1</sup>H NMR (600 MHz, DMSO-*d*<sub>6</sub>) signals include (C1H, δ (ppm) 4.81, *J* = 6.3 Hz, d) and (C5H, δ (ppm) 5.15, s) and a diagnostic NOE correlation between C13H(β) and C5H.
- [73] Scepttrin isolation: Walker, R. P.; Faulkner, D. J.; van Engen, D.; Clardy, J. *J. Am. Chem. Soc.* **1981**, *103*, 5772.
- [74] Ageliferin isolation: (a) Rinehart, K. L. U.S. Patent 4737510, Apr. 12, **1988**; (b) Rinehart, K. L. *Pure Appl. Chem.* **1989**, *61*, 525; (c) Kobayashi, J.; Tsuda, H.; Murayama, T.; Nakamura, H.; Ohizumi, Y.; Ishibashi, M.; Iwamura, M. *Tetrahedron* **1990**, *46*, 5579.
- [76] For examples and discussion of similar vinyl halides in synthesis: Coleman, R. S.; Carpenter, A. J. *J. Org. Chem.* **1993**, *58*, 4452 and see Ref. 11a
- [77] Spoering, R. M. Studies Toward a Synthesis of Palau'amine. Ph.D. Thesis, Harvard University, **2005**.

## 2.5 Experimental.

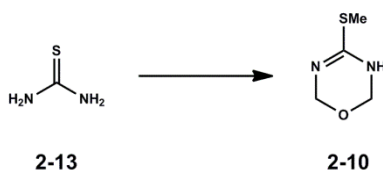
### 2.5.1 Materials and Methods.

Unless stated otherwise, reactions were performed under an argon (Ar) atmosphere in flame-dried glassware. Tetrahydrofuran (THF), chloroform (CHCl<sub>3</sub>), methylene chloride (CH<sub>2</sub>Cl<sub>2</sub>), diethyl ether (Et<sub>2</sub>O), toluene (PhCH<sub>3</sub>), benzene (PhH), dimethoxyethane (DME), dimethyl formamide (DMF) and acetonitrile (CH<sub>3</sub>CN) were dried and deoxygenated through activated alumina solvent drying systems or distilled prior to use. 2,2,2-Trichloro-1-(1H-pyrrol-2-yl)ethanone was obtained from Oakwood Chemicals. 2-(trimethylsilyl)ethoxymethyl chloride (SEMCl) was obtained from Combi-Blocks. Potassium hexamethyldisilazide (KHMDS) was obtained as a 0.5M solution in toluene from Sigma-Aldrich. Column chromatography was performed on silica gel 60 (SiliCycle, 240-400 mesh). Thin layer chromatography (TLC) and preparative thin layer chromatography (pTLC) utilized pre-coated plates (silica gel 60 PF254, 0.25 mm or 0.5 mm). Purification of advanced intermediates employed an Agilent 1200 Preparative HPLC (pHPLC) system equipped with an Agilent Quadrupole 6130 ESI-MS detector and an automated fraction collector. Mobile phases (Mobile phase A: H<sub>2</sub>O, Mobile Phase B: CH<sub>3</sub>CN) were prepared with 0.1% or 1% trifluoroacetic acid (CF<sub>3</sub>CO<sub>2</sub>H) or 0.1% formic acid (HCO<sub>2</sub>H) as indicated. Advanced intermediates isolated and characterized as trifluoroacetate salts are denoted as (2·CF<sub>3</sub>CO<sub>2</sub>H) in data tables. The trifluoroacetate salt may be omitted from structures in schemes for clarity. NMR spectra were recorded on Bruker Avance spectrometers (500 MHz or 600 MHz). Data for <sup>1</sup>H NMR spectra are reported as follows: chemical shift (δ ppm) (multiplicity, coupling constant (Hz), integration) at 298K, unless stated otherwise, and are referenced to a residual solvent peak. Data for <sup>13</sup>C NMR spectra are reported in terms of chemical shift (δ ppm) and are referenced to residual solvent peak. Melting points were measured using a Barnstead/Electrothermal 9100 apparatus and are uncorrected. IR spectra were recorded on a Perkin-Elmer 100 spectrometer.



## 2.5.2 Experimental Procedures and Characterization Data

### 4-(Methylthio)-3,6-dihydro-2H-1,3,5-oxadiazine (2-10).

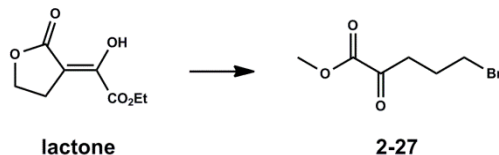


A 1-L flask was charged with thiourea **2-13** (76 g, 1.0 mol, 1.0 equiv) and 37 wt % aqueous formaldehyde solution (470-mL, 6.0 mol, 6.0 equiv). 40 wt % aqueous NaOH solution (10-mL) was added and the clear solution was heated at 60°C for 2h. The reaction was cooled to RT and neutralized (pH = 6) with formic acid (0.3-mL). Concentration in vacuo gave a crude off-white sticky oil that was dissolved in MeOH (760-mL). Concentrated HCl (20-mL) was added and stirred at RT for 12h. The clear solution was neutralized (pH = 7) with 50 wt% NaOH. Concentration of the cloudy precipitous solution in vacuo at 50°C yielded a pasty white solid. This material was dissolved in MeOH (2.4-L) and H<sub>2</sub>O (0.6-L) and added to a 5-L three-necked flask fitted with a thermometer, reflux condenser and exit bubbler. The solution was adjusted to pH = 8 with 40 wt % aqueous NaOH solution and then treated with CH<sub>3</sub>I (64-mL, 1.0 mol). The clear, colorless solution was slowly brought to 65°C and stirred at this temperature for 18h. The solution was cooled to 50°C and concentrated in vacuo at 50°C to give a clear aqueous solution (~250-mL). The aqueous solution was washed with EtOAc (8 × 150-mL). (**Note:** the discarded organic layer slowly turns orange with exposure to air.) The aqueous solution was neutralized with 50 wt % NaOH to pH = 8.5 and washed with CH<sub>2</sub>Cl<sub>2</sub> (3 × 15-mL). (**Note:** after the first wash the organic layer is on top.) The aqueous layer was concentrated in vacuo to give a crude white solid **2-10** (~230 g) which was combined with another 1 mol batch of crude **2-10** (prepared in the same manner). The combined crude solid **2-10** (2 mol) was dissolved in 2-propanol / hexanes (4:1) (1.6-L) and refluxed for 20 min at which point insoluble inorganic salts were filtered off while hot. The white solution was refluxed for 20 min until clear and cooled slowly to RT. The clear solution was placed in a -20°C freezer to allow for crystallization over 48h. Pure **2-10** was isolated as a crystalline white solid (85 g, 32%) after filtration, washing with hexanes and drying overnight in vacuo. (**Note:** Additional **2-10** can be obtained from the mother liquor by the addition of hexanes and subsequent cooling to -20°C.)

### 4-(Methylthio)-3,6-dihydro-2H-1,3,5-oxadiazine (2-10):

**R<sub>f</sub>** = 0.1, CHCl<sub>3</sub> / MeOH (9:1); opaque needles from 2-propanol / hexanes (4:1) (m.p. 124–126°C); <sup>1</sup>H NMR (500 MHz, DMSO-*d*<sub>6</sub>): δ (ppm) 10.45 (bs, 1H), 5.01 (s, 4H), 2.60 (s, 3H); <sup>13</sup>C NMR (125 MHz, DMSO-*d*<sub>6</sub>): δ (ppm) 163.4, 73.8, 13.5; **HRMS-ESI** (*m/z*) calcd for [C<sub>4</sub>H<sub>8</sub>N<sub>2</sub>OS+H]<sup>+</sup>: 133.0436; found: 133.0442; **IR** (neat)  $\nu_{\max}$  (cm<sup>-1</sup>): 3105, 3046, 2923, 1603, 1550.

### Methyl 5-bromo-2-oxopentanoate (2-27).



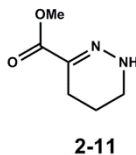
A solution of lactone (46.6 g, 249 mmol – prepared according to Cushman, M.; Gerhardt, S.; Huber, R.; Fischer, M.; Kis, K.; Bacher, A. *J. Org. Chem.* **2002**, *67*, 5807) in 30% HBr / HOAc (150-mL) was heated at 110°C for 2h. An additional 100-mL of 30% HBr / HOAc was added and the reaction maintained at 110°C for 14h. The mixture was concentrated in vacuo to afford a brown oil that was dissolved in 250-mL MeOH. Concentrated aqueous H<sub>2</sub>SO<sub>4</sub> (0.5-mL) was added and the solution stirred at RT for 14h. The reaction was concentrated and the incipient residue dissolved in Et<sub>2</sub>O. Saturated aqueous NaHCO<sub>3</sub> was carefully added until gas evolution ceased. The organic layer was separated and washed with H<sub>2</sub>O and dried over Na<sub>2</sub>SO<sub>4</sub>. Concentration in vacuo provided **2-27** as a brown oil that was used without further purification.

**Note:** the EtOH used was freshly distilled from Mg turnings.

### Methyl 5-bromo-2-oxopentanoate (2-27):

<sup>1</sup>H NMR (500 MHz, CHCl<sub>3</sub>-d<sub>1</sub>): δ (ppm) 3.86 (s, 3H), 3.46-3.44 (t, *J* = 4.9 Hz, 2H), 3.06-3.04 (t, *J* = 7.0 Hz, 2H), 2.20-2.17 (m, 2H); LRMS-ESI (*m/z*) calcd for [C<sub>6</sub>H<sub>9</sub>BrO<sub>3</sub>+H]<sup>+</sup>: 209.0; found: 209.0.

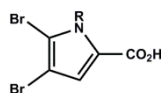
### Methyl-1,4,5,6-tetrahydro-3-pyridazinecarboxylate (2-11).



Hydrazine hydrate (20.4 g, 398 mmol) was dissolved in a mixture of MeOH (300-mL) and H<sub>2</sub>O (37.5-mL). Glacial HOAc (7-mL) was added and the solution cooled in an ice-bath. A solution of crude **2-27** in MeOH (50-mL) was added over 30 min wherein a white precipitate formed. The ice-bath was removed wherein the solids dissolved. The pH of the mixture was maintained between 4 and 7 with 3 M aqueous K<sub>2</sub>CO<sub>3</sub>. After the pH had stabilized at RT, the reaction was immersed into an oil-bath pre-heated to 60°C and 3 M aqueous K<sub>2</sub>CO<sub>3</sub> was used to adjust the pH to ~5. The reaction was heated at 60°C for 1h at which time the pH was 6. After removing MeOH in vacuo, the residue was dissolved in a minimum amount of H<sub>2</sub>O and extracted with EtOAc. The organic layer was dried over Na<sub>2</sub>SO<sub>4</sub>, filtered and concentrated to afford a solid that was recrystallized from EtOAc to afford **2-11** (42.5 g, 81%).

**Methyl-1,4,5,6-tetrahydro-3-pyridazinecarboxylate (2-11):**

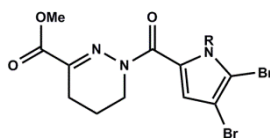
$R_f = 0.5$ , EtOAc/CH<sub>2</sub>Cl<sub>2</sub> (2:3); colorless crystals from EtOAc (m.p. 72°C); <sup>1</sup>H NMR (400 MHz, CHCl<sub>3</sub>-*d*<sub>1</sub>): δ (ppm) 5.90 (bs, 1H), 3.78 (s, 3H), 3.23 (t, *J* = 5.2 Hz, 2H), 2.45 (t, *J* = 6.8 Hz, 2H), 1.90 (m, 2H); <sup>13</sup>C NMR (75 MHz, CHCl<sub>3</sub>-*d*<sub>1</sub>): δ (ppm) 165.8, 132.0, 52.1, 41.9, 21.2, 17.6; LRMS-ESI (*m/z*) calcd for [C<sub>6</sub>H<sub>10</sub>N<sub>2</sub>O<sub>2</sub>+H]<sup>+</sup>: 143.07; found: 143.06; IR (neat)  $\nu_{\max}$  (cm<sup>-1</sup>): 3200, 2957, 1694, 1588, 1442, 1303, 1237, 1190, 115, 972, 743.

**4,5-dibromo-1-((2-(trimethylsilyl)ethoxy)methyl)-1H-pyrrole-2-carboxylic acid (2-12a).****2-12a**

A solution of NaOH (17.6 g, 439 mmol) in H<sub>2</sub>O (218 mL) was added to a solution of 4,5-dibromo-1-((2-(trimethylsilyl)ethoxy)methyl)-1H-pyrrole-2-carboxylate ethyl ester (94.4 g, 221 mmol) in THF / MeOH (1000-mL / 70-mL). The resulting solution was stirred at 65°C for 5h. The reaction was quenched with 10% aqueous citric acid. The solvents were removed in vacuo and the residue taken up in CH<sub>2</sub>Cl<sub>2</sub>. The solution was washed with saturated aqueous NH<sub>4</sub>Cl, H<sub>2</sub>O and brine. The organic layer was dried over Na<sub>2</sub>SO<sub>4</sub>, filtered and concentrated in vacuo to give **2-12a** as an off white solid (86.5g, 98%). This material was used without purification.

**4,5-dibromo-1-((2-(trimethylsilyl)ethoxy)methyl)-1H-pyrrole-2-carboxylic acid (2-12a):**

<sup>1</sup>H NMR (400 MHz, CHCl<sub>3</sub>-*d*<sub>1</sub>): δ (ppm) 7.21 (s, 1H), 5.81 (s, 2H), 3.60 (t, *J* = 8.4Hz, 2H), 0.91 (t, *J* = 8.4Hz, 2H), 0.02 (s, 9H); <sup>13</sup>C NMR (75 MHz, CHCl<sub>3</sub>-*d*<sub>1</sub>): δ (ppm) 164.3, 123.2, 122.7, 115.3, 101.1, 75.5, 66.3, 17.8, -1.5; LRMS-ESI (*m/z*) calcd for [C<sub>11</sub>H<sub>17</sub>Br<sub>2</sub>NO<sub>3</sub>Si+H]<sup>+</sup>: 399.93; found: 400.10; IR (neat)  $\nu_{\max}$  (cm<sup>-1</sup>): 3400, 1652, 1635, 1338, 1250, 1148, 667.

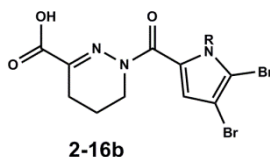
**Preparation of 1-(4,5-dibromo-1-((2-(trimethylsilyl)ethoxy)methyl)-1H-pyrrole-2-carbonyl)-1,4,5,6-tetrahydropyridazine-3-carboxylic acid (2-16b).****2-16a**

Oxalyl chloride (20.3-mL, 236 mmol) was added to a solution of acid **2-12a** (47.1 g, 118 mmol) in CH<sub>2</sub>Cl<sub>2</sub> (400 mL). DMF (0.5-mL) was added and the resulting mixture was stirred at RT for 1 h. The solvent was removed in vacuo to give a brown oily residue that was dissolved in CH<sub>3</sub>CN (370-mL). To this solution was added **2-11** (16.8 g, 118 mmol), pyridine (19-mL, 236 mmol) and DMAP (50 mg) and the resulting mixture was stirred at RT overnight. The solvent was removed in vacuo and the residue taken up in CH<sub>2</sub>Cl<sub>2</sub>. The solution was washed with H<sub>2</sub>O and brine. The organic layer was dried over Na<sub>2</sub>SO<sub>4</sub>, filtered and concentrated in vacuo. Purification by flash

column chromatography (gradient hexanes/EtOAc (9:1) to (4:1)) provided methyl ester **2-16a** (58 g, 94%) as a white solid.

**Ester (2-16a):**

$R_f = 0.3$ , EtOAc/CH<sub>2</sub>Cl<sub>2</sub> (1:4); <sup>1</sup>H NMR (400 MHz, ):  $\delta$  (ppm) 7.50 (s, 1H), 5.84 (s, 2H), 3.88 (s, 3H), 3.86 (m, 2H), 3.56 (t,  $J = 8.0$  Hz, 2H), 2.56 (t,  $J = 6.4$  Hz, 2H), 1.96 (td,  $J = 12.4, 6.3$  Hz, 2H), 0.89 (t,  $J = 8.0$  Hz, 2H), 0.04 (s, 9H); <sup>13</sup>C NMR (75 MHz, CHCl<sub>3</sub>-*d*<sub>1</sub>):  $\delta$  (ppm) 164.5, 160.0, 139.3, 125.2, 124.1, 113.2, 100.3, 76.0, 66.0, 52.5, 39.6, 21.8, 17.8, 16.6, -1.5; HRMS-ESI ( $m/z$ ) calcd for [C<sub>17</sub>H<sub>25</sub>Br<sub>2</sub>N<sub>3</sub>O<sub>4</sub>Si+H]<sup>+</sup>: 522.0054; found: 522.0057; IR (neat)  $\nu_{\max}$  (cm<sup>-1</sup>): 1711, 1648, 1413, 1337, 1267, 1239, 1090, 973, 834.

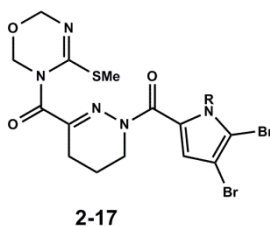


A solution of ester **2-16a** (66 g, 126 mmol) in THF/H<sub>2</sub>O (520-mL/250-mL) was stirred for 30 min in an ice-water bath. A solution of LiOH (30-mL, aqueous 0.5 M) was added and the resulting mixture stirred at 4°C for 1h. The reaction was quenched with 10% aqueous citric acid and concentrated in vacuo. The residue was taken up in EtOAc and washed with saturated aqueous NH<sub>4</sub>Cl, H<sub>2</sub>O and brine. The organic layer was dried over Na<sub>2</sub>SO<sub>4</sub>, filtered and concentrated in vacuo. The resulting white solid **2-16b** (62.2 g, 97%) was used without further purification.

**1-(4,5-dibromo-1-((2-(trimethylsilyl)ethoxy)methyl)-1H-pyrrole-2-carbonyl)-1,4,5,6-tetrahydropyridazine-3-carboxylic acid (2-16b):**

<sup>1</sup>H NMR (400 MHz, CHCl<sub>3</sub>-*d*<sub>1</sub>):  $\delta$  (ppm) 7.36 (s, 1H), 6.95 (bs, 1H), 5.74 (s, 2H), 3.86 (t,  $J = 5.6$  Hz, 2H), 3.55 (t,  $J = 8.0$  Hz, 2H), 2.61 (t,  $J = 6.4$  Hz, 2H), 2.01 (td,  $J = 12.3, 6.3$  Hz, 2H), 0.88 (t,  $J = 8.0$  Hz, 2H), -0.06 (s, 9H); <sup>13</sup>C NMR (75MHz, CHCl<sub>3</sub>-*d*<sub>1</sub>):  $\delta$  (ppm) 163.8, 160.5, 139.8, 128.3, 125.2, 121.5, 113.0, 100.4, 75.8, 66.4, 40.0, 21.0, 17.7, 16.4, -1.5; HRMS-ESI ( $m/z$ ) calcd for [C<sub>16</sub>H<sub>23</sub>Br<sub>2</sub>N<sub>3</sub>O<sub>4</sub>Si+H]<sup>+</sup>: 507.9897; found: 507.9898.; IR (neat)  $\nu_{\max}$  (cm<sup>-1</sup>): 3203, 2951, 1715, 1652, 1422, 1240, 1179, 1096, 1096, 969, 860, 742, 684, 612.

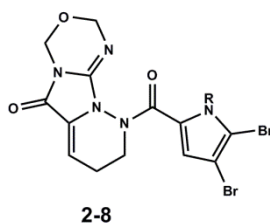
**(4,5-dibromo-1-((2-(trimethylsilyl)ethoxy)methyl)-1H-pyrrol-2-yl)(3-(4-(methylthio)-3,6-dihydro-2H-1,3,5-oxadiazine-3-carbonyl)-5,6-dihydropyridazin-1(4H)-yl)methanone (2-17).**



Solid **2-10** (5.8 g, 43.6 mmol) was added to a solution of **2-16b** (21.2 g, 41.6 mmol) in DMF (275-mL) at 0°C. N,N,N',N'-Tetramethyl-O-(benzotriazol-1-yl)uronium tetrafluoroborate (TBTU) (14.7 g, 45.7 mmol) was added, followed by the slow addition of (*i*-Pr)<sub>2</sub>NEt (14.4-mL, 83.1 mmol). The resulting mixture was stirred at RT overnight. The reaction mixture was diluted with EtOAc (1-L) and washed with saturated aqueous NH<sub>4</sub>Cl (2 × 200-mL), H<sub>2</sub>O (8 × 200-mL) and brine (200-mL). The organic layer was dried over Na<sub>2</sub>SO<sub>4</sub>, filtered and concentrated in vacuo to afford a red-brown oil further purified by flash column chromatography to give **2-17** as a yellow oil (24.20 g, 93%).

**(4,5-dibromo-1-((2-(trimethylsilyl)ethoxy)methyl)-1H-pyrrol-2-yl)(3-(4-(methylthio)-3,6-dihydro-2H-1,3,5-oxadiazine-3-carbonyl)-5,6-dihydropyridazin-1(4H)-yl)methanone (2-17):** <sup>1</sup>H NMR (500 MHz, CHCl<sub>3</sub>-*d*<sub>1</sub>): δ (ppm) 6.91 (s, 1H), 5.74 (s, 2H), 5.23 (s, 2H), 5.09 (s, 2H), 3.89-3.86 (t, *J* = 5.6 Hz, 2H), 3.50-3.47 (t, *J* = 8.1 Hz, 2H), 2.59-2.56 (t, *J* = 6.4 Hz, 2H), 2.03 (s, 3H), 1.23-1.26 (t, *J* = 7.1 Hz, 2H), -0.07 (s, 9H); **LRMS-ESI** (*m/z*) calcd for [C<sub>20</sub>H<sub>29</sub>Br<sub>2</sub>N<sub>5</sub>O<sub>4</sub>SSi+H]<sup>+</sup>: 622.02; found: 622.1.

### Monomer (2-8).

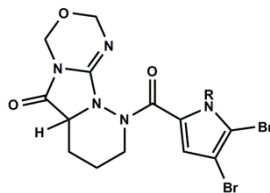


A mixture of **2-17** (24.2 g, 38.8 mmol), HgCl<sub>2</sub> (17.9 g, 67.0 mmol) and pyridine (9.5-mL, 116.4 mmol) in CH<sub>3</sub>CN (180-mL) was heated at reflux for 48h. Upon cooling to RT, a white solid was removed by filtration and the solvent evaporated in vacuo. The reaction mixture was taken up in EtOAc and insoluble inorganic solids were removed by filtration. The organic layer was washed with 1 M NaOH whereupon a white precipitate formed. The precipitate was filtered and the NaOH wash / filtration sequence continued until no further solid formed (6-7×). The organic layer was washed with H<sub>2</sub>O and brine and dried over NaSO<sub>4</sub>. Concentration in vacuo and purification by flash column chromatography (hexanes/EtOAc) afforded **2-8** as a yellow solid (4.5 g, 20%) and recovered **2-17** (6.1 g, 20%).

### Monomer (2-8):

<sup>1</sup>H NMR (500 MHz, CH<sub>3</sub>CN-*d*<sub>3</sub>): δ (ppm) 6.93 (s, 1H), 5.93-5.91 (t, *J* = 4.6 Hz, 2H), 5.60 (s, 2H), 5.21 (s, 2H), 4.94-4.81 (m, 2H), 3.88 (m, 2H), 3.59-3.56 (t, *J* = 8.0 Hz, 2H), 2.36 (m, 2H), 0.89-0.86 (t, *J* = 7.1 Hz, 2H), -0.05 (s, 9H); <sup>13</sup>C NMR (125 MHz, CH<sub>3</sub>CN-*d*<sub>3</sub>): δ (ppm) 164.9, 157.6, 141.9, 134.3, 130.1, 126.5, 120.4, 114.1, 101.1, 79.4, 77.1, 73.0, 67.6, 30.8, 24.2, 18.9, -0.8; **LRMS-ESI** (*m/z*) calcd for [C<sub>19</sub>H<sub>25</sub>Br<sub>2</sub>N<sub>5</sub>O<sub>4</sub>Si+H]<sup>+</sup>: 576.01; found: 576.0.

### Reduced Monomer (2-21).



2-21



To a solution of monomer **2-8** (100 mg, 0.17 mmol, 1.0 equiv) in THF (0.87-mL) was added Zn dust (25 mg, 0.38 mmol, 2.2 equiv) and glacial HOAc (104 mg, 1.73 mmol, 10 equiv) and the resultant heterogeneous mixture was heated to 75°C in an oil bath for 1h. The reaction was judged complete by TLC analysis ( $R_f = 0.3$ , hexanes / EtOAc (1:1)) and cooled to RT. The mixture was diluted with CH<sub>2</sub>Cl<sub>2</sub> and washed with saturated aqueous NaHCO<sub>3</sub>, dried over Na<sub>2</sub>SO<sub>4</sub>, filtered and concentrated in vacuo to give crude reduced monomer **2-21**. Purification by flash column chromatography eluting with gradient hexanes / EtOAc (2:1 to 1:1) provided **2-21** (72 mg, 72%) as a colorless foam.

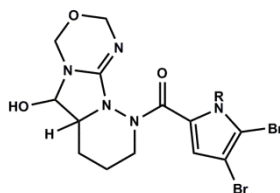
**Note:** Similar reduction conditions including 1 atm H<sub>2</sub>, cat. Pd/C, MeOH, RT / 1 atm H<sub>2</sub>, cat. PtO<sub>2</sub>, EtOAc, RT were also effective, although slow de-halogenation was commonly observed.

### Reduced Monomer (2-21):

<sup>1</sup>H NMR (500 MHz, CHCl<sub>3</sub>-d<sub>1</sub>): δ (ppm) 6.90 (s, 1H), 5.83 (d, *J* = 10.4 Hz, 1H), 5.51 (d, *J* = 10.4 Hz, 1H), 5.42 (d, 8.9 Hz, 1H), 5.14-4.98 (m, 3H), 4.55-4.43 (m, 1H), 3.91-3.81 (m, 1H), 3.53 (t, *J* = 8.3 Hz, 2H), 3.11-3.00 (m, 1H), 2.24-2.14 (m, 1H), 1.85-1.68 (m, 2H), 0.97-0.78 (m, 2H), -0.01 (s, 9H); LRMS-ESI (*m/z*) calcd for [C<sub>19</sub>H<sub>27</sub>Br<sub>2</sub>N<sub>5</sub>O<sub>4</sub>Si+H]<sup>+</sup>: 578.03; found: 578.0.

### Preparation of Aminal (2-22) and 2-aminoimidazole (2-23).

#### Aminal (2-22).



2-22



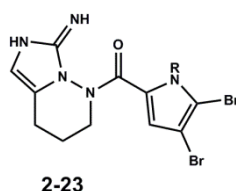
Reduced monomer **2-21** (88 mg, 0.15 mmol, 1.0 equiv) was dissolved in toluene (0.76-mL) and cooled to -78°C followed by the dropwise addition of LiHBET<sub>3</sub> (0.76-mL, 0.76 mmol, 5.0 equiv, 1.0 M in THF). The amber colored solution slowly faded to a light yellow as stirring was continued for 1h at -78°C. The reaction was quenched by the addition of saturated aqueous NH<sub>4</sub>Cl (1.2-mL) and allowed to reach RT. The mixture was diluted with H<sub>2</sub>O and extracted with

EtOAc. Combined organics were washed with brine, dried over Na<sub>2</sub>SO<sub>4</sub>, filtered and concentrated in vacuo to give the crude hemiaminal **2-22**. Purification by flash column chromatography eluting with CH<sub>2</sub>Cl<sub>2</sub> / MeOH (20:1) provided **2-22** (60 mg, 68%) as a white foam.

**Aminal (2-22):**

<sup>1</sup>H NMR (500 MHz, CH<sub>3</sub>CN-*d*<sub>3</sub>, 343 K): δ (ppm) 7.05 (s, 1H), 5.71 (ABq, *J*<sub>AB</sub> = 10.1 Hz, 2H), 4.98-4.71 (m, 5H), 4.32-4.28 (m, 1H), 3.88 (bs, 1H), 3.67-3.60 (m, 2H), 3.45-3.40 (m, 1H), 2.87-2.82 (m, 1H), 1.90-1.44 (m, 3H), 0.95-0.90 (m, 2H), -0.01 (s, 9H); LRMS-ESI (*m/z*) calcd for [C<sub>19</sub>H<sub>29</sub>Br<sub>2</sub>N<sub>5</sub>O<sub>4</sub>Si+H]<sup>+</sup>: 580.04; found: 580.0.

**2-aminoimidazole (2-23).**



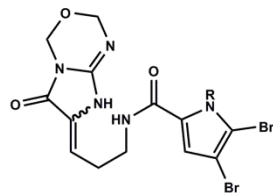
To a solution of hemiaminal **2-22** (165 mg, 0.28 mmol, 1.0 equiv) dissolved in CH<sub>3</sub>CN (2.5-mL) was added Cl<sub>3</sub>CCO<sub>2</sub>H (1.4-mL, 1.42 mmol, 5 equiv, 1.0 M in CH<sub>3</sub>CN / H<sub>2</sub>O (1:1)) and the resultant reddish solution was heated at 110°C (sealed vessel) in an oil bath for 9h. The mixture was cooled to RT and concentrated in vacuo. Purification by flash column chromatography (short silica plug) eluting with gradient CH<sub>2</sub>Cl<sub>2</sub> / MeOH (20:1 to 10:1) provided crude **2-23**. Further purification by preparative TLC (1000-μm SiO<sub>2</sub>) eluting isocratic CH<sub>2</sub>Cl<sub>2</sub> / MeOH (12:1) provided 2-aminoimidazole **2-23** (34 mg, 21%) as an off-white solid.

**Note:** Following the above procedures, 2-aminoimidazole **2-23** (0.39 g, 39%, 3 steps from **2-8**) was prepared from monomer **2-8** (1.12 g, 1.94 mmol) in 3 steps without purification of intermediates **2-21** and **2-22**.

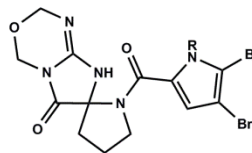
**2-aminoimidazole (2-23):**

<sup>1</sup>H NMR (500 MHz, CH<sub>3</sub>CN-*d*<sub>3</sub>): δ (ppm) 8.41 (bs, 1H), 6.86 (bs, 1H), 6.41 (bs, 1H), 5.66 (bs, 2H), 3.91 (bs, 2H), 3.53 (dd, *J* = 9.4, 8.3 Hz, 2H), 2.82-2.73 (m, 2H), 1.91-1.81 (m, 2H), 0.93-0.82 (m, 2H), -0.01 (s, 9H) (resonance at 3.91 ppm significantly broadened at RT); <sup>13</sup>C NMR (125 MHz, CH<sub>3</sub>CN-*d*<sub>3</sub>, 343 K): δ (ppm) 164.5, 147.1, 127.4, 123.0, 119.8, 113.3, 101.2, 77.5, 67.9, 50.8, 30.7, 22.8, 19.3, -0.9 (missing 1C resonance at 343K); LRMS-ESI (*m/z*) calcd for [C<sub>17</sub>H<sub>25</sub>Br<sub>2</sub>N<sub>5</sub>O<sub>2</sub>Si+H]<sup>+</sup>: 518.0223; found: 518.0217.

### Monoalkylidene (2-24a).



2-24a



2-24b

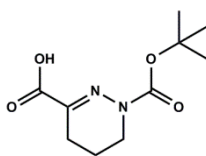


To a suspension of KH (9 mg, 0.07 mmol, 1.3 equiv) and 18-crown-6 (20 mg, 0.08 mmol, 1.45 equiv, dried azeotropically with benzene) in THF (0.1-mL) at RT was added a solution of reduced monomer **2-21** (30 mg, 0.05 mmol, 1.0 equiv, in THF (0.25-mL)) dropwise. The mixture became light yellow and homogeneous and was stirred at RT for 10 min followed by direct purification by preparative TLC (1000- $\mu$ M, SiO<sub>2</sub>) eluting with CH<sub>2</sub>Cl<sub>2</sub>: MeOH (12:1) to provide a band containing **2-24a** (14 mg, 47%) as an off-white film. Monoalkylidene **2-24a** was the major isomer in this experiment, <sup>1</sup>H NMR analysis of a minor band (impure) from preparative TLC was tentatively assigned as spirocycle **2-24b**.

### Monoalkylidene (2-24a):

<sup>1</sup>H NMR (500 MHz, CH<sub>3</sub>CN-*d*<sub>3</sub>):  $\delta$  (ppm) 7.31 (bs, 1H), 6.78 (s, 1H), 5.76 (s, 2H), 5.62 (t, *J* = 8.2 Hz, 1H), 5.16 (s, 2H), 4.91 (s, 2H), 3.51 (t, *J* = 8.1 Hz, 2H), 3.43-3.35 (m, 2H), 2.50-2.41 (m, 2H), 0.81 (t, *J* = 8.1 Hz, 2H), -0.07 (s, 9H); LRMS-ESI (*m/z*) calcd for [C<sub>19</sub>H<sub>27</sub>Br<sub>2</sub>N<sub>5</sub>O<sub>4</sub>Si+H]<sup>+</sup>: 578.03; found: 578.0.

### 1-(tert-butoxycarbonyl)-1,4,5,6-tetrahydropyridazine-3-carboxylic acid (2-34).



2-34b

*Tert*-butyl hydrazinecarboxylate (5.05 g, 38.2 mmol, 1.0 equiv) was dissolved in MeOH (50-mL) and cooled to 0°C with an ice-water bath, followed by the addition of glacial HOAc (1.2-mL). A second solution containing methyl 5-bromo-2-oxopentanoate **2-27** (8.00 g, 38.2 mmol, 1.0 equiv) in MeOH (25-mL) was added dropwise to the cooled reaction over 15 min. The reaction was allowed to reach RT and stirred for an additional 30 min. TLC analysis indicates consumption of **2-27** and a product indicative of intermediate hydrazone formation. The mixture was neutralized with 3 M aqueous K<sub>2</sub>CO<sub>3</sub> and immersed into an oil-bath preheated to 60°C. The pH of the mixture was maintained between 4 and 7 with 3 M aqueous K<sub>2</sub>CO<sub>3</sub>. The reaction was heated at 60°C for 2h. After cooling to RT, the reaction was concentrated in vacuo and diluted with CH<sub>2</sub>Cl<sub>2</sub> (200-mL). The organic layer was washed with saturated aqueous NaHCO<sub>3</sub>, H<sub>2</sub>O, brine, dried over Na<sub>2</sub>SO<sub>4</sub>, filtered and concentrated in vacuo to give crude 1-*tert*-butyl 3-methyl 5,6-dihydropyridazine-1,3(4H)-dicarboxylate **2-34a** (9.25 g, crude weight, LRMS-ESI (*m/z*) calcd



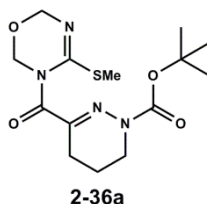
for  $[C_{11}H_{18}N_2O_4+H]^+$ : 243.13; found: 243.1) as a yellow solid that was used in the subsequent step without further purification.

The crude ester **2-34a** was dissolved in THF (90-mL) at RT followed by the addition of LiOH (1.05 g, 45.8 mmol, 1.2 equiv in H<sub>2</sub>O (15-mL)). The reaction mixture was stirred at RT for 15 min until judged complete by TLC analysis. The mixture was concentrated in vacuo to remove THF (approx. 90-mL) and neutralized with 3 M aqueous HCl to pH = 3. The precipitous acidic solution was extracted with CH<sub>2</sub>Cl<sub>2</sub> (2 × 200-mL) and combined organics were washed with brine (2 × 20-mL), dried over Na<sub>2</sub>SO<sub>4</sub>, filtered and concentrated in vacuo to give crude acid **2-34b** (7.2 g, 82%, crude) as an off-white solid that was used in the subsequent step without further purification.

**1-(tert-butoxycarbonyl)-1,4,5,6-tetrahydropyridazine-3-carboxylic acid (2-34b):**

<sup>1</sup>H NMR (500 MHz, CHCl<sub>3</sub>-d<sub>1</sub>): δ (ppm) 3.70-3.67 (m, 2H), 2.51 (t, J = 6.0 Hz, 2H), 1.91 (m, 2H), 1.54 (s, 9H); <sup>13</sup>C NMR (125 MHz, DMSO-d<sub>6</sub>): δ (ppm) 165.4, 151.9, 140.6, 81.1, 41.2, 27.8, 21.3, 16.6; LRMS-ESI (m/z) calcd for  $[C_{10}H_{16}N_2O_4+H]^+$ : 229.12; found: 229.1.

**tert-butyl 3-(4-(methylthio)-3,6-dihydro-2H-1,3,5-oxadiazine-3-carbonyl)-5,6-dihydropyridazine-1(4H)-carboxylate (2-36a).**

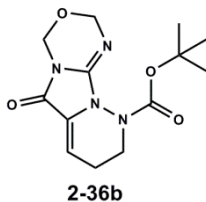


Crude acid **2-34b** (4.30 g, 18.8 mmol, 1.0 equiv), heterocycle **2-10** (2.98 g, 22.6 mmol, 1.2 equiv) and TBTU (6.35 g, 19.8 mmol, 1.05 equiv) were dissolved in DMF (95-mL) and cooled to 0°C with an ice-water bath followed by the addition of (*i*-Pr)<sub>2</sub>NEt (6.6-mL, 37.7 mmol, 2.0 equiv). The reaction was slowly warmed to RT and allowed to stir overnight. The mixture was diluted with EtOAc (200-mL) and washed with saturated aqueous NH<sub>4</sub>Cl (2 × 10-mL), H<sub>2</sub>O (8 × 10-mL), brine, dried over Na<sub>2</sub>SO<sub>4</sub>, filtered and concentrated in vacuo to give a crude foam further purified by flash column chromatography (hexanes/EtOAc gradient, 100% to (3:2)) to afford **2-36a** as a white solid (1.94 g, 30%).

**tert-butyl 3-(4-(methylthio)-3,6-dihydro-2H-1,3,5-oxadiazine-3-carbonyl)-5,6-dihydropyridazine-1(4H)-carboxylate (2-36a):**

<sup>1</sup>H NMR (400 MHz, CHCl<sub>3</sub>-d<sub>1</sub>): δ (ppm) 5.37 (s, 2H), 5.16 (s, 2H), 3.69 (t, J = 3.6 Hz, 2H), 2.48 (t, J = 6.8 Hz, 2H), 2.30 (s, 3 H), 1.92-1.90 (m, 2H), 1.53 (s, 9H); LRMS-ESI (m/z) calcd for  $[C_{14}H_{22}N_4O_4S+H]^+$ : 342.14; found: 342.1.

### Boc Monomer (2-36b).



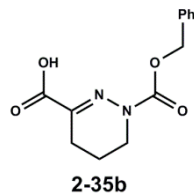
Purified **2-36a** (1.70 g, 5.0 mmol, 1.0 equiv) was dissolved in CH<sub>2</sub>Cl<sub>2</sub> (50-mL) at RT followed by the addition of oxalyl chloride (0.45-mL, 5.2 mmol, 1.05 equiv) via syringe. After stirring at RT for 1h, the reaction mixture was quenched by the addition of saturated aqueous NaHCO<sub>3</sub>. The mixture was diluted with CHCl<sub>3</sub> (50-mL) and the organic layer was separated, washed with H<sub>2</sub>O, brine, dried over Na<sub>2</sub>SO<sub>4</sub>, filtered and concentrated in vacuo to give a crude foam further purified by flash column chromatography (hexanes/EtOAc gradient, (4:1) to 100% EtOAc) to afford **2-36b** as a white solid (1.2 g, 82%).

**Note:** A repeated experiment with **2-36a** (12.4 g, 36.3 mmol) and oxalyl chloride (3.43-mL, 40.0 mmol, 1.1 equiv) afforded **2-36b** (9.28 g, 87%).

### Boc Monomer (2-36b):

<sup>1</sup>H NMR (500 MHz, CH<sub>3</sub>CN-*d*<sub>3</sub>): δ (ppm) 5.92 (t, *J* = 4.7 Hz, 1H), 5.23 (s, 2H), 5.01 (s, 2H), 4.27 (bs, 1H), 3.03 (bs, 1H), 2.35-2.31 (m, 2H), 1.46 (s, 9H); LRMS-ESI (*m/z*) calcd for [C<sub>13</sub>H<sub>18</sub>N<sub>4</sub>O<sub>4</sub>+H]<sup>+</sup>: 295.14; found: 295.1.

### 1-((benzyloxy)carbonyl)-1,4,5,6-tetrahydropyridazine-3-carboxylic acid (2-35b).



Benzyl hydrazinecarboxylate (6.35 g, 38.2 mmol, 1.0 equiv) was dissolved in MeOH (50-mL) and cooled to 0°C with an ice-water bath, followed by the addition of glacial HOAc (1.2-mL). A second solution containing methyl 5-bromo-2-oxopentanoate **2-27** (8.00 g, 38.2 mmol, 1.0 equiv) in MeOH (25-mL) was added dropwise to the cooled reaction over 15 min. The reaction was allowed to reach RT and stirred for an additional 30 min. TLC analysis indicates consumption of **2-27** and a product indicative of intermediate hydrazone formation. The mixture was neutralized with 3 M aqueous K<sub>2</sub>CO<sub>3</sub> and immersed into an oil-bath preheated to 60°C. The pH of the mixture was maintained between 4 and 7 with 3 M aqueous K<sub>2</sub>CO<sub>3</sub>. The reaction was heated at 60°C for 2h. After cooling to RT, the reaction was concentrated in vacuo and diluted with CH<sub>2</sub>Cl<sub>2</sub> (200-mL). The organic layer was washed with saturated aqueous NaHCO<sub>3</sub>, H<sub>2</sub>O, brine, dried over Na<sub>2</sub>SO<sub>4</sub>, filtered and concentrated in vacuo to give crude 1-benzyl 3-methyl 5,6-dihydropyridazine-1,3(4H)-dicarboxylate **2-35a** (11.4 g, crude weight, LRMS-ESI (*m/z*) calcd

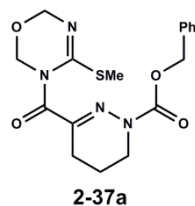
for  $[C_{14}H_{16}N_2O_4+H]^+$ : 277.12; found: 277.1.) as a yellow oil that was used in the subsequent step without further purification.

The crude ester **2-35a** was dissolved in THF (90-mL) at RT followed by the addition of LiOH (1.05 g, 45.8 mmol, 1.2 equiv, in H<sub>2</sub>O (15-mL)). The reaction mixture was stirred at RT for 15 min until judged complete by TLC analysis. The mixture was concentrated in vacuo to remove THF (approx. 90-mL) and neutralized with 3 M aqueous HCl to pH = 3. The precipitous acidic solution was extracted with CH<sub>2</sub>Cl<sub>2</sub> (2 × 200-mL) and combined organics were washed with brine (2 × 20-mL), dried over Na<sub>2</sub>SO<sub>4</sub>, filtered and concentrated in vacuo to give crude 1-((benzyloxy)carbonyl)-1,4,5,6-tetrahydropyridazine-3-carboxylic acid **2-35b** (8.5 g, 85%, crude) that was used in the subsequent step without further purification.

**1-((benzyloxy)carbonyl)-1,4,5,6-tetrahydropyridazine-3-carboxylic acid (2-35b):**

<sup>1</sup>H NMR (500 MHz, CHCl<sub>3</sub>-*d*<sub>1</sub>): δ (ppm) 7.43-7.29 (m, 5H), 5.29 (s, 2H), 3.79-3.74 (m, 2H), 2.53 (t, *J* = 6.4 Hz, 2H), 1.98-1.89 (m, 2H); LRMS-ESI (*m/z*) calcd for  $[C_{13}H_{14}N_2O_4+H]^+$ : 263.1; found: 263.1.

**benzyl 3-(4-(methylthio)-3,6-dihydro-2H-1,3,5-oxadiazine-3-carbonyl)-5,6-dihydropyridazine-1(4H)-carboxylate (2-37a)**

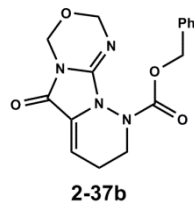


Crude acid **2-35b** (4.00 g, 15.3 mmol, 1.0 equiv), heterocycle **2-10** (2.41 g, 18.3 mmol, 1.2 equiv) and TBTU (5.14 g, 16.0 mmol, 1.05 equiv) were dissolved in DMF (76-mL) and cooled to 0°C with an ice-water bath followed by the addition of (*i*-Pr)<sub>2</sub>NEt (5.3-mL, 30.5 mmol, 2.0 equiv). The reaction was slowly warmed to RT and allowed to stir overnight. The mixture was diluted with EtOAc (200-mL) and washed with saturated aqueous NH<sub>4</sub>Cl (2 × 10-mL), H<sub>2</sub>O (8 × 10-mL), brine, dried over Na<sub>2</sub>SO<sub>4</sub>, filtered and concentrated in vacuo to give a crude foam further purified by flash column chromatography (hexanes/EtOAc gradient, 100% to (3:2)) to afford **2-37a** as a white solid (2.20 g, 38%).

**benzyl 3-(4-(methylthio)-3,6-dihydro-2H-1,3,5-oxadiazine-3-carbonyl)-5,6-dihydropyridazine-1(4H)-carboxylate (2-37a):**

<sup>1</sup>H NMR (500 MHz, CHCl<sub>3</sub>-*d*<sub>1</sub>): δ (ppm) 7.41-7.33 (m, 5H), 5.30 (s, 2H), 5.28 (s, 2H), 5.08 (s, 2H), 3.81-3.75 (t, *J* = 5.5 Hz, 2H), 2.51-2.49 (t, *J* = 6.4 Hz, 2H), 2.28 (s, 3H), 1.96-1.91 (m, 2H); LRMS-ESI (*m/z*) calcd for  $[C_{17}H_{20}N_4O_4S+H]^+$ : 377.13; found: 377.1.

### Cbz Monomer (2-37b).



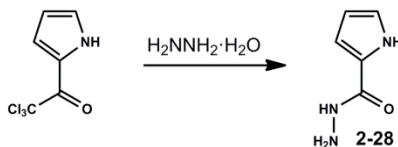
Purified **2-37a** (134 mg, 0.36 mmol, 1.0 equiv) was dissolved in CH<sub>2</sub>Cl<sub>2</sub> (3.6-mL) at RT followed by the addition of oxalyl chloride (34  $\mu$ L, 0.39 mmol, 1.05 equiv) via syringe. After stirring at RT for 1h, the reaction mixture was quenched by the addition of saturated aqueous NaHCO<sub>3</sub>. The mixture was diluted with CHCl<sub>3</sub> (10-mL) and the organic layer was separated, washed with H<sub>2</sub>O, brine, dried over Na<sub>2</sub>SO<sub>4</sub>, filtered and concentrated in vacuo to give **2-37b** as a crude foam (140 mg, quant. yield, >85% purity as determined by <sup>1</sup>H NMR)

**Note:** A purified yield was not obtained for **2-37b**.

### Cbz Monomer (2-37b):

<sup>1</sup>H NMR (500 MHz, CH<sub>3</sub>CN-*d*<sub>3</sub>):  $\delta$  (ppm) 7.38-7.33 (m, 5H), 5.99 (t, *J* = 4.6 Hz, 1H), 5.22 (s, 4H), 5.00 (s, 2H), 3.72 (bs, 2H) 2.46-2.43 (m, 2H); LRMS-ESI (*m/z*) calcd for [C<sub>16</sub>H<sub>16</sub>N<sub>4</sub>O<sub>4</sub>+H]<sup>+</sup>: 329.12; found: 329.1.

### 1H-pyrrole-2-carbohydrazide (2-28).

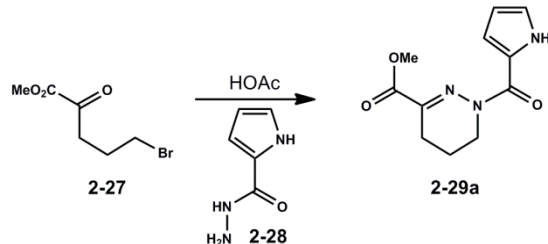


2,2,2-Trichloro-1-(1H-pyrrol-2-yl)ethanone (400 g, 1.9 mol) was suspended in H<sub>2</sub>O (200-mL) in a 5-L three-necked flask fitted with a mechanical stirring apparatus, reflux condenser and a 500-mL addition funnel. A solution of hydrazine hydrate (1-L, 11.3 mol, 6.0 equiv, 55 wt % in H<sub>2</sub>O) was added over 10 min. The heterogeneous reaction was heated to 70°C for 50 min with vigorous stirring. The gray suspension was cooled to RT, and the crude product was isolated by filtration, washed with H<sub>2</sub>O (3  $\times$  250-mL) and Et<sub>2</sub>O (3  $\times$  500-mL) and dried in vacuo to afford **2-28** as a gray solid (219 g, 93%). This material showed spectroscopic data consistent with literature and was used without further purification.<sup>[1]</sup>

### 1H-pyrrole-2-carbohydrazide (2-28):

<sup>1</sup>H NMR (500 MHz, DMSO-*d*<sub>6</sub>):  $\delta$  (ppm) 11.45 (bs, 1H), 9.27 (s, 1H), 6.86-6.83 (m, 1H), 6.77-6.74 (m, 1H), 6.08-6.03 (m, 1H), 4.33 (bs, 2H); <sup>13</sup>C NMR (125 MHz, DMSO-*d*<sub>6</sub>):  $\delta$  (ppm) 161.3, 124.9, 121.3, 109.6, 108.6; HRMS-ESI (*m/z*) calcd for [C<sub>5</sub>H<sub>7</sub>N<sub>3</sub>O+H]<sup>+</sup>: 126.0667; found: 126.0667; IR (neat)  $\nu_{\text{max}}$  (cm<sup>-1</sup>): 3302, 1618, 1508, 734.

## Methyl 1-(1H-pyrrole-2-carbonyl)-1,4,5,6-tetrahydropyridazine-3-carboxylate (2-29a).



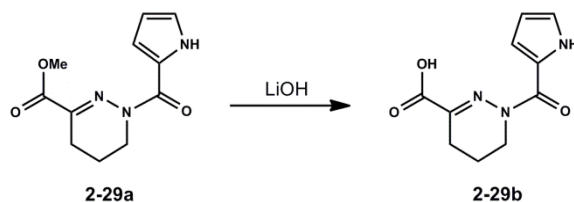
1H-pyrrole-2-carbohydrazide **2-28** (212 g, 1.7 mol, 1.0 equiv) was suspended in MeOH (1.6-L) in a 5-L three-necked flask fitted with a mechanical stirring apparatus, reflux condenser and a 500-mL addition funnel. The reaction was cooled to an internal temperature of 5°C with an ice-water bath. Acetic acid (49-mL) was added in a single portion followed by the dropwise addition of methyl 5-bromo-2-oxopentanoate **2-27** (354 g, 1.7 mol, 1.0 equiv) as a light brown solution in MeOH (950-mL) over 45 min.<sup>[2]</sup> The reaction becomes thick after approximately 20 min at which point the stirring rate was increased to afford a heterogeneous gray mixture. The ice-water bath was removed and the reaction was allowed to warm to RT over 1h. 3M aqueous K<sub>2</sub>CO<sub>3</sub> (150-mL) was added carefully and the reaction was stirred at RT for 15 min. The reaction was slowly heated to 65°C and additional 3M aqueous K<sub>2</sub>CO<sub>3</sub> (300-mL) was added slowly to maintain pH = 6. The reaction became dark and homogeneous. The dark solution was kept at 65°C for 1h (reaction complete by TLC). The mixture was cooled to 40°C and concentrated in vacuo to give a gray solid. The crude solid was dissolved in CHCl<sub>3</sub> (3-L) and H<sub>2</sub>O (750-mL). The biphasic mixture was filtered through a sintered glass funnel (medium frit) and partitioned in a separatory funnel. The aqueous phase was back-extracted with CHCl<sub>3</sub> (2 × 250-mL). Organics were combined and washed with H<sub>2</sub>O (2 × 500-mL), brine (250-mL), dried over Na<sub>2</sub>SO<sub>4</sub>, and concentrated in vacuo to give crude **2-29a** as a light yellow solid (382 g, 96%) that was used without further purification.

An analytical sample was obtained after purification by recrystallization from EtOAc.

### Methyl 1-(1H-pyrrole-2-carbonyl)-1,4,5,6-tetrahydropyridazine-3-carboxylate (2-29a):

*R<sub>f</sub>* = 0.50 hexanes / EtOAc (1:1); yellow needles from EtOAc (m.p. 143–145°C); <sup>1</sup>H NMR (600 MHz, CH<sub>3</sub>CN-*d*<sub>3</sub>): δ (ppm) 10.73 (bs, 1H), 7.26 (ddd, *J* = 2.8, 1.5, 0.8 Hz, 1H), 7.03 (ddd, *J* = 3.7, 1.5, 0.8 Hz, 1H), 6.23 (ddd, *J* = 3.7, 2.8, 0.8 Hz, 1H) 3.87 (s, 3H), 3.83-3.79 (m, 2H), 2.50 (t, *J* = 6.4 Hz, 2H), 1.93-1.88 (m, 2H); <sup>13</sup>C NMR (125 MHz, CH<sub>3</sub>CN-*d*<sub>3</sub>): δ (ppm) 165.3, 160.7, 140.1, 125.9, 124.0, 119.8, 110.4, 53.1, 40.2, 22.4, 17.0; HRMS-ESI (*m/z*) calcd for [C<sub>11</sub>H<sub>13</sub>N<sub>3</sub>O<sub>3</sub>+H]<sup>+</sup>: 236.1035; found: 236.1015; IR (neat) *v*<sub>max</sub> (cm<sup>-1</sup>): 3312, 1733, 1584, 1413.

### 1-(1H-pyrrole-2-carbonyl)-1,4,5,6-tetrahydropyridazine-3-carboxylic acid (2-29b).



Ester **2-29a** (407 g, 1.7 mol, 1.0 equiv) was suspended in a solution of THF/MeOH (2:1) (3.2-L) and cooled to an internal temperature of 5°C with an ice-water bath. A solution of LiOH (79 g, 3.5 mol, 2.0 equiv) in H<sub>2</sub>O (800-mL) was cooled to an internal temperature of 5°C and added to the suspension over 5 min via an addition funnel. The temperature was maintained and the reaction became homogeneous in 3 min. After 5 min, 3M HCl was added until pH = 6. The suspension was concentrated in vacuo to remove volatile organics and acidified to pH = 3 (3M HCl). The acidic solution was saturated with solid NaCl and extracted with CHCl<sub>3</sub> / MeOH (9:1) (3 × 1-L). Combined organics were washed with H<sub>2</sub>O, brine, dried over Na<sub>2</sub>SO<sub>4</sub> and concentrated in vacuo to give crude **2-29b** as a light tan solid (340 g, 89%) that was used without further purification.

An analytical sample was obtained after purification by recrystallization from CH<sub>2</sub>Cl<sub>2</sub>.

**1-(1H-pyrrole-2-carbonyl)-1,4,5,6-tetrahydropyridazine-3-carboxylic acid (2-29b):**

$R_f$  = 0.10 (streaks), CHCl<sub>3</sub> / MeOH (9:1); opaque needles from CHCl<sub>3</sub> (m.p. 208–209°C); <sup>1</sup>H NMR (500 MHz, DMSO-*d*<sub>6</sub>): δ (ppm) 13.00 (bs, 1H), 11.55 (bs, 1H), 7.43 (ddd, *J* = 2.8, 1.5, 0.8 Hz, 1H), 7.01 (ddd, *J* = 3.7, 1.5, 0.8 Hz, 1H), 6.17 (ddd, *J* = 3.7, 2.8, 0.8 Hz, 1H), 3.79-3.75 (m, 2H), 2.45 (t, *J* = 6.4 Hz, 2H), 1.87-1.81 (m, 2H); <sup>13</sup>C NMR (125 MHz, DMSO-*d*<sub>6</sub>): δ (ppm) 165.5, 160.2, 140.1, 123.8, 123.3, 119.0, 109.6, 39.0, 21.4, 16.2; HRMS-ESI (*m/z*) calcd for [C<sub>10</sub>H<sub>11</sub>N<sub>3</sub>O<sub>3</sub>+H]<sup>+</sup>: 222.0879; found: 222.0876; IR (neat)  $\nu_{\max}$  (cm<sup>-1</sup>): 3417, 3360, 2504, 1676, 1598.

**(1-(1H-pyrrole-2-carbonyl)-1,4,5,6-tetrahydropyridazin-3-yl)(4-(methylthio)-2H-1,3,5-oxadiazin-3(6H)-yl)methanone (2-30).**



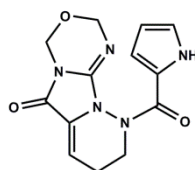
Crude acid **2-29b** (86 g, 0.39 mol, 1.0 equiv) was suspended in CH<sub>2</sub>Cl<sub>2</sub> (1.1-L) in a 3-L three-necked flask fitted with a mechanical stirring apparatus and an addition funnel. Oxalyl chloride (35-mL, 0.41 mol, 1.05 equiv) was added to the suspension via syringe over 2 min, followed by the addition of catalytic DMF (4 mmol, 0.01 equiv). The reaction color darkened over 30 min and was vigorously stirred at RT for 3h until formation of the acid chloride was determined complete by TLC / LC-MS analysis of a reaction aliquot quenched with MeOH. A solution of **2-10** (88 g, 0.66 mol, 1.7 equiv) in saturated aqueous NaHCO<sub>3</sub> (1.1-L) was carefully added to the reaction mixture over 5 min. The biphasic reaction mixture was stirred vigorously at RT for 12h. The two phases were separated and the aqueous layer was extracted with CHCl<sub>3</sub> (2 × 750-mL). Organics were combined and washed with saturated aqueous NaHCO<sub>3</sub> (250-mL), H<sub>2</sub>O (5 × 250-mL), brine (250-mL), dried over Na<sub>2</sub>SO<sub>4</sub> and concentrated in vacuo to give crude **2-30** as a light brown foam (87 g) that was used without further purification.

An analytical sample was obtained after purification by flash column chromatography (hexanes / EtOAc gradient, (4:1) to (1:1)).

**(1-(1H-pyrrole-2-carbonyl)-1,4,5,6-tetrahydropyridazin-3-yl)(4-(methylthio)-2H-1,3,5-oxadiazin-3(6H)-yl)methanone (2-30):**

$R_f$  = 0.45, hexanes / EtOAc (1:1);  $^1\text{H NMR}$  (600 MHz, benzene- $d_6$ ):  $\delta$  (ppm) 9.53 (bs, 1H), 7.51-7.48 (m, 1H), 6.41-6.39 (m, 1H), 6.18-6.15 (m, 1H), 4.99 (s, 2H), 4.91 (s, 2H), 3.50-3.46 (m, 2H), 2.00 (t,  $J$  = 6.8 Hz, 2H), 1.98 (s, 3H), 1.06-1.01 (m, 2H);  $^{13}\text{C NMR}$  (125 MHz,  $\text{CHCl}_3$ - $d_1$ ): 166.5, 160.5, 151.4, 142.9, 124.0, 122.7, 118.8, 110.3, 81.0, 74.0, 39.9, 22.5, 16.5, 14.7; **HRMS-ESI** ( $m/z$ ) calcd for  $[\text{C}_{14}\text{H}_{17}\text{N}_5\text{O}_3\text{S}+\text{H}]^+$ : 336.1130; found: 336.1144; **IR** (neat)  $\nu_{\text{max}}$  ( $\text{cm}^{-1}$ ): 3286, 2847, 1668, 1618, 1584.

**Monomer (2-26).**



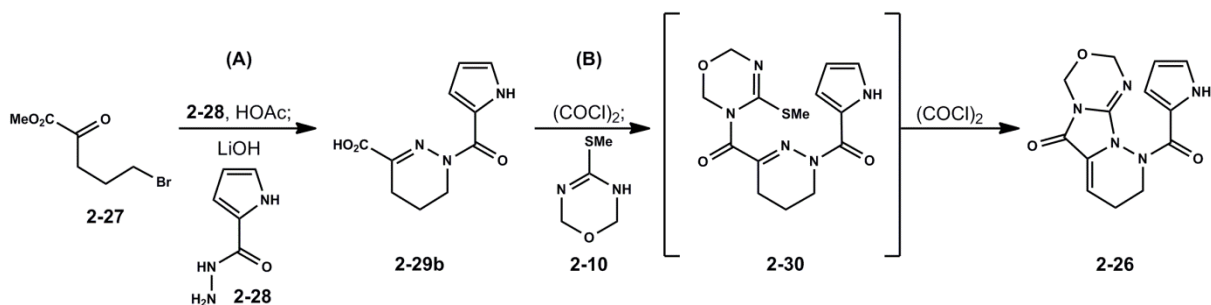
2-26

Crude **2-30** (87 g, 0.26 mol, 1.0 equiv) was dissolved in  $\text{CH}_2\text{Cl}_2$  (1.7-L) followed by the addition of oxalyl chloride (22-mL, 0.26 mol, 1.0 equiv) via syringe over 2 min. The reaction was stirred at RT and developed a deep red-orange color within 20 min. The solution began to precipitate the product as an orange solid as the reaction progressed. After 1h at RT the reaction was carefully quenched with saturated aqueous  $\text{NaHCO}_3$  (1-L). The biphasic mixture was separated and the aqueous layer extracted with  $\text{CHCl}_3$  ( $2 \times 750$ -mL). Organics were combined and washed with saturated aqueous  $\text{NaHCO}_3$  ( $3 \times 250$ -mL),  $\text{H}_2\text{O}$  ( $3 \times 250$ -mL), dried over  $\text{Na}_2\text{SO}_4$  and concentrated in vacuo to give crude **2-26** as a tan solid. The crude solid was dissolved in  $\text{CHCl}_3$  / MeOH (9:1) and adsorbed onto dry silica gel. Purification by flash column chromatography (hexanes / EtOAc gradient, (4:1) to 100% EtOAc) afforded **2-26** as a light yellow solid (53 g, 47% from **2-29b**).

**Monomer (2-26):**

$R_f$  = 0.3, hexanes / EtOAc (1:1); needles from EtOAc (m.p. 186–188°C);  $^1\text{H NMR}$  (600 MHz, DMSO- $d_6$ ):  $\delta$  (ppm) 11.79 (bs, 1H), 7.04 (ddd,  $J$  = 2.8, 1.5, 0.8 Hz, 1H), 6.73 (ddd,  $J$  = 3.7, 1.5, 0.8 Hz, 1H), 6.19 (ddd,  $J$  = 3.7, 2.8, 0.8 Hz, 1H), 5.98 (t,  $J$  = 4.7 Hz, 1H), 5.30 (s, 2H), 4.93 (s, 2H), 4.58 (bs, 1H), 3.21 (bs, 1H), 2.26 (bs, 2H);  $^1\text{H NMR}$  (600 MHz, DMSO- $d_6$ , 343K):  $\delta$  (ppm) 11.37 (bs, 1H), 7.02-6.99 (m, 1H), 6.74-6.70 (m, 1H), 6.20-6.17 (m, 1H), 5.95 (t,  $J$  = 4.7 Hz, 1H), 5.28 (s, 2H), 4.95 (s, 2H), 3.90 (bs, 2H), 2.32-2.29 (m, 2H);  $^{13}\text{C NMR}$  (125 MHz, DMSO- $d_6$ ):  $\delta$  (ppm) 164.1, 155.9, 139.9, 128.5, 124.2, 122.1, 115.1, 109.9, 106.6, 77.5, 71.0, 44.3, 22.2; **HRMS-ESI** ( $m/z$ ) calcd for  $[\text{C}_{13}\text{H}_{13}\text{N}_5\text{O}_3+\text{H}]^+$ : 288.1082; found: 288.1096; **IR** (neat)  $\nu_{\text{max}}$  ( $\text{cm}^{-1}$ ): 3183, 1751, 1691, 1386.

## Synthesis of Monomer (2-29).



### Procedure (A).

#### 1-(1H-pyrrole-2-carbonyl)-1,4,5,6-tetrahydropyridazine-3-carboxylic acid (2-29b).

**2-28** (19.6 g, 0.16 mmol, 1.0 equiv) was suspended in MeOH (155-mL) in a 500-mL three-necked flask fitted with a reflux condenser and a 150-mL addition funnel. The reaction was cooled to an internal temperature of 5°C with an ice-water bath. Acetic acid (2.4-mL) was added in a single portion followed by the dropwise addition of **2-27** (34.5 g, 0.16 mol, 1.0 equiv) as a light brown solution in MeOH (95-mL) over 45 min. The reaction solidifies after approximately 20 min at which point the stirring rate was increased to afford a heterogeneous gray mixture. The ice-water bath was removed and the reaction allowed to stir at RT for 1h. An aqueous solution of 3M K<sub>2</sub>CO<sub>3</sub> (30-mL) was carefully added and the reaction was stirred at RT for 15 min. The reaction was slowly heated to 65°C and an additional volume of 3M K<sub>2</sub>CO<sub>3</sub> (5-mL) was added slowly to maintain a pH = 6. The reaction became dark and homogeneous. The dark solution was kept at 65°C for 1h until complete by TLC analysis. The reaction was cooled to RT and diluted with THF (200-mL). The solution was cooled to an internal temperature of -5°C with an ice / saturated aqueous NH<sub>4</sub>Cl bath. A solution of LiOH (7.2 g, 0.31 mol, 2.0 equiv, 100-mL H<sub>2</sub>O) was added in a single portion and stirred for 1h at -5°C until hydrolysis was judged complete by TLC analysis. The reaction was adjusted with 3M HCl to pH = 6 and volatiles were removed in vacuo. The aqueous solution was acidified with 3M HCl to pH = 3. The acidic solution was saturated with NaCl and extracted CHCl<sub>3</sub> / MeOH (9:1) (3×500-mL). Combined organics were washed with H<sub>2</sub>O, brine, dried over Na<sub>2</sub>SO<sub>4</sub> and concentrated in vacuo to give crude **2-29** as a light tan solid (30.9 g, 89%) that was used without further purification.

### Procedure (B).

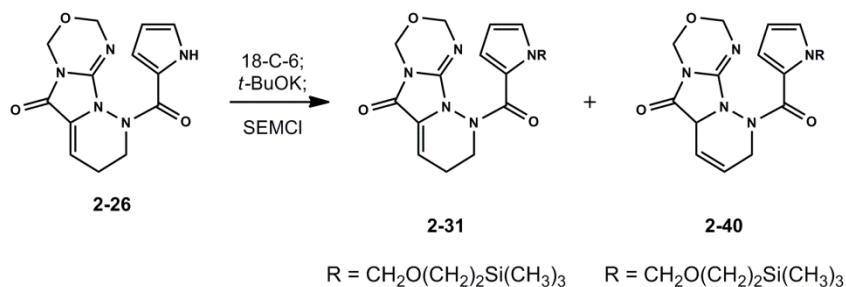
#### Monomer (2-26).

A portion of crude acid **2-29b** (26.9 g, 0.12 mol, 1.0 equiv) was suspended in CH<sub>2</sub>Cl<sub>2</sub> (350-mL) in a 1-L flask. Oxalyl chloride (9.9-mL, 0.12 mol, 0.95 equiv) was added to the heterogeneous solution via syringe over 2 min, followed by the addition of catalytic DMF (94-μL, 1 mmol, 0.01 equiv). The reaction color darkened over 30 min and was vigorously stirred at RT for 3h until formation of the acid chloride was determined by complete by TLC/LC-MS analysis of a reaction aliquot quenched with MeOH. The heterogeneous solution was cooled to an internal temperature of 5°C with an ice-water bath. A solution of **2-10** (28.9 g, 0.22 mol, 1.8 equiv) and



Et<sub>3</sub>N (30.5-mL, 0.22 mol, 1.8 equiv) in CH<sub>3</sub>CN (350-mL) was added to the reaction via cannula. The reaction was allowed to reach RT and stirred for 5h until coupling was judged complete by TLC analysis (via intermediate **2-30**). A second portion of oxalyl chloride (9.9-mL, 0.12 mol, 0.95 equiv) was added via syringe and the dark solution was stirred for 45 min. The reaction was diluted with CHCl<sub>3</sub> (1-L) and washed with H<sub>2</sub>O (2 × 250-mL), saturated aqueous NH<sub>4</sub>Cl (2 × 250-mL), saturated aqueous NaHCO<sub>3</sub> (2 × 250-mL), dried over Na<sub>2</sub>SO<sub>4</sub> and concentrated in vacuo to give crude **2-26** as a tan solid. The crude solid was dissolved in CHCl<sub>3</sub> / MeOH (9:1) and adsorbed onto dry silica gel. Purification by flash column chromatography (hexanes / EtOAc gradient, (4:1) to 100% EtOAc) afforded **2-26** as a light yellow solid (19.3 g, 55% from **2-29b**).

### SEM Monomer (**2-31**).



A 3-L three-necked flask fitted with a mechanical stirring apparatus was charged with **2-26** (72.5 g, 0.25 mol, 1.0 equiv) and 18-crown-6 ether (70.1 g, 0.27 mol, 1.05 equiv, azeotroped from benzene) suspended in THF (2.5-L). The heterogeneous yellow solution was cooled to an internal temperature of -5°C with an ice / saturated aqueous NH<sub>4</sub>Cl bath. Potassium tert-butoxide (28.9 g, 0.26 mol, 1.02 equiv) was added in a single portion. The reaction became immediately homogeneous with a dark reddish-purple color. The temperature was maintained by the addition of ice to the bath. The solution was stirred for 3 min followed by the addition of 2-(trimethylsilyl)ethoxymethyl chloride (48.4-mL, 0.273 mol, 1.08 equiv) via syringe over 5 min. The solution became gradually lighter in color and was quenched after 10 min with saturated aqueous NH<sub>4</sub>Cl. The volume of THF was reduced in vacuo and the reaction was diluted with EtOAc (1.5-L) and washed with H<sub>2</sub>O (2 × 200-mL), 0.5M KH<sub>2</sub>PO<sub>4</sub> buffer (pH = 7.8) (3 × 200-mL), dried over Na<sub>2</sub>SO<sub>4</sub> and concentrated in vacuo to give a crude orange oil which was purified by flash column chromatography (hexanes / EtOAc gradient, (9:1) to (3:7)) providing deconjugated isomer **2-40** (7.4 g, 7%) as a yellow oil followed by **2-31** (63.3 g, 60%) as a yellow foam.

### Deconjugated monomer (**2-40**):

$R_f = 0.75$ , hexanes / EtOAc (1:1); <sup>1</sup>H NMR (500 MHz, CH<sub>3</sub>CN-*d*<sub>3</sub>): δ (ppm) 7.03 (dd, *J* = 2.6, 1.7 Hz, 1H), 6.94 (dd, *J* = 3.8, 1.7 Hz, 1H), 6.18-6.14 (m, 1H), 6.12 (dd, *J* = 3.8, 2.7 Hz, 1H), 5.90 (dddd, *J* = 6.5, 2.2, 2.2, 2.2 Hz, 1H), 5.62 (d, *J* = 10.2 Hz, 1H) 5.52 (d, *J* = 10.2 Hz, 1H), 5.25 (d, *J* = 8.8 Hz, 1H), 5.03 (d, *J* = 8.8 Hz, 1H), 4.96, 4.92 (ABq, *J*<sub>AB</sub> = 11.6 Hz, 2H), 4.71-4.63 (m, 1H), 4.58-4.54 (m, 1H), 3.77-3.70 (m, 1H), 3.46-3.40 (m, 2H), 0.85-0.80 (m, 2H), -0.05 (s, 9H); <sup>13</sup>C NMR (125 MHz, CH<sub>3</sub>CN-*d*<sub>3</sub>): δ (ppm) 166.5, 164.5, 146.5, 128.7, 128.4, 123.8, 121.1, 117.6, 108.5, 79.2, 77.8, 72.4, 66.5, 58.9, 39.3, 18.4, -1.4; HRMS-ESI (*m/z*) calcd for [C<sub>19</sub>H<sub>27</sub>N<sub>5</sub>O<sub>4</sub>Si+H]<sup>+</sup>: 418.1911; found: 418.1913; IR (neat)  $\nu_{\text{max}}$  (cm<sup>-1</sup>): 2953, 2896, 1763, 1694, 1643.

**SEM Monomer (2-31):**

$R_f = 0.7$ , hexanes / EtOAc (1:1);  $^1\text{H NMR}$  (500 MHz,  $\text{CH}_3\text{CN}-d_3$ ):  $\delta$  (ppm) 7.13 (dd,  $J = 2.8$ , 1.5 Hz, 1H), 6.87 (dd,  $J = 3.7$ , 1.5 Hz, 1H), 6.19 (dd,  $J = 3.7$ , 2.8 Hz, 1H), 5.89 (t,  $J = 4.6$  Hz, 1H), 5.23 (bs, 2H), 4.93 (s, 2H), 3.39 (t,  $J = 8.3$  Hz, 2H), 2.30-2.26 (m, 2H), 0.82 (t,  $J = 8.3$  Hz, 2H), -0.05 (s, 9H). (some  $^1\text{H}$  signals too broad to observe at RT – see  $^1\text{H NMR}$  @ 343K)  $^1\text{H NMR}$  (600 MHz,  $\text{CH}_3\text{CN}-d_3$ , 343K):  $\delta$  (ppm) 7.14-7.10 (m, 1H), 6.87-6.82 (m, 1H), 6.24-6.19 (m, 1H), 5.94-5.90 (m, 1H), 5.53 (s, 2H), 5.25 (s, 2H), 4.97 (s, 2H), 4.05-3.88 (m, 2H), 3.60-3.49 (m, 2H), 2.39-2.32 (m, 2H), 0.94-0.85 (m, 2H), 0.01 (s, 9H). (resolution broadened @ 343K);  $^{13}\text{C NMR}$  (125 MHz,  $\text{CH}_3\text{CN}-d_3$ ):  $\delta$  (ppm) 166.1, 157.3, 141.0, 130.3, 130.0, 123.0, 119.0, 109.1, 106.5, 79.1, 77.6, 72.3, 66.5, 48.1, 23.4, 18.3, -1.5; **HRMS-ESI** ( $m/z$ ) calcd for  $[\text{C}_{19}\text{H}_{27}\text{N}_5\text{O}_4\text{Si}+\text{H}]^+$ : 418.1911; found: 418.1904; **IR** (neat)  $\nu_{\text{max}}$  ( $\text{cm}^{-1}$ ): 2953, 2893, 1747, 1704, 1685.

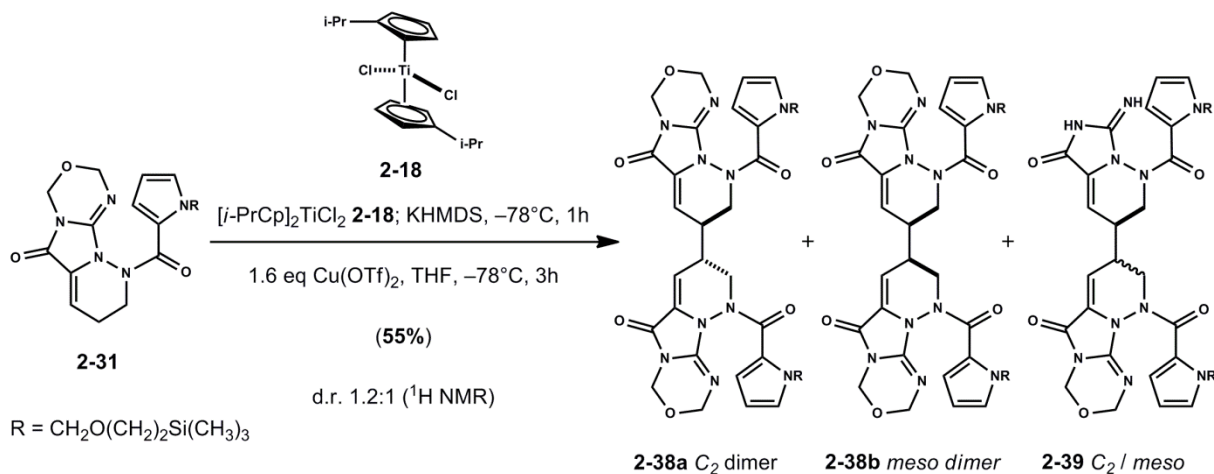
**Table 2.1** Optimization of silylethylmethoxylation procedure for the preparation of **2-31**  
Conversion of monomer **2-26** to derivative **2-31**

Entry	$\text{E}^+$ / Equiv	Base / Equiv	Solvent	Additive / Notes	Yield (%)
1	SEMCl / 1.1	KHMDS / 1.05	THF (0.15 M)	-20°C to RT (1h) + (21%) <b>2-26</b>	(41%)
2	SEMCl / 1.1	KHMDS / 1.05	THF (0.15 M)	-20°C to RT (1h)	(36%)
3	SEMCl / 1.1	<i>t</i> -BuOK / 1.1	THF (0.15 M)	-10°C to RT (1.5h)	(48%)
4	SEMCl / 1.2	<i>t</i> -BuOK / 1.02	THF (0.15 M)	-10°C to RT (10 min)	(60%)

**For record:** with regard to the conversion of **2-26** to **2-31** the following alternative conditions afforded **2-31** in poor yield.

Entry	Poor reactions: (yield not determined, TLC / $^1\text{H NMR}$ analysis of crude reaction)
1a	KHMDS (1.05 equiv), THF (0.2 M), -40°C; SEMCl (1.1 equiv), to RT
1b	inverse addition: same as 1a, addition of KHMDS to substrate with SEMCl, THF (0.2 M), -40°C
2	KH (1.1 equiv, 30 wt % disp. in oil), THF (0.2M), 0°C to RT; SEMCl (1.1 equiv), 0°C to RT
3	NaH (1.2 equiv, solid), DMF (0.3 M), 0°C to RT; SEMCl (1.1 equiv), 0°C to RT
4	substrate in DMF (0.2 M) with SEMCl (1.1 equiv) at RT (forms precipitate, not product)
5	<i>t</i> -BuOK (1.0 equiv), THF (0.2 M), RT; SEMCl (1.1 equiv), RT (initial attempt at 'standard conditions')

## Dimerization of SEM Monomer (2-31).



A 250-mL flask was charged with **2-31** (5.62 g, 13.5 mmol, 1.0 equiv) and *i*-PrCp<sub>2</sub>TiCl<sub>2</sub> (4.71 g, 14.2 mmol, 1.05 equiv) and dried azeotropically from benzene (3×20-mL).<sup>[3]</sup> The dried red solid was dissolved in degassed THF (100-mL) and cooled to  $-78^\circ\text{C}$ .<sup>[4]</sup> KHMDS (32.4-mL, 16.2 mmol, 1.2 equiv, 0.5 M in toluene) was added via syringe over 5 min. The homogeneous red solution became dark green upon addition of KHMDS. The enolate solution was stirred at  $-78^\circ\text{C}$  for 45 min at which point a slurry of Cu(OTf)<sub>2</sub> in degassed THF (55-mL) was added quickly via syringe (13 gauge needle). The heterogeneous dark brown mixture was stirred at  $-78^\circ\text{C}$  for 3h and quenched with 20-mL of 0.5M EDTA (pH = 8.5). The resultant slurry was warmed to RT, diluted with EtOAc (300-mL) and washed with 0.5M EDTA (3×100-mL), H<sub>2</sub>O (2×50-mL), brine (50-mL), dried over Na<sub>2</sub>SO<sub>4</sub> and concentrated in vacuo to give a crude red solid. Purification by flash column chromatography (hexanes / EtOAc gradient, (7:3) to 100% EtOAc) gave **2-38a**:**2-38b** (1.2:1) (3.21 g, 55%) followed by impure **2-39** (1.33 g, 25%) after column flushing (EtOAc / MeOH (9:1)). The mixture **2-38a**:**2-38b** was dissolved in CH<sub>3</sub>CN (13-mL) and allowed to crystallize out **2-38b** at 4°C over 12h. The mother liquor enriched in **2-38a** was concentrated in vacuo and separated from remaining **2-38b** by flash column chromatography (CHCl<sub>3</sub> / EtOAc slow gradient, (9:1) to 100% EtOAc) to provide **2-38a** (1.69 g, 30%) as a yellow foam.

### $\text{C}_2$ -Dimer (**2-38a**):

$R_f = 0.45$ , CHCl<sub>3</sub> / EtOAc (1:3);  $^1\text{H NMR}$  (500 MHz, DMSO-*d*<sub>6</sub>, 373K):  $\delta$  (ppm) 7.22 (s, 2H), 6.75-6.73 (m, 2H), 6.20-6.17 (m, 2H), 5.82 (d,  $J = 2.4$  Hz, 2H), 5.51 (d,  $J = 9.9$  Hz, 2H), 5.42 (d,  $J = 9.9$  Hz, 2H), 5.26, 5.24 (ABq,  $J_{AB} = 8.5$  Hz, 4H), 4.92 (s, 4H), 4.05-3.97 (m, 2H), 3.72-3.64 (m, 2H), 3.46 (t,  $J = 8.1$  Hz, 4H), 2.56-2.52 (m, 2H), 0.82-0.77 (m, 4H), -0.03 (s, 18H);  $^{13}\text{C NMR}$  (150 MHz, CH<sub>3</sub>CN-*d*<sub>3</sub>, 343K):  $\delta$  (ppm) 164.0, 155.8, 139.6, 129.8, 128.7, 122.2, 117.4, 108.3, 104.9, 78.1, 76.7, 71.3, 65.8, 47.6, 35.4, 17.5, -2.5; **HRMS-ESI** ( $m/z$ ) calcd for [C<sub>38</sub>H<sub>52</sub>N<sub>10</sub>O<sub>8</sub>Si<sub>2</sub>+H]<sup>+</sup>: 833.3586; found: 833.3685; **IR** (neat)  $\nu_{\text{max}}$  (cm<sup>-1</sup>): 2953, 2893, 1749, 1703, 1682, 1415, 1080.

### Meso -Dimer (2-38b):

$R_f = 0.45$ ,  $\text{CHCl}_3 / \text{EtOAc}$  (1:3); light yellow needles from  $\text{CH}_3\text{CN}$  (m.p. 238–241°C);  $^1\text{H NMR}$  (500 MHz,  $\text{DMSO-}d_6$ , 373K):  $\delta$  (ppm) 7.24–7.22 (m, 2H), 6.79 (dd,  $J = 3.8, 1.4$  Hz, 2H), 6.19 (dd,  $J = 3.8, 2.7$  Hz, 2H), 5.60–5.58 (m, 2H), 5.51, 5.45 (ABq,  $J_{AB} = 10.1$  Hz, 4H), 5.26, 5.21 (ABq,  $J_{AB} = 8.6$  Hz, 4H), 4.91 (s, 4H), 4.06–3.97 (m, 2H), 3.86–3.78 (m, 2H), 3.46 (t, 8.0 Hz, 4H), 2.52–2.48 (m, 2H), 0.82–0.78 (m, 4H), -0.03 (s, 18H);  $^{13}\text{C NMR}$  (150 MHz,  $\text{DMSO-}d_6$ , 343K):  $\delta$  (ppm) 163.8, 155.7, 139.5, 130.0, 128.6, 122.7, 117.0, 108.4, 105.2, 78.0, 76.7, 71.3, 65.7, 47.2, 35.9, 17.8, -1.4; **HRMS-ESI** ( $m/z$ ) calcd for  $[\text{C}_{38}\text{H}_{52}\text{N}_{10}\text{O}_8\text{Si}_2+\text{H}]^+$ : 833.3586; found: 833.3594; **IR** (neat)  $\nu_{\text{max}}$  ( $\text{cm}^{-1}$ ): 3100, 2955, 1748, 1707, 1671, 1409, 1080.

Crystals of **2-38b** suitable for X-ray diffraction analysis were obtained from a standing solution of **2-38b** in  $\text{CH}_3\text{CN}$  at 4°C. (CCDC 859079)

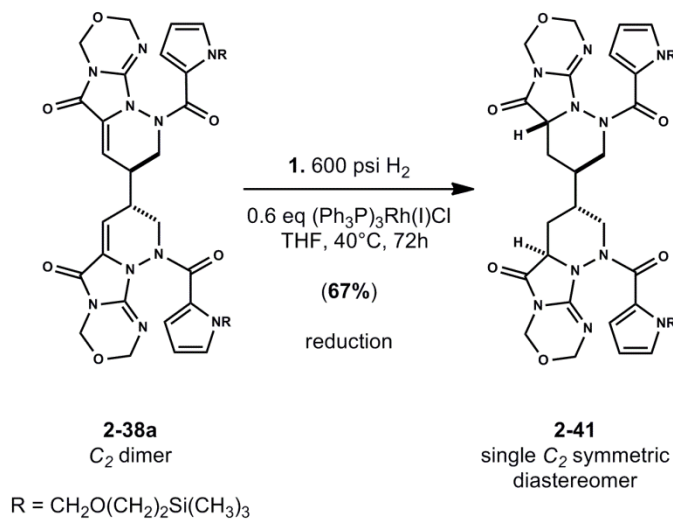
An analytical sample of **2-39** (**2-HCO<sub>2</sub>H**) was obtained after purification by HPLC.

**HPLC Conditions:** Waters Sunfire C18 column (19 × 250-mm) with UV detection at 280-nm; Solution A:  $\text{H}_2\text{O}$  w/0.1% formic acid and Solution B:  $\text{CH}_3\text{CN}$  w/0.1% formic acid; increase gradient of Solution B from 20% to 100%, 0-15 min; flow rate: 20-mL/min.

### (2-39) (2-HCO<sub>2</sub>H):

$R_f = 0.1$  (streaks),  $\text{EtOAc} / \text{MeOH}$  (2:1);  $^1\text{H NMR}$  (600 MHz,  $\text{DMSO-}d_6$ , 373K):  $\delta$  (ppm) 7.91–7.47 (bs, 1H), 7.25–7.20 (m, 2H), 6.80–6.69 (m, 2H), 6.23–6.16 (m, 2H), 5.82–5.67 (m, 1H), 5.57–5.40 (m, 6H), 5.27–5.19 (m, 2H), 4.94–4.88 (m, 2H), 4.10–3.56 (m, 4H), 3.53–3.42 (m, 4H), 2.46–2.40 (m, 2H), 0.86–0.77 (m, 4H), -0.03 (18H); **HRMS-ESI** ( $m/z$ ) calcd for  $[\text{C}_{36}\text{H}_{50}\text{N}_{10}\text{O}_7\text{Si}_2+\text{H}]^+$ : 791.3481; found: 791.3514.

### Reduced C<sub>2</sub> Dimer (2-41).



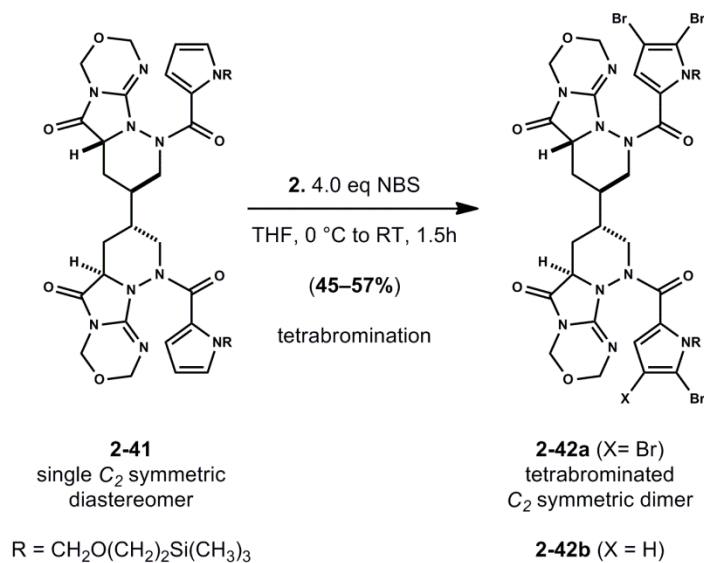
$\text{ClRh}(\text{PPh}_3)_3$  (2.07 g, 22 mmol, 0.4 equiv) was suspended in THF (100-mL, sparged with Ar) and sparged with H<sub>2</sub> (1 atm) via syringe until the red solution became homogeneous (15 min). The

catalyst solution was added to a 600-mL Parr bomb vessel followed by a yellow solution of **2-38a** (4.67 g, 56 mmol, 180-mL THF). The reaction vessel was sealed and purged with H<sub>2</sub> (3 × 600 psi) while stirring. The reaction vessel was pressurized with H<sub>2</sub> (600 psi), slowly heated to 40°C, and allowed to stir for 48h. A second portion of catalyst (1.03 g, 11 mmol, 0.2 equiv, 20-mL THF) was added at RT and the reaction was stirred at 40°C under H<sub>2</sub> (600 psi) for an additional 24h until completion. The red solution was concentrated in vacuo and diluted with EtOAc (300 mL). The organic solution was washed with saturated aqueous NaHCO<sub>3</sub> (3×50-mL), H<sub>2</sub>O (50-mL), dried over Na<sub>2</sub>SO<sub>4</sub> and concentrated in vacuo to give a crude red solid. The crude solid was dissolved in CHCl<sub>3</sub> and filtered before purification by flash column chromatography (CHCl<sub>3</sub>/ EtOAc gradient, 100% CHCl<sub>3</sub> to (1:4)) afforded **2-41** (3.16 g, 67%) as a light tan foam.

#### Reduced C<sub>2</sub> Dimer (**2-41**):

$R_f = 0.3$ , CHCl<sub>3</sub> / EtOAc (1:4); <sup>1</sup>H NMR (500 MHz, CH<sub>3</sub>CN-*d*<sub>3</sub>): δ (ppm) 7.03 (dd, *J* = 2.8, 1.6 Hz, 2H), 6.89 (dd, *J* = 3.8, 1.6 Hz, 2H), 6.08 (dd, *J* = 3.8, 2.8 Hz, 2H), 5.67 (d, *J* = 10.1 Hz, 2H), 5.44 (d, *J* = 10.1 Hz, 2H), 5.21 (d, *J* = 8.7 Hz, 2H), 5.10 (*J* = 8.7 Hz, 2H), 4.96 (bs, 4H), 4.53-4.49 (m, 2H), 3.82 (dd, *J* = 11.7, 5.0 Hz, 2H) 3.48-3.39 (m, 4H), 2.64 (dd, *J* = 12.9, 11.1 Hz, 2H), 2.19-2.13 (m, 2H), 1.76-1.67 (m, 2H), 1.53-1.44 (m, 2H), 0.89-0.78 (m, 4H), -0.04 (s, 18H); <sup>13</sup>C NMR (125 MHz, CH<sub>3</sub>CN-*d*<sub>3</sub>): δ (ppm) 168.3, 165.4, 145.4, 128.7, 124.0, 117.2, 108.5, 79.2, 77.8, 72.4, 66.4, 56.9, 44.5, 36.0, 30.0, 18.4, -1.3; HRMS-ESI (*m/z*) calcd for [C<sub>38</sub>H<sub>56</sub>N<sub>10</sub>O<sub>8</sub>Si<sub>2</sub>+H]<sup>+</sup>: 837.3900; found: 837.3918; IR (neat)  $\nu_{\max}$  (cm<sup>-1</sup>): 3056, 2953, 1759, 1695, 1948, 1436.

#### Oxidation of (**2-41**) to provide brominated dimers (**2-42a**) and (**2-42b**).



N-bromosuccinimide (NBS) (3.96 g, 22.3 mmol, 4.05 equiv) was added in a single portion to a solution of **2-41** (4.60 g, 5.5 mmol, 1.0 equiv) in THF (27.5-mL) at 0°C in a 100-mL flask wrapped in aluminum foil. The dark brown solution was stirred at 0°C for 1.5h and quenched with Na<sub>2</sub>S<sub>2</sub>O<sub>3</sub> (5.0-mL, 0.3M in H<sub>2</sub>O) and allowed to warm to RT. The reaction mixture was diluted with EtOAc (250-mL) and washed with H<sub>2</sub>O (8×20-mL), dried over Na<sub>2</sub>SO<sub>4</sub> and concentrated in vacuo to give a crude tan solid. The crude solid was purified by flash column

chromatography (CHCl<sub>3</sub> / EtOAc gradient, 100% CHCl<sub>3</sub> to (1:4)) to give tetrabrominated **2-42a** (3.50 g, 55%) as a light tan solid followed by tribrominated **2-42b** (0.60 g, 9%) as a light tan solid.

**(2-42a):**

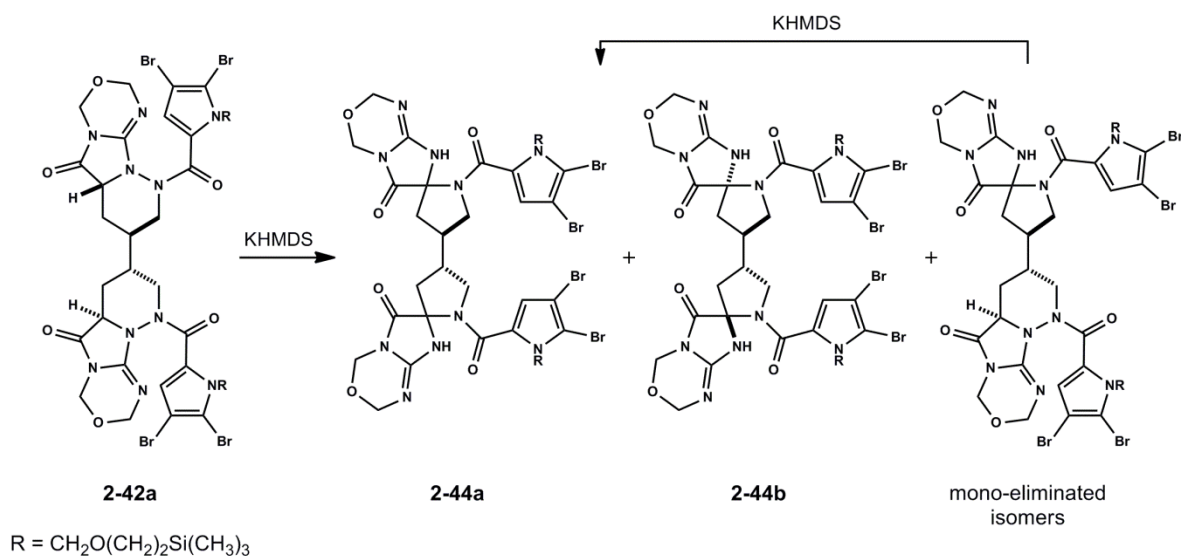
$R_f = 0.6$ , CHCl<sub>3</sub> / EtOAc (1:4); <sup>1</sup>H NMR (600 MHz, CHCl<sub>3</sub>-d<sub>1</sub>): δ (ppm) 6.96 (s, 2H), 5.86 (d, *J* = 10.5 Hz, 2H), 5.45 (d, *J* = 10.5 Hz, 2H), 5.40 (d, *J* = 8.7 Hz, 2H), 5.13 (d, *J* = 10.9, 2H), 5.06 (d, *J* = 10.9 Hz, 2H), 5.04 (d, *J* = 8.7 Hz, 2H), 4.61-4.57 (m, 2H), 3.76 (dd, *J* = 11.7, 4.9 Hz, 2H), 3.53-3.49 (m, 4H), 2.73-2.66 (m, 2H), 2.28-2.22 (m, 2H), 1.77-1.70 (m, 2H), 1.41-1.34 (m, 2H), 0.95-0.78 (m, 4H), -0.01 (s, 18H); <sup>13</sup>C NMR (150 MHz, CHCl<sub>3</sub>-d<sub>1</sub>): δ (ppm) 166.9, 164.1, 144.2, 125.3, 117.8, 111.9, 99.9, 78.7, 75.5, 71.6, 66.5, 56.3, 44.3, 35.0, 30.0, 18.2, -1.2; **HRMS-ESI** (*m/z*) calcd for [C<sub>38</sub>H<sub>52</sub>Br<sub>4</sub>N<sub>10</sub>O<sub>8</sub>Si<sub>2</sub>+H]<sup>+</sup>: 1153.0286; found: 1153.0455; **IR** (neat)  $\nu_{\max}$  (cm<sup>-1</sup>): 2952, 2884, 1759, 1695, 1655, 1423.

**(2-42b):**

$R_f = 0.55$ , CHCl<sub>3</sub> / EtOAc (1:4); <sup>1</sup>H NMR (600 MHz, CH<sub>3</sub>CN-d<sub>3</sub>): δ (ppm) 6.99 (s, 1H), 6.93 (d, *J* = 4.0 Hz, 1H), 6.22 (d, *J* = 4.0 Hz, 1H), 5.69 (dd, *J* = 10.6, 8.5 Hz, 2H), 5.58 (dd, *J* = 10.6, 8.5 Hz, 2H), 5.20 (dd, *J* = 8.7, 2.6 Hz, 2H), 5.10, 5.09 (ABq, *J*<sub>AB</sub> = 8.6, 2H), 4.98-4.94 (m, 4H), 4.51-4.48 (m, 1H), 4.48-4.46 (m, 1H), 3.84 (dd, *J* = 11.7, 5.0 Hz, 1H), 3.81 (dd, *J* = 11.7, 5.0 Hz, 1H), 3.55-3.48 (m, 4H), 2.66 (t, *J* = 4.6 Hz, 2H), 2.20-2.16 (m, 2H), 1.77- 1.70 (m, 2H), 1.51, 1.47 (ABq, *J*<sub>AB</sub> = 4.0 Hz, 2H), 0.91-0.79 (m, 4H), -0.031 (s, 9H), -0.03 (s, 9H); **HRMS-ESI** (*m/z*) calcd for [C<sub>38</sub>H<sub>53</sub>Br<sub>3</sub>N<sub>10</sub>O<sub>8</sub>Si<sub>2</sub>+H]<sup>+</sup>: 1073.1198; found: 1073.1224; **IR** (neat)  $\nu_{\max}$  (cm<sup>-1</sup>): 2952, 2889, 1761, 1698, 1659, 1426.

**Note:** Typical yields for **2-42a** ranged from (45–57%). Lower yields are due to incomplete bromination, in which case **2-42b** was isolated as a minor product. **2-42b** can be resubjected to NBS bromination conditions although this process is not optimized.

### Synthesis of Spiroaminals (2-44) via base promoted hydrazide fragmentation



A solution of KHMDS (8.4-mL, 4.2 mmol, 3.2 equiv, 0.5M in toluene) was added to a suspension of 18-crown-6 (1.4 g, 5.3 mmol, 4.0 equiv) in THF (2-mL) cooled to  $-78^{\circ}\text{C}$ . After stirring at  $-78^{\circ}\text{C}$  for 5 min, a solution of **2-42a** (1.52 g, 1.3 mmol) in THF (22-mL) was added dropwise via syringe over 15 min. The reaction mixture was stirred at  $-78^{\circ}\text{C}$  for 140 min. The reaction was quenched with the addition of EtOAc (5-mL) followed by 0.5M  $\text{KH}_2\text{PO}_4$  buffer (20-mL, pH = 7.8). The mixture was warmed to RT and diluted with EtOAc (250-mL). The organic phase was washed with 0.5M  $\text{KH}_2\text{PO}_4$  buffer (3 $\times$ 50-mL),  $\text{H}_2\text{O}$ , brine, dried over  $\text{Na}_2\text{SO}_4$  and concentrated in vacuo to give a crude tan solid which was purified by flash column chromatography (pre-treated silica with 1%  $\text{Et}_3\text{N}$  in hexanes) and eluted (2% to 6% to 15% MeOH in  $\text{CHCl}_3$ ) to give bis-spirocycle **2-44a** as a pale yellow foam (220 mg, 15%) and  $\text{C}_2$  bis-spirocycle **2-44b** as a pale yellow foam (604 mg, 39%). Tentatively assigned mono-eliminated isomers were also recovered (310 mg, 20%) and could be resubjected to the above reaction conditions to afford **2-44a** and **2-44b**.

**Bis-spirocycle (2-44a):**

$^1\text{H NMR}$  (500 MHz,  $\text{CH}_3\text{CN}-d_3$ ):  $\delta$  (ppm) 6.70 (s, 2H), 5.81 (s, 1H), 5.49 (s, 1H), 5.37 (s, 2H), 5.21-4.78 (m, 10H), 3.9 (s, 2H), 3.60-3.28 (m, 8H), 2.48-2.10 (m, 4H), 0.82 (s, 4H), -0.03 (s, 18H);  $^{13}\text{C NMR}$  (125 MHz,  $\text{CH}_3\text{CN}-d_3$ ):  $\delta$  (ppm) 170.3, 169.3, 159.6, 147.5, 127.6, 127.5, 115.8, 111.1, 110.3, 99.2, 99.1, 78.5, 77.8, 76.9, 75.5, 72.2, 72.1, 66.0, 54.5, 53.6, 41.53, 40.9, 39.7, 17.47, 17.35, -0.18; **HRMS-ESI** ( $m/z$ ) calcd for  $[\text{C}_{38}\text{H}_{52}\text{Br}_4\text{N}_{10}\text{O}_8\text{Si}_2+\text{H}]^+$ : 1153.0286; found: 1153.0409; **IR** (neat)  $\nu_{\text{max}}$  ( $\text{cm}^{-1}$ ): 2952, 2920, 2847, 1761, 1702, 1641, 1431.

**$\text{C}_2$  Bis-spirocycle (2-44b):**

$^1\text{H NMR}$  (500 MHz, acetone- $d_6$ ):  $\delta$  (ppm) 6.80 (s, 2H), 5.64-5.50 (m, 4H), 5.25-5.08 (m, 4H), 4.89 (s, 4H), 4.16 (s, 2H), 3.68-3.51 (m, 6H), 2.67 (s, 2H), 2.28-2.09 (m, 4H), 0.86-0.75 (m, 4H), -0.01 (s, 18H);  $^{13}\text{C NMR}$  (125 MHz, acetone- $d_6$ ):  $\delta$  (ppm) 168.5, 159.7, 148.0, 127.8, 115.9, 110.4, 99.1, 78.1, 76.5, 75.5, 72.2, 65.9, 53.4, 41.2, 39.8, 17.5, -1.9;  $^{13}\text{C NMR}$  (125 MHz,  $\text{CHCl}_3-d_1$ ):  $\delta$  (ppm) 169.1, 160.8, 148.7, 128.6, 116.9, 111.7, 99.8, 78.4, 76.5, 75.5, 72.7, 66.6, 53.5, 41.0, 39.7, 17.9, -1.8.

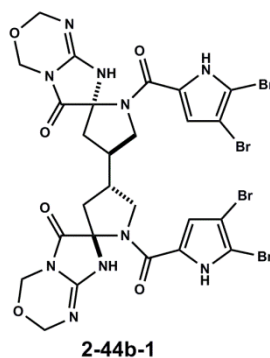
An analytical sample of **2-44b (2 $\cdot$ HCO $_2$ H)** was obtained after purification by HPLC.

**HPLC Conditions:** Waters Sunfire C18 column (19  $\times$  250 mm) with UV detection at 280 nm; Solution A:  $\text{H}_2\text{O}$ , w/0.1% formic acid and Solution B:  $\text{CH}_3\text{CN}$  w/0.1% formic acid; increase gradient of Solution B from 40% to 100%, 0-15 min; flow rate: 20-mL/min.

**$\text{C}_2$  bis-spirocycle (2-44b) (2 $\cdot$ HCO $_2$ H):**

$^1\text{H NMR}$  (600 MHz,  $\text{CH}_3\text{CN}-d_3$ ):  $\delta$  (ppm) 6.87 (s, 2H), 5.63 (d,  $J = 10.4$  Hz, 2H), 5.45 (d,  $J = 10.4$  Hz, 2H), 5.28 (d,  $J = 8.2$  Hz, 2H), 5.21 (d,  $J = 8.2$  Hz, 2H), 5.00 (d,  $J = 4.9$  Hz, 2H), 4.95 (d,  $J = 4.9$  Hz, 2H), 4.03-3.98 (m, 2H), 3.47-3.43 (m, 6H), 2.53-2.46 (m, 2H), 2.32-2.27 (m, 2H), 2.12-2.06 (m, 2H), 0.87-0.76 (m, 4H), -0.04 (s, 18H);  $^{13}\text{C NMR}$  (150 MHz,  $\text{CH}_3\text{CN}-d_3$ ):  $\delta$  (ppm) 169.3, 161.0, 151.8, 127.9, 117.2, 112.1, 100.3, 79.2, 76.7, 75.9, 73.6, 67.0, 54.6, 41.9, 40.9, 18.3, -1.2. **HRMS-ESI** ( $m/z$ ) calcd for  $[\text{C}_{38}\text{H}_{52}\text{Br}_4\text{N}_{10}\text{O}_8\text{Si}_2+\text{H}]^+$ : 1153.0286; found: 1153.0393. **IR** (neat)  $\nu_{\text{max}}$  ( $\text{cm}^{-1}$ ): 2952, 2863, 1761, 1699, 1639, 1430.

## C<sub>2</sub> bis-spirocycle (2-44b):



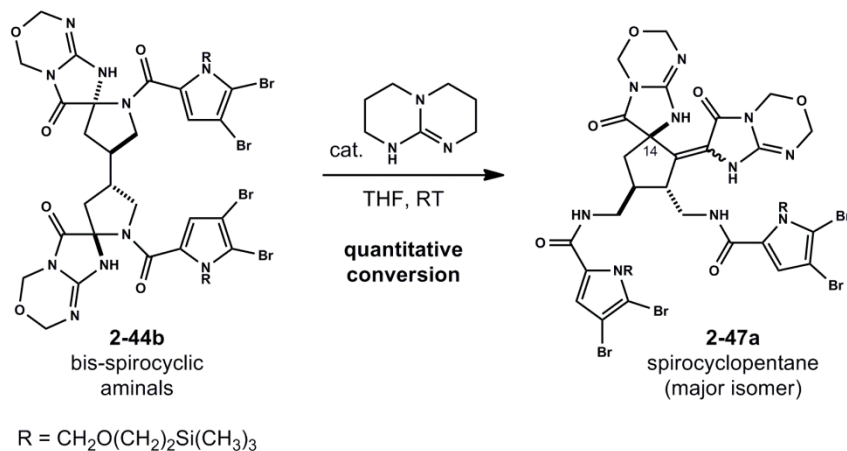
A solution of **2-44b** (28 mg, 0.0243 mmol) in CH<sub>2</sub>Cl<sub>2</sub> (2.5-mL) was stirred with CF<sub>3</sub>CO<sub>2</sub>H (180-μL, 2.35 mmol) at RT for 100 min. The reaction was diluted with EtOAc (20-mL) and washed with saturated aqueous NaHCO<sub>3</sub> (4 × 20-mL), H<sub>2</sub>O and brine. The organic phase was dried over Na<sub>2</sub>SO<sub>4</sub> and concentrated in vacuo to give the crude product **2-44b-1**. The crude product was dissolved in THF (2.4-mL) and evenly distributed into 6 vials (2-dram). Each vial was placed in a 20-mL vial containing one of the following solvents: EtOH, 2-propanol, H<sub>2</sub>O, hexanes, toluene and CHCl<sub>3</sub>. The vials were sealed and stored at RT.

Crystals of **2-44b-1** suitable for X-ray diffraction analysis were obtained from slow evaporation of 2-propanol / THF at RT. (CCDC 859080)

## C<sub>2</sub> bis-spirocycle (2-44b-1):

<sup>1</sup>H NMR (500 MHz, HOAc-*d*<sub>4</sub>): δ (ppm) 7.08 (s, 2H), 5.40 (s, 4H), 5.15 (s, 4H), 4.49-4.45 (m, 2H), 3.78-3.72 (m, 2H), 2.91 (s, 2H), 2.51-2.32 (m, 4H); <sup>13</sup>C NMR (125 MHz, HOAc-*d*<sub>4</sub>): δ (ppm) 167.5, 159.3, 152.8, 124.4, 117.8, 109.0, 100.4, 78.9, 73.4, 73.0, 52.7, 40.3, 39.7. HRMS-ESI (*m/z*) calcd for [C<sub>26</sub>H<sub>24</sub>Br<sub>4</sub>N<sub>10</sub>O<sub>4</sub>+H]<sup>+</sup>: 892.8654; found: 892.8681.

## Isomerization of Spirocycle (12b)



TBD (6.0 mg, 0.043 mmol) was added to a solution of **2-44b** (32 mg, 0.028 mmol) in THF (1.0-mL) at RT. After stirring at RT for 1h, the reaction was quenched with saturated aqueous NH<sub>4</sub>Cl



(2-mL) and diluted with EtOAc (30-mL). The organic phase was washed with saturated aqueous NH<sub>4</sub>Cl, H<sub>2</sub>O, brine, dried over Na<sub>2</sub>SO<sub>4</sub> and concentrated in vacuo. The crude mixture was purified by pTLC (pre-treated with 1% Et<sub>3</sub>N in hexanes, eluted with CHCl<sub>3</sub> / MeOH (15:1)) to afford **2-47a** (7.6 mg, 24%) and **2-47b** (5.5 mg, 17%).

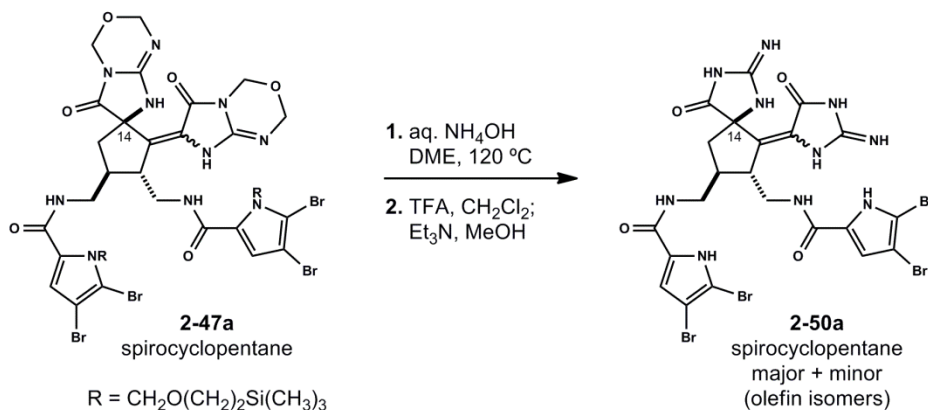
**(2-47a):**

<sup>1</sup>H NMR (600 MHz, CH<sub>3</sub>CN-*d*<sub>3</sub>): δ (ppm) 7.80 (s, 1H), 7.70 (s, 1H), 6.80 (s, 1H), 6.76 (s, 1H), 5.88 (d, *J* = 8.8 Hz, 1H), 5.84 (d, *J* = 8.8 Hz, 1H), 5.68 (d, *J* = 8.8 Hz, 1H), 5.67 (d, *J* = 8.8 Hz, 1H), 5.20-5.14 (m, 4H), 4.94-4.88 (m, 4H), 3.56-3.43 (m, 5H), 3.40-3.33 (m, 1H), 3.32-3.27 (m, 1H), 3.25-3.18 (m, 1H), 3.14 (t, *J* = 5.0 Hz, 1H), 2.56-2.49 (m, 1H), 2.46 (dd, *J* = 6.0, 6.0 Hz, 1H), 0.88-0.76 (m, 4H), -0.02 (s, 18H); <sup>13</sup>C NMR (125 MHz, CH<sub>3</sub>CN-*d*<sub>3</sub>): δ (ppm) 174.6, 164.3, 162.0, 161.9, 161.4, 151.9, 148.9, 135.2, 130.3, 129.5, 129.3, 116.6, 116.4, 111.8, 111.7, 100.2, 100.0, 76.6, 76.3, 75.9, 73.6, 73.5, 69.2, 66.8, 66.7, 49.3, 43.8, 42.9, 42.2, 18.3, -1.4. HRMS-ESI (*m/z*) calcd for [C<sub>38</sub>H<sub>52</sub>Br<sub>4</sub>N<sub>10</sub>O<sub>8</sub>Si<sub>2</sub>+H]<sup>+</sup>: 1153.0286; found: 1153.0350. IR (neat) ν<sub>max</sub> (cm<sup>-1</sup>): 3258, 2952, 2888, 1693, 1610, 1543.

**(2-47b):**

<sup>1</sup>H NMR (500 MHz, CH<sub>3</sub>CN-*d*<sub>3</sub>): δ (ppm) 8.01 (s, 1H), 7.49 (s, 1H), 6.79 (s, 1H), 6.73 (s, 1H), 5.91 (d, *J* = 10.5 Hz, 1H), 5.87 (d, *J* = 10.5 Hz, 1H), 5.67-5.59 (m, 2H), 5.18-5.06 (m, 4H), 4.89-4.80 (m, 4H), 3.63-3.26 (m, 8H), 3.11-3.05 (m, 1H), 2.50-2.01 (m, 2H), 0.88 (t, *J* = 7.5 Hz, 4H), -0.02 (s, 18H); <sup>13</sup>C NMR (125 MHz, CH<sub>3</sub>CN-*d*<sub>3</sub>): δ (ppm) 170.3, 169.3, 159.6, 147.5, 127.6, 127.5, 115.8, 111.1, 110.3, 99.2, 99.1, 78.5, 77.8, 76.9, 75.5, 72.2, 72.1, 66.0, 54.5, 53.6, 41.5, 40.9, 39.7, 17.5, 17.4, -0.18. HRMS-ESI (*m/z*) calcd for [C<sub>38</sub>H<sub>52</sub>Br<sub>4</sub>N<sub>10</sub>O<sub>8</sub>Si<sub>2</sub>+H]<sup>+</sup>: 1153.0286; found: 1153.0386.

**Preparation of spirocycloalkylidene isomers (2-50a) from purified (2-47a).**



A solution of NH<sub>4</sub>OH (23-μL, 0.34 mmol, 14.8 M in H<sub>2</sub>O) was added to a solution of **2-47a** (7.6 mg, 6.6 μmol) in DME / H<sub>2</sub>O (4:1) (625-μL) in a screw-cap vial (1-dram). The vial was sealed and stirred in a 120°C pre-heated oil bath for 90 min. After cooling to RT, the reaction mixture was concentrated in vacuo. The residue was co-evaporated with THF and dried in vacuo for 1h. The residue was dissolved in CH<sub>2</sub>Cl<sub>2</sub> (0.65-mL) and stirred with CF<sub>3</sub>CO<sub>2</sub>H (50-μL, 0.65 mmol) at RT for 1h. The mixture was concentrated and co-evaporated with MeOH, then redissolved in MeOH (0.5-mL) and stirred with Et<sub>3</sub>N (50-μL, 0.36 mmol) at RT for 30 min. Evaporation of

volatiles and co-evaporation with MeOH gave the crude product (free base), which was treated with CF<sub>3</sub>CO<sub>2</sub>H (0.3-mL) in MeOH (1 mL) for 5 min, concentrated to remove excess CF<sub>3</sub>CO<sub>2</sub>H and redissolved in MeOH (1.5-mL) followed by purification by HPLC to give the desired major **2-50a** (1.8 mg, 26%) and the minor **2-50a** (1.2 mg, 17%).

**Major isomer 2-50a (2·CF<sub>3</sub>CO<sub>2</sub>H):**

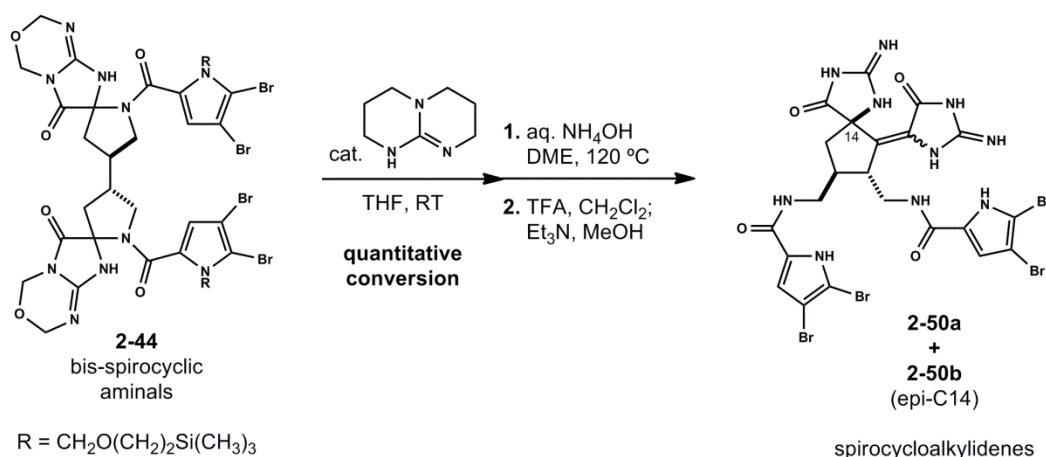
<sup>1</sup>H NMR (500 MHz, MeOH-*d*<sub>4</sub>): δ (ppm) 6.77 (s, 1H), 6.66 (s, 1H), 3.52 (d, *J* = 14.0 Hz, 1H), 3.32-3.20 (m, 3H), 3.17-3.15 (m, 1H), 2.66 (dd, *J* = 14.0, 7.0 Hz, 1H), 2.52-2.49 (m, 1H), 2.16-2.14 (m, 1H); <sup>13</sup>C NMR (125 MHz, MeOH-*d*<sub>4</sub>): δ (ppm) 176.2, 161.2, 160.7, 159.5, 126.7, 113.4, 113.0, 105.5, 105.1, 98.9, 98.7, 69.3, 42.2, 41.9, 41.4, 41.1. HRMS-ESI (*m/z*) calcd for [C<sub>22</sub>H<sub>20</sub>Br<sub>4</sub>N<sub>10</sub>O<sub>4</sub>+H]<sup>+</sup>: 808.8442; found: 808.8449.

**Minor isomer 2-50a (2·CF<sub>3</sub>CO<sub>2</sub>H):**

<sup>1</sup>H NMR (500 MHz, MeOH-*d*<sub>4</sub>): δ (ppm) 6.70 (s, 1H), 6.68 (s, 1H), 3.74-3.67 (m, 1H), 3.60-3.52 (bs, 1H), 3.30-3.22 (m, 2H), 3.07 (dd, *J* = 12.5, 6.0 Hz, 1H), 2.56-2.46 (m, 1H), 2.45-2.37 (m, 1H), 1.85 (d, *J* = 13.5 Hz, 1H); <sup>13</sup>C NMR (125 MHz, MeOH-*d*<sub>4</sub>): δ (ppm) 178.5, 169.6, 162.2, 161.9, 161.0, 159.7, 128.7, 128.3, 114.6, 114.5, 106.5, 106.1, 102.5, 100.1, 100.0, 72.4, 47.2, 42.9, 42.5, 41.8, 40.1. HRMS-ESI (*m/z*) calcd for [C<sub>22</sub>H<sub>20</sub>Br<sub>4</sub>N<sub>10</sub>O<sub>4</sub>+H]<sup>+</sup>: 808.8442; found: 808.8508.

**HPLC Conditions:** Waters Sunfire C18 column (19 × 250-mm) with UV detection at 280-nm; Solution A: H<sub>2</sub>O w/1% CF<sub>3</sub>CO<sub>2</sub>H and Solution B: CH<sub>3</sub>CN w/1% CF<sub>3</sub>CO<sub>2</sub>H; increase gradient of Solution B from 10% to 30%, 0-2 min; then to 60%, 12 min; flow rate: 20-mL/min.

**Base Promoted Isomerization of Bis-spiroaminals (12).**



To a solution of **2-44a** (330 mg, 0.286 mmol) and **2-44b** (870 mg, 0.755 mmol) in THF (38-mL) was added a solution of TBD (4.0-mL, 0.33M in THF, 1.32 mmol) at RT. After stirring for 1h, the reaction was quenched with saturated aqueous NH<sub>4</sub>Cl (20-mL) and extracted with EtOAc. The organic phase was washed with saturated aqueous NH<sub>4</sub>Cl, H<sub>2</sub>O, brine, dried over Na<sub>2</sub>SO<sub>4</sub> and concentrated in vacuo to give a yellow powder (~1.1 g).

The crude product was dissolved in DME / H<sub>2</sub>O (4:1) (87.5 mL) and evenly distributed into five 20-mL vials (microwave reaction vials). A solution of NH<sub>4</sub>OH (0.59-mL, 8.73 mmol, 14.8 M in H<sub>2</sub>O) was added to each vial, which was then sealed and stirred in a pre-heated oil bath (120°C) for 90 min. After cooling to RT, the reaction mixtures were combined and concentrated in vacuo. The residue was co-evaporated with THF (3×50-mL) and dried in vacuo, redissolved in CH<sub>2</sub>Cl<sub>2</sub> (103-mL) and stirred with CF<sub>3</sub>CO<sub>2</sub>H (7.9-mL, 103 mmol) at RT for 70 min. The mixture was concentrated and co-evaporated with MeOH (20-mL), then redissolved in MeOH (50-mL) and stirred with Et<sub>3</sub>N (2.7-mL, 19.4 mmol) at RT for 30 min. Evaporation of volatiles followed by co-evaporation with MeOH (2×20-mL) gave the crude product (free base), which was treated with CF<sub>3</sub>CO<sub>2</sub>H (3-mL) in MeOH (20-mL). The mixture was concentrated, redissolved in MeOH (25-mL) and purified by HPLC to give minor isomer **2-50a** (32 mg, 3%) and a mixture of major isomer **2-50a** and *epi*-C14-**2-50b** (430 mg, 40%).

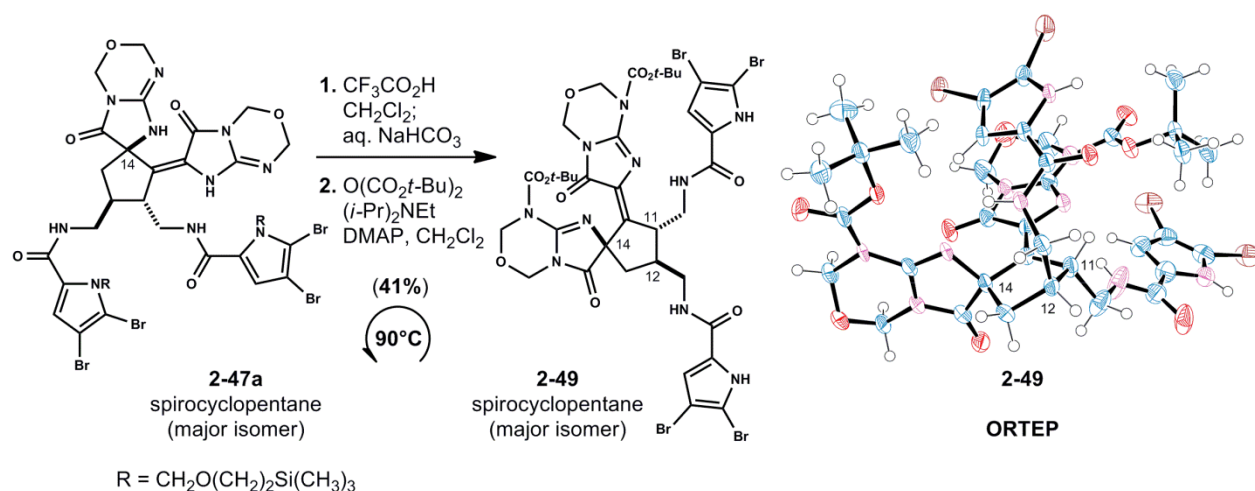
A small portion of the above mixture was further purified by HPLC to give an analytical sample of major isomer **2-50a**.

#### Major isomer **2-50a** (**2-CF<sub>3</sub>CO<sub>2</sub>H**):

<sup>1</sup>H NMR (500 MHz, MeOH-*d*<sub>4</sub>): δ (ppm) 6.71 (s, 1H), 6.61 (s, 1H), 3.65 (dd, *J* = 13.8, 4.8 Hz, 1H), 3.56-3.47 (m, 1H), 3.30-3.21 (m, 2H), 3.17-3.12 (m, 1H), 2.59-2.52 (m, 2H), 2.38 (d, *J* = 11.7 Hz, 1H); <sup>13</sup>C NMR (125 MHz, MeOH-*d*<sub>4</sub>): δ (ppm) 175.4, 161.2, 160.5, 158.3, 126.9, 126.4, 113.5, 112.8, 105.6, 104.9, 99.0, 98.6, 68.9, 42.4, 41.9, 41.8. LRMS-ESI (*m/z*) calcd for [C<sub>22</sub>H<sub>20</sub>Br<sub>4</sub>N<sub>10</sub>O<sub>4</sub>+H]<sup>+</sup>: 808.8; found: 808.8.

**HPLC Conditions:** Phenomenex Luna PFP (2) column (10 × 250-mm) with UV detection at 280-nm; Solution A: H<sub>2</sub>O w/0.1% CF<sub>3</sub>CO<sub>2</sub>H and Solution B: CH<sub>3</sub>CN w/0.1% CF<sub>3</sub>CO<sub>2</sub>H; increase gradient of Solution B from 10% to 30%, 0-2 min; then to 42%, 22min; flow rate: 5-mL/min.

#### Derivatization of (**2-47a**) to (**2-49**).



A solution of **2-47a** (6.0 mg, 0.0052 mmol) in CH<sub>2</sub>Cl<sub>2</sub> (0.54-mL) was stirred with CF<sub>3</sub>CO<sub>2</sub>H (40-μL, 0.52 mmol) at RT for 70 min. The reaction was diluted with EtOAc (30-mL) and washed

with saturated aqueous NaHCO<sub>3</sub> (4×20-mL), H<sub>2</sub>O, brine, dried over Na<sub>2</sub>SO<sub>4</sub> and concentrated in vacuo. The residue was redissolved in DMF (0.1-mL) and THF (0.3-mL). A solution of Boc<sub>2</sub>O (23-μL, 0.023 mmol, 1.0M in THF) was added, followed by a solution of TBD (24-μL, 0.024 mmol, 0.33 M in THF) and a solution of DMAP (1.0-μL, 0.005 mmol, 0.5M in THF) at RT. After stirring at RT for 80 min, the reaction mixture was quenched with saturated aqueous NH<sub>4</sub>Cl and extracted with EtOAc. The organic phase was washed with saturated aqueous NH<sub>4</sub>Cl (3×), H<sub>2</sub>O, brine, dried over Na<sub>2</sub>SO<sub>4</sub> and concentrated in vacuo to give a yellow oil which was purified by pTLC (pre-treated with 1% Et<sub>3</sub>N in hexanes, eluted with CHCl<sub>3</sub> / MeOH (20:1) to afford **2-49** (2.3 mg, 41%) as a light yellow solid.

**(2-49):**

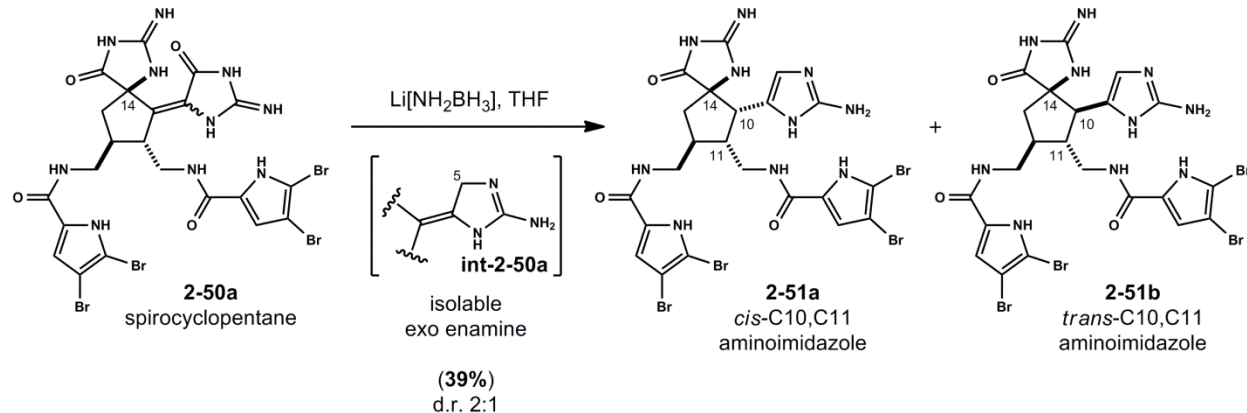
<sup>1</sup>H NMR (500 MHz, CH<sub>3</sub>CN-*d*<sub>3</sub>): δ (ppm) 10.43 (bs, 2H), 8.61 (d, *J* = 9.8 Hz, 1H), 7.77 (s, 1H), 6.73 (s, 1H), 6.55 (s, 1H), 5.34-5.02 (m, 8H), 4.05 (dd, *J* = 14.2, 7.1 Hz, 1H), 3.65-3.36 (m, 3H), 2.99 (d, *J* = 8.7 Hz, 1H), 2.71 (dd, *J* = 13.9, 7.6 Hz, 1H), 2.49-2.45 (m, 1H), 2.01-1.95 (m, 1H), 1.49 (s, 9H), 1.47 (s, 9H). HRMS-ESI (*m/z*) calcd for [C<sub>36</sub>H<sub>40</sub>Br<sub>4</sub>N<sub>10</sub>O<sub>10</sub>+H]<sup>+</sup>: 1092.9706; found: 1092.9741.

**Note:** Compound **2-49** was also prepared from a mixture of **2-44a** and **2-44b** via a similar procedure. To a solution of **2-44a** and **2-44b** (318 mg, 0.276 mmol, 1:2) in THF (10.5-mL) was added a solution of TBD (1.0-mL, 0.33 mmol, 0.33 M in THF) at RT. After stirring at RT for 1h, the reaction was quenched by saturated aqueous NH<sub>4</sub>Cl (20-mL) and extracted with EtOAc. The organic phase was washed with saturated aqueous NH<sub>4</sub>Cl, H<sub>2</sub>O, brine, dried over Na<sub>2</sub>SO<sub>4</sub> and concentrated in vacuo to give the crude product as a yellow solid.

A solution of the above crude in CH<sub>2</sub>Cl<sub>2</sub> (28-mL) was stirred with CF<sub>3</sub>CO<sub>2</sub>H (2.1-mL, 27.4 mmol) at RT for 70 min. It was diluted with EtOAc (300-mL) and washed with saturated aqueous NaHCO<sub>3</sub> (4×30-mL), H<sub>2</sub>O and brine. The organic phase was dried over Na<sub>2</sub>SO<sub>4</sub>, concentrated in *vacuo* and redissolved in DMF (2.2-mL) and THF (6.6-mL). A solution of Boc<sub>2</sub>O (1.24 mL, 1.24 mmol, 1.0 M in THF) was added, followed by a solution of TBD (1.15-mL, 0.38 mmol, 0.33 M in THF) and a solution of DMAP (50-μL, 0.025 mmol, 0.5 M in THF) at RT. After stirring at RT for 80 min, the reaction mixture was quenched with saturated aqueous NH<sub>4</sub>Cl and extracted with EtOAc. The organic phase was washed with saturated aqueous NH<sub>4</sub>Cl (3×), H<sub>2</sub>O, brine, dried over Na<sub>2</sub>SO<sub>4</sub>, concentrated in *vacuo* and purified by pTLC (pre-treated with 1% Et<sub>3</sub>N in hexanes, eluted with CHCl<sub>3</sub> / MeOH (20:1)) to afford **2-49** (78 mg, 26%) and a minor compound (58 mg, 19%) (LRMS-ESI (*m/z*) calcd for [C<sub>36</sub>H<sub>40</sub>Br<sub>4</sub>N<sub>10</sub>O<sub>10</sub>+H]<sup>+</sup>: 1092.97 found: 1092.40).

Crystals of **2-49** suitable for X-ray diffraction analysis were obtained from a standing solution of (**2-49**) in CH<sub>3</sub>CN at 4°C. (CCDC 859078).

## Reduction of Glycoamidines (2-50a) with lithium amidotrihydroborate (LAB)



Preparation of lithium amidotrihydroborate (LAB) solution: To a suspension of  $\text{BH}_3 \cdot \text{NH}_3$  (0.50 g, 14.5 mmol, 90% reagent purity) in THF (3.2-mL) cooled to  $-20^\circ\text{C}$  was added a solution of *n*-BuLi (5.6-mL, 14.0 mmol, 2.5 M in hexanes) dropwise. The mixture was warmed to RT, stirred for 1h and used directly ( $\sim 1.60$  M) in the following reaction.

A portion of the above LAB solution (4.1-mL, 1.59 M, 6.5 mmol) was added to a solution of **2-50ab** (201 mg, 0.194 mmol) in THF (6.6-mL) at RT. Gentle gas evolution was observed. The mixture was stirred in a pre-heated oil-bath ( $60^\circ\text{C}$ ) for 4h. A second portion of the LAB solution (2.0-mL, 3.2 mmol) was added and the cloudy mixture was stirred at  $60^\circ\text{C}$  for another 6h. After cooling to  $-40^\circ\text{C}$ , the reaction was quenched with slow addition of 10%  $\text{CF}_3\text{CO}_2\text{H}$  in  $\text{H}_2\text{O}$  (10-mL). (**Note:** gas evolution is vigorous if the addition is too fast). The mixture was warmed to RT and stirred at  $60^\circ\text{C}$  for 4h and purified directly by HPLC to give the desired **2-51b** (20.6 mg, 10%), **2-51a** (57 mg, 39%) mixed with other diastereomers and recovered **2-50a** (15.5 mg, 8%).

**HPLC Conditions:** Waters Sunfire C18 column (19  $\times$  250-mm) with UV detection at 280-nm; Solution A:  $\text{H}_2\text{O}$  w/1%  $\text{CF}_3\text{CO}_2\text{H}$  and Solution B:  $\text{CH}_3\text{CN}$ , w/1%  $\text{CF}_3\text{CO}_2\text{H}$ ; increase gradient of Solution B from 10% to 30%, 0-2 min; then to 60%, 12 min; flow rate: 20-mL/min.

### (2-51b) (2- $\text{CF}_3\text{CO}_2\text{H}$ ):

$^1\text{H}$  NMR (600 MHz,  $\text{D}_2\text{O}$ ):  $\delta$  (ppm) 6.75 (s, 1H), 6.62 (s, 1H), 6.50 (s, 1H), 3.56-3.40 (m, 4H), 3.28 (d,  $J = 11.6$  Hz, 1H), 2.59 (dd,  $J = 14.6, 9.7$  Hz, 1H), 2.48-2.35 (m, 2H), 1.91 (dd,  $J = 14.6, 6.1$  Hz, 1H);  $^{13}\text{C}$  NMR (125 MHz,  $\text{D}_2\text{O}$ ):  $\delta$  (ppm) 178.0, 161.5, 160.9, 157.9, 146.9, 126.1, 125.8, 121.5, 113.6, 113.2, 111.8, 106.08, 106.02, 99.0, 98.9, 71.8, 49.6, 46.5, 42.4, 41.9, 40.6, 38.4. **HRMS-ESI** ( $m/z$ ) calcd for  $[\text{C}_{22}\text{H}_{22}\text{Br}_4\text{N}_{10}\text{O}_3 + \text{H}]^+$ : 794.8649; found: 794.8697.

A portion of the mixed **2-51a** was further purified by HPLC to give an analytical sample of **2-51a**.

**HPLC Conditions:** Waters X-Select Fluoro-phenyl column (19  $\times$  250-mm) with UV detection at 280-nm; Solution A:  $\text{H}_2\text{O}$  w/1%  $\text{CF}_3\text{CO}_2\text{H}$  and Solution B:  $\text{CH}_3\text{CN}$  w/1%  $\text{CF}_3\text{CO}_2\text{H}$ ; increase gradient of Solution B from 10% to 22%, 0-2 min; then to 26.5%, 14 min; flow rate: 30-mL/min.

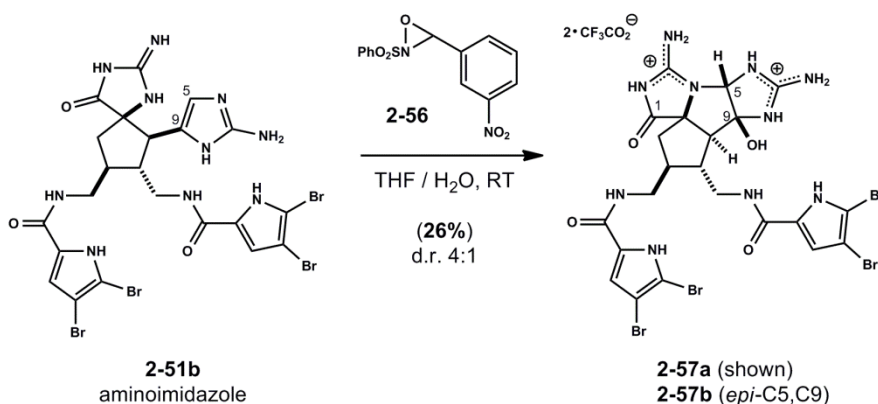
**(2-51b) (2·CF<sub>3</sub>CO<sub>2</sub>H):**

<sup>1</sup>H NMR (500 MHz, MeOH-*d*<sub>4</sub>): δ (ppm) 6.81 (s, 1H), 6.78 (s, 1H), 6.52 (s, 1H), 3.71 (d, *J* = 9.5 Hz, 1H), 3.53-3.41 (m, 4H), 2.74-2.63 (m, 2H), 2.48 (dd, *J* = 13.0, 7.5 Hz, 1H), 2.04 (dd, *J* = 12.0, 9.5 Hz, 1H); <sup>13</sup>C NMR (125 MHz, MeOH-*d*<sub>4</sub>): δ (ppm) 176.0, 160.8, 160.2, 157.8, 147.4, 127.05, 127.01, 120.7, 113.1, 111.2, 105.0, 104.9, 98.6, 72.3, 46.0, 42.4, 42.3, 41.5, 40.9, 38.6. HRMS-ESI (*m/z*) calcd for [C<sub>22</sub>H<sub>22</sub>Br<sub>4</sub>N<sub>10</sub>O<sub>3</sub>+H]<sup>+</sup>: 794.8649; found: 794.8641.

**Preparation of 2-aminoimidazoles (2-51ab) from glycoamidines (2-50a).**

Starting from the major isomer of **2-50a** (14 mg, 0.0135 mmol) via the above procedure, compound **2-51b** was obtained (2.1 mg, 15%), along with **2-51a** (3.7 mg, 27%) and recovered major isomer of **2-50a** (2.5 mg, 18%).

Starting from the minor isomer of **2-50a** (108 mg, 0.104 mmol) via the above procedure, compound **2-51b** was obtained (7.0 mg, 6.6%), along with **2-51a** (10.0 mg, 9.4%) and recovered major isomer of **2-50a** (9.0 mg, 8%). The lower yields are attributed to poor solubility of the minor isomer of **2-50a** in THF.

**Oxidation of (2-51b) – Formation of (2-57a) and (2-57b).**

To a solution of **2-51b** (24 mg, 0.0235 mmol) in THF / H<sub>2</sub>O (9:1) (1.09-mL) was added 3-(3-nitrophenyl)-2-(phenylperoxythio)-1,2-oxaziridine **2-56** (10.0 mg, 0.0326 mmol).<sup>[5]</sup> The flask was flushed with Ar, sealed and stirred at 55°C. A second portion of **2-56** (3.7 mg, 0.0121 mmol) was added after 3h and a third portion (3.0 mg, 0.0098 mmol) was added after 6h. After stirring at RT for 10h (total time), the reaction mixture was diluted with THF (10-mL) and 10% CF<sub>3</sub>CO<sub>2</sub>H in H<sub>2</sub>O (0.2-mL). The mixture was purified by HPLC to give desired major diastereomer **2-57a** (5.2 mg, 21%), the minor diastereomer **2-57b** (1.2 mg, 5%) and recovered **2-51b** mixed with two tentatively assigned ketone isomers (5.5 mg, 23%).

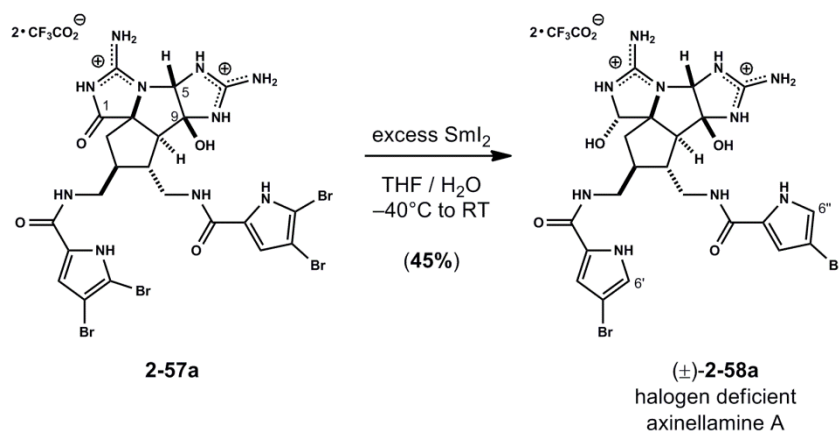
**HPLC Conditions:** Phenomenex Luna PFP (2) column (10 × 250 mm) with UV detection at 280 nm; Solution A: H<sub>2</sub>O w/0.1% CF<sub>3</sub>CO<sub>2</sub>H and Solution B: CH<sub>3</sub>CN w/0.1% CF<sub>3</sub>CO<sub>2</sub>H; increase gradient of Solution B from 10% to 30%, 0-2 min; then to 42%, 26 min; flow rate: 5-mL/min.

**Dehydro des-chloro Axinellamine A (2-57a) (2·CF<sub>3</sub>CO<sub>2</sub>H):**

<sup>1</sup>H NMR (600 MHz, MeOH-*d*<sub>4</sub>): δ (ppm) 6.93 (s, 1H), 6.82 (s, 1H), 5.28 (s, 1H), 3.65 (dd, *J* = 13.8, 4.8 Hz, 1H), 3.54-3.42 (m, 3H), 2.75-2.71 (m, 1H), 2.68-2.62 (m, 1H), 2.57-2.49 (m, 1H), 2.22-2.13 (m, 1H), 1.93-1.88 (m, 1H); <sup>13</sup>C NMR (125 MHz, MeOH-*d*<sub>4</sub>): δ (ppm) 160.9, 160.7, 157.5, 127.3, 113.3, 113.0, 104.8, 100.4, 98.7, 98.6, 80.9, 78.9, 55.5, 43.0, 42.0, 41.3, 40.9, 40.6. HRMS-ESI (*m/z*) calcd for [C<sub>22</sub>H<sub>22</sub>Br<sub>4</sub>N<sub>10</sub>O<sub>4</sub>+H]<sup>+</sup>: 810.8599; found: 810.8583.

**Dehydro des-chloro Axinellamine B (2-57b) (2·CF<sub>3</sub>CO<sub>2</sub>H):**

<sup>1</sup>H NMR (600 MHz, MeOH-*d*<sub>4</sub>): δ (ppm) 6.90 (s, 1H), 6.80 (s, 1H), 5.32 (s, 1H), 3.50 (dd, *J* = 15.0, 6.0 Hz, 2H), 3.47-3.30 (m, 3H), 2.77-2.70 (m, 2H), 2.45-2.36 (m, 1H), 2.23-2.14 (m, 1H), 2.22-2.13 (m, 1H), 1.68-1.52 (m, 1H); <sup>1</sup>H NMR (DMSO-*d*<sub>6</sub>): δ (ppm) 12.59 (s, 2H), 9.45 (s, 1H), 8.37 (s, 2H), 8.10-8.06 (m, 3H), 7.95 (s, 1H), 7.05 (s, 1H), 6.93 (s, 1H), 6.90 (s, 1H), 5.14 (s, 1H), 3.40-3.10 (m, 4H), 2.50-2.46 (m, 2H), 2.22 (bs, 1H), 2.01-1.92 (m, 1H), 1.40 (t, *J* = 12.0 Hz, 1H); <sup>13</sup>C NMR (125 MHz, MeOH-*d*<sub>4</sub>): δ (ppm) 173.3, 160.8, 160.5, , 157.4, 127.2, 127.0, 113.3, 112.9, 104.8, 104.6, 100.6, 98.6, 98.5, 81.3, 81.0, 56.3, 44.0, 43.0, 42.5, 39.3. HRMS-ESI (*m/z*) calcd for [C<sub>22</sub>H<sub>22</sub>Br<sub>4</sub>N<sub>10</sub>O<sub>4</sub>+H]<sup>+</sup>: 810.8599; found: 810.8594.

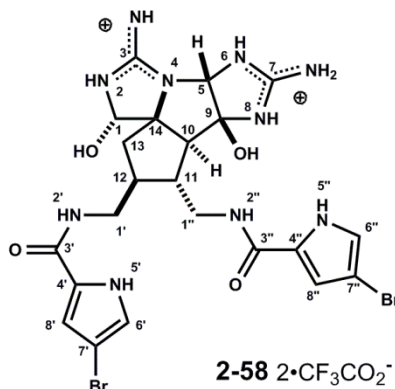
**SmI<sub>2</sub> reduction of (2-57a) to access (2-58).**

To a solution of **2-57a** (5.2 mg, 0.005 mmol) in THF / H<sub>2</sub>O (2:1) (150-μL) was added a solution of SmI<sub>2</sub> (174-μL, 0.04 mmol, 0.23 M in THF) at -78°C. The initially purple mixture became yellow after several minutes. LC-MS analysis indicated partial debromination occurred to give a debrominated intermediate (LRMS-ESI (*m/z*) calcd for [C<sub>22</sub>H<sub>24</sub>Br<sub>2</sub>N<sub>10</sub>O<sub>4</sub>+H]<sup>+</sup>: 653.04; found: 653.1). The solvent volume was reduced by a stream of Ar and the mixture was cooled to -40°C. A solution of SmI<sub>2</sub> (110-μL, 0.0253 mmol, 0.23 M in THF) was added and the mixture was warmed to RT. The solvent was evaporated with a stream of Ar and an additional portion of SmI<sub>2</sub> (110-μL, 0.0253 mmol, 0.23M in THF) was added at -40°C. This concentration-addition procedure was repeated until LC-MS analysis indicated >80% conversion of the debrominated intermediate to the desired product **2-58**. The reaction was quenched with 10% CF<sub>3</sub>CO<sub>2</sub>H in H<sub>2</sub>O and the resulting yellow solution was purified by HPLC. The desired **2-58** was obtained (2.0 mg, 45%), along with an over-reduced compound (1.0 mg, 22%) (LRMS-ESI (*m/z*) calcd for [C<sub>22</sub>H<sub>28</sub>Br<sub>2</sub>N<sub>10</sub>O<sub>4</sub>+H]<sup>+</sup>: 657.07; found: 657.0).

**HPLC Conditions:** Phenomenex Luna PFP (2) column (10 × 250-mm) with UV detection at 280 -nm; Solution A: H<sub>2</sub>O w/0.1% CF<sub>3</sub>CO<sub>2</sub>H and Solution B: CH<sub>3</sub>CN w/0.1% CF<sub>3</sub>CO<sub>2</sub>H; increase gradient of Solution B from 10% to 30%, 0-2 min; then to 33.5%, 12 min; flow rate: 5- mL/min.

**(2-58) (2·CF<sub>3</sub>CO<sub>2</sub>H):**

<sup>1</sup>H NMR (600 MHz, MeOH-*d*<sub>4</sub>): δ (ppm) 6.94 (s, 1H), 6.93 (s, 1H), 6.87 (s, 1H), 6.87 (s, 1H), 5.28 (s, 1H), 4.93 (s, 1H), 3.67 (dd, *J* = 13.9, 5.4 Hz, 1H), 3.55-3.42 (m, 3H), 3.09 (d, *J* = 7.5 Hz, 1H), 2.64-2.57 (m, 1H), 2.15 (dd, *J* = 12.8, 5.4 Hz, 1H), 2.09-2.01 (m, 1H), 1.75 (t, *J* = 12.4 Hz, 1H); <sup>1</sup>H NMR (600 MHz, DMSO-*d*<sub>6</sub>): δ (ppm) 11.75 (s, 2H), 9.42 (s, 1H), 9.38 (s, 1H), 8.61 (bs, 1H), 8.60 (s, 1H), 8.30 (bs, 2H), 8.08-8.03 (m, 2H), 7.61 (s, 1H), 7.05 (d, *J* = 6.0 Hz, 1H), 6.95 (s, 1H), 6.83 (s, 1H), 6.81 (s, 1H), 5.15 (s, 1H), 4.81 (d, *J* = 6.3 Hz, 1H), 3.47 (ddd, *J* = 12.6, 6.3, 6.3 Hz, 1H), 3.33-3.28 (m, 3H), 2.84 (d, *J* = 6.5 Hz, 1H), 2.45-2.39 (m, 1H), 1.97 (dd, *J* = 12.4, 5.4 Hz, 1H), 1.88-1.80 (m, 1H), 1.55 (t, *J* = 12.6 Hz, 1H); <sup>13</sup>C NMR (125 MHz, DMSO-*d*<sub>6</sub>): δ (ppm) 160.5, 160.4, 156.9, 155.5, 127.4, 127.2, 121.8, 121.7, 112.1, 111.7, 100.9, 95.5, 95.4, 84.5, 82.7, 78.5, 53.2, 43.4, 43.4, 42.5, 41.8. **HRMS-ESI** (*m/z*) calcd for [C<sub>22</sub>H<sub>26</sub>Br<sub>2</sub>N<sub>10</sub>O<sub>4</sub>+H]<sup>+</sup>: 655.0565; found: 655.0586.



(see data tables)



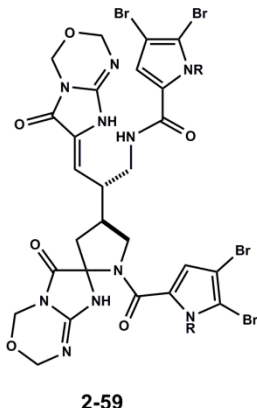
NMR Data for **2-58** in MeOH-*d*<sub>4</sub>

Atom #	<sup>13</sup> C NMR	<sup>1</sup> H NMR, $\delta$ (mult, <i>J</i> in Hz)	HMBC (C no.)
1	83.5	4.93 (s)	C3, C13, C14
2			
3	156.2		
4			
5	78.3	5.28 (s)	C7, C9, C14
6			
7	157.1		
8			
9	100.3		
10	52.5	3.09 (d, <i>J</i> = 7.5 Hz)	C1, C5, C9, C11, C13, C14, C1''
11	40.8	2.64-2.57 (m)	C9
12	41.6	2.09-2.01 (m)	
13 $\beta$	41.1	2.15 (dd, <i>J</i> = 12.8, 5.4 Hz)	C1, C10, C12
13 $\alpha$		1.75 (t, <i>J</i> = 12.4 Hz)	C1, C11, C14, C1'
14	82.3		
1'	42.8	3.67 (dd, <i>J</i> = 13.9, 5.4 Hz)	C10, C13, C3'
1''		3.55-3.45 (m)	
2'	N-amide		
3'	161.3		
4'	126		
5'	N-pyrrole		
6'	112	6.87 (s)	C4', C8'
7'	96.1		
8'	121.3	6.94 (s)	C4', C6', C7'
1''	42.3	3.45-3.42 (m)	C10, C12, C3'
2''	N-amide		
3''	161.3		
4''	126		
5''	N-pyrrole		
6''	112	6.81 (s)	C4'', C8''
7''	96.1		
8''	121.3	6.93 (s)	C4'', C6'', C7''

NMR Data for **2-58** in DMSO-*d*<sub>6</sub>

Atom #	<sup>13</sup> C NMR	<sup>1</sup> H NMR, $\delta$ (mult, J in Hz)	g-COSY	T-ROESY
1	84.5	4.81 (d, <i>J</i> = 6.3 Hz)	2-NH	2-NH, 3-NH <sub>2</sub> , H12, H13 $\alpha$
2		7.05 (d, <i>J</i> = 6.0 Hz)	H1	H1, H10
3	155.5	9.42, 8.61 (bs)-NH <sub>2</sub>		H1
4				
5	78.5	5.15 (s)	6-NH	6-NH, 9-OH, H13 $\beta$
6		8.60 (s)	H5, 8-NH	H5
7	156.9	8.30 (bs)-NH <sub>2</sub>		
8		9.38 (s)	6-NH	9-OH, H10
9	100.9	7.65 (s, 1H)-9-OH		H5, 8-NH, H11
10	53.2	2.84 (d, <i>J</i> = 6.5 Hz)	H11	2-NH, 8-NH
11	under solvent	2.45-2.39 (m)	H10, H12, (H1'') <sub>2</sub>	
12	42.5	1.88-1.80 (m)	H11, (H13) <sub>2</sub>	H1
13 $\beta$	41.8	1.55 (t, <i>J</i> = 12.6 Hz)	H13 $\alpha$	H13 $\alpha$
13 $\alpha$		1.97 (dd, <i>J</i> = 12.4, 5.4 Hz)	H13 $\beta$	H1, H13 $\beta$
14	82.7			
1'	43.4	3.47 (ddd, <i>J</i> = 12.6, 6.3, 6.3 Hz)		
1'		3.33-3.28 (m)		
2'	N-amide	8.08-8.03 (m)	(H1') <sub>2</sub>	H1', H6'
3'	160.5			
4'	127.2			
5'	N-pyrrole	11.75 (s)	6'-NH	H8'
6'	121.8	6.83 (s)	5'-NH	2'-NH
7'	95.5			
8'	111.7	7.05 (s)		5'-NH
1''	43.4	3.40-3.20 (m)		
2''	N-amide	8.08-8.03 (m)	(H1'') <sub>2</sub>	H1'', H6''
3''	160.4			
4''	127.4			
5''	N-pyrrole	11.75 (s)	6''-NH	H8''
6''	121.7	6.81 (s)	5''-NH	2''-NH
7''	95.4			
8''	112.1	6.95 (s)		5''-NH

### Preparation of mono-alkylidene (**2-59**) (major isomer) from bis-spirocycle (**2-44b**).



A 0.5 M stock solution containing tetramethylguanidine (TMG) (59 mg) in THF (1.0-mL) was prepared. Purified **2-44b** was dissolved in THF (0.51-mL) followed by the addition of the above TMG stock solution (7.8- $\mu$ L, 0.35 equiv of TMG). The reaction vial was sealed under Ar and stirred at 50°C for 2h. At 2h the reaction was run to partial conversion. The desired mono-alkylidene **2-59** (major isomer) was observed by LC-MS as the major compound in the presence of spirocycloalkylidene isomers **2-47** and unreacted **2-44b**. The reaction solution was directly purified by HPLC (2  $\times$  300- $\mu$ L injections). The desired **2-59** (major isomer) (4.8 mg, 37%) was obtained (retention time:  $\sim$ 12.1 min) after lyophilization of aqueous fractions.

**HPLC Conditions:** Waters Sunfire C18 column (19  $\times$  250-mm) with UV detection at 254-nm; Solution A: H<sub>2</sub>O w/0.1% formic acid and Solution B: CH<sub>3</sub>CN w/0.1% formic acid; increase gradient of Solution B from 40% to 100%, 0.5-17 min; flow rate: 20-mL/min.

Repeat experiments conducted with **2-44b** afforded desired mono-alkylidene **2-59** (major isomer) in 27–40% yield. The reaction also proceeds in CH<sub>3</sub>CN and DME albeit in lower yield.

#### **Mono-alkylidene (2-59) (2·HCO<sub>2</sub>H) (major isomer):**

<sup>1</sup>H NMR (600 MHz, CH<sub>3</sub>CN-*d*<sub>3</sub>):  $\delta$  (ppm) 7.32 (bs, 1H), 6.86 (bs, 1H), 6.78 (bs, 1H), 5.83 (d, *J* = 10.3 Hz, 1H), 5.79-5.70 (m, 2H), 5.66 (d, *J* = 11.2 Hz, 1H), 5.43 (d, *J* = 11.0 Hz, 1H), 5.36 (d, *J* = 8.9 Hz, 1H), 5.28-5.20 (m, 3H), 5.08 (d, *J* = 9.6 Hz, 1H), 5.04-4.96 (m, 3H), 4.17-4.11 (m, 1H), 3.59-3.37 (m, 7H), 2.97-2.91 (m, 1H), 2.77-2.69 (m, 1H), 0.86-0.73 (m, 4H), -0.71 (s, 18H)  
\*2H under residual CH<sub>3</sub>CN peak – obtained from COSY; **LRMS-ESI** (*m/z*) calcd for [C<sub>38</sub>H<sub>52</sub>Br<sub>4</sub>N<sub>10</sub>O<sub>8</sub>Si<sub>2</sub>+H]<sup>+</sup>: 1153.0; found: 1153.1.

### Preparation of mono-alkylidene (**2-59**) (two isomers) from bis-spirocycles (**2-44**).

A 0.5 M stock solution of tetramethylguanidine (TMG) (59 mg) in THF (1.0-mL) was prepared. A mixture of purified **2-44a** and purified **2-44b** (57 mg, 0.049 mmol,  $\sim$ 1:1) was dissolved in THF (2.2-mL) followed by the addition of the above TMG stock solution (31- $\mu$ L, 0.3 equiv of TMG). The reaction vial was sealed under Ar and stirred at 50°C for 2h. An additional amount of TMG stock solution was added (31- $\mu$ L, 0.3 equiv) and the reaction was stirred for 2.5h at 50°C

(total time 4.5h). The reaction converts both isomers of **2-44** into a major and minor isomer of desired **2-59**. The reaction was cooled to RT and split into equal portions (~1.1-mL each).

Half of the material was purified by pTLC. The pTLC plates were pretreated with a solution of 1% Et<sub>3</sub>N in hexanes and dried prior to use. The crude material was loaded onto two plates and eluted with CHCl<sub>3</sub> / MeOH (15:1). The desired mono-alkylidenes **2-59** (major isomer, R<sub>f</sub> = 0.6) and (minor isomer, R<sub>f</sub> = 0.62) were separable, however co-elute with unreacted bispirocycles **2-44** and spirocycloalkylidene isomers **2-47**. It was discovered that direct chlorination of crude mixtures (containing desired **2-59** in the presence of **2-44** and **2-47**) was a more efficient process (*vide infra*).

For characterization purposes, the remaining half of crude material was purified by HPLC (3 × 300-μL injections). The desired mono-alkylidenes **2-59** (minor isomer, retention time: ~12.3 min) and (major isomer, retention time: ~12.8 min) were obtained after lyophilization of aqueous fractions. Yield was not determined.

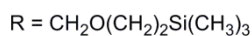
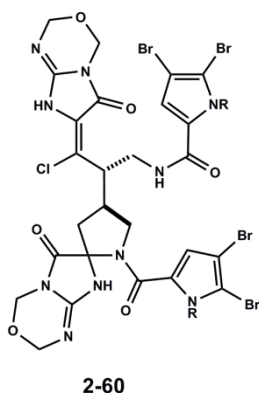
**HPLC Conditions:** Waters Sunfire C18 column (19 × 250-mm) with UV detection at 254-nm; Solution A: H<sub>2</sub>O w/0.1% formic acid and Solution B: CH<sub>3</sub>CN w/0.1% formic acid; increase gradient of Solution B from 30% to 100%, 0.5-17 min; flow rate: 20-mL/min.

**Mono-alkylidene (2-59) (2·HCO<sub>2</sub>H) (major isomer):** see above.

**Mono-alkylidene (2-59) (2·HCO<sub>2</sub>H) (minor isomer):**

<sup>1</sup>H NMR (600 MHz, CH<sub>3</sub>CN-*d*<sub>3</sub>): δ (ppm) 7.21 (bs, 1H), 6.94 (bs, 1H), 6.77 (bs, 1H), 5.85 (d, *J* = 10.4 Hz, 1H), 5.80-5.68 (m, 3H), 5.42-5.33 (m, 2H), 5.31-5.19 (m, 3H), 5.11-4.93 (m, 4H), 4.03-3.97 (m, 1H), 3.88-3.81 (m, 1H), 3.54-3.30 (m, 7H), 2.65-2.57 (m, 1H), 0.84-0.77 (m, 4H), -0.04 (s, 9H), -0.08 (s, 9H) \*2H under residual CH<sub>3</sub>CN peak – obtained from COSY; LRMS-ESI (*m/z*) calcd for [C<sub>38</sub>H<sub>52</sub>Br<sub>4</sub>N<sub>10</sub>O<sub>8</sub>Si<sub>2</sub>+H]<sup>+</sup>: 1153.0; found: 1153.1.

**Preparation of chlorinated alkylidene (2-60) from mono-alkylidene (2-59) (major isomer).**



A 0.17 M stock solution of *t*-BuOCl was prepared by the dissolution of *t*-BuOCl (5-μL) in CH<sub>2</sub>Cl<sub>2</sub> (250-μL). Purified mono-alkylidene **2-59** (major isomer) (14.0 mg, 0.012 mmol, 1.0

equiv) was dissolved in CH<sub>2</sub>Cl<sub>2</sub> (0.85-mL) and cooled to -78°C in a dry ice / acetone bath. To this solution was added *t*-BuOCl stock solution (73-μL, 1.0 equiv). The reaction was stirred at -78°C for 45 min at which point the bath was removed and allowed to reach RT. The reaction was judged complete after 1.5h at RT by LC-MS analysis (>90% conversion, UV analysis with detection at 254-nm). The reaction was concentrated with a stream of Ar and dissolved in CH<sub>3</sub>CN-*d*<sub>3</sub> (500-μL) for characterization by <sup>1</sup>H NMR analysis. The crude sample showed a set of resonances which suggested the crude mixture contained multiple diastereomers. The sample was concentrated and redissolved in acetic acid-*d*<sub>4</sub>.

Crystals of **2-60** (apparent major isomer by <sup>1</sup>H NMR) suitable for X-ray diffraction analysis were obtained from this sample in acetic acid-*d*<sub>4</sub> at RT. (CCDC 942603)

For characterization purposes, two isomers of **2-60** identified by LC-MS analysis (**LRMS-ESI** (*m/z*) calcd for [C<sub>38</sub>H<sub>51</sub>Br<sub>4</sub>ClN<sub>10</sub>O<sub>8</sub>Si<sub>2</sub>+H]<sup>+</sup>: 1187.0 ; found: 1186.9) were separated by HPLC. Major isomer (retention time: ~ 9.3 min) and minor isomer (retention time: ~ 9.6 min) in approx. 1.2:1 ratio.

**HPLC Conditions:** Waters Sunfire C18 column (19 × 250-mm) with UV detection at 254-nm; Solution A: H<sub>2</sub>O w/0.1% formic acid and Solution B: CH<sub>3</sub>CN w/0.1% formic acid; increase gradient of Solution B from 40% to 100%, 0.5-17 min; flow rate: 20-mL/min.

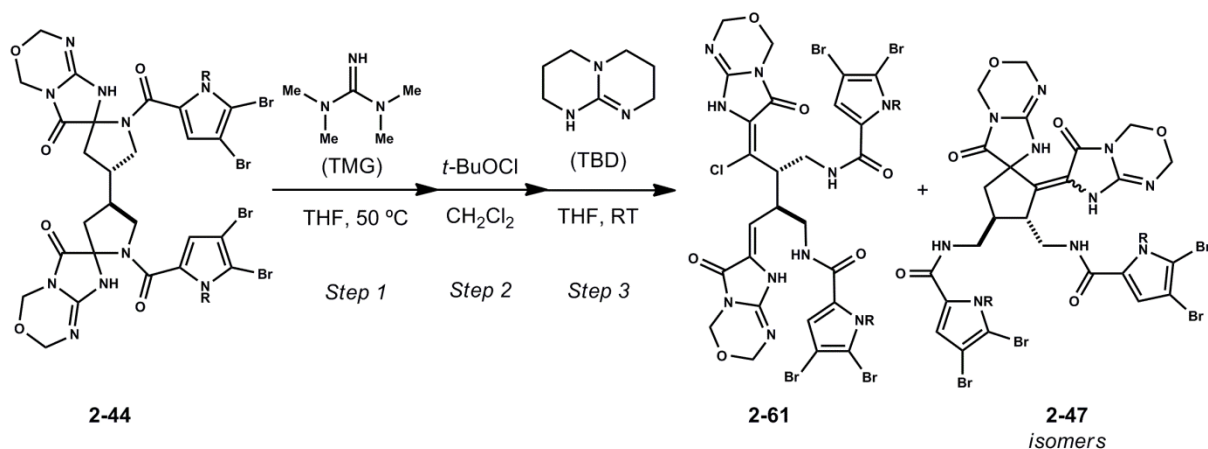
**Chlorinated alkylidene (2-60) (2·HCO<sub>2</sub>H) (major isomer):**

<sup>1</sup>H NMR (600 MHz, CH<sub>3</sub>CN-*d*<sub>3</sub>): δ (ppm) 8.07 (s, 1H), 7.03-6.96 (m, 1H), 6.86-6.75 (m, 1H), 6.65 (s, 1H), 5.78-5.64 (m, 2H), 5.64-5.54 (m, 1H), 5.47-5.34 (m, 1H), 5.21-4.99 (m, 4H), 4.93-4.77 (m, 4H), 4.38-4.31 (m, 1H), 4.13-4.07 (m, 1H), 3.59-3.37 (m, 6H), 2.78-2.68 (m, 2H), 0.89-0.77 (m, 4H), -0.03 (s, 9H), -0.06 (s, 9H) \*2H under residual CH<sub>3</sub>CN peak; **LRMS-ESI** (*m/z*) calcd for [C<sub>38</sub>H<sub>51</sub>Br<sub>4</sub>ClN<sub>10</sub>O<sub>8</sub>Si<sub>2</sub>+H]<sup>+</sup>: 1187.0 ; found: 1186.9.

**Chlorinated alkylidene (2-60) (2·HCO<sub>2</sub>H) (minor isomer):**

<sup>1</sup>H NMR (600 MHz, CH<sub>3</sub>CN-*d*<sub>3</sub>): δ (ppm) 8.07 (s, 1H), 7.02-6.93 (m, 1H), 6.86-6.77 (m, 1H), 6.63 (s, 1H), 5.83 (d, *J* = 11.0 Hz, 1H), 5.77 (d, *J* = 10.6 Hz, 1H), 5.63 (d, *J* = 10.6 Hz, 1H), 5.36 (d, *J* = 11.0 Hz, 1H), 5.20-5.06 (m, 4H), 4.94-4.81 (m, 4H), 4.34-4.27 (m, 1H), 4.08-4.02 (m, 1H), 3.79-3.70 (m, 1H), 3.53-3.37 (m, 4H), 3.36-3.28 (m, 1H), 2.71-2.60 (m, 2H), 0.90-0.74 (m, 4H), -0.00 (s, 9H), -0.07 (s, 9H) \*2H under residual CH<sub>3</sub>CN peak; **LRMS-ESI** (*m/z*) calcd for [C<sub>38</sub>H<sub>51</sub>Br<sub>4</sub>ClN<sub>10</sub>O<sub>8</sub>Si<sub>2</sub>+H]<sup>+</sup>: 1187.0 ; found: 1186.9.

## Preparation of chlorinated bis-alkylidene (**2-61**) from bis-spirocycles (**2-44**).

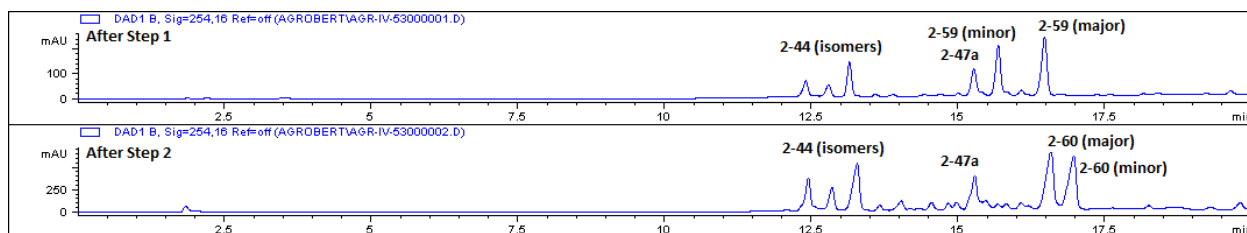


**Step 1** – A 0.48 M stock solution of tetramethylguanidine (TMG) (55.5 mg) in THF (1.0-mL) was prepared. A mixture of purified **2-44a** and purified **2-44b** (195 mg, 0.17 mmol, ~1:1) was dissolved in THF (7.5-mL) followed by the addition of the above TMG stock solution (106- $\mu$ L, 0.3 equiv of TMG). The reaction vial was sealed under Ar and stirred at 50°C for 2h. An additional amount of TMG stock solution was added (106- $\mu$ L, 0.3 equiv) and the reaction was stirred for 2.5h at 50°C (total time 4.5h). The reaction converts both isomers of **2-44** into a major and minor isomer of desired **2-59**. The reaction was cooled to RT and an aliquot (~1.2-mL) was taken and concentrated for use in the subsequent chlorination reaction (assumed 0.050 mmol of crude **2-59**).

**Step 2** – A 0.44 M stock solution of *t*-BuOCl was prepared by the dissolution of *t*-BuOCl (50- $\mu$ L) in CH<sub>2</sub>Cl<sub>2</sub> (1.0-mL). Crude mono-alkylidene isomers **2-59** (0.050 mmol, 1.0 equiv) were dissolved in CH<sub>2</sub>Cl<sub>2</sub> (3.3-mL) and cooled to -78°C in a dry ice / acetone bath. To this solution was added *t*-BuOCl stock solution (102- $\mu$ L, calcd 0.9 equiv). The reaction was stirred at -78°C for 1h at which point the bath was removed and allowed to reach 0°C in an ice-water bath. The reaction was stirred at 0°C for 1h and allowed to warm to RT. After 1h at RT the reaction was judged complete by LC-MS analysis. The crude reaction contains a mixture of desired chlorinated isomers **2-60** (approx. 40–50% by LC-MS UV analysis with detection at 254-nm) and spirocycloalkylidene isomers **2-47** (approx. 20%) and residual bis-spirocycles **2-44**. The crude mixture of chlorinated isomers **2-60** was concentrated with a stream of Ar and used directly in the subsequent reaction.

### Crude Reaction Analysis (after Step 1 and after Step 2):

**HPLC Conditions:** Waters Sunfire C18 analytical column (5  $\mu$ m, 4.6  $\times$  250-mm) with UV detection at 254-nm; Solution A: H<sub>2</sub>O w/0.1% formic acid and Solution B: CH<sub>3</sub>CN w/0.1% formic acid; increase gradient of Solution B from 30% to 100%, 0.2-17 min; flow rate: 1.0-mL/min.

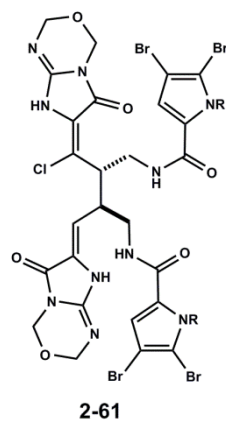


*Step 3* – A 0.3 M stock solution of TBD in THF was prepared. The crude mixture of chlorinated isomers **2-60** (assumed 0.050 mmol, 1.0 equiv) was dissolved in THF (1.0-mL) and toluene (0.98-mL) at RT. To this solution was added TBD stock solution (196- $\mu$ L, calcd 1.2 equiv) via syringe in a single portion. The reaction was stirred at RT for 3h and judged complete by LC-MS analysis. The reaction was quenched by the addition of saturated aqueous  $\text{NH}_4\text{Cl}$  (1-mL) and diluted with EtOAc (5-mL). The organic layer was separated and washed with saturated aqueous  $\text{NH}_4\text{Cl}$  (2-mL),  $\text{H}_2\text{O}$  (2-mL), brine, dried over  $\text{Na}_2\text{SO}_4$  and concentrated in vacuo. The crude material was purified by pTLC. The pTLC plates (500- $\mu$ m) were pretreated with a solution of 1%  $\text{Et}_3\text{N}$  in hexanes and dried prior to use. The crude material was dissolved in  $\text{CHCl}_3$ , loaded onto two plates and eluted with  $\text{CHCl}_3$  / MeOH (15:1). After elution, three major bands were identified by UV detection at 254-nm. These bands were isolated and characterized as spirocycloalkylidene **2-47b** (6.0 mg, 13%, yield calcd. from **2-44**,  $R_f = 0.65$ ), chlorinated bis-alkylidene **2-61** (6.5 mg, 14%, 3 steps from **2-44**,  $R_f = 0.60$ ) and spirocycloalkylidene **2-47a** (7.4 mg, 16%, yield calcd. from **2-44**,  $R_f = 0.58$ ).

The conversion of both isomers **2-60** to chlorinated bis-alkylidene **2-61** is presumed. Independent experiments with individual isomers (**2-60**) and TBD to afford chlorinated bis-alkylidene **2-61** were not conducted.

For characterization purposes, a portion of chlorinated bis-alkylidene **2-61** obtained from pTLC was purified by HPLC. (retention time: ~13 min).

**HPLC Conditions:** Waters Sunfire C18 column (19  $\times$  250-mm) with UV detection at 254-nm; Solution A:  $\text{H}_2\text{O}$  w/0.1% formic acid and Solution B:  $\text{CH}_3\text{CN}$  w/0.1% formic acid; increase gradient of Solution B from 50% to 100%, 0.5-17 min; flow rate: 20-mL/min.



**Chlorinated bis-alkylidene (2-60) (2·HCO<sub>2</sub>H):**

<sup>1</sup>H NMR (600 MHz, CH<sub>3</sub>CN-*d*<sub>3</sub>): δ (ppm) 7.57 (bs, 1H), 7.47 (bs, 1H), 6.86 (s, 1H), 6.73 (s, 1H), 5.84-5.77 (m, 2H), 5.73-5.66 (m, 2H), 5.50 (d, *J* = 9.9 Hz, 1H), 5.22-5.05 (m, 4H), 4.99-4.86 (m, 4H), 4.59-4.52 (m, 1H), 3.64-3.35 (m, 8H), 3.16-3.03 (m, 1H), 0.86-0.73 (m, 4H), -0.07 (s, 18H); LRMS-ESI (*m/z*) calcd for [C<sub>38</sub>H<sub>51</sub>Br<sub>4</sub>ClN<sub>10</sub>O<sub>8</sub>Si<sub>2</sub>+H]<sup>+</sup>: 1187.0; found: 1186.9,



### 2.5.3 Experimental References

[1] Dydio, P.; Zielinski, T.; Jurczak, J. *J. Org. Chem.* **2009**, *74*, 1525.

[2] For the preparation of methyl 5-bromo-2-oxopentanoate **2-27** see: (a) Li, Q.; Hurley, P.; Ding, H.; Roberts, A. G.; Akella, R.; Harran, P. G. *J. Org. Chem.* **2009**, *74*, 5909. (b) Cushman, M.; Gerhardt, S.; Huber, R.; Fischer, M.; Kis, K.; Bacher, A. *J. Org. Chem.* **2002**, *67*, 5807.

[3] For the preparation of *i*-PrCp<sub>2</sub>TiCl<sub>2</sub> refer to: Giolando, D. M.; Rauchfuss, T. B.; Rheingold, A. L.; Wilson, S. R. *Organometallics* **1987**, *6*, 667.

[4] Sparging THF with Ar for 20 min was as effective as the freeze-pump-thaw method for this reaction.

[5] For the preparation of 3-(3-nitrophenyl)-2-(phenylperoxythio)-1,2-oxaziridine **2-56** refer to Vishwakarma, L. C.; Stringer, O. D.; Davis, F. A. *Org. Syn.* **1988**, *66*, 203; **1993**, *8*, 543.

## APPENDIX ONE

### Spectra Relevant to Chapter Two:

#### Chapter 2 – Symmetry-Based Logic for the Synthesis of Axinellamines and Palau'amine

adapted in part from

#### Synthetic ( $\pm$ )-Axinellamines Deficient in Halogen

*Hui Ding, Andrew G. Roberts and Patrick G. Harran*

*Angew. Chem. Int. Ed.* **2012**, *51*, 4416 – 4419.

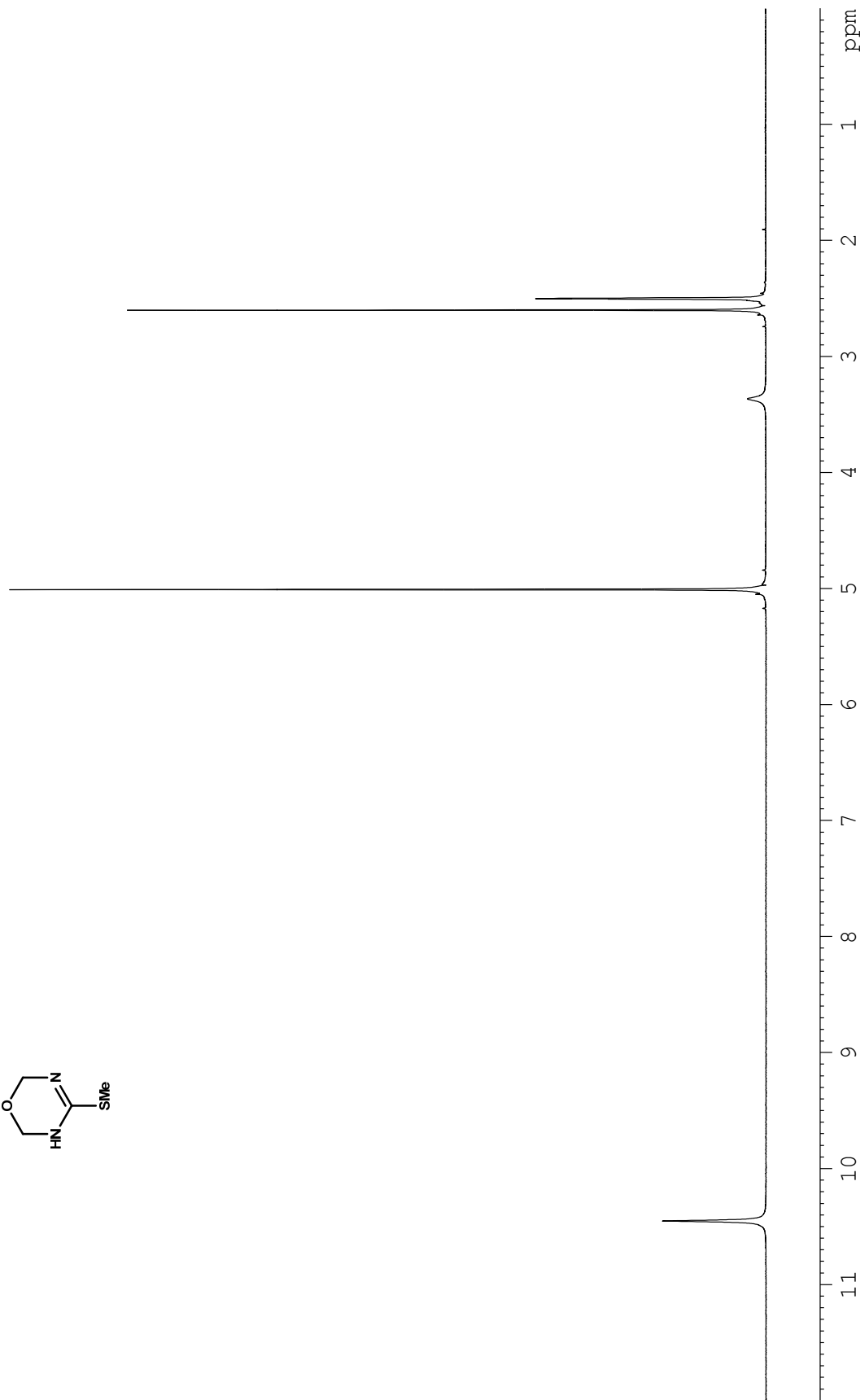
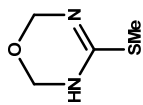


**Figure A1.1.** <sup>1</sup>H NMR (500 MHz, DMSO-*d*<sub>6</sub>) spectrum of compound 2-10.

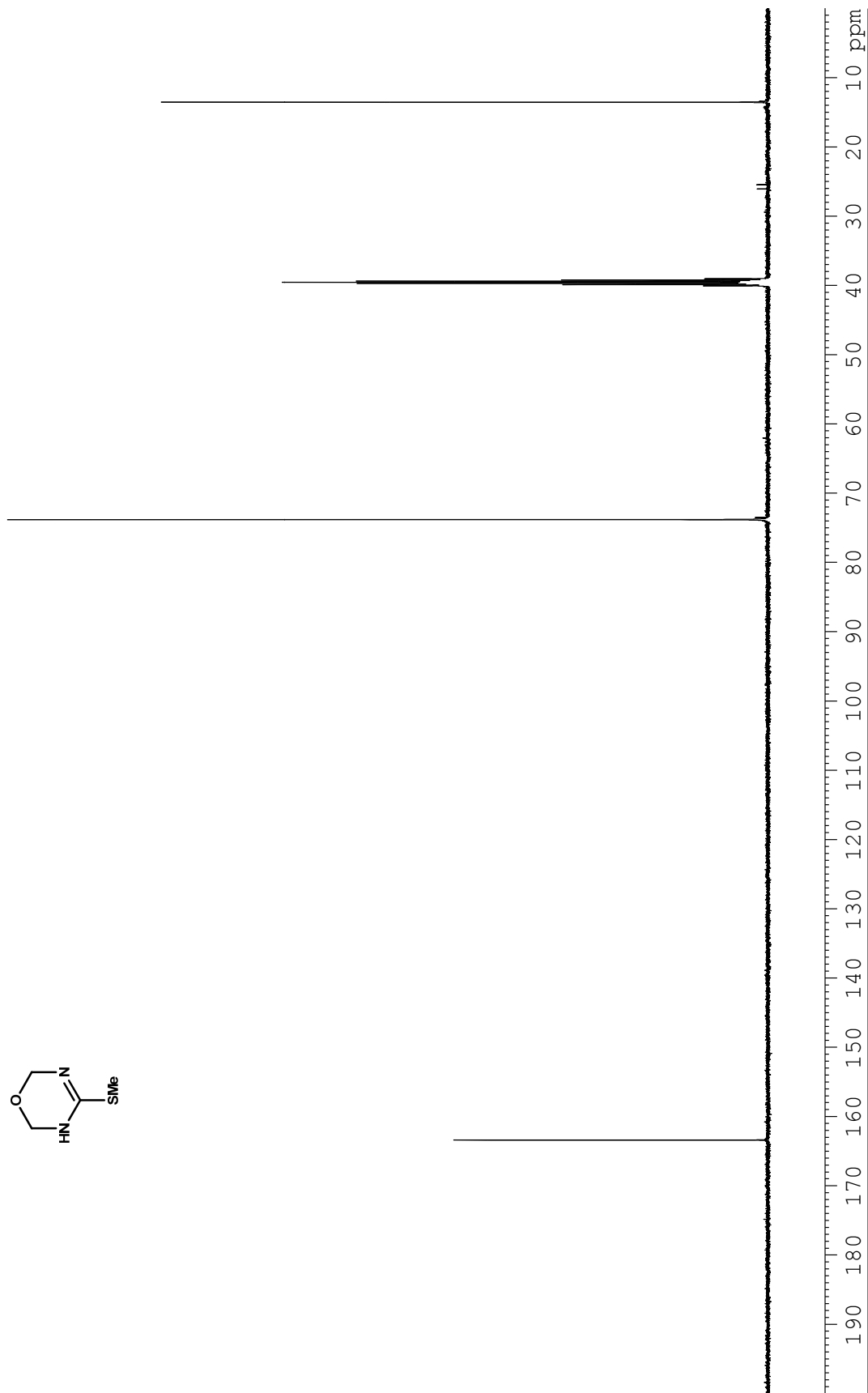
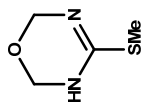


**Figure A1.2.**  $^{13}\text{C}$  NMR (125 MHz,  $\text{DMSO-}d_6$ ) spectrum of compound 2-10.

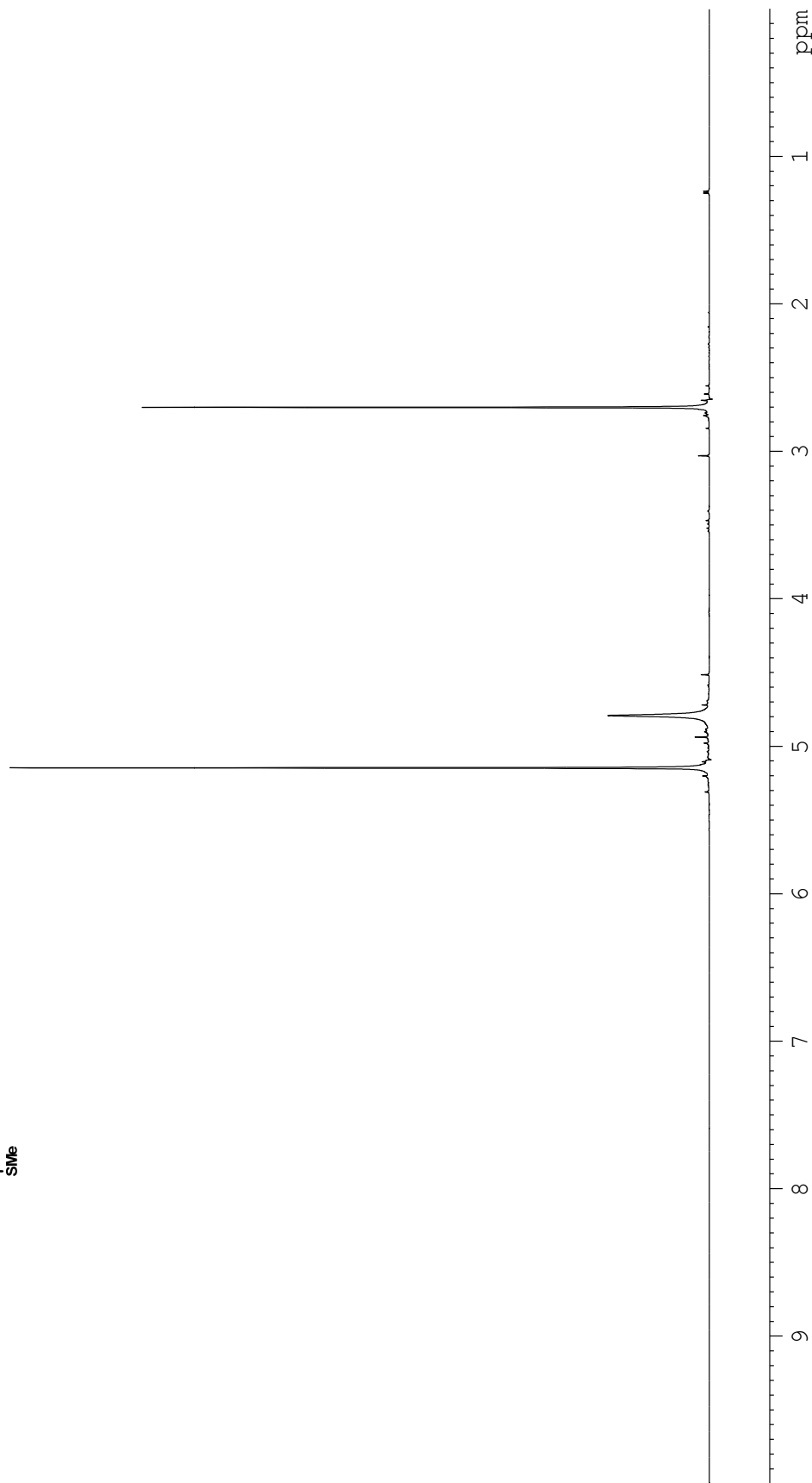
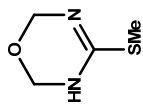


**Figure A1.3.** <sup>1</sup>H NMR (600 MHz, H<sub>2</sub>O-*d*<sub>2</sub>) spectrum of compound 2-10.

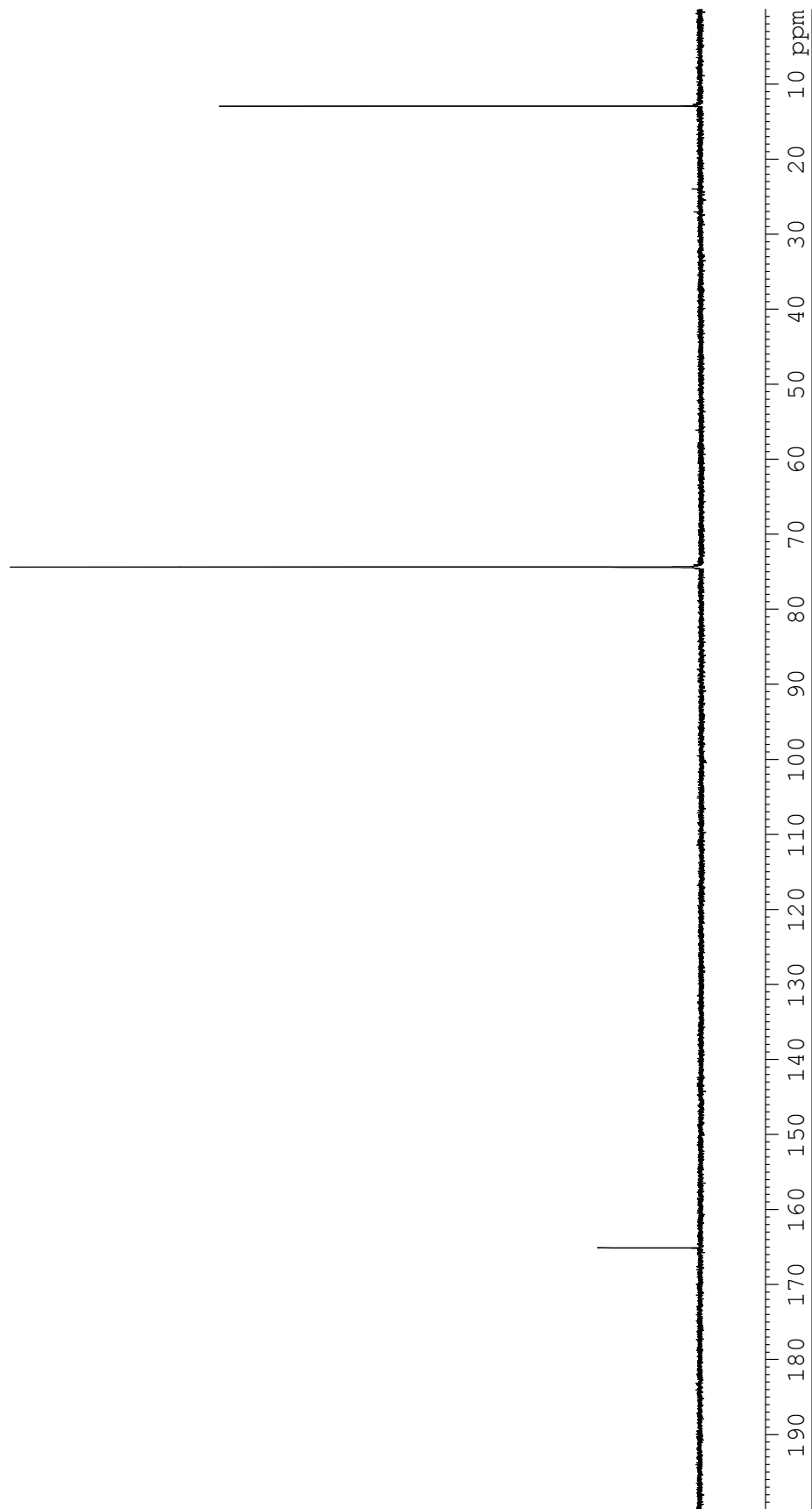
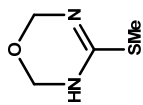
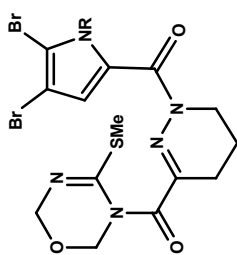


**Figure A1.4.**  $^{13}\text{C}$  NMR (125 MHz,  $\text{H}_2\text{O}-d_2$ ) spectrum of compound 2-10.



R = CH<sub>2</sub>O(CH<sub>2</sub>)<sub>2</sub>Si(CH<sub>3</sub>)<sub>3</sub>

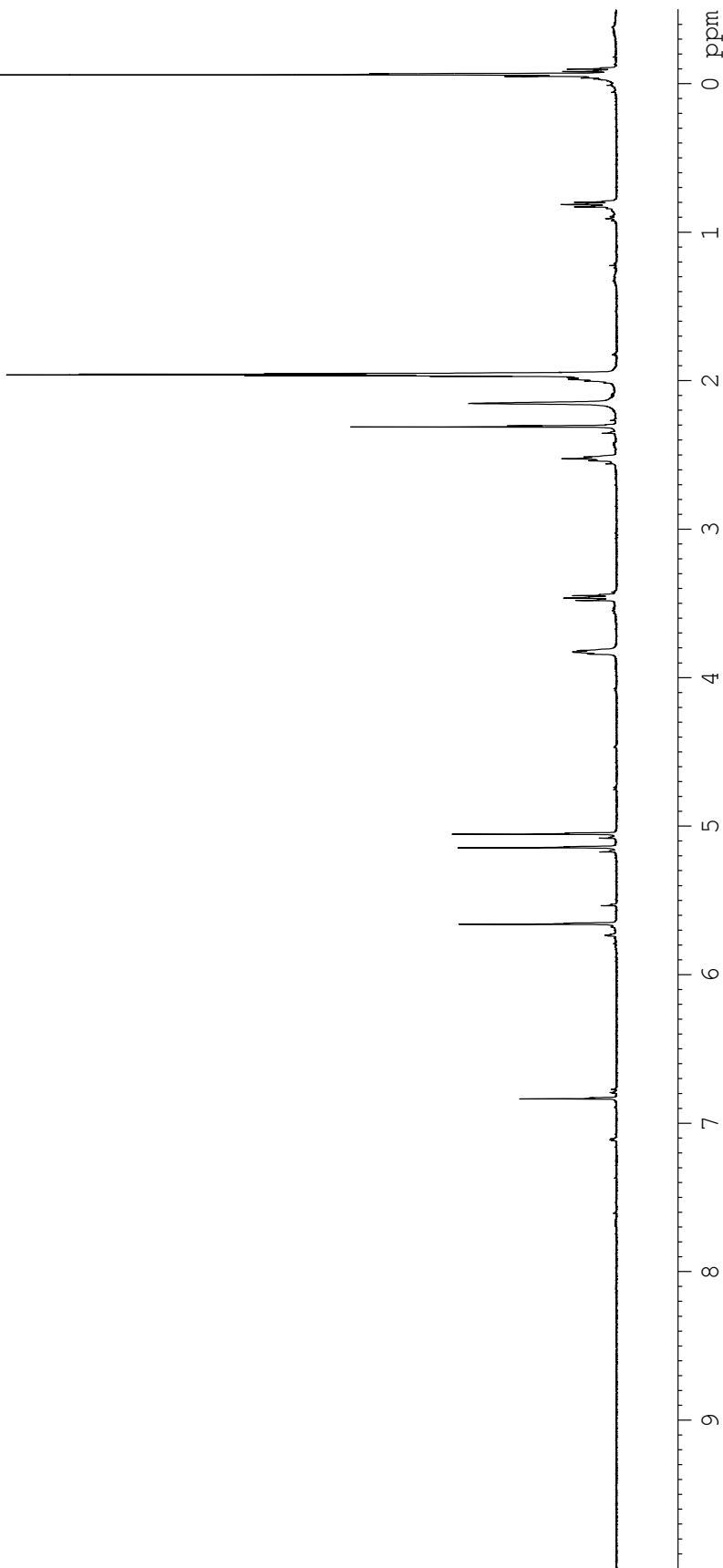
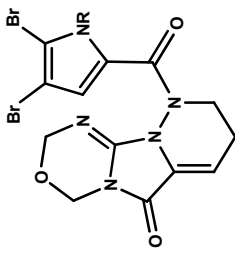


**Figure A1.5.** <sup>1</sup>H NMR (500 MHz, CH<sub>3</sub>CN-*d*<sub>3</sub>) spectrum of compound 2-17.



R = CH<sub>2</sub>O(CH<sub>2</sub>)<sub>2</sub>Si(CH<sub>3</sub>)<sub>3</sub>

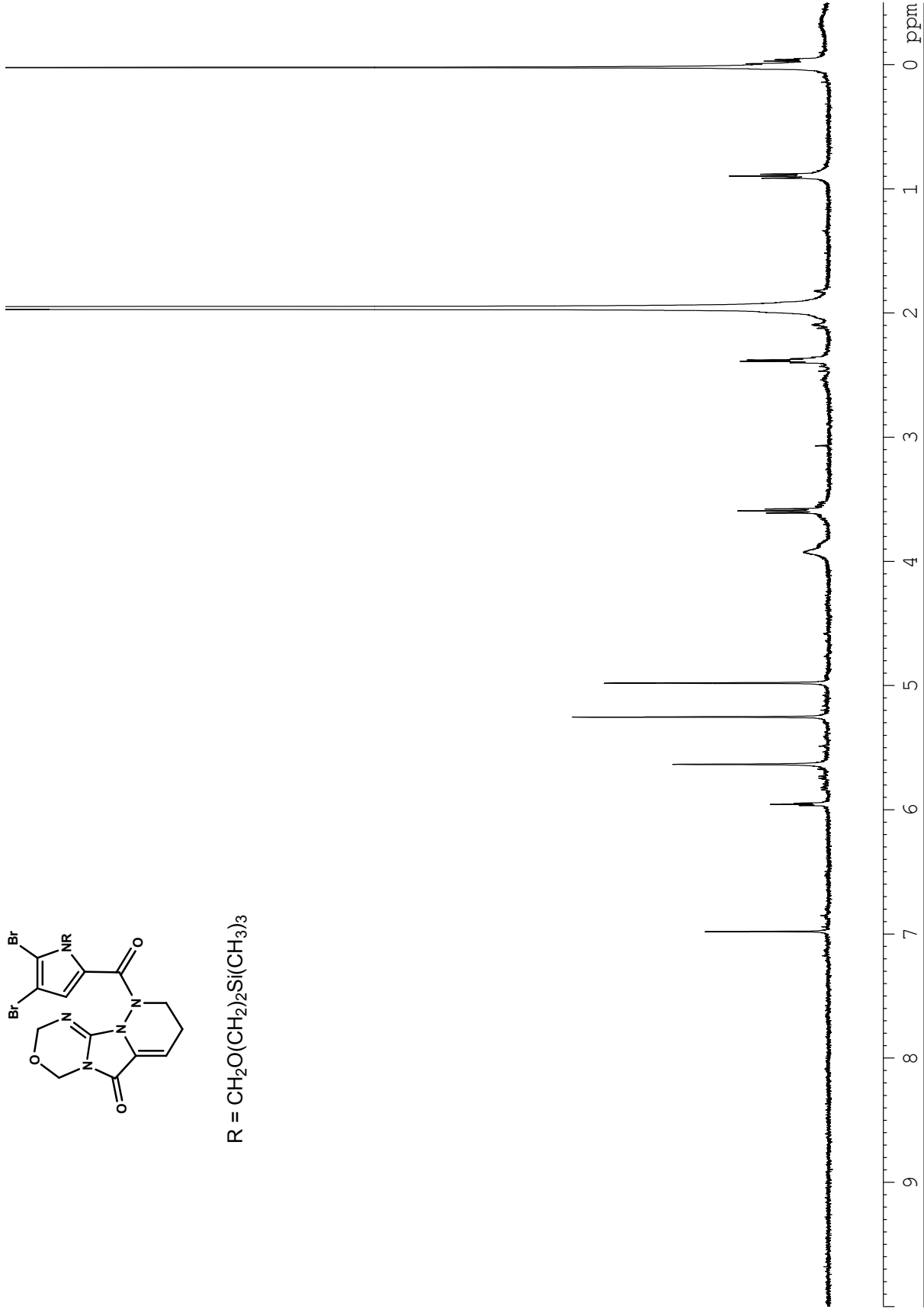
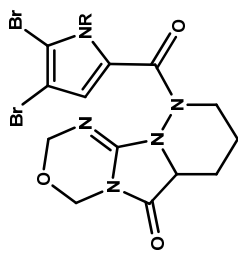


**Figure A1.6.** <sup>1</sup>H NMR (500 MHz, CH<sub>3</sub>CN-*d*<sub>3</sub>) spectrum of compound **2-8**.





R = CH<sub>2</sub>O(CH<sub>2</sub>)<sub>2</sub>Si(CH<sub>3</sub>)<sub>3</sub>

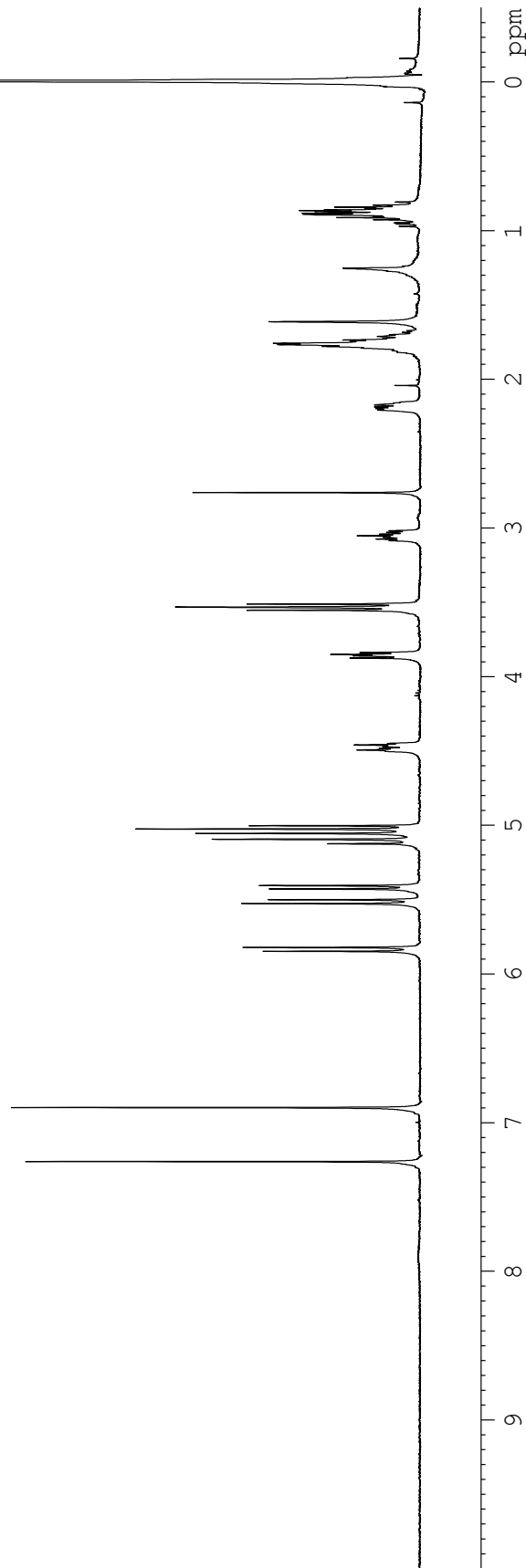
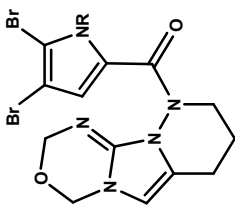


**Figure A1.7.** <sup>1</sup>H NMR (500 MHz, CHCl<sub>3</sub>-d<sub>1</sub>) spectrum of compound **2-21**.



R = CH<sub>2</sub>O(CH<sub>2</sub>)<sub>2</sub>Si(CH<sub>3</sub>)<sub>3</sub>

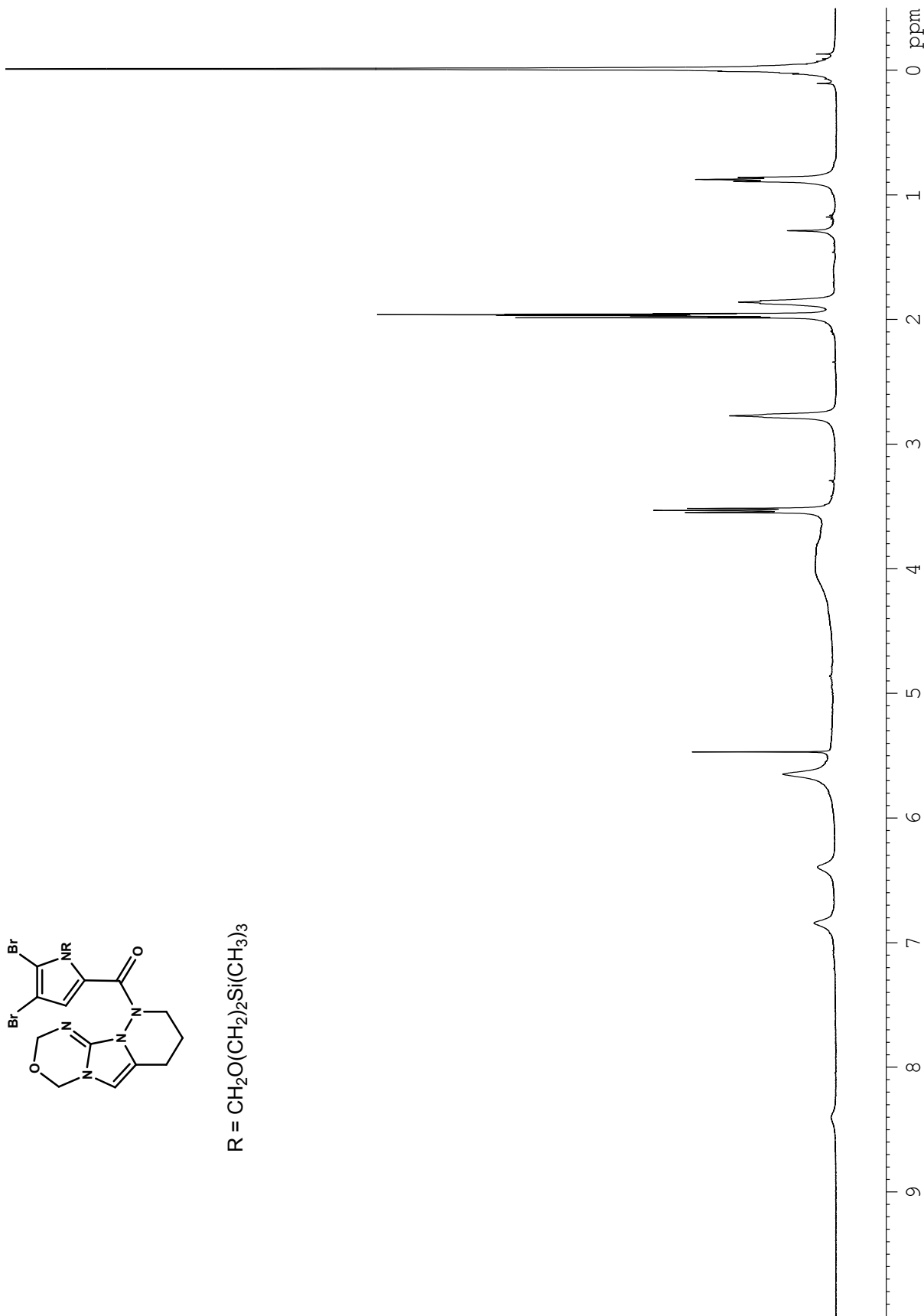
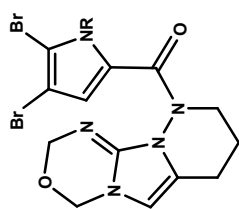


**Figure A1.8.** <sup>1</sup>H NMR (500 MHz, CH<sub>3</sub>CN-*d*<sub>3</sub>) spectrum of compound **2-23**.



R = CH<sub>2</sub>O(CH<sub>2</sub>)<sub>2</sub>Si(CH<sub>3</sub>)<sub>3</sub>

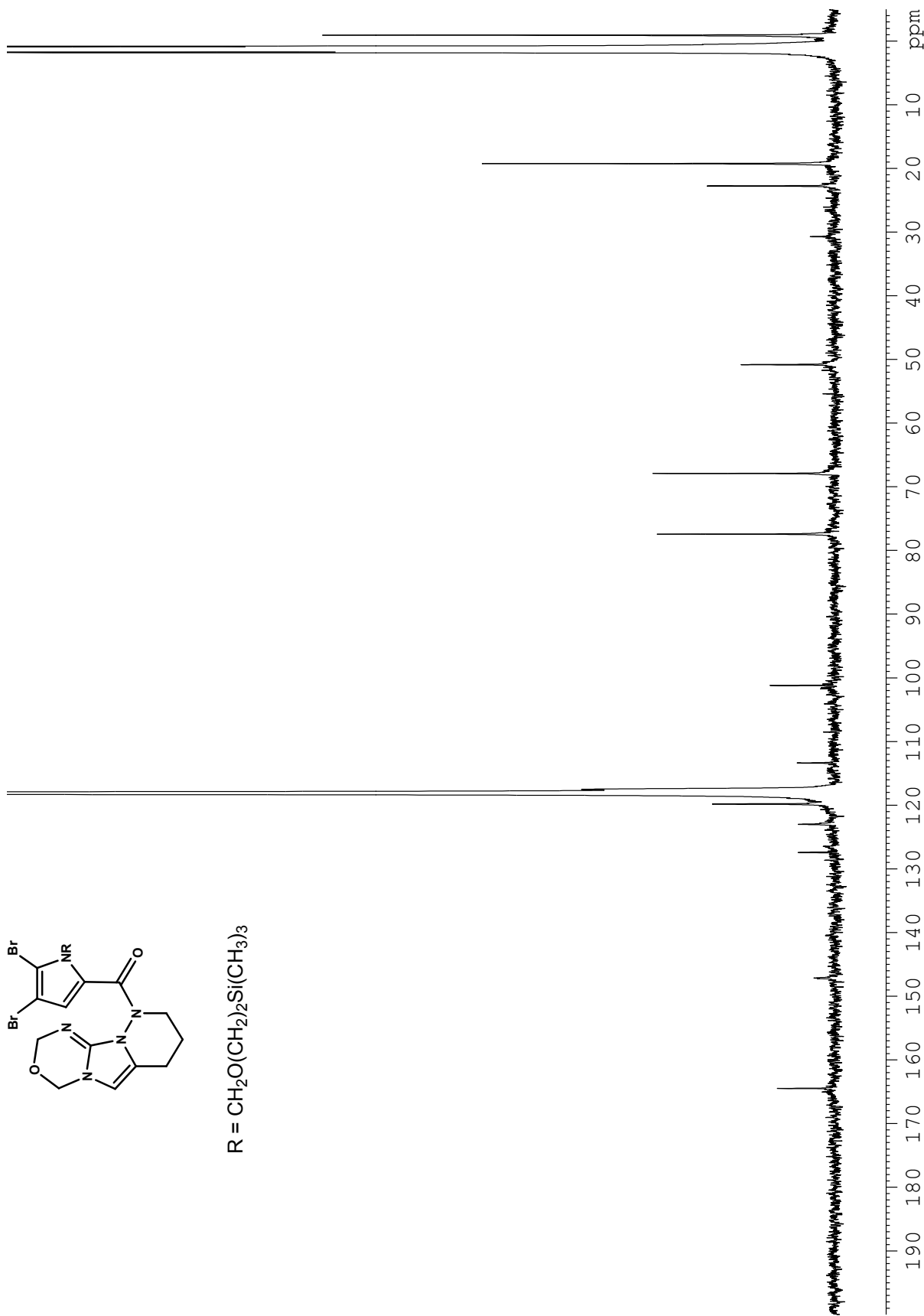
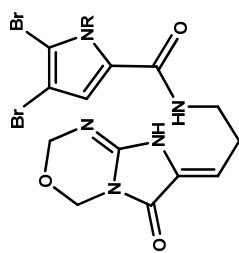


**Figure A1.9.** <sup>13</sup>C NMR (125 MHz, CH<sub>3</sub>CN-*d*<sub>3</sub>, 343 K) spectrum of compound **2-23**.



R = CH<sub>2</sub>O(CH<sub>2</sub>)<sub>2</sub>Si(CH<sub>3</sub>)<sub>3</sub>

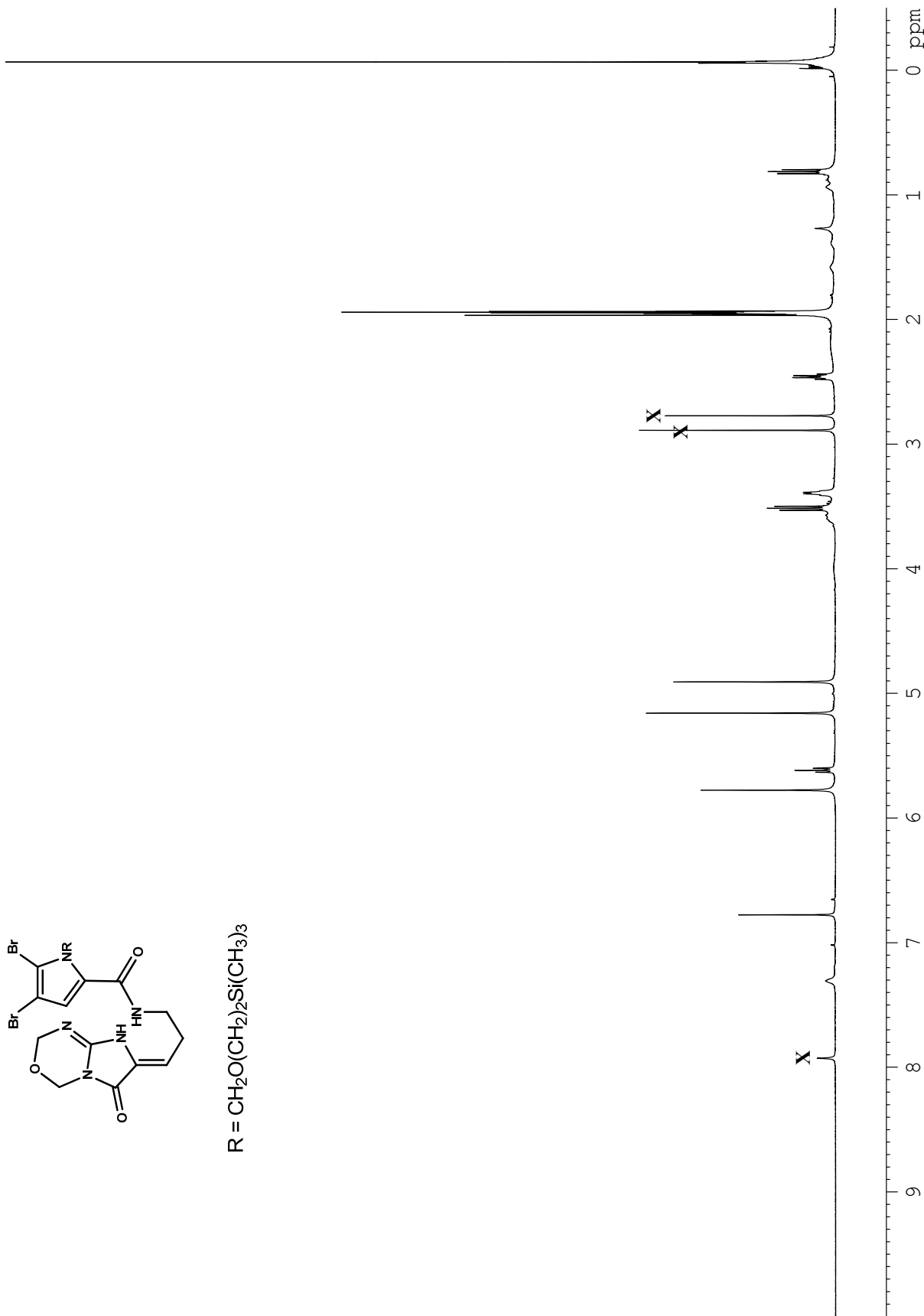


**Figure A1.10.** <sup>1</sup>H NMR (500 MHz, CH<sub>3</sub>CN-*d*<sub>3</sub>) spectrum of compound **2-24a**.

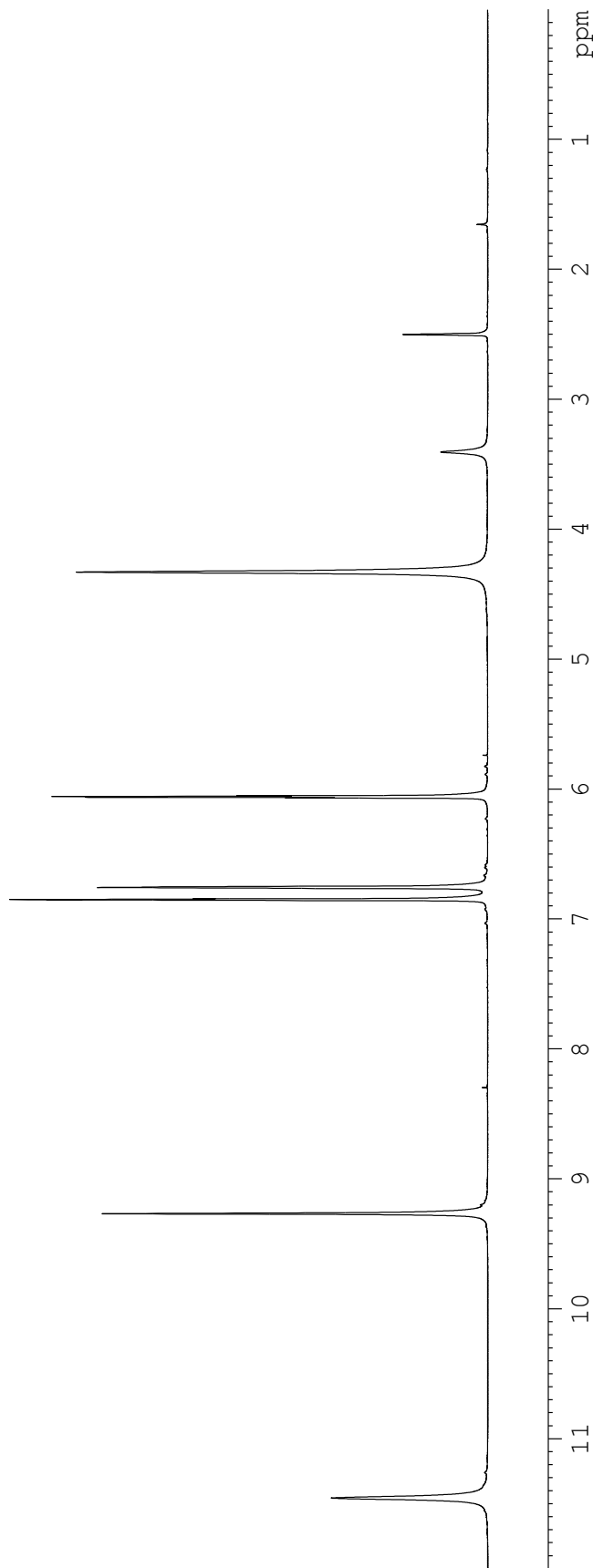
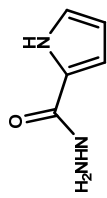


**Figure A1.11.** <sup>1</sup>H NMR (500 MHz, DMSO-*d*<sub>6</sub>) spectrum of compound 2-28.

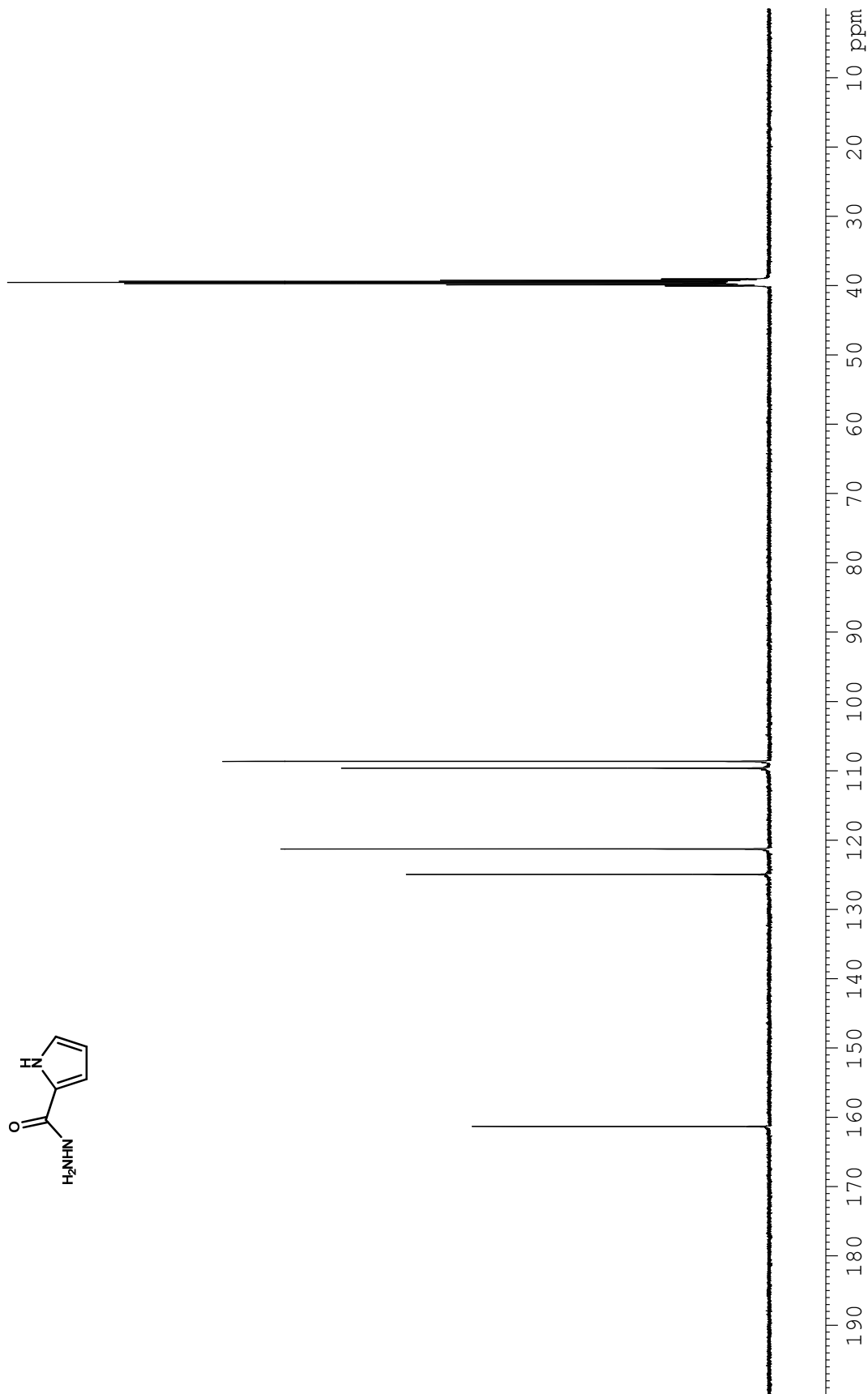
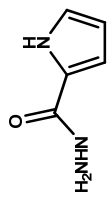


**Figure A1.12.**  $^{13}\text{C}$  NMR (125 MHz, DMSO- $d_6$ ) spectrum of compound 2-28.

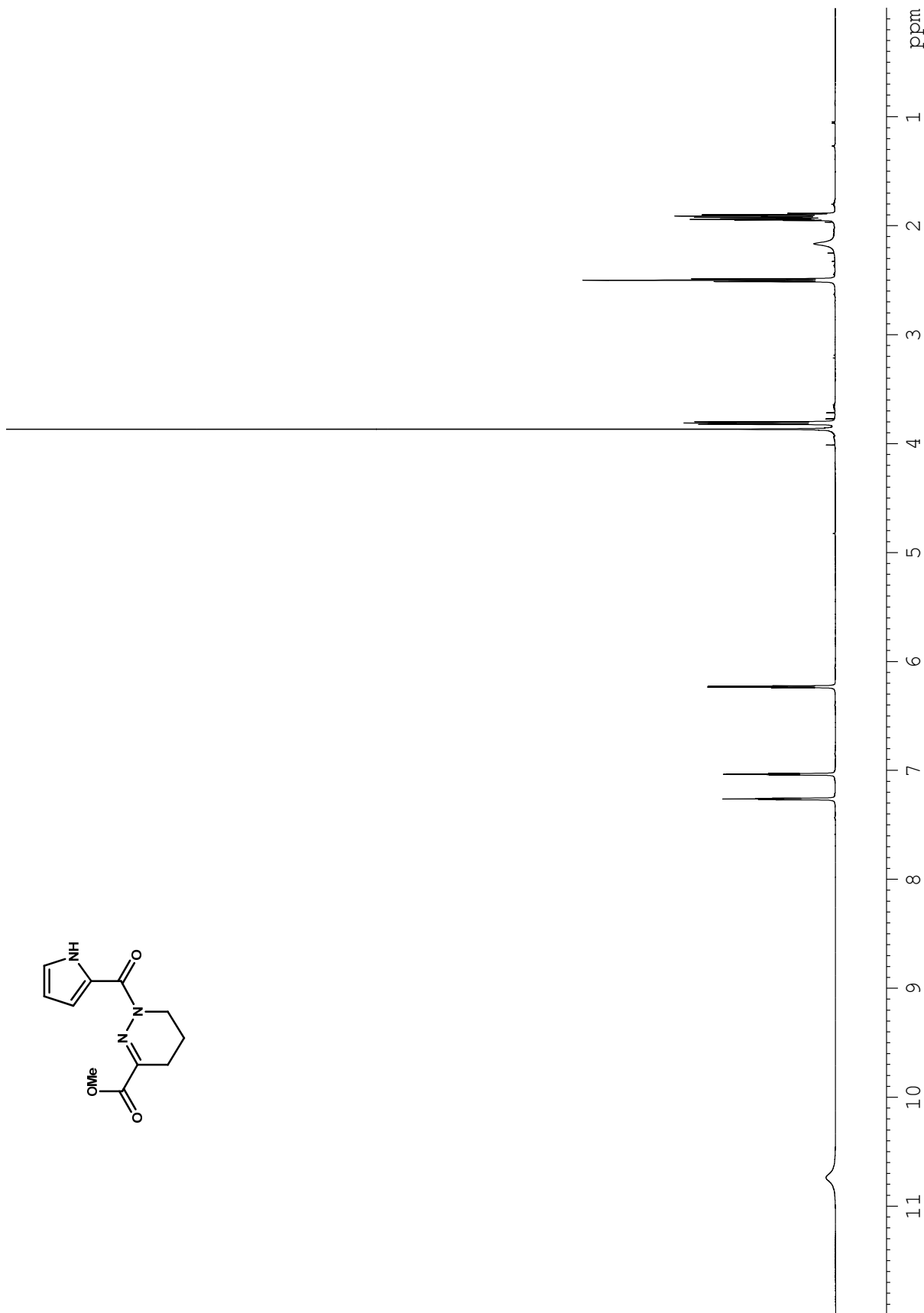
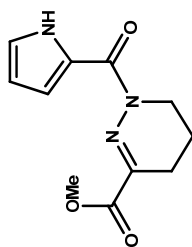


**Figure A1.13.**  $^1\text{H}$  NMR (500 MHz,  $\text{CH}_3\text{CN-}d_3$ ) spectrum of compound **2-29a**.

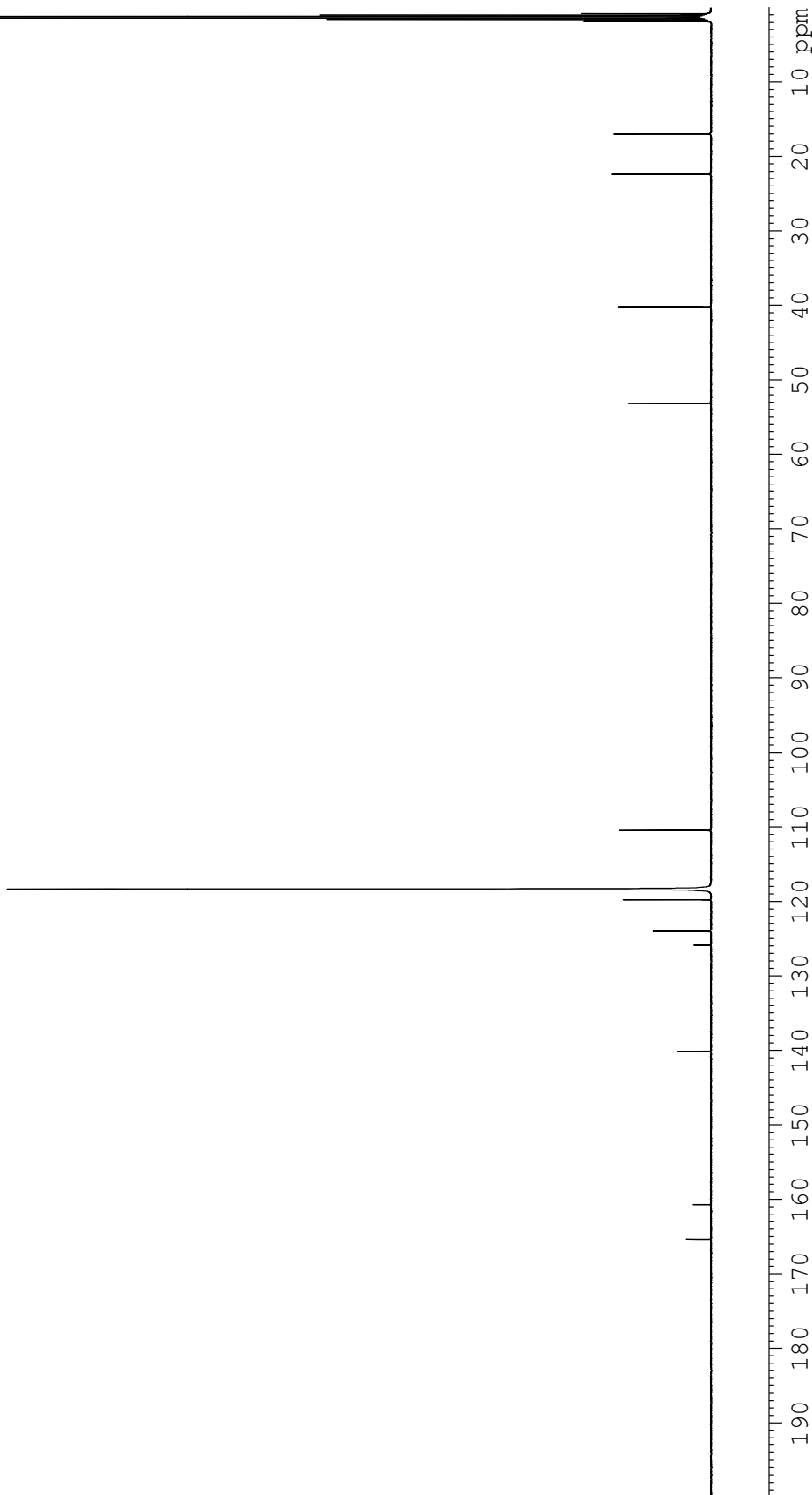
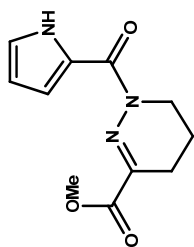


**Figure A1.14.**  $^{13}\text{C}$  NMR (125 MHz,  $\text{CH}_3\text{CN}-d_3$ ) spectrum of compound 2-29a.



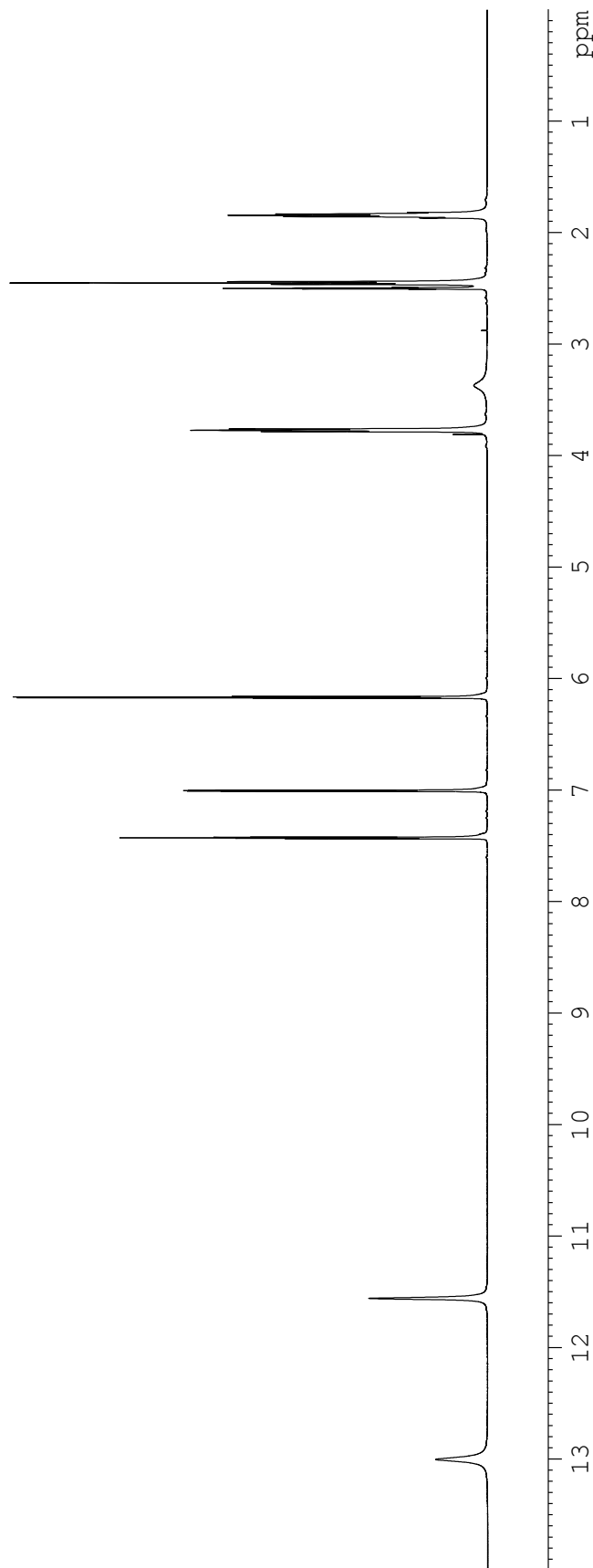
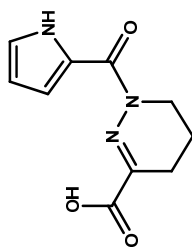


**Figure A1.15.**  $^1\text{H}$  NMR (500 MHz,  $\text{DMSO-}d_6$ ) spectrum of compound **2-29b**.

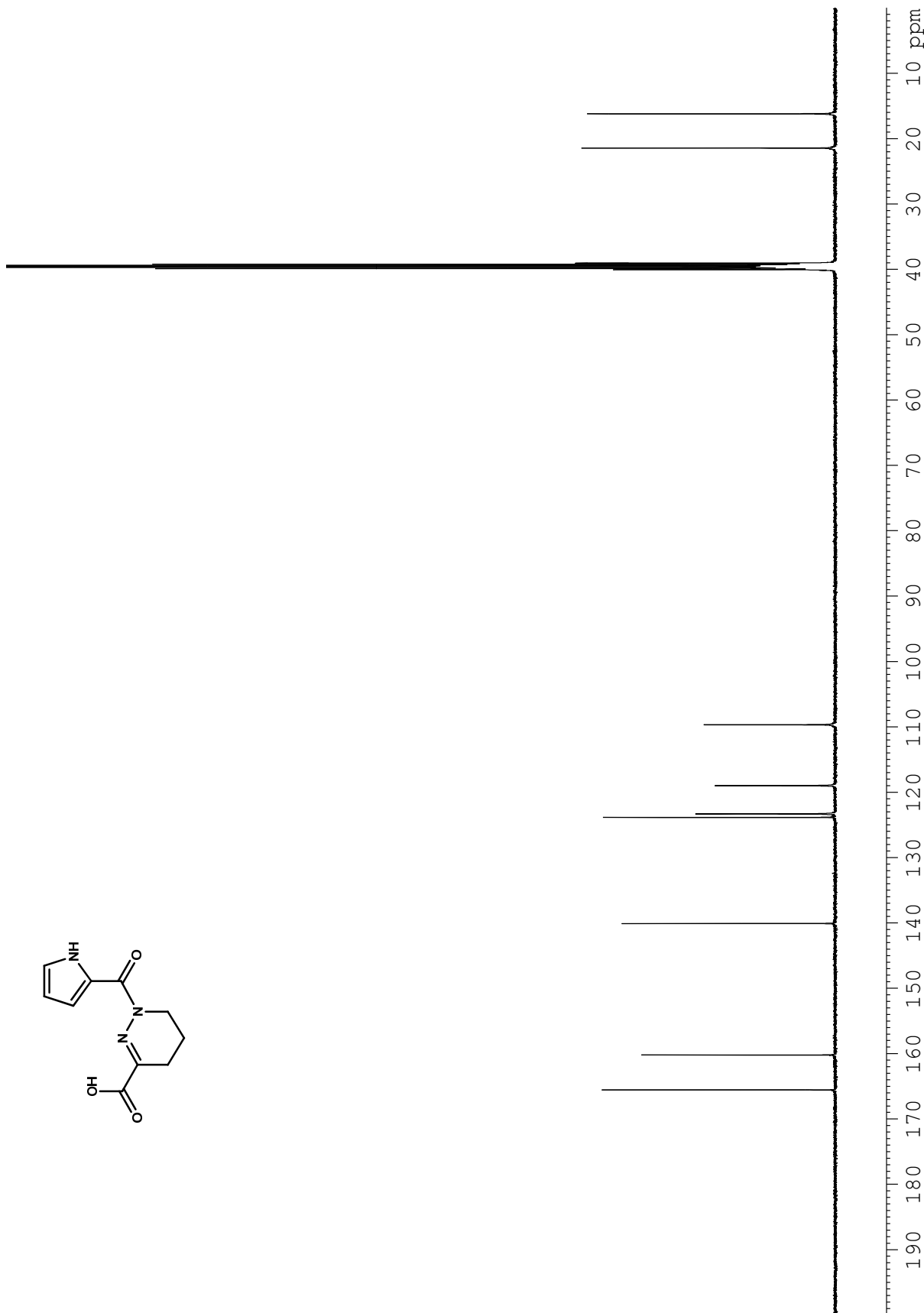
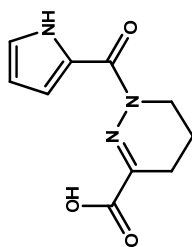


**Figure A1.16.**  $^{13}\text{C}$  NMR (125 MHz,  $\text{DMSO-}d_6$ ) spectrum of compound 2-29b.

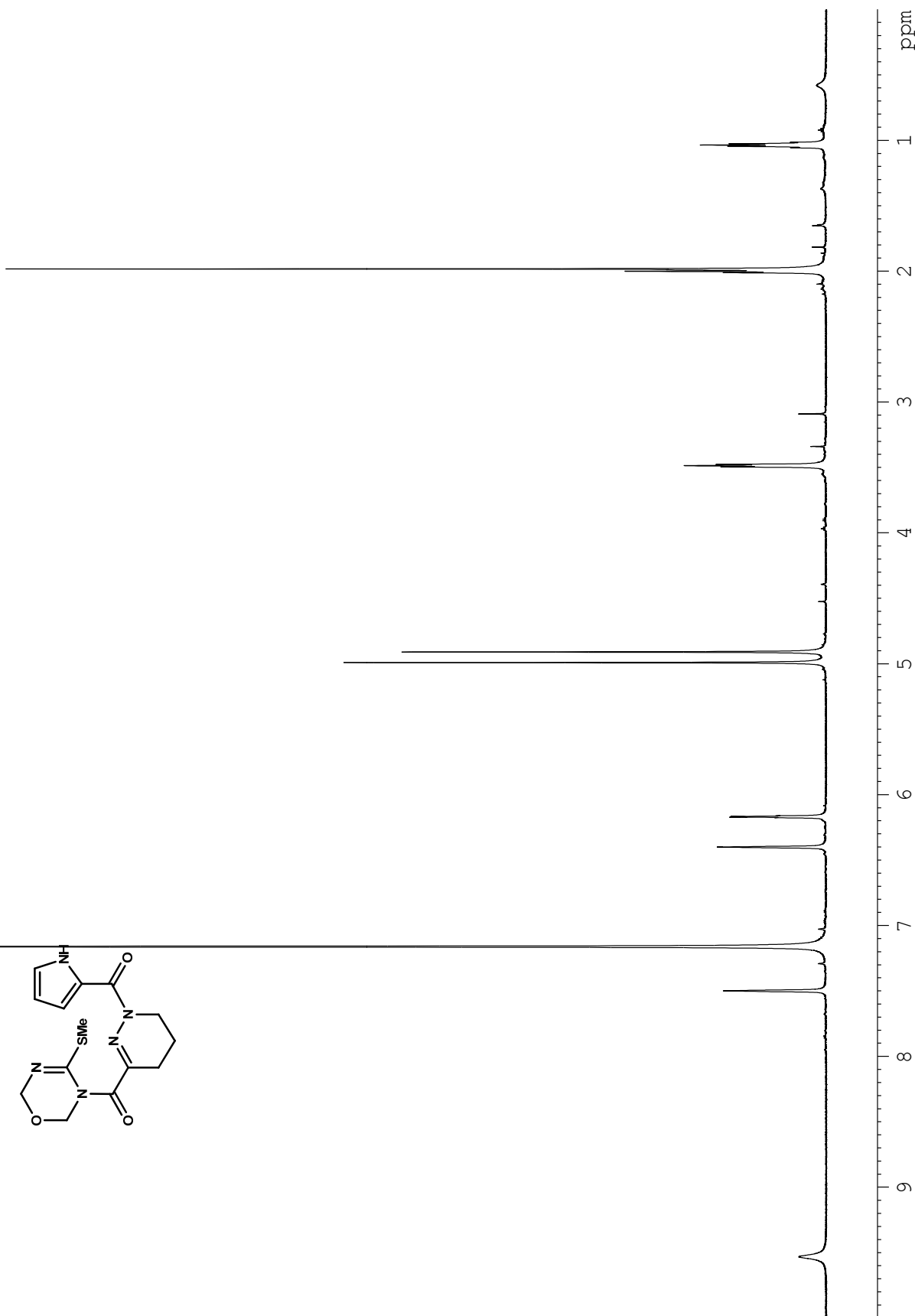
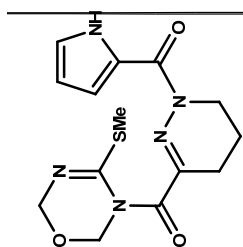


**Figure A1.17.**  $^1\text{H}$  NMR (600 MHz, benzene- $d_6$ ) spectrum of compound **2-30**.

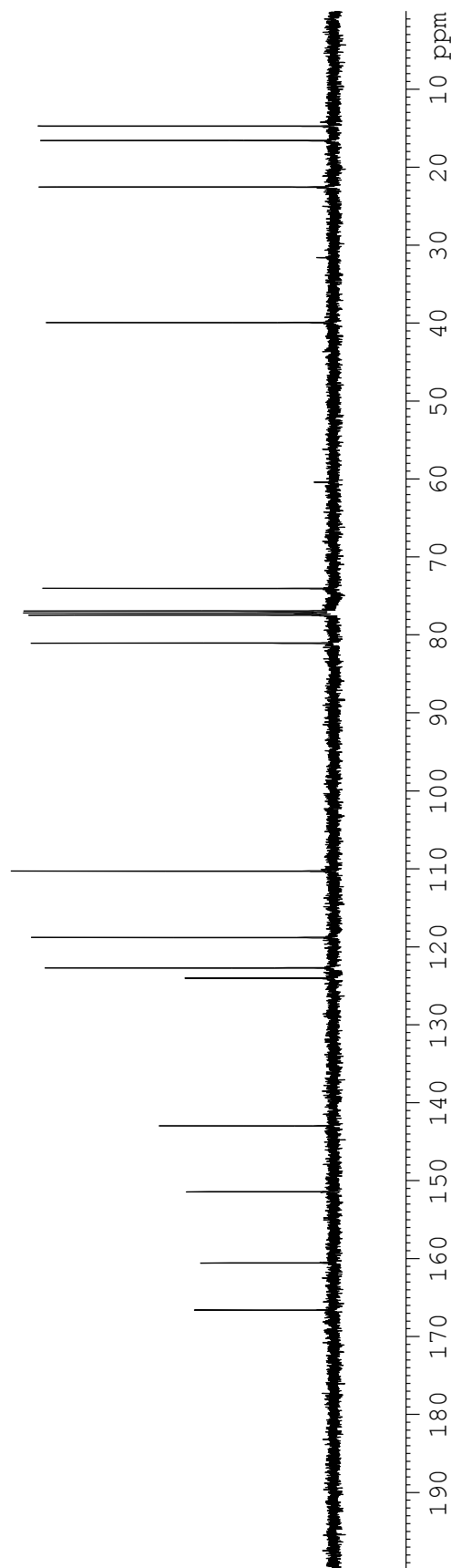
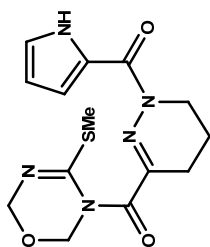


**Figure A1.18.**  $^{13}\text{C}$  NMR (125 MHz,  $\text{CH}_3\text{CN}-d_3$ ) spectrum of compound 2-30.

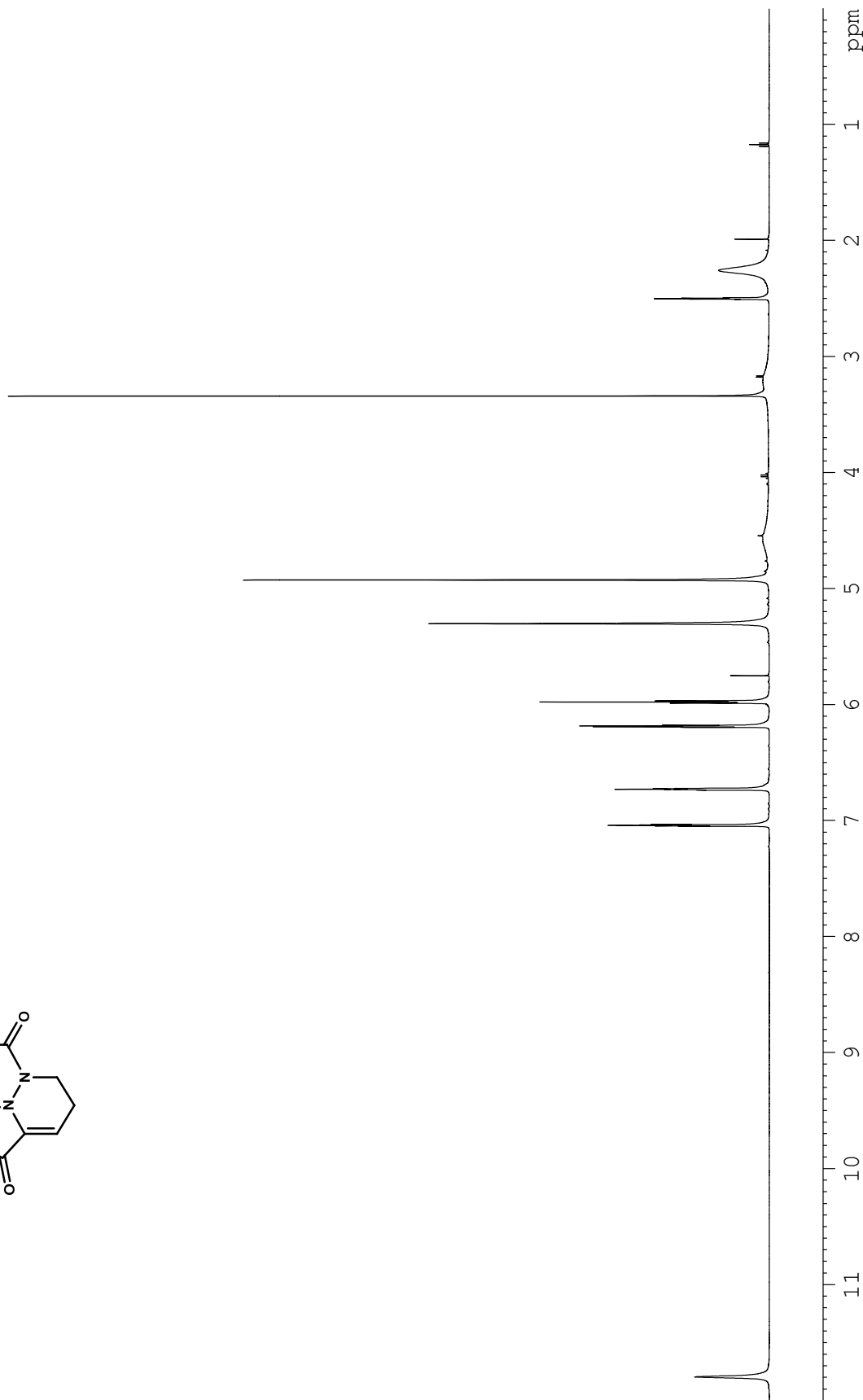
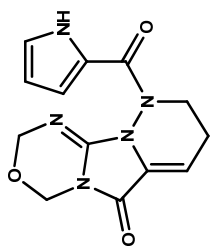


**Figure A1.19.**  $^1\text{H}$  NMR (600 MHz,  $\text{DMSO-}d_6$ ) spectrum of compound **2-26**.

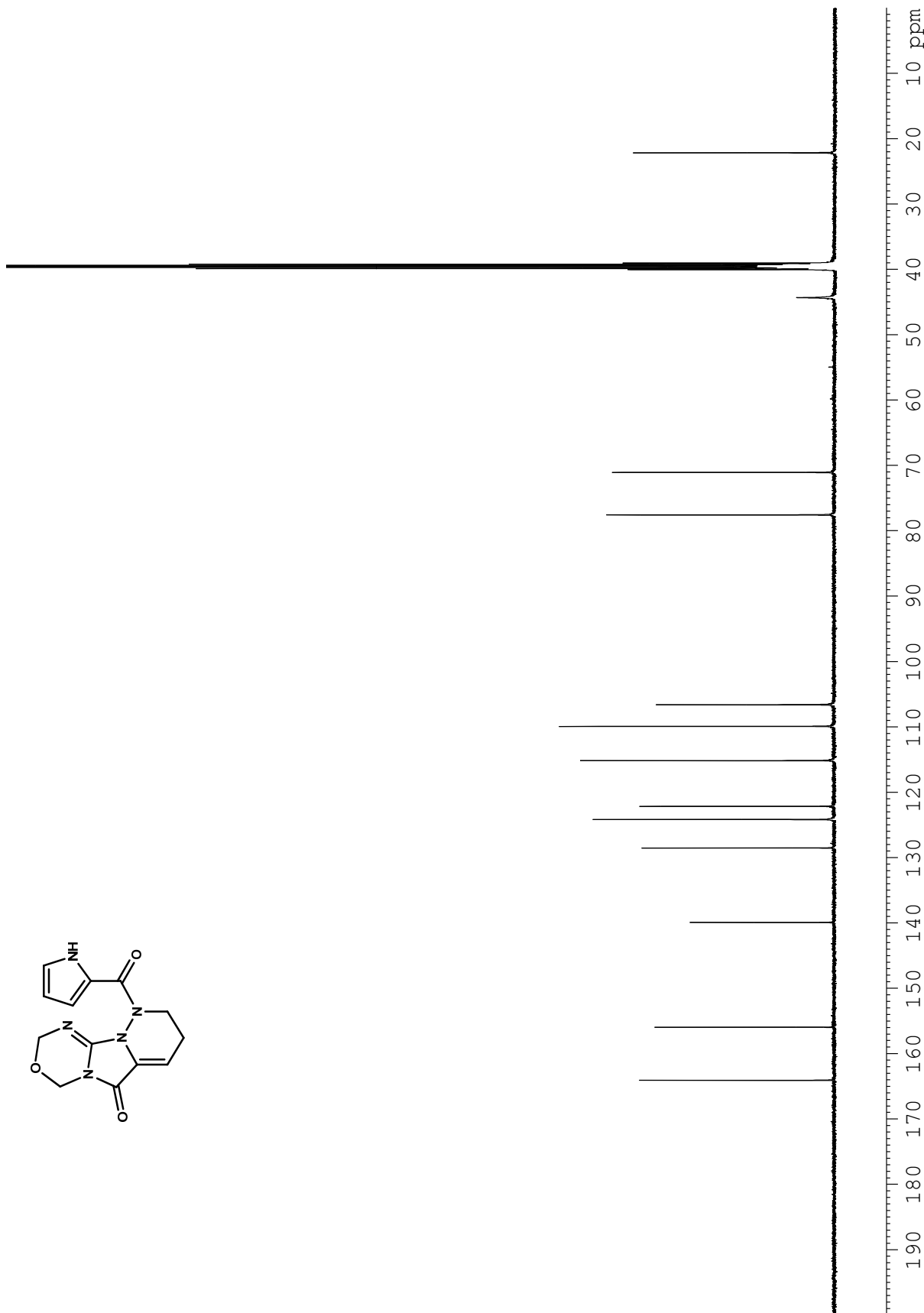
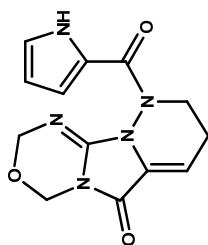
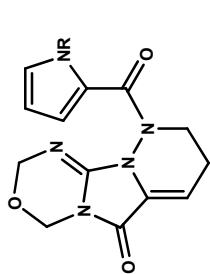


**Figure A1.20.**  $^{13}\text{C}$  NMR (125 MHz,  $\text{DMSO-}d_6$ ) spectrum of compound **2-26**.



R = CH<sub>2</sub>O(CH<sub>2</sub>)<sub>2</sub>Si(CH<sub>3</sub>)<sub>3</sub>

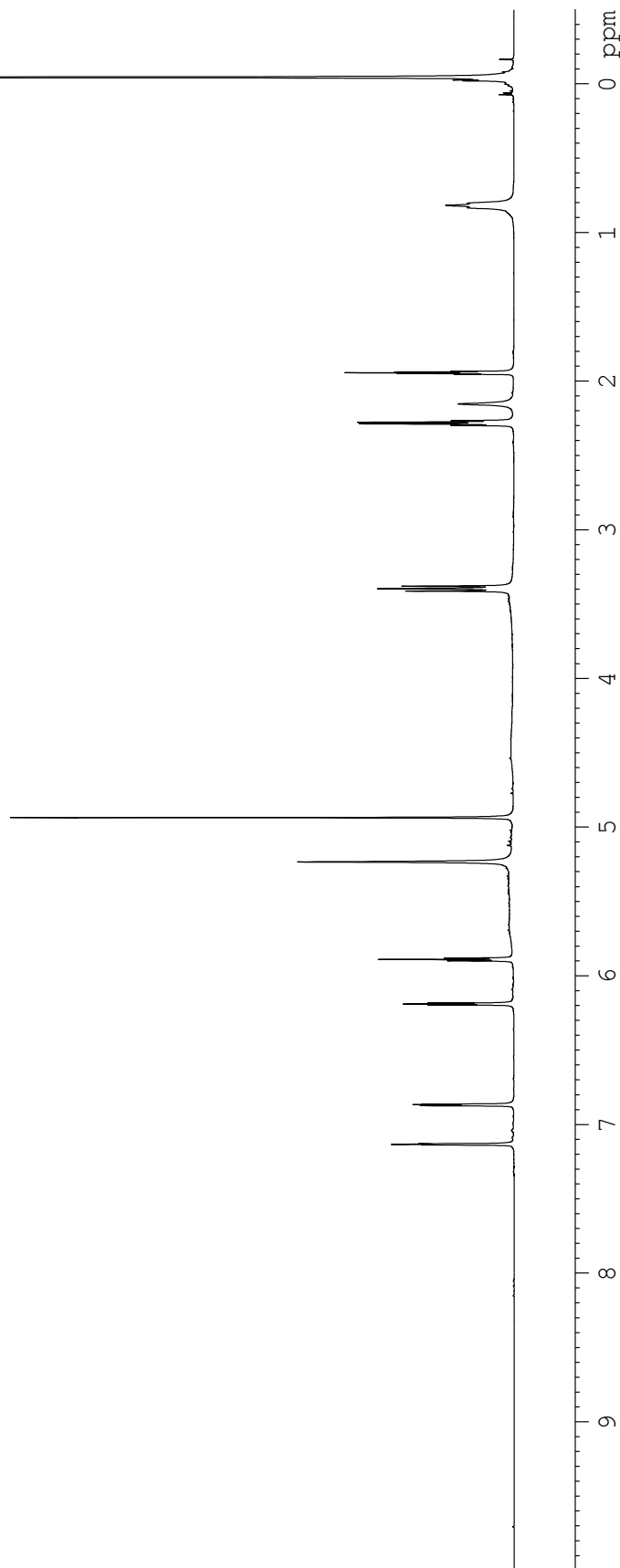
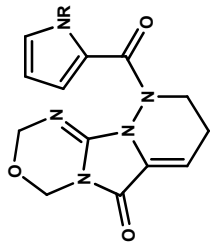


**Figure A1.21.** <sup>1</sup>H NMR (500 MHz, CH<sub>3</sub>CN-*d*<sub>3</sub>) spectrum of compound **2-31**.



R = CH<sub>2</sub>O(CH<sub>2</sub>)<sub>2</sub>Si(CH<sub>3</sub>)<sub>3</sub>

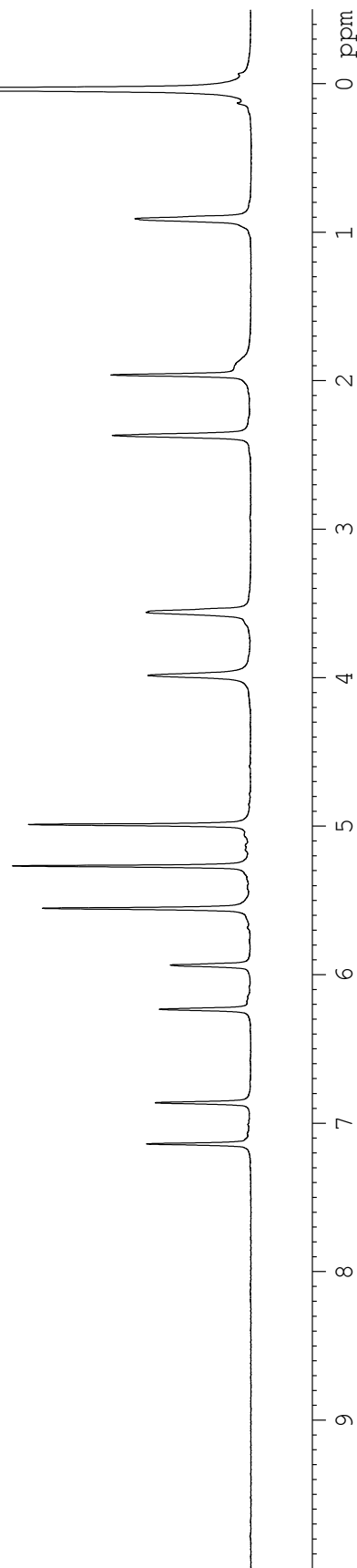
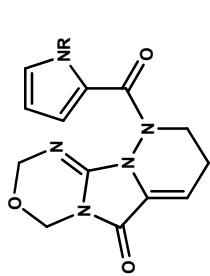
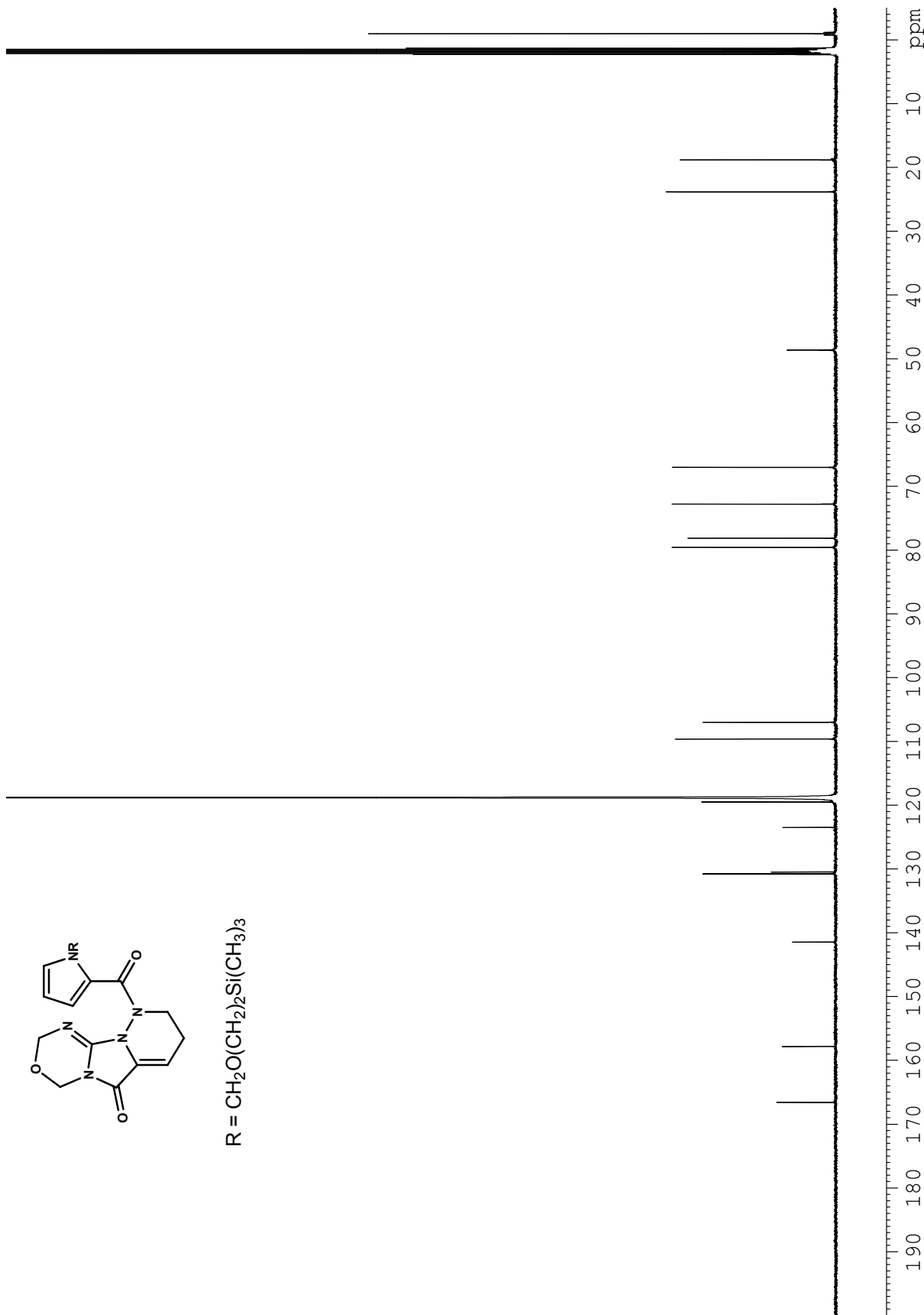


**Figure A1.22.** <sup>1</sup>H NMR (600 MHz, CH<sub>3</sub>CN-*d*<sub>3</sub>, 343 K) spectrum of compound **2-31**.

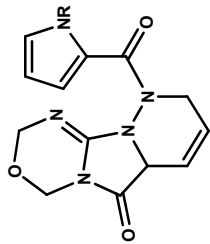




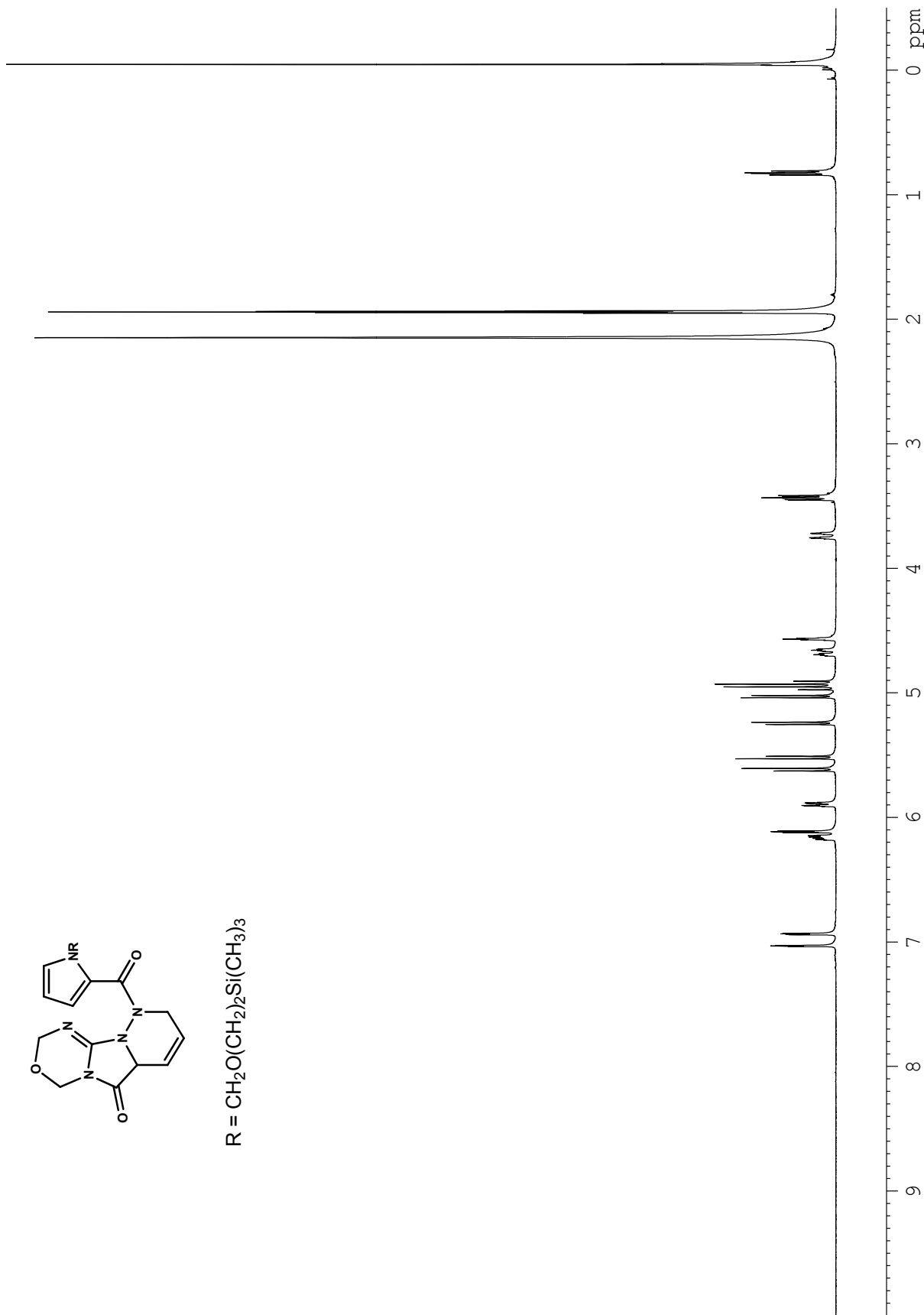
R = CH<sub>2</sub>O(CH<sub>2</sub>)<sub>2</sub>Si(CH<sub>3</sub>)<sub>3</sub>



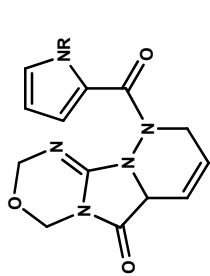
**Figure A1.23.** <sup>13</sup>C NMR (125 MHz, CH<sub>3</sub>CN-*d*<sub>3</sub>) spectrum of compound **2-31**.



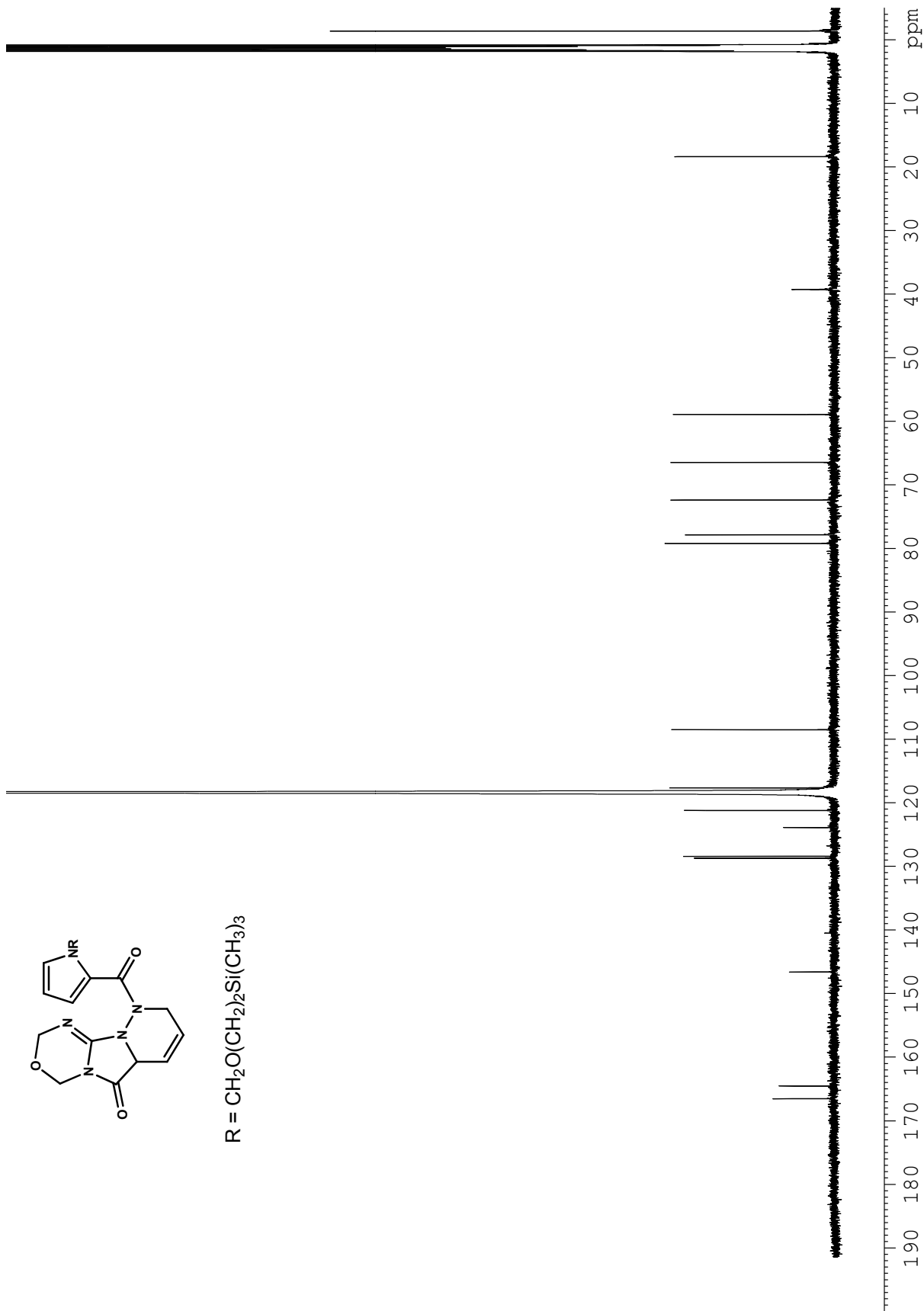
R = CH<sub>2</sub>O(CH<sub>2</sub>)<sub>2</sub>Si(CH<sub>3</sub>)<sub>3</sub>



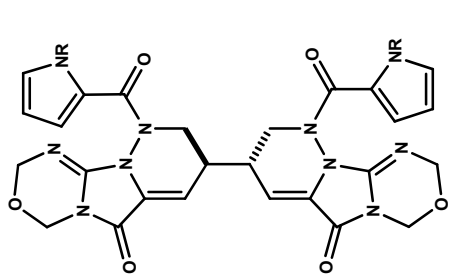
**Figure A1.24.** <sup>1</sup>H NMR (500 MHz, CH<sub>3</sub>CN-*d*<sub>3</sub>) spectrum of compound **2-40**.



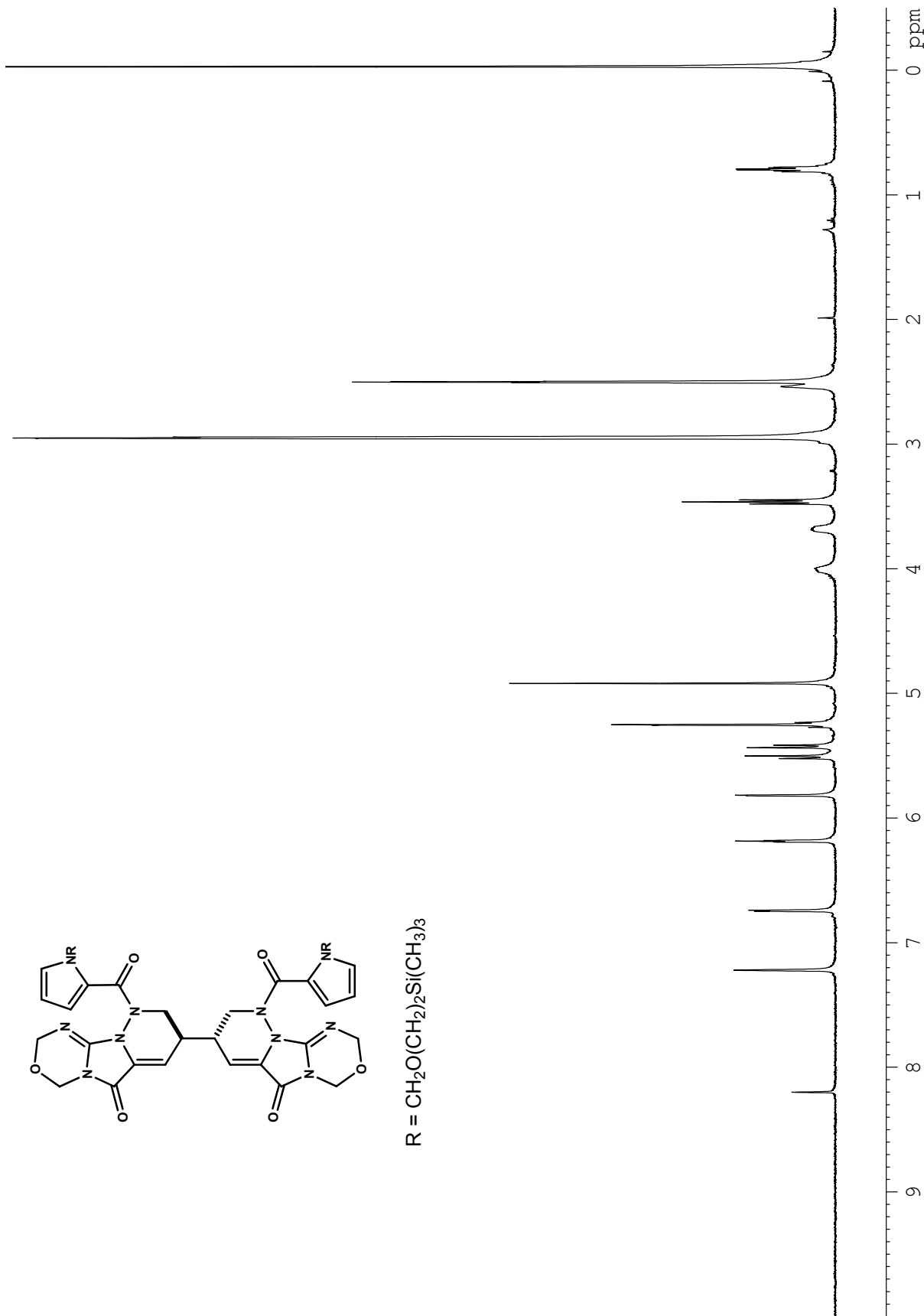
R = CH<sub>2</sub>O(CH<sub>2</sub>)<sub>2</sub>Si(CH<sub>3</sub>)<sub>3</sub>



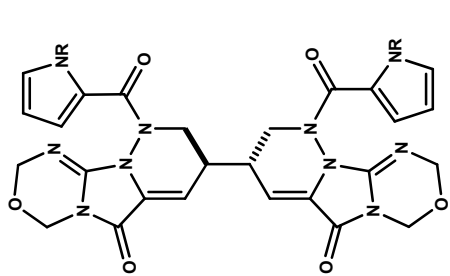
**Figure A1.25.** <sup>13</sup>C NMR (125 MHz, CH<sub>3</sub>CN-*d*<sub>3</sub>) spectrum of compound **2-40**.



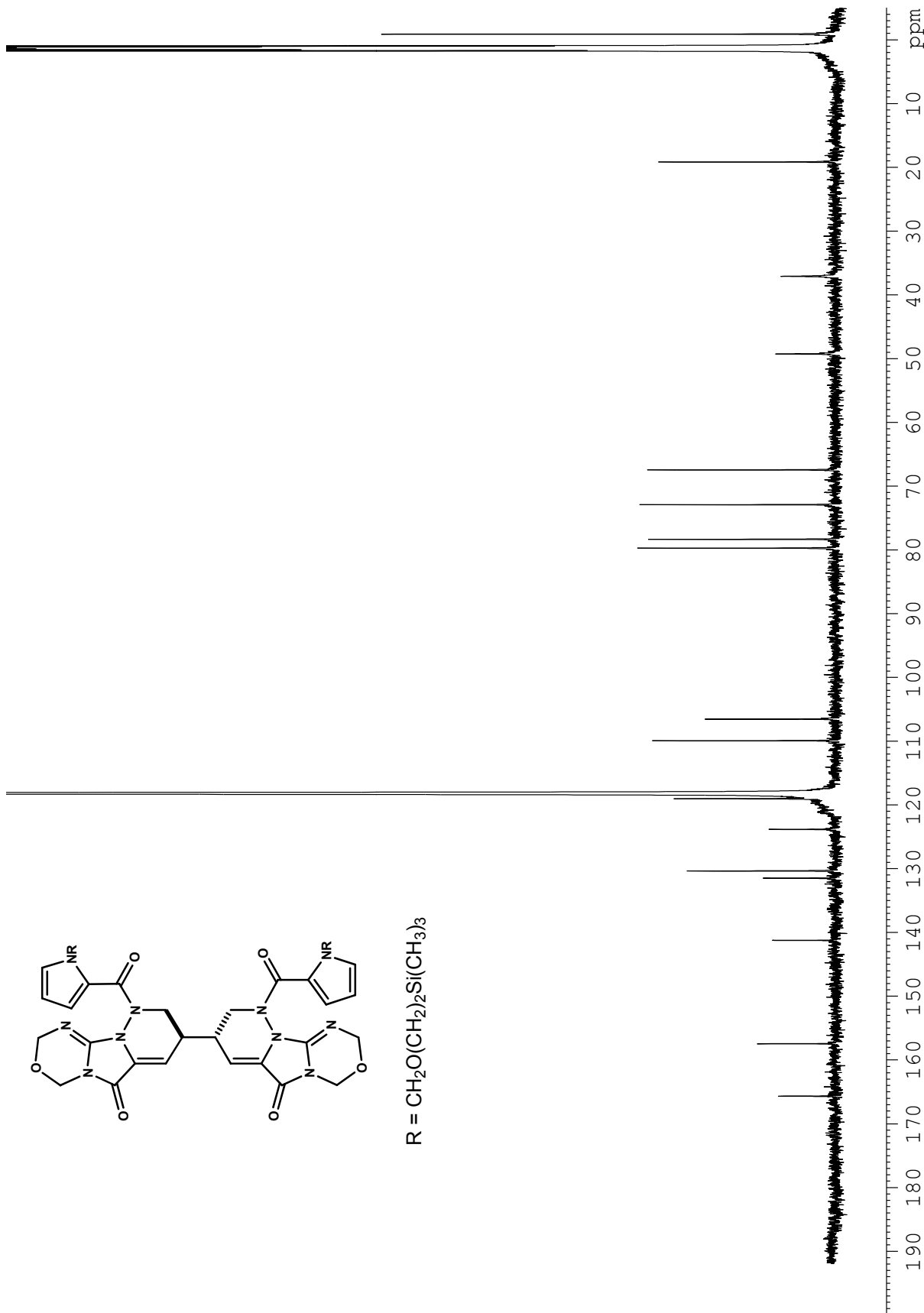
R = CH<sub>2</sub>O(CH<sub>2</sub>)<sub>2</sub>Si(CH<sub>3</sub>)<sub>3</sub>



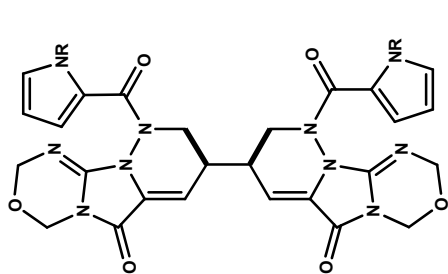
**Figure A1.26.** <sup>1</sup>H NMR (600 MHz, DMSO-*d*<sub>6</sub>, 343 K) spectrum of compound **2-38a**.



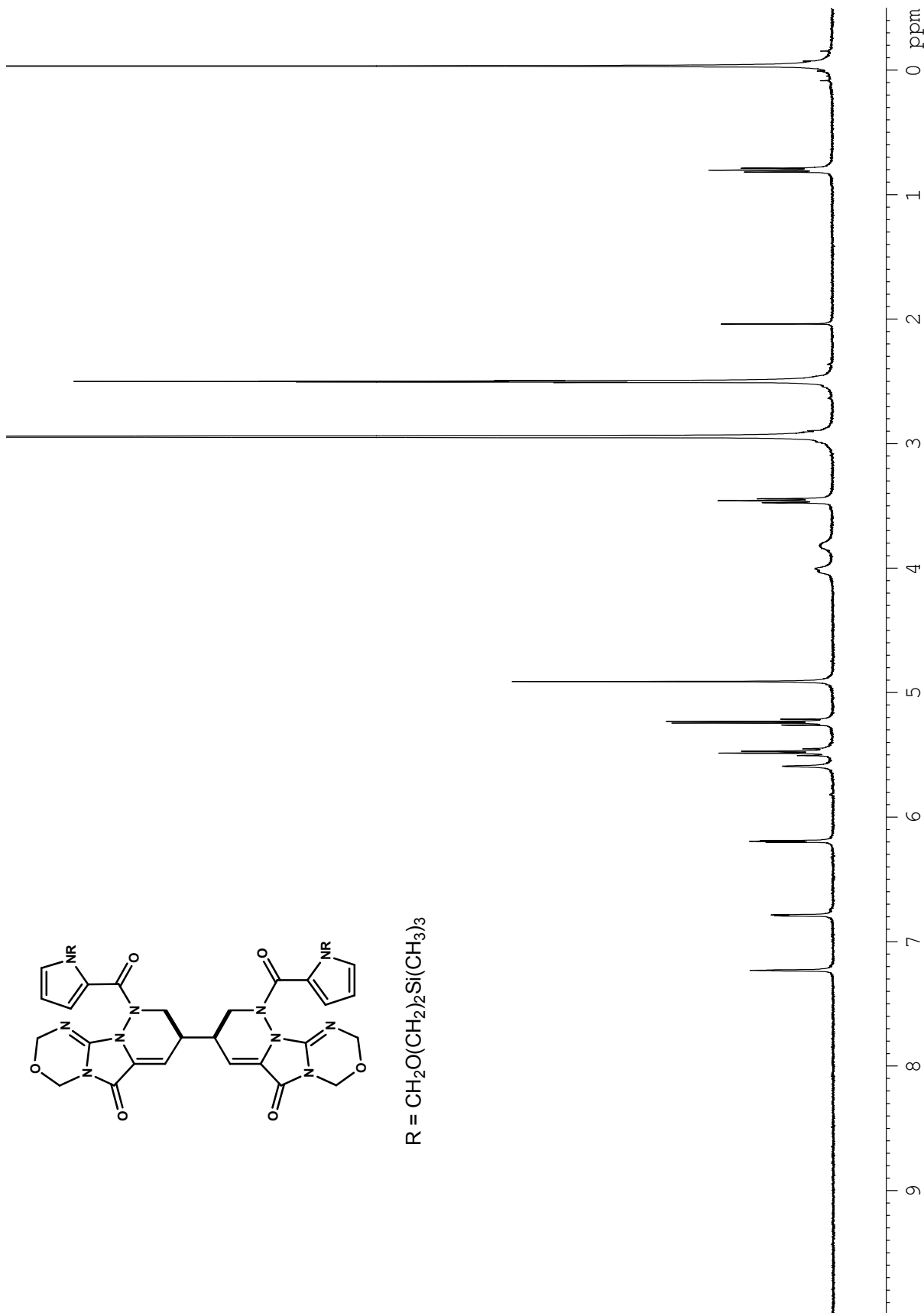
R = CH<sub>2</sub>O(CH<sub>2</sub>)<sub>2</sub>Si(CH<sub>3</sub>)<sub>3</sub>



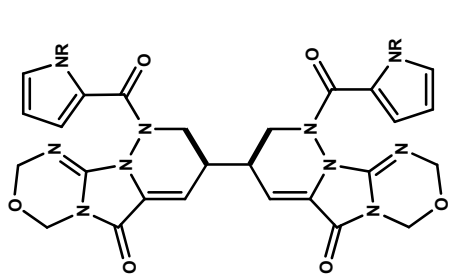
**Figure A1.27.** <sup>13</sup>C NMR (125 MHz, CH<sub>3</sub>CN-*d*<sub>3</sub>, 343 K) spectrum of compound **2-38a**.



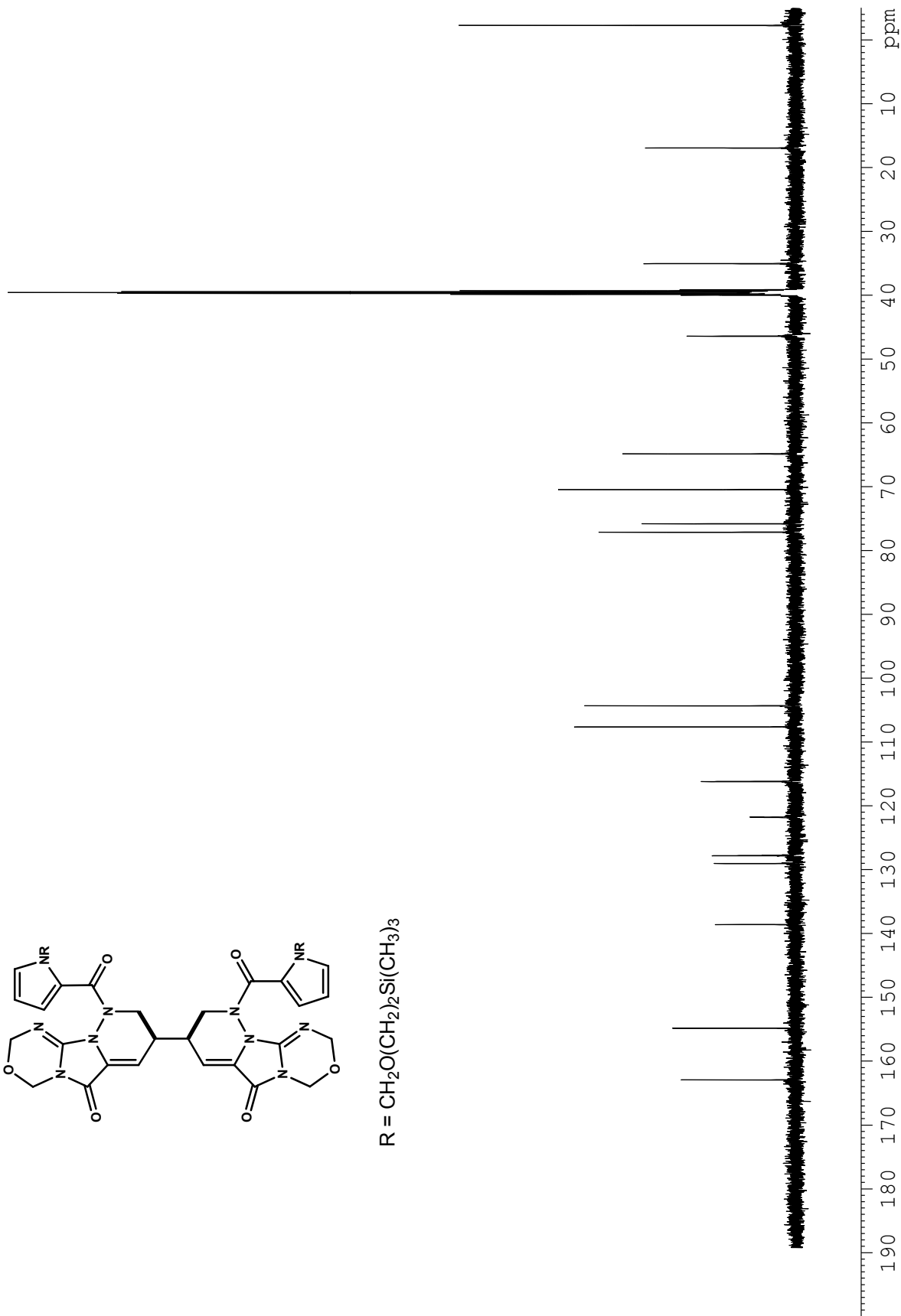
R =  $\text{CH}_2\text{O}(\text{CH}_2)_2\text{Si}(\text{CH}_3)_3$



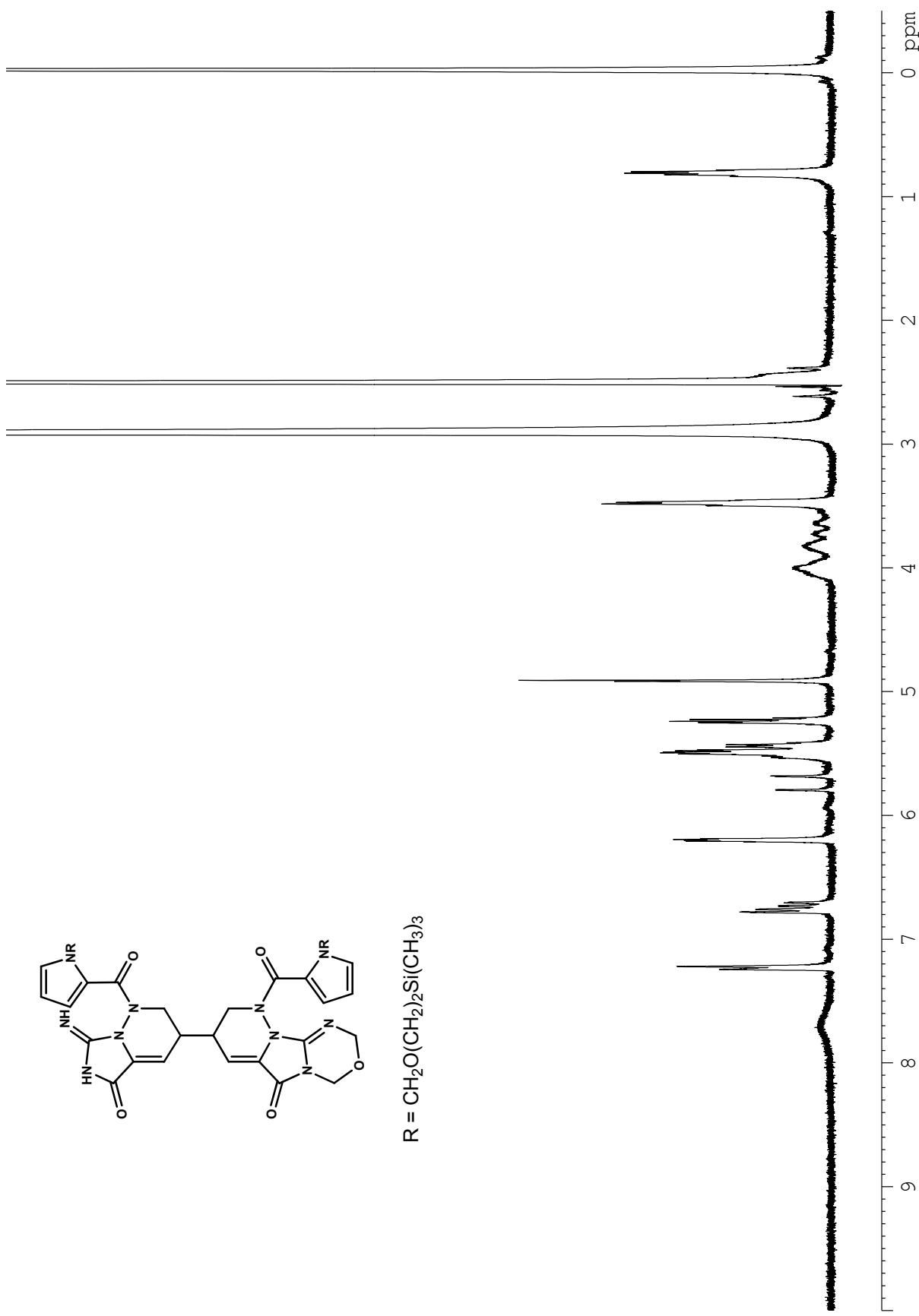
**Figure A1.28.**  $^1\text{H}$  NMR (600 MHz,  $\text{DMSO-}d_6$ , 373 K) spectrum of compound **2-38b**.



R =  $\text{CH}_2\text{O}(\text{CH}_2)_2\text{Si}(\text{CH}_3)_3$



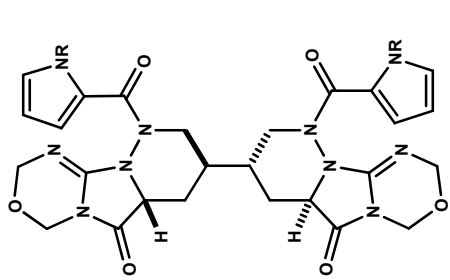
**Figure A1.29.**  $^{13}\text{C}$  NMR (150 MHz,  $\text{DMSO-}d_6$ , 373 K) spectrum of compound **2-38b**.



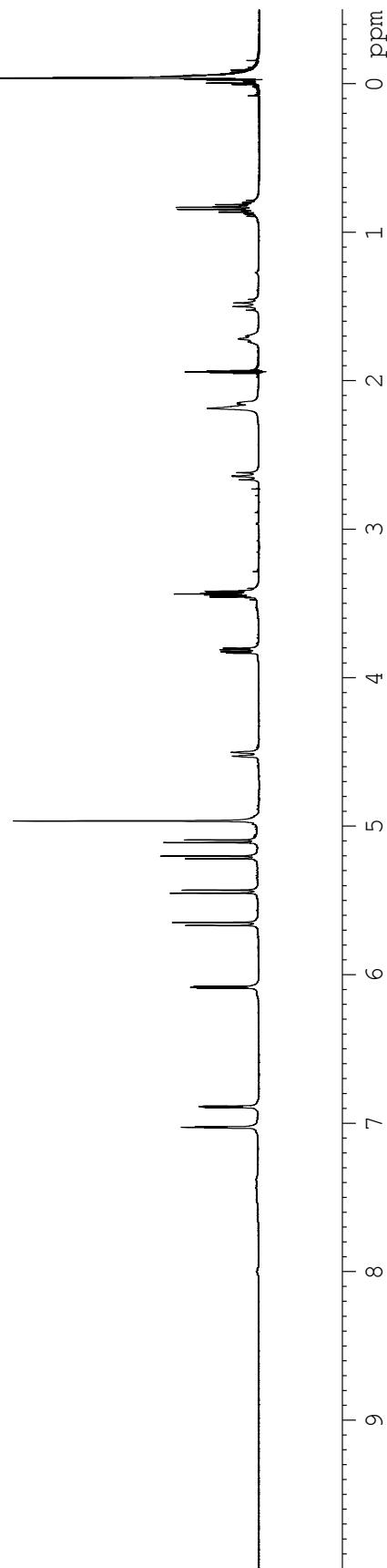
R = CH<sub>2</sub>O(CH<sub>2</sub>)<sub>2</sub>Si(CH<sub>3</sub>)<sub>3</sub>

Figure A1.30. <sup>1</sup>H NMR (600 MHz, DMSO-*d*<sub>6</sub>, 373 K) spectrum of compound 2-39.

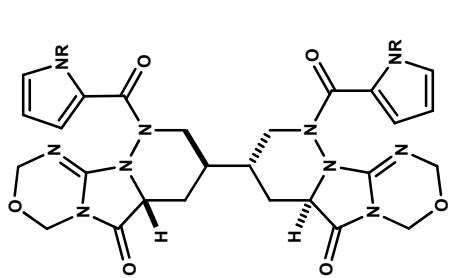




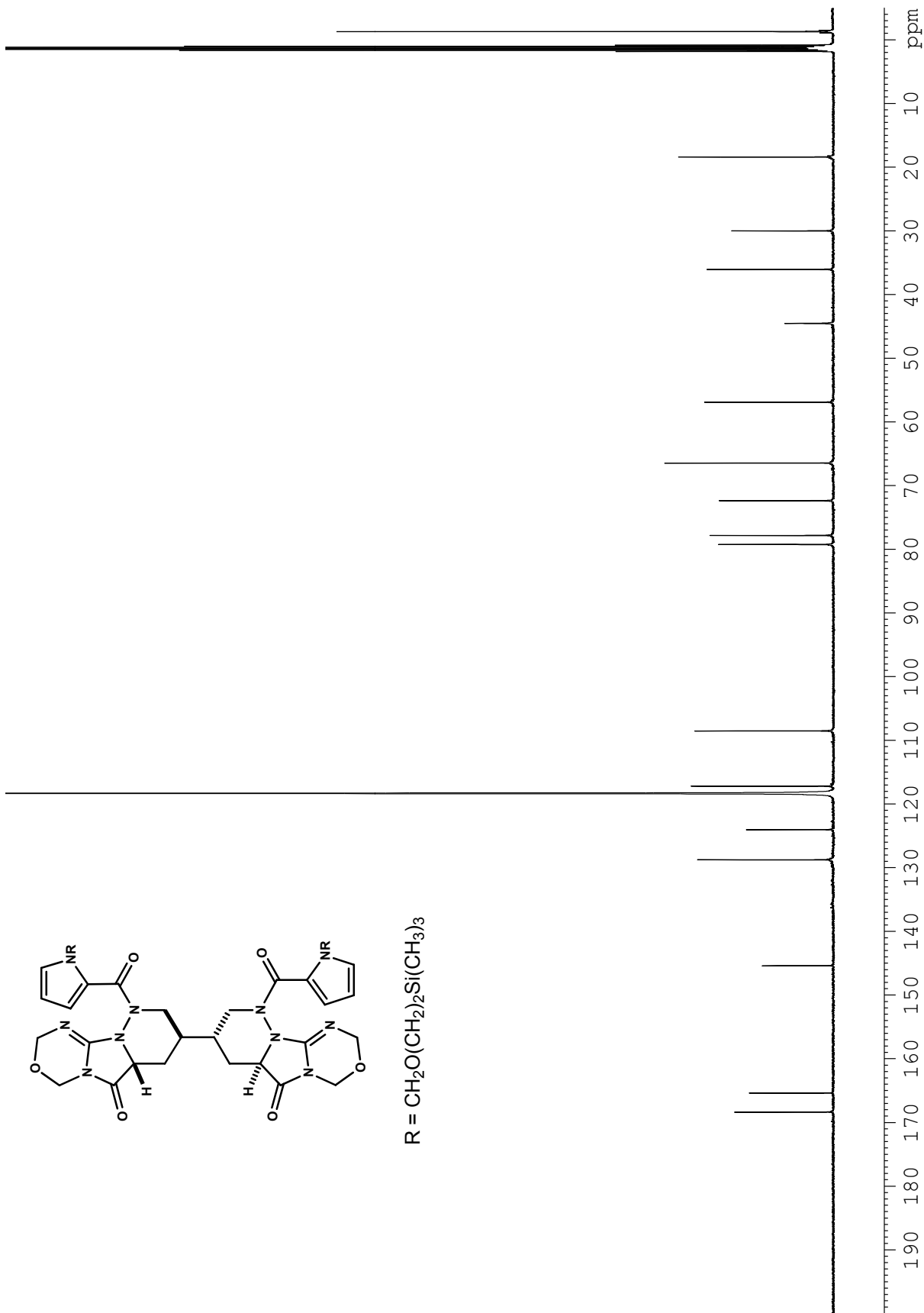
R = CH<sub>2</sub>O(CH<sub>2</sub>)<sub>2</sub>Si(CH<sub>3</sub>)<sub>3</sub>



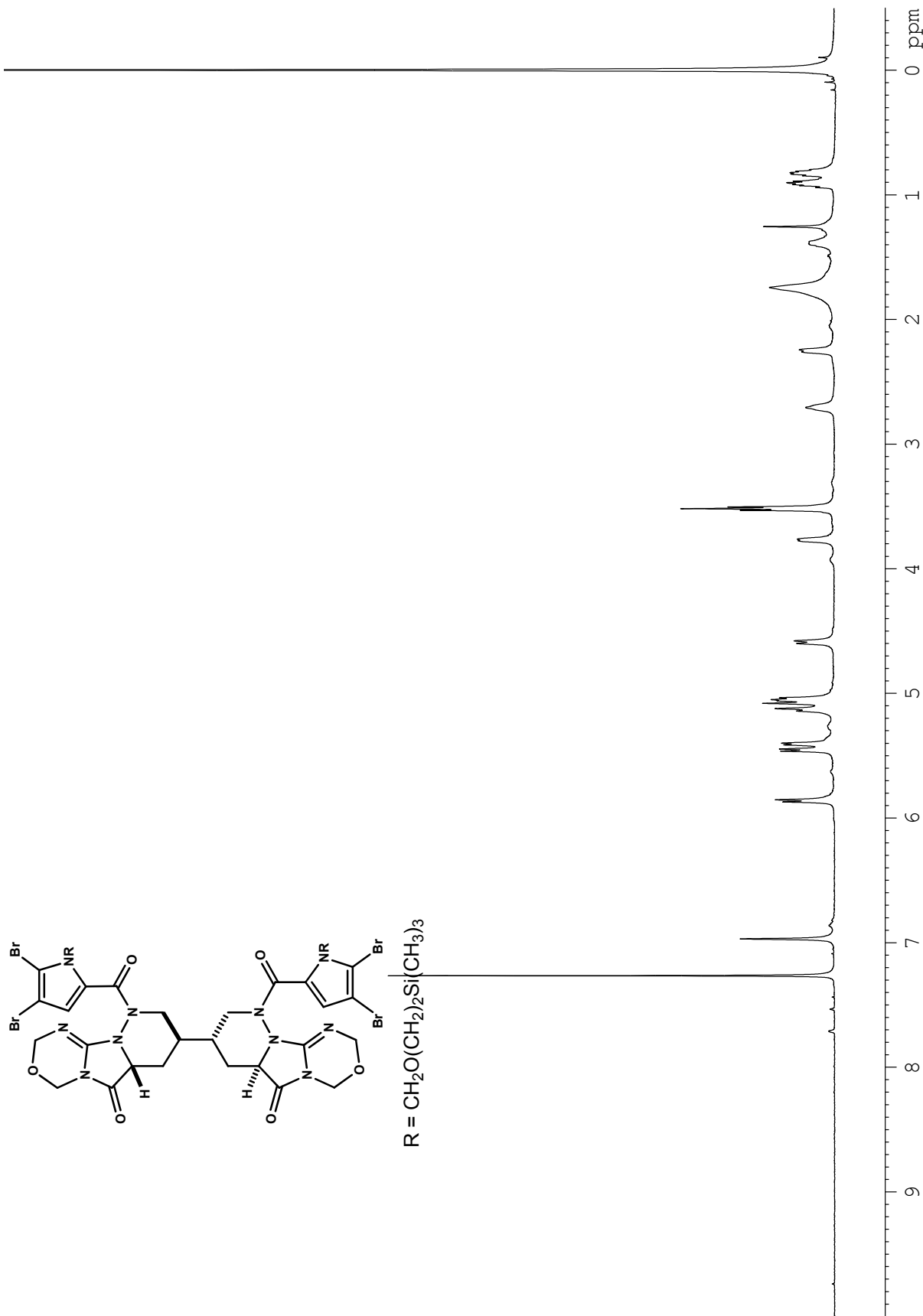
**Figure A1.31.** <sup>1</sup>H NMR (500 MHz, CH<sub>3</sub>CN-*d*<sub>3</sub>) spectrum of compound **2-41**.



R = CH<sub>2</sub>O(CH<sub>2</sub>)<sub>2</sub>Si(CH<sub>3</sub>)<sub>3</sub>



**Figure A1.32.** <sup>13</sup>C NMR (125 MHz, CH<sub>3</sub>CN-*d*<sub>3</sub>) spectrum of compound **2-41**.



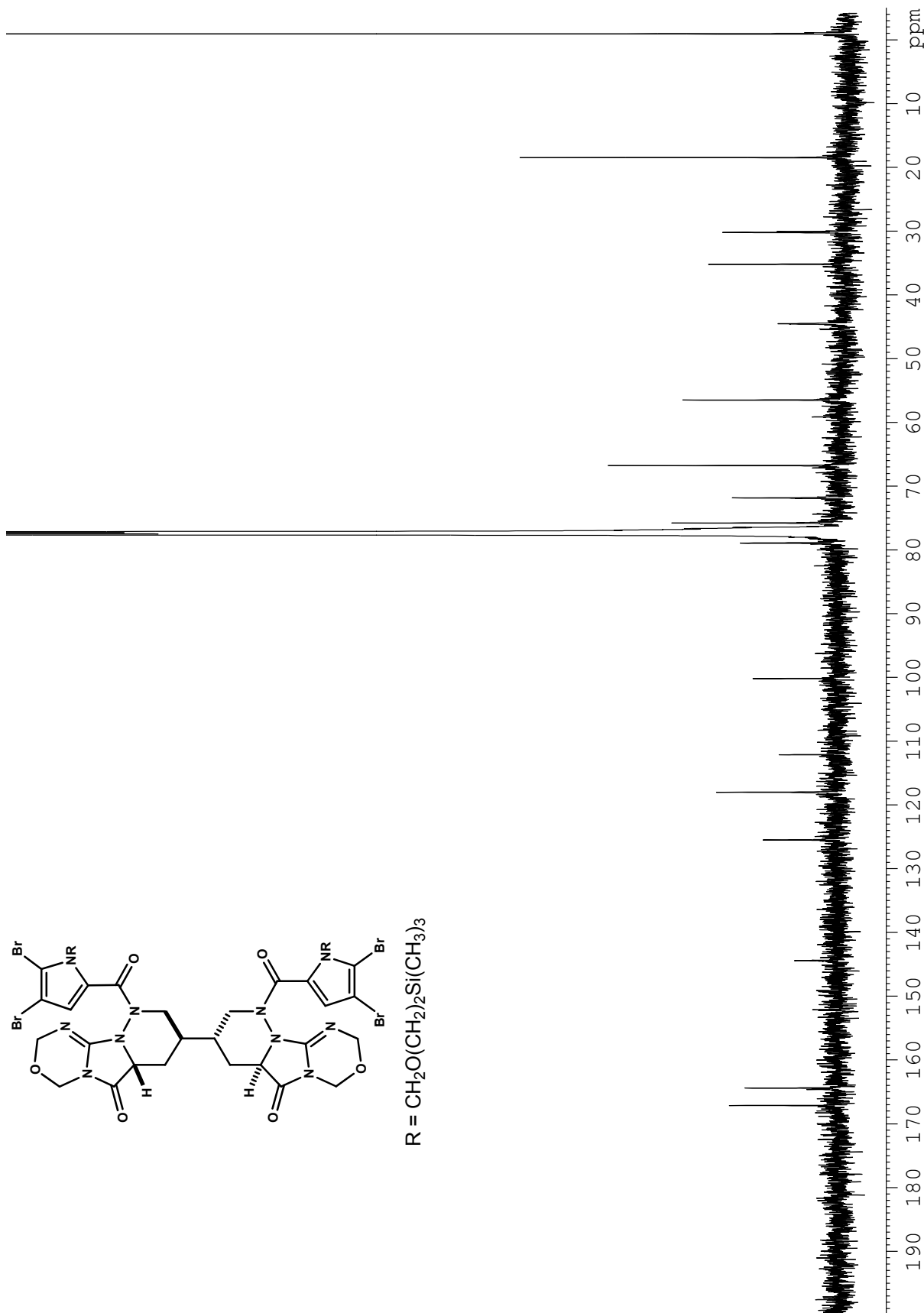
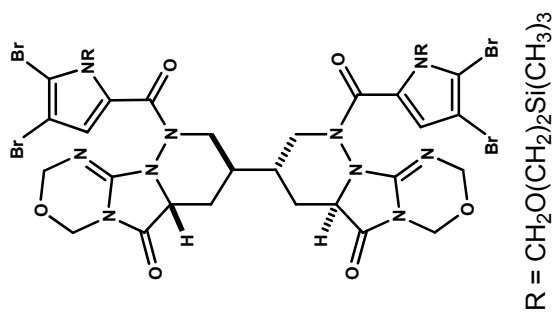
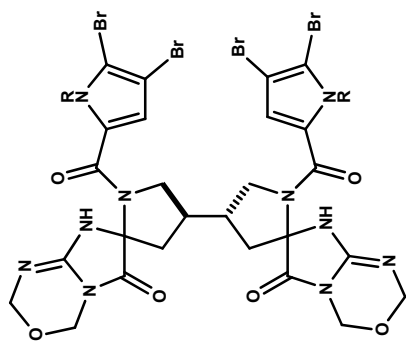


**Figure A1.34.** <sup>13</sup>C NMR (125 MHz, CHCl<sub>3</sub>-d<sub>1</sub>) spectrum of compound **2-42a**.



R =  $\text{CH}_2\text{O}(\text{CH}_2)_2\text{Si}(\text{CH}_3)_3$

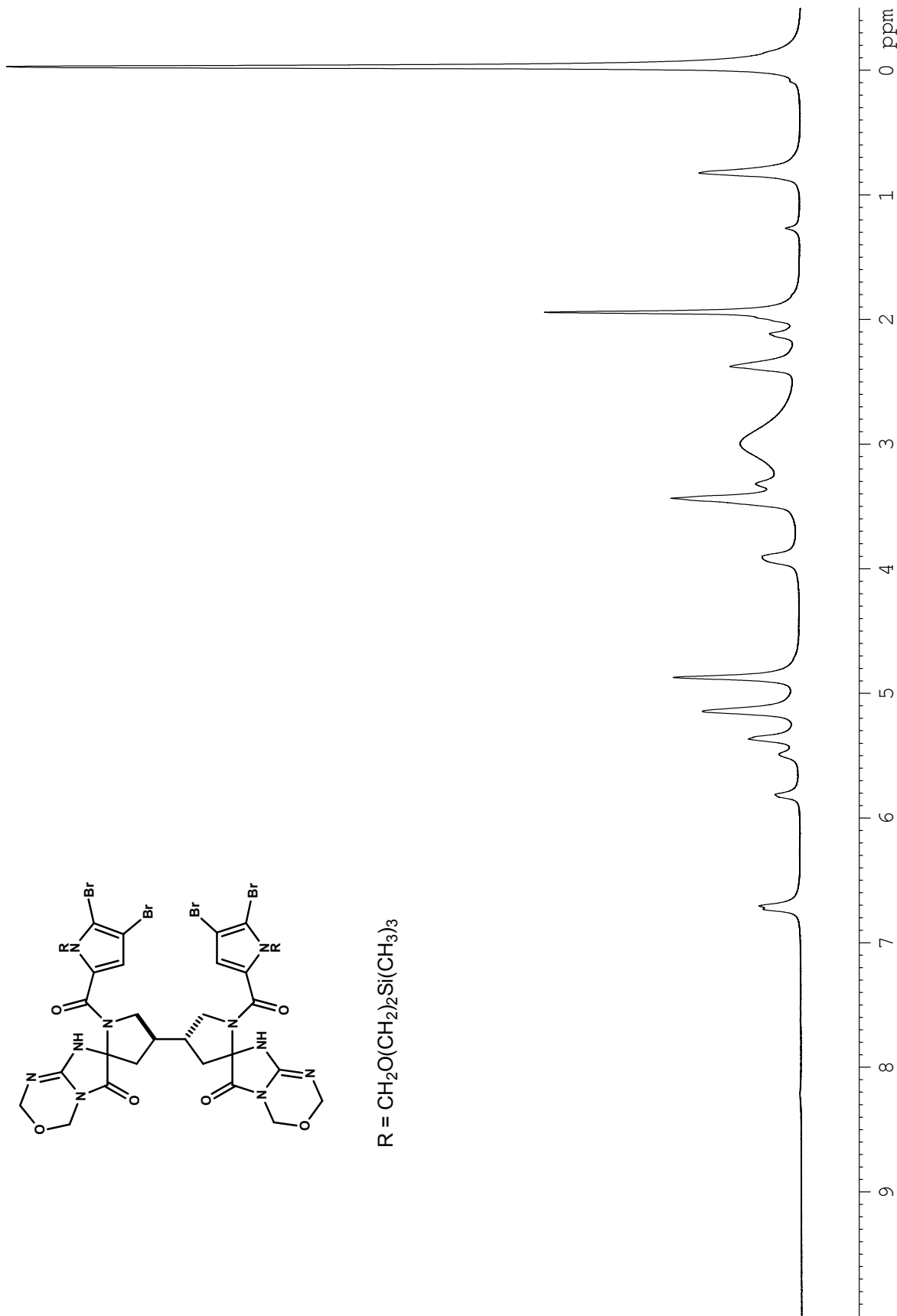
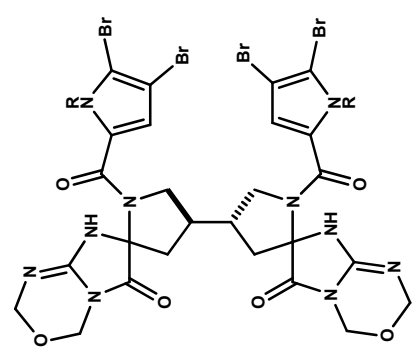
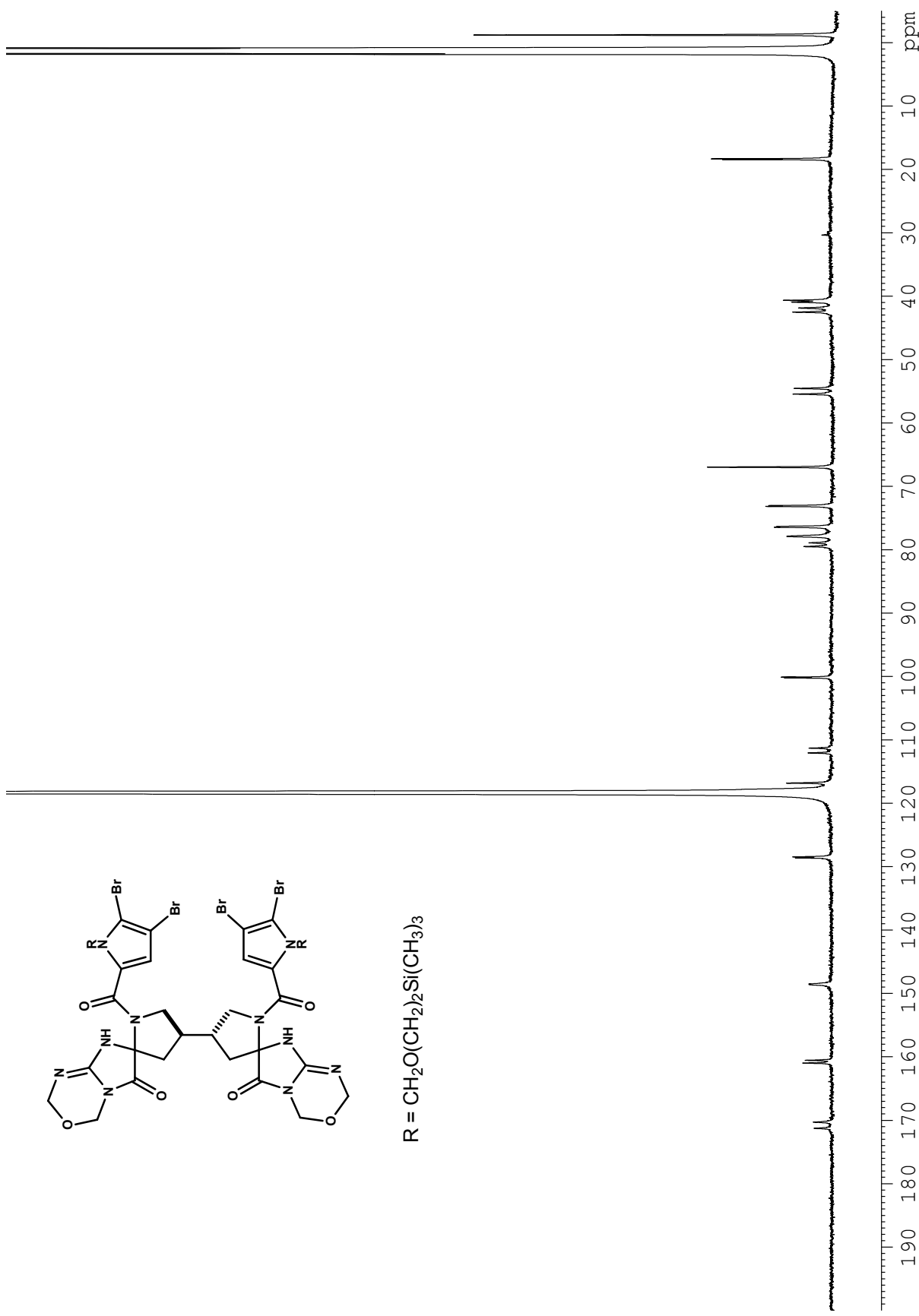
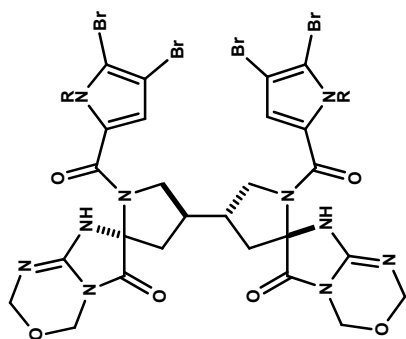


**Figure A1.35.**  $^1\text{H}$  NMR (500 MHz,  $\text{CH}_3\text{CN}-d_3$ ) spectrum of compound **2-44a**.



R = CH<sub>2</sub>O(CH<sub>2</sub>)<sub>2</sub>Si(CH<sub>3</sub>)<sub>3</sub>

**Figure A1.36.** <sup>13</sup>C NMR (125 MHz, CH<sub>3</sub>CN-*d*<sub>3</sub>) spectrum of compound **2-44a**.



R =  $\text{CH}_2\text{O}(\text{CH}_2)_2\text{Si}(\text{CH}_3)_3$

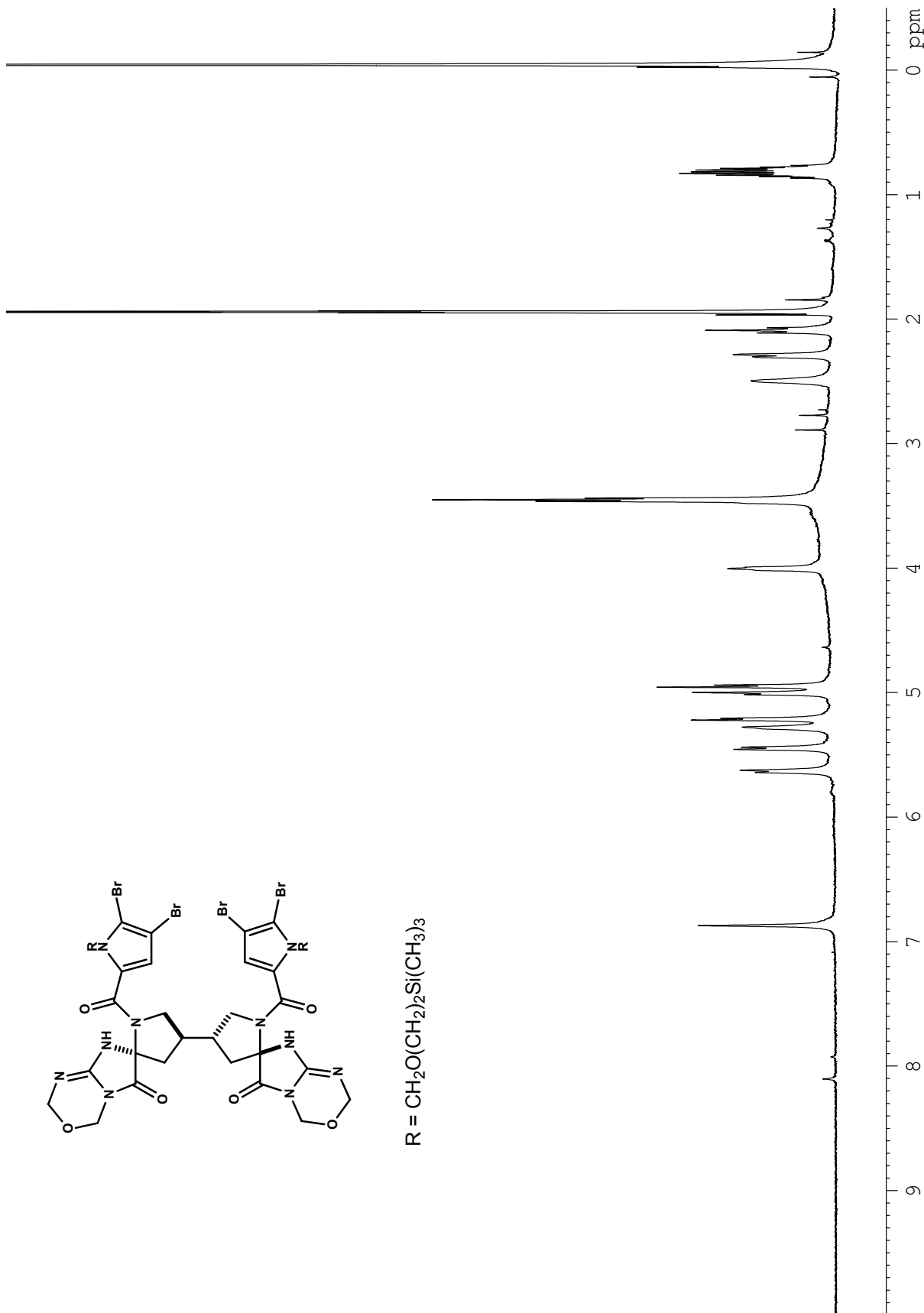
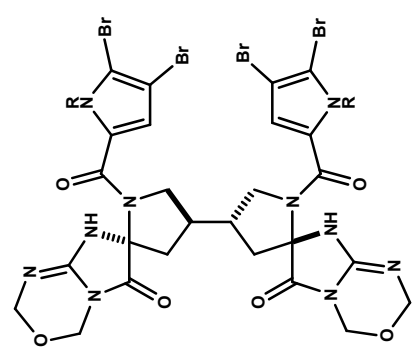
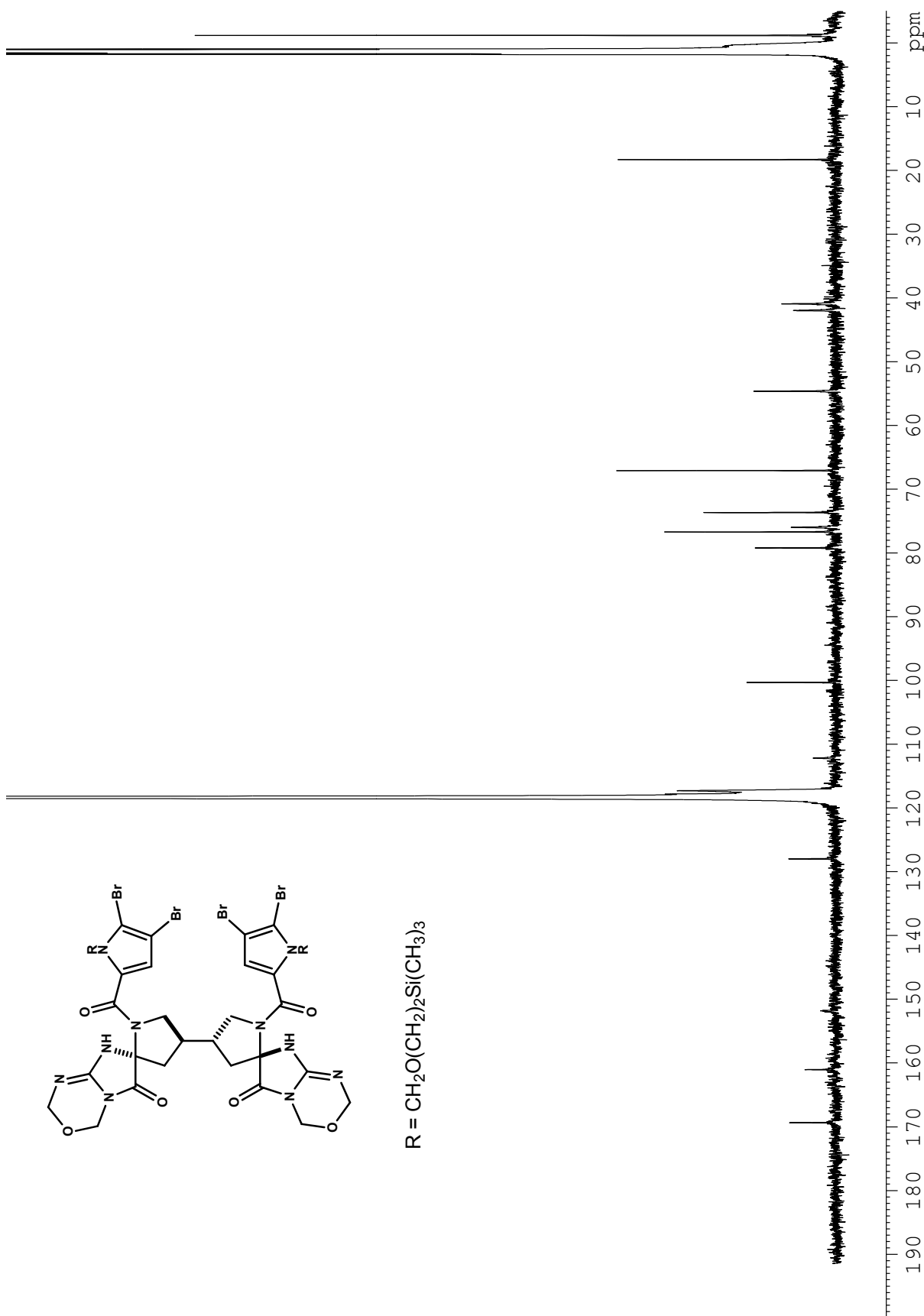


**Figure A1.37.**  $^1\text{H}$  NMR (600 MHz,  $\text{CH}_3\text{CN}-d_3$ ) spectrum of compound **2-44b**.



R = CH<sub>2</sub>O(CH<sub>2</sub>)<sub>2</sub>Si(CH<sub>3</sub>)<sub>3</sub>

**Figure A1.38.** <sup>13</sup>C NMR (150 MHz, CH<sub>3</sub>CN-*d*<sub>3</sub>) spectrum of compound **2-44b**.



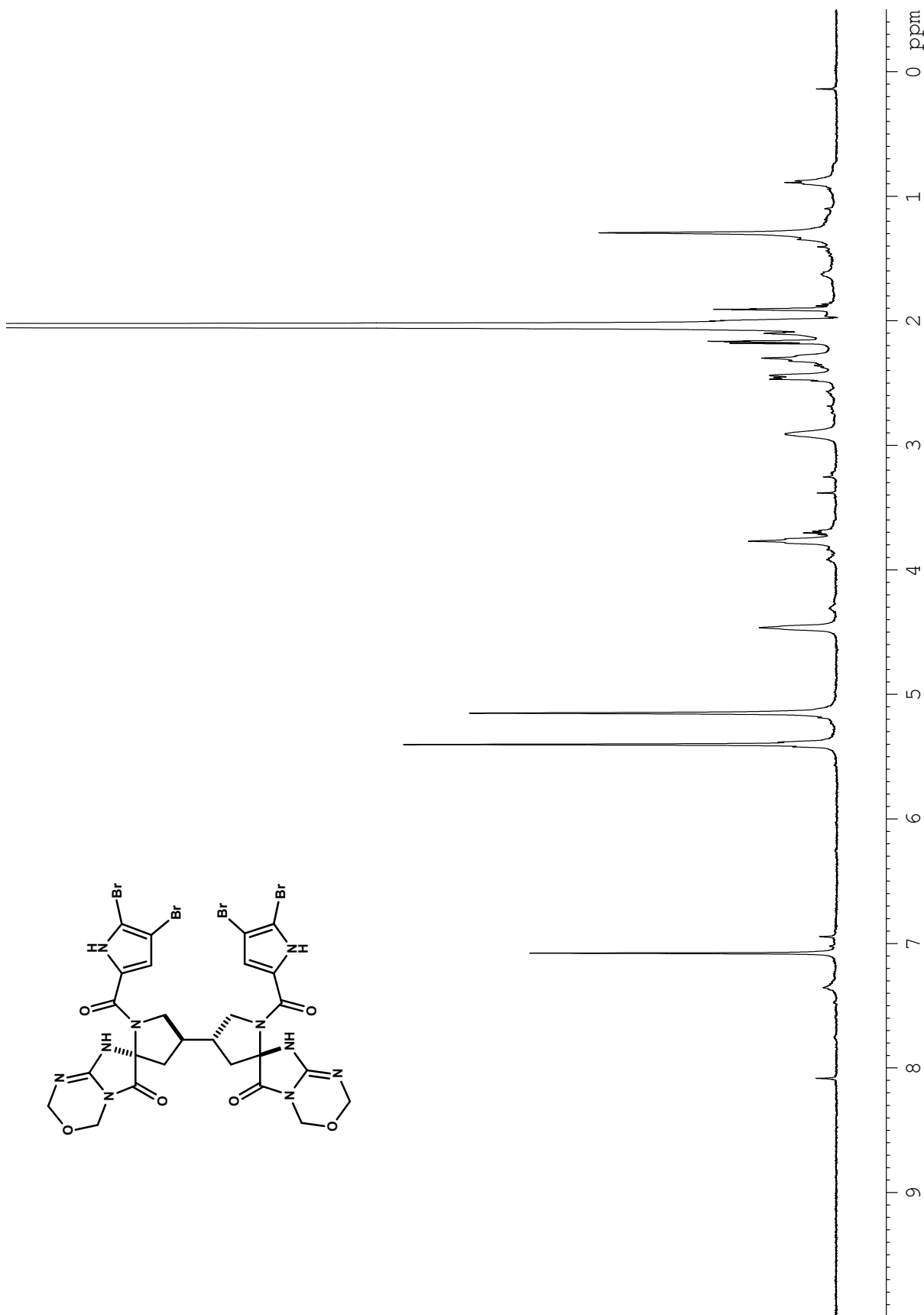


**Figure A1.39.** <sup>1</sup>H NMR (500 MHz, acetic acid-*d*<sub>4</sub>) spectrum of compound 2-44b-1.

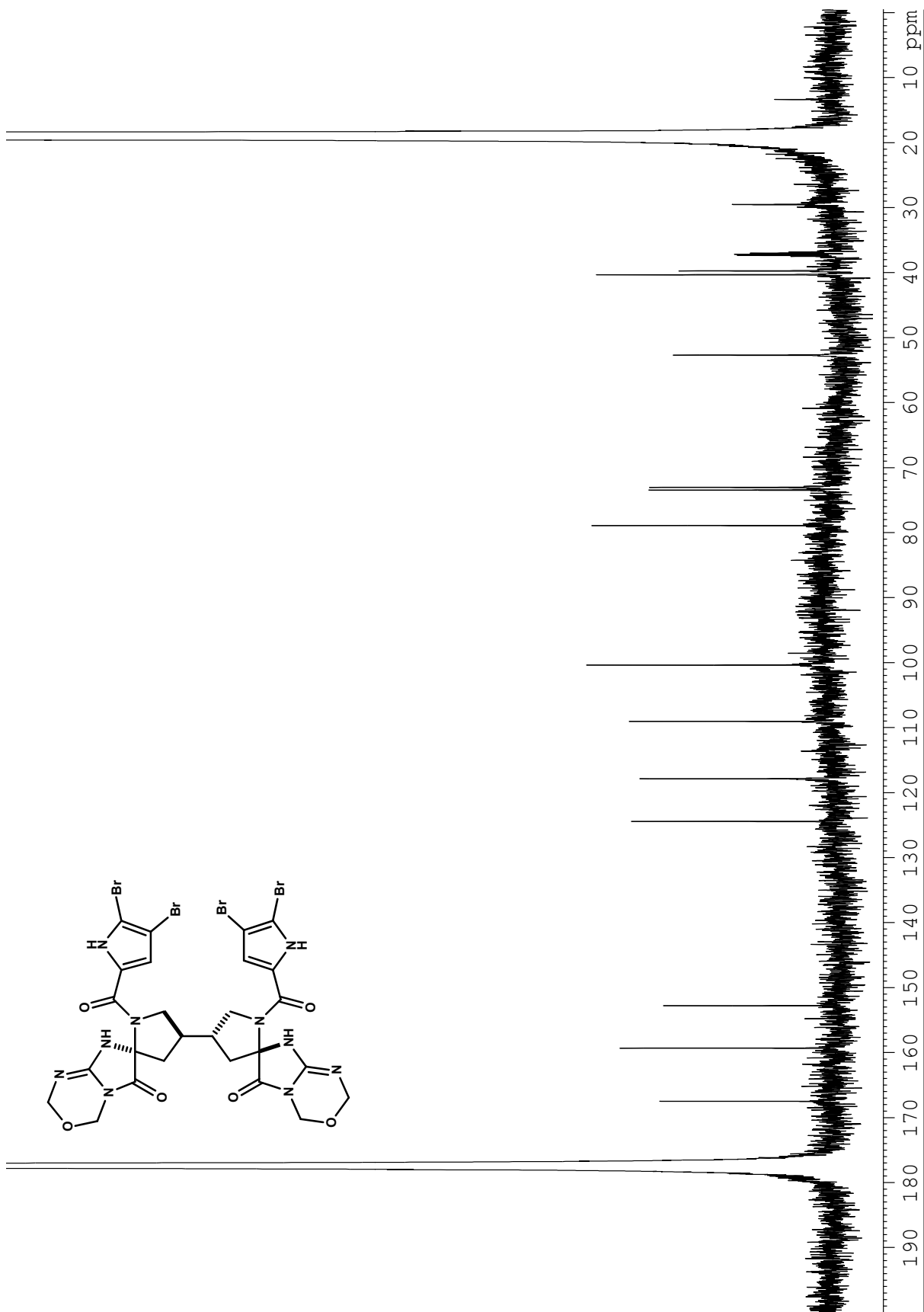
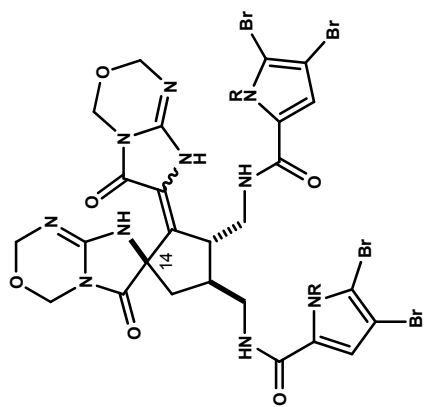


**Figure A1.40.** <sup>13</sup>C NMR (125 MHz, acetic acid-*d*<sub>4</sub>) spectrum of compound 2-44b-1.



R = CH<sub>2</sub>O(CH<sub>2</sub>)<sub>2</sub>Si(CH<sub>3</sub>)<sub>3</sub>

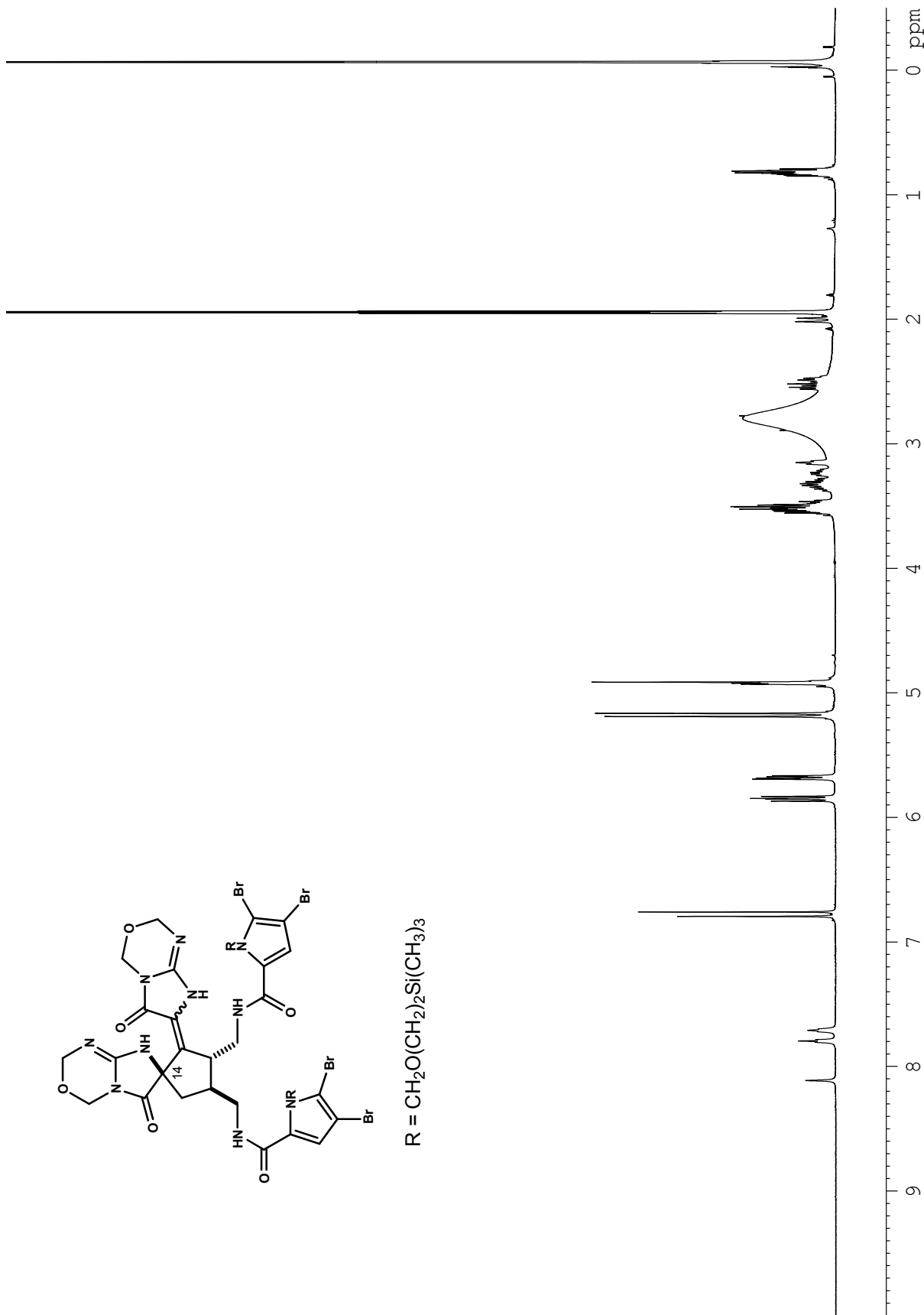
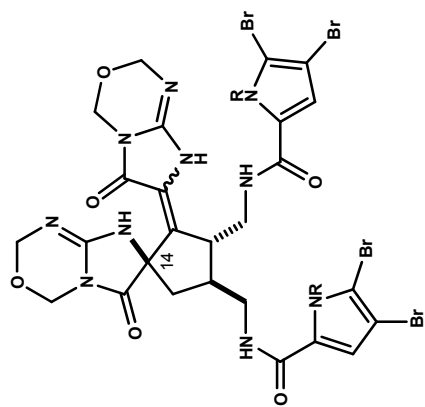
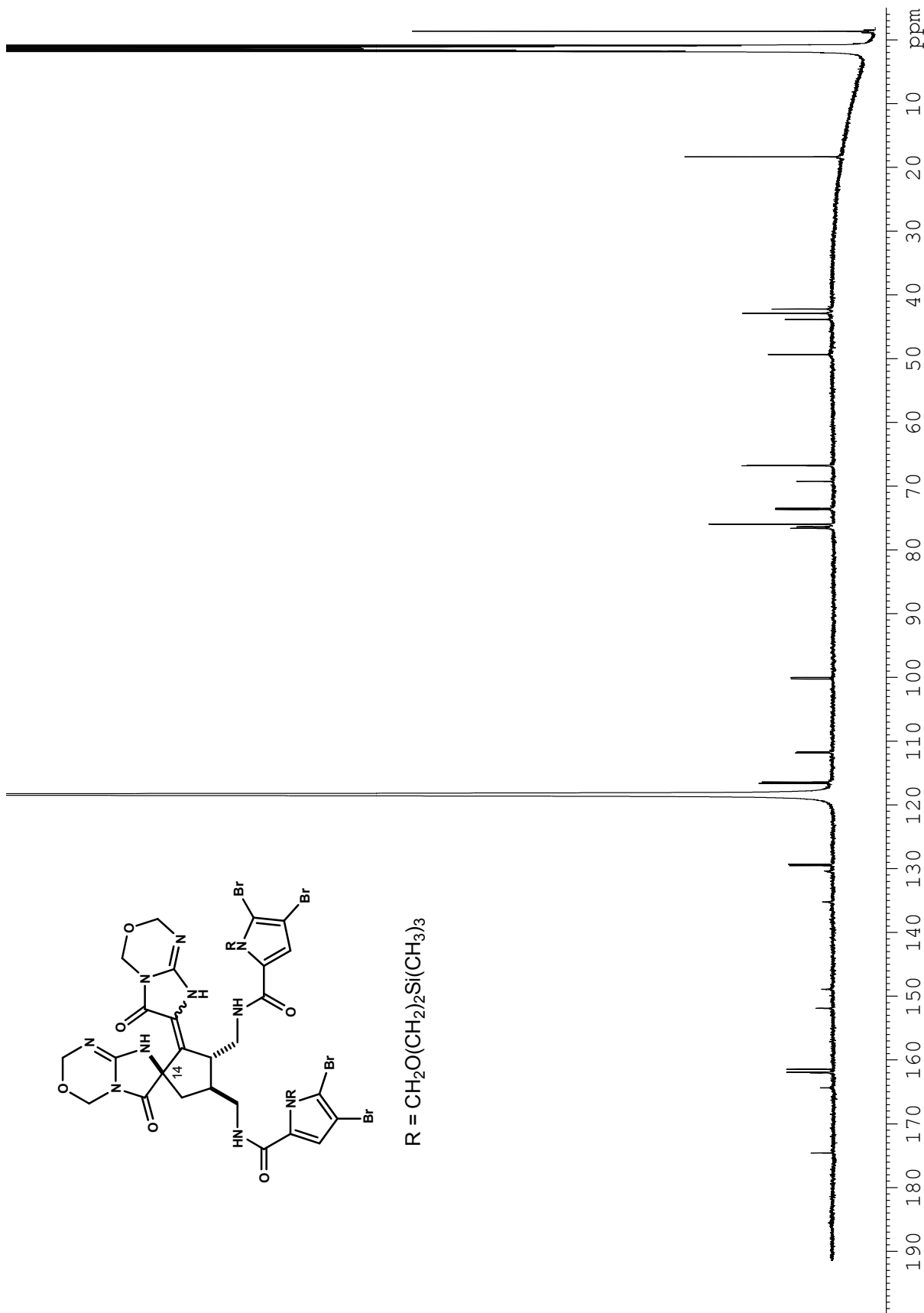


**Figure A1.41.** <sup>1</sup>H NMR (500 MHz, CH<sub>3</sub>CN-*d*<sub>3</sub>) spectrum of compound **2-47a**.



R = CH<sub>2</sub>O(CH<sub>2</sub>)<sub>2</sub>Si(CH<sub>3</sub>)<sub>3</sub>

**Figure A1.42.** <sup>13</sup>C NMR (125 MHz, CH<sub>3</sub>CN-*d*<sub>3</sub>) spectrum of compound 2-47a.

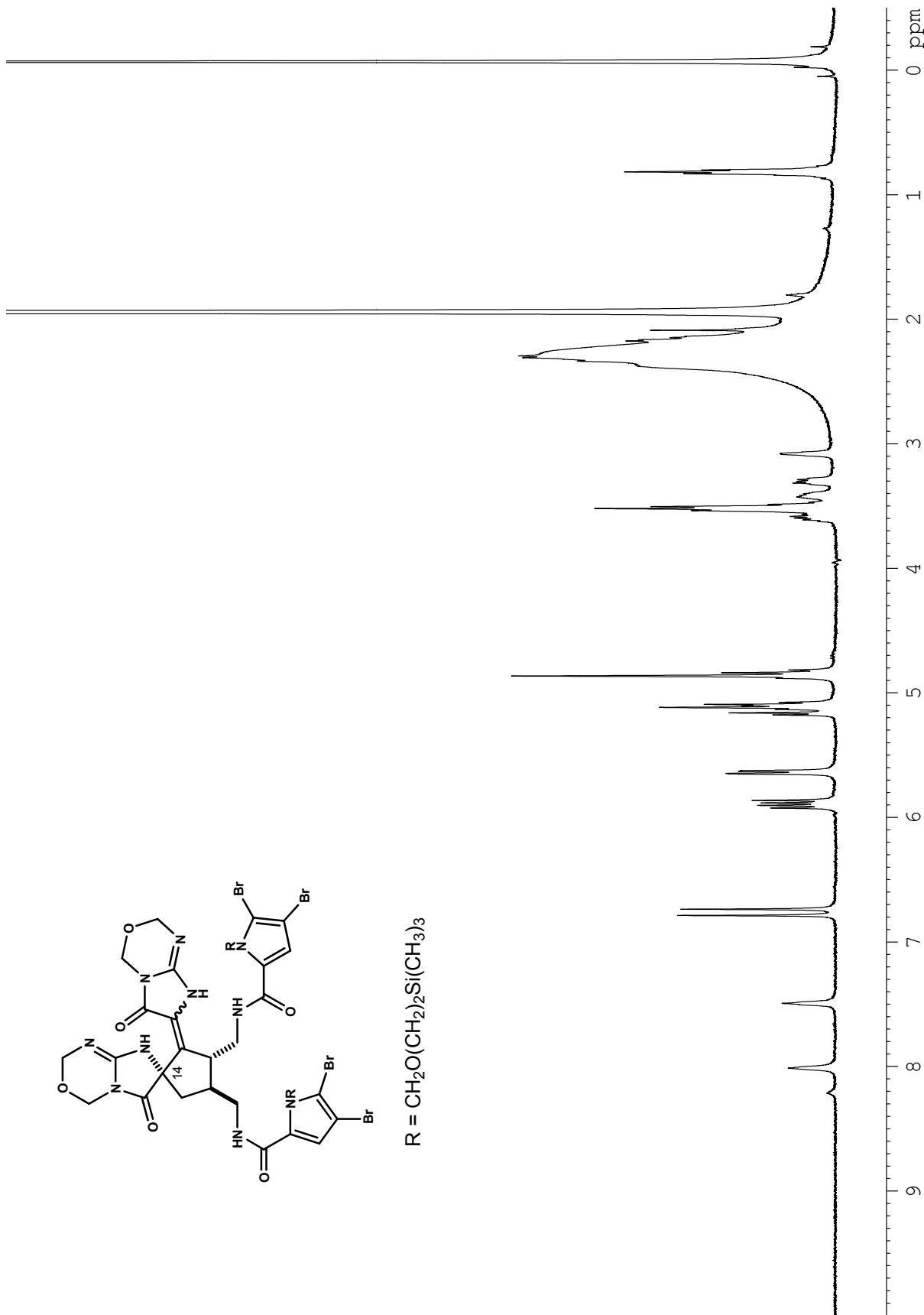


**Figure A1.43.**  $^1\text{H}$  NMR (500 MHz,  $\text{CH}_3\text{CN}-d_3$ ) spectrum of compound **2-47b**.

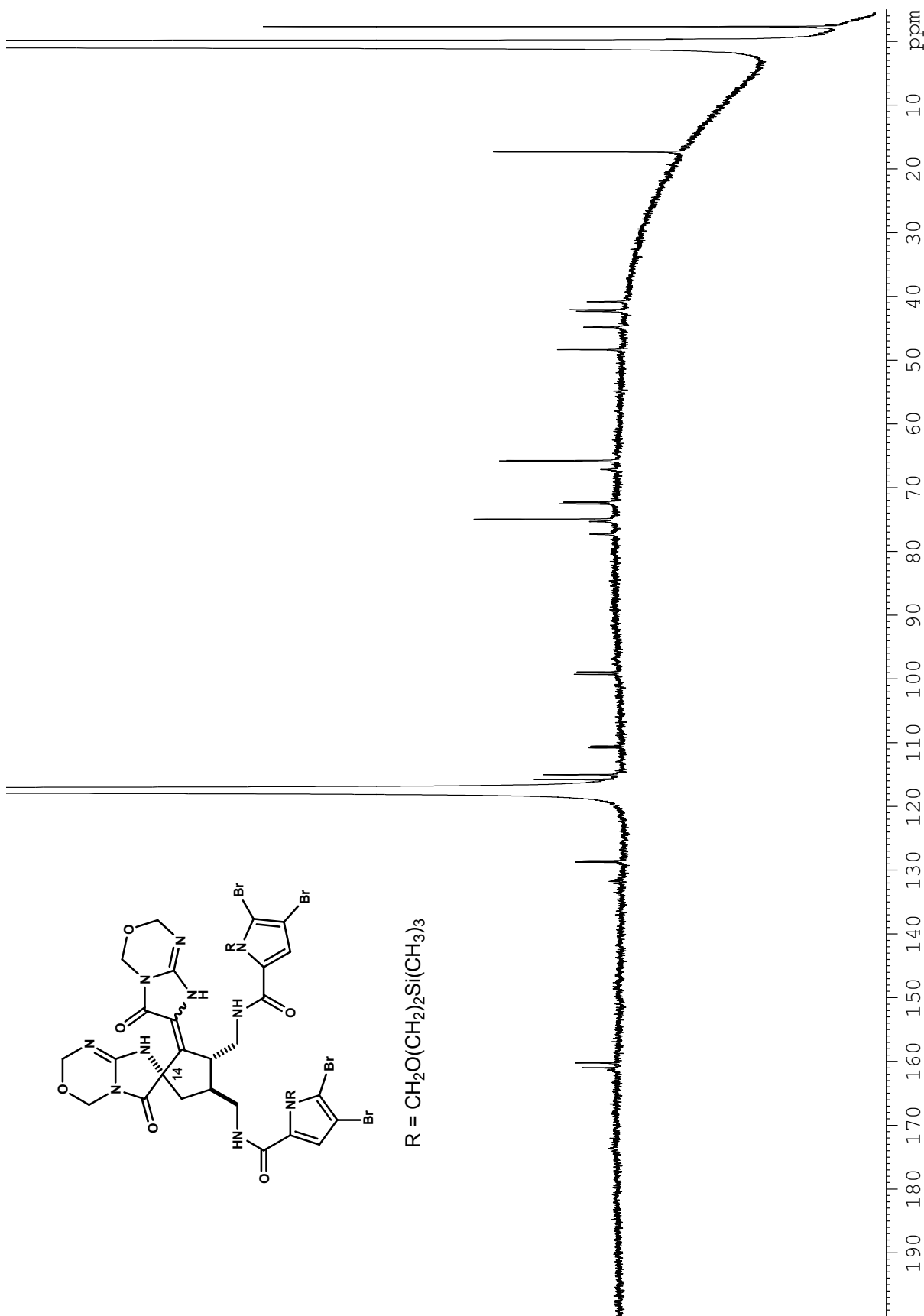


**Figure A1.44.**  $^{13}\text{C}$  NMR (125 MHz,  $\text{CH}_3\text{CN}-d_3$ ) spectrum of compound 2-47b.

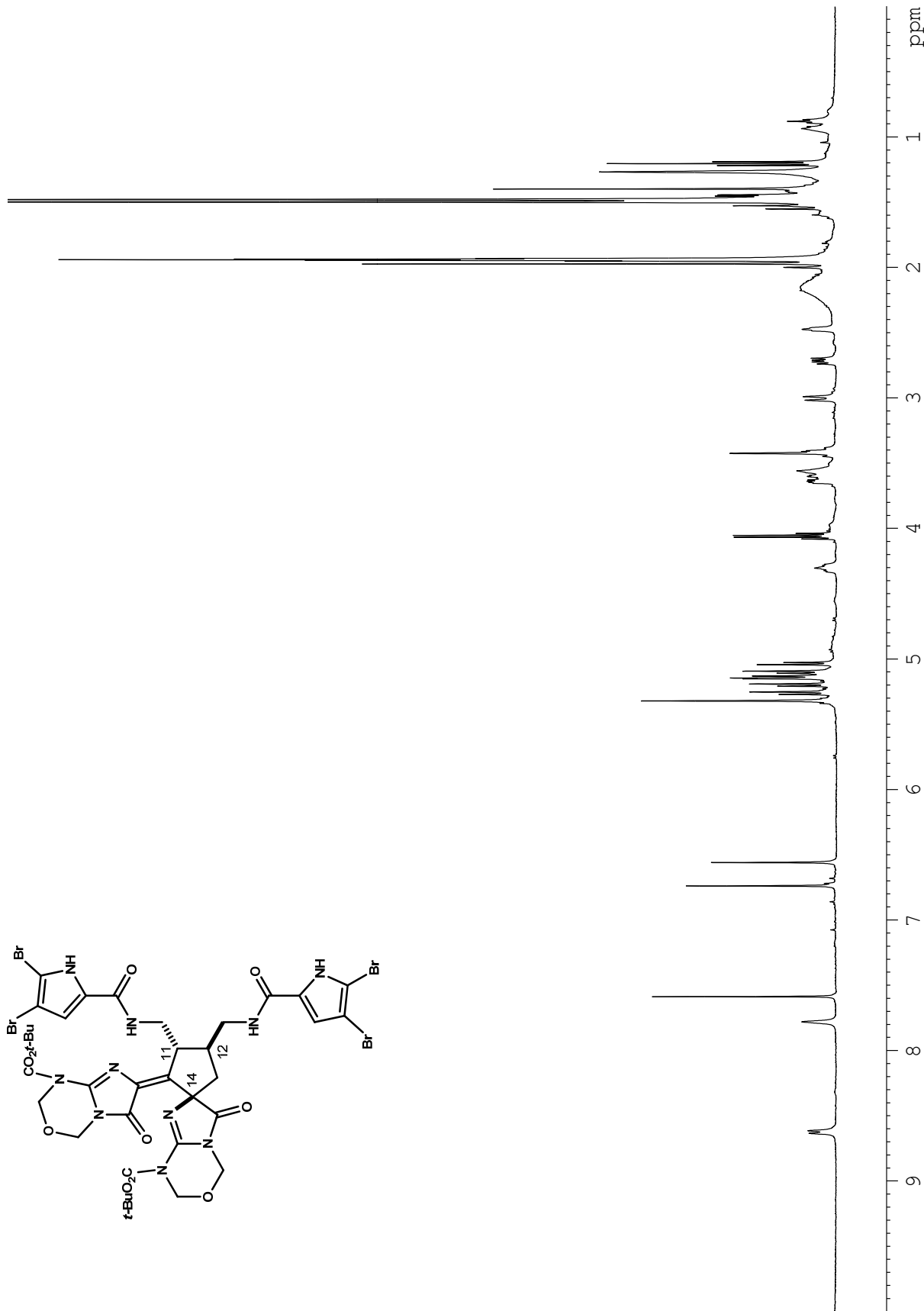
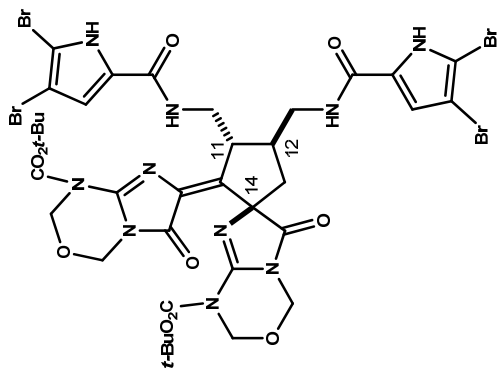


**Figure A1.45.**  $^1\text{H}$  NMR (500 MHz,  $\text{CH}_3\text{CN}-d_3$ ) spectrum of compound **2-49**.

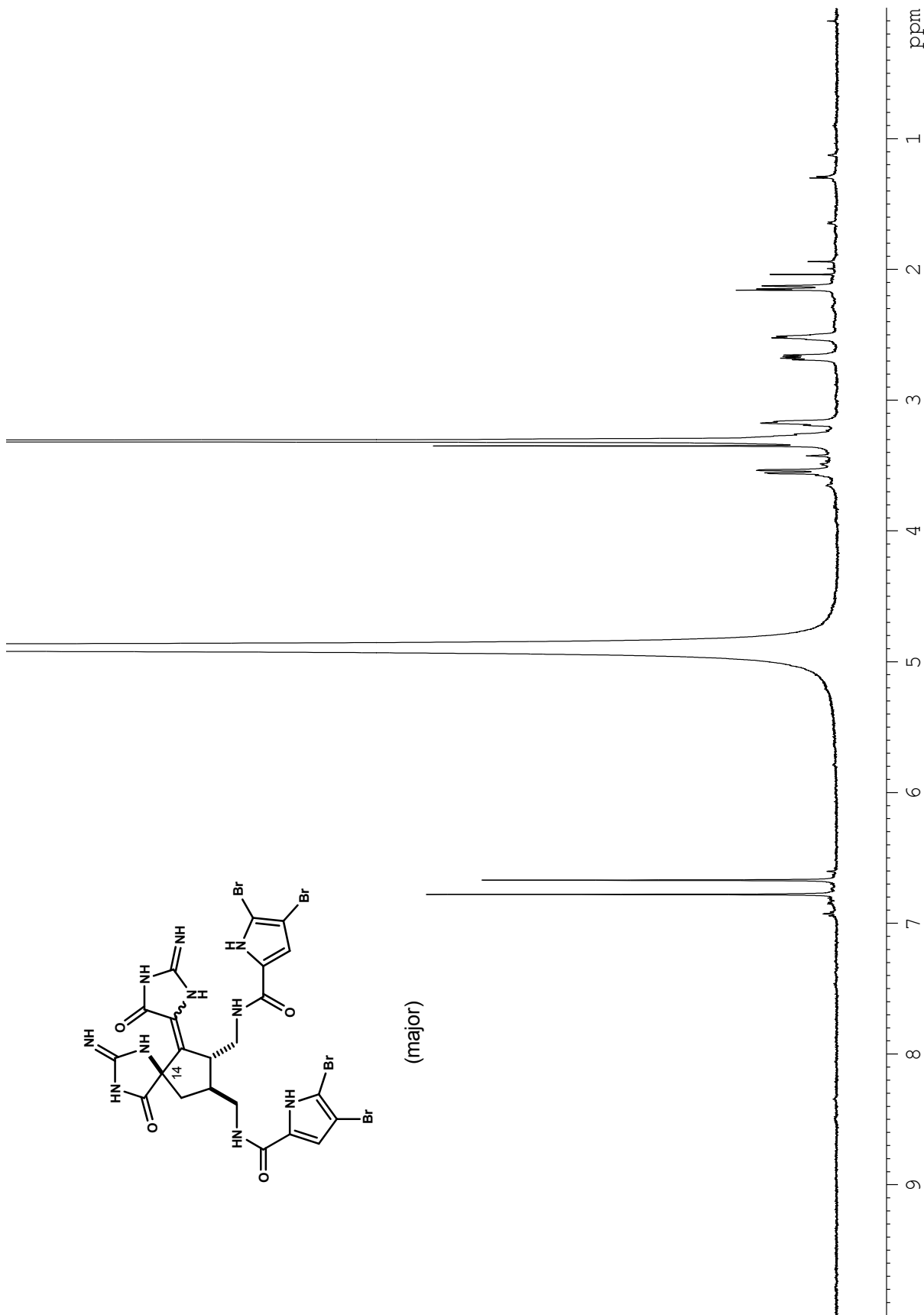


**Figure A1.46.**  $^1\text{H NMR}$  (500 MHz,  $\text{MeOH-}d_4$ ) spectrum of compound **2-50a** ( $2 \cdot \text{CF}_3\text{CO}_2\text{H}$ ) (major).



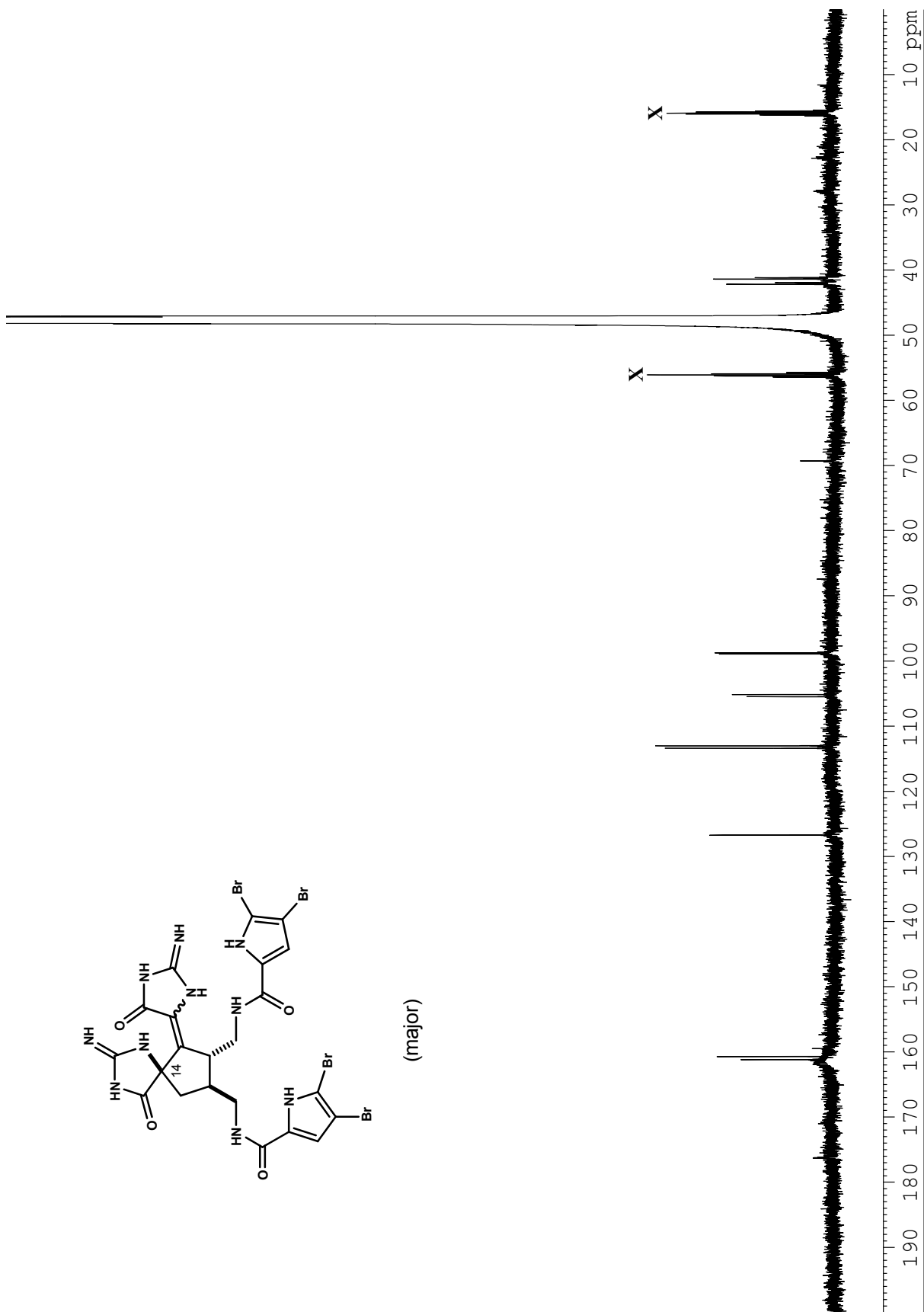


**Figure A1.47.** <sup>13</sup>C NMR (125 MHz, MeOH-*d*<sub>4</sub>) spectrum of compound **2-50a** (**2·CF<sub>3</sub>CO<sub>2</sub>H**) (major).

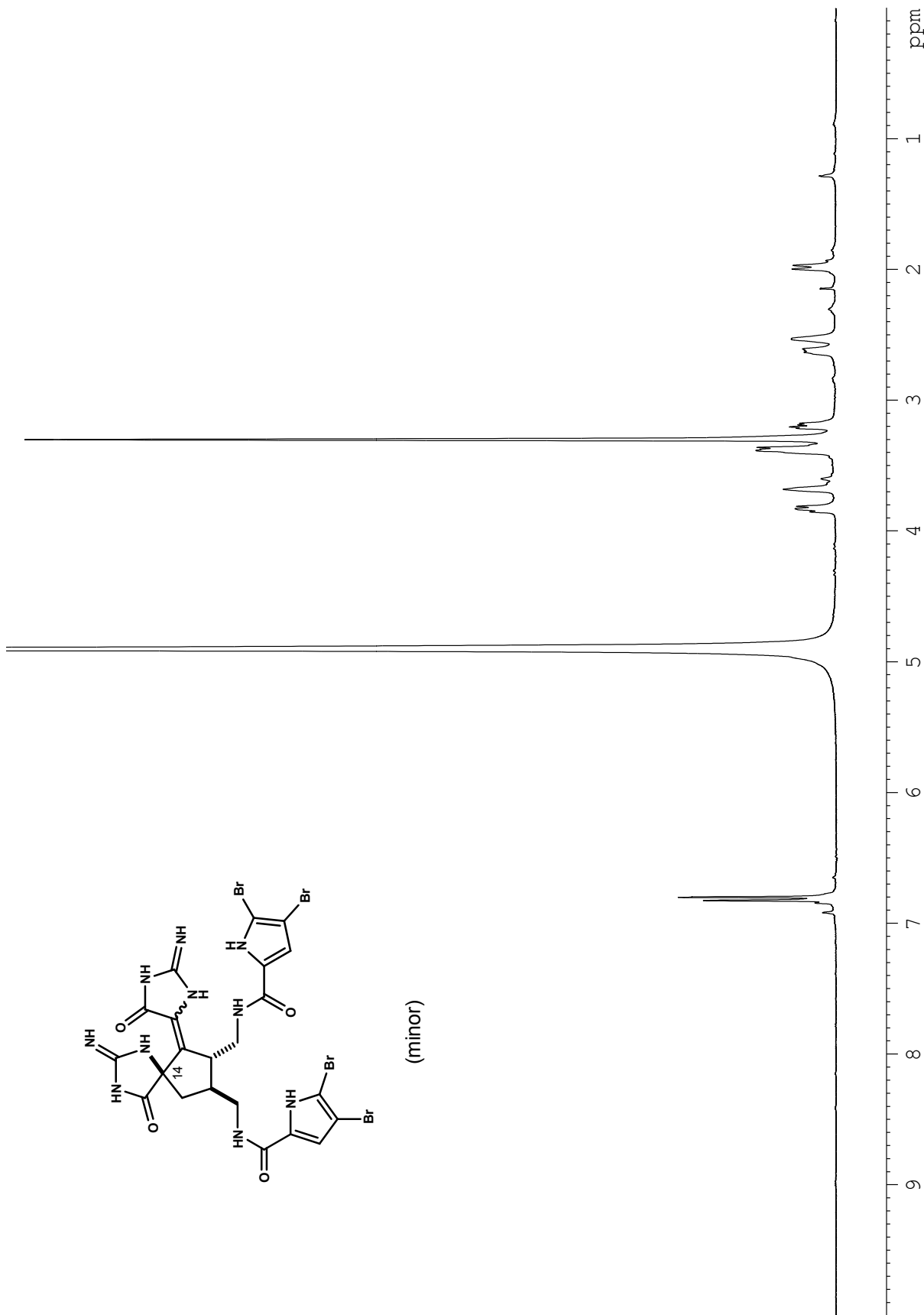


**Figure A1.48.** <sup>1</sup>H NMR (500 MHz, MeOH-*d*<sub>4</sub>) spectrum of compound 2-50a (2·CF<sub>3</sub>CO<sub>2</sub>H) (minor).

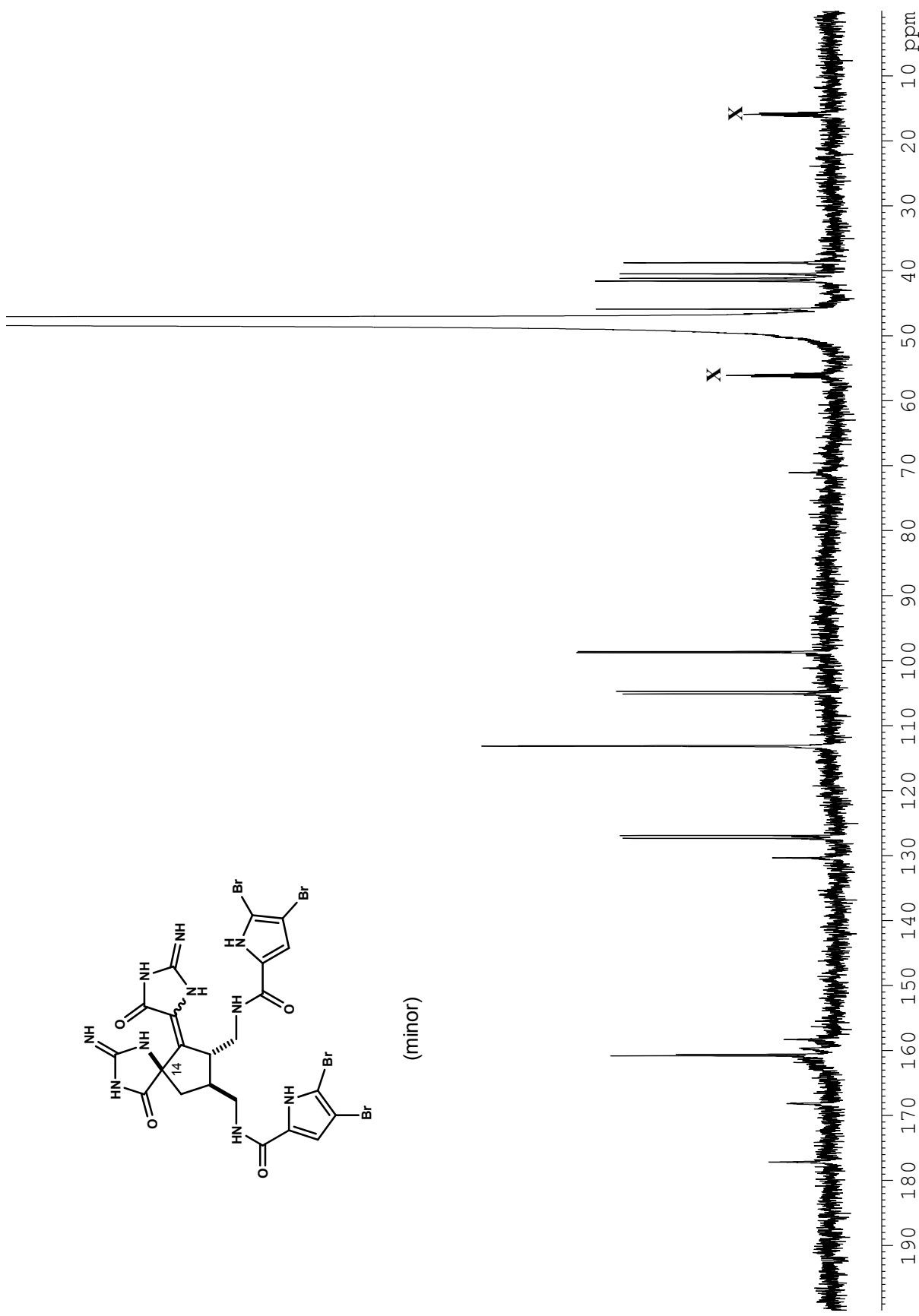


**Figure A1.49.** <sup>13</sup>C NMR (125 MHz, MeOH-*d*<sub>4</sub>) spectrum of compound 2-50a (2·CF<sub>3</sub>CO<sub>2</sub>H) (minor).

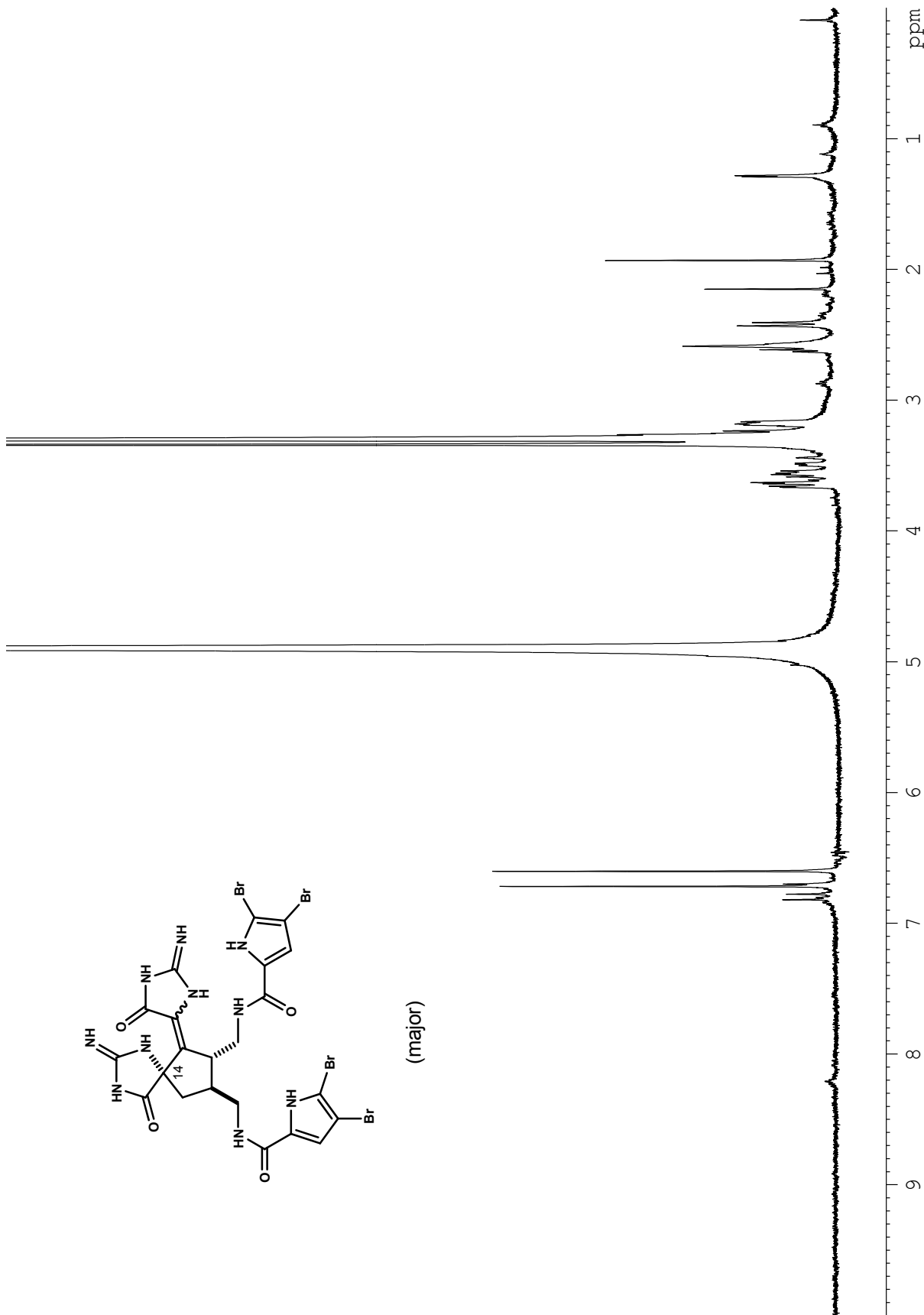


**Figure A1.50.** <sup>1</sup>H NMR (500 MHz, MeOH-*d*<sub>4</sub>) spectrum of compound 2-50b (2·CF<sub>3</sub>CO<sub>2</sub>H) (minor).

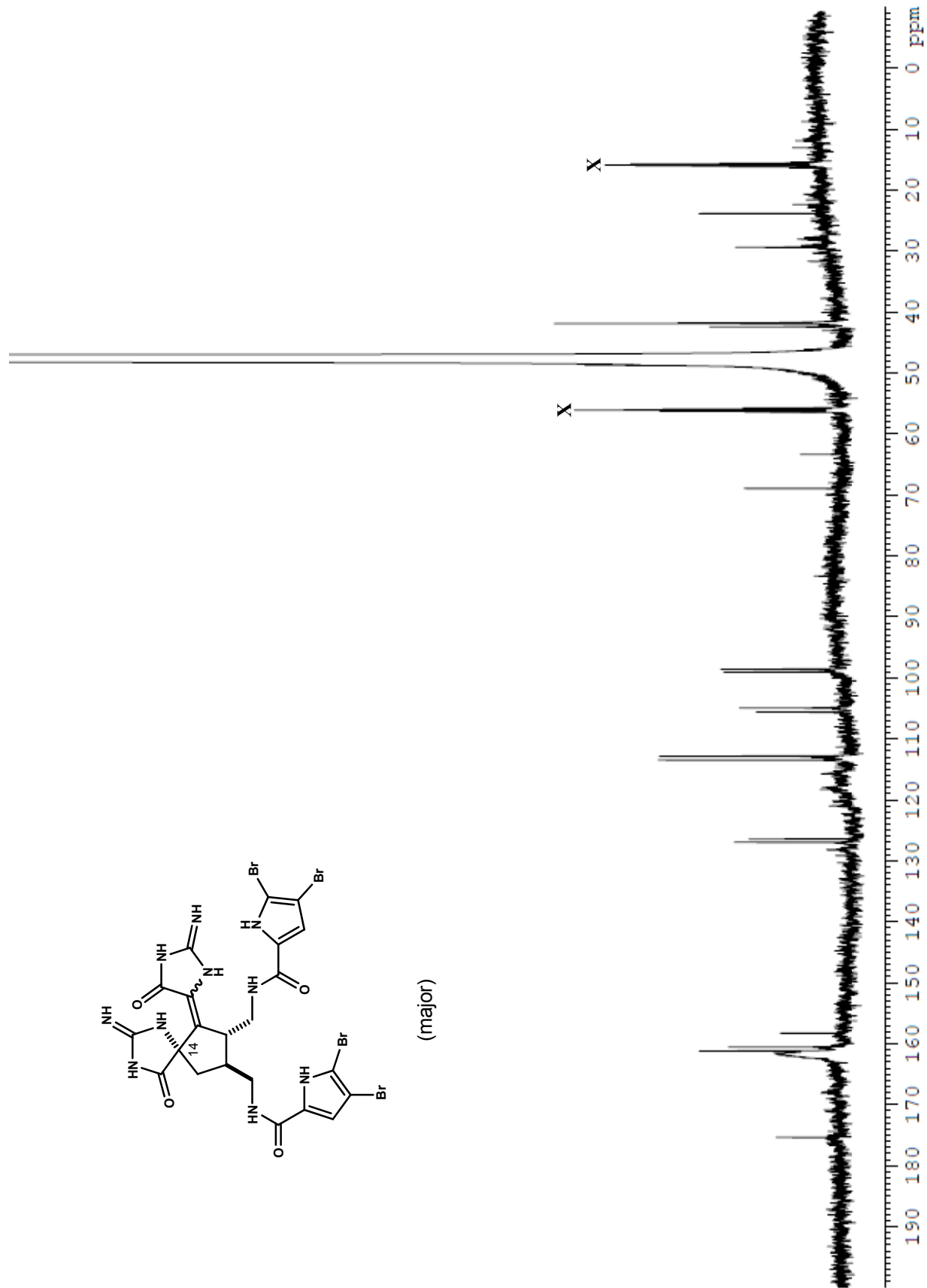


**Figure A1.51.**  $^{13}\text{C}$  NMR (125 MHz,  $\text{MeOH-}d_4$ ) spectrum of compound **2-50b** ( $2\cdot\text{CF}_3\text{CO}_2\text{H}$ ) (minor).

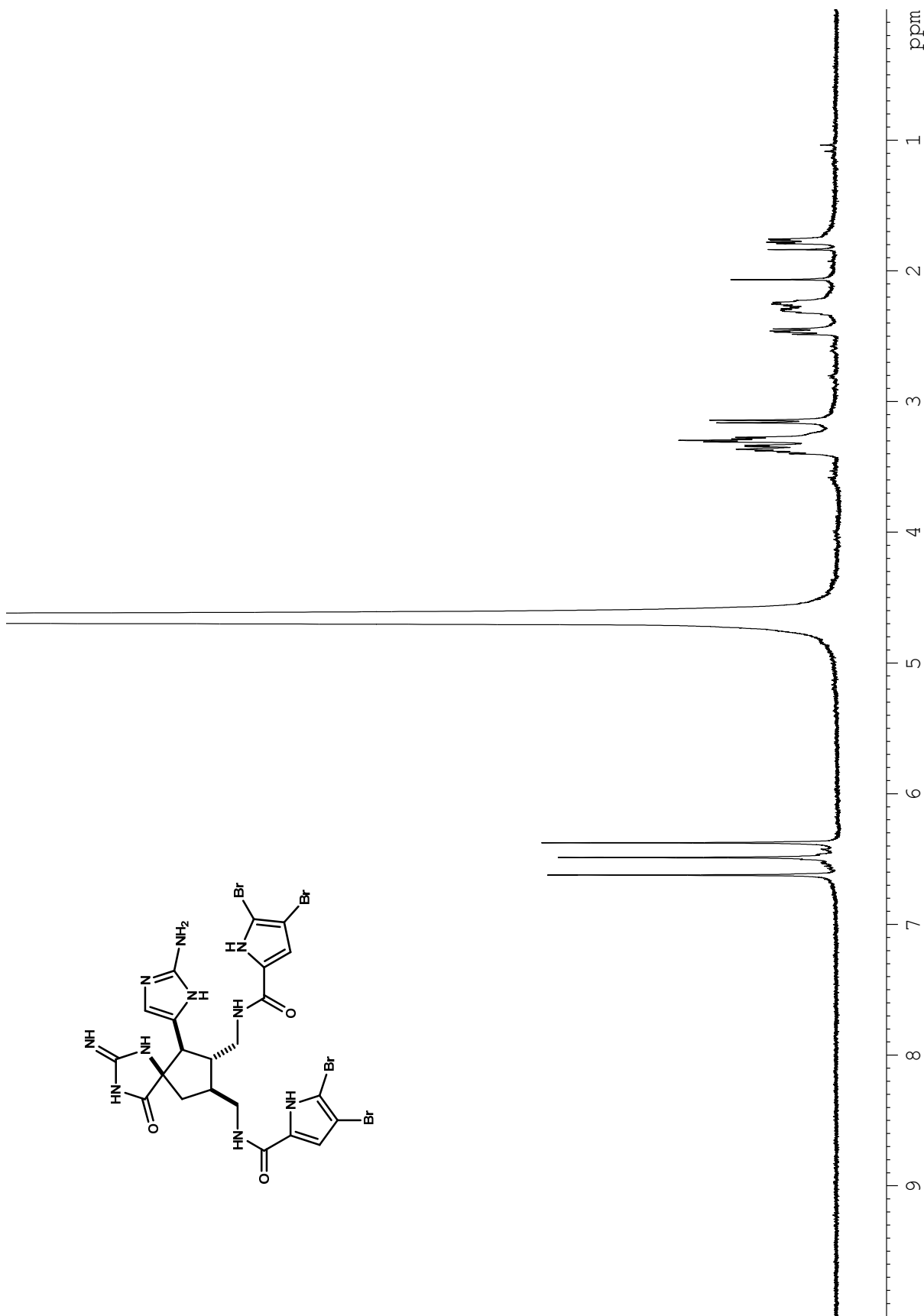


**Figure A1.52.** <sup>1</sup>H NMR (500 MHz, H<sub>2</sub>O-*d*<sub>2</sub>) spectrum of compound 2-51b (2·CF<sub>3</sub>CO<sub>2</sub>H).

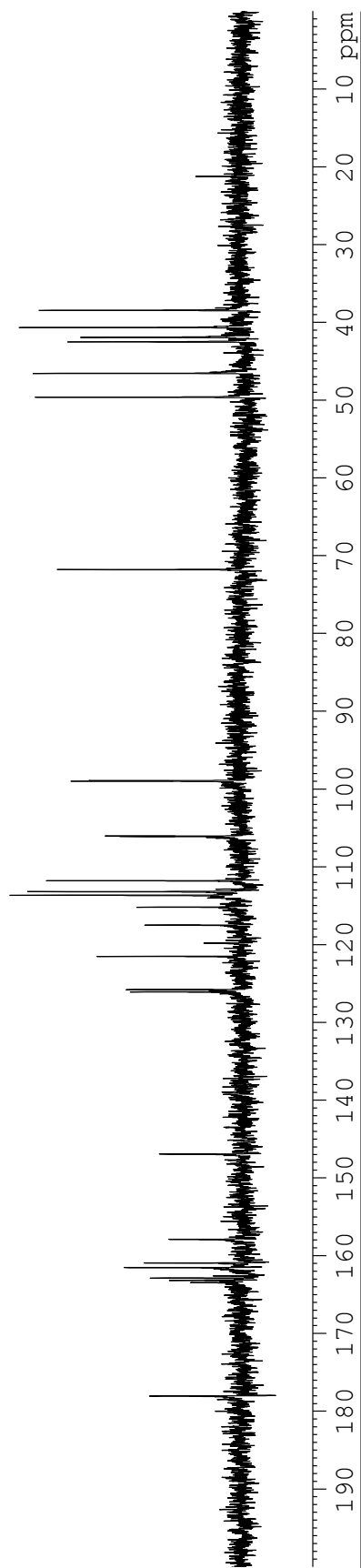
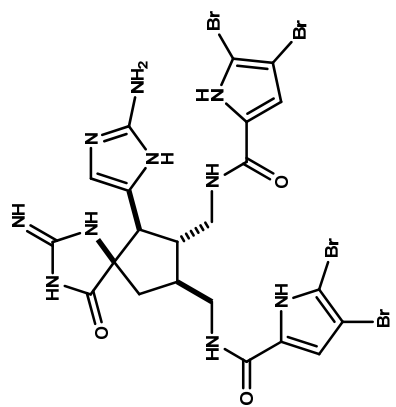


**Figure A1.53.** <sup>13</sup>C NMR (125 MHz, H<sub>2</sub>O-*d*<sub>2</sub>) spectrum of compound **2-51b** (2·CF<sub>3</sub>CO<sub>2</sub>H).

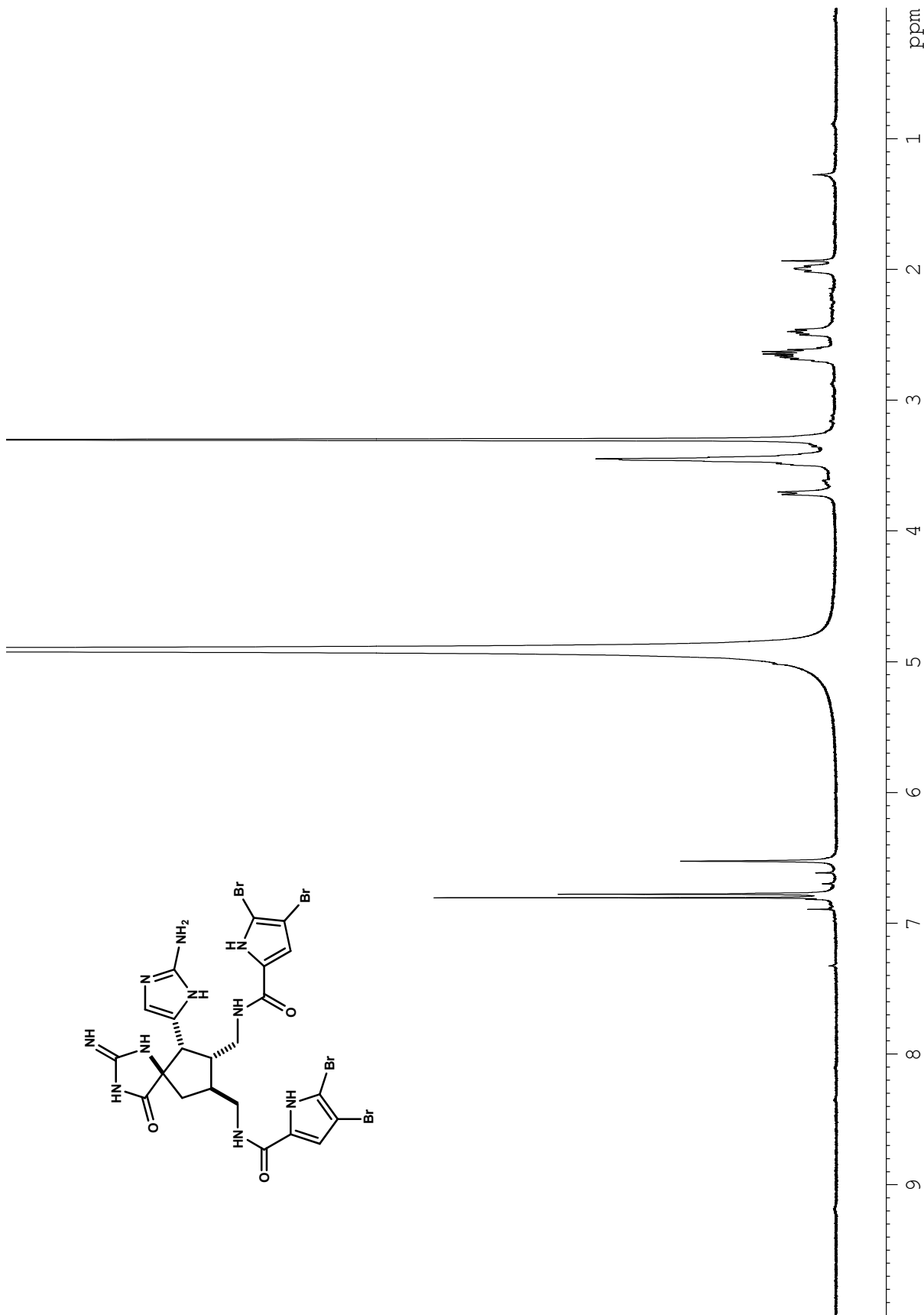


**Figure A1.54.** <sup>1</sup>H NMR (500 MHz, MeOH-*d*<sub>4</sub>) spectrum of compound 2-51a (2·CF<sub>3</sub>CO<sub>2</sub>H).



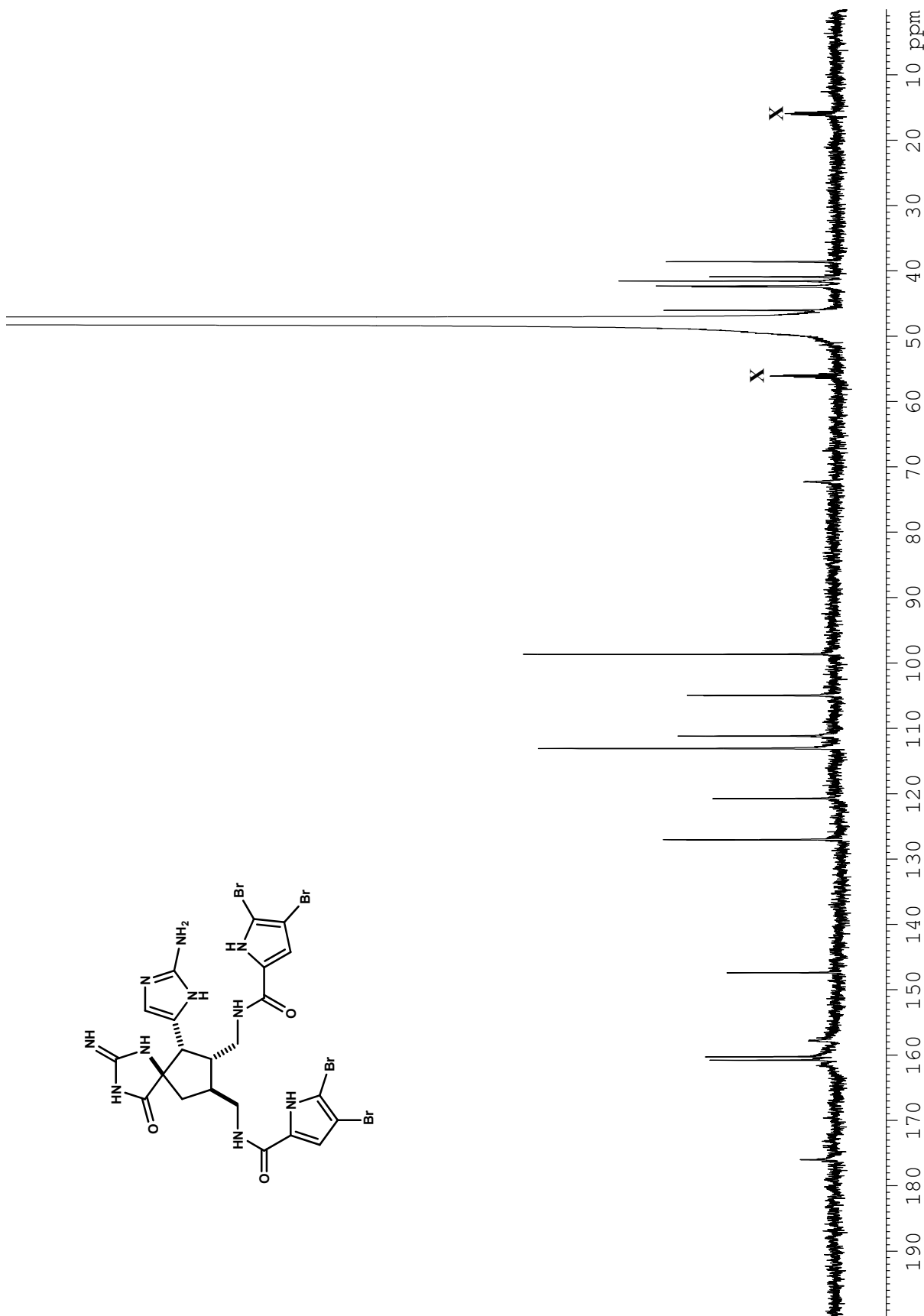


**Figure A1.55.**  $^{13}\text{C}$  NMR (125 MHz,  $\text{MeOH-}d_4$ ) spectrum of compound **2-51a** ( $2\text{-CF}_3\text{CO}_2\text{H}$ ).

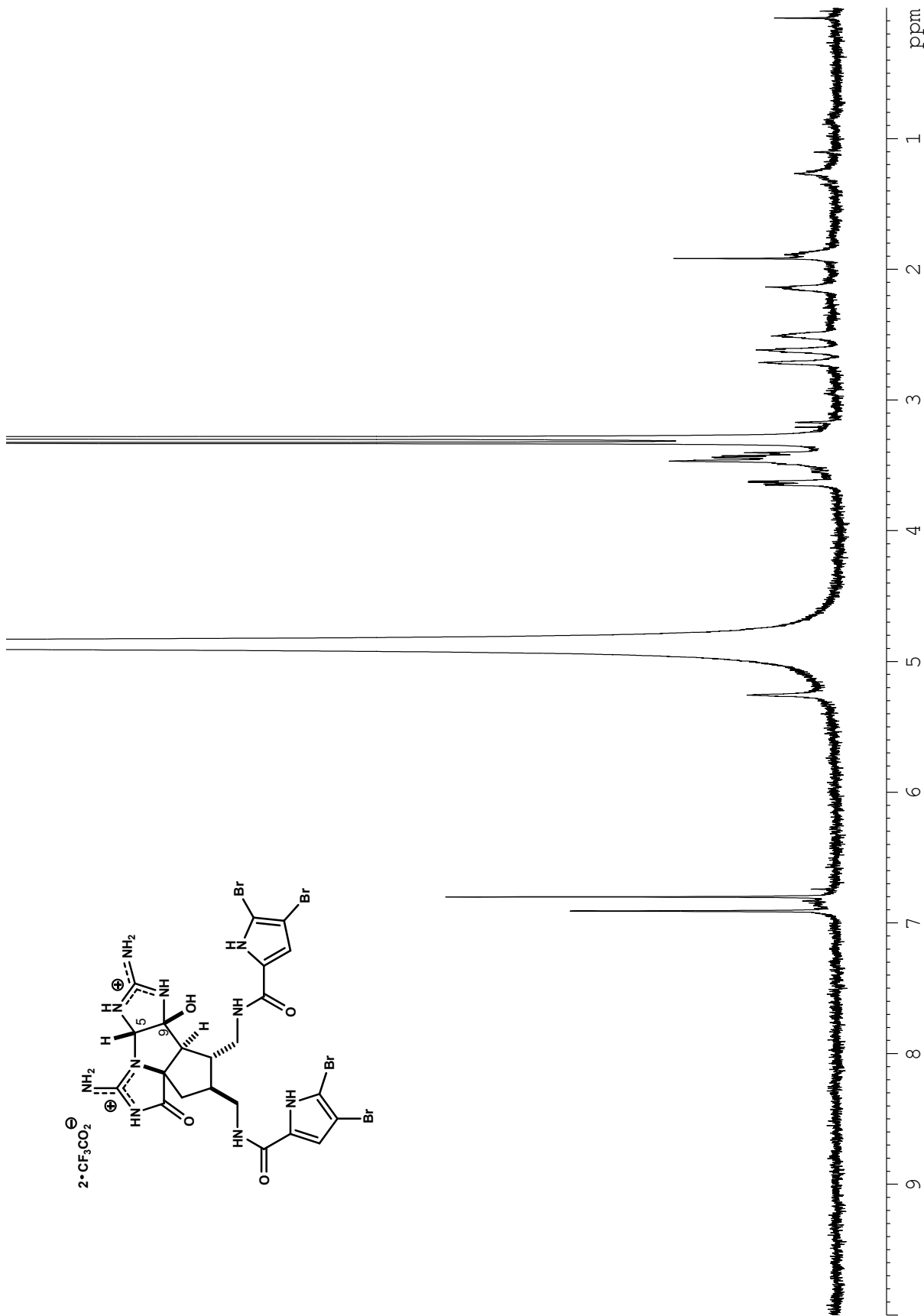


**Figure A1.56.**  $^1\text{H}$  NMR (600 MHz,  $\text{MeOH-}d_4$ ) spectrum of compound **2-57a** ( $2 \cdot \text{CF}_3\text{CO}_2\text{H}$ ).

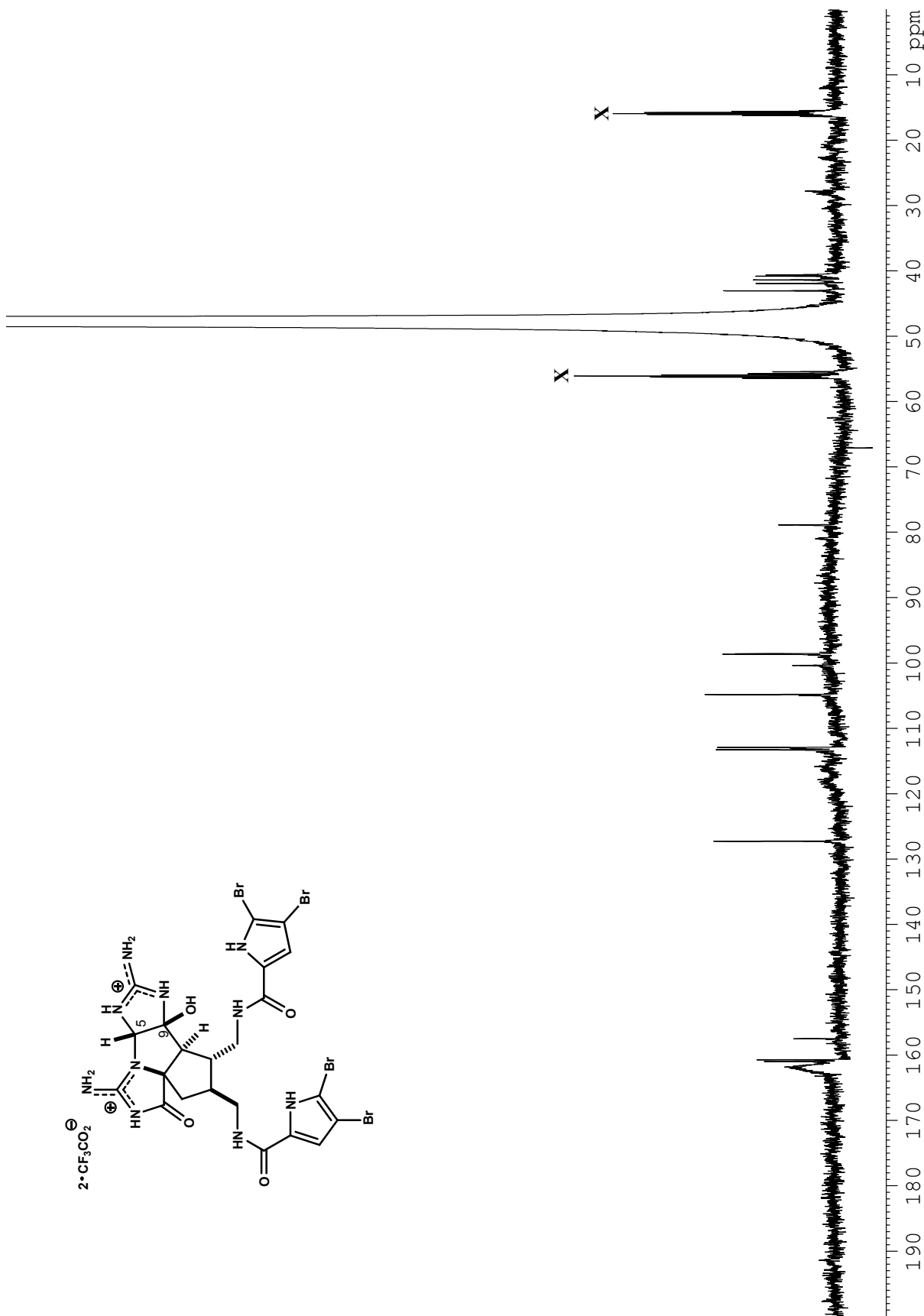


**Figure A1.57.**  $^{13}\text{C}$  NMR (125 MHz, MeOH-*d*<sub>4</sub>) spectrum of compound 2-57a (2-CF<sub>3</sub>CO<sub>2</sub>H).

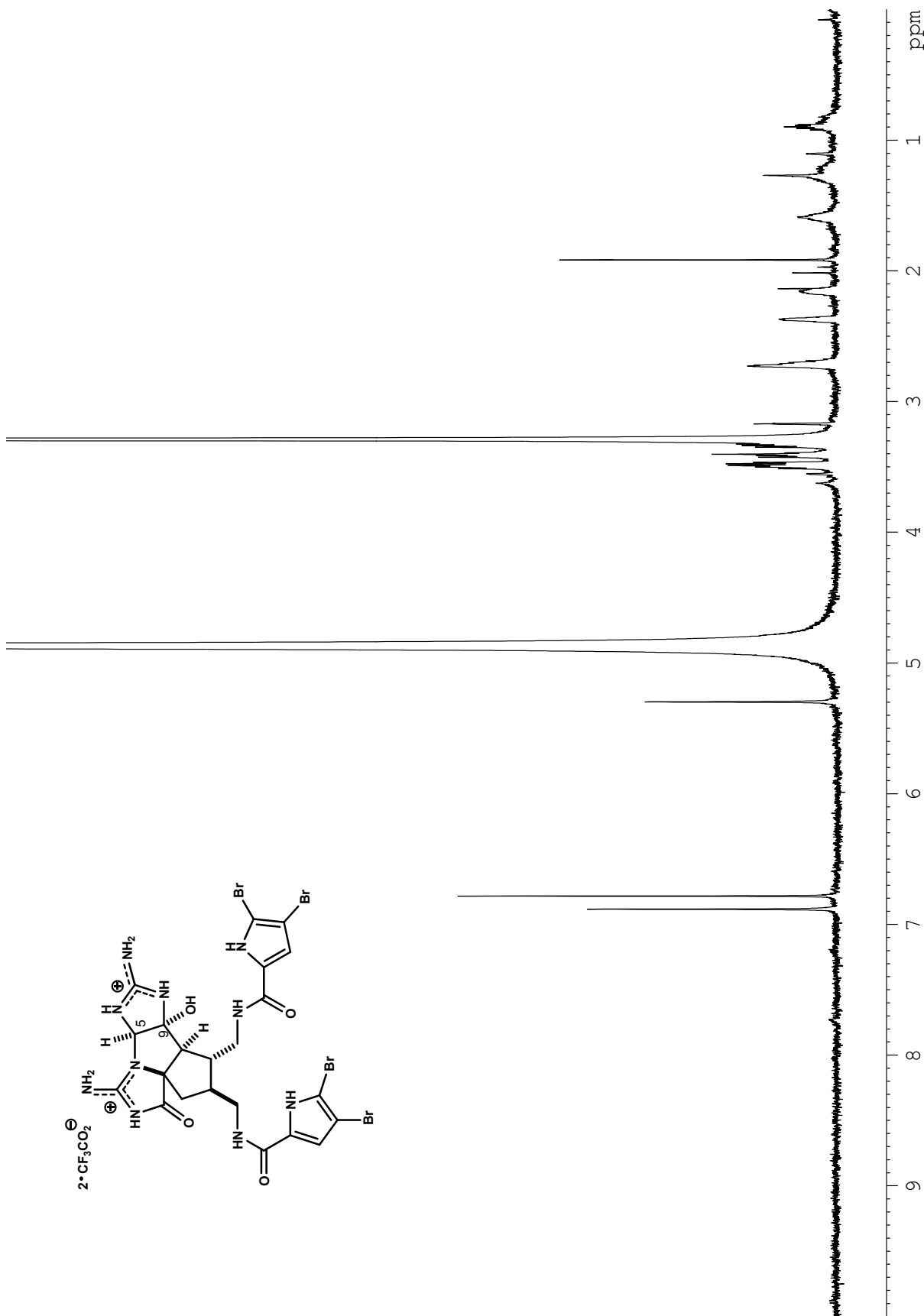


**Figure A1.58.** <sup>1</sup>H NMR (600 MHz, MeOH-*d*<sub>4</sub>) spectrum of compound 2-57b (2·CF<sub>3</sub>CO<sub>2</sub>H).

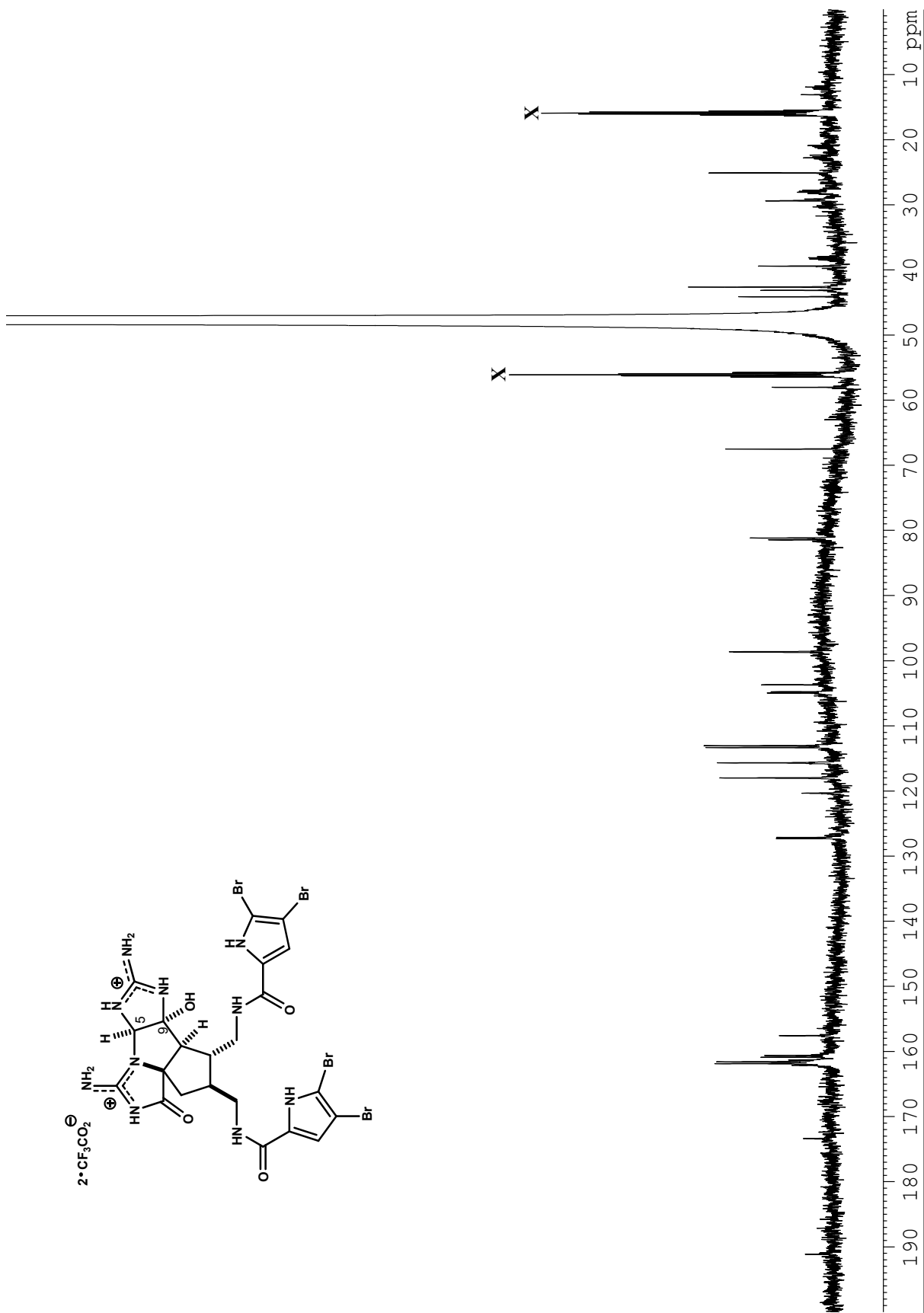


**Figure A1.59.**  $^{13}\text{C}$  NMR (125 MHz,  $\text{MeOH-}d_4$ ) spectrum of compound **2-57b** ( $2\text{-CF}_3\text{CO}_2\text{H}$ ).

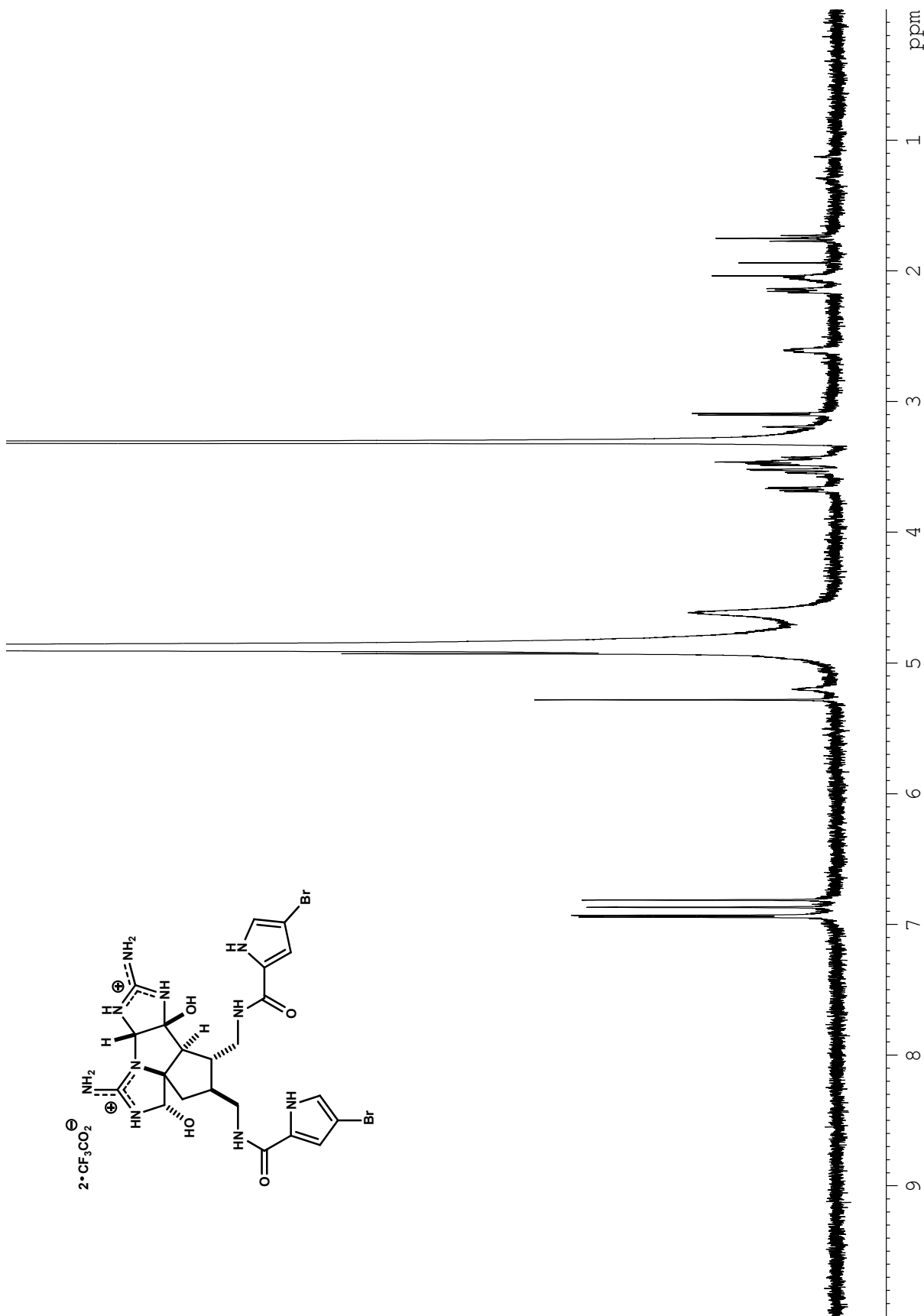


**Figure A1.60.** <sup>1</sup>H NMR (500 MHz, MeOH-*d*<sub>4</sub>) spectrum of compound 2-58a (2·CF<sub>3</sub>CO<sub>2</sub>H).

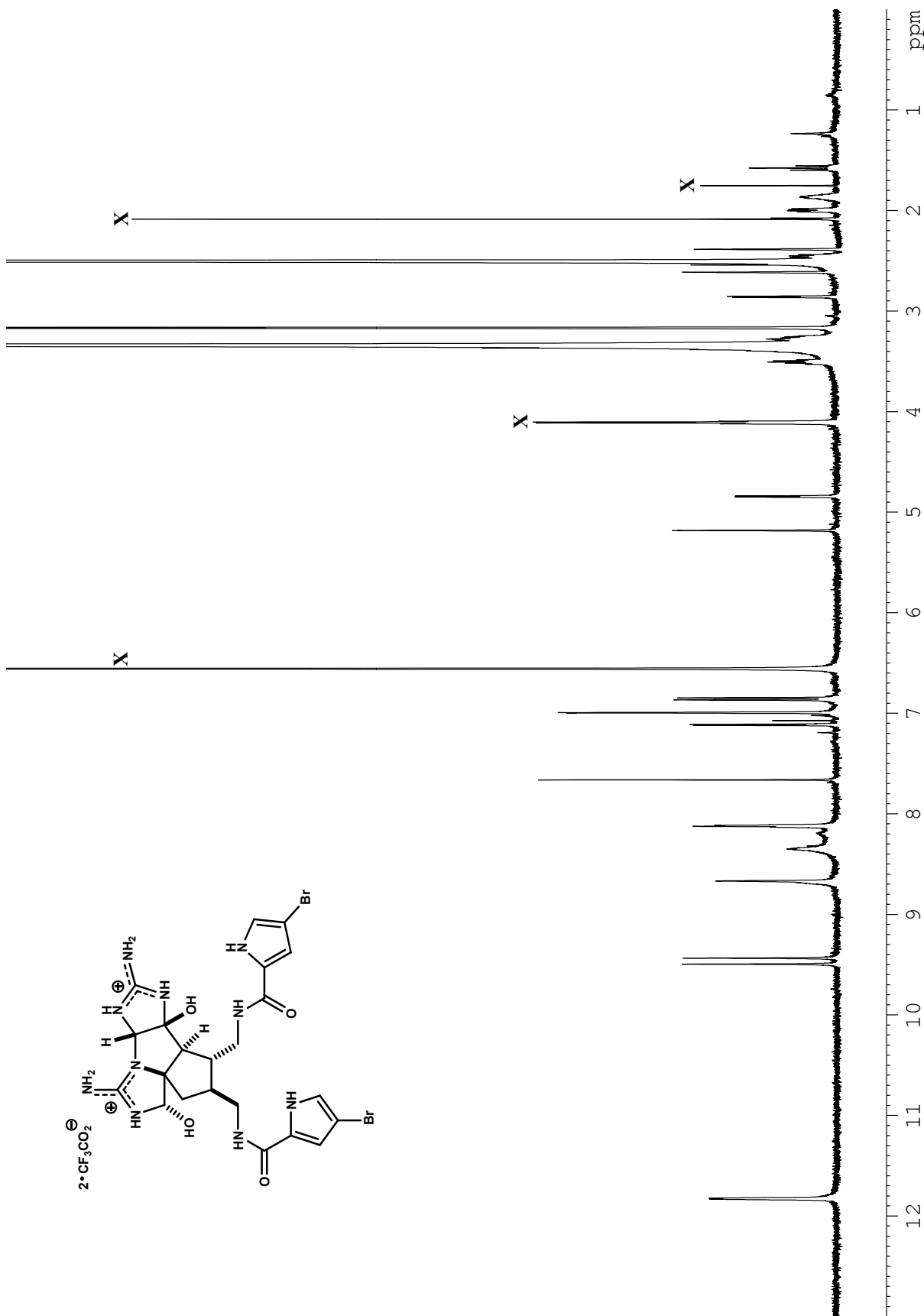


**Figure A1.61.** <sup>1</sup>H NMR (500 MHz, DMSO-*d*<sub>6</sub>) spectrum of compound 2-58a (2·CF<sub>3</sub>CO<sub>2</sub>H).

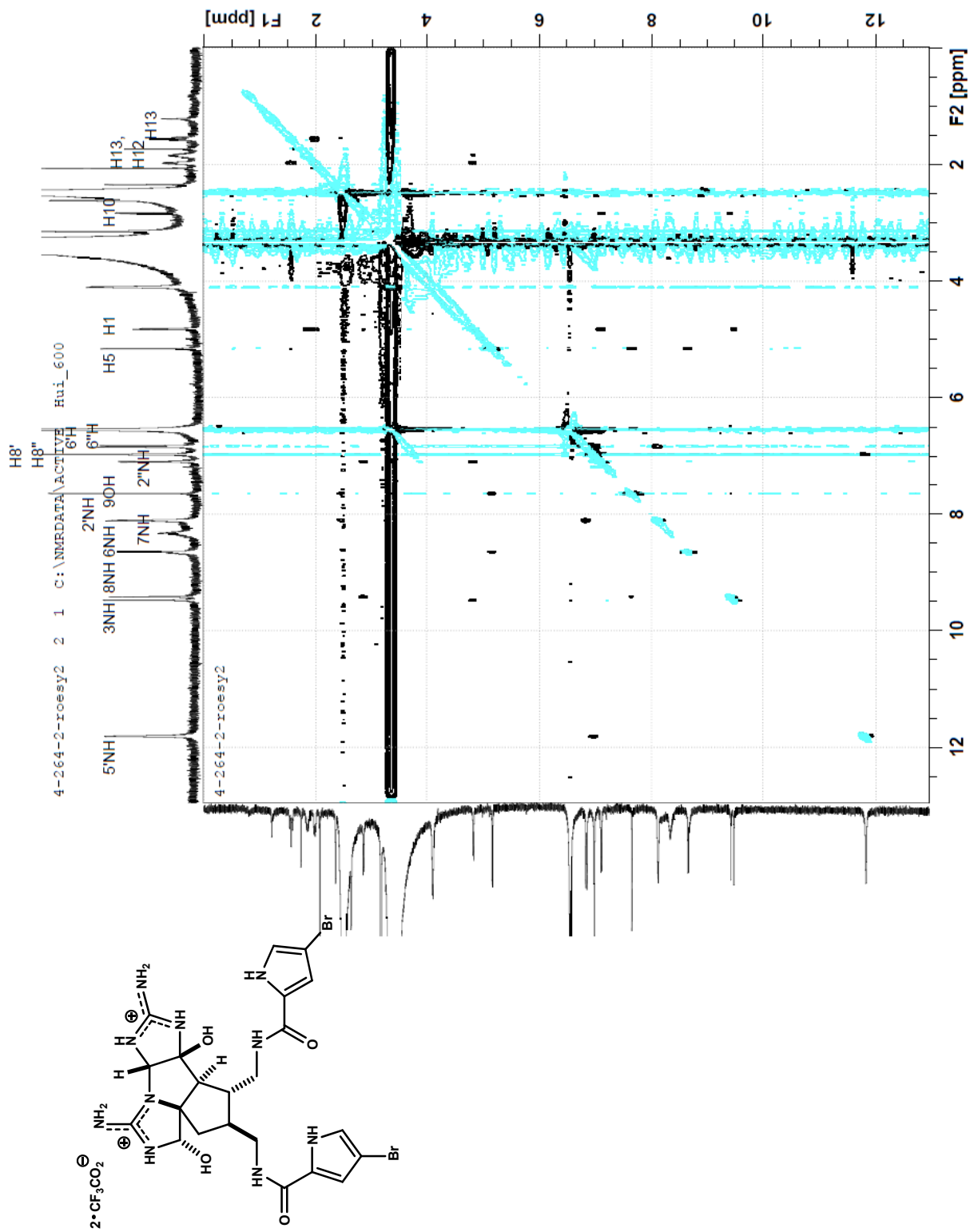


Figure A1.62. ROESY (600 MHz, DMSO-*d*<sub>6</sub>) spectrum of compound 2-58a (2·CF<sub>3</sub>CO<sub>2</sub>H).



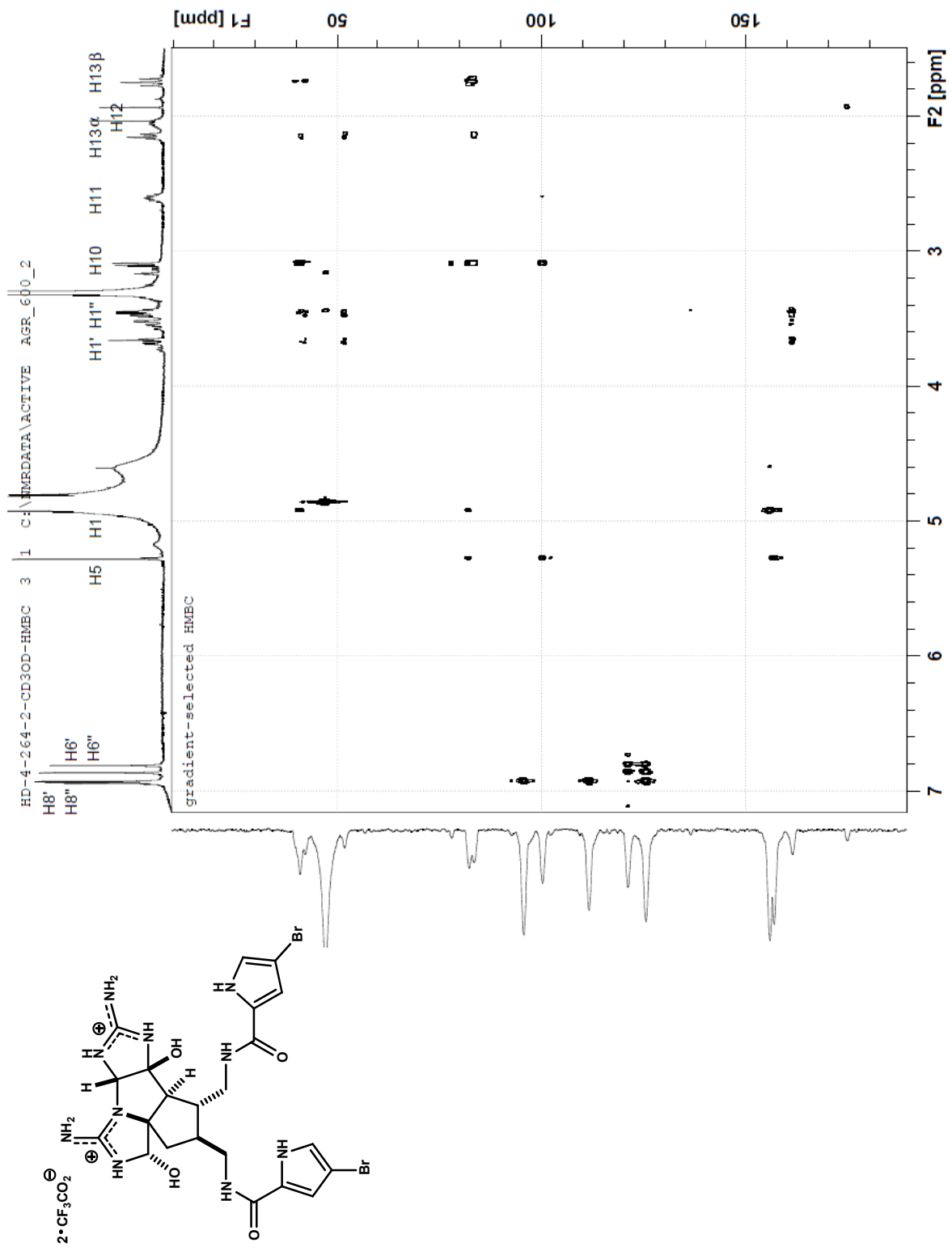


Figure A1.63. HMBC (600 MHz, MeOH-*d*<sub>4</sub>) spectrum of compound 2-58a (2·CF<sub>3</sub>CO<sub>2</sub>H).

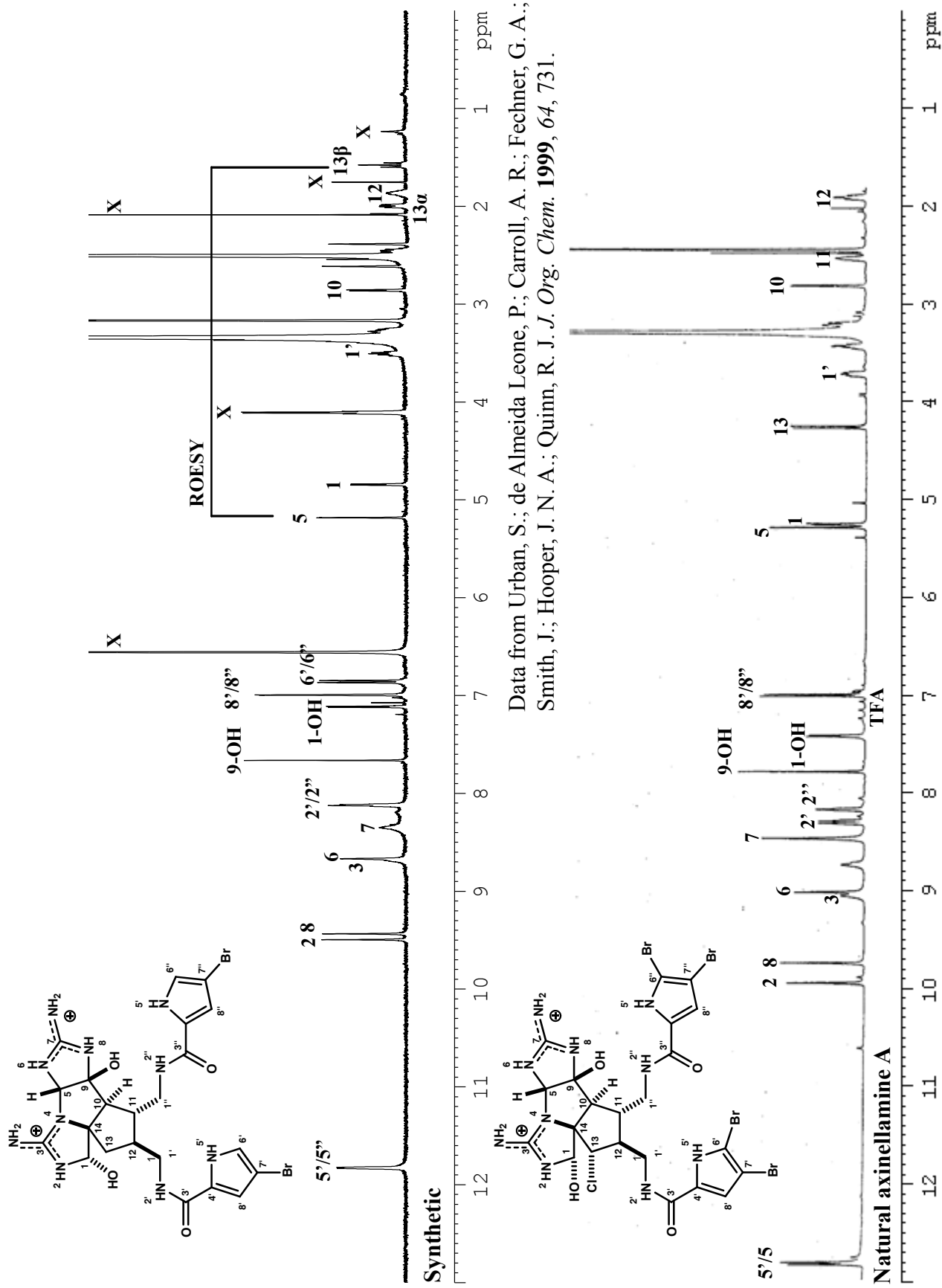
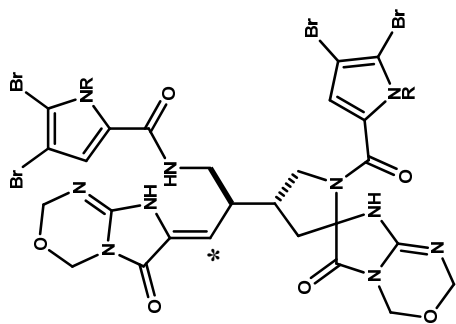
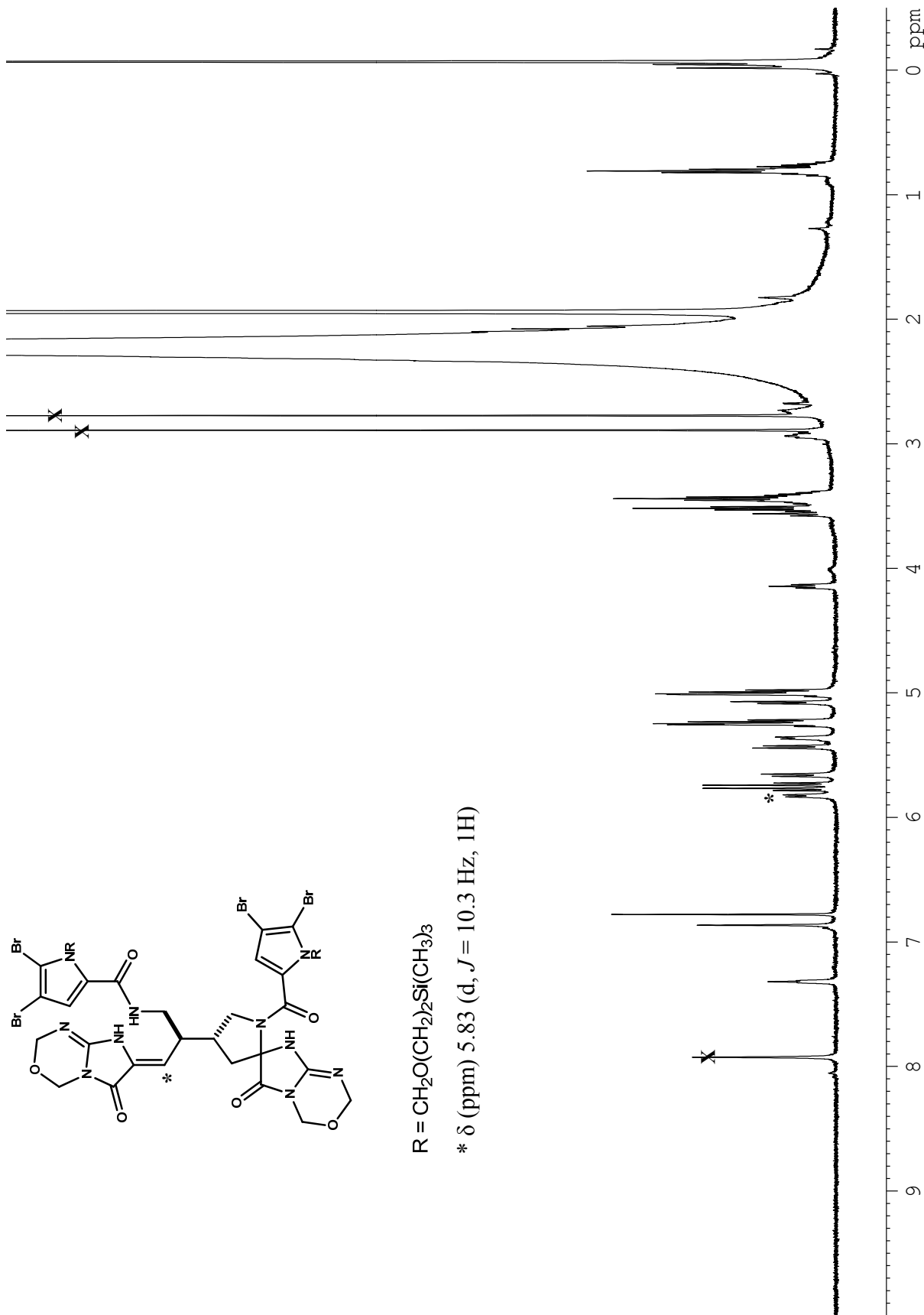


Figure A1.64. Comparison of <sup>1</sup>H NMR (DMSO-*d*<sub>6</sub>) spectra (Top: synthetic 2-58a, Bottom: natural axinellamine A 2-5a)

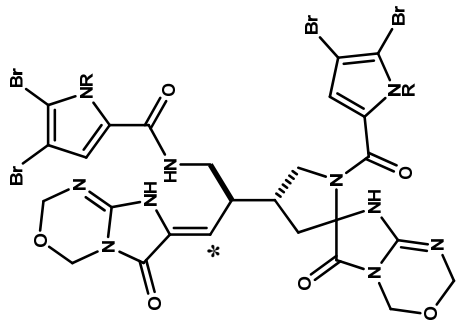


R = CH<sub>2</sub>O(CH<sub>2</sub>)<sub>2</sub>Si(CH<sub>3</sub>)<sub>3</sub>

\* δ (ppm) 5.83 (d, J = 10.3 Hz, 1H)



**Figure A1.65.** <sup>1</sup>H NMR (600 MHz, CH<sub>3</sub>CN-*d*<sub>3</sub>) spectrum of compound 2-59 (HCO<sub>2</sub>H) (major isomer).



R = CH<sub>2</sub>O(CH<sub>2</sub>)<sub>2</sub>Si(CH<sub>3</sub>)<sub>3</sub>

\* δ (ppm) 5.83 (d, J = 10.3 Hz, 1H)

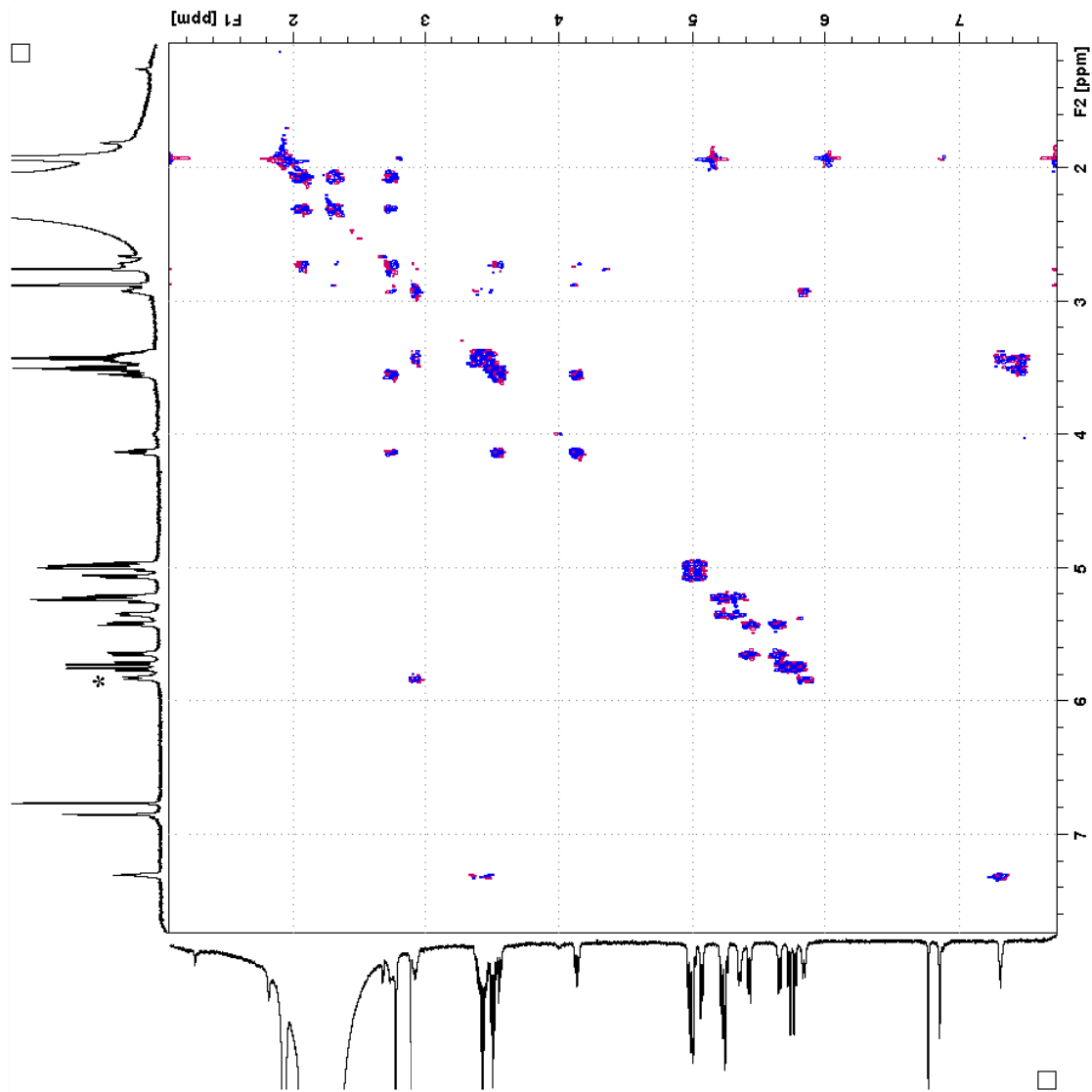
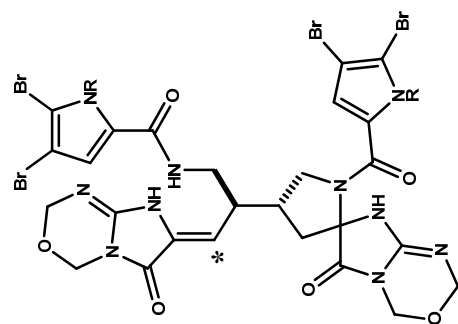


**Figure A1.66.** COSY (600 MHz, CH<sub>3</sub>CN-*d*<sub>3</sub>) spectrum of compound 2-59 (HCO<sub>2</sub>H) (major isomer).



R = CH<sub>2</sub>O(CH<sub>2</sub>)<sub>2</sub>Si(CH<sub>3</sub>)<sub>3</sub>

\* δ (ppm) 5.85 (d, J = 10.4 Hz, 1H)

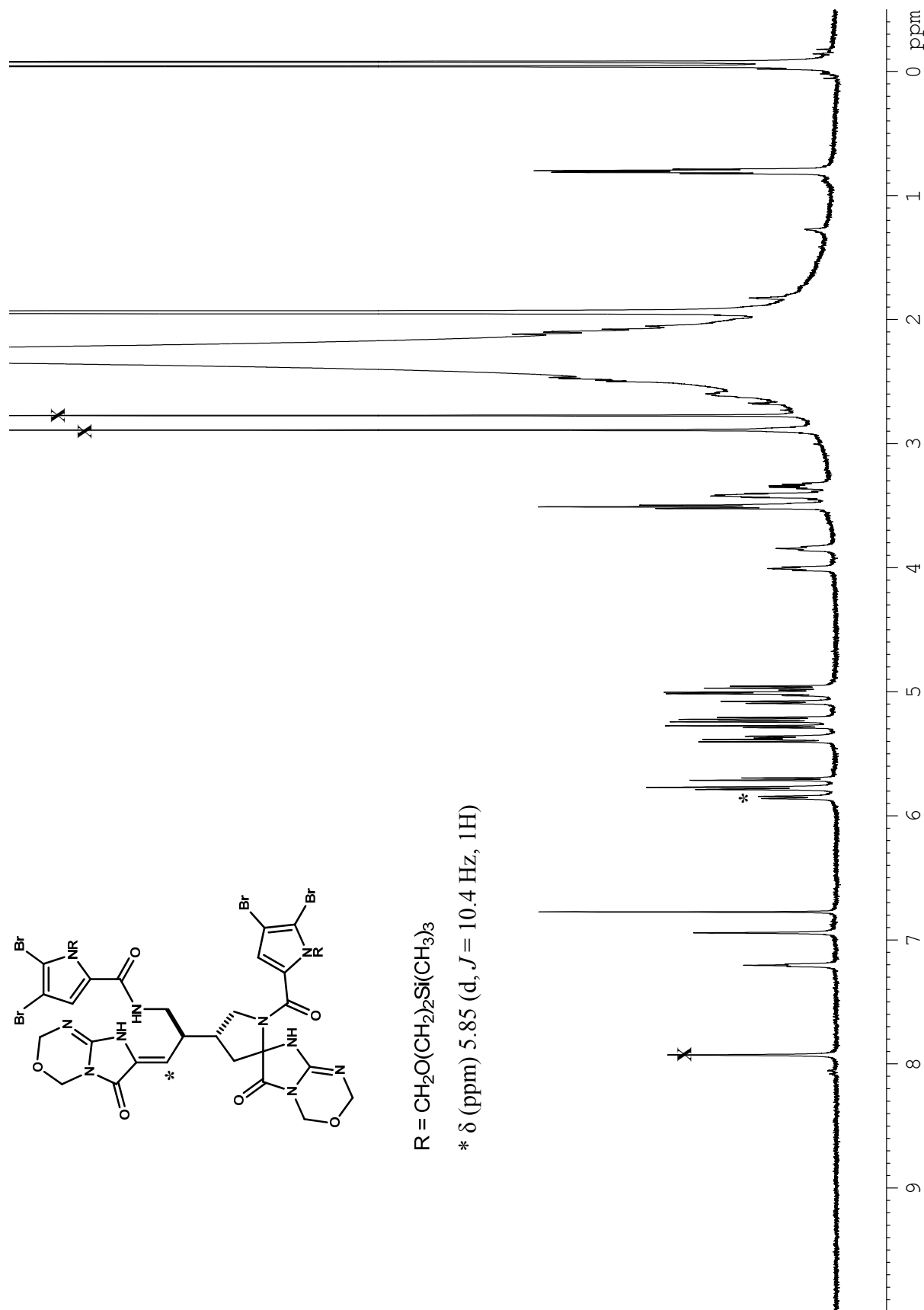
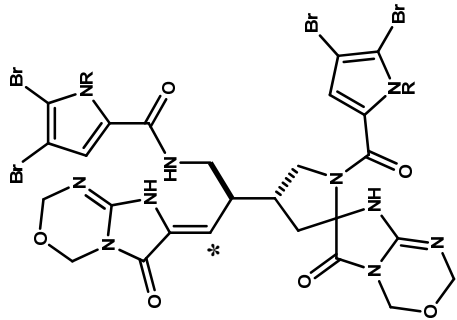


**Figure A1.67.** <sup>1</sup>H NMR (600 MHz, CH<sub>3</sub>CN-*d*<sub>3</sub>) spectrum of compound 2-59 (HCO<sub>2</sub>H) (minor isomer).



R = CH<sub>2</sub>O(CH<sub>2</sub>)<sub>2</sub>Si(CH<sub>3</sub>)<sub>3</sub>

\* δ (ppm) 5.85 (d, J = 10.4 Hz, 1H)

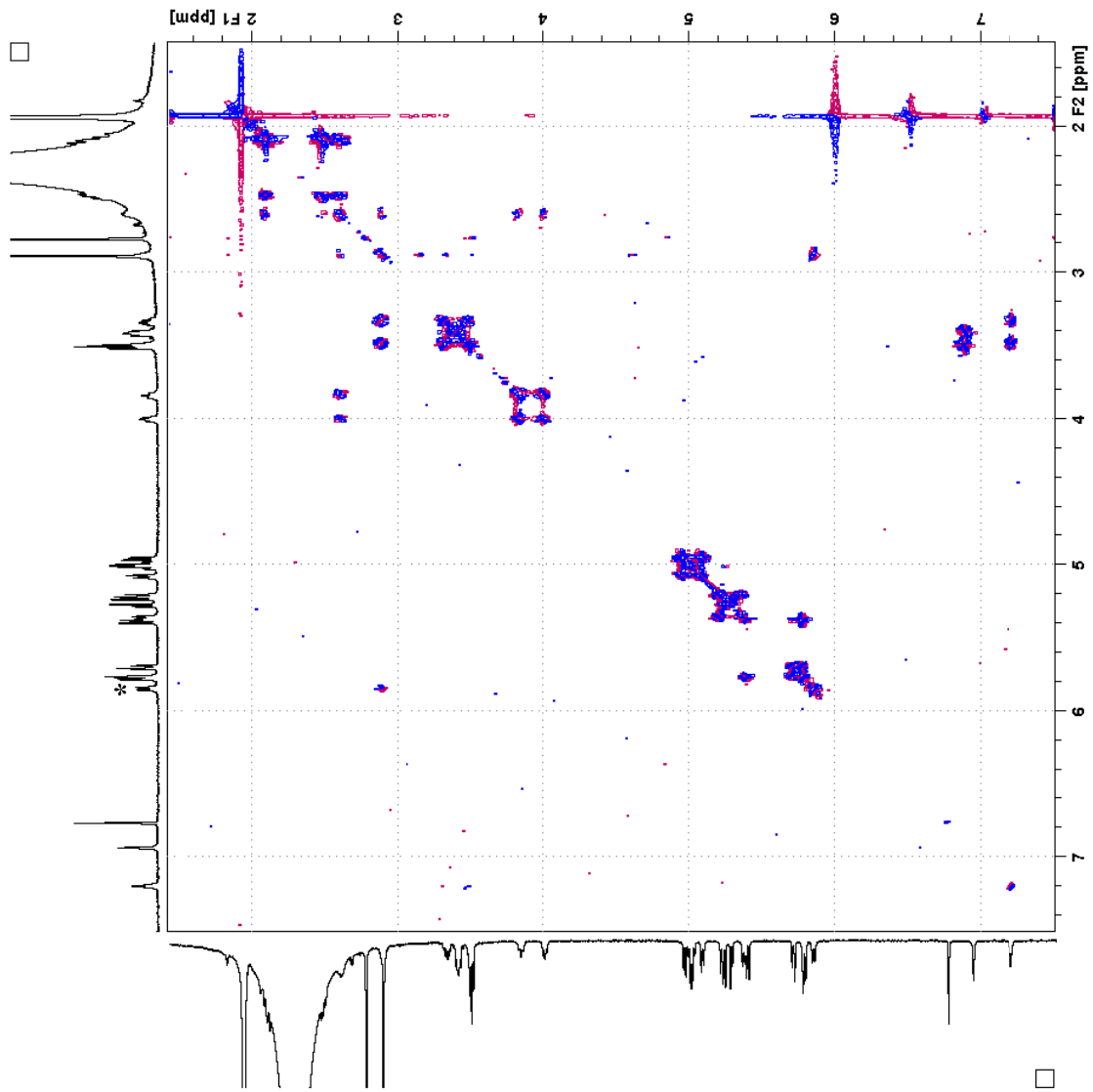
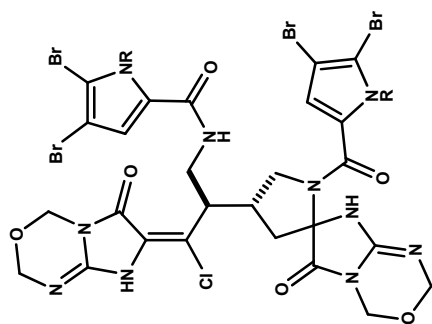


**Figure A1.68.** COSY (600 MHz, CH<sub>3</sub>CN-*d*<sub>3</sub>) spectrum of compound 2-59 (HCO<sub>2</sub>H) (minor isomer).



R = CH<sub>2</sub>O(CH<sub>2</sub>)<sub>2</sub>Si(CH<sub>3</sub>)<sub>3</sub>

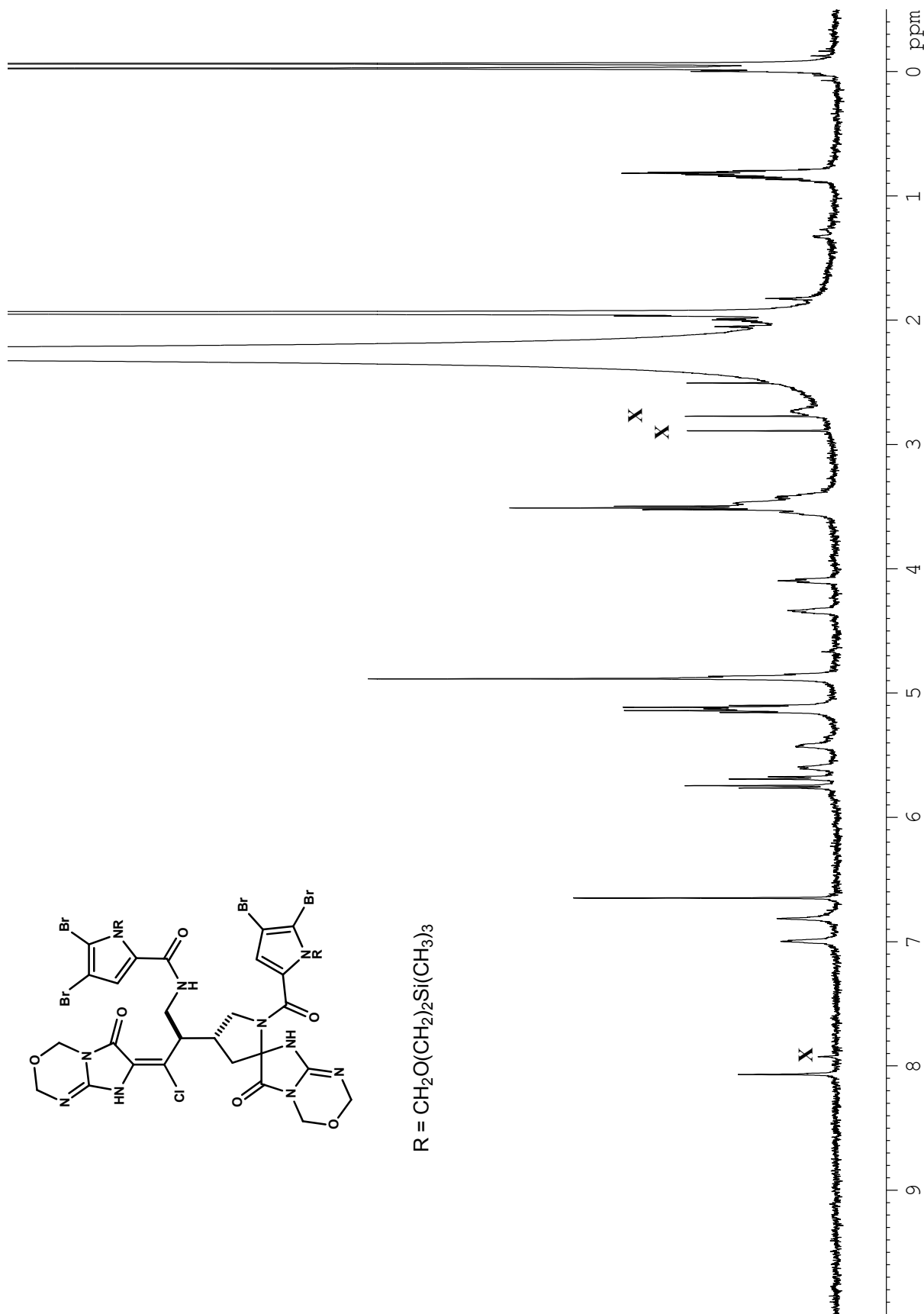
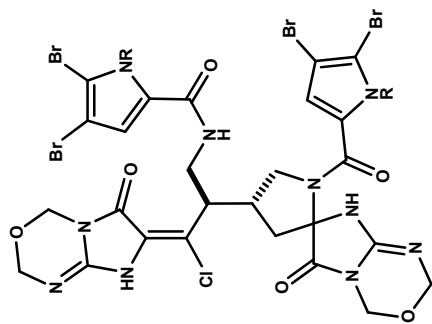


**Figure A1.69.** <sup>1</sup>H NMR (600 MHz, CH<sub>3</sub>CN-*d*<sub>3</sub>) spectrum of compound **2-60** (HCO<sub>2</sub>H) (major isomer).



R = CH<sub>2</sub>O(CH<sub>2</sub>)<sub>2</sub>Si(CH<sub>3</sub>)<sub>3</sub>

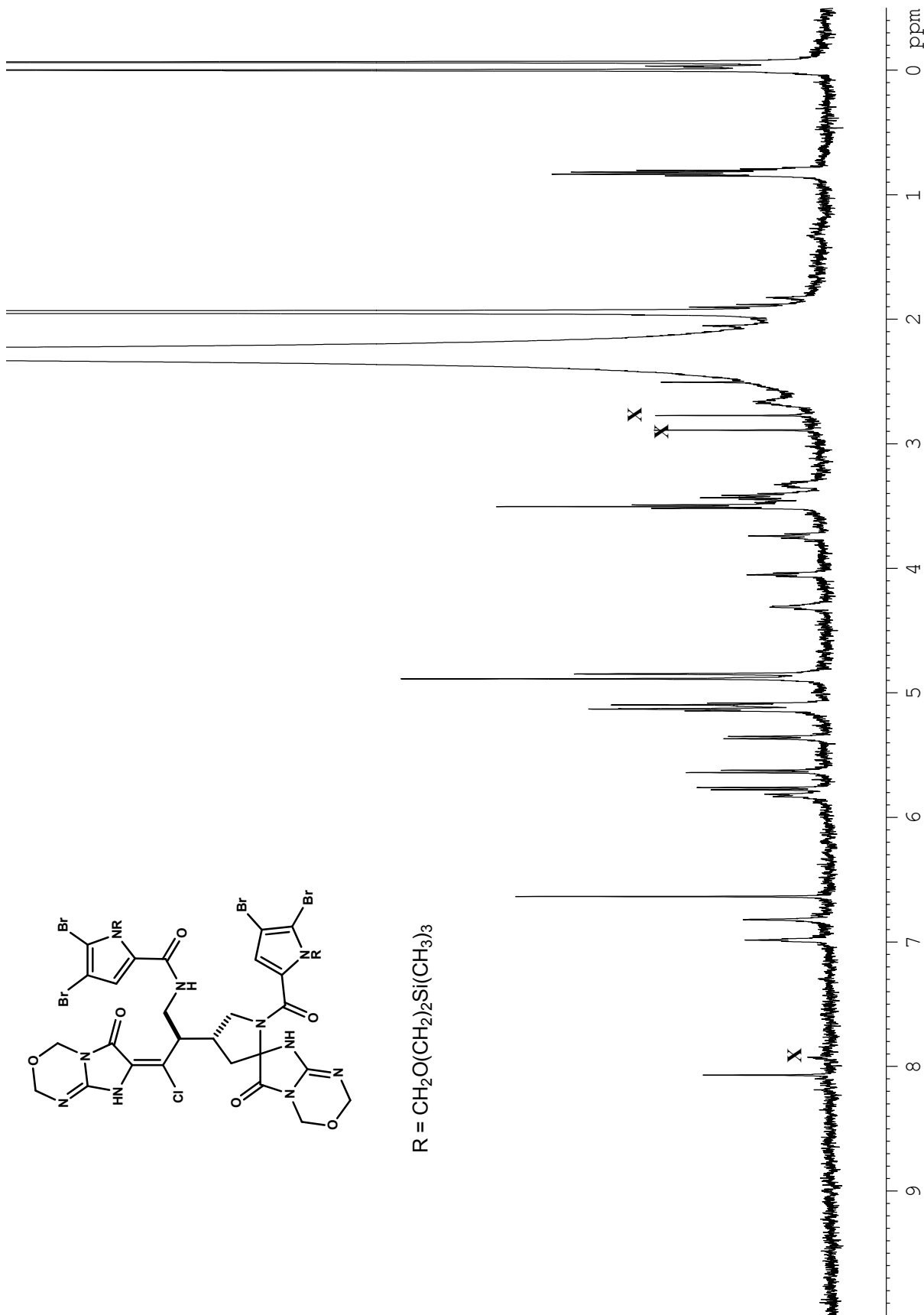
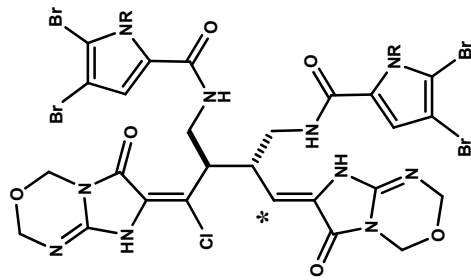


**Figure A1.70.** <sup>1</sup>H NMR (600 MHz, CH<sub>3</sub>CN-*d*<sub>3</sub>) spectrum of compound **2-60** (HCO<sub>2</sub>H) (minor isomer).





R =  $\text{CH}_2\text{O}(\text{CH}_2)_2\text{Si}(\text{CH}_3)_3$

\*  $\delta$  (ppm) 5.50 (d,  $J = 9.9$  Hz, 1H)

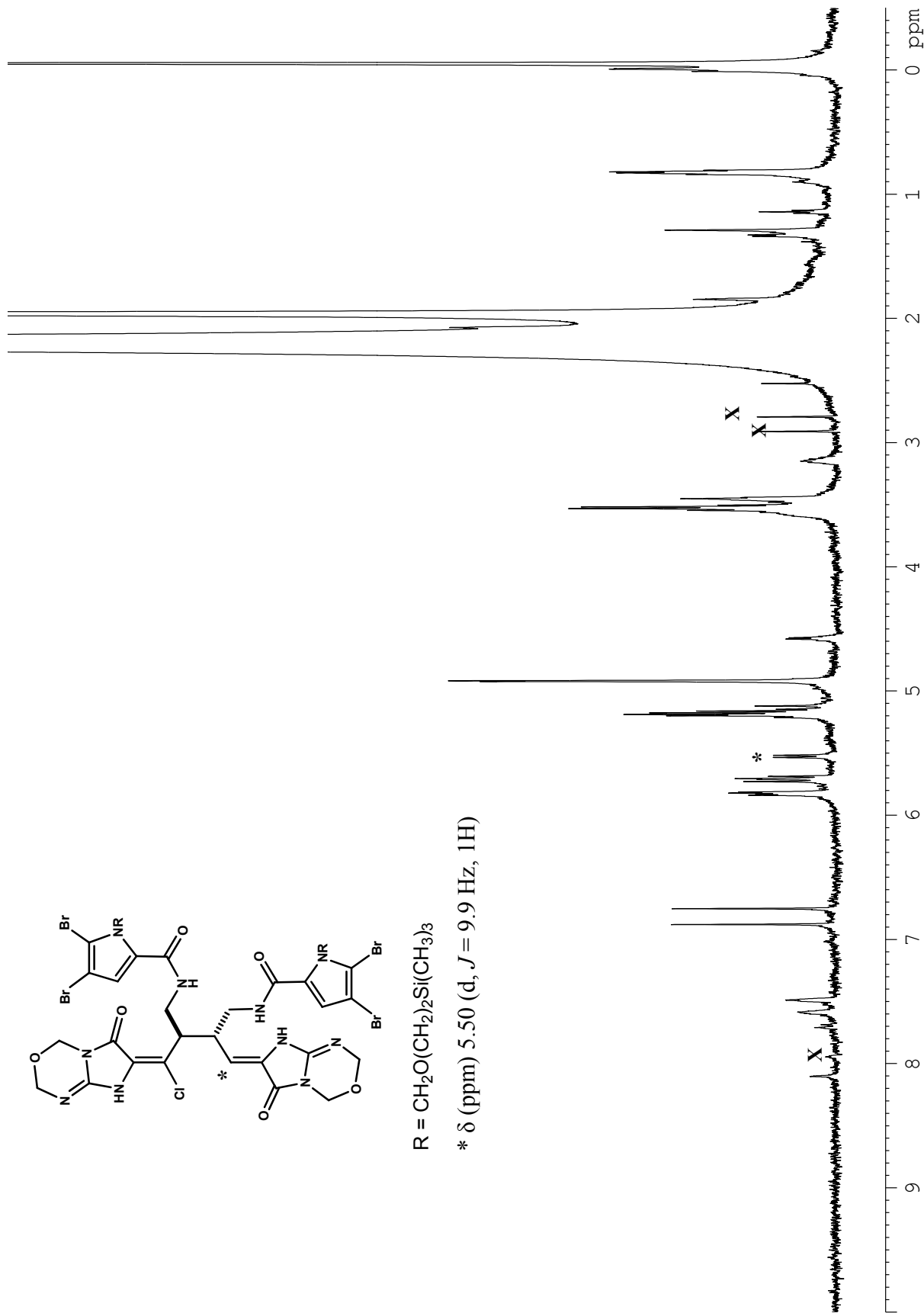


**Figure A1.71.**  $^1\text{H}$  NMR (600 MHz,  $\text{CH}_3\text{CN}-d_3$ ) spectrum of compound 2-61 ( $2 \cdot \text{HCO}_2\text{H}$ ) (tentative).

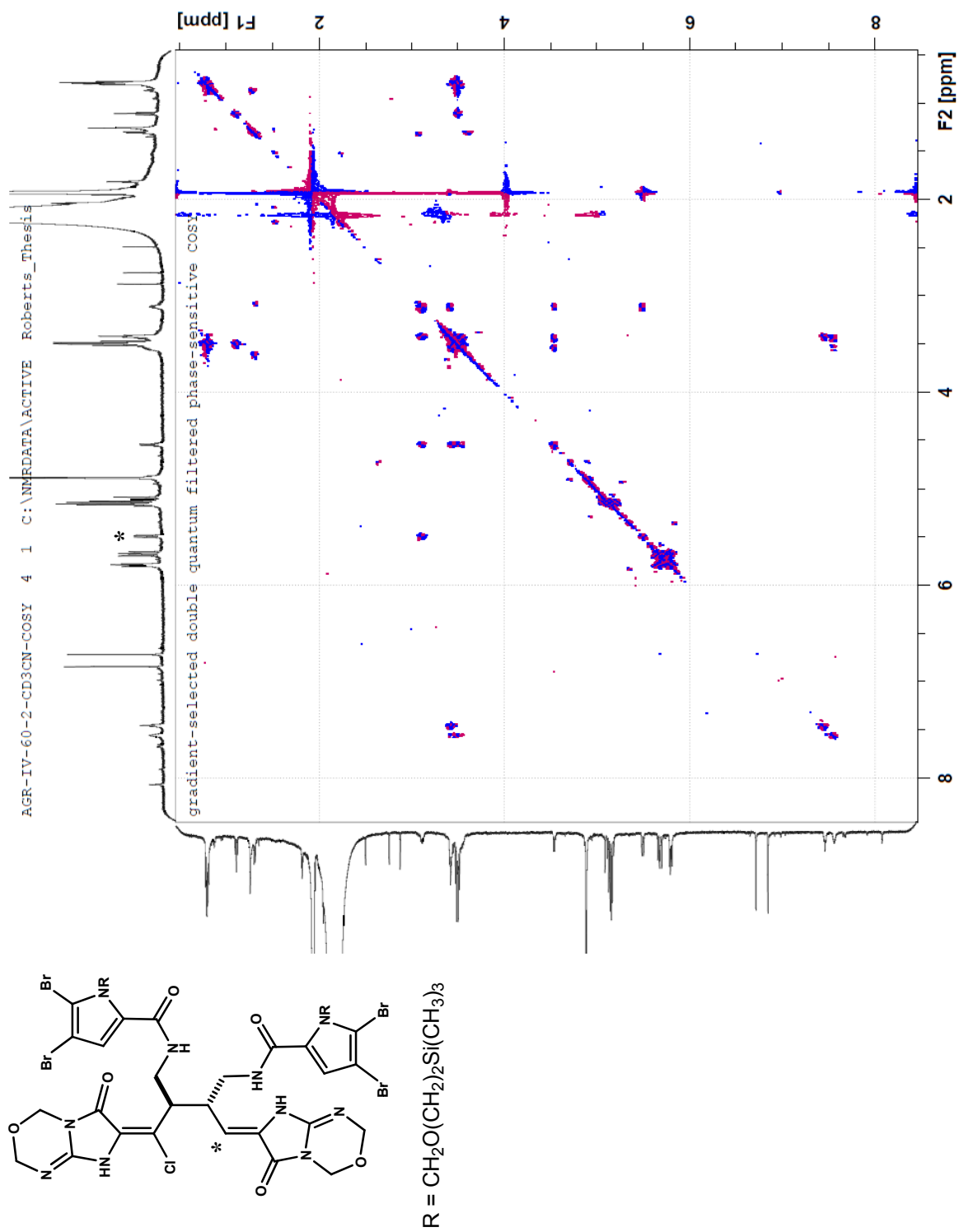


**Figure A1.72.** COSY (600 MHz, CH<sub>3</sub>CN-*d*<sub>3</sub>) spectrum of compound 2-61 (2·HCO<sub>2</sub>H) (tentative).

## APPENDIX ONE

### 2.6.2 X-ray crystallographic data for Compound 2-46b.

Table 1. Crystal data and structure refinement for har710.

Identification code	har710	
Empirical formula	C <sub>44</sub> H <sub>62</sub> Br <sub>4</sub> N <sub>13</sub> O <sub>8</sub> Si <sub>2</sub>	
Formula weight	1276.89	
Temperature	100(2) K	
Wavelength	0.71073 Å	
Crystal system	Triclinic	
Space group	P-1	
Unit cell dimensions	a = 7.541(3) Å	α = 112.402(4)°.
	b = 17.267(6) Å	β = 92.443(4)°.
	c = 23.527(9) Å	γ = 91.072(4)°.
Volume	2827.8(18) Å <sup>3</sup>	
Z	2	
Density (calculated)	1.500 Mg/m <sup>3</sup>	
Absorption coefficient	2.948 mm <sup>-1</sup>	
F(000)	1298	
Crystal size	0.30 x 0.08 x 0.04 mm <sup>3</sup>	
Theta range for data collection	3.79 to 28.47°.	
Index ranges	-10 ≤ h ≤ 10, -23 ≤ k ≤ 21, 0 ≤ l ≤ 31	
Reflections collected	13842	
Independent reflections	13842 [R(int) = 0.0000]	
Completeness to theta = 25.00°	98.9 %	
Absorption correction	Semi-empirical from equivalents	
Max. and min. transmission	0.8912 and 0.4177	
Refinement method	Full-matrix least-squares on F <sup>2</sup>	
Data / restraints / parameters	13842 / 56 / 610	
Goodness-of-fit on F <sup>2</sup>	1.036	
Final R indices [I > 2σ(I)]	R1 = 0.1193, wR2 = 0.3040	
R indices (all data)	R1 = 0.2228, wR2 = 0.3432	
Largest diff. peak and hole	1.990 and -1.339 e.Å <sup>-3</sup>	

Table 2. Atomic coordinates ( $\times 10^4$ ) and equivalent isotropic displacement parameters ( $\text{\AA}^2 \times 10^3$ ) for har710.  $U(\text{eq})$  is defined as one third of the trace of the orthogonalized  $U^{ij}$  tensor.

	x	y	z	$U(\text{eq})$
Br(1)	8213(1)	10951(1)	826(1)	40(1)
Br(2)	9284(2)	4625(1)	3670(1)	48(1)
Br(3)	3461(2)	11053(1)	664(1)	40(1)
Br(4)	14014(2)	4537(1)	3496(1)	47(1)
Si(1)	16970(8)	3859(3)	1665(2)	83(2)
Si(2)	746(11)	11479(5)	3029(4)	90(3)
Si(2A)	2440(20)	11541(9)	2871(7)	82(6)
O(1)	13416(9)	7910(4)	3870(3)	35(2)
O(2)	13257(9)	8819(4)	2957(3)	33(2)
O(3)	14332(10)	11079(4)	4455(3)	40(2)
O(4)	5968(9)	6236(4)	521(3)	36(2)
O(5)	1489(16)	5016(8)	837(5)	40(4)
O(5A)	800(30)	5299(14)	574(10)	41(9)
O(6)	3556(9)	7793(4)	695(3)	36(2)
O(7)	14986(10)	6193(5)	2702(4)	39(2)
O(8)	1441(10)	9457(5)	1414(4)	52(2)
N(1)	13181(11)	6129(5)	3487(4)	31(2)
N(2)	10663(10)	7897(5)	3452(4)	27(2)
N(3)	10789(10)	9280(5)	4265(4)	31(2)
N(4)	12324(11)	10492(6)	4982(4)	35(2)
N(5)	13199(11)	9750(5)	3962(4)	31(2)
N(6)	5704(10)	8037(5)	1442(4)	30(2)
N(7)	3433(10)	7302(5)	1775(4)	32(2)
N(8)	925(11)	6378(5)	1591(4)	33(2)
N(9)	3313(10)	6134(5)	943(4)	26(2)
N(10)	3922(11)	9545(5)	859(4)	33(2)
C(1)	12576(12)	5390(7)	3513(5)	31(2)
C(2)	10786(12)	5431(7)	3568(5)	32(2)
C(3)	10267(14)	6205(7)	3568(5)	34(3)
C(4)	11774(13)	6629(6)	3514(5)	32(2)
C(5)	12018(12)	7516(6)	3610(4)	27(2)

C(6)	9204(12)	7520(6)	2993(4)	29(2)
C(7)	8966(13)	8144(6)	2699(5)	31(2)
C(8)	9299(12)	8960(6)	3232(4)	27(2)
C(9)	10801(12)	8807(6)	3621(5)	27(2)
C(10)	12616(13)	9086(6)	3451(5)	28(2)
C(11)	14759(15)	10283(6)	4050(5)	36(3)
C(12)	13798(13)	11074(7)	5032(5)	34(3)
C(13)	12105(12)	9899(7)	4453(5)	32(2)
C(14)	7142(12)	8044(6)	2350(5)	27(2)
C(15)	6967(12)	8544(6)	1936(4)	25(2)
C(16)	5158(12)	7264(6)	1514(4)	26(2)
C(17)	6697(12)	7155(6)	1903(4)	26(2)
C(18)	4902(13)	6496(6)	908(5)	27(2)
C(19)	2513(15)	5349(6)	511(5)	39(3)
C(20)	165(14)	5598(7)	1160(6)	44(3)
C(21)	2415(12)	6595(6)	1451(4)	25(2)
C(22)	4760(12)	8287(6)	1029(5)	28(2)
C(23)	5231(13)	9090(7)	1006(5)	33(2)
C(24)	6850(14)	9490(7)	1035(5)	33(2)
C(25)	6516(14)	10200(6)	914(5)	35(3)
C(26)	4704(14)	10248(7)	824(5)	37(3)
C(27)	14971(15)	6285(8)	3316(5)	41(3)
C(28)	14979(16)	5344(9)	2254(6)	53(3)
C(29)	16738(18)	4958(8)	2228(6)	51(3)
C(30)	16390(30)	3795(12)	885(8)	101(6)
C(31)	19390(30)	3647(14)	1753(9)	110(7)
C(32)	15450(30)	3109(16)	1890(11)	139(9)
C(33)	2024(14)	9375(7)	848(5)	33(2)
C(34)	1570(20)	10283(9)	1835(6)	59(4)
C(35)	1110(20)	10381(9)	2435(7)	93(5)
C(36)	-160(30)	11447(14)	3788(8)	90(8)
C(37)	3120(30)	12092(17)	3249(13)	210(20)
C(38)	-810(40)	12090(30)	2683(17)	200(20)
C(39)	4930(30)	11360(20)	2916(17)	82(6)
C(40)	1870(60)	12320(30)	2480(20)	82(6)
C(41)	1240(50)	11510(30)	3590(16)	82(6)

N(1S)	9038(17)	7842(9)	-400(7)	81(4)
C(1S)	9277(18)	7494(9)	-69(7)	59(4)
C(2S)	9580(20)	7083(13)	324(8)	92(6)
N(2S)	7300(20)	6877(8)	4634(6)	77(4)
C(3S)	7416(19)	6431(10)	4867(7)	60(4)
C(4S)	7590(40)	5842(17)	5176(11)	173(14)
N(3S)	6870(20)	3556(14)	4223(13)	164(11)
C(5S)	7030(30)	3214(13)	4543(12)	115(8)
C(6S)	7300(20)	2728(11)	4925(7)	81(5)

---

Table 3. Bond lengths [Å] and angles [°] for har710.

---

Br(1)-C(25)	1.880(10)
Br(2)-C(2)	1.870(10)
Br(3)-C(26)	1.836(11)
Br(4)-C(1)	1.834(11)
Si(1)-C(30)	1.829(18)
Si(1)-C(29)	1.871(13)
Si(1)-C(31)	1.89(2)
Si(1)-C(32)	1.95(3)
Si(2)-C(35)	1.911(15)
Si(2)-C(36)	1.958(17)
Si(2)-C(38)	1.949(18)
Si(2)-C(37)	2.009(17)
Si(2A)-C(39)	1.917(18)
Si(2A)-C(40)	1.947(18)
Si(2A)-C(41)	1.967(18)
Si(2A)-C(35)	2.085(16)
O(1)-C(5)	1.245(10)
O(2)-C(10)	1.201(12)
O(3)-C(11)	1.395(12)
O(3)-C(12)	1.434(13)
O(4)-C(18)	1.202(12)
O(5)-C(19)	1.373(15)
O(5)-C(20)	1.451(16)
O(5)-H(19D)	1.3599
O(5)-H(20C)	1.4234
O(5A)-C(19)	1.31(2)
O(5A)-C(20)	1.39(2)
O(6)-C(22)	1.253(10)
O(7)-C(27)	1.394(13)
O(7)-C(28)	1.443(15)
O(8)-C(33)	1.377(13)
O(8)-C(34)	1.391(15)
N(1)-C(4)	1.369(13)
N(1)-C(1)	1.371(13)

N(1)-C(27)	1.474(13)
N(2)-C(5)	1.341(12)
N(2)-C(6)	1.461(11)
N(2)-C(9)	1.466(12)
N(3)-C(13)	1.373(11)
N(3)-C(9)	1.422(12)
N(3)-H(3)	0.8800
N(4)-C(13)	1.277(13)
N(4)-C(12)	1.456(12)
N(5)-C(10)	1.357(12)
N(5)-C(13)	1.394(13)
N(5)-C(11)	1.437(12)
N(6)-C(22)	1.382(12)
N(6)-C(15)	1.457(11)
N(6)-C(16)	1.462(12)
N(7)-C(21)	1.366(11)
N(7)-C(16)	1.454(12)
N(7)-H(7)	0.8800
N(8)-C(21)	1.274(11)
N(8)-C(20)	1.432(12)
N(8)-H(8)	0.8800
N(9)-C(18)	1.361(12)
N(9)-C(21)	1.372(12)
N(9)-C(19)	1.450(11)
N(10)-C(26)	1.372(13)
N(10)-C(23)	1.385(13)
N(10)-C(33)	1.453(13)
C(1)-C(2)	1.362(13)
C(2)-C(3)	1.400(15)
C(3)-C(4)	1.376(13)
C(3)-H(3)	0.9500
C(4)-C(5)	1.467(14)
C(6)-C(7)	1.496(14)
C(6)-H(6A)	0.9900
C(6)-H(6B)	0.9900
C(7)-C(8)	1.494(13)



C(7)-C(14)	1.544(13)
C(7)-H(7A)	1.0000
C(8)-C(9)	1.515(14)
C(8)-H(8A)	0.9900
C(8)-H(8B)	0.9900
C(9)-C(10)	1.560(13)
C(11)-H(11A)	0.9900
C(11)-H(11B)	0.9900
C(12)-H(12A)	0.9900
C(12)-H(12B)	0.9900
C(14)-C(17)	1.514(12)
C(14)-C(15)	1.531(13)
C(14)-H(14)	1.0000
C(15)-H(15A)	0.9900
C(15)-H(15B)	0.9900
C(16)-C(17)	1.507(12)
C(16)-C(18)	1.533(14)
C(17)-H(17A)	0.9900
C(17)-H(17B)	0.9900
C(19)-H(19A)	0.9900
C(19)-H(19B)	0.9900
C(19)-H(19C)	0.9900
C(19)-H(19D)	0.9900
C(19)-H(35C)	1.2121
C(19)-H(35D)	1.0563
C(20)-H(20A)	0.9900
C(20)-H(20B)	0.9900
C(20)-H(20C)	0.9900
C(20)-H(20D)	0.9900
C(22)-C(23)	1.445(13)
C(23)-C(24)	1.378(13)
C(24)-C(25)	1.383(14)
C(24)-H(24)	0.9500
C(25)-C(26)	1.382(14)
C(27)-H(27A)	0.9900
C(27)-H(27B)	0.9900

C(28)-C(29)	1.489(18)
C(28)-H(28A)	0.9900
C(28)-H(28B)	0.9900
C(29)-H(29A)	0.9900
C(29)-H(29B)	0.9900
C(30)-H(30A)	0.9800
C(30)-H(30B)	0.9800
C(30)-H(30C)	0.9800
C(31)-H(31A)	0.9800
C(31)-H(31B)	0.9800
C(31)-H(31C)	0.9800
C(32)-H(32A)	0.9800
C(32)-H(32B)	0.9800
C(32)-H(32C)	0.9800
C(33)-H(33A)	0.9900
C(33)-H(33B)	0.9900
C(34)-C(35)	1.417(19)
C(34)-H(34A)	0.9900
C(34)-H(34B)	0.9900
C(35)-H(35A)	0.9900
C(35)-H(35B)	0.9900
C(36)-H(36A)	0.9800
C(36)-H(36B)	0.9800
C(36)-H(36C)	0.9800
C(37)-H(37A)	0.9800
C(37)-H(37B)	0.9800
C(37)-H(37C)	0.9800
C(38)-H(38A)	0.9800
C(38)-H(38B)	0.9800
C(38)-H(38C)	0.9800
C(39)-H(39A)	0.9800
C(39)-H(39B)	0.9800
C(39)-H(39C)	0.9800
C(40)-H(40A)	0.9800
C(40)-H(40B)	0.9800
C(40)-H(40C)	0.9800

C(41)-H(41A)	0.9800
C(41)-H(41B)	0.9800
C(41)-H(41C)	0.9800
N(1S)-C(1S)	1.161(18)
C(1S)-C(2S)	1.38(2)
C(2S)-H(2S1)	0.9800
C(2S)-H(2S2)	0.9800
C(2S)-H(2S3)	0.9800
N(2S)-C(3S)	1.104(17)
C(3S)-C(4S)	1.46(2)
C(4S)-H(4S1)	0.9801
C(4S)-H(4S2)	0.9801
C(4S)-H(4S3)	0.9801
N(3S)-C(5S)	1.12(3)
C(5S)-C(6S)	1.46(3)
C(6S)-H(6S1)	0.9800
C(6S)-H(6S2)	0.9800
C(6S)-H(6S3)	0.9800
C(30)-Si(1)-C(29)	109.7(8)
C(30)-Si(1)-C(31)	111.1(9)
C(29)-Si(1)-C(31)	104.3(8)
C(30)-Si(1)-C(32)	111.4(10)
C(29)-Si(1)-C(32)	108.9(9)
C(31)-Si(1)-C(32)	111.2(10)
C(35)-Si(2)-C(36)	112.0(7)
C(35)-Si(2)-C(38)	110.9(15)
C(36)-Si(2)-C(38)	111.0(9)
C(35)-Si(2)-C(37)	107.4(8)
C(36)-Si(2)-C(37)	107.4(8)
C(38)-Si(2)-C(37)	107.9(9)
C(39)-Si(2A)-C(40)	113.3(11)
C(39)-Si(2A)-C(41)	112.3(11)
C(40)-Si(2A)-C(41)	123(2)
C(39)-Si(2A)-C(35)	108.4(9)
C(40)-Si(2A)-C(35)	112.3(17)

C(41)-Si(2A)-C(35)	82.4(17)
C(11)-O(3)-C(12)	111.9(8)
C(19)-O(5)-C(20)	110.9(11)
C(19)-O(5)-H(19D)	42.5
C(20)-O(5)-H(19D)	149.4
C(19)-O(5)-H(20C)	147.3
C(20)-O(5)-H(20C)	40.3
H(19D)-O(5)-H(20C)	153.1
C(19)-O(5A)-C(20)	119.3(18)
C(27)-O(7)-C(28)	116.1(9)
C(33)-O(8)-C(34)	112.3(10)
C(4)-N(1)-C(1)	109.2(8)
C(4)-N(1)-C(27)	124.3(9)
C(1)-N(1)-C(27)	125.2(9)
C(5)-N(2)-C(6)	128.2(8)
C(5)-N(2)-C(9)	119.0(8)
C(6)-N(2)-C(9)	110.9(8)
C(13)-N(3)-C(9)	111.0(8)
C(13)-N(3)-H(3)	124.5
C(9)-N(3)-H(3)	124.5
C(13)-N(4)-C(12)	113.8(9)
C(10)-N(5)-C(13)	112.9(8)
C(10)-N(5)-C(11)	128.4(9)
C(13)-N(5)-C(11)	118.7(8)
C(22)-N(6)-C(15)	127.2(8)
C(22)-N(6)-C(16)	119.6(7)
C(15)-N(6)-C(16)	111.6(7)
C(21)-N(7)-C(16)	110.7(8)
C(21)-N(7)-H(7)	124.6
C(16)-N(7)-H(7)	124.6
C(21)-N(8)-C(20)	114.8(9)
C(21)-N(8)-H(8)	122.6
C(20)-N(8)-H(8)	122.6
C(18)-N(9)-C(21)	113.5(8)
C(18)-N(9)-C(19)	127.4(9)
C(21)-N(9)-C(19)	119.0(8)

C(26)-N(10)-C(23)	108.5(8)
C(26)-N(10)-C(33)	125.7(9)
C(23)-N(10)-C(33)	125.0(9)
C(2)-C(1)-N(1)	107.7(10)
C(2)-C(1)-Br(4)	128.2(8)
N(1)-C(1)-Br(4)	124.0(7)
C(1)-C(2)-C(3)	108.1(9)
C(1)-C(2)-Br(2)	126.4(9)
C(3)-C(2)-Br(2)	125.4(8)
C(4)-C(3)-C(2)	107.3(9)
C(4)-C(3)-H(3)	126.3
C(2)-C(3)-H(3)	126.3
N(1)-C(4)-C(3)	107.6(9)
N(1)-C(4)-C(5)	122.1(8)
C(3)-C(4)-C(5)	128.9(10)
O(1)-C(5)-N(2)	121.4(9)
O(1)-C(5)-C(4)	120.0(9)
N(2)-C(5)-C(4)	118.4(8)
N(2)-C(6)-C(7)	103.0(8)
N(2)-C(6)-H(6A)	111.2
C(7)-C(6)-H(6A)	111.2
N(2)-C(6)-H(6B)	111.2
C(7)-C(6)-H(6B)	111.2
H(6A)-C(6)-H(6B)	109.1
C(6)-C(7)-C(8)	102.3(8)
C(6)-C(7)-C(14)	112.9(8)
C(8)-C(7)-C(14)	115.1(8)
C(6)-C(7)-H(7A)	108.7
C(8)-C(7)-H(7A)	108.7
C(14)-C(7)-H(7A)	108.7
C(7)-C(8)-C(9)	105.2(8)
C(7)-C(8)-H(8A)	110.7
C(9)-C(8)-H(8A)	110.7
C(7)-C(8)-H(8B)	110.7
C(9)-C(8)-H(8B)	110.7
H(8A)-C(8)-H(8B)	108.8

N(3)-C(9)-N(2)	113.9(8)
N(3)-C(9)-C(8)	115.8(8)
N(2)-C(9)-C(8)	103.0(7)
N(3)-C(9)-C(10)	102.7(7)
N(2)-C(9)-C(10)	111.7(8)
C(8)-C(9)-C(10)	110.1(8)
O(2)-C(10)-N(5)	128.0(9)
O(2)-C(10)-C(9)	127.1(8)
N(5)-C(10)-C(9)	104.5(8)
O(3)-C(11)-N(5)	106.5(9)
O(3)-C(11)-H(11A)	110.4
N(5)-C(11)-H(11A)	110.4
O(3)-C(11)-H(11B)	110.4
N(5)-C(11)-H(11B)	110.4
H(11A)-C(11)-H(11B)	108.6
O(3)-C(12)-N(4)	114.7(8)
O(3)-C(12)-H(12A)	108.6
N(4)-C(12)-H(12A)	108.6
O(3)-C(12)-H(12B)	108.6
N(4)-C(12)-H(12B)	108.6
H(12A)-C(12)-H(12B)	107.6
N(4)-C(13)-N(3)	126.8(10)
N(4)-C(13)-N(5)	125.9(9)
N(3)-C(13)-N(5)	107.3(9)
C(17)-C(14)-C(15)	102.4(8)
C(17)-C(14)-C(7)	113.4(8)
C(15)-C(14)-C(7)	115.0(8)
C(17)-C(14)-H(14)	108.6
C(15)-C(14)-H(14)	108.6
C(7)-C(14)-H(14)	108.6
N(6)-C(15)-C(14)	103.7(7)
N(6)-C(15)-H(15A)	111.0
C(14)-C(15)-H(15A)	111.0
N(6)-C(15)-H(15B)	111.0
C(14)-C(15)-H(15B)	111.0
H(15A)-C(15)-H(15B)	109.0

N(7)-C(16)-N(6)	113.5(8)
N(7)-C(16)-C(17)	115.0(8)
N(6)-C(16)-C(17)	101.5(7)
N(7)-C(16)-C(18)	102.2(7)
N(6)-C(16)-C(18)	114.5(8)
C(17)-C(16)-C(18)	110.6(8)
C(16)-C(17)-C(14)	102.8(8)
C(16)-C(17)-H(17A)	111.2
C(14)-C(17)-H(17A)	111.2
C(16)-C(17)-H(17B)	111.2
C(14)-C(17)-H(17B)	111.2
H(17A)-C(17)-H(17B)	109.1
O(4)-C(18)-N(9)	128.2(9)
O(4)-C(18)-C(16)	126.4(9)
N(9)-C(18)-C(16)	105.0(8)
O(5A)-C(19)-O(5)	46.0(11)
O(5A)-C(19)-N(9)	111.7(13)
O(5)-C(19)-N(9)	107.6(9)
O(5A)-C(19)-H(19A)	66.0
O(5)-C(19)-H(19A)	110.2
N(9)-C(19)-H(19A)	110.2
O(5A)-C(19)-H(19B)	136.7
O(5)-C(19)-H(19B)	110.2
N(9)-C(19)-H(19B)	110.2
H(19A)-C(19)-H(19B)	108.5
O(5A)-C(19)-H(19C)	108.7
O(5)-C(19)-H(19C)	141.5
N(9)-C(19)-H(19C)	109.5
H(19A)-C(19)-H(19C)	46.1
H(19B)-C(19)-H(19C)	65.8
O(5A)-C(19)-H(19D)	109.3
O(5)-C(19)-H(19D)	68.1
N(9)-C(19)-H(19D)	109.3
H(19A)-C(19)-H(19D)	138.7
H(19B)-C(19)-H(19D)	44.9
H(19C)-C(19)-H(19D)	108.3

O(5A)-C(19)-H(35C)	119.7
O(5)-C(19)-H(35C)	150.0
N(9)-C(19)-H(35C)	102.4
H(19A)-C(19)-H(35C)	55.9
H(19B)-C(19)-H(35C)	59.5
H(19C)-C(19)-H(35C)	11.0
H(19D)-C(19)-H(35C)	103.8
O(5A)-C(19)-H(35D)	125.3
O(5)-C(19)-H(35D)	84.8
N(9)-C(19)-H(35D)	104.1
H(19A)-C(19)-H(35D)	135.3
H(19B)-C(19)-H(35D)	30.3
H(19C)-C(19)-H(35D)	96.0
H(19D)-C(19)-H(35D)	16.8
H(35C)-C(19)-H(35D)	89.8
O(5A)-C(20)-N(8)	117.1(13)
O(5A)-C(20)-O(5)	43.3(10)
N(8)-C(20)-O(5)	113.0(9)
O(5A)-C(20)-H(20A)	67.1
N(8)-C(20)-H(20A)	109.0
O(5)-C(20)-H(20A)	109.0
O(5A)-C(20)-H(20B)	132.8
N(8)-C(20)-H(20B)	109.0
O(5)-C(20)-H(20B)	109.0
H(20A)-C(20)-H(20B)	107.8
O(5A)-C(20)-H(20C)	107.7
N(8)-C(20)-H(20C)	107.5
O(5)-C(20)-H(20C)	68.3
H(20A)-C(20)-H(20C)	140.8
H(20B)-C(20)-H(20C)	45.5
O(5A)-C(20)-H(20D)	107.8
N(8)-C(20)-H(20D)	109.3
O(5)-C(20)-H(20D)	136.8
H(20A)-C(20)-H(20D)	46.5
H(20B)-C(20)-H(20D)	63.8
H(20C)-C(20)-H(20D)	107.2



N(8)-C(21)-N(7)	127.4(9)
N(8)-C(21)-N(9)	125.2(8)
N(7)-C(21)-N(9)	107.5(8)
O(6)-C(22)-N(6)	117.0(9)
O(6)-C(22)-C(23)	124.6(9)
N(6)-C(22)-C(23)	118.3(8)
C(24)-C(23)-N(10)	108.3(9)
C(24)-C(23)-C(22)	132.0(10)
N(10)-C(23)-C(22)	119.3(8)
C(23)-C(24)-C(25)	106.9(9)
C(23)-C(24)-H(24)	126.6
C(25)-C(24)-H(24)	126.6
C(26)-C(25)-C(24)	109.2(9)
C(26)-C(25)-Br(1)	124.0(8)
C(24)-C(25)-Br(1)	126.7(8)
N(10)-C(26)-C(25)	107.1(9)
N(10)-C(26)-Br(3)	123.6(8)
C(25)-C(26)-Br(3)	129.3(8)
O(7)-C(27)-N(1)	111.8(9)
O(7)-C(27)-H(27A)	109.3
N(1)-C(27)-H(27A)	109.3
O(7)-C(27)-H(27B)	109.3
N(1)-C(27)-H(27B)	109.2
H(27A)-C(27)-H(27B)	107.9
O(7)-C(28)-C(29)	112.7(10)
O(7)-C(28)-H(28A)	109.0
C(29)-C(28)-H(28A)	109.1
O(7)-C(28)-H(28B)	109.1
C(29)-C(28)-H(28B)	109.1
H(28A)-C(28)-H(28B)	107.8
C(28)-C(29)-Si(1)	118.3(10)
C(28)-C(29)-H(29A)	107.7
Si(1)-C(29)-H(29A)	107.7
C(28)-C(29)-H(29B)	107.7
Si(1)-C(29)-H(29B)	107.7
H(29A)-C(29)-H(29B)	107.1

Si(1)-C(30)-H(30A)	109.5
Si(1)-C(30)-H(30B)	109.4
H(30A)-C(30)-H(30B)	109.5
Si(1)-C(30)-H(30C)	109.5
H(30A)-C(30)-H(30C)	109.5
H(30B)-C(30)-H(30C)	109.5
Si(1)-C(31)-H(31A)	109.5
Si(1)-C(31)-H(31B)	109.5
H(31A)-C(31)-H(31B)	109.5
Si(1)-C(31)-H(31C)	109.5
H(31A)-C(31)-H(31C)	109.5
H(31B)-C(31)-H(31C)	109.5
Si(1)-C(32)-H(32A)	109.5
Si(1)-C(32)-H(32B)	109.5
H(32A)-C(32)-H(32B)	109.5
Si(1)-C(32)-H(32C)	109.5
H(32A)-C(32)-H(32C)	109.5
H(32B)-C(32)-H(32C)	109.5
O(8)-C(33)-N(10)	113.1(8)
O(8)-C(33)-H(33A)	109.0
N(10)-C(33)-H(33A)	108.9
O(8)-C(33)-H(33B)	109.0
N(10)-C(33)-H(33B)	109.0
H(33A)-C(33)-H(33B)	107.8
O(8)-C(34)-C(35)	113.7(12)
O(8)-C(34)-H(34A)	108.8
C(35)-C(34)-H(34A)	109.0
O(8)-C(34)-H(34B)	108.9
C(35)-C(34)-H(34B)	108.6
H(34A)-C(34)-H(34B)	107.7
C(34)-C(35)-Si(2)	119.4(12)
C(34)-C(35)-Si(2A)	94.9(11)
Si(2)-C(35)-Si(2A)	39.5(5)
C(34)-C(35)-H(35A)	107.7
Si(2)-C(35)-H(35A)	107.5
Si(2A)-C(35)-H(35A)	88.5

C(34)-C(35)-H(35B)	107.3
Si(2)-C(35)-H(35B)	107.3
Si(2A)-C(35)-H(35B)	146.9
H(35A)-C(35)-H(35B)	107.0
Si(2)-C(36)-H(36A)	109.4
Si(2)-C(36)-H(36B)	109.7
H(36A)-C(36)-H(36B)	109.5
Si(2)-C(36)-H(36C)	109.3
H(36A)-C(36)-H(36C)	109.5
H(36B)-C(36)-H(36C)	109.5
Si(2)-C(37)-H(37A)	109.2
Si(2)-C(37)-H(37B)	109.5
H(37A)-C(37)-H(37B)	109.5
Si(2)-C(37)-H(37C)	109.7
H(37A)-C(37)-H(37C)	109.5
H(37B)-C(37)-H(37C)	109.5
Si(2)-C(38)-H(38A)	109.5
Si(2)-C(38)-H(38B)	109.5
H(38A)-C(38)-H(38B)	109.5
Si(2)-C(38)-H(38C)	109.4
H(38A)-C(38)-H(38C)	109.5
H(38B)-C(38)-H(38C)	109.5
Si(2A)-C(39)-H(39A)	109.7
Si(2A)-C(39)-H(39B)	109.4
H(39A)-C(39)-H(39B)	109.5
Si(2A)-C(39)-H(39C)	109.4
H(39A)-C(39)-H(39C)	109.5
H(39B)-C(39)-H(39C)	109.5
Si(2A)-C(40)-H(40A)	109.8
Si(2A)-C(40)-H(40B)	109.5
H(40A)-C(40)-H(40B)	109.5
Si(2A)-C(40)-H(40C)	109.2
H(40A)-C(40)-H(40C)	109.5
H(40B)-C(40)-H(40C)	109.5
Si(2A)-C(41)-H(41A)	109.4
Si(2A)-C(41)-H(41B)	109.3

H(41A)-C(41)-H(41B)	109.5
Si(2A)-C(41)-H(41C)	109.7
H(41A)-C(41)-H(41C)	109.5
H(41B)-C(41)-H(41C)	109.5
N(1S)-C(1S)-C(2S)	179.5(15)
C(1S)-C(2S)-H(2S1)	109.5
C(1S)-C(2S)-H(2S2)	109.4
H(2S1)-C(2S)-H(2S2)	109.5
C(1S)-C(2S)-H(2S3)	109.5
H(2S1)-C(2S)-H(2S3)	109.5
H(2S2)-C(2S)-H(2S3)	109.5
N(2S)-C(3S)-C(4S)	179(2)
C(3S)-C(4S)-H(4S1)	109.4
C(3S)-C(4S)-H(4S2)	109.5
H(4S1)-C(4S)-H(4S2)	109.5
C(3S)-C(4S)-H(4S3)	109.5
H(4S1)-C(4S)-H(4S3)	109.5
H(4S2)-C(4S)-H(4S3)	109.5
N(3S)-C(5S)-C(6S)	176(3)
C(5S)-C(6S)-H(6S1)	109.4
C(5S)-C(6S)-H(6S2)	109.6
H(6S1)-C(6S)-H(6S2)	109.5
C(5S)-C(6S)-H(6S3)	109.5
H(6S1)-C(6S)-H(6S3)	109.5
H(6S2)-C(6S)-H(6S3)	109.5

---

Symmetry transformations used to generate equivalent atoms:

Table 4. Anisotropic displacement parameters ( $\text{\AA}^2 \times 10^3$ ) for har710. The anisotropic displacement factor exponent takes the form:  $-2\pi^2 [h^2 a^{*2} U^{11} + \dots + 2 h k a^* b^* U^{12}]$

	U <sup>11</sup>	U <sup>22</sup>	U <sup>33</sup>	U <sup>23</sup>	U <sup>13</sup>	U <sup>12</sup>
Br(1)	26(1)	36(1)	66(1)	28(1)	-4(1)	-7(1)
Br(2)	23(1)	48(1)	87(1)	44(1)	0(1)	-9(1)
Br(3)	30(1)	33(1)	59(1)	21(1)	-8(1)	2(1)
Br(4)	28(1)	43(1)	85(1)	40(1)	10(1)	4(1)
Si(1)	122(5)	47(2)	69(3)	8(2)	36(3)	-10(3)
O(1)	20(4)	26(4)	52(5)	8(3)	-11(3)	-9(3)
O(2)	18(4)	32(4)	43(5)	9(3)	1(3)	-3(3)
O(3)	36(4)	25(4)	54(5)	11(4)	0(3)	-5(3)
O(4)	24(4)	32(4)	44(5)	6(3)	8(3)	-13(3)
O(6)	20(4)	35(4)	47(5)	11(3)	-8(3)	-4(3)
O(7)	31(4)	36(4)	59(5)	29(4)	10(3)	1(3)
O(8)	30(5)	57(6)	58(5)	9(4)	-2(4)	-19(4)
N(1)	21(4)	27(5)	45(5)	13(4)	3(4)	-7(4)
N(2)	14(4)	29(5)	35(5)	7(4)	-2(3)	0(3)
N(3)	15(4)	34(5)	41(5)	10(4)	0(3)	-12(4)
N(4)	24(5)	37(5)	41(6)	14(4)	-10(4)	-14(4)
N(5)	17(4)	30(5)	44(5)	12(4)	-3(3)	-11(4)
N(6)	19(4)	28(5)	42(5)	15(4)	-7(3)	-10(4)
N(7)	15(4)	27(5)	42(5)	1(4)	3(3)	-10(3)
N(8)	22(4)	34(5)	34(5)	4(4)	7(3)	-9(4)
N(9)	16(4)	23(4)	33(5)	3(4)	0(3)	-7(3)
N(10)	18(4)	27(5)	51(6)	14(4)	-5(4)	1(4)
C(1)	10(5)	43(6)	41(6)	16(5)	5(4)	-6(4)
C(2)	14(5)	45(7)	44(7)	26(5)	2(4)	-4(4)
C(3)	26(6)	42(7)	32(6)	13(5)	-9(4)	-4(5)
C(4)	26(6)	31(6)	38(6)	13(5)	-4(4)	-10(5)
C(5)	14(5)	28(5)	40(6)	15(5)	-2(4)	0(4)
C(6)	16(5)	36(6)	29(6)	4(5)	2(4)	-4(4)
C(7)	17(5)	25(5)	47(7)	9(5)	-2(4)	-8(4)
C(8)	14(5)	24(5)	39(6)	7(4)	2(4)	-1(4)
C(9)	17(5)	18(5)	41(6)	7(4)	2(4)	-6(4)

C(10)	19(5)	20(5)	42(7)	10(5)	-5(4)	-3(4)
C(11)	34(6)	21(5)	45(7)	5(5)	1(5)	-8(5)
C(12)	16(5)	42(6)	37(6)	8(5)	-10(4)	-18(5)
C(13)	10(5)	39(6)	48(7)	18(5)	-10(4)	-11(4)
C(14)	16(5)	28(5)	36(6)	10(4)	-1(4)	-4(4)
C(15)	11(4)	28(5)	37(6)	16(4)	-7(4)	-7(4)
C(16)	13(5)	29(5)	37(6)	15(4)	-4(4)	-8(4)
C(17)	12(4)	24(5)	41(6)	12(4)	-5(4)	-11(4)
C(18)	21(5)	26(5)	37(6)	14(5)	4(4)	3(4)
C(19)	31(6)	27(6)	46(7)	0(5)	6(5)	-13(5)
C(20)	26(6)	29(6)	60(8)	-3(5)	4(5)	-10(5)
C(21)	12(4)	25(5)	36(6)	8(4)	-1(4)	-7(4)
C(22)	11(4)	22(5)	46(6)	9(5)	-6(4)	-3(4)
C(23)	16(5)	32(6)	52(7)	19(5)	-1(4)	-4(4)
C(24)	24(5)	32(6)	40(6)	13(5)	-1(4)	-5(4)
C(25)	26(6)	21(5)	60(7)	20(5)	-5(5)	-7(4)
C(26)	28(6)	31(6)	53(7)	20(5)	-13(5)	-9(5)
C(27)	30(6)	43(7)	52(8)	19(6)	4(5)	0(5)
C(28)	34(7)	78(10)	55(8)	34(7)	3(5)	-12(7)
C(29)	56(8)	47(8)	56(8)	23(6)	16(6)	0(6)
N(1S)	65(9)	81(10)	105(11)	47(9)	-21(7)	17(7)
C(1S)	37(8)	53(9)	90(11)	34(8)	-7(7)	-10(6)
C(2S)	41(9)	138(17)	134(15)	97(14)	-2(9)	-30(10)
N(2S)	103(11)	58(8)	78(9)	31(7)	26(8)	23(8)
C(3S)	47(8)	60(10)	82(11)	39(8)	-4(7)	1(7)
C(4S)	230(30)	210(30)	170(20)	170(20)	130(20)	170(20)
N(3S)	53(10)	167(19)	380(30)	220(20)	42(14)	22(11)
C(5S)	96(16)	87(14)	190(20)	81(15)	59(15)	-13(12)
C(6S)	54(10)	93(13)	90(12)	30(10)	-14(8)	-31(9)

---

Table 5. Hydrogen coordinates ( $\times 10^4$ ) and isotropic displacement parameters ( $\text{\AA}^2 \times 10^3$ ) for newtwin4.

	x	y	z	U(eq)
H(3)	10039	9188	4510	38
H(7)	3092	7723	2098	38
H(8)	404	6683	1928	39
H(3)	9093	6402	3599	41
H(6A)	8113	7448	3190	35
H(6B)	9521	6969	2688	35
H(7A)	9920	8075	2403	38
H(8A)	8224	9126	3471	33
H(8B)	9645	9408	3089	33
H(11A)	15766	10072	4227	43
H(11B)	15095	10300	3653	43
H(12A)	13460	11647	5293	41
H(12B)	14830	10932	5243	41
H(14)	6204	8219	2657	33
H(15A)	6510	9106	2164	30
H(15B)	8124	8608	1773	30
H(17A)	7715	6912	1650	31
H(17B)	6350	6792	2122	31
H(19A)	1769	5447	190	47
H(19B)	3447	4958	309	47
H(19C)	2708	5299	86	47
H(19D)	3089	4877	577	47
H(20A)	-627	5710	856	53
H(20B)	-570	5336	1382	53
H(20C)	369	5169	1338	53
H(20D)	-1136	5645	1117	53
H(24)	7980	9313	1121	39
H(27A)	15397	6861	3583	49
H(27B)	15797	5889	3388	49
H(28A)	14631	5341	1843	64

H(28B)	14078	5000	2357	64
H(29A)	17066	4972	2644	62
H(29B)	17623	5320	2138	62
H(30A)	15116	3654	790	151
H(30B)	17072	3360	590	151
H(30C)	16661	4336	858	151
H(31A)	19530	3044	1640	165
H(31B)	19827	3950	2181	165
H(31C)	20079	3836	1482	165
H(32A)	14344	3384	2040	209
H(32B)	16064	2973	2214	209
H(32C)	15184	2593	1528	209
H(33A)	1381	9765	702	40
H(33B)	1731	8797	549	40
H(34A)	785	10625	1684	70
H(34B)	2805	10501	1856	70
H(35A)	2050	10132	2610	112
H(35B)	2	10040	2393	112
H(35C)	3048	5318	25	112
H(35D)	3429	4896	517	112
H(36A)	619	11118	3944	135
H(36B)	-1363	11189	3702	135
H(36C)	-195	12020	4097	135
H(37A)	3612	12122	2878	314
H(37B)	3933	11793	3424	314
H(37C)	2984	12661	3552	314
H(38A)	-436	12027	2274	304
H(38B)	-746	12690	2952	304
H(38C)	-2036	11875	2649	304
H(39A)	5467	11355	2543	122
H(39B)	5109	10818	2953	122
H(39C)	5502	11808	3277	122
H(40A)	576	12352	2436	122
H(40B)	2355	12126	2069	122
H(40C)	2387	12878	2729	122
H(41A)	-41	11544	3525	122



H(41B)	1674	11992	3958	122
H(41C)	1501	10991	3644	122
H(2S1)	8551	7138	577	138
H(2S2)	10640	7329	591	138
H(2S3)	9749	6488	83	138
H(4S1)	8669	5986	5447	259
H(4S2)	7652	5271	4868	259
H(4S3)	6553	5874	5422	259
H(6S1)	6147	2513	4992	122
H(6S2)	7873	3086	5323	122
H(6S3)	8053	2257	4719	122

---

Table 6. Torsion angles [°] for har710.

---

C(4)-N(1)-C(1)-C(2)	-1.0(12)
C(27)-N(1)-C(1)-C(2)	-168.4(9)
C(4)-N(1)-C(1)-Br(4)	-179.5(7)
C(27)-N(1)-C(1)-Br(4)	13.1(14)
N(1)-C(1)-C(2)-C(3)	0.7(12)
Br(4)-C(1)-C(2)-C(3)	179.1(8)
N(1)-C(1)-C(2)-Br(2)	-176.2(7)
Br(4)-C(1)-C(2)-Br(2)	2.2(15)
C(1)-C(2)-C(3)-C(4)	-0.2(12)
Br(2)-C(2)-C(3)-C(4)	176.8(8)
C(1)-N(1)-C(4)-C(3)	0.9(11)
C(27)-N(1)-C(4)-C(3)	168.4(9)
C(1)-N(1)-C(4)-C(5)	168.5(9)
C(27)-N(1)-C(4)-C(5)	-24.1(15)
C(2)-C(3)-C(4)-N(1)	-0.5(11)
C(2)-C(3)-C(4)-C(5)	-166.9(10)
C(6)-N(2)-C(5)-O(1)	159.3(10)
C(9)-N(2)-C(5)-O(1)	-3.5(14)
C(6)-N(2)-C(5)-C(4)	-25.3(15)
C(9)-N(2)-C(5)-C(4)	171.9(9)
N(1)-C(4)-C(5)-O(1)	-24.2(15)
C(3)-C(4)-C(5)-O(1)	140.4(11)
N(1)-C(4)-C(5)-N(2)	160.3(9)
C(3)-C(4)-C(5)-N(2)	-35.0(16)
C(5)-N(2)-C(6)-C(7)	-140.8(10)
C(9)-N(2)-C(6)-C(7)	23.1(10)
N(2)-C(6)-C(7)-C(8)	-37.0(9)
N(2)-C(6)-C(7)-C(14)	-161.3(8)
C(6)-C(7)-C(8)-C(9)	38.3(9)
C(14)-C(7)-C(8)-C(9)	161.2(8)
C(13)-N(3)-C(9)-N(2)	133.8(9)
C(13)-N(3)-C(9)-C(8)	-107.1(9)
C(13)-N(3)-C(9)-C(10)	12.9(10)
C(5)-N(2)-C(9)-N(3)	-67.9(11)

C(6)-N(2)-C(9)-N(3)	126.6(8)
C(5)-N(2)-C(9)-C(8)	166.0(8)
C(6)-N(2)-C(9)-C(8)	0.4(10)
C(5)-N(2)-C(9)-C(10)	47.9(12)
C(6)-N(2)-C(9)-C(10)	-117.7(9)
C(7)-C(8)-C(9)-N(3)	-149.0(8)
C(7)-C(8)-C(9)-N(2)	-24.1(10)
C(7)-C(8)-C(9)-C(10)	95.1(9)
C(13)-N(5)-C(10)-O(2)	178.4(10)
C(11)-N(5)-C(10)-O(2)	-2.6(18)
C(13)-N(5)-C(10)-C(9)	4.9(11)
C(11)-N(5)-C(10)-C(9)	-176.1(10)
N(3)-C(9)-C(10)-O(2)	175.9(10)
N(2)-C(9)-C(10)-O(2)	53.4(14)
C(8)-C(9)-C(10)-O(2)	-60.3(13)
N(3)-C(9)-C(10)-N(5)	-10.5(10)
N(2)-C(9)-C(10)-N(5)	-133.0(9)
C(8)-C(9)-C(10)-N(5)	113.3(9)
C(12)-O(3)-C(11)-N(5)	58.8(11)
C(10)-N(5)-C(11)-O(3)	147.2(10)
C(13)-N(5)-C(11)-O(3)	-33.9(13)
C(11)-O(3)-C(12)-N(4)	-55.8(12)
C(13)-N(4)-C(12)-O(3)	21.3(13)
C(12)-N(4)-C(13)-N(3)	-177.3(10)
C(12)-N(4)-C(13)-N(5)	4.5(15)
C(9)-N(3)-C(13)-N(4)	171.1(10)
C(9)-N(3)-C(13)-N(5)	-10.5(11)
C(10)-N(5)-C(13)-N(4)	-178.6(10)
C(11)-N(5)-C(13)-N(4)	2.3(16)
C(10)-N(5)-C(13)-N(3)	2.9(12)
C(11)-N(5)-C(13)-N(3)	-176.2(9)
C(6)-C(7)-C(14)-C(17)	-51.0(12)
C(8)-C(7)-C(14)-C(17)	-168.0(9)
C(6)-C(7)-C(14)-C(15)	-168.3(9)
C(8)-C(7)-C(14)-C(15)	74.7(12)
C(22)-N(6)-C(15)-C(14)	163.3(9)

C(16)-N(6)-C(15)-C(14)	-2.0(10)
C(17)-C(14)-C(15)-N(6)	26.5(9)
C(7)-C(14)-C(15)-N(6)	149.9(8)
C(21)-N(7)-C(16)-N(6)	133.9(9)
C(21)-N(7)-C(16)-C(17)	-109.8(9)
C(21)-N(7)-C(16)-C(18)	10.1(10)
C(22)-N(6)-C(16)-N(7)	-66.0(11)
C(15)-N(6)-C(16)-N(7)	100.6(9)
C(22)-N(6)-C(16)-C(17)	170.0(9)
C(15)-N(6)-C(16)-C(17)	-23.4(10)
C(22)-N(6)-C(16)-C(18)	50.8(12)
C(15)-N(6)-C(16)-C(18)	-142.6(8)
N(7)-C(16)-C(17)-C(14)	-83.6(9)
N(6)-C(16)-C(17)-C(14)	39.4(9)
C(18)-C(16)-C(17)-C(14)	161.3(8)
C(15)-C(14)-C(17)-C(16)	-41.2(9)
C(7)-C(14)-C(17)-C(16)	-165.6(8)
C(21)-N(9)-C(18)-O(4)	179.6(11)
C(19)-N(9)-C(18)-O(4)	-1.1(18)
C(21)-N(9)-C(18)-C(16)	6.2(11)
C(19)-N(9)-C(18)-C(16)	-174.4(10)
N(7)-C(16)-C(18)-O(4)	177.0(10)
N(6)-C(16)-C(18)-O(4)	53.8(14)
C(17)-C(16)-C(18)-O(4)	-60.2(13)
N(7)-C(16)-C(18)-N(9)	-9.5(10)
N(6)-C(16)-C(18)-N(9)	-132.6(8)
C(17)-C(16)-C(18)-N(9)	113.4(9)
C(20)-O(5A)-C(19)-O(5)	54.2(17)
C(20)-O(5A)-C(19)-N(9)	-40(2)
C(20)-O(5)-C(19)-O(5A)	-46.3(15)
C(20)-O(5)-C(19)-N(9)	57.2(13)
C(18)-N(9)-C(19)-O(5A)	-161.1(15)
C(21)-N(9)-C(19)-O(5A)	18.2(18)
C(18)-N(9)-C(19)-O(5)	150.0(11)
C(21)-N(9)-C(19)-O(5)	-30.6(14)
C(19)-O(5A)-C(20)-N(8)	42(3)

C(19)-O(5A)-C(20)-O(5)	-53.5(17)
C(21)-N(8)-C(20)-O(5A)	-18.5(18)
C(21)-N(8)-C(20)-O(5)	29.4(15)
C(19)-O(5)-C(20)-O(5A)	45.6(15)
C(19)-O(5)-C(20)-N(8)	-60.1(14)
C(20)-N(8)-C(21)-N(7)	-179.9(10)
C(20)-N(8)-C(21)-N(9)	-2.0(15)
C(16)-N(7)-C(21)-N(8)	171.4(10)
C(16)-N(7)-C(21)-N(9)	-6.9(11)
C(18)-N(9)-C(21)-N(8)	-178.2(10)
C(19)-N(9)-C(21)-N(8)	2.4(16)
C(18)-N(9)-C(21)-N(7)	0.1(12)
C(19)-N(9)-C(21)-N(7)	-179.3(9)
C(15)-N(6)-C(22)-O(6)	-170.1(9)
C(16)-N(6)-C(22)-O(6)	-5.9(14)
C(15)-N(6)-C(22)-C(23)	10.4(15)
C(16)-N(6)-C(22)-C(23)	174.7(9)
C(26)-N(10)-C(23)-C(24)	-2.9(12)
C(33)-N(10)-C(23)-C(24)	-173.4(9)
C(26)-N(10)-C(23)-C(22)	-175.8(10)
C(33)-N(10)-C(23)-C(22)	13.7(15)
O(6)-C(22)-C(23)-C(24)	-138.6(12)
N(6)-C(22)-C(23)-C(24)	40.8(17)
O(6)-C(22)-C(23)-N(10)	32.3(16)
N(6)-C(22)-C(23)-N(10)	-148.2(10)
N(10)-C(23)-C(24)-C(25)	1.0(12)
C(22)-C(23)-C(24)-C(25)	172.7(11)
C(23)-C(24)-C(25)-C(26)	1.2(13)
C(23)-C(24)-C(25)-Br(1)	-174.7(8)
C(23)-N(10)-C(26)-C(25)	3.5(12)
C(33)-N(10)-C(26)-C(25)	173.9(9)
C(23)-N(10)-C(26)-Br(3)	-178.0(8)
C(33)-N(10)-C(26)-Br(3)	-7.6(15)
C(24)-C(25)-C(26)-N(10)	-2.9(13)
Br(1)-C(25)-C(26)-N(10)	173.0(8)
C(24)-C(25)-C(26)-Br(3)	178.7(8)

Br(1)-C(25)-C(26)-Br(3)	-5.3(16)
C(28)-O(7)-C(27)-N(1)	-78.7(12)
C(4)-N(1)-C(27)-O(7)	-67.1(13)
C(1)-N(1)-C(27)-O(7)	98.4(12)
C(27)-O(7)-C(28)-C(29)	-75.5(12)
O(7)-C(28)-C(29)-Si(1)	-179.4(8)
C(30)-Si(1)-C(29)-C(28)	57.8(13)
C(31)-Si(1)-C(29)-C(28)	176.9(11)
C(32)-Si(1)-C(29)-C(28)	-64.4(13)
C(34)-O(8)-C(33)-N(10)	67.5(13)
C(26)-N(10)-C(33)-O(8)	-106.6(12)
C(23)-N(10)-C(33)-O(8)	62.3(13)
C(33)-O(8)-C(34)-C(35)	-175.6(12)
O(8)-C(34)-C(35)-Si(2)	-167.6(10)
O(8)-C(34)-C(35)-Si(2A)	159.6(11)
C(36)-Si(2)-C(35)-C(34)	173.0(13)
C(38)-Si(2)-C(35)-C(34)	48.4(17)
C(37)-Si(2)-C(35)-C(34)	-69.3(17)
C(36)-Si(2)-C(35)-Si(2A)	-128.9(11)
C(38)-Si(2)-C(35)-Si(2A)	106.5(13)
C(37)-Si(2)-C(35)-Si(2A)	-11.2(12)
C(39)-Si(2A)-C(35)-C(34)	-76.8(16)
C(40)-Si(2A)-C(35)-C(34)	49.3(19)
C(41)-Si(2A)-C(35)-C(34)	172.2(17)
C(39)-Si(2A)-C(35)-Si(2)	151.2(14)
C(40)-Si(2A)-C(35)-Si(2)	-82.8(17)
C(41)-Si(2A)-C(35)-Si(2)	40.2(15)

---

Symmetry transformations used to generate equivalent atoms:

## Chapter 3 – Total Synthesis of (±)-Ageliferin via N-amidinyliminium Ion Rearrangement

*adapted in part from*

### Total Synthesis of Ageliferin via N-amidinyliminium Ion Rearrangement

*Hui Ding, Andrew G. Roberts and Patrick G. Harran*

*Chem. Sci.* **2013**, *4*, 303 – 306.

#### 3.1 Introduction.

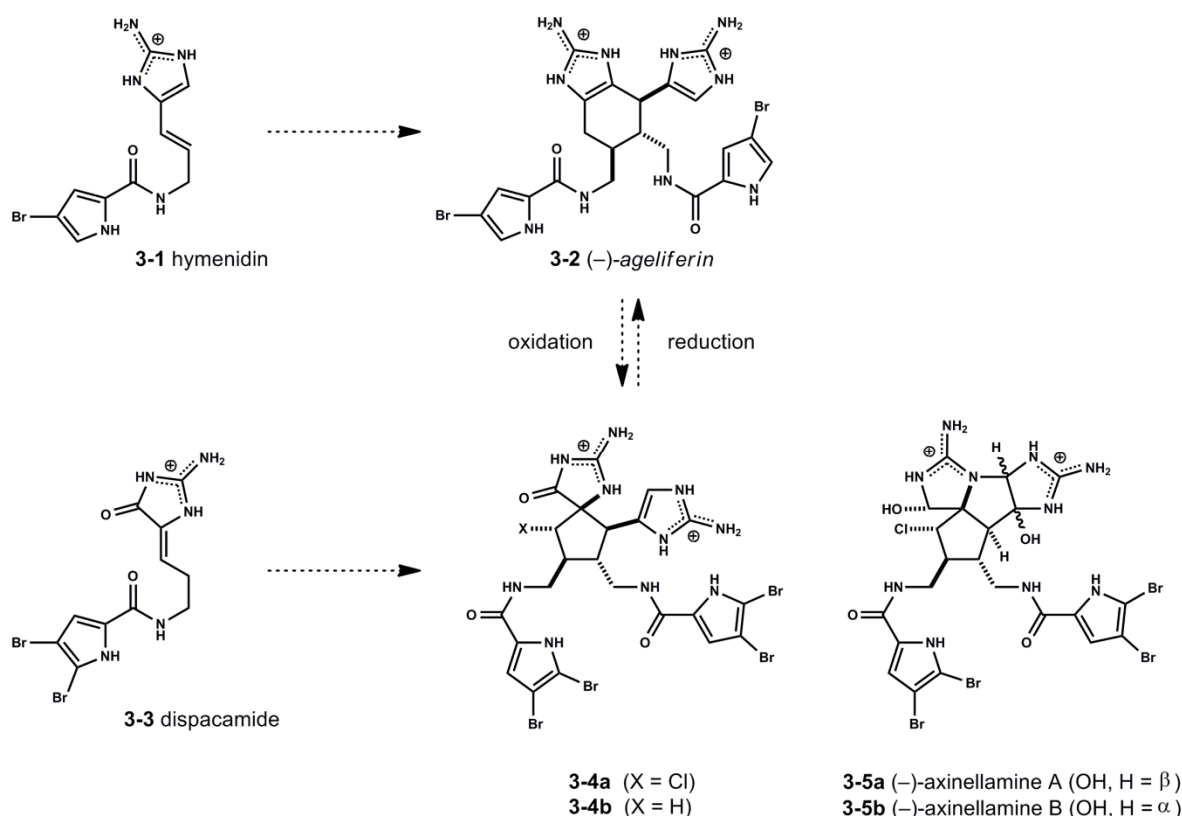


**Figure 3.1.** Pyrrole-imidazole alkaloids: monomer oxidation state (3-1, 3-3) and the interrelatedness of derived dimers.

(-)-Ageliferin (3-2, Figure 3.1) is a pyrrole-imidazole alkaloid discovered in extracts of *Agelas coniferin*. It has since been identified in numerous *Agelas* sponges; routinely alongside isomers such as sceptrin (not shown) and nagelamides (not shown).<sup>[1]</sup> The molecule is a prototypic oroidin (confer hymenidin 3-1) dimer and features prominently in discussions as to

how, or if, its structure is biosynthetically intermediate en route to more complex relatives.<sup>[2]</sup> Regarding the origin of **3-2** itself, two pathways have been advocated: 1) a net two-carbon ring expansion of sceptrin<sup>[3]</sup> and 2) formal Diels–Alder dimerization of hymenidin **3-1** followed by tautomerization.<sup>[1b]</sup> Both constructions have been emulated in the laboratory. Baran has synthesized **3-2** by executing the former, while Ohta has prepared a dimethylated congener (unnatural) using a variant of the latter (see Chapter 1).<sup>[4,5]</sup> Chen’s recent asymmetric synthesis of (–)-ageliferin **3-2** and related variants is not aligned with either pathway.<sup>[6]</sup>

The 2-aminotetrahydrobenzimidazole motif in ageliferin **3-2** is thought a reduced precursor to ring-contracted spirocycles such as those observed in palau’amine (not shown), konbu’acidin (not shown), axinellamines **3-5** and massadine (not shown).<sup>[2]</sup> Several laboratories have adopted similar logic for converting ageliferin synthons into congeners of dehydro ‘pre-axinellamine’ (i.e. **3-4a**, X = Cl).<sup>[7]</sup> Our own observations have led us to pursue the reverse outcome. Namely, we find that  $C_2$ -symmetric dimers of the natural product dispacamide **3-3** readily isomerize to oxidized precursors of **3-4b**; wherein X = H (*vide infra*). We recently discovered methods to partially reduce these materials<sup>[8b]</sup>, and herein demonstrate novel ring expansion of the resultant hemiaminals to (±)-ageliferin **3-2**. Depending upon intermediate stereochemistry, we also create previously unknown structural isomers of the axinellamine ring system.



## 3.2 Results and Discussion.

### 3.2.1 Synthesis and Equilibration of Spirocyclopentane Aminoimidazoles (3-12).

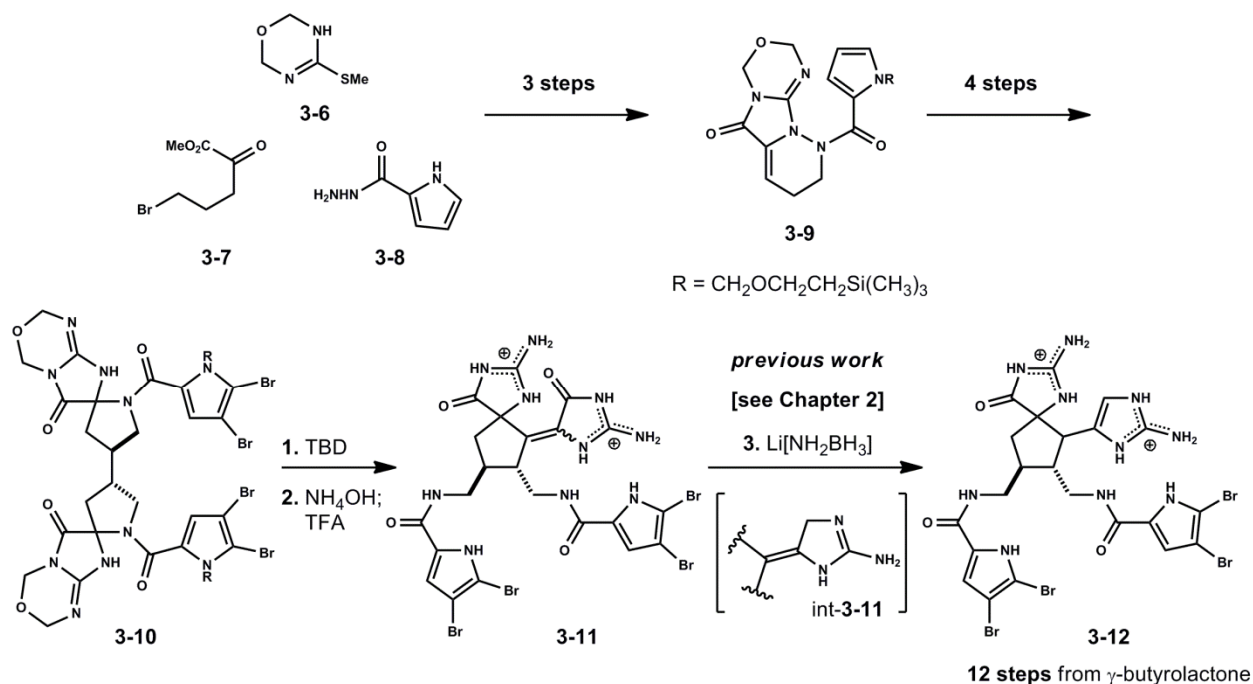
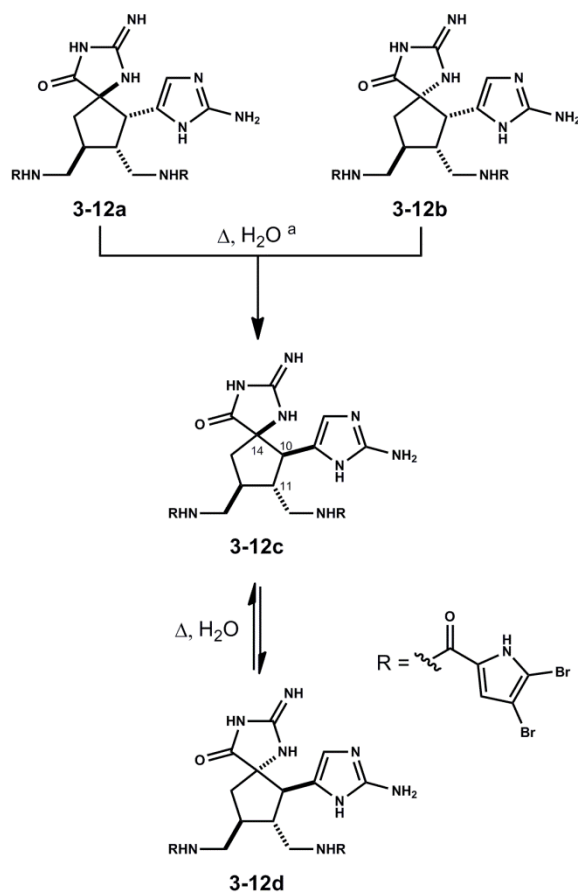


**Figure 3.2.** Spirocycles **3-12** are prepared in 12 steps from  $\gamma$ -butyrolactone, utilizing thiourea **3-6** and carbohydrazide **3-8** as key building blocks.

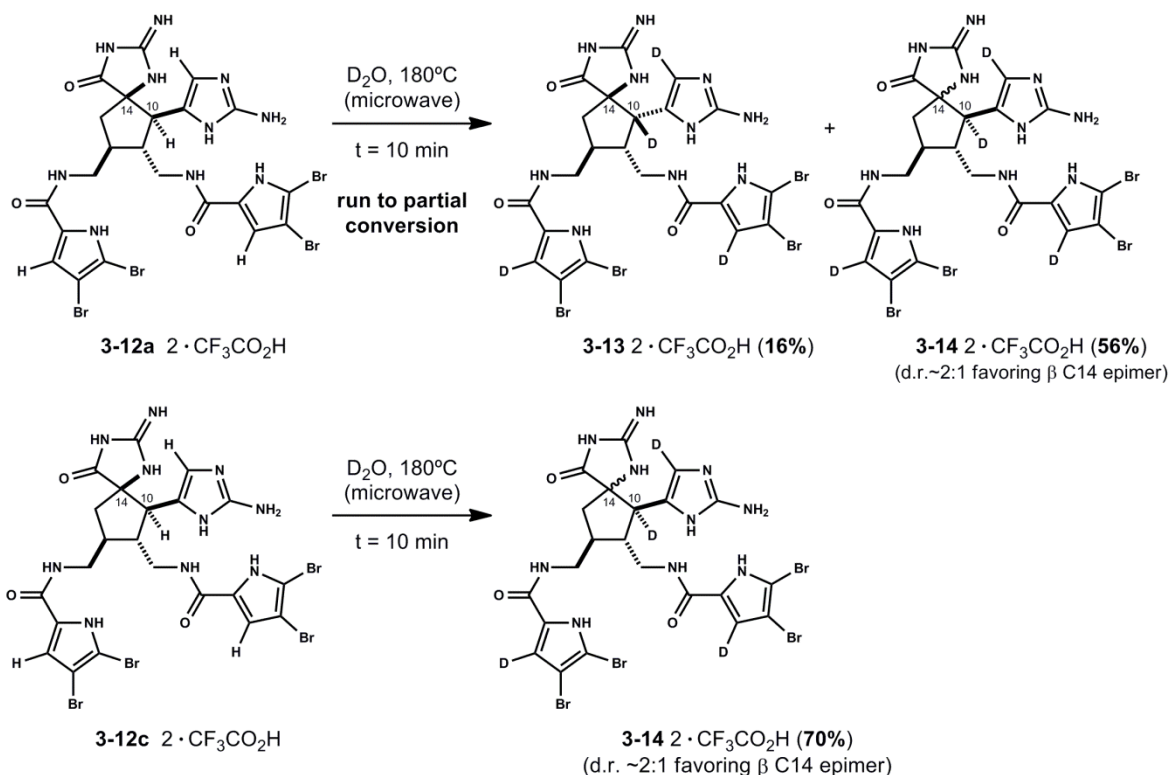
The assembly of  $C_2$ -symmetric spiroaminals **3-10** requires twelve steps beginning with  $\gamma$ -butyrolactone, thiourea and carbohydrazide **3-8** (Figure 3.2). As we've shown previously,<sup>[8b]</sup> the aminal units in **3-10** are moderately stable to acid, but not base. In fact, all diastereomers of this structure are susceptible to a base mediated rearrangement cascade; funneling ultimately to alkydienes **3-11** following degradation of the oxadiazine rings. In earlier studies, we advanced individual isomers of **3-11** to axinellamine structures.<sup>[8b]</sup> In the current work, separation is not necessary. Geometric isomers of each C14 epimer of **3-11** can be reduced as a mixture; initially to alkyldiene aminoimidazolines **int-3-11**. These subsequently tautomerize to aminoimidazoles **3-12**.



**Scheme 3.1.** Bistrifluoroacetate salt forms of diastereomers **3-12** thermally equilibrate in water. Reagents and conditions: (a) e.g. pure **3-12a**,  $\text{H}_2\text{O}$ ,  $180^\circ\text{C}$  (microwave), 15 min, **42%** of **3-12c**, **23%** of **3-12d**. Isolated yields for variations of this experiment are detailed in experimental of this chapter and **Scheme 3.2**.

A valuable finding was made while experimenting with **3-12**. The structure is isolated as a mixture of four diastereomers. It turns out the stereochemistry at C10 and C14 can be equilibrated. This is achieved simply by heating salt forms of **3-12** in water. For example, microwave heating an aqueous solution of pure **3-12a** ( $2 \cdot \text{CF}_3\text{CO}_2\text{H}$ ,  $180^\circ\text{C}$ , 1.0 mM) converts it fully to **3-12c** and its C14 epimer **3-12d** (65% isolated by HPLC, d.r. 2:1) within 15 minutes (Scheme 3.1). A similar result is observed when the experiment is repeated on pure **3-12d**, a mixture of **3-12a** and **3-12b**, or a mixture containing diastereomers **3-12a**, **3-12b** and **3-12d**. In each case, the system converges on C10,C11 *trans* diastereomers **3-12c** and **3-12d**, wherein **3-12c** predominates in roughly a 2:1 ratio.<sup>[9]</sup> Mechanistic details are not yet known, although data

is consistent with reversible cleavage of the C10,C14 bond (*vide infra*).<sup>[10]</sup> To further understand this equilibration process several deuterium incorporation studies were conducted.

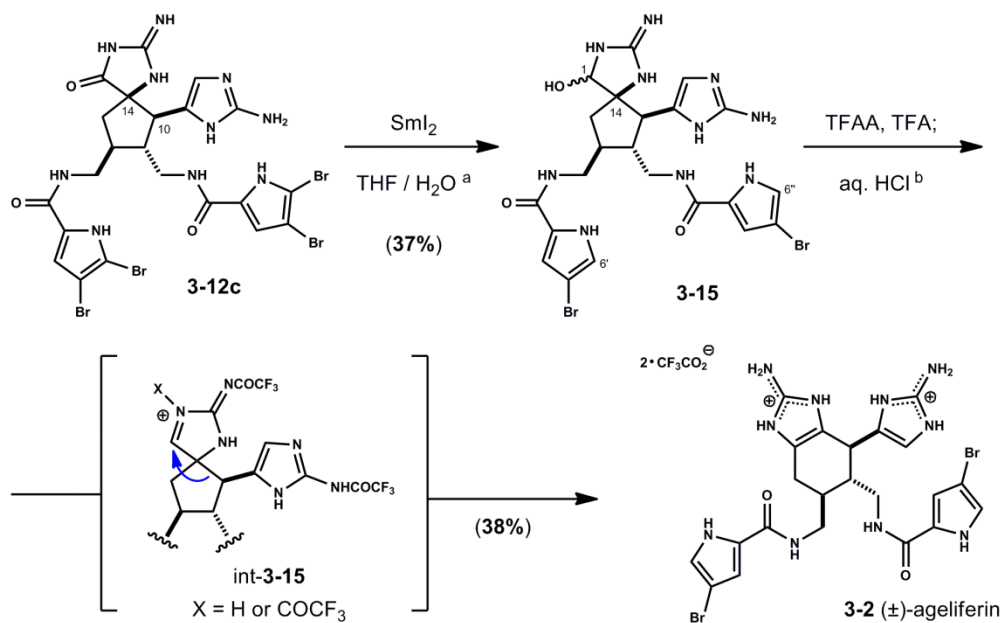


**Scheme 3.2.** Thermolysis of **3-12a** in  $\text{D}_2\text{O}$  results in rapid tetradeuteration (as labeled, >95% D at each position as determined by  $^1\text{H}$  NMR and MS) concomitant with epimerization at C10 and C14. Data reflects product mixture at ~75% conversion. The same experiment carried out on **3-12c** results in tetradeuteration and loss of stereochemical integrity at C14. The ratio of C14 epimers is ~2:1, comparable to that produced from **3-12a**, suggesting equilibrium has been established. No C10 epimers (e.g. **3-12b**, **3-12d**) are observed. Yields refer to isolated material following preparative reverse phase HPLC.

Thermolysis of **3-12a** (Scheme 3.2) in  $\text{D}_2\text{O}$  results in rapid tetradeuteration (as labeled ( $\geq 95\%$  D incorporation, at each position as determined by  $^1\text{H}$  NMR and MS analysis) concomitant with epimerization at C10 and C14 to provide tetradeuterated isomers **3-13** and **3-14**. Data from this experiment reflects a product mixture at approximately 75% conversion. The same experiment carried out on **3-12c** results in tetradeuteration and loss of stereochemical integrity at C14. The ratio of C14 epimers is ~2:1, comparable to that produced from **3-12a**, suggesting equilibrium has been established. No C10 epimers are observed. Yields in these experiments refer to isolated

material following preparative reverse phase HPLC. Further support for deuterium incorporation in a related model system is discussed in Section 3.2.4 Results and Discussion (*vide infra*).

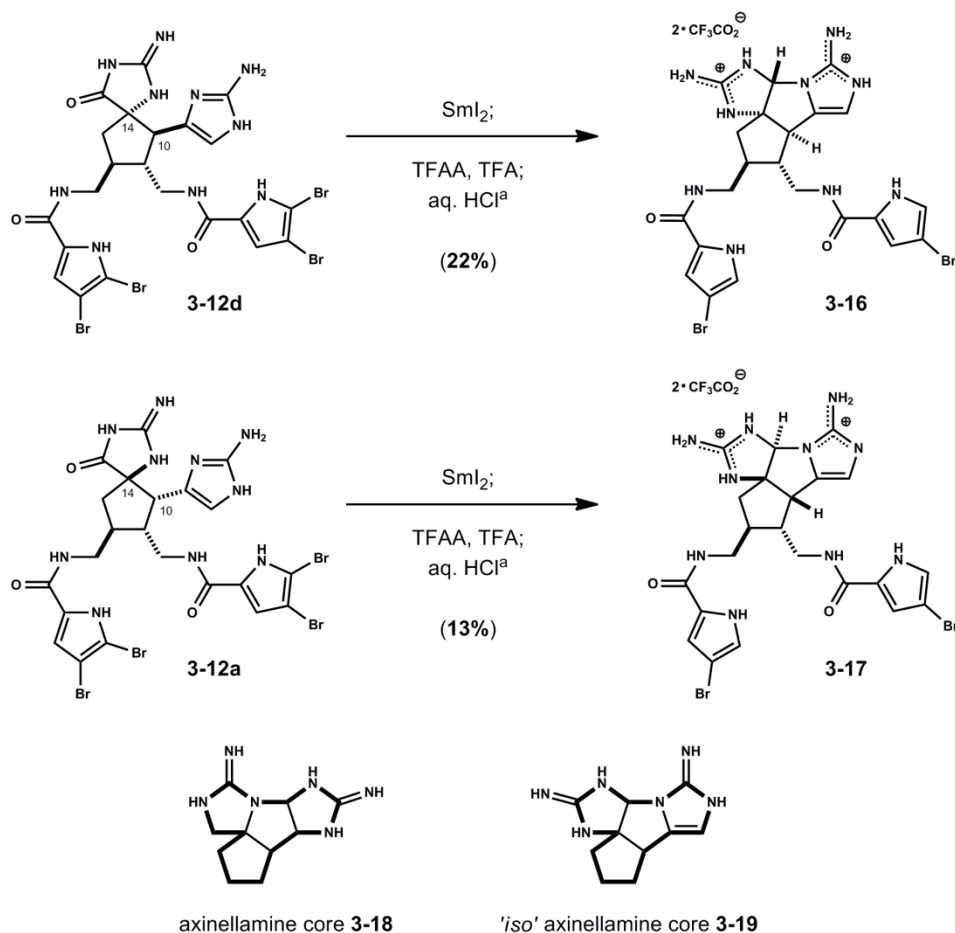
### 3.2.2 Synthesis of (±)-ageliferin (**3-2**) and 'iso'axinellamines (**3-16**, **3-17**).



**Scheme 3.3.** Total synthesis of (±)-ageliferin **3-2** - Reagents and conditions: (a) **3-12c**, excess  $\text{SmI}_2$ , THF /  $\text{H}_2\text{O}$ ,  $-40^\circ\text{C}$  to RT, 37%; (b) TFAA / TFA, THF,  $70^\circ\text{C}$ ; aq. 1M HCl, 38% from **3-15**.

The equilibration process (*vide supra*) converts four isomers of **3-12** to two (**3-12c**, **3-12d**), and the major isomer is used to synthesize (±)-ageliferin **3-2**. Major diastereomer **3-12c** is treated with excess  $\text{SmI}_2$  in aqueous THF (Scheme 3.3). This results in rapid debromination at C6' and C6'' followed by gradual reduction of the glycohydrazide carbonyl (C1). The resultant epimeric hemiaminals **3-15** (d.r. 1:1) are freed from samarium salts by preparative HPLC and exposed to trifluoroacetic anhydride (TFAA) in  $\text{CF}_3\text{CO}_2\text{H}$ .<sup>[11]</sup> This initiates ring-expanding rearrangement to a trifluoroacetylated tetrahydrobenzimidazole, from which the racemic natural product (±)-ageliferin **3-2** is isolated following hydrolytic (1 M HCl) workup.<sup>[12]</sup>

Each C1 epimer of **3-15** converts to ( $\pm$ )-ageliferin **3-2** using this protocol (Scheme 3.3), which we rationalize in terms of 1,2-alkyl migration occurring within an intermediate acyl N-amidinyliminium ion (**int-3-15**, X = H or COCF<sub>3</sub>). The result is analogous to acylation-induced ring expansion of partially reduced 1,3-diazaspiro[4.4]nonan-2,4-diones (*vide infra*).<sup>[13,14]</sup>



**Scheme 3.4.** Synthesis of 'iso' axinellamines (**3-19**) - Reagents and conditions: (a) TFAA / TFA, THF, 60 °C; aq. 1M HCl. Products **3-16** and **3-17** isolated as bistrifluoroacetate salts (**22%** and **13%** respectively over two steps, >95% purity) following two rounds of preparative reverse phase HPLC. Lowered yields reflect competing air oxidation of intermediates during isolation.

However, in the current complex, non-symmetric system, substrate stereochemistry provides for varying outcomes. For example, minor C14 epimer **3-12d** does not lead to ( $\pm$ )-ageliferin **3-2**. Rather, upon SmI<sub>2</sub> reduction and TFAA/TFA treatment, this molecule gives polycycle **3-16**, wherein a putative N-amidinyliminium ion intermediate is trapped by the proximal, *cis*-disposed aminoimidazole (Scheme 3.4). When the original mixture of **3-12** is separated by HPLC rather

than equilibrated, we observe a similar result beginning with major component **3-12a**. Like **3-12d**, the C14-C10 bond and the aminoimidazole substituent are oriented *cis* on the cyclopentane ring in **3-12a**. SmI<sub>2</sub> reduction and TFAA/TFA treatment of this material affords aminal **3-17**.<sup>[15]</sup>

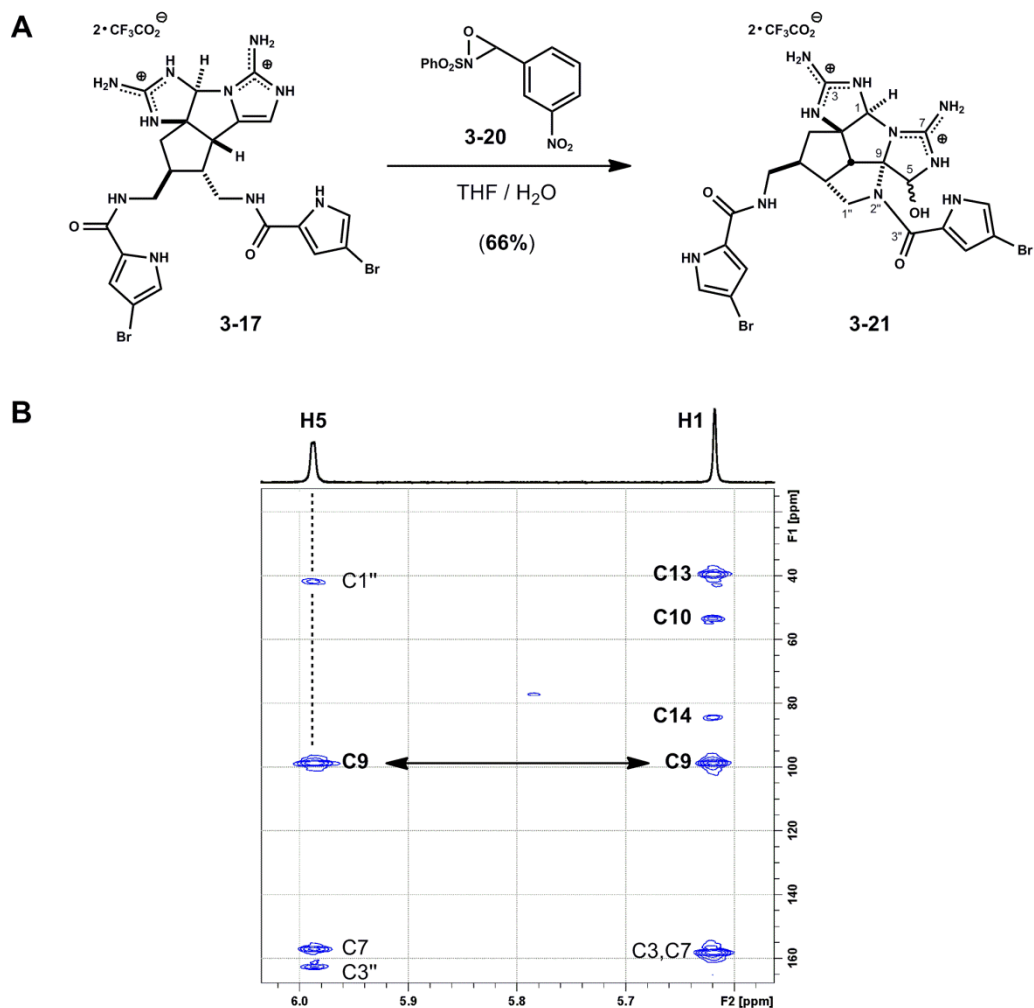


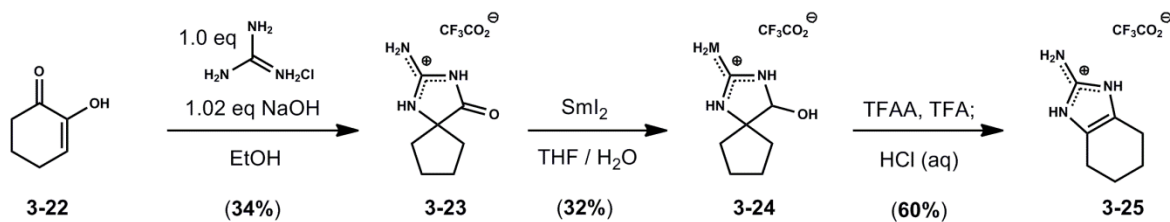
**Figure 3.3.** Reactivity and characterization of pentacycle **3-21** - **A** Reagents and conditions: **3-20**, THF, 60°C, 2h, 66%, d.r.~1.4:1. **B** Partial HMBC data for **3-21** (500 MHz, CH<sub>3</sub>OH-*d*<sub>4</sub>); Key correlations: H5–C1'', H5–C3'', H5–C9 and H1–C9.

Structures **3-16** and **3-17** have inverted core topologies and represent new synthetic isosteres (**3-19**) of the axinellamine (**3-18**) ring system (Scheme 3.4). They exist at the oxidation state of ageliferin **3-2**, yet this parameter is easily adjusted. For example, exposure of **3-17** to oxaziridine **3-20** (55°C, 2h) in aqueous THF smoothly oxidizes the aminoimidazole ring (Figure 3.3, A).<sup>[7b,8b]</sup> Following preparative HPLC, we isolate two hemiaminal epimers of pentacycle **3-21**

(66%, d.r. 1.4:1); a remarkable substance having two imbedded aminal linkages sharing a common nitrogen atom. This unusual connectivity is assigned with the aid of HMBC spectra (Figure 3.3, B), wherein C1 and C5 aminal protons correlate to C9. Relative to precursor **3-17**, a new long-range correlation linking C5H to C1" and C3" is reflective of the installed C9-N2" bond.

### 3.2.3 Related Rearrangements in Hydantoin and Model Glycohydantoin Systems.

#### A Model System Confirms Reactivity and Structure



#### B Preparation of 3-28 from 2-aminocyclohexanone (3-26) confirms structure of (3-25)

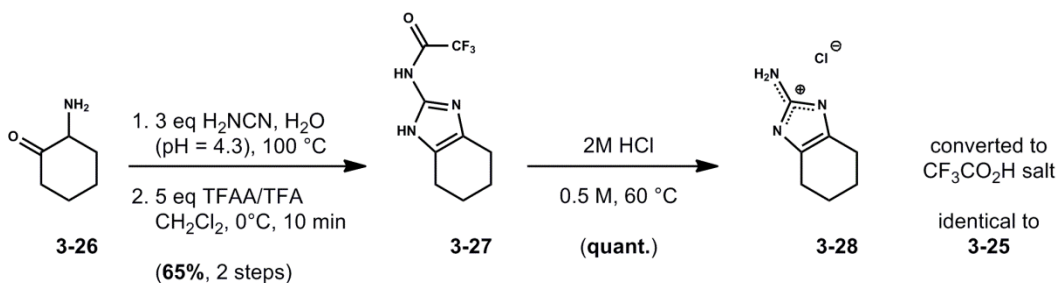


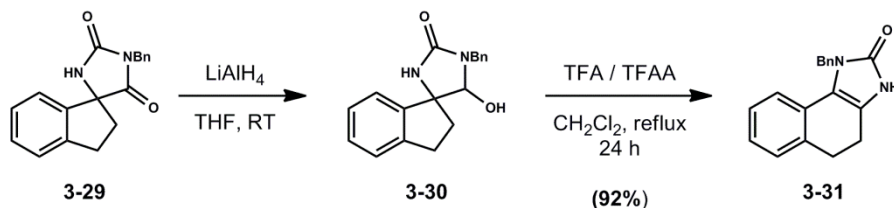
Figure 3.4. Model studies.

Additionally, we examined the observed rearrangement and 2-aminobenzimidazole product formation (confer ageliferin **3-2**) in the simplest model system 2-amino-1,3-diazaspiro[4.4]non-1-en-4-ol **3-24** derived from the  $\text{SmI}_2$  mediated reduction of 2-imino-1,3-diazaspiro[4.4]nonan-4-one **3-23**. As anticipated, the results confirm that 1,2-alkyl migration occurs within an intermediate acyl N-amindinylium ion (not shown, from **3-24**) to provide 2-aminotetrahydrobenzimidazole **3-25**. For further assurance, 2-aminotetrahydrobenzimidazole **3-28** (Figure 3.4, Part B) prepared from the condensation of 2-aminocyclohexanone **3-26** with cyanamide was in spectroscopic agreement with 2-aminotetrahydrobenzimidazole **3-25**. The moderate yield obtained for **3-25** (Part A) suggests that optimization of these dehydration conditions may provide a method of general utility for the synthesis of substituted 2-aminotetrahydrobenzimidazoles that may be difficult to access by alternative methods. The method is analogous to acylation-induced ring expansion of partially reduced 1,3-



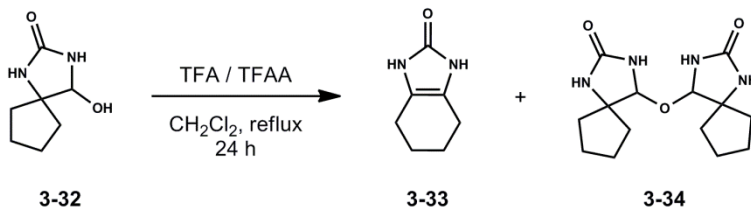
diazaspiro[4.4]nonan-2,4-diones (Figure 3.5) as studied in aryl and vinyl systems by Pesquet and co-workers.<sup>[13b]</sup> Notably, precedent provided by Salazar and co-workers<sup>[13a]</sup> was influential in our proposed synthesis of ageliferin **3-2**.

Reductive Ring Expansion: Aryl and Vinyl Precedent



Pesquet, A.; Daich, A.; Van Hijfte, L. *J. Org. Chem.* **2006**, *71*, 5303.

Reductive Ring Expansion: Alkyl Precedent



Salazar, L.; Rubido, J.; Espada, M.; Pedregal, C.; Trigo, G. *J. Heterocycl. Chem.* **1986**, *23*, 481.

**Figure 3.5.** Precedent for reductive ring expansions in hydantoin systems (**3-29**, **3-32**)

### 3.2.4 Deuterium Exchange Reactions in a Model 2-aminoimidazole (3-38).

We became interested in further understanding the results of our deuterium incorporation experiments (see Scheme 3.2, **3-12a** and **3-12c**). Specifically, we questioned the feasibility of deuterium incorporation at the 2-aminoimidazole benzylic position (see Scheme 3.2, **3-12a** or **3-12c**, confer C10) upon heating in D<sub>2</sub>O. We prepared 5-cyclopentyl-1H-imidazol-2-amine **3-38** (CF<sub>3</sub>CO<sub>2</sub>H) as a model system (Figure 3.6). It was synthesized by the addition of cyclopentylmagnesium bromide to a cold solution of metalated Boc-Gly-N(OCH<sub>3</sub>)(CH<sub>3</sub>) **3-36** in THF.<sup>[16]</sup> The resultant  $\alpha$ -amino ketone **3-37** was treated with trifluoroacetic acid and condensed with excess cyanamide in buffered aqueous media to form **3-38** in good yield. Isolated **3-38** was converted to its trifluoroacetate salt for further experiments. We conducted preliminary thermolysis experiments in D<sub>2</sub>O at 180°C. Figure 3.6 shows the time course of deuterium incorporation as analyzed by <sup>1</sup>H NMR analysis (600 MHz, H<sub>2</sub>O-*d*<sub>2</sub>, reaction aliquot after cooling to RT). The initial study suggests deuterium is readily incorporated at position (a) within 1 minute (t = 1 min) of heating in D<sub>2</sub>O at 180°C to provide intermediate **3-39**. Interestingly, complete deuterium exchange occurs more slowly at position (b) (see t = 9 h) with prolonged heating as intermediate **3-39** proceeds to **3-40**. After 9 hours (t = 9 h), deuterium exchange at positions (a) and (b) was > 95% as determined by <sup>1</sup>H NMR integration. Purification by preparative HPLC provided dideuterated 2-aminoimidazole **3-40**. These results are consistent with deuterium incorporation observed in intermediates **3-12** at positions C10 and C5. The requirement for prolonged thermolysis in model substrate (conversion of **3-39** to **3-40**, position (b)) is interesting.<sup>[17]</sup>

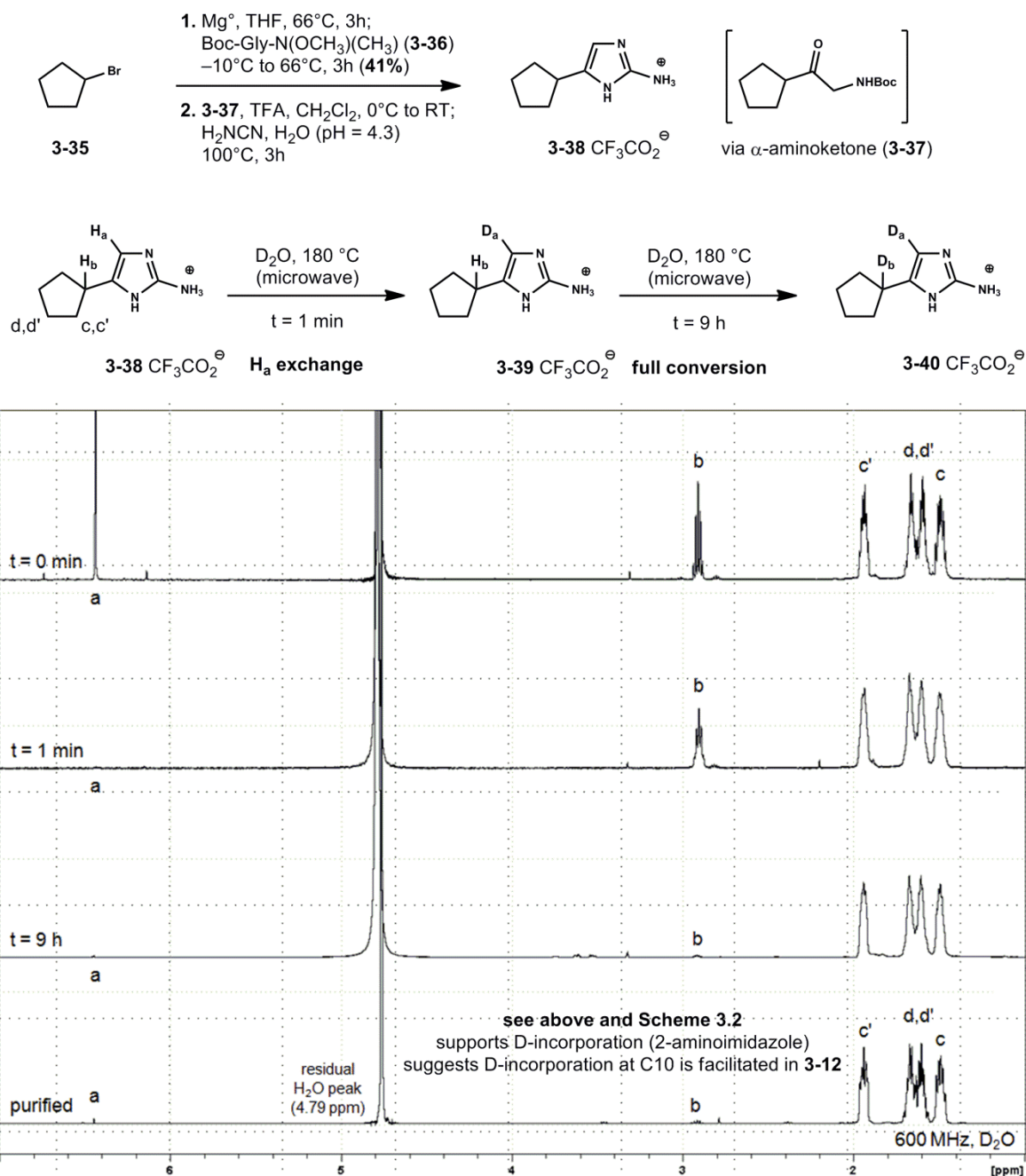


**Figure 3.6.** Synthesis of **3-38** from bromocyclopentane (**3-35**) and Boc-Gly-N(OCH<sub>3</sub>)(CH<sub>3</sub>) (**3-36**). Microwave heating deuterium incorporation study (time course) on model 5-cyclopentyl-1*H*-imidazol-2-amine (**3-38**) CF<sub>3</sub>CO<sub>2</sub>H. Crude reaction mixture analysis using <sup>1</sup>H NMR in D<sub>2</sub>O (t = 0 min, 1 min, 9 h and purified **3-40** CF<sub>3</sub>CO<sub>2</sub>H).

As previously mentioned, the equilibration of isomers **3-12** is consistent with reversible cleavage of the C10,C14 bond. The requirement for prolonged thermolysis of model **3-39** (D-incorporation at position (b), ~8-9 h) versus the observed rapid deuterium exchange in **3-12** (D-

incorporation at position C10, < 10 min) can be rationalized in two ways (Figure 3.7). The zwitterionic species (**int-3-12**) formed from heterolysis of the C10,C14 bond and biradical species (**int-3-12**) formed from the respective homolysis are two viable intermediates. Either intermediate might facilitate deuterium exchange at position C10 in **3-12**. However, these reaction modes are not reasonable for model 2-aminoimidazoles **3-38** and **3-39** (Figure 3.6).

Both mechanistic proposals account for the equilibration of C14 (d.r. 2:1)

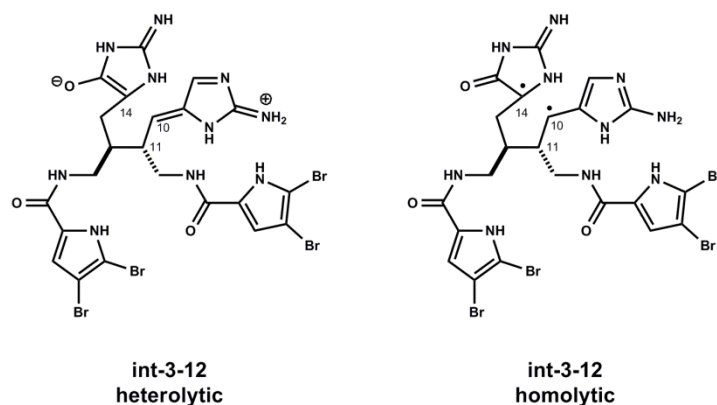


**Figure 3.7.** Mechanistic proposals for the equilibration of C10 and C14 in isomers **3-12** (see Scheme 3.2).

### 3.3 Conclusion

One can envision numerous oxidative manipulations in this series, providing access to a range of designed congeners. When combined with a short and flexible synthesis of ( $\pm$ )-ageliferin **3-2**, the chemistry provides a wide platform to explore biological functions of complex pyrrole–imidazole natural products; ideally while uncovering synthetic variants having superior and/or more selective activity. Initial screens suggest moderate antibacterial activity for the group. We suspect other venues may be more fruitful. Particularly interactions with gated ion channels, for which there is intriguing precedent.<sup>[18]</sup> Work along these lines is ongoing, as are attempts to exploit these key findings for total syntheses of axinellamine **3-5** and palau'amine structures (*see Chapter 4*).

### 3.4 References and Notes

- [1] (a) Rinehart, K. L. U.S. Patent 4737510, Apr. 12, 1988; (b) Rinehart, K. L. *Pure Appl. Chem.* **1989**, *61*, 525; (c) Kobayashi, J.; Tsuda, H.; Murayama, T.; Nakamura, H.; Ohizumi, Y.; Ishibashi, M.; Iwamura, M. *Tetrahedron* **1990**, *46*, 5579; (d) Keifer, P. A.; Schwartz, R. E.; Koker, M. E. S.; Hughes, Jr., R. G.; Rittschof, D.; Rinehart, K. L. *J. Org. Chem.* **1991**, *56*, 2965; (e) Williams, D. H.; Faulkner, D. J. *Tetrahedron*, **1996**, *52*, 5381; (f) Ageliferin has drawn attention due to reported antiviral and antimicrobial activities, particularly an intriguing impact on drug resistant biofilms: Stern, V. *Sci. Am.* **2009**, *19*, 7 and (g) Rogers, S. A.; Huigens III, R. W.; Cavanagh, J.; Melander, C. *Antimicrob. Agents Chemother.* **2010**, *54*, 2112 and references cited therein.
- [2] O'Malley, D. P.; Li, K.; Maue, M.; Zografos, A. L.; Baran, P. S. *J. Am. Chem. Soc.* **2007**, *129*, 4762.
- [3] (a) Baran, P. S.; O'Malley, D. P.; Zografos, A. L. *Angew. Chem. Int. Ed.* **2004**, *43*, 2674; (b) Ma, Z.; Lu, J.; Wang, X.; Chen, C. *Chem. Commun.* **2011**, *47*, 427.
- [4] (a) Baran, P. S.; Li, K.; O'Malley, D. P.; Mitsos, C. *Angew. Chem., Int. Ed.* **2006**, *45*, 249; (b) Northrop, B. H.; O'Malley, D. P.; Zografos, A. L.; Baran, P. S.; Houk, K. N. *Angew. Chem. Int. Ed.* **2006**, *45*, 4126.
- [5] (a) Kawasaki, I.; Sakaguchi, N.; Fukushima, N.; Fujioka, N.; Nikaido, F.; Yamashita, M.; Ohta, S. *Tetrahedron Lett.*, **2002**, *43*, 4377; (b) Kawasaki, I.; Sakaguchi, N.; Khadeer, A.; Yamashita, M.; Ohta, S. *Tetrahedron* **2006**, *62*, 10182.
- [6] (a) Wang, X. ; Ma, Z.; Lu, J.; Tan, X.; Chen, C. *J. Am. Chem. Soc.* **2011**, *133*, 15350; (b) Wang, X. ; Wang, X.; Tan, X.; Lu, J.; Cormier, K. W.; Ma, Z.; Chen, C. *J. Am. Chem. Soc.* **2012**, *134*, 18834.
- [7] (a) Sivappa, R.; Hernandez, N. M.; He, Y.; Lovely, C. J. *Org. Lett.* **2007**, *9*, 3861; (b) Sivappa, R.; Koswatta, P.; Lovely, C. J. *Tetrahedron Lett.* **2007**, *48*, 5771; (c) Zancanella, M. A.; Romo, D. *Org. Lett.* **2008**, *10*, 3685; (d) He, Y.; Krishnamoorthy, P.; Lima, H.; Chen, Y.; Wu, H.; Sivappa, R.; Dias, H. V. R.; Lovely, C. J. *Org. Biomol. Chem.* **2011**, *9*, 2685; (e) The term "pre-axinellamine" was coined by P. S. Baran *et al.*: Yamaguchi, J.; Seiple, I.; Young, I. S.; O'Malley, D. P.; Maue, M.; Baran, P. S. *Angew. Chem. Int. Ed.* **2008**, *47*, 3578.
- [8] (a) Li, Q.; Hurley, P.; Ding, H.; Roberts, A. G.; Akella, R.; Harran, P. G. *J. Org. Chem.* **2009**, *74*, 5909; (b) Ding, H.; Roberts, A. G.; Harran, P. G. *Angew. Chem., Int. Ed.* **2012**, *51*, 4340; (c) Ding, H.; Roberts, A. G.; Harran, P. G. *Chem. Sci.* **2013**, *4*, 303.
- [9] Equilibration experiments conducted with **3-12a**, **3-12b** and **3-12d** uniformly provide **3-12c** and **3-12d** in a ~2:1 ratio. In certain instances, competitive hydrolysis providing hydantoin derivatives of **3-12c** and **3-12d** is observed upon prolonged heating.
- [10] See Experimental of this chapter for details.

[11] Desalted hemiaminals **3-15** show diagnostic (see Ref. 8b) C1 methine <sup>1</sup>H resonances at  $\delta$  (ppm) 5.23 and 5.14 (500 MHz, MeOH-*d*<sub>4</sub>). Because the materials degrade readily, seemingly through auto-oxidation, they are reacted with TFAA/CF<sub>3</sub>CO<sub>2</sub>H immediately after isolation.

[12] <sup>13</sup>C NMR data for synthetic ( $\pm$ )-ageliferin **3-2** is identical to that reported for natural (–)-ageliferin **3-2**, except for a 3.8 ppm discrepancy in chemical shift for C11 (Scheme 3.3). The same phenomenon is observed by Baran (Ref. 2) and Chen (Ref. 6). We attribute the difference to the natural product being purified and characterized as an acetate salt, whereas we isolate **3-2** by preparative HPLC eluting with 0.1% CF<sub>3</sub>CO<sub>2</sub>H in CH<sub>3</sub>CN/H<sub>2</sub>O. For further discussion see: (a) Pugmire, R. J.; Grant, D. M. *J. Am. Chem. Soc.* **1968**, *90*, 697; (b) Olofson, A.; Yakushijin, K.; Horne, D. A. *J. Org. Chem.* **1998**, *63*, 5787.

[13] (a) Pedregal, C.; Espada, M.; Salazar, L. Elguero, J. *J. Heterocycl. Chem.* **1986**, *23*, 487; (b) Pesquet, A.; Daïch, A.; Van Hijfte, L. *J. Org. Chem.* **2006**, *71*, 5303; (c) An interesting base promoted ring expansion of 4-amino-1,3-diaza-2-(methylthio)spiro[4.4]non-1-ene has been observed: Lanman, B. A.; Overman, L. E. *Heterocycles* **2006**, *70*, 557.

[14] The analogous SmI<sub>2</sub> mediated reduction on model 2-imino-1,3-diazaspiro[4.4]nonan-4-one **3-23** provides 2-amino-1,3-diazaspiro[4.4]non-1-en-4-ol **3-24** which undergoes efficient ring expanding rearrangement to 2-aminotetrahydrobenzimidazole **3-25** (See Figure 3.5 and Experimental).

[15] Based on results for **3-12a**, **3-12c** and **3-12d**, we anticipated the remaining series diastereomer, namely **3-12b**, would lead to nagelamide E (*i.e.* C10 *epi*-**3-2**) upon SmI<sub>2</sub> reduction and ring expansion. Interestingly, a mixture (as yet inseparable) of **3-12b** and its C14 epimer (*i.e.* **3-12a**) gives only **3-17** and ageliferin **3-2** following these two operations. To the extent **3-12a** leads only to **3-17** (Scheme 3.4), the ageliferin **3-2** produced is derived from **3-12b**. This implies C10 epimerization occurs during and/or prior to ring expansion. Note: thermal equilibration of ageliferin **3-2** and nagelamide E (not shown) has been demonstrated (See Ref. 2 and O'Malley, D. P. Ph.D. Dissertation, the Scripps Research Institute, **2008**, UMI #3313886).

[16] Synthesis of  $\alpha$ -Boc-aminoketones from  $\alpha$ -Boc-amino-Weinreb amides using a pre-deprotonation protocol: Liu, J.; Ikemoto, N.; Petrillo, D.; Armstrong III, J. D. *Tetrahedron Lett.* **2002**, *43*, 8223.

[17] For deuterium exchange studies in comparable systems see: (a) Abou-Jneid, R.; Ghouli, S.; Martin, M.-T.; Dau, E. T. H.; Travert, N.; Al-Mourabit, A. *Org. Lett.* **2004**, *6*, 3933; (b) Comparable D-incorporation in agelastatin systems: Movassaghi, M.; Siegal, D.; Han, S. *Chem. Sci.* **2010**, *1*, 561 and see Refs. 2, 15 (O'Malley, Ph.D. Dissertation)

[18] Bickmeyer, U. *Toxicon*, **2005**, *45*, 627.

## 3.5 Experimental.

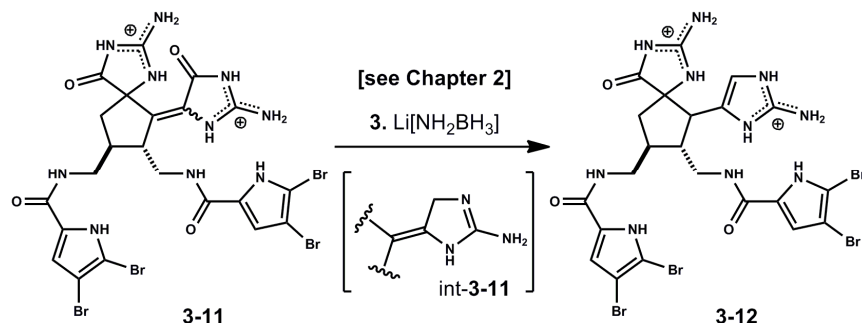
### 3.5.1 Materials and Methods.

Unless stated otherwise, reactions were performed under an argon (Ar) atmosphere in flame-dried glassware. Tetrahydrofuran (THF), chloroform (CHCl<sub>3</sub>), methylene chloride (CH<sub>2</sub>Cl<sub>2</sub>), diethyl ether (Et<sub>2</sub>O), toluene (PhCH<sub>3</sub>), benzene (PhH), dimethoxyethane (DME), dimethyl formamide (DMF) and acetonitrile (CH<sub>3</sub>CN) were dried and deoxygenated through activated alumina solvent drying systems or distilled prior to use. Column chromatography was performed on silica gel 60 (SiliCycle, 240-400 mesh). Thin layer chromatography (TLC) and preparative thin layer chromatography (pTLC) utilized pre-coated plates (silica gel 60 PF254, 0.25 mm or 0.5 mm). Purification of advanced intermediates employed an Agilent 1200 Preparative HPLC (pHPLC) system equipped with an Agilent Quadrupole 6130 ESI-MS detector and an automated fraction collector. Mobile phases (Mobile phase A: H<sub>2</sub>O, Mobile Phase B: CH<sub>3</sub>CN) were prepared with 0.1% or 1% trifluoroacetic acid (CF<sub>3</sub>CO<sub>2</sub>H) or 0.1% formic acid as indicated. Advanced intermediates isolated and characterized as trifluoroacetate salts are denoted as (2·CF<sub>3</sub>CO<sub>2</sub>H) in data tables. The trifluoroacetate salt may be omitted from structures in schemes for clarity. NMR spectra were recorded on Bruker Avance spectrometers (500 MHz or 600 MHz). Data for <sup>1</sup>H NMR spectra are reported as follows: chemical shift (δ ppm) (multiplicity, coupling constant (Hz), integration) at 298K, unless stated otherwise, and are referenced to a residual solvent peak. Data for <sup>13</sup>C NMR spectra are reported in terms of chemical shift (δ ppm) and are referenced to residual solvent peak.



### 3.5.2 Experimental Procedures and Characterization Data.

Compounds **3-6**, **3-7**, **3-8**, **3-10**, **3-11**, **int-3-11**, **3-12a** and **3-12c** are reported in **Chapter 2.5 Experimental**.<sup>[1]</sup>



#### Reduction of glycoamidines (**3-11**) to provide a 2-aminoimidazoles (**3-12**).

Preparation of lithium amidotrihydroborate (LAB) solution: To a suspension of BH<sub>3</sub>·NH<sub>3</sub> (0.57 g, 16.5 mmol, 90% purity) in THF (3.6-mL) cooled to -20°C was added a solution of *n*-BuLi (2.5 M in hexanes, 6.4-mL, 16.0 mmol) dropwise. The mixture was warmed to RT, stirred for 1h and used directly (~1.6 M) in the following reaction.

A portion of the above LAB solution (3.8-mL, 1.6 M, 6.1 mmol) was added to a solution of **3-11** (207 mg, 0.20 mmol) in THF (6.8-mL) at RT. Gentle gas evolution was observed. The mixture was stirred in a pre-heated oil-bath (60°C) for 4h. A second portion of the LAB solution (1.9-mL, 3.0 mmol) was added and the cloudy mixture was stirred at 60°C for another 4h. After cooling to -40°C, the reaction was quenched by the slow addition of 10% CF<sub>3</sub>CO<sub>2</sub>H in H<sub>2</sub>O (10-mL) (**Note:** gas evolution can be vigorous if the addition is too fast). The mixture was warmed to RT and stirred at 60°C for 4h, then purified by HPLC to give **3-12a** + **3-12b** (46 mg, 22.5%), **3-12c** (21.0 mg, 11%), **3-12d** (19 mg, 9.3%) and recovered **3-11** (9.0 mg, 4.3%).

**HPLC conditions:** Waters Sunfire C18 column (19 × 250-mm) with UV detection at 280-nm, Solution A: H<sub>2</sub>O w/1% CF<sub>3</sub>CO<sub>2</sub>H and Solution B: CH<sub>3</sub>CN w/1% CF<sub>3</sub>CO<sub>2</sub>H; increase gradient of Solution B from 10% to 30%, 0-2 min; then to 60%, 12 min; flow rate: 20-mL/min.

Compounds **3-12a** and **3-12c** are reported in Chapter 2, Section 2.5.2 Experimental.

For characterization purposes, a portion of the **3-12a** + **3-12b** mixture was further purified by HPLC to provide pure **3-12b**.

**HPLC conditions:** Waters XSelect Fluoro-phenyl column (19 × 250-mm) with UV detection at 280-nm, Solution A: H<sub>2</sub>O w/1% CF<sub>3</sub>CO<sub>2</sub>H and Solution B: CH<sub>3</sub>CN w/1% CF<sub>3</sub>CO<sub>2</sub>H; increase gradient of Solution B from 10% to 22%, 0-2 min; then to 26.5%, 14 min; flow rate: 30-mL/min.

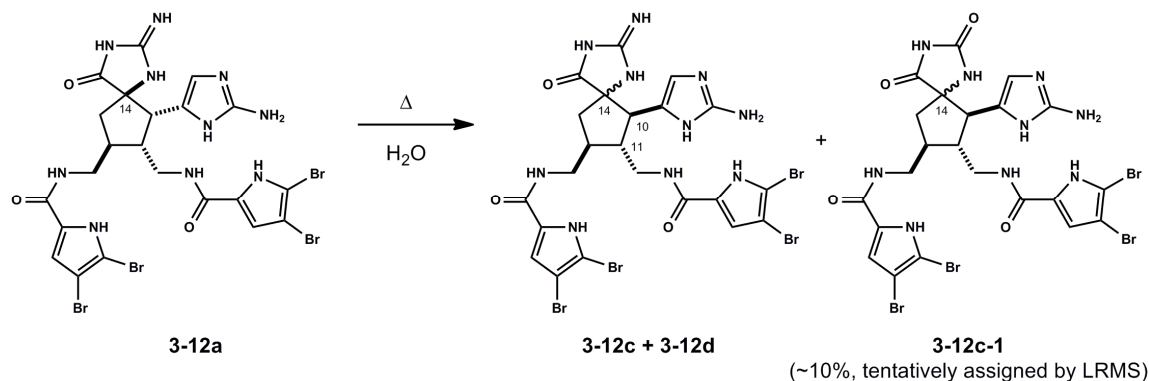
Compound (**3-12b**):

$^1\text{H NMR}$  (MeOH- $d_4$ ):  $\delta$  (ppm) 6.82 (s, 1H), 6.77 (s, 1H), 6.61 (s, 1H), 3.55 (d,  $J = 8.6$  Hz, 1H), 3.47 (d,  $J = 5.9$  Hz, 2H), 3.34-3.27 (m, partially coincident with residual MeOH peak), 2.78 (dd,  $J = 15.8, 7.9$  Hz, 1H), 2.56-2.46 (m, 1H), 2.27-2.21 (m, 1H), 2.12-2.05 (m, 1H);  $^{13}\text{C NMR}$  (MeOH- $d_4$ ):  $\delta$  (ppm) 162.2, 161.7, 148.5, 128.6, 128.4, 122.8, 114.54, 114.48, 112.3, 106.34, 106.29, 100.1, 100.0, 73.6, 47.2, 44.4, 43.7, 43.4, 41.9, 39.7; **HRMS-ESI** ( $m/z$ ) calcd for  $[\text{C}_{22}\text{H}_{22}\text{Br}_4\text{N}_{10}\text{O}_3+\text{H}]^+$ : 794.8649; found: 794.8619.

Compound (**3-12d**):

$^1\text{H NMR}$  (MeOH- $d_4$ ):  $\delta$  (ppm) 6.90 (s, 1H), 6.77 (s, 1H), 6.61 (s, 1H), 3.64 (dd,  $J = 13.7, 4.9$  Hz, 1H), 3.51-3.45 (m, 3H), 3.25 (d,  $J = 12.5$  Hz, 1H), 2.69-2.59 (m, 1H), 2.47-2.39 (m, 1H), 2.33-2.18 (m, 2H);  $^{13}\text{C NMR}$  (MeOH- $d_4$ ):  $\delta$  (ppm) 162.2, 162.1, 149.0, 128.6, 128.3, 123.5, 114.6, 114.4, 112.7, 106.5, 106.3, 100.06, 100.02, 73.1, 50.0, 45.9, 43.0, 41.0, 40.7, 38.2; **HRMS-ESI** ( $m/z$ ) calcd for  $[\text{C}_{22}\text{H}_{22}\text{Br}_4\text{N}_{10}\text{O}_3+\text{H}]^+$ : 794.8649; found: 794.8666.

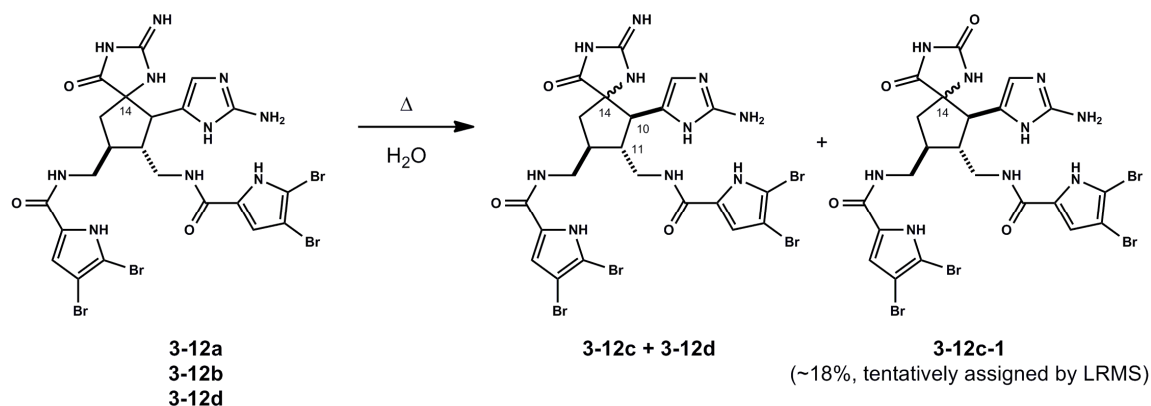
**Preparation of (3-12c) and (3-12d) from (3-12a).**



Purified **3-12a** (8.0 mg, 0.0078 mmol) was dissolved in MeOH (3-mL) and evenly distributed into three 10-mL microwave reaction vials. Each sample was concentrated, dissolved in DI- $\text{H}_2\text{O}$  and stirred at  $180^\circ\text{C}$  for 15 min in a CEM microwave reactor. The mixtures were combined, diluted with MeOH and purified by HPLC. Two *trans*-C10, C11 compounds were obtained **3-12c** (3.4 mg, 42%) and **3-12d** (1.9 mg, 23%) along with two epimeric-C14 compounds tentatively assigned as hydantoin (**3-12c-1**) (~1 mg total, 10%) (**LRMS-ESI** ( $m/z$ ) calcd for  $[\text{C}_{22}\text{H}_{21}\text{Br}_4\text{N}_9\text{O}_4+\text{H}]^+$ : 795.9; found: 795.6).

**HPLC conditions:** Waters XBridge RP-18 column (19  $\times$  250-mm) with UV detection at 280-nm; Solution A: w/0.1%  $\text{CF}_3\text{CO}_2\text{H}$  and Solution B:  $\text{CH}_3\text{CN}$  w/0.1%  $\text{CF}_3\text{CO}_2\text{H}$ ; increase gradient of Solution B from 10% to 33%, 0-2 min; then to 36%, 15 min; flow rate: 20-mL/min.

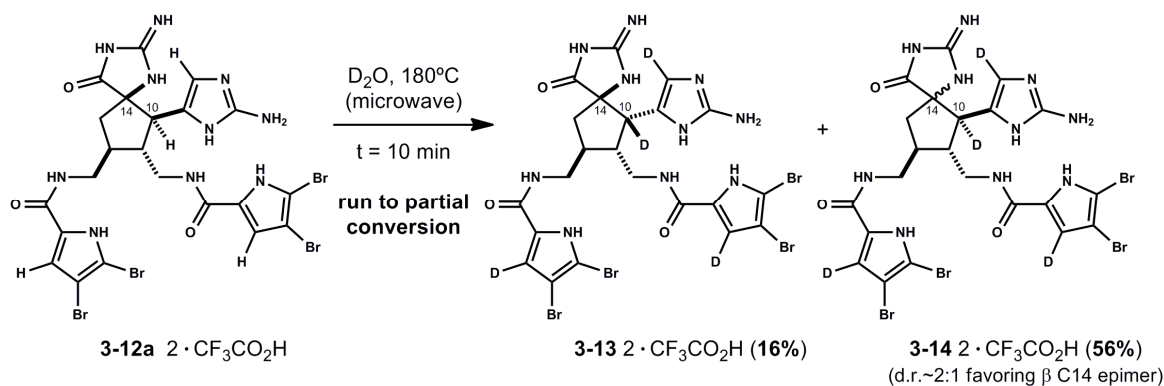
## Preparation of (3-12c) and (3-12d) from a mixture of (3-12a, 3-12b, 3-12d).



A mixture of (**3-12a** + **3-12b** + **3-12d**) (16.5 mg, 0.016 mmol, d.r. 4:1:1.5) was dissolved in MeOH (3-mL) and evenly distributed into three 10-mL microwave reaction vials. Each sample was concentrated and re-dissolved in DI-H<sub>2</sub>O (4.5-mL each) and stirred at 180°C for 18 min in a CEM microwave reactor. The mixtures were combined, diluted with MeOH and purified by HPLC. Two *trans*-C10,C11 compounds were obtained **3-12c** (2.4 mg, 16%) and **3-12d** (2.2 mg, 14%) along with two epimeric-C14 compounds tentatively assigned as hydantoin compounds (**3-12c-1**) (~3 mg total, 18%); (LRMS-ESI (*m/z*) for [C<sub>22</sub>H<sub>21</sub>Br<sub>4</sub>N<sub>9</sub>O<sub>4</sub>+H]<sup>+</sup>: 795.9; found: 795.6).

**HPLC conditions:** Waters XBridge RP-18 column (19 × 250-mm) with UV detection at 280-nm; Solution A: H<sub>2</sub>O w/0.1% CF<sub>3</sub>CO<sub>2</sub>H and Solution B: CH<sub>3</sub>CN w/0.1% CF<sub>3</sub>CO<sub>2</sub>H, increase gradient of Solution B from 10% to 33%, 0-2 min; then to 36%, 15 min; flow rate: 20-mL/min.

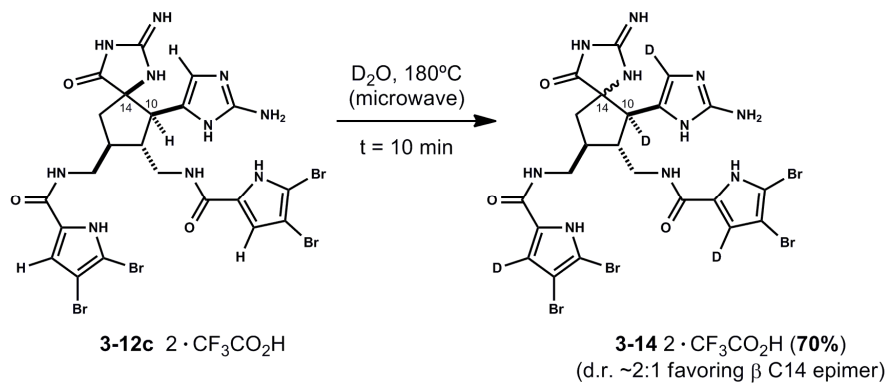
## Thermolysis of 3-12a in D<sub>2</sub>O by heating in a microwave reactor.



Purified **3-12a** (4.0 mg, 0.004 mmol) was dissolved in D<sub>2</sub>O (3-mL) and evenly distributed into two 10-mL microwave reaction vials and stirred at 180°C for 10 min in a CEM microwave reactor. The mixtures were combined, diluted with MeOH and purified by HPLC. Two fractions were collected. The first fraction contains **3-13** and α-C14-**3-14** (1.4 mg, 34%, d.r. 1:1.1) and the second fraction is β-C14-**3-14** (1.6 mg, 38%).

**HPLC conditions:** Waters XBridge RP-18 column (19 × 250-mm) with UV detection at 280-nm; Solution A: H<sub>2</sub>O w/0.1% CF<sub>3</sub>CO<sub>2</sub>H and B: CH<sub>3</sub>CN w/0.1% CF<sub>3</sub>CO<sub>2</sub>H; increase gradient of Solution B from 10% to 32%, 0-2 min; then to 36%, 15 min; flow rate: 20-mL/min.

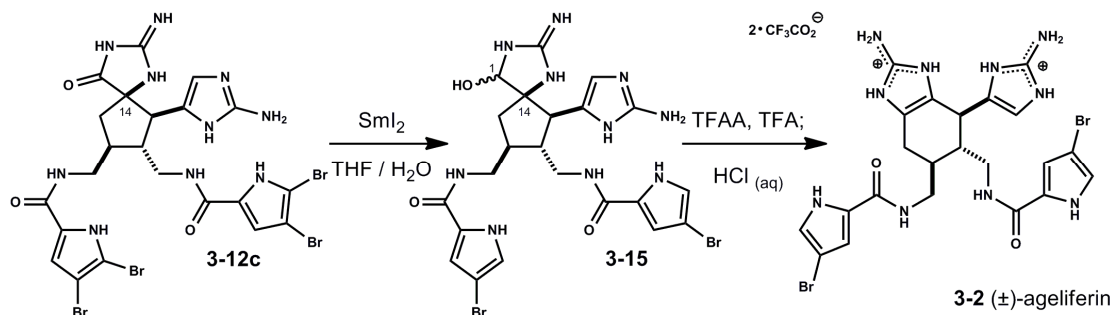
### Thermolysis of 3-12c in D<sub>2</sub>O by heating in a microwave reactor.



Pure **3-12c** (4.2 mg, 0.0042 mmol) was dissolved in D<sub>2</sub>O (5-mL) and evenly distributed into two 10-mL microwave reaction vials and stirred at 180°C for 10 min in a CEM microwave reactor. The mixtures were combined, diluted with MeOH and purified by HPLC. Two *trans*-C10,C11 compounds were obtained α-C14-**3-14** (0.9 mg, 21%) and β-C14-**3-14** (2.1 mg, 49%).

**HPLC conditions:** Waters XBridge RP-18 column (19 × 250-mm) with UV detection at 280-nm; Solution A: H<sub>2</sub>O w/0.1% CF<sub>3</sub>CO<sub>2</sub>H and Solution B: CH<sub>3</sub>CN w/0.1% CF<sub>3</sub>CO<sub>2</sub>H; increase gradient of Solution B from 10% to 32%, 0-2 min; then to 36%, 15 min; flow rate: 20-mL/min.

### Synthesis of (±)-ageliferin (3-2).



To a solution of **3-12c** (20.0 mg, 0.019 mmol) in THF / H<sub>2</sub>O (100-μL) was added a freshly-prepared solution of SmI<sub>2</sub> (700-μL, 0.196 mmol, 0.28M in THF) at -40°C. The initially blue mixture became purple after degassed H<sub>2</sub>O (100-μL) was added. It turned to pale yellow after a few minutes. LCMS analysis indicated partial debromination occurred to give partially debrominated intermediates (LRMS-ESI (*m/z*) calcd for [C<sub>22</sub>H<sub>24</sub>Br<sub>2</sub>N<sub>10</sub>O<sub>4</sub>+H]<sup>+</sup>: 653.04; found: 653.1). The solvent volume was reduced by a stream of Ar and the mixture was cooled to -40°C. Another portion of SmI<sub>2</sub> (750-μL, 0.21 mmol, 0.28 M in THF) was added and the mixture was warmed to RT. The reaction was quenched with degassed THF and H<sub>2</sub>O (1.2-mL each) under Ar.

The crude solution was diluted with 10% CF<sub>3</sub>CO<sub>2</sub>H in H<sub>2</sub>O and purified by HPLC. The desired C1-hemiaminal compounds **3-15** (LRMS-ESI (*m/z*) calcd for [C<sub>22</sub>H<sub>27</sub>Br<sub>2</sub>N<sub>10</sub>O<sub>3</sub>+H]<sup>+</sup>: 639.06; found: 639.1) were obtained (6.2 mg, 37%, d.r. 1:1). Compounds **3-15** in solution are prone to auto-oxidation so no further purification was performed.

**HPLC conditions:** Waters XSelect Fluoro-phenyl column (19 × 250-mm) with UV detection at 280-nm; Solution A: H<sub>2</sub>O w/0.1% CF<sub>3</sub>CO<sub>2</sub>H and Solution B: CH<sub>3</sub>CN w/ 0.1% CF<sub>3</sub>CO<sub>2</sub>H; increase gradient of Solution B from 10% to 25%, 0-2 min; then to 28%, 8 min; flow rate: 20-mL/min.

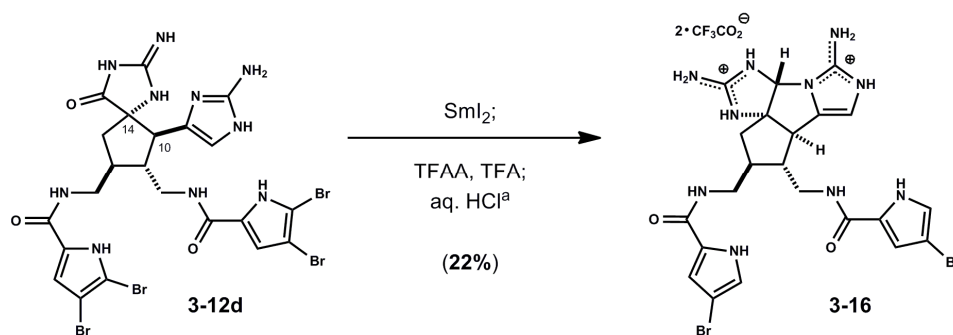
The above mixture **3-15** (6.2 mg) was dissolved in anhydrous THF (0.24-mL). TFAA (100-μL, 0.71 mmol) was added, followed by CF<sub>3</sub>CO<sub>2</sub>H (50-μL, 0.78 mmol). The vial was sealed and stirred at 70°C for 27h. The reaction mixture was concentrated and dissolved in DME (0.3-mL), then treated with 2M HCl in H<sub>2</sub>O (0.4-mL, 0.8 mmol) at 45°C for 14h. It was diluted with H<sub>2</sub>O and purified by HPLC to afford (±)-ageliferin **3-2** (2.2 mg, 38% from **3-12c**).

**HPLC conditions:** Waters XBridge RP-18 column (19 × 250-mm) with UV detection at 280-nm; Solution A: H<sub>2</sub>O w/0.1% CF<sub>3</sub>CO<sub>2</sub>H and Solution B: CH<sub>3</sub>CN w/0.1% CF<sub>3</sub>CO<sub>2</sub>H; increase gradient of Solution B from 10% to 28%, 0-2 min; then to 34%, 25 min; flow rate: 20-mL/min.

**(±)-ageliferin (3-2):**

<sup>1</sup>H NMR (MeOH-*d*<sub>4</sub>): δ (ppm) 6.97 (d, *J* = 1.5 Hz, 1H), 6.94 (d, *J* = 1.5 Hz, 1H), 6.91 (d, *J* = 1.5 Hz, 1H), 6.81 (d, *J* = 1.5 Hz, 1H), 6.77 (bs, 1H), 3.80 (d, *J* = 7.0 Hz, 1H), 3.76 (dd, *J* = 14.6, 4.4 Hz, 1H), 3.64 (dd, *J* = 14.0, 3.5 Hz, 1H), 3.49 (dd, *J* = 14.5, 4.9 Hz, 1H), 3.33 (m, partially coincident with residual MeOH peak), 2.76 (ddd, *J* = 16.5, 5.7, 1.1 Hz, 1H), 2.45 (ddd, *J* = 16.6, 8.1, 1.9 Hz, 1H), 2.28-2.22 (m, 1H), 2.14-2.09 (m, 1H); <sup>13</sup>C NMR (MeOH-*d*<sub>4</sub>): δ (ppm) 163.3, 163.0, 149.26, 149.19, 127.6, 127.2, 127.1, 123.3, 123.1, 122.8, 119.1, 114.2, 113.6, 113.0, 97.7, 97.6, 44.1, 42.8, 40.0, 37.2, 33.3, 23.7; HRMS-ESI (*m/z*) calcd for [C<sub>22</sub>H<sub>24</sub>Br<sub>2</sub>N<sub>10</sub>O<sub>2</sub>+H]<sup>+</sup>: 621.0510; found: 621.0500.

**Synthesis of 'iso' axinellamine (3-16).**



To a solution of **3-12d** (16.7 mg, 0.016 mmol) in THF (100-μL) was added a freshly-prepared solution of SmI<sub>2</sub> (290-μL, 0.0667 mmol, 0.23 M in THF) at RT. The initially blue mixture became purple after degassed H<sub>2</sub>O (80-μL) was added. It turned to pale yellow after a few minutes. LCMS analysis indicated partial debromination occurred to give partially debrominated

intermediates (**LRMS-ESI** ( $m/z$ ) calcd for  $[C_{22}H_{24}Br_2N_{10}O_4+H]^+$ : 653.04; found: 653.1). The solvent volume was reduced by a stream of Ar. A solution of  $SmI_2$  (750- $\mu$ L, 0.21 mmol, 0.28 M in THF) was added at RT. The solvent was removed by a stream of Ar and more  $SmI_2$  in THF (290  $\mu$ L, 0.23 M, 0.0667 mmol) was added at RT. This concentration-addition procedure was repeated 4 more times and LC shows >60% conversion of the debrominated compounds to the desired product. The reaction was quenched with THF and  $H_2O$  (1.2-mL each) under Ar. The crude solution was diluted with 10%  $CF_3CO_2H$  in  $H_2O$  and purified by HPLC. The desired C1-hemi-aminal compounds (5.5 mg, 39%, d.r. 1:1) (**LRMS-ESI** ( $m/z$ ) calcd for  $[C_{22}H_{27}Br_2N_{10}O_3+H]^+$ : 639.06; found: 639.0) were obtained. These compounds in solution are prone to auto-oxidation so no further purification was performed.

**HPLC conditions:** Waters XBridge RP-18 column (19  $\times$  250-mm) with UV detection at 280-nm; Solution A:  $H_2O$  w/0.1%  $CF_3CO_2H$  and Solution B:  $CH_3CN$  w/0.1%  $CF_3CO_2H$ ; increase gradient of Solution B from 10% to 32%, 0-2 min; then to 33.5%, 7 min; flow rate: 20-mL/min.

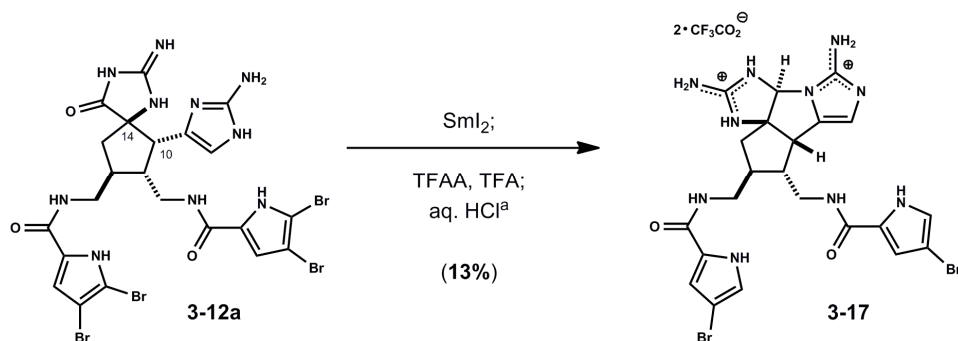
The above mixture (5.5 mg) was dissolved in anhydrous THF (0.28-mL). TFAA (45- $\mu$ L, 0.32 mmol) was added, followed by  $CF_3CO_2H$  (50- $\mu$ L, 0.65 mmol). The vial was sealed and stirred at 60°C for 80 min. The reaction mixture was concentrated and dissolved in MeOH (50- $\mu$ L), then treated with 2M HCl in  $H_2O$  (0.25-mL, 0.5 mmol) at 60°C for 4h. The mixture was diluted with  $H_2O$  and purified by HPLC to afford **3-16** (3.0 mg, 22% from **3-12d**).

**HPLC conditions:** Waters Sunfire C18 column (19  $\times$  250-mm) with UV detection at 280-nm; Solution A:  $H_2O$  w/1%  $CF_3CO_2H$  and Solution B:  $CH_3CN$  w/1%  $CF_3CO_2H$ ; increase gradient of Solution B from 10% to 50%, 0-2 min; then to 51%, 6 min; flow rate: 20- mL/min.

#### 'iso' axinellamine (**3-16**):

$^1H$  NMR (MeOH- $d_4$ ):  $\delta$  (ppm) 6.96 (d,  $J = 1.5$  Hz, 1H), 6.92 (d,  $J = 1.5$  Hz, 1H), 6.88 (d,  $J = 1.5$  Hz, 1H), 6.80 (d,  $J = 1.5$  Hz, 1H), 6.51 (d,  $J = 1.2$  Hz, 1H), 6.00 (s, 1H), 3.76 (dd,  $J = 14.0, 4.2$  Hz, 1H), 3.57 (dd,  $J = 14.0, 4.2$  Hz, 1H), 3.51 (dd,  $J = 13.0, 6.5$  Hz, 1H), 3.44 (d,  $J = 9.3$  Hz, 1H), 3.34 (m, partially coincident with residual MeOH peak), 2.48-2.37 (m, 1H), 2.34-2.17 (m, 2H), 1.94-1.89 (m, 1H);  $^{13}C$  NMR (MeOH- $d_4$ ):  $\delta$  (ppm) 163.0, 162.9, 158.6, 144.3, 133.1, 127.25, 127.21, 123.3, 123.0, 113.4, 106.8, 97.7, 97.5, 85.0, 77.0, 53.3, 51.4, 44.9, 42.6, 41.5, 40.1; **HRMS-ESI** ( $m/z$ ) calcd for  $[C_{22}H_{24}Br_2N_{10}O_2+H]^+$ : 621.0510; found: 621.0500.

#### Synthesis of 'iso' axinellamine (**3-17**).



To a solution of **3-12a** (23.0 mg, 0.022 mmol) in THF (110- $\mu$ L) was added a freshly-prepared solution of SmI<sub>2</sub> (800- $\mu$ L, 0.224 mmol, 0.28M in THF) at -40°C. The initially blue mixture became purple after addition of degassed H<sub>2</sub>O (100- $\mu$ L). The mixture turned to pale yellow after a few minutes. LCMS analysis indicated partial debromination occurred to give partially debrominated intermediate (**LRMS-ESI** (*m/z*) calcd for [C<sub>22</sub>H<sub>24</sub>Br<sub>2</sub>N<sub>10</sub>O<sub>4</sub>+H]<sup>+</sup>: 653.04; found: 653.1). The solvent volume was reduced by a stream of Ar. A solution of SmI<sub>2</sub> (750- $\mu$ L, 0.21 mmol, 0.28 M in THF) was added at RT. The solvent was removed by a stream of Ar and more SmI<sub>2</sub> in THF (800- $\mu$ L, 0.28 M, 0.224 mmol) was added at RT. This concentration-addition procedure was repeated two more times and LCMS analysis shows >60% conversion of the partially debrominated compounds relative to the desired product. The reaction was quenched with degassed THF and H<sub>2</sub>O (1.2-mL each) under Ar. The crude solution was diluted with 10% CF<sub>3</sub>CO<sub>2</sub>H in H<sub>2</sub>O and purified by HPLC. The desired aminal compounds (**LRMS-ESI** (*m/z*) calcd for [C<sub>22</sub>H<sub>27</sub>Br<sub>2</sub>N<sub>10</sub>O<sub>3</sub>+H]<sup>+</sup>: 639.06; found: 639.0) were obtained (8.2 mg, 42%, d.r. 1:1). These compounds in solution are prone to auto-oxidation so no further purification was performed.

**HPLC conditions:** Waters XSelect Fluoro-phenyl column (19 × 250-mm) with UV detection at 280-nm; Solution A: H<sub>2</sub>O w/0.1% CF<sub>3</sub>CO<sub>2</sub>H and Solution B: CH<sub>3</sub>CN w/ 0.1% CF<sub>3</sub>CO<sub>2</sub>H; increase gradient of Solution B from 10% to 25%, 0-2 min; then to 28%, 8 min; flow rate: 20-mL/min.

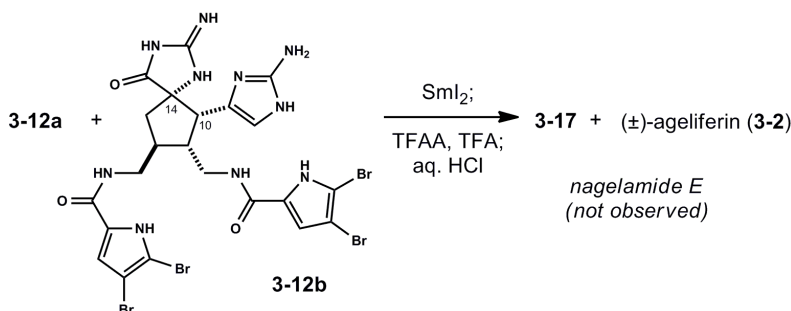
The above mixture (8.2 mg) was dissolved in anhydrous THF (0.28-mL). TFAA (100- $\mu$ L, 0.71 mmol) was added, followed by CF<sub>3</sub>CO<sub>2</sub>H (120- $\mu$ L, 1.57 mmol). The vial was sealed and stirred at 60°C for 7h. The reaction mixture was concentrated and dissolved in THF (0.1-mL), then treated with 2M HCl in H<sub>2</sub>O (0.2-mL, 0.4 mmol) at 60°C for 4h. The reaction mixture was diluted with H<sub>2</sub>O and purified by HPLC to afford **3-17** (2.4 mg, 13% from **3-12a**).

**HPLC conditions:** Waters XBridge RP-18 column (19 × 250-mm) with UV detection at 280-nm; Solution A: H<sub>2</sub>O w/0.1% CF<sub>3</sub>CO<sub>2</sub>H and Solution B: CH<sub>3</sub>CN w/0.1% CF<sub>3</sub>CO<sub>2</sub>H; increase gradient of Solution B from 10% to 31%, 0-2 min; then to 33.3%, 11 min; flow rate: 20-mL/min.

**'iso' axinellamine (3-17):**

**<sup>1</sup>H NMR** (MeOH-*d*<sub>4</sub>):  $\delta$  (ppm) 6.94 (d, *J* = 1.2 Hz, 1H), 6.93 (d, *J* = 1.2 Hz, 1H), 6.88 (d, *J* = 1.2 Hz, 1H), 6.83 (d, *J* = 1.2 Hz, 1H), 6.66 (s, 1H), 5.95 (s, 1H), 3.83 (d, *J* = 9.3 Hz, 1H), 3.56-3.36 (m, 4H), 2.51-2.38 (m, 2H), 2.03-1.96 (m, 2H); **<sup>13</sup>C NMR** (MeOH-*d*<sub>4</sub>):  $\delta$  (ppm) 163.1, 162.9, 158.9, 144.6, 129.4, 127.29, 127.23, 123.11, 123.06, 113.7, 113.6, 108.8, 97.7, 97.5, 84.8, 76.9, 50.8, 43.9, 43.6, 41.5, 40.8, 40.5; **HRMS-ESI** (*m/z*) calcd for [C<sub>22</sub>H<sub>24</sub>Br<sub>2</sub>N<sub>10</sub>O<sub>2</sub>+H]<sup>+</sup>: 621.0510; found: 621.0519.

## Synthesis of 'iso' axinellamine (**3-17**) and ( $\pm$ )-ageliferin (**3-2**) from a mixture of **3-12a** and **3-12b**.



To a solution of **3-12a** and **3-12b** (57 mg, 0.056 mmol; d.r. 4:1) in THF (200- $\mu\text{L}$ ) was added a freshly-prepared solution of  $\text{SmI}_2$  (2.0-mL, 0.56 mmol, 0.28M in THF) at  $-40^\circ\text{C}$ . The initially blue mixture became purple after degassed  $\text{H}_2\text{O}$  (200- $\mu\text{L}$ ) was added. It turned to pale yellow after a few minutes. LCMS analysis indicated partial debromination occurred to give debrominated intermediates **C** (LRMS-ESI ( $m/z$ ) calcd for  $[\text{C}_{22}\text{H}_{24}\text{Br}_2\text{N}_{10}\text{O}_4+\text{H}]^+$ : 653.04; found: 653.1). The solvent volume was reduced by a stream of Ar. A solution of  $\text{SmI}_2$  (1.8-mL, 0.50 mmol, 0.28 M in THF) was added at RT. The reaction was quenched with degassed THF and  $\text{H}_2\text{O}$  (2.0-mL each) under Ar. The crude solution was diluted with 10%  $\text{CF}_3\text{CO}_2\text{H}$  in  $\text{H}_2\text{O}$  and purified by HPLC. The desired *CI*-hemi-aminal compounds were obtained (23.5 mg, 41%) as a mixture of diastereomers.

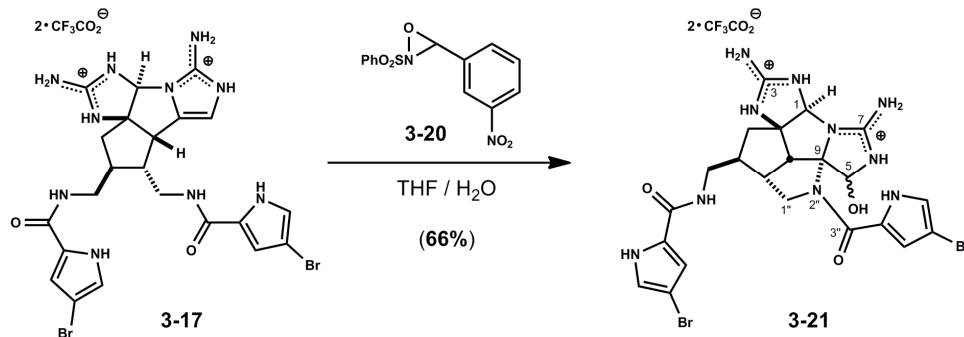
**HPLC conditions:** Waters XSelect Fluoro-phenyl column (19  $\times$  250-mm) with UV detection at 280-nm; Solution A:  $\text{H}_2\text{O}$  w/0.1%  $\text{CF}_3\text{CO}_2\text{H}$  and Solution B:  $\text{CH}_3\text{CN}$  w/ 0.1%  $\text{CF}_3\text{CO}_2\text{H}$ ; increase gradient of Solution B from 10% to 25%, 0-2 min; then to 28%, 8 min; flow rate: 20-mL/min.

Part of the above mixture (22.0 mg, 0.025 mmol) was dissolved in anhydrous THF (0.9-mL). TFAA (360- $\mu\text{L}$ , 2.59 mmol) was added, followed by  $\text{CF}_3\text{CO}_2\text{H}$  (360- $\mu\text{L}$ , 4.7 mmol). The vial was sealed and stirred at  $60^\circ\text{C}$  for 5h. The reaction mixture was concentrated and dissolved in DME (0.6-mL), then treated with 2M HCl in  $\text{H}_2\text{O}$  (1.0-mL, 2.0 mmol) at  $60^\circ\text{C}$  for 14h. It was diluted with  $\text{H}_2\text{O}$  and purified by HPLC to afford **3-17** (6.3 mg, 18% from **3-12a**) and ( $\pm$ )-ageliferin **3-2** (2.0 mg, 22% from **3-12b**).

**HPLC conditions:** Waters XBridge RP-18 column (19  $\times$  250-mm) with UV detection at 280-nm; Solution A:  $\text{H}_2\text{O}$  w/0.1%  $\text{CF}_3\text{CO}_2\text{H}$  and Solution B:  $\text{CH}_3\text{CN}$  w/0.1%  $\text{CF}_3\text{CO}_2\text{H}$ ; increase gradient of Solution B from 10% to 31%, 0-2 min; then to 33.3%, 11 min; flow rate: 20-mL/min.



## Synthesis of pentacyclic aminals (3-21).



To a solution of **3-17** (4.3 mg, 0.0051 mmol) in THF-H<sub>2</sub>O (5:1, 360- $\mu$ L) was added 3-(3-nitrophenyl)-2-(phenylperoxythio)-1,2-oxaziridine (**3-20**) (3.2 mg, 0.010 mmol) at RT. The mixture was stirred at 55°C for 2h. The mixture was diluted with 10% CF<sub>3</sub>CO<sub>2</sub>H in H<sub>2</sub>O and purified by HPLC to give **3-21a** (1.7 mg, 39%) and **3-21b** (1.2 mg, 27%).

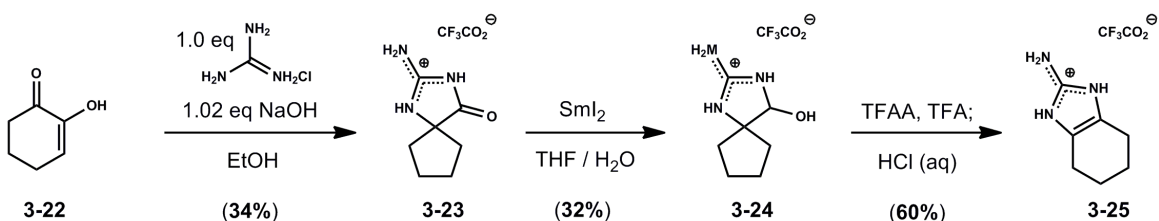
**HPLC conditions:** Waters XBridge RP18 column (19  $\times$  250-mm) with UV detection at 280-nm; Solution A: H<sub>2</sub>O w/0.1% CF<sub>3</sub>CO<sub>2</sub>H and Solution B: CH<sub>3</sub>CN w/0.1% CF<sub>3</sub>CO<sub>2</sub>H; increase gradient of Solution B from 10% to 28%, 0-2 min; then to 30%, 10 min; flow rate: 20-mL/min.

### Aminal (**3-21a**):

<sup>1</sup>H NMR (MeOH-*d*<sub>4</sub>):  $\delta$  (ppm) 7.03 (d, *J* = 1.4 Hz, 1H), 6.91 (d, *J* = 1.5 Hz, 1H), 6.77 (d, *J* = 1.5 Hz, 1H), 6.76 (d, *J* = 1.4 Hz, 1H), 5.99 (s, 1H), 5.62 (s, 1H), 4.49 (dd, *J* = 14.4, 8.1 Hz, 1H), 3.50-3.35 (m, 2H), 2.79 (d, *J* = 12.2 Hz, 1H), 2.74-2.65 (m, 1H), 2.46 (dd, *J* = 14.0, 14.0 Hz, 1H), 2.35-2.28 (m, 1H), 1.99-1.94 (m, 2H); <sup>1</sup>H NMR (DMSO-*d*<sub>6</sub>):  $\delta$  (ppm) 12.04 (s, 1H), 11.76 (s, 1H), 9.84 (s, 1H), 8.97 (s, 1H), 8.90 (bs, 2H), 8.36 (s, 1H), 8.25 (dd, *J* = 6.0, 6.0 Hz, 1H), 8.17 (bs, 2H), 7.30 (s, 1H), 7.16 (s, 1H), 6.96 (s, 1H), 6.83 (s, 1H), 6.78 (s, 1H), 5.82 (s, 1H), 5.53 (s, 1H), 4.35 (dd, *J* = 14.5, 9.0 Hz, 1H), 3.50 (m, 2H, coincident with residual H<sub>2</sub>O peak; refer to data in MeOH-*d*<sub>4</sub>), 2.63-2.60 (m, 1H), 2.52 (m, 1H, coincident with residual DMSO peak), 2.29-2.24 (m, 1H), 2.18-2.15 (m, 1H), 1.99-1.93 (m, 1H), 1.84-1.78 (m, 1H); <sup>13</sup>C NMR (MeOH-*d*<sub>4</sub>):  $\delta$  (ppm) 163.0, 158.6, 157.5, 127.2, 124.5, 124.4, 123.1, 115.9, 113.4, 99.2, 97.9, 97.6, 84.8, 77.6, 72.4 (weak), 54.0, 44.7, 42.8, 40.0, 38.1; HRMS-ESI (*m/z*) calcd for [C<sub>22</sub>H<sub>24</sub>Br<sub>2</sub>N<sub>10</sub>O<sub>3</sub>+H]<sup>+</sup>: 637.0459; found: 637.0442.

**Aminal (3-21b):**

<sup>1</sup>H NMR (MeOH-*d*<sub>4</sub>): δ (ppm) 6.97 (d, *J* = 1.4 Hz, 1H), 6.93 (d, *J* = 1.5 Hz, 1H), 6.77 (d, *J* = 1.5 Hz, 1H), 6.62 (d, *J* = 1.4 Hz, 1H), 5.41 (s, 1H), 5.22 (s, 1H), 4.11 (d, *J* = 10.6 Hz, 1H), 4.01 (d, *J* = 10.4 Hz, 1H), 3.92 (dd, *J* = 10.6, 7.0 Hz, 1H), 3.56-3.44 (m, 2H), 2.80-2.75 (m, 1H), 2.49-2.46 (m, 1H), 2.21-2.15 (m, 1H), 1.90 (dd, *J* = 12.5, 12.5 Hz, 1H); <sup>1</sup>H NMR (DMSO-*d*<sub>6</sub>): δ (ppm) 11.97 (s, 1H), 11.81 (s, 1H), 9.89 (s, 1H), 9.04 (s, 1H), 8.88 (s, 1H), 8.68 (s, 1H), 8.42 (bs, 2H), 8.22 (dd, *J* = 6.0, 6.0 Hz, 1H), 7.18 (d, *J* = 5.2 Hz, 1H), 7.10 (dd, *J* = 3.2, 1.6 Hz, 1H), 6.96 (dd, *J* = 2.8, 1.5 Hz, 1H), 6.83 (s, 1H), 6.65 (s, 1H), 5.30 (s, 1H), 5.07 (dd, *J* = 5.3, 2.1 Hz, 1H), 3.94 (d, *J* = 10.6 Hz, 1H), 3.81 (dd, *J* = 10.6, 6.8 Hz, 1H), 3.78 (d, *J* = 10.4 Hz, 1H), 3.42-3.38 (m, 2H), 2.60-2.57 (m, 1H), 2.15 (dd, *J* = 13.0, 5.4 Hz, 1H), 2.05-1.93 (m, 1H), 1.75 (dd, *J* = 12.9, 12.9 Hz, 1H); <sup>13</sup>C NMR (MeOH-*d*<sub>4</sub>): δ (ppm) 162.9, 162.1, 158.7, 158.6, 127.1, 126.8, 123.9, 116.6, 113.3, 99.9, 98.0, 97.7, 84.6, 83.4, 81.4, 57.1, 54.2, 45.1, 44.6, 42.1, 41.3.; HRMS-ESI (*m/z*) calcd for [C<sub>22</sub>H<sub>24</sub>Br<sub>2</sub>N<sub>10</sub>O<sub>3</sub>+H]<sup>+</sup>: 637.0459; found: 637.0449.

**Procedures for the synthesis of model system 2-amino-1,3-diazaspiro[4.4]non-1-en-4-ol (3-24) and ring-expansive rearrangement to provide 4,5,6,7-tetrahydro-1H-benzo[d]imidazol-2-amine (3-25).**

1,2-Cyclohexanedione was prepared from cyclohexanone according to literature procedures.<sup>[2]</sup>

**2-Imino-1,3-diazaspiro[4.4]nonan-4-one (3-23).**

Guanidine hydrochloride (6.81 g, 71 mmol) was stirred with granulated sodium hydroxide (2.92 g, 73 mmol, 1.02 equiv) in EtOH (355-mL, 0.2 M) at RT for 5 min. 1,2-cyclohexanedione (8.25 g, 71 mmol) was added to the opaque white solution and the reaction was heated to reflux. The solution became clear and light yellow and was heated for 2.5h until judged complete by TLC analysis. The reaction was cooled to RT and concentrated in vacuo to provide a crude brown foam. The crude free base was dissolved in 10-mL MeOH, filtered to remove salts and loaded onto a dry silica gel column. Purification by flash column chromatography, isocratic CH<sub>2</sub>Cl<sub>2</sub> / MeOH / conc. NH<sub>4</sub>OH (90:9:1) for 8 column volumes followed by column flush with isocratic CH<sub>2</sub>Cl<sub>2</sub> / MeOH / conc. NH<sub>4</sub>OH (50:49:1) gave **3-23** as a tan solid (3.70 g, 34%). This material showed spectroscopic data consistent with literature.<sup>[3]</sup>

**2-Imino-1,3-diazaspiro[4.4]nonan-4-one (3-23):**

<sup>1</sup>H NMR (500 MHz, MeOH-*d*<sub>4</sub>): δ (ppm) 2.04-1.95 (m, 2H), 1.89-1.71 (m, 6H); <sup>13</sup>C NMR (125 MHz, MeOH-*d*<sub>4</sub>): δ (ppm) 195.8, 170.9, 73.3, 38.4, 26.5.

The isolated free base (**3-23**) can be readily converted to the trifluoroacetate salt (**3-23**) CF<sub>3</sub>CO<sub>2</sub>H by dissolution in MeOH and addition of 1.2 equiv CF<sub>3</sub>CO<sub>2</sub>H followed by concentration in vacuo.

**2-Imino-1,3-diazaspiro[4.4]nonan-4-one (3-23) CF<sub>3</sub>CO<sub>2</sub>H:**

<sup>1</sup>H NMR (500 MHz, MeOH-*d*<sub>4</sub>): δ (ppm) 2.16-2.08 (m, 2H), 1.98-1.85 (m, 6H); <sup>13</sup>C NMR (125 MHz, MeOH-*d*<sub>4</sub>): δ (ppm) 179.5, 158.5, 71.6, 38.4, 26.2; HRMS-ESI (*m/z*) calcd for [C<sub>7</sub>H<sub>11</sub>N<sub>3</sub>O+H]<sup>+</sup>: 154.0980; found: 154.0986.

**2-Amino-1,3-diazaspiro[4.4]non-1-en-4-ol (3-24):**

To a solution of **3-23** (14 mg, 0.052 mmol) in degassed THF (0.2-mL) was added a freshly prepared solution of SmI<sub>2</sub> (2.0-mL, 0.56 mmol, 0.28 M in THF) at -40°C. The initially blue mixture became purple after addition of degassed H<sub>2</sub>O (0.2-mL). The reaction turned to pale yellow after a few min. The solvent volume was reduced by a stream of Ar. A solution of SmI<sub>2</sub> (2.0-mL, 0.56 mmol, 0.28 M in THF) was added at RT. This concentration-addition procedure was repeated two more times. The reaction was diluted with 10% CF<sub>3</sub>CO<sub>2</sub>H in H<sub>2</sub>O and purified by HPLC. The desired hemiaminal **3-24** was obtained (4.5 mg, 32%). This material showed spectroscopic data consistent with literature.<sup>[4]</sup>

**HPLC conditions:** Waters Sunfire C18 column (19 × 250-mm) with UV detection at 280-nm; Solution A: H<sub>2</sub>O w/1% CF<sub>3</sub>CO<sub>2</sub>H and Solution B: CH<sub>3</sub>CN w/1% CF<sub>3</sub>CO<sub>2</sub>H; increase gradient of Solution B from 10% to 25%, 0-2 min; then to 28.8%, 9 min; flow rate: 20-mL/min.

**4,5,6,7-Tetrahydro-1H-benzo[d]imidazol-2-amine (3-25).**

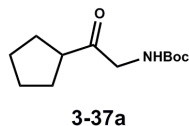
2-Amino-1,3-diazaspiro[4.4]non-1-en-4-ol (**3-24**) (4.5 mg, 0.0167 mmol, CF<sub>3</sub>CO<sub>2</sub>H salt) was dissolved in anhydrous THF (0.8-mL). TFAA (120-μL, 0.86 mmol) was added followed by CF<sub>3</sub>CO<sub>2</sub>H (120-μL, 1.57 mmol). The reaction vial was sealed and stirred at 70°C for 6h. The reaction mixture was concentrated and treated with aqueous 2M HCl (0.6-mL, 1.2 mmol) at RT for 2h. The resultant solution was diluted with H<sub>2</sub>O and purified by HPLC to afford **3-25** (2.7 mg, 64%). This material showed spectroscopic data consistent with literature<sup>[5]</sup> and an authentic sample (**3-38**) which was prepared from the condensation reaction of 2-aminocyclohexanone<sup>[6]</sup> and cyanamide (5 equiv) in H<sub>2</sub>O (0.1 M, pH = 4.3, adjusted with 10 % NaOH) at 100°C for 3h.

**HPLC conditions:** Waters XBridge RP18 column (19 × 250-mm) with UV detection at 280-nm; Solution A: H<sub>2</sub>O w/0.1% CF<sub>3</sub>CO<sub>2</sub>H and Solution B: CH<sub>3</sub>CN w/0.1% CF<sub>3</sub>CO<sub>2</sub>H; increase gradient of Solution B from 10% to 32%, 0-2 min; then to 33.5%, 6 min; flow rate: 20-mL/min.

**4,5,6,7-Tetrahydro-1H-benzo[d]imidazol-2-amine (3-25) CF<sub>3</sub>CO<sub>2</sub>H:**

<sup>1</sup>H NMR (500 MHz, MeOH-*d*<sub>4</sub>): δ (ppm) 2.43-2.41 (m, 4H), 1.82-1.80 (m, 4H); <sup>13</sup>C NMR (125 MHz, MeOH-*d*<sub>4</sub>): δ (ppm) 148.0, 121.9, 23.2, 21.1; HRMS-ESI (*m/z*) calcd for [C<sub>7</sub>H<sub>11</sub>N<sub>3</sub>+H]<sup>+</sup>: 138.1031; found: 138.1044.

### Preparation of *tert*-butyl (2-cyclopentyl-2-oxoethyl)carbamate (**3-37a**).

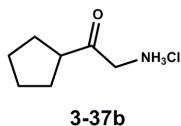


To a cooled solution of Boc-Gly-N(OCH<sub>3</sub>)(CH<sub>3</sub>) (4.0 g, 18.3 mmol, 1.0 equiv) in THF (91.5-mL) was added EtMgBr (6.1-mL, 18.3 mmol, 1.0 equiv, 3.0 M in THF) dropwise. Mild gas formation was observed and the solution was allowed to stir at -10°C for 10 min. A solution of cyclopentyl magnesium bromide (44-mL, 22.0 mmol, 1.2 equiv, as prepared above in THF) was added via syringe and the reaction temperature was maintained at 0°C with an ice-water bath. After 30 min, the reaction was warmed to RT and immersed in a pre-heated oil bath at 70°C for 3h. The reaction was judged complete by TLC analysis and cooled to 0°C, carefully quenched with saturated aqueous NaHCO<sub>3</sub> and diluted with EtOAc (150-mL). The bi-phasic mixture was allowed to separate and the aqueous layer was discarded. The organic layer was washed with H<sub>2</sub>O, brine, dried over Na<sub>2</sub>SO<sub>4</sub>, filtered and concentrated in vacuo. The residue was purified by flash column chromatography eluting with gradient hexanes/EtOAc (100% to (3:2)) to provide side product *tert*-butyl (2-oxobutyl)carbamate (650 mg, 19%) followed by desired *tert*-butyl (2-cyclopentyl-2-oxoethyl)carbamate **3-37a** (1.71 g, 41%) as an off-white waxy solid.

#### *tert*-butyl (2-cyclopentyl-2-oxoethyl)carbamate (**3-37a**):

<sup>1</sup>H NMR (500 MHz, CHCl<sub>3</sub>-*d*<sub>1</sub>): δ (ppm) 5.26 (bs, 1H), 4.05 (d, *J* = 4.6 Hz, 2H), 2.86 (ddd, *J* = 16.1, 8.4, 7.6 Hz, 1H), 1.87-1.79 (m, 2H), 1.77-1.54 (m, 6H), 1.43 (s, 9H); <sup>13</sup>C NMR (125 MHz, CHCl<sub>3</sub>-*d*<sub>1</sub>): δ (ppm) 208.2, 155.8, 79.8, 49.7, 49.1, 29.2, 28.5, 26.1.

### Preparation of 2-amino-1-cyclopentylethanone (**3-37b**) (HCl).

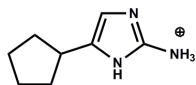


To a cooled solution of *tert*-butyl (2-cyclopentyl-2-oxoethyl)carbamate **3-37a** (1.6 g, 7.0 mmol, 1.0 equiv) in CH<sub>2</sub>Cl<sub>2</sub> (39.1-mL) was added CF<sub>3</sub>CO<sub>2</sub>H (5.0-mL) at 0°C. The reaction was stirred for 1h and subsequently warmed to RT for an additional 1h. The light yellow solution was concentrated in vacuo to provide a crude residue. The residue was dissolved in MeOH (15-mL) followed by the addition of anhydrous HCl (5-mL, 4.0 M in 1,4-dioxane) at RT. The acidic solution was concentrated in vacuo to provide 2-amino-1-cyclopentylethanone **3-37b** (HCl) (1.1 g, 99%) as a white powder that was used in the following step without purification.

#### 2-amino-1-cyclopentylethanone (**3-37b**) (HCl):

<sup>1</sup>H NMR (500 MHz, MeOH-*d*<sub>4</sub>): δ (ppm) 4.01 (s, 2H), 3.05 (ddd, *J* = 15.9, 8.6, 7.4 Hz, 1H), 1.96-1.87 (m, 2H), 1.83-1.75 (m, 2H), 1.73-1.61 (m, 4H); <sup>13</sup>C NMR (125 MHz, MeOH-*d*<sub>4</sub>): δ (ppm) 206.6, 49.8, 47.5, 29.7, 26.9.

## Preparation of 5-cyclopentyl-1H-imidazol-2-amine (3-38) (CF<sub>3</sub>CO<sub>2</sub>H).



3-38 CF<sub>3</sub>CO<sub>2</sub><sup>⊖</sup>

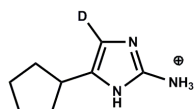
An aqueous solution (47-mL) of 2-amino-1-cyclopentylethanone **3-37b (HCl)** (1.1 g, 7.0 mmol, 1.0 equiv) and cyanamide (867 mg, 21.0 mmol, 3.0 equiv) was adjusted from pH = 2.5 to pH = 4.3 with 10 wt % aqueous NaOH. The solution was immersed in a pre-heated oil bath (105°C) and allowed to reflux for 3h. The cloudy solution was cooled to RT, diluted with anhydrous EtOH (50-mL) and concentrated in vacuo at 50°C to provide crude 5-cyclopentyl-1H-imidazol-2-amine (**3-38**) (**HCl**) as a light brown oil.

### 5-cyclopentyl-1H-imidazol-2-amine (3-38) (CF<sub>3</sub>CO<sub>2</sub>H):

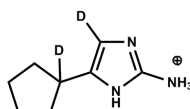
<sup>1</sup>H NMR (500 MHz, H<sub>2</sub>O-*d*<sub>2</sub>): δ (ppm) 6.48 (d, *J* = 1.1 Hz, 1H), 2.96 (q, *J* = 7.9 Hz, 1H), 2.02-1.94 (m, 2H), 1.74-1.47 (m, 6H); <sup>13</sup>C NMR (125 MHz, H<sub>2</sub>O-*d*<sub>2</sub>)\*: δ (ppm) 146.3, 132.1, 107.0, 35.0, 31.3, 24.4; LRMS-ESI (*m/z*) calcd for [C<sub>8</sub>H<sub>13</sub>N<sub>3</sub>+H]<sup>+</sup>: 152.1; found: 152.1.

\*<sup>13</sup>C NMR obtained with HCl salt of **3-38**.

### Deuterium Incorporation Studies: Preparation of deuterated 2-aminoimidazoles (3-39) and (3-40).



3-39 CF<sub>3</sub>CO<sub>2</sub><sup>⊖</sup>



3-40 CF<sub>3</sub>CO<sub>2</sub><sup>⊖</sup>

A portion of crude 5-cyclopentyl-1H-imidazol-2-amine (**3-38**) was purified by HPLC to afford 5-cyclopentyl-1H-imidazol-2-amine (**3-38**) (CF<sub>3</sub>CO<sub>2</sub>H).

**HPLC conditions:** Waters Sunfire C18 column (19 × 250-mm) with UV detection at 280-nm; Solution A: H<sub>2</sub>O w/1% CF<sub>3</sub>CO<sub>2</sub>H and Solution B: CH<sub>3</sub>CN w/1% CF<sub>3</sub>CO<sub>2</sub>H; increase gradient of Solution B from 5% to 10%, 0.5-2 min; 10% to 60%, 2-10 min; flow rate: 20-mL/min.

A solution of 5-cyclopentyl-1H-imidazol-2-amine (CF<sub>3</sub>CO<sub>2</sub>H) (**3-38**) (50.1 mg, 0.189 mmol) in H<sub>2</sub>O-*d*<sub>2</sub> (5.0-mL) was dispersed into a 10-mL microwave reaction vial and sealed. The sample was stirred at 180°C for 1 min in a CEM microwave reactor. The reaction was cooled to RT and a 500-μL was taken for <sup>1</sup>H NMR analysis. Deuterium exchange at *t* = 1 min was judged complete by <sup>1</sup>H NMR analysis as depicted in 5-cyclopentyl-1H-imidazol-2-amine (**3-39**)-*d*<sub>1</sub> (CF<sub>3</sub>CO<sub>2</sub>H).

**5-cyclopentyl-1H-imidazol-2-amine (3-39)-*d*<sub>1</sub> (CF<sub>3</sub>CO<sub>2</sub>H):**

<sup>1</sup>H NMR (500 MHz, H<sub>2</sub>O-*d*<sub>2</sub>): δ (ppm) 2.96 (q, *J* = 7.9 Hz, 1H), 2.02-1.94 (m, 2H), 1.74-1.47 (m, 6H). LRMS-ESI (*m/z*) calcd for [C<sub>8</sub>H<sub>12</sub>D<sub>1</sub>N<sub>3</sub>+H]<sup>+</sup>: 153.1; found: 153.1.

The reaction solution was sealed and stirred 180°C for 5 min in a CEM microwave reactor and analyzed as described above. This process was repeated with the same reaction solution at further time points (t = 10 min, 30 min, 180 min, 360 min, 540 min). The deuterium exchange was judged complete (>95%) at 540 min (t = 9h). A portion of the remaining solution was purified by HPLC to obtain 5-cyclopentyl-1H-imidazol-2-amine (3-40)-*d*<sub>2</sub> (CF<sub>3</sub>CO<sub>2</sub>H) as a white film after lyophilization of aqueous fractions. A yield was not obtained for this reaction.

**HPLC conditions:** Waters Sunfire C18 column (19 × 250-mm) with UV detection at 280-nm; Solution A: H<sub>2</sub>O w/1% CF<sub>3</sub>CO<sub>2</sub>H and Solution B: CH<sub>3</sub>CN w/1% CF<sub>3</sub>CO<sub>2</sub>H; increase gradient of Solution B from 5% to 10%, 0.5-2 min; 10% to 60%, 2-10 min; flow rate: 20-mL/min.

**5-cyclopentyl-1H-imidazol-2-amine (3-40)-*d*<sub>2</sub> (CF<sub>3</sub>CO<sub>2</sub>H):**

<sup>1</sup>H NMR (500 MHz, H<sub>2</sub>O-*d*<sub>2</sub>): δ (ppm) 1.98-1.91 (m, 2H), 1.74-1.47 (m, 6H); LRMS-ESI (*m/z*) calcd for [C<sub>8</sub>H<sub>11</sub>D<sub>2</sub>N<sub>3</sub>+H]<sup>+</sup>: 154.1; found: 154.1.

### 3.5.3 Experimental References.

[1] (a) Ding, H.; Roberts, A. G.; Harran, P. G. *Angew. Chem., Int. Ed.* **2012**, 51, 4340; (b) Li, Q.; Hurley, P.; Ding, H.; Roberts, A. G.; Akella, R.; Harran, P. G. *J. Org. Chem.* **2009**, 74, 5909.

[2] For the preparation of 1,2-cyclohexanedione (CAS Registry Number: 765-87-7): Hach, C. C.; Banks, C. V.; Diehl, H. *Org. Syn.*, **1963** *Coll. Vol. 4*, 229; **1952** Vol. 32, 35.

[3] The conversion of 1,2-cyclohexanedione to **3-23** via an  $\alpha$ -diketone rearrangement with guanidines has been reported previously. The reported procedure was modified to provide adequate quantities of model substrate **3-23**. Anzai, K. *Bull. Chem. Soc. Jap.* **1969**, 42, 3314. (Compound **VIII** in text)

[4] Su, S.; Sieple, I. B.; Young, I. S.; Baran, P. S. *J. Am. Chem. Soc.*, **2008**, 130, 16490–16491. (Compound **11** in text).

[5] 4,5,6,7-Tetrahydro-1H-benzo[d]imidazol-2-amine (**3-25**) was previously prepared and characterized as the ethyl sulfate salt. Little, T. L.; Webber, S. E. *J. Org. Chem.* **1994**, 59, 7299.

[6] For the preparation of 2-aminocyclohexanone (CAS Registry Number: 22374-48-7): (a) Baumgarten, H. E.; Peterson, J. M. *J. Am. Chem. Soc.* **1960**, 82, 459; (b) Alt, G. H.; Knowles, W. S. *Org. Syn.*, **1973** *Coll. Vol. 5*, 208; **1965** Vol. 45, 16.

## APPENDIX TWO

### Spectra Relevant to Chapter Three:

#### Chapter 3 – Total Synthesis of (±)-Ageliferin *via* N-amidinyliminium Ion Rearrangement

*adapted in part from*

#### Total Synthesis of Ageliferin *via* N-amidinyliminium Ion Rearrangement

*Hui Ding, Andrew G. Roberts and Patrick G. Harran*

*Chem. Sci.* **2013**, *4*, 303 – 306.



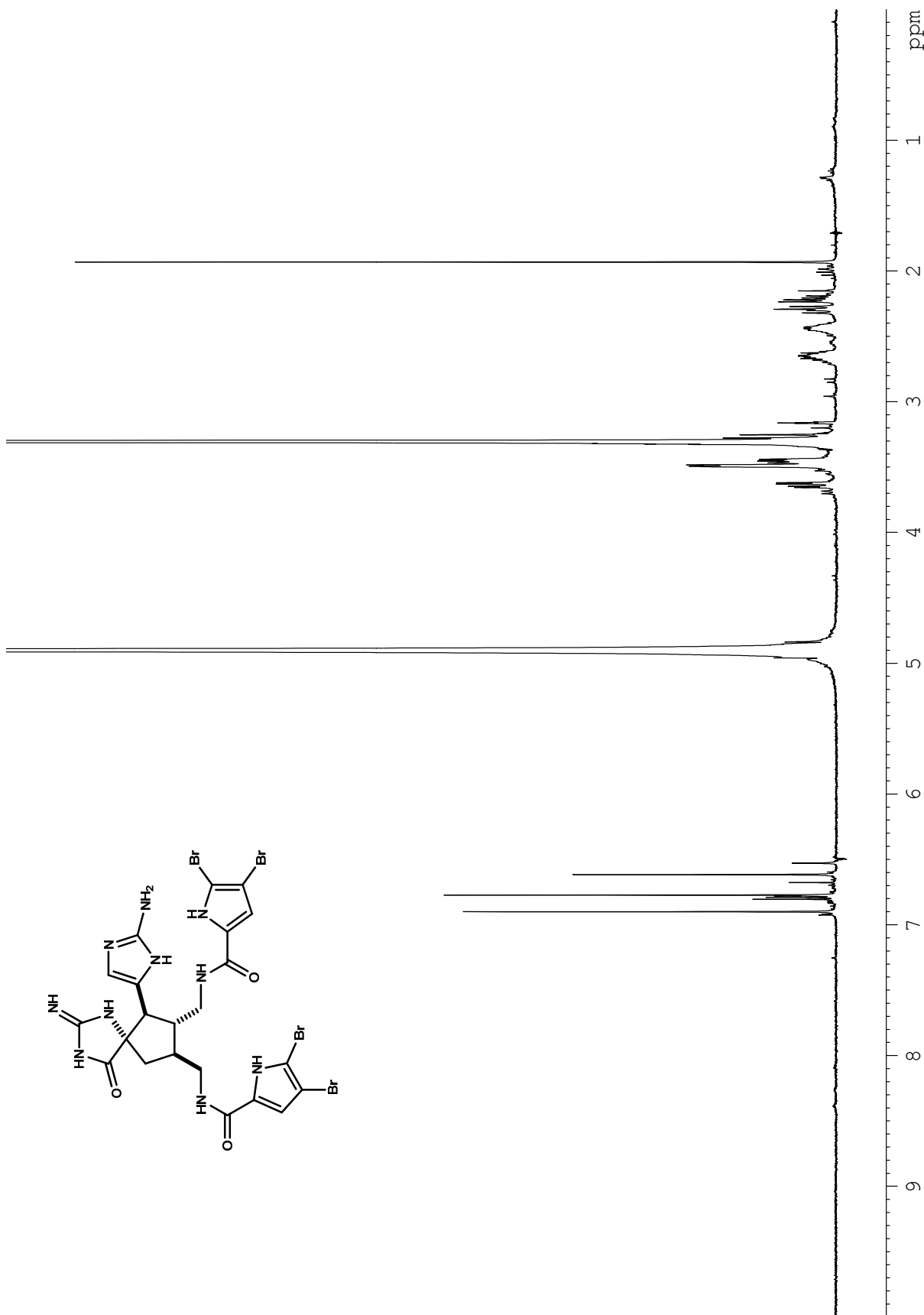


**Figure A2.1.** <sup>1</sup>H NMR (500 MHz, MeOH-*d*<sub>4</sub>) spectrum of compound 3-12d (2·CF<sub>3</sub>CO<sub>2</sub>H).

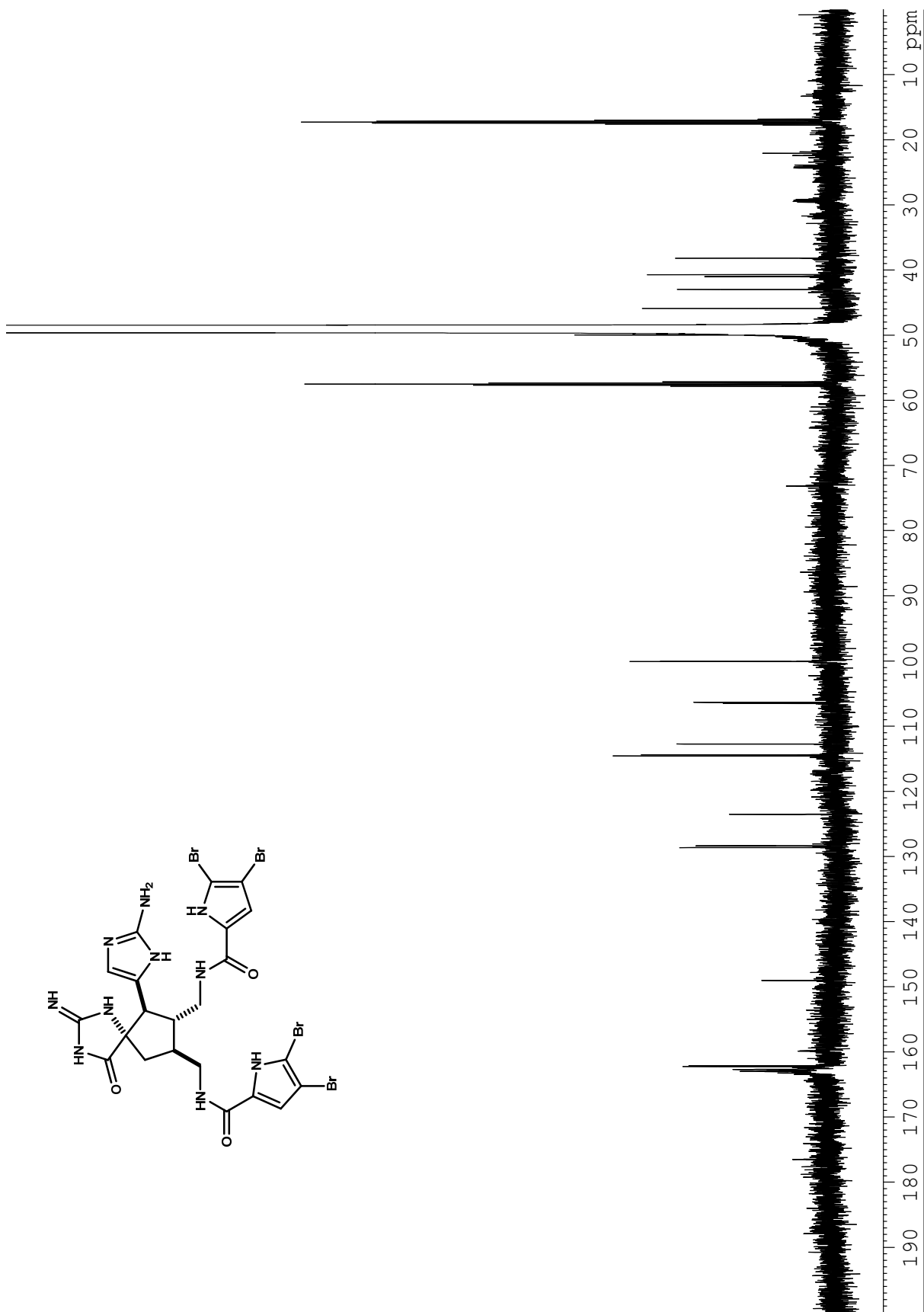


**Figure A2.2.**  $^{13}\text{C}$  NMR (125 MHz,  $\text{MeOH-}d_4$ ) spectrum of compound 3-12d ( $2 \cdot \text{CF}_3\text{CO}_2\text{H}$ ).

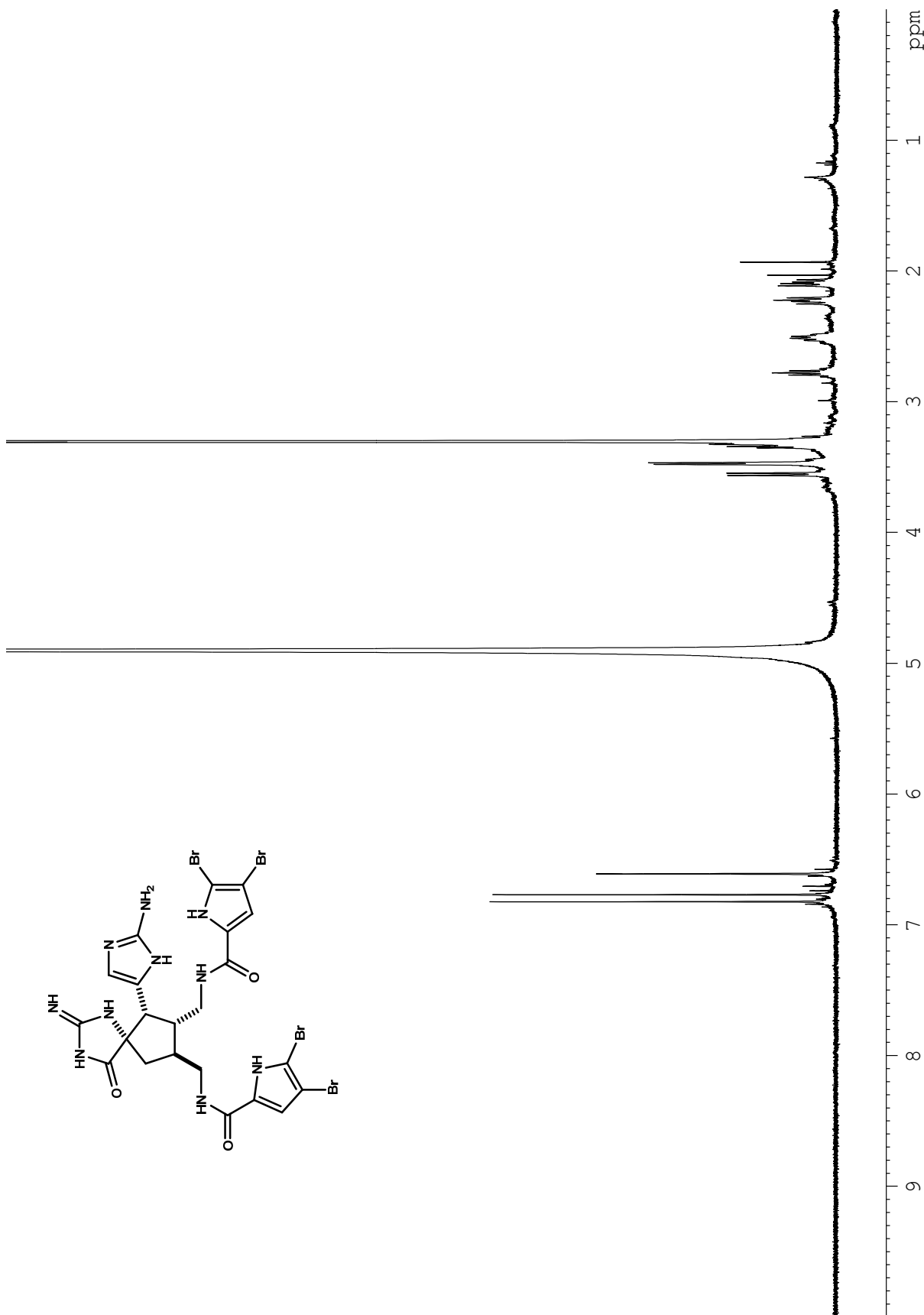


**Figure A2.3.** <sup>1</sup>H NMR (500 MHz, MeOH-*d*<sub>4</sub>) spectrum of compound 3-12b (2·CF<sub>3</sub>CO<sub>2</sub>H).

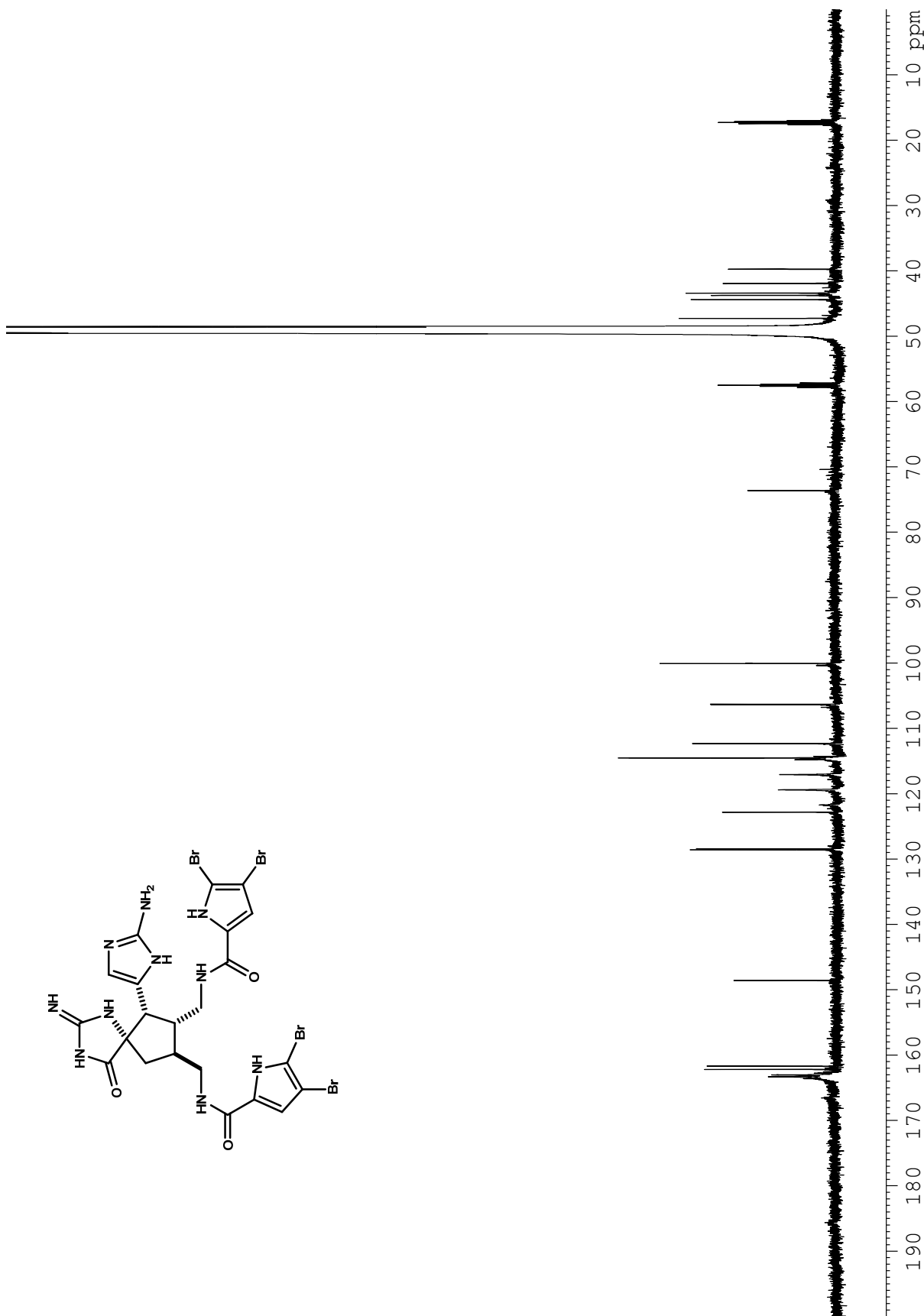


**Figure A2.4.** <sup>13</sup>C NMR (125 MHz, MeOH-*d*<sub>4</sub>) spectrum of compound 3-12b (2·CF<sub>3</sub>CO<sub>2</sub>H).

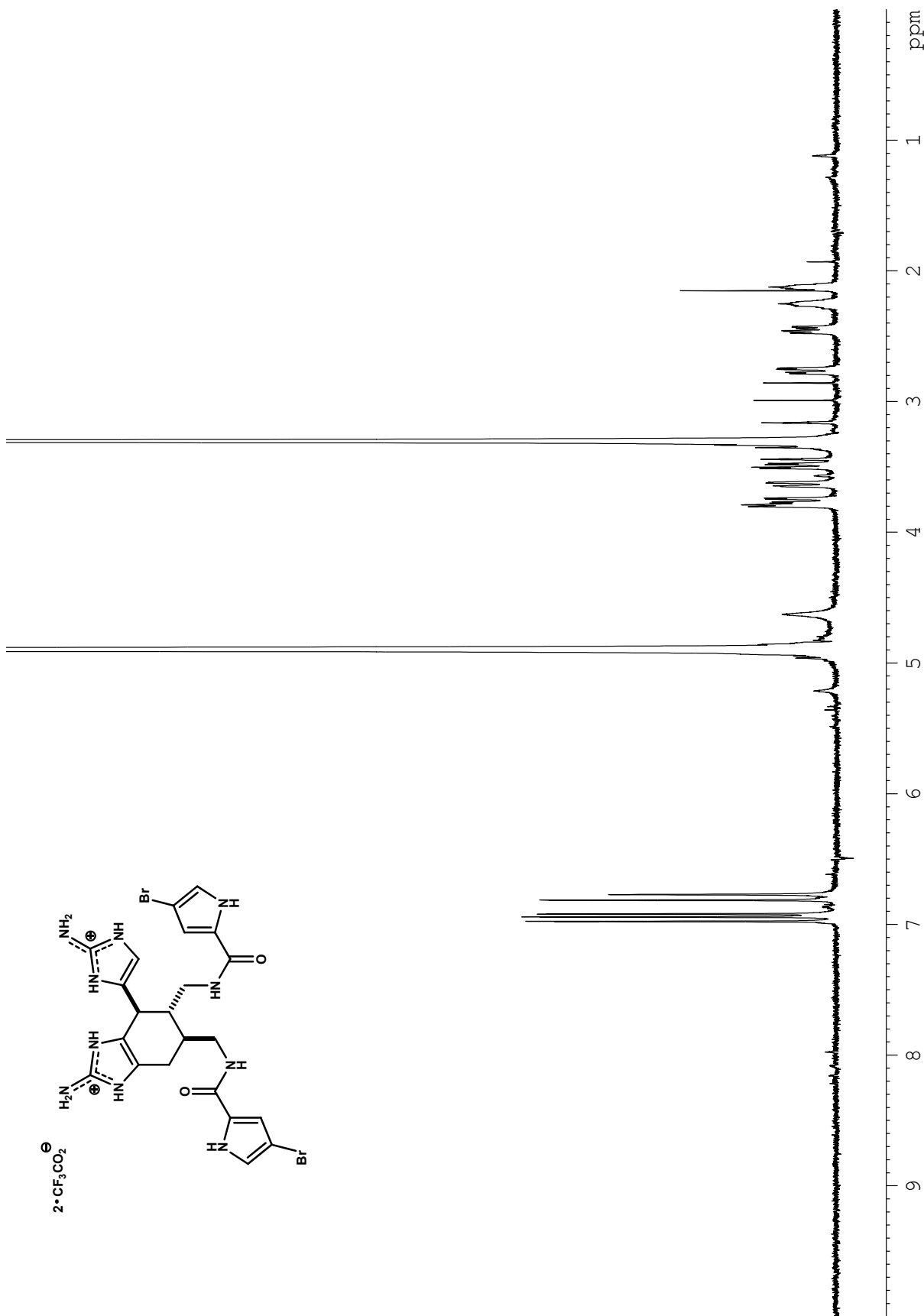


**Figure A2.5.** <sup>1</sup>H NMR (500 MHz, MeOH-*d*<sub>4</sub>) spectrum of compound 3-2 (2·CF<sub>3</sub>CO<sub>2</sub>H).

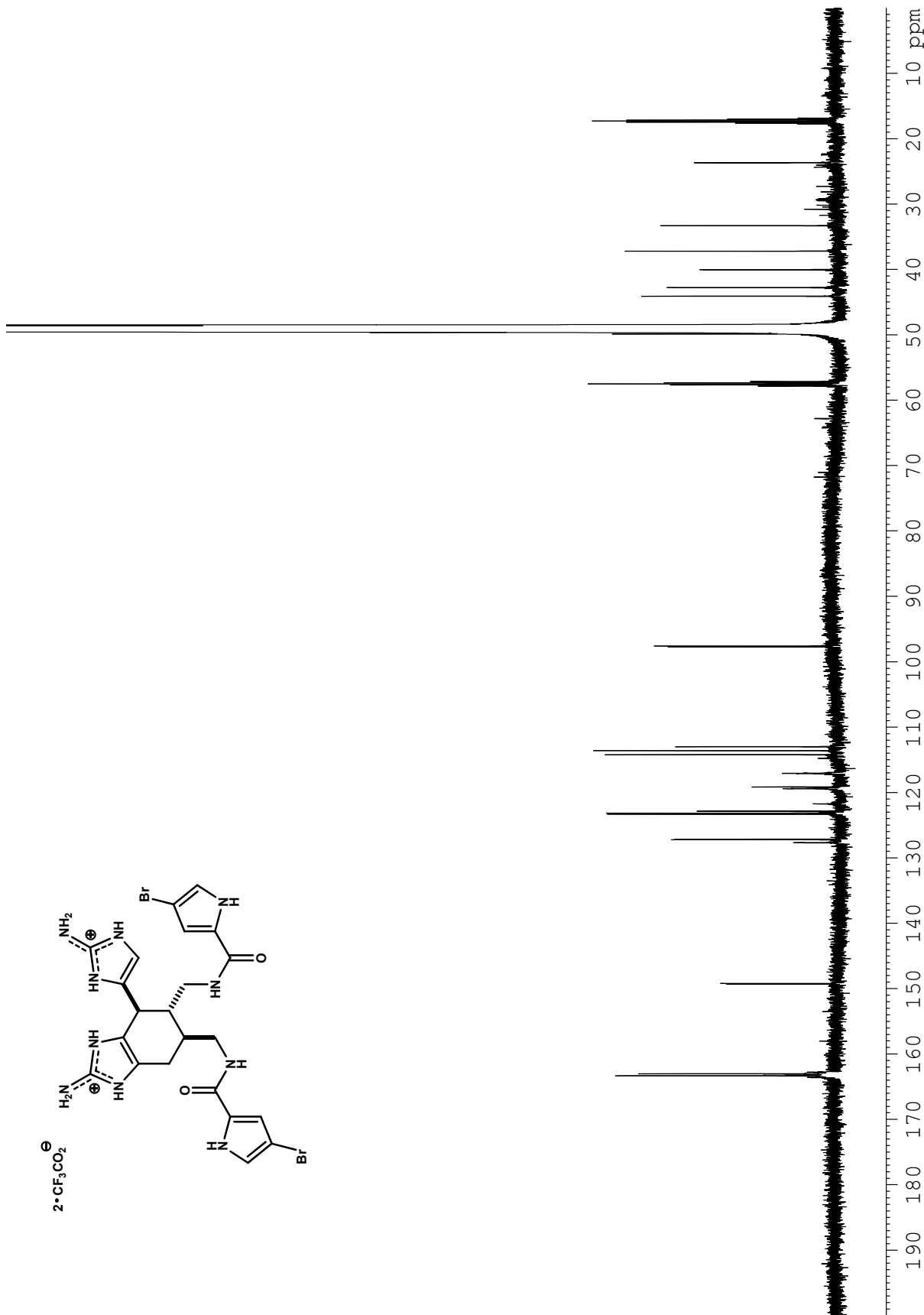


**Figure A2.6.** <sup>13</sup>C NMR (125 MHz, MeOH-*d*<sub>4</sub>) spectrum of compound 3-2 (2·CF<sub>3</sub>CO<sub>2</sub>H).

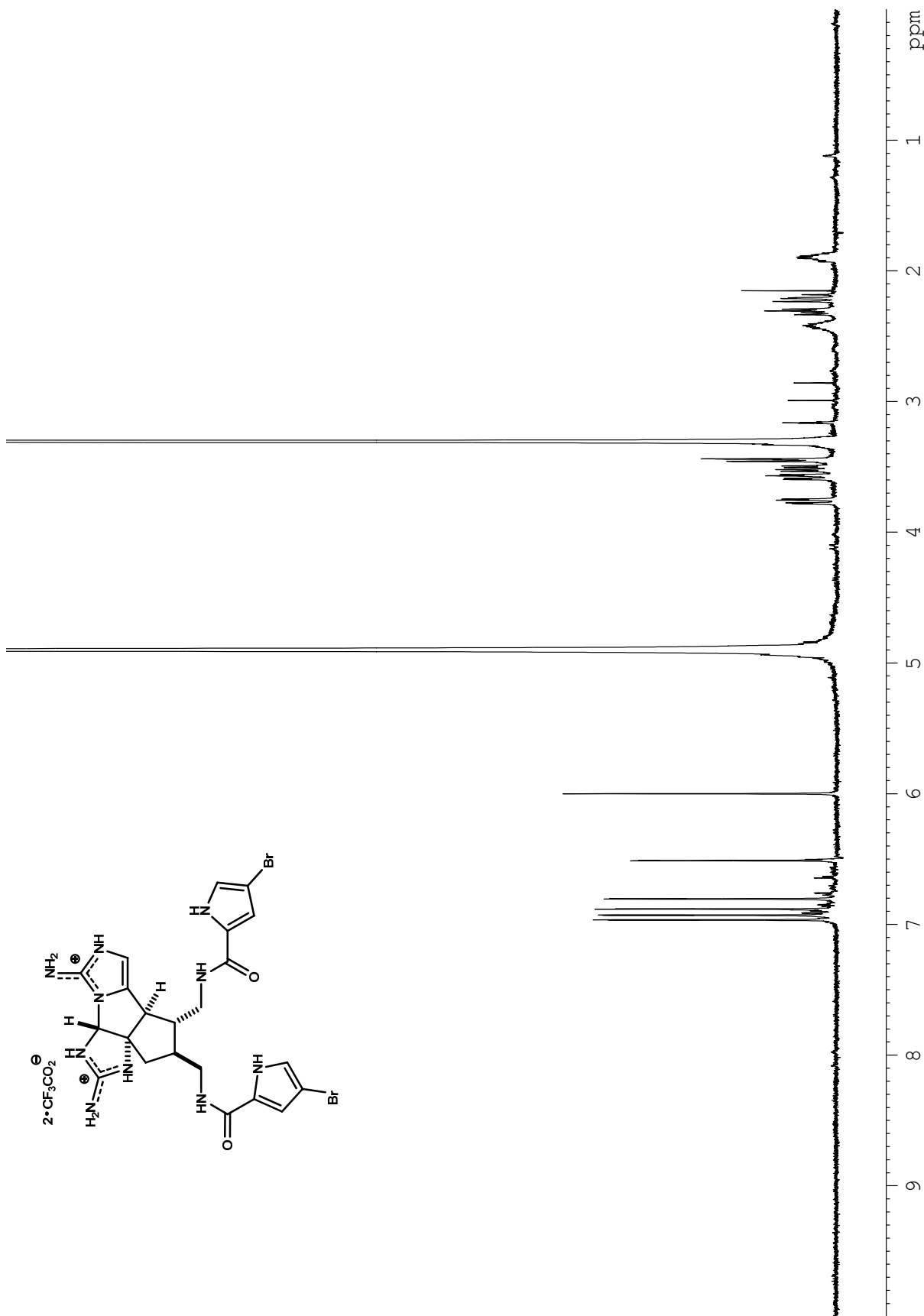


**Figure A2.7.** <sup>1</sup>H NMR (500 MHz, MeOH-*d*<sub>4</sub>) spectrum of compound 3-16 (2·CF<sub>3</sub>CO<sub>2</sub>H).

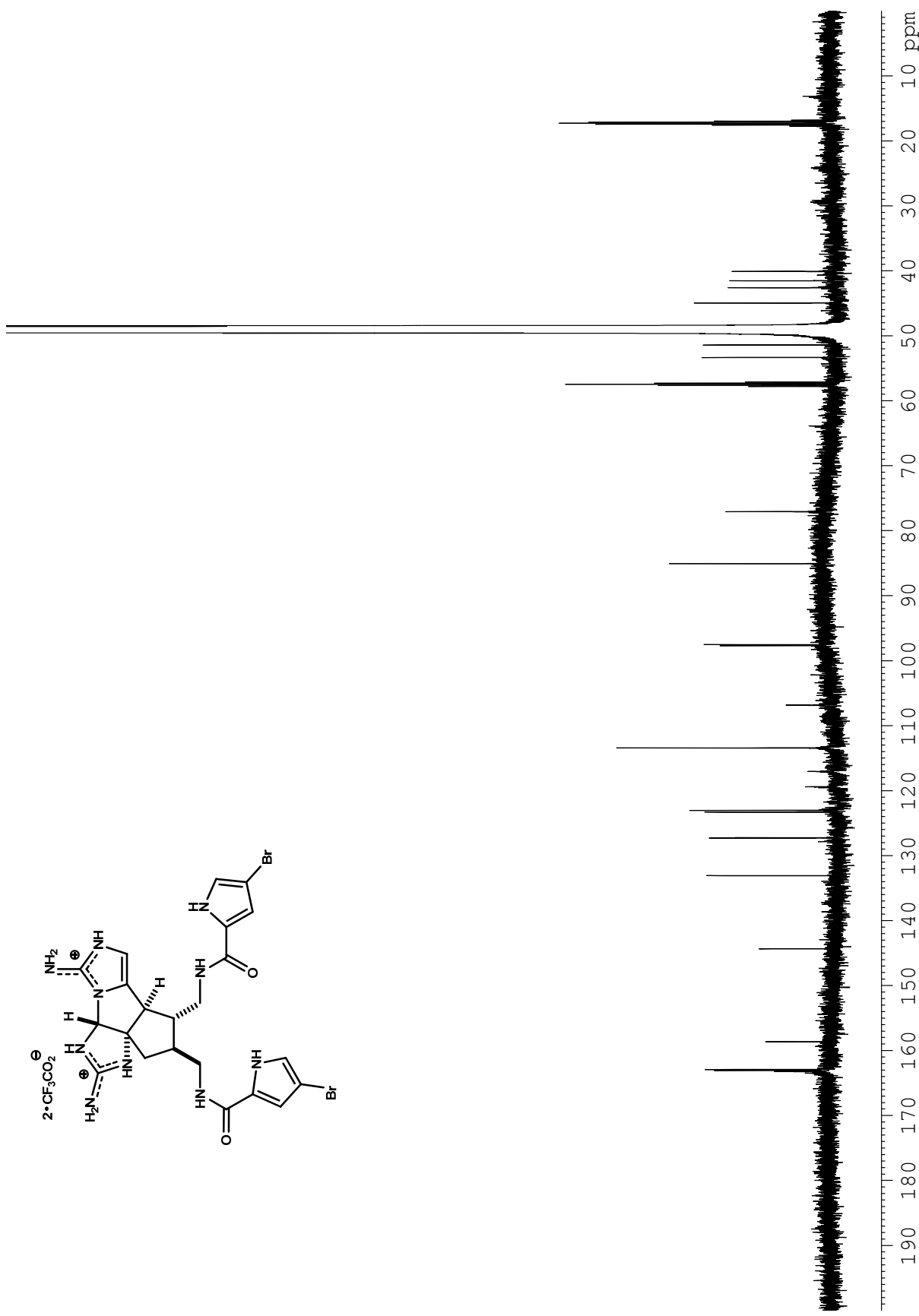


**Figure A2.8.** <sup>13</sup>C NMR (125 MHz, MeOH-*d*<sub>4</sub>) spectrum of compound 3-16 (2·CF<sub>3</sub>CO<sub>2</sub>H).



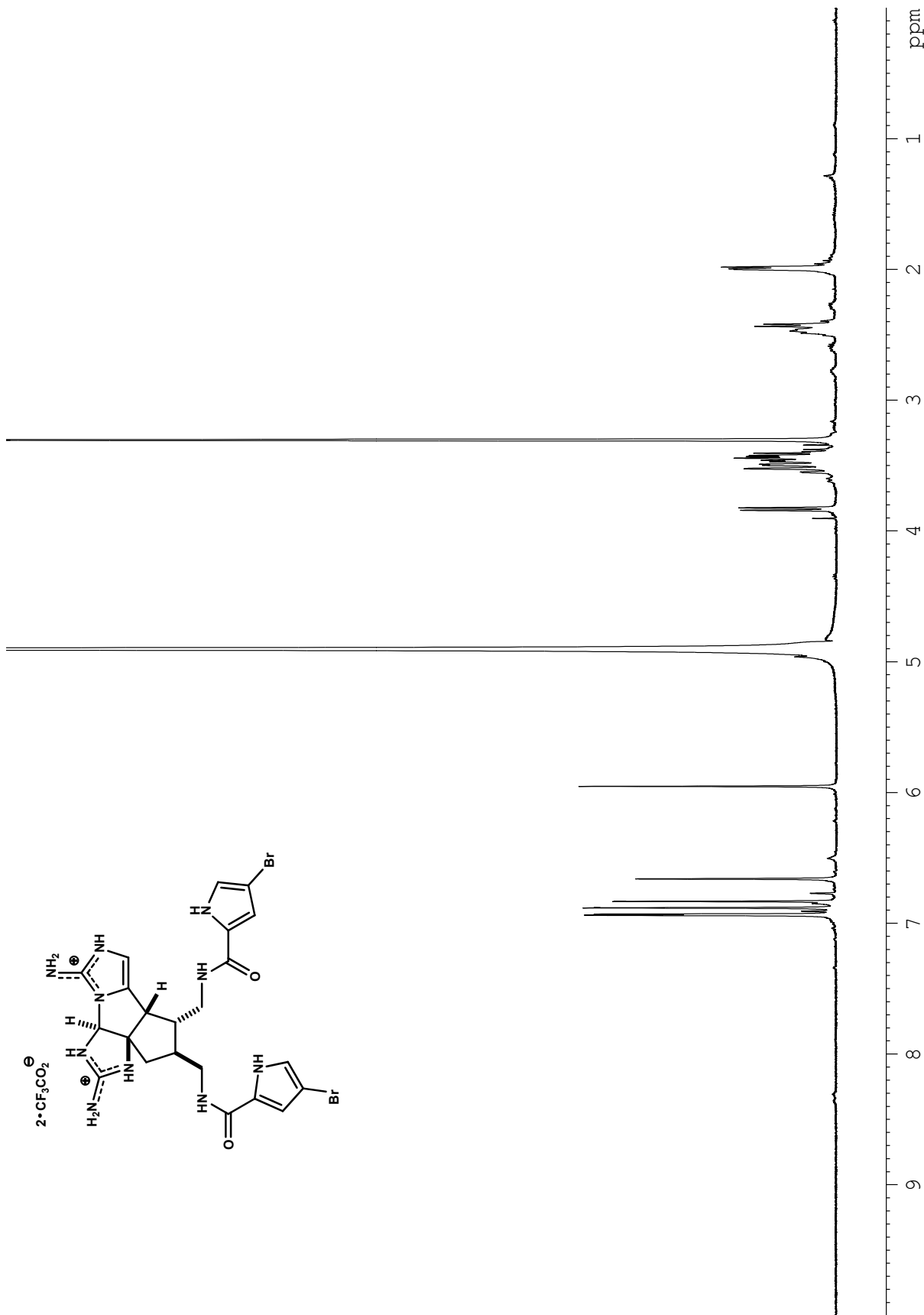


**Figure A2.9.**  $^1\text{H}$  NMR (500 MHz,  $\text{MeOH-}d_4$ ) spectrum of compound **3-17** ( $2 \cdot \text{CF}_3\text{CO}_2\text{H}$ ).

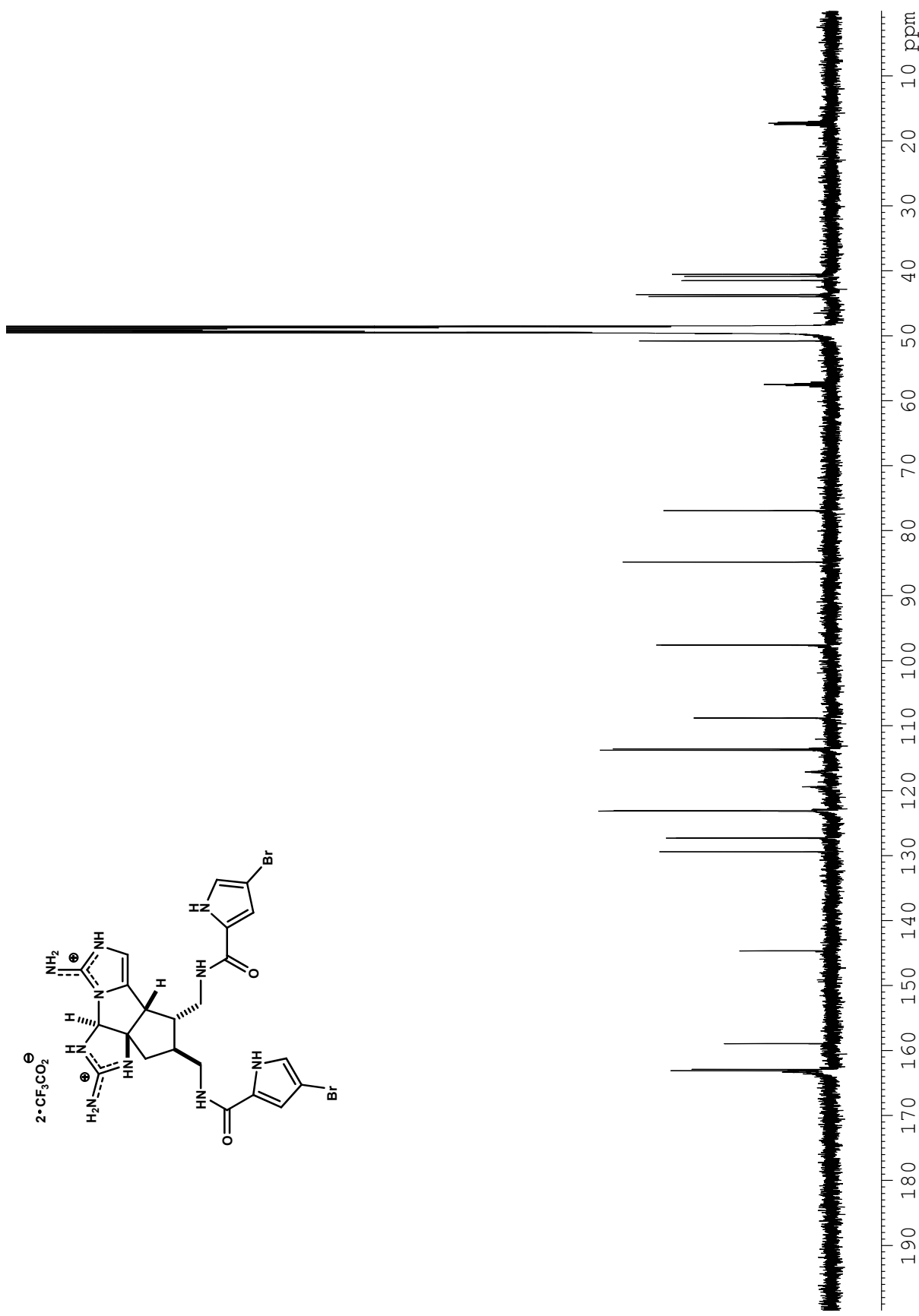


**Figure A2.10.** <sup>13</sup>C NMR (125 MHz, MeOH-*d*<sub>4</sub>) spectrum of compound 3-17 (2·CF<sub>3</sub>CO<sub>2</sub>H).

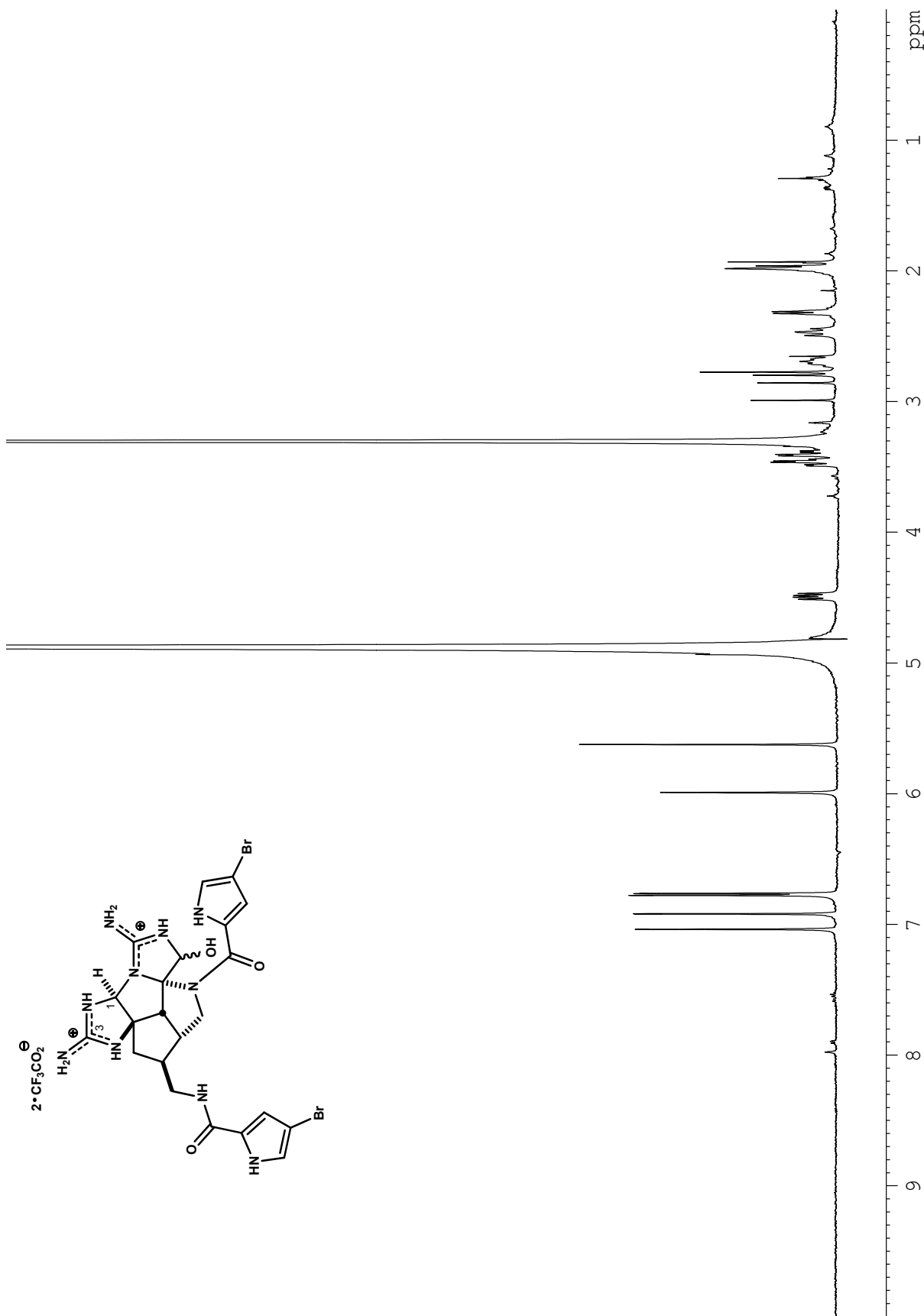


**Figure A2.11.** <sup>1</sup>H NMR (500 MHz, MeOH-*d*<sub>4</sub>) spectrum of compound **3-21a** (2·CF<sub>3</sub>CO<sub>2</sub>H).

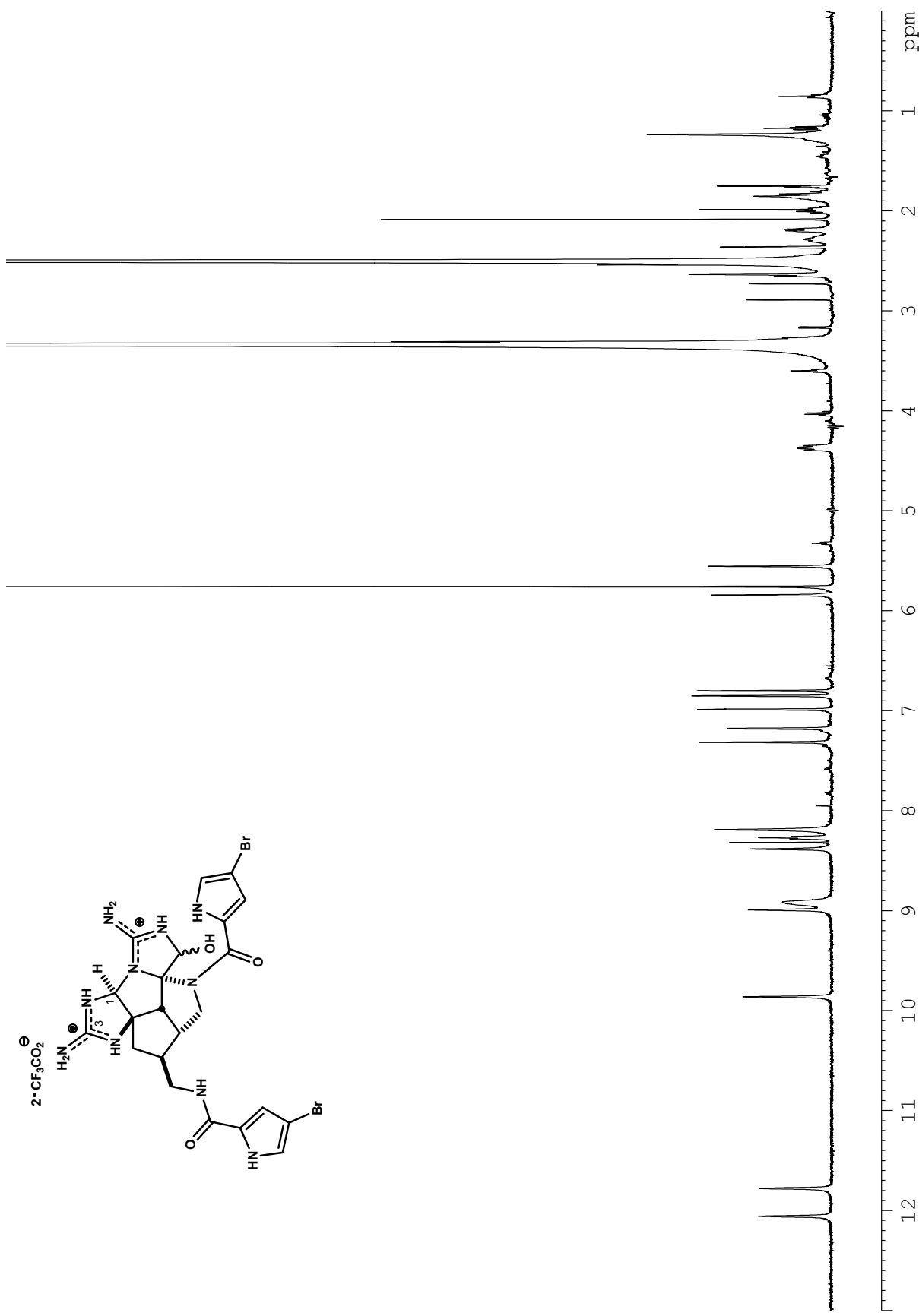


**Figure A2.12.** <sup>1</sup>H NMR (500 MHz, DMSO-*d*<sub>6</sub>) spectrum of compound 3-21a (2·CF<sub>3</sub>CO<sub>2</sub>H).

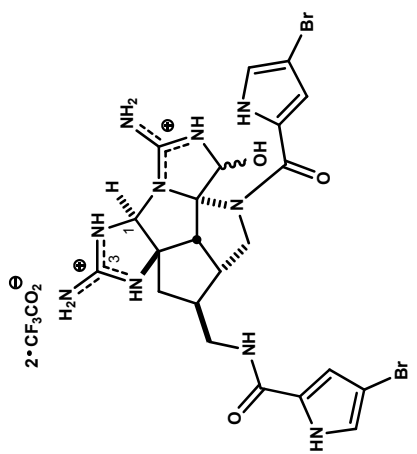
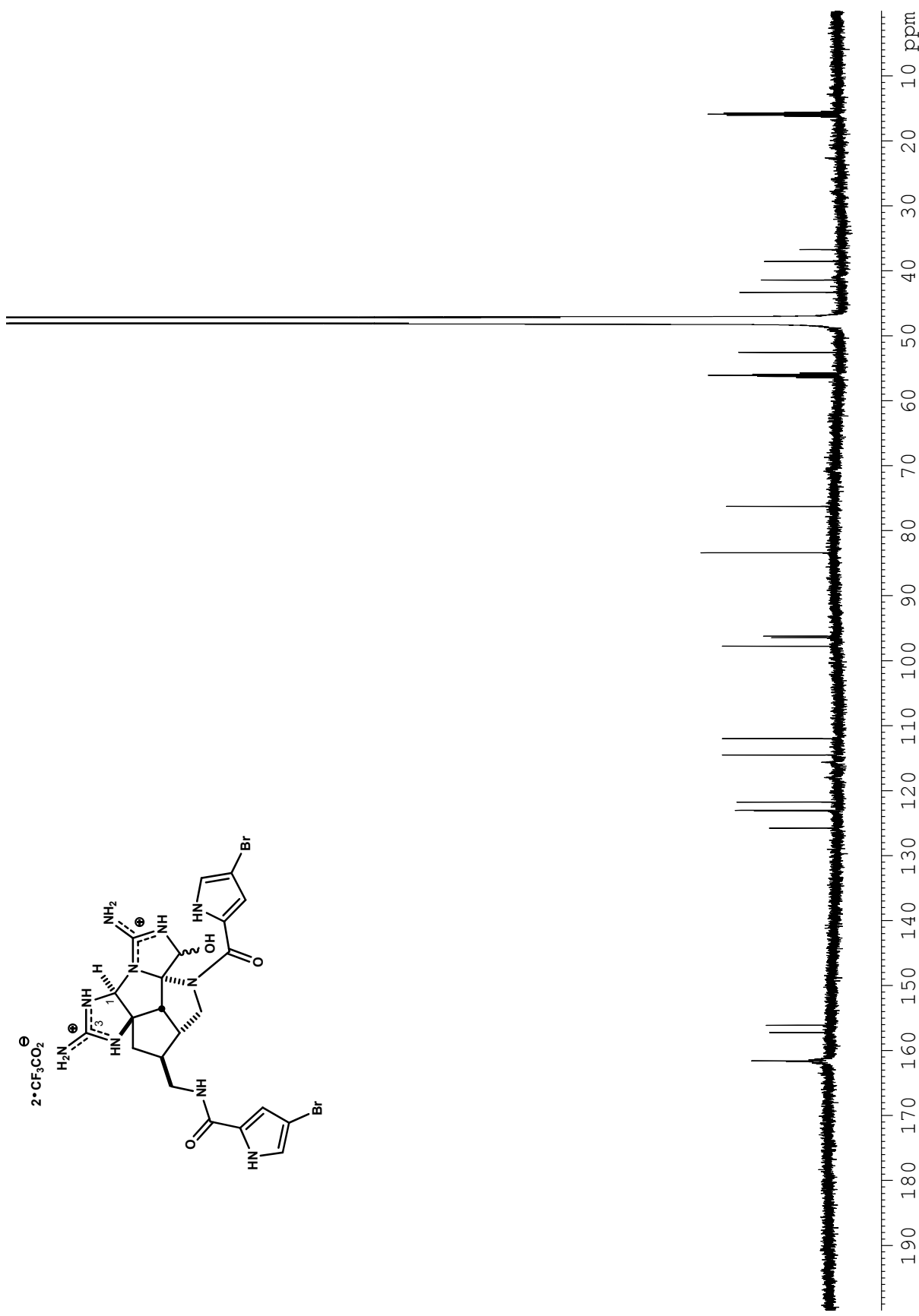


**Figure A2.13.** <sup>13</sup>C NMR (125 MHz, MeOH-*d*<sub>4</sub>) spectrum of compound **3-21a** (2-CF<sub>3</sub>CO<sub>2</sub>H).

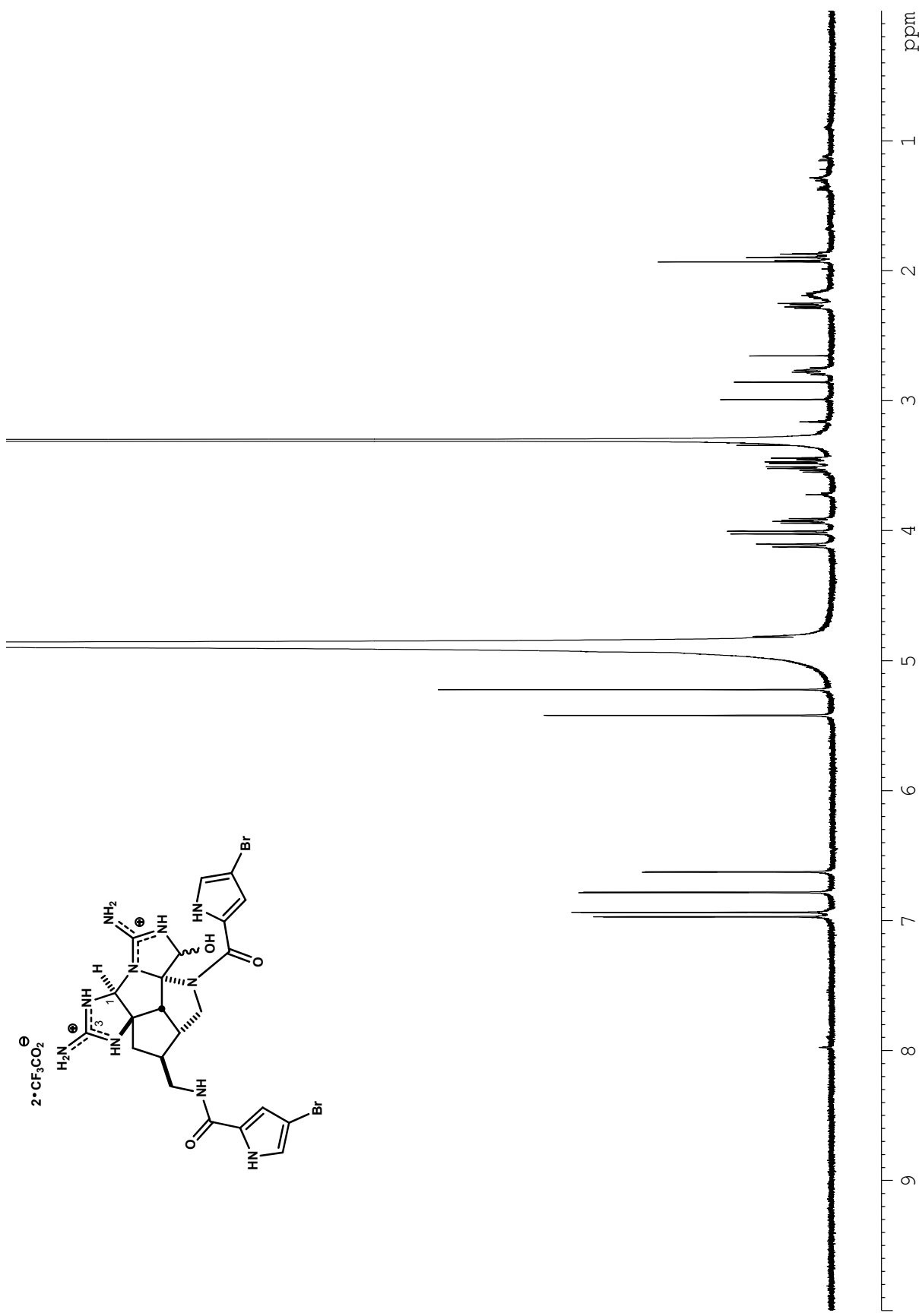


**Figure A2.14.** <sup>1</sup>H NMR (500 MHz, MeOH-*d*<sub>4</sub>) spectrum of compound 3-21b (2·CF<sub>3</sub>CO<sub>2</sub>H).

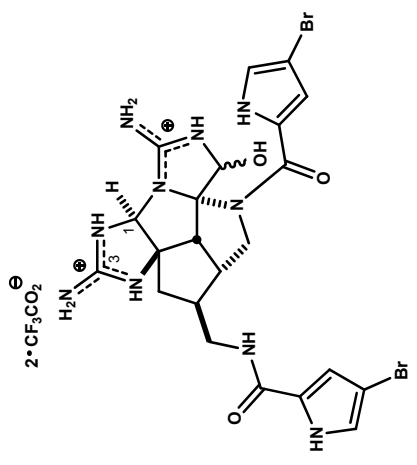
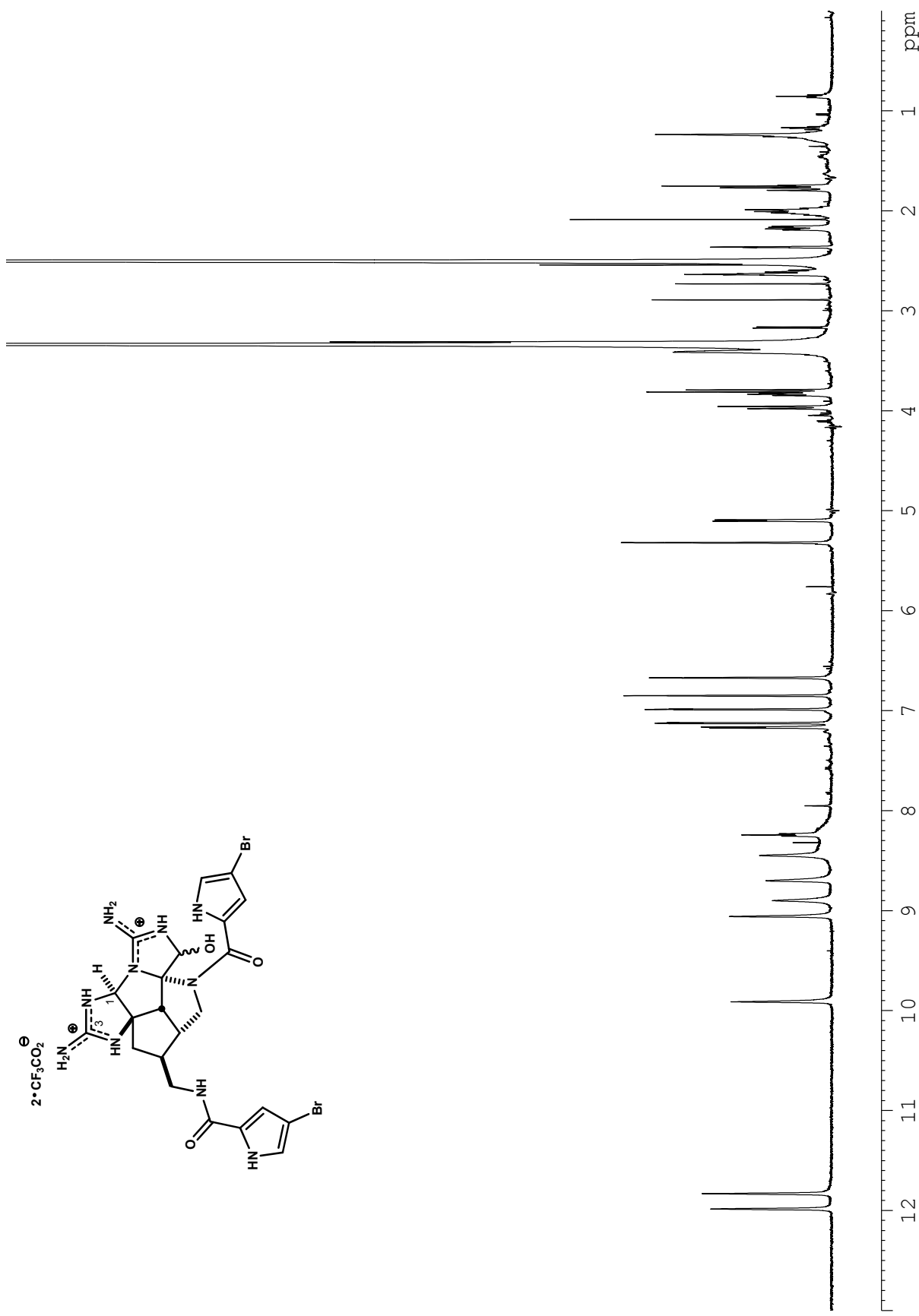


**Figure A2.15.** <sup>1</sup>H NMR (500 MHz, DMSO-*d*<sub>6</sub>) spectrum of compound 3-21b (2 · CF<sub>3</sub>CO<sub>2</sub>H).

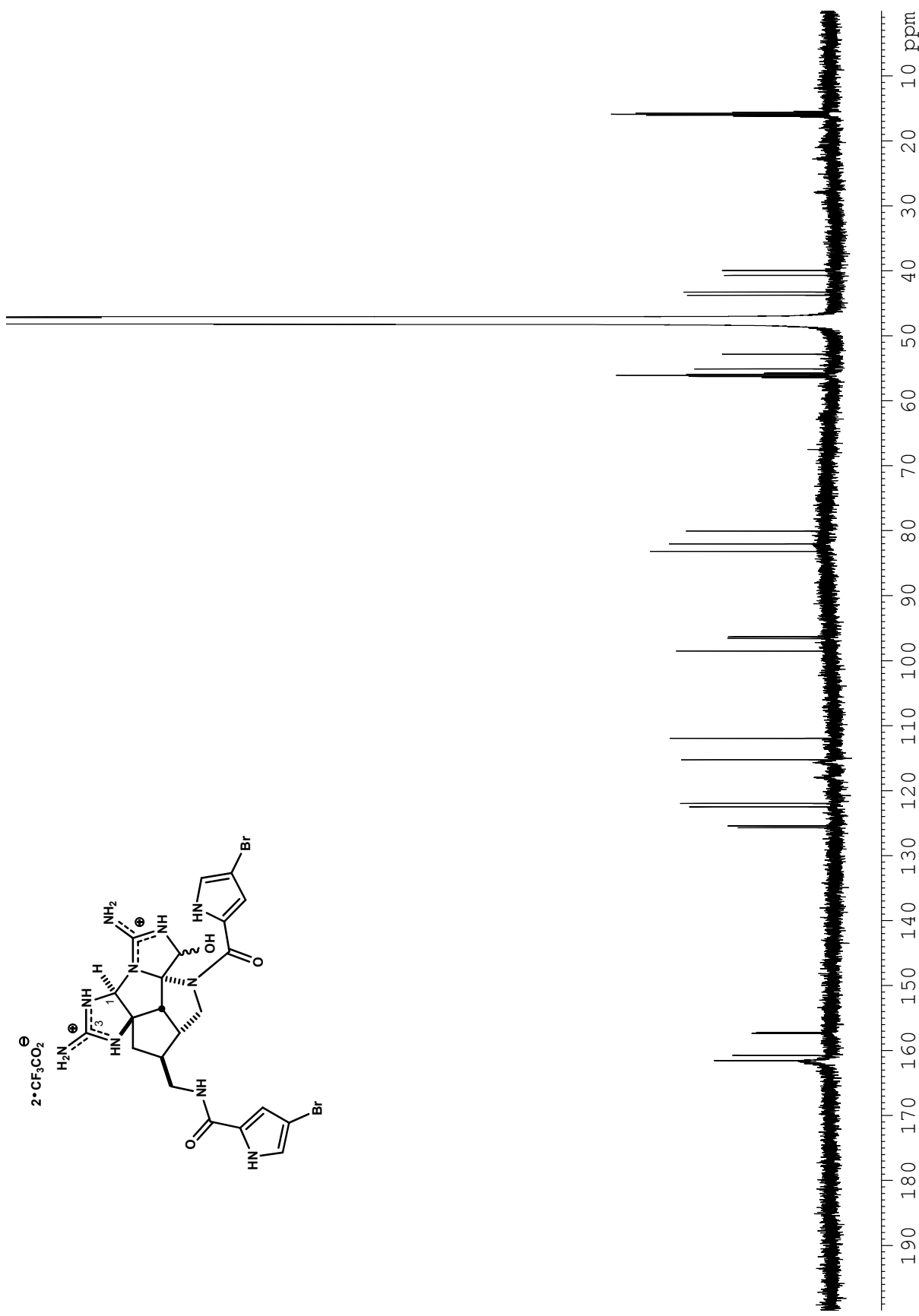


**Figure A2.16.** <sup>13</sup>C NMR (125 MHz, MeOH-*d*<sub>4</sub>) spectrum of compound 3-21b (2·CF<sub>3</sub>CO<sub>2</sub>H).



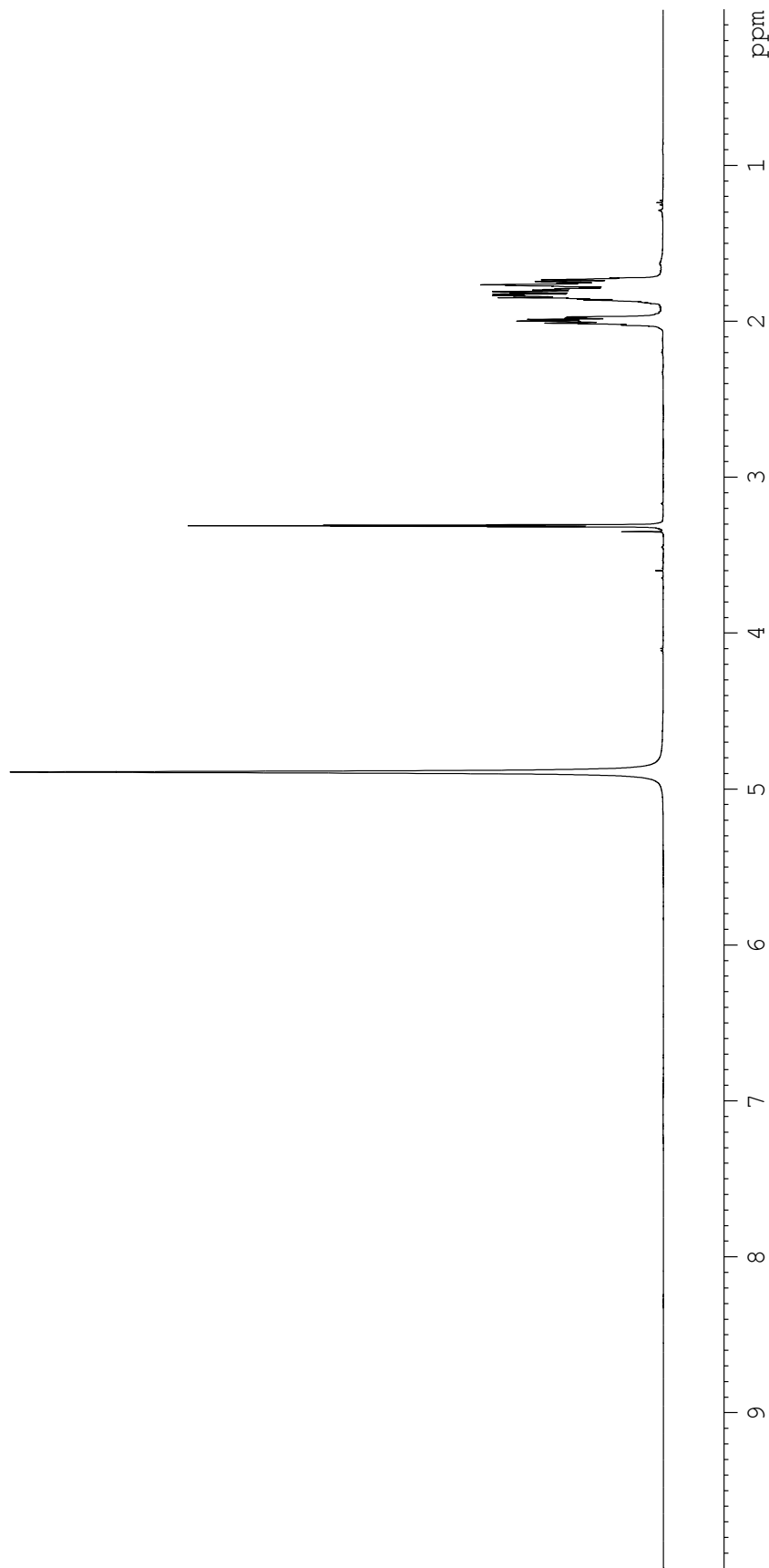
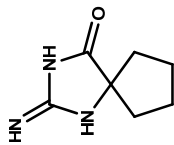


**Figure A2.17.** <sup>1</sup>H NMR (500 MHz, MeOH-*d*<sub>4</sub>) spectrum of compound 3-23 (freebase).

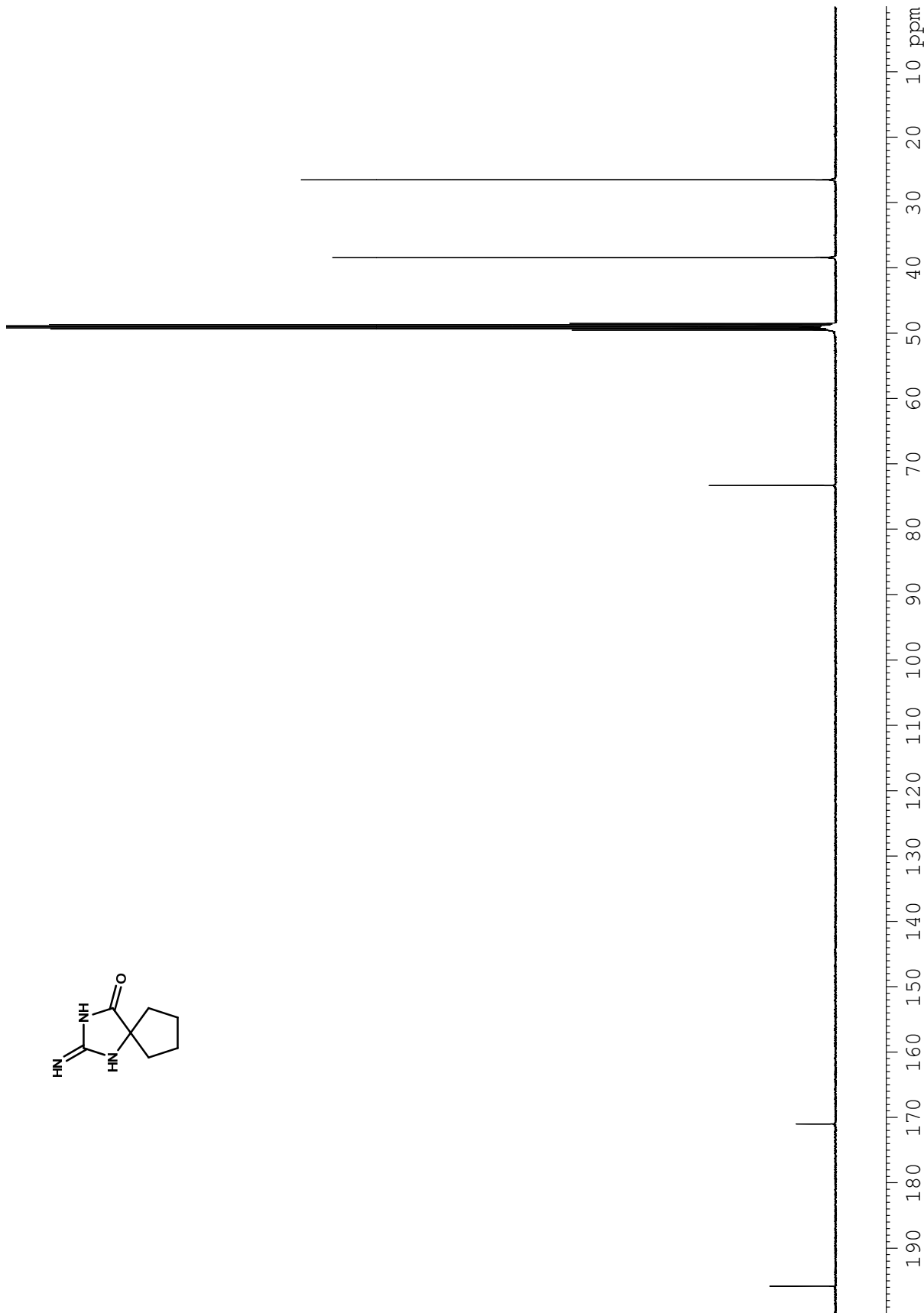
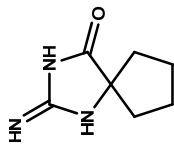


**Figure A2.18.**  $^{13}\text{C}$  NMR (125 MHz,  $\text{MeOH-}d_4$ ) spectrum of compound 3-23 (freebase).

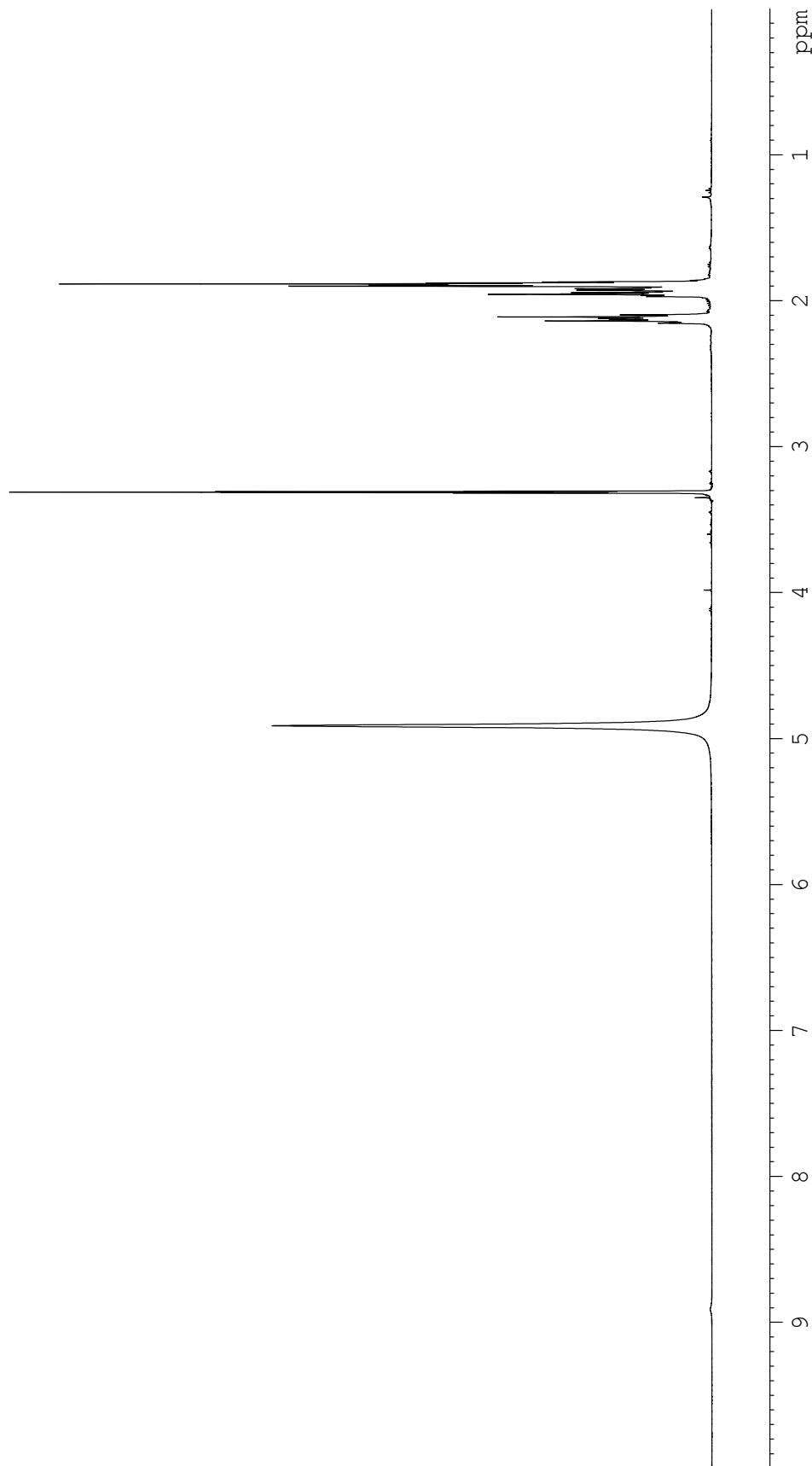
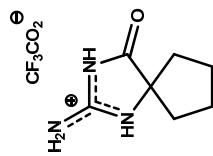


**Figure A2.19.** <sup>1</sup>H NMR (500 MHz, MeOH-*d*<sub>4</sub>) spectrum of compound **3-23** (CF<sub>3</sub>CO<sub>2</sub>H).

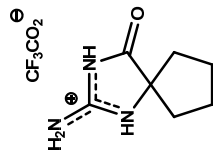


**Figure A2.20.** <sup>13</sup>C NMR (125 MHz, MeOH-*d*<sub>4</sub>) spectrum of compound 3-23 (CF<sub>3</sub>CO<sub>2</sub>H).

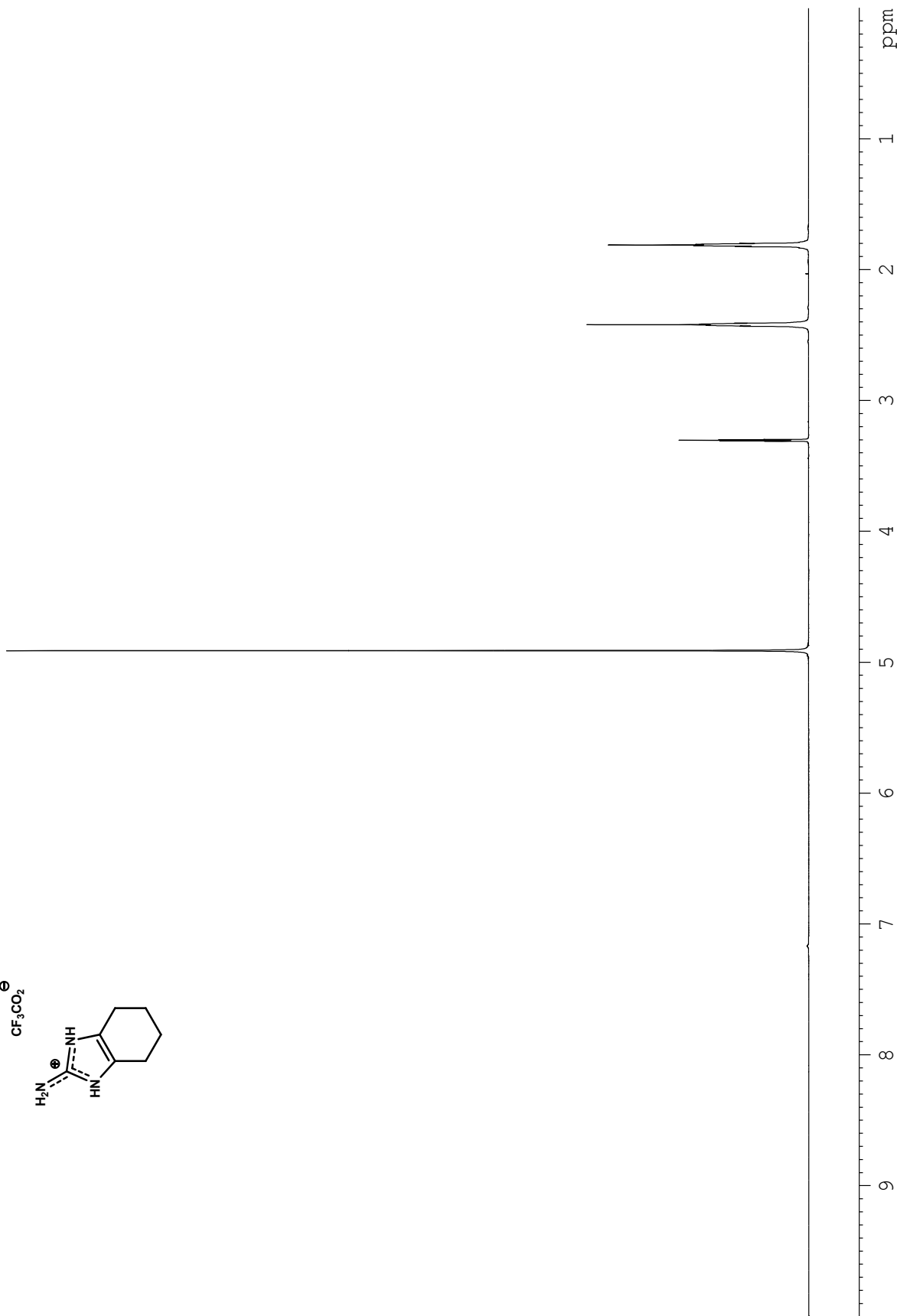
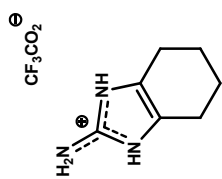


**Figure A2.21.** <sup>1</sup>H NMR (500 MHz, MeOH-*d*<sub>4</sub>) spectrum of compound 3-25 (CF<sub>3</sub>CO<sub>2</sub>H).

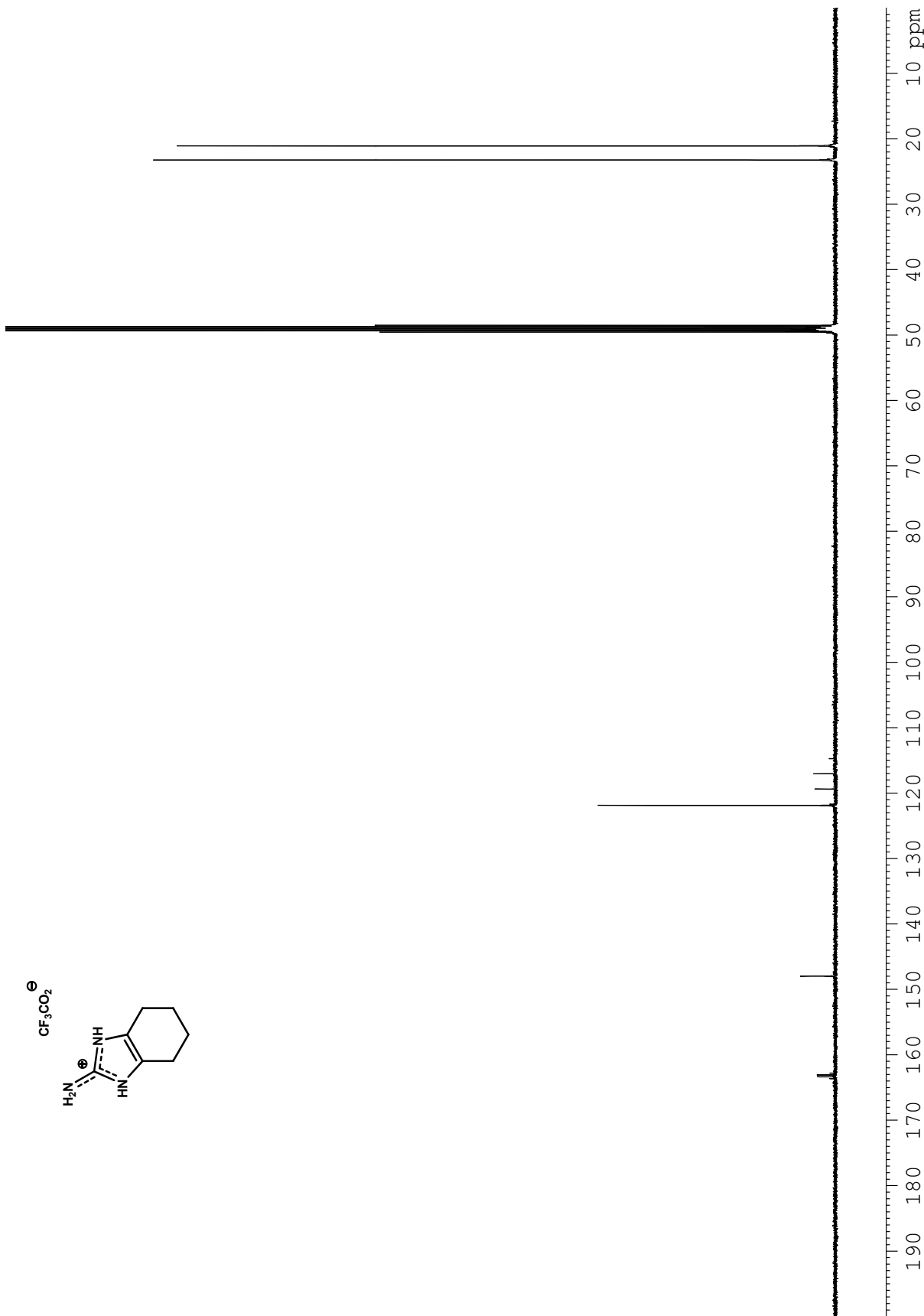
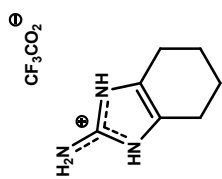


**Figure A2.22.** <sup>13</sup>C NMR (125 MHz, MeOH-*d*<sub>4</sub>) spectrum of compound **3-25** (CF<sub>3</sub>CO<sub>2</sub>H).

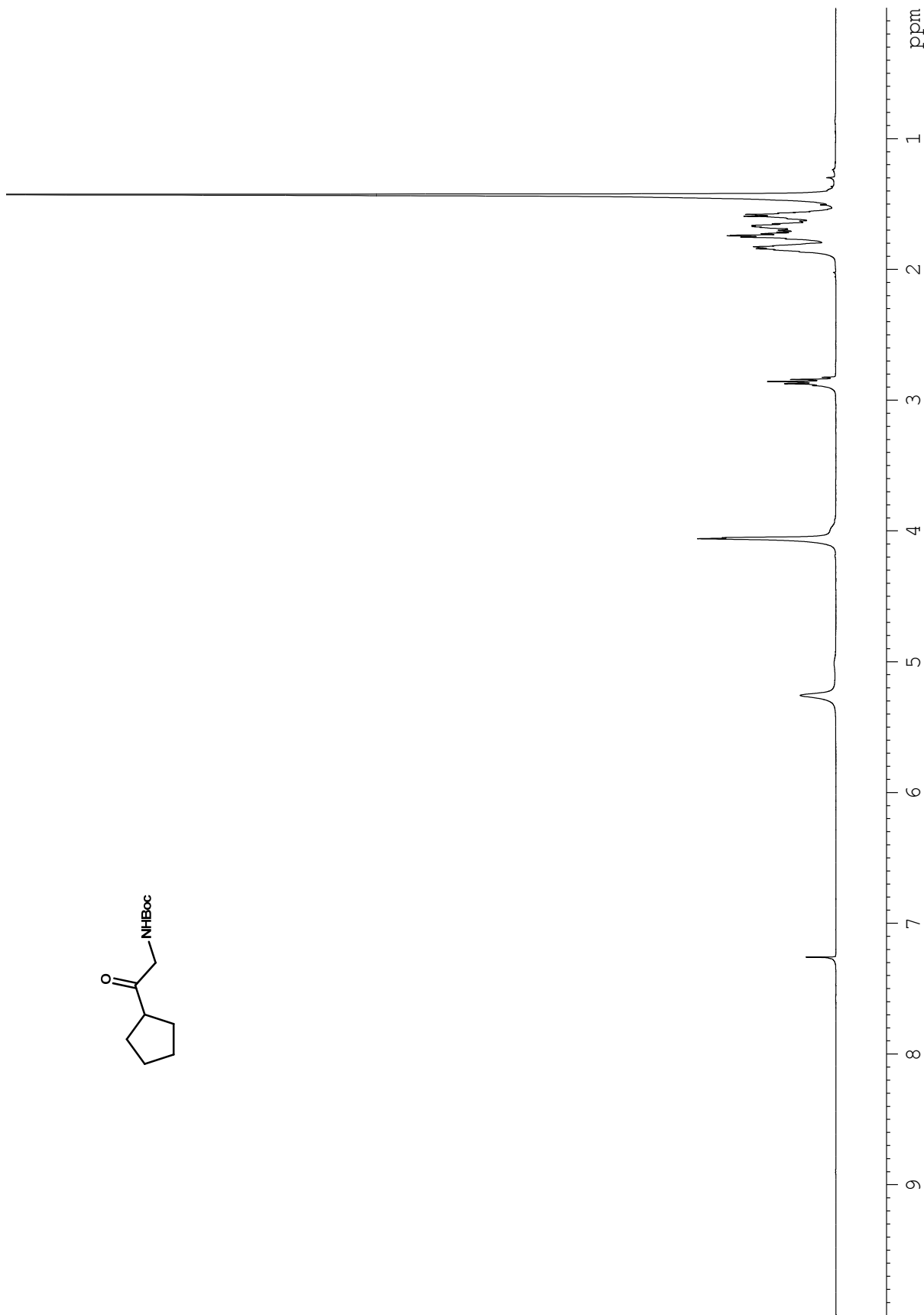
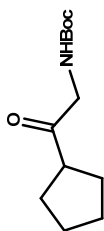


**Figure A2.23.**  $^1\text{H}$  NMR (500 MHz,  $\text{CHCl}_3-d_1$ ) spectrum of compound **3-37a**.

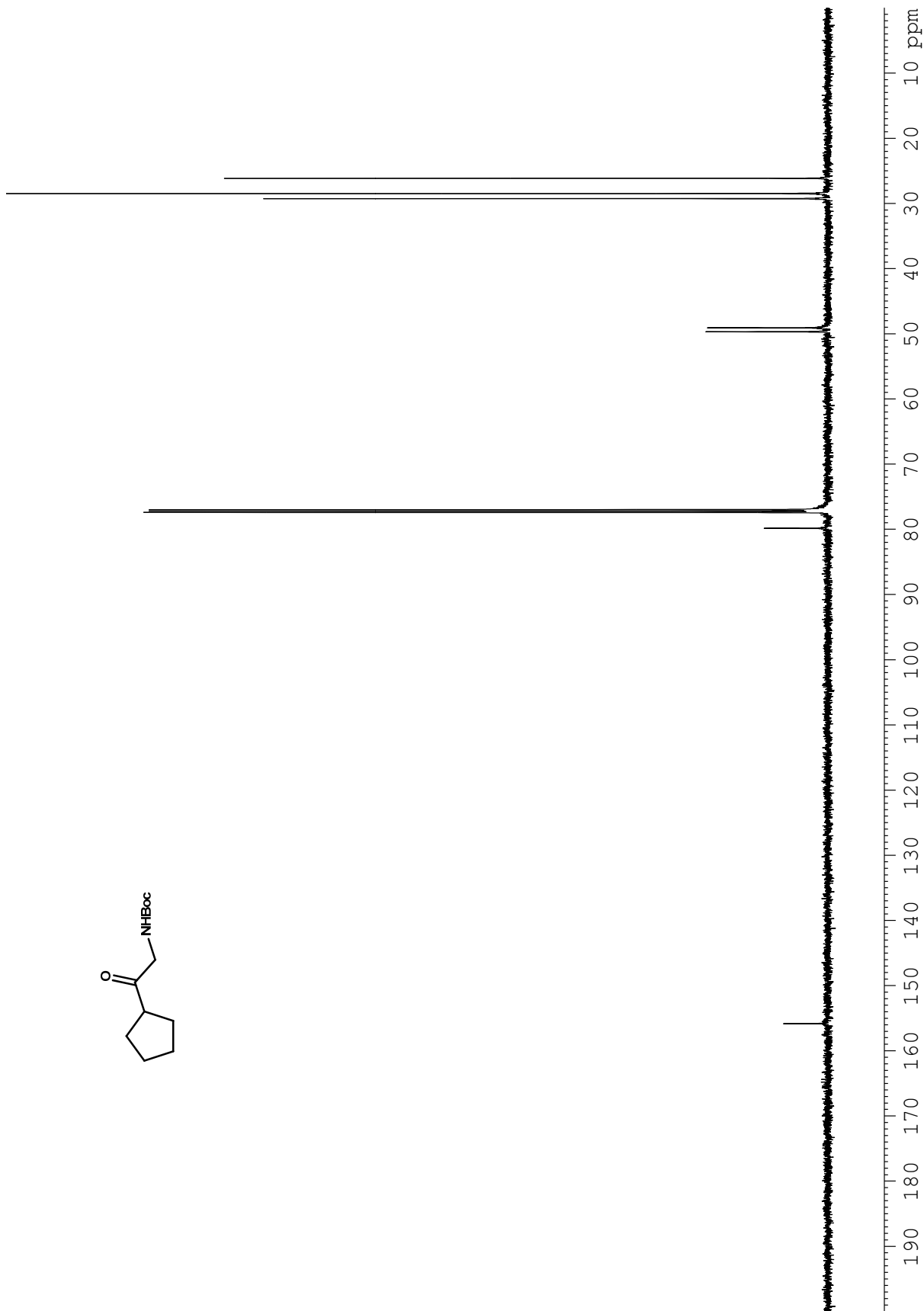
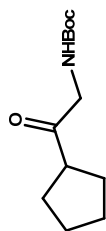


**Figure A2.24.**  $^{13}\text{C}$  NMR (150 MHz,  $\text{CHCl}_3$ - $d_1$ ) spectrum of compound 3-37a.



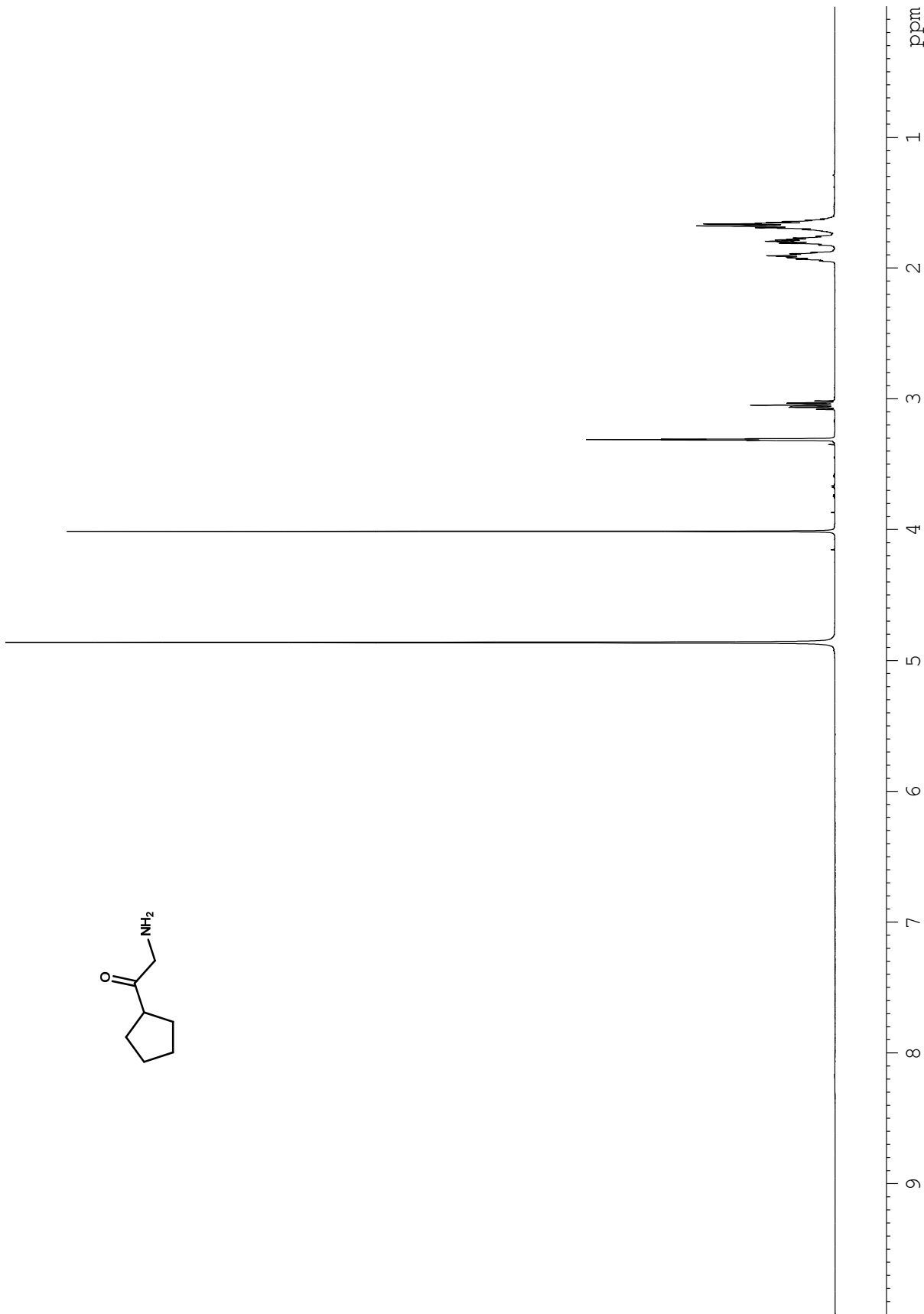
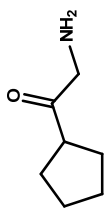


**Figure A2.25.** <sup>1</sup>H NMR (500 MHz, MeOH-*d*<sub>4</sub>) spectrum of compound 3-37b (crude).

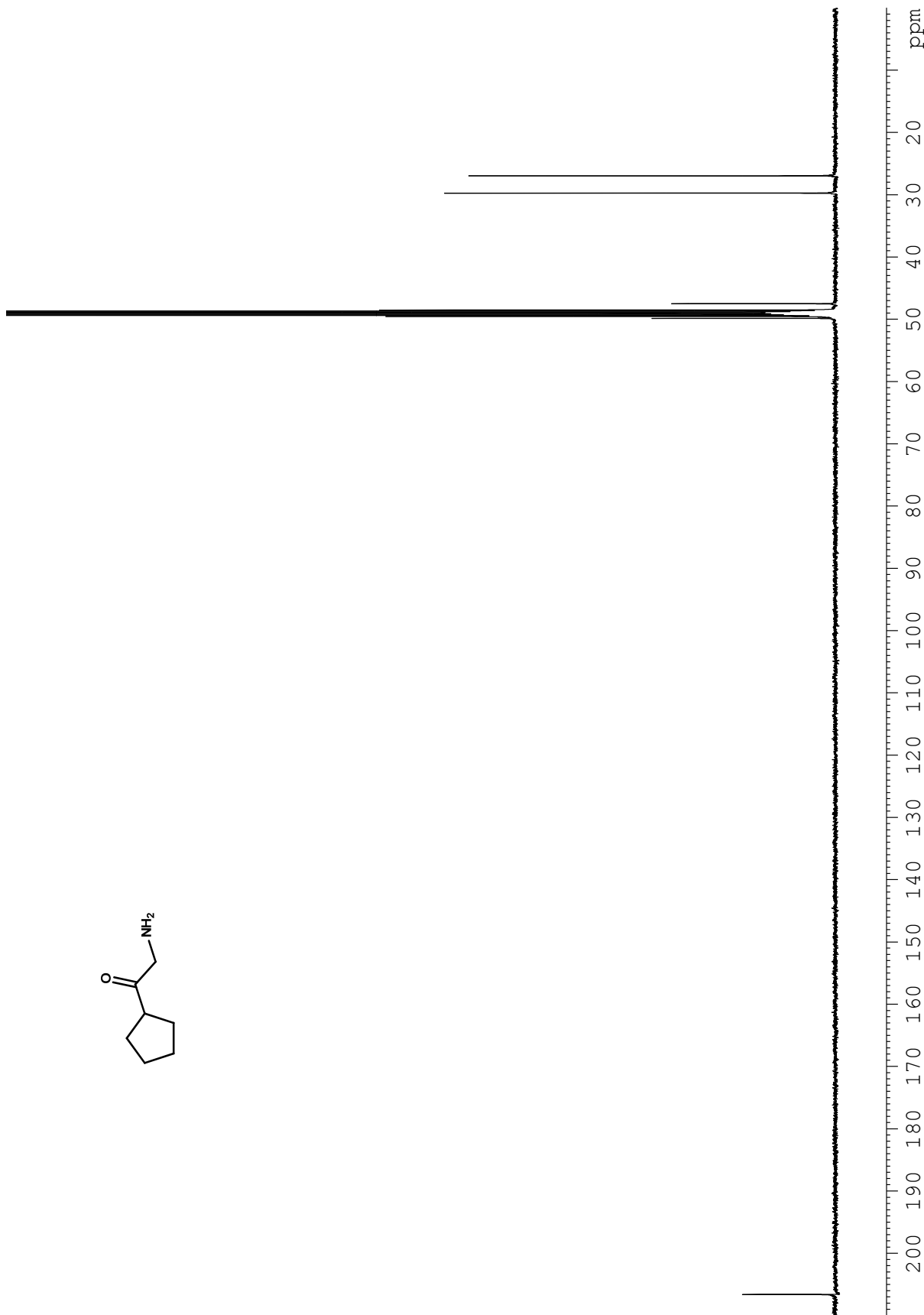
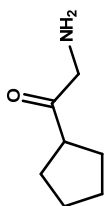


**Figure A2.26.**  $^{13}\text{C}$  NMR (125 MHz,  $\text{MeOH-}d_4$ ) spectrum of compound 3-37b (crude).

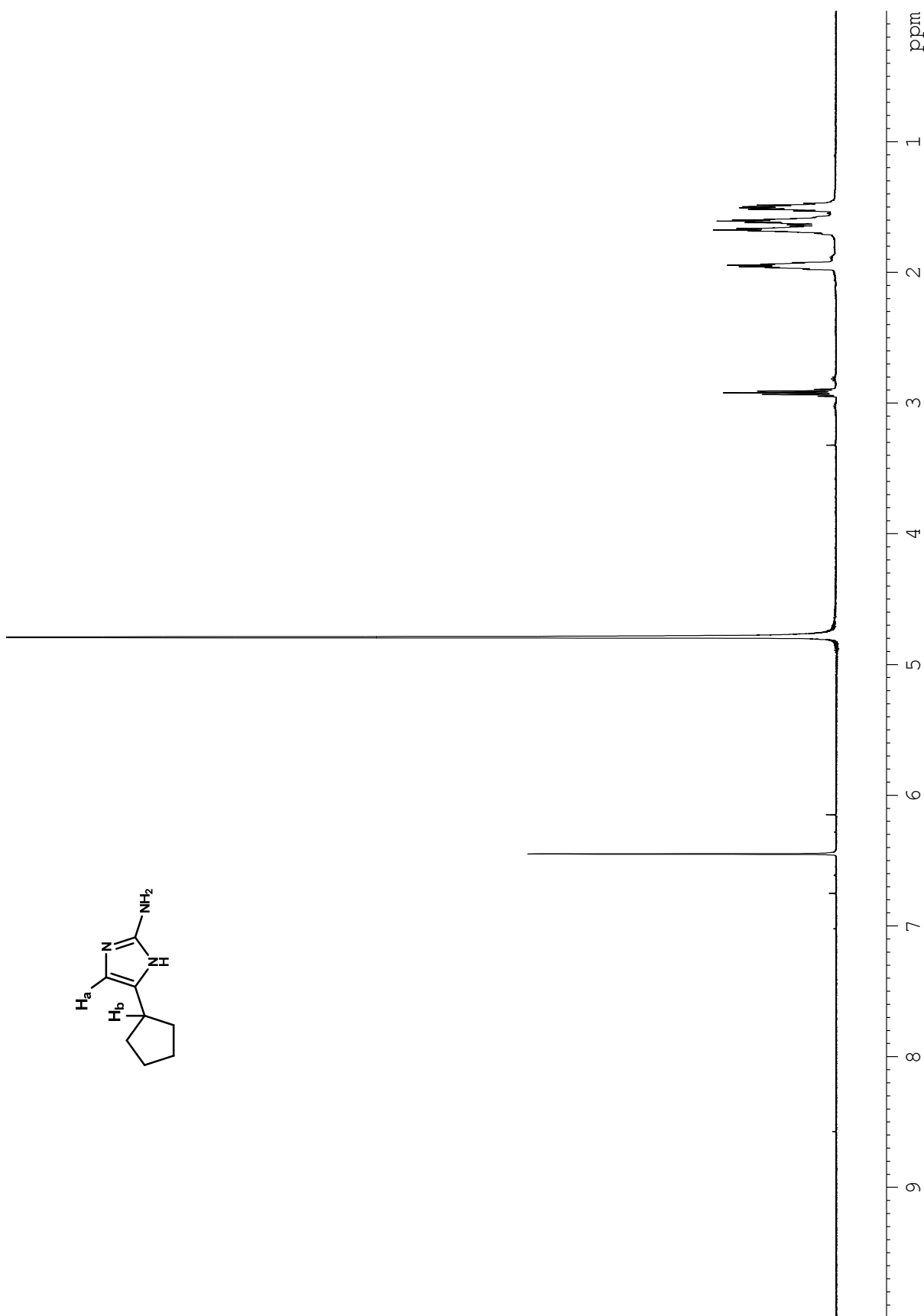


**Figure A2.27.** <sup>1</sup>H NMR (600 MHz, H<sub>2</sub>O-*d*<sub>2</sub>) spectrum of compound 3-38 (CF<sub>3</sub>CO<sub>2</sub>H).

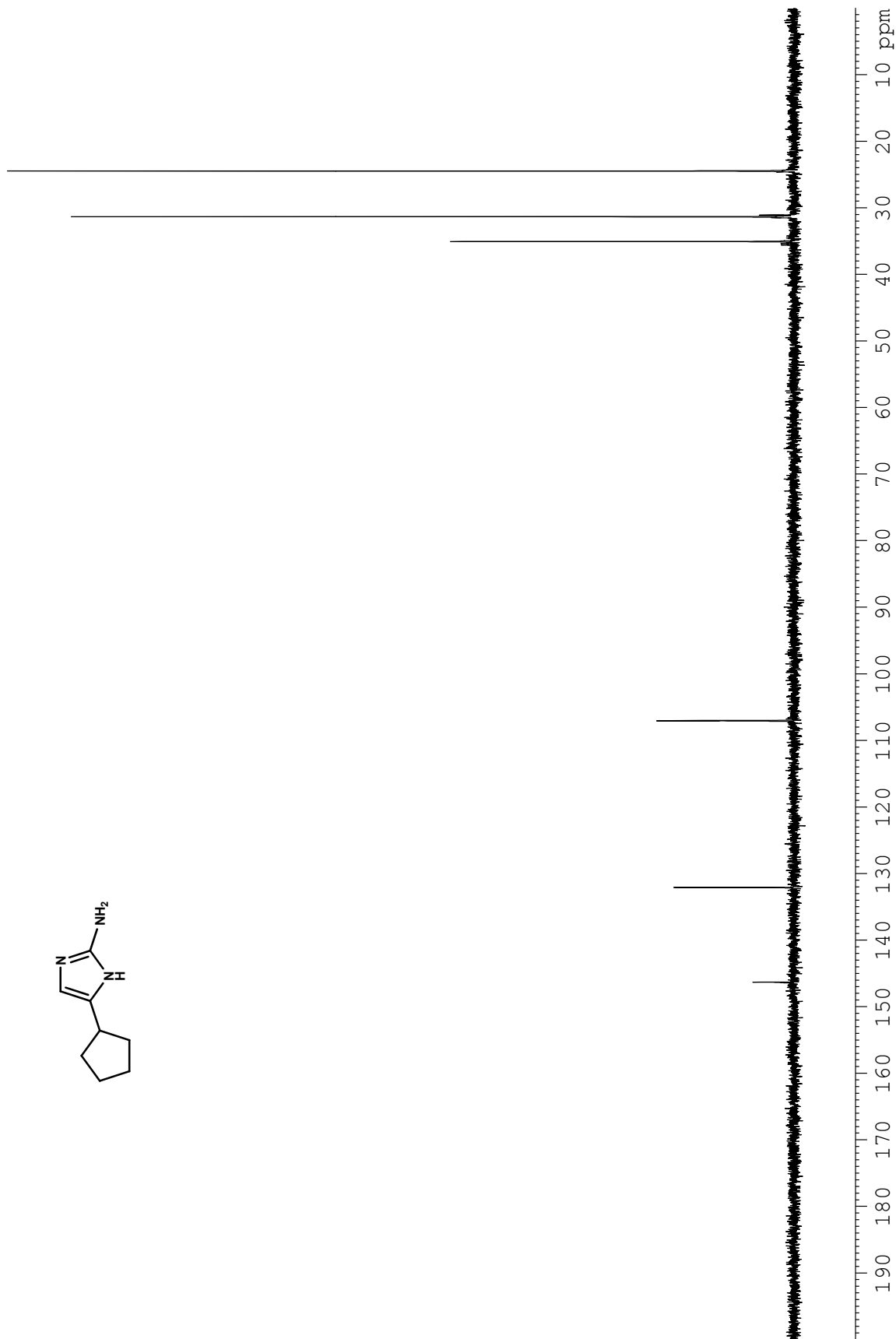
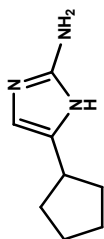


**Figure A2.28.**  $^{13}\text{C}$  NMR (125 MHz,  $\text{H}_2\text{O}-d_2$ ) spectrum of compound 3-38 ( $\text{CF}_3\text{CO}_2\text{H}$ ).

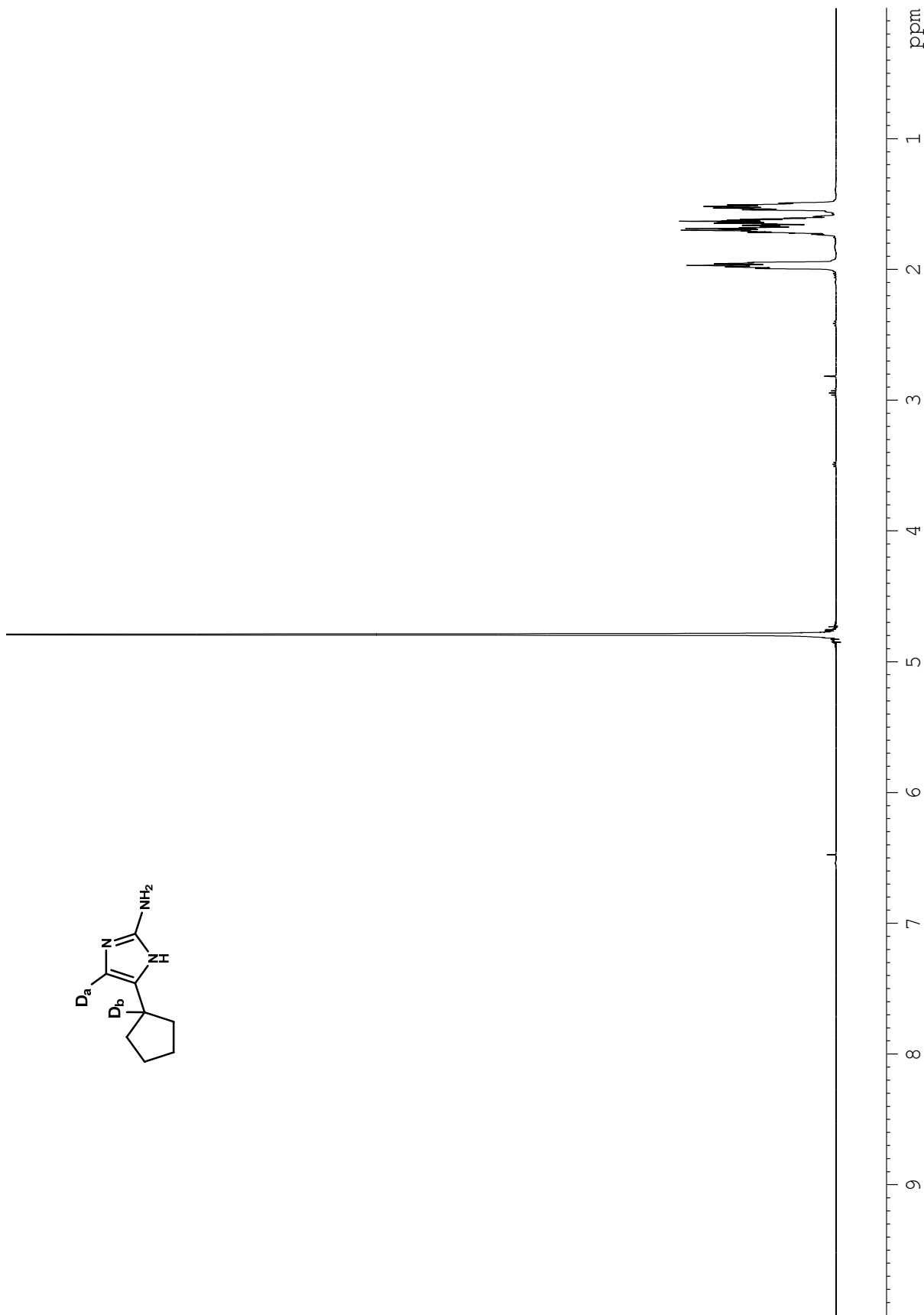


**Figure A2.29.**  $^1\text{H}$  NMR (600 MHz,  $\text{H}_2\text{O}-d_2$ ) spectrum of compound 3-40 ( $\text{CF}_3\text{CO}_2\text{H}$ ).

## Chapter 4 – Regarding an Alternative Route to (±)-Axinellamine A from (±)-Ageliferin

### Controlled, oxidative transformations of 2-aminoimidazoles (Part I)

Andrew G. Roberts, Hui Ding and Patrick G. Harran

#### 4.1 Introduction.

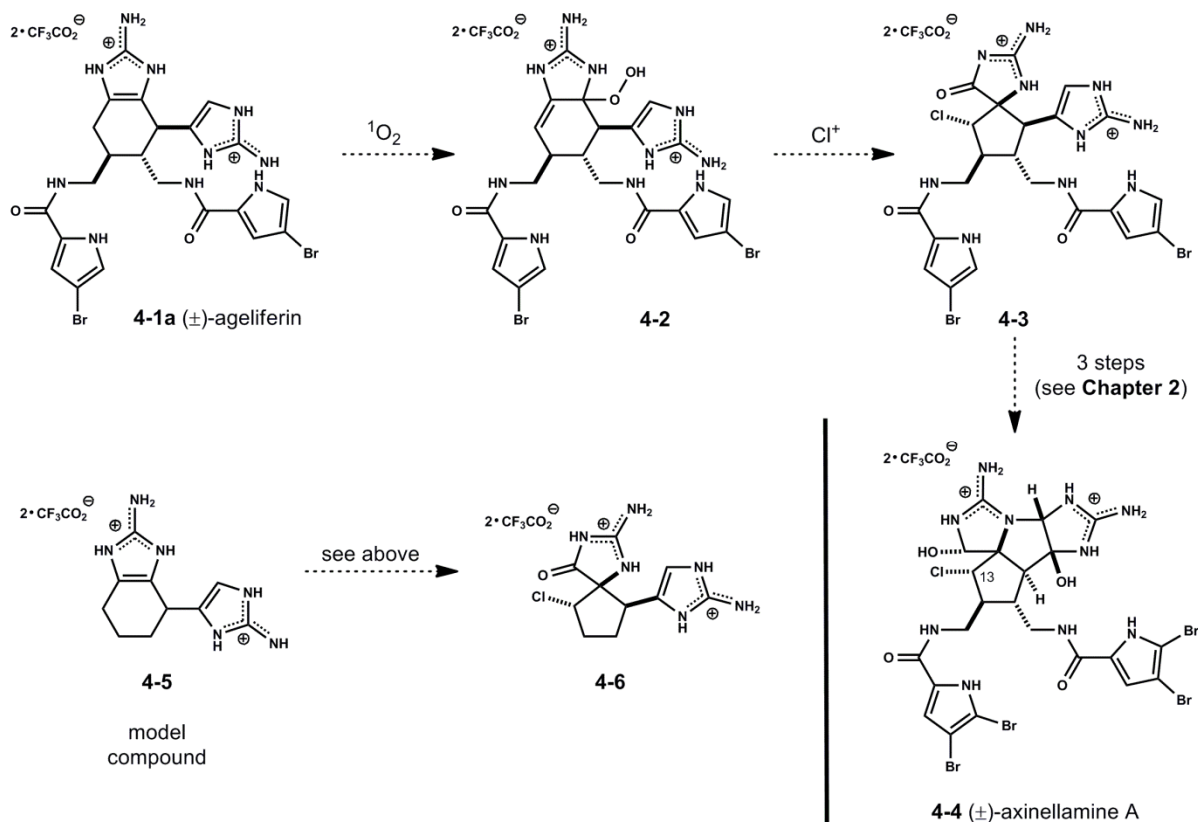


Figure 4.1. Proposed access to chlorospirocyclopentane (4-3) via oxidative ring contraction of (±)-ageliferin (4-1a)

#### 4.1.1 Proposed Synthesis of (±)-Axinellamine A 4-4 from (±)-Ageliferin 4-1a.

Having demonstrated access to (±)-ageliferin 4-1a from common spirocyclopentane intermediate via ring-expansion (Chapter 3), we considered the feasibility of converting (±)-ageliferin 4-1a to a chlorinated spirocyclopentane 4-3 (Figure 4.1).<sup>[1]</sup> Such a transformation would require a regio- and facially selective oxidation of the 2-aminotetrahydrobenzimidazole core present in ageliferin 4-1a with subsequent enamine halogenation (of type 4-2) and ring-

contraction to provide desired chlorinated (C13) spirocyclopentane **4-3**. If realized, chlorinated spirocyclopentane (**4-3**) could be converted to ( $\pm$ )-axinellamine A **4-4**.<sup>[1b]</sup> We were intrigued by the use of singlet oxygen or similar reagents to access structures (of type **4-3**) via Schenck ene-type reactivity.<sup>[2]</sup> Additionally, the intermediate peroxy hemiaminal **4-2** may serve as an oxygen donor in the requisite epoxidation of the pendant 2-aminoimidazole.<sup>[3]</sup> Certainly, one should also consider the regio- and stereochemical product outcome of ene-type reactivity in asymmetric systems.<sup>[4]</sup>

We were initially inspired by the ene-type transformations present in the work of Foote and Burrows with regard to biologically relevant oxidations of guanine. Since the initial understanding of singlet oxygen<sup>[5]</sup> and its practical use<sup>[6]</sup>, many synthetic transformations and methods have been reported.<sup>[2b]</sup> We became increasingly drawn to methods that demonstrate the use of singlet oxygen within the context of highly polar substrates, more specifically, densely nitrogenous heterocycles.<sup>[7]</sup> Foote and co-workers have demonstrated such utility in studying the low-temperature photosensitized (methylene blue) singlet oxygen reactions of guanosine derivatives.<sup>[7b]</sup> In the same report, an intriguing reaction between 4-methyl-1,2,4-triazoline-3,5-dione (MTAD) and a guanosine derivative lends credence to the analogous involvement of singlet oxygen in such systems. The ability to generate singlet oxygen under aqueous conditions, wherein substrates (*e.g.* **4-1a**) would be soluble, were attractive.<sup>[6]</sup> In an elegant extension of related research, Burrows and co-workers reported several oxidative transformations of guanosine and 8-oxoguanine via the photosensitized (rose bengal) generation of singlet oxygen in dilute buffered aqueous solutions.<sup>[8]</sup> These reaction modes parallel the desired 2-aminoimidazole activation required to transform **4-1a** to peroxy intermediate **4-2**.

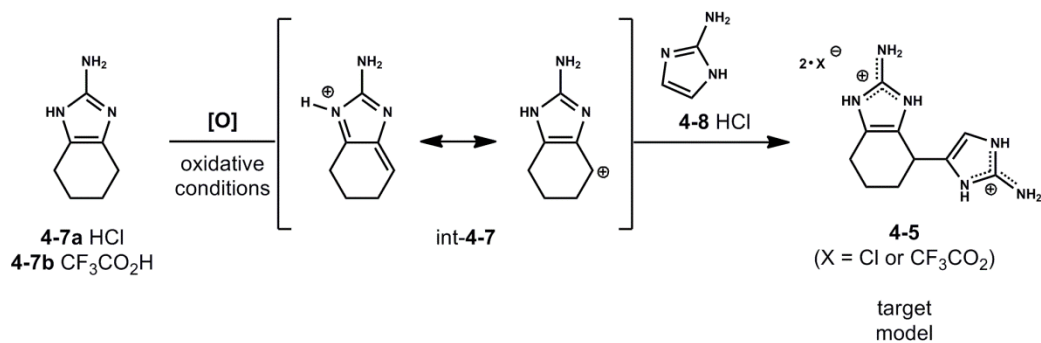


**Figure 4.2.** Proposed study to understand reactivity towards oxidations - Synthesis of ageliferin model compound (**4-5**)

In addition to singlet oxygen, we reasoned that cyclic diazo dienophiles explored by Foote may undergo analogous ene-type reactions with ageliferin **4-1a**.<sup>[9,10a]</sup> Specifically, we sought to explore oxidations with 1,2,4-triazoline-3,5-diones, such as MTAD or 4-phenyl-1,2,4-triazoline-3,5-dione (PTAD) with reactivity reportedly analogous to that of singlet oxygen.<sup>[11]</sup> Corey and co-workers have demonstrated significant utility of MTAD for similar ene-type oxidative transformations in indole derived substrates.<sup>[10b,c]</sup> In planning, we realized a model bis-guanidine **4-5** would be an ideal system to explore these potential oxidative transformations. Presented with several challenging transformations, we proposed the preparation of bis-guanidine **4-5** via the intermediacy of resonance stabilized **int-4-7** (Figure 4.2) as a unique opportunity to understand the reactivity of oxidants such as singlet oxygen and 1,2,4-triazoline-3,5-diones, in a simple 2-aminoimidazole system (**4-7**). Related oxidative transformations with nucleophilic (**4-8**) capture in situ were precedented.<sup>[12]</sup> With access to ageliferin core **4-5**, we sought to develop regio- and facially selective oxidative reactions with subsequent chlorinative ring-contraction to access model axinellamine-type core **4-6**, a sequence that would ideally translate to **4-1a**. The use of ene-type reactivity in this setting distinguishes this proposal from related oxidative ring-contraction strategies.



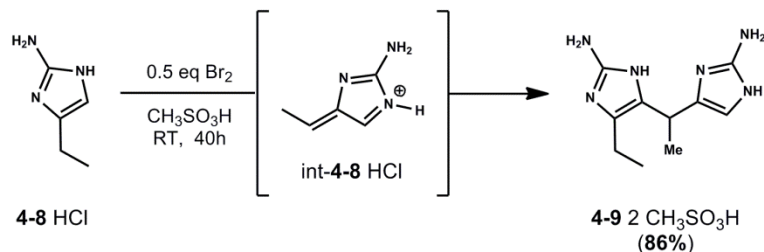
#### 4.1.2 Related Synthetic Efforts.

Several groups have pursued transformations of this type wherein the general strategy involves a type of oxidative ring-contraction, reminiscent of the early Kinnel–Scheuer hypothesis for the incorporation of chlorine (C13) in palau'amine (not shown).<sup>[13]</sup> Early efforts disclosed by the Baran and co-workers demonstrated ( $\pm$ )-ageliferin **4-1a** underwent regioselective oxidations at the more substituted 2-aminoimidazole.<sup>[14]</sup> Ultimately, after screening many oxidants<sup>[15]</sup>, the group concluded that aqueous magnesium monoperoxyphthalate was effective in the regioselective generation of a bis-hemiaminal intermediate that could be thermally induced to undergo ring-contraction (6 to 5-membered ring) to afford a des-chlorinated (C13) spirocyclopentane.<sup>[14]</sup> The research groups of Lovely, Chen and Romo have proposed access to chlorinated spirocyclopentanes (of type **4-3**) via similar oxidative ring contraction strategies. Lovely and co-workers have demonstrated efficient ring-contractions of 2-aminoimidazoles initiated by oxidations with either dimethyldioxirane (DMDO) or Davis oxaziridines.<sup>[16]</sup> An elegant solution to this general problem was disclosed by the Romo group wherein oxidation with DMDO and subsequent enamine-type chlorination (confer conversion of **4-1** to **4-3**) provided access to chlorinated spirocyclopentanes and ultimately a functionalized *trans*-azabicyclo[3.3.0]octane core.<sup>[17]</sup> Inspired by these promising methods, and informed by failed Büchi-type cyclizations<sup>[18]</sup>, the Chen laboratory has described access to an interesting ageliferin-palau'amine hybrid structure (not shown) thought relevant as an alternative to the original Kinnel–Scheuer Diels–Alder biosynthetic hypothesis.<sup>[19]</sup>

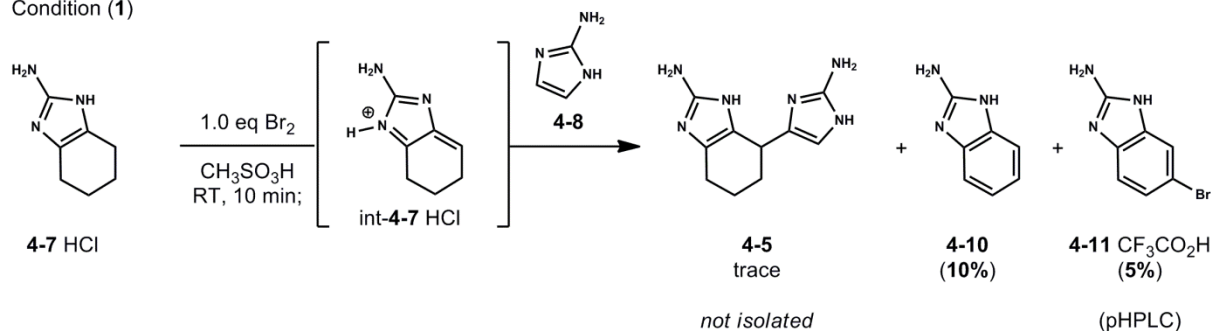
## 4.2 Results and Discussion (Part I).

### 4.2.1 Synthesis of the Ageliferin Core (4-5).

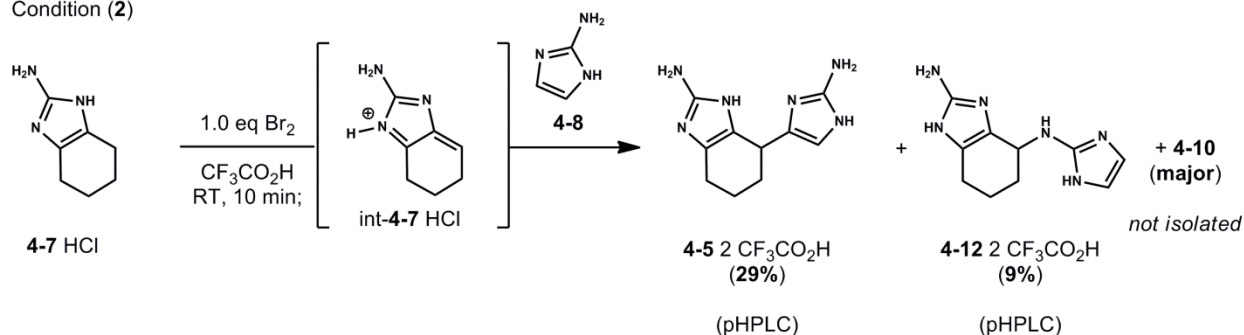
Horne (1996)



Condition (1)



Condition (2)

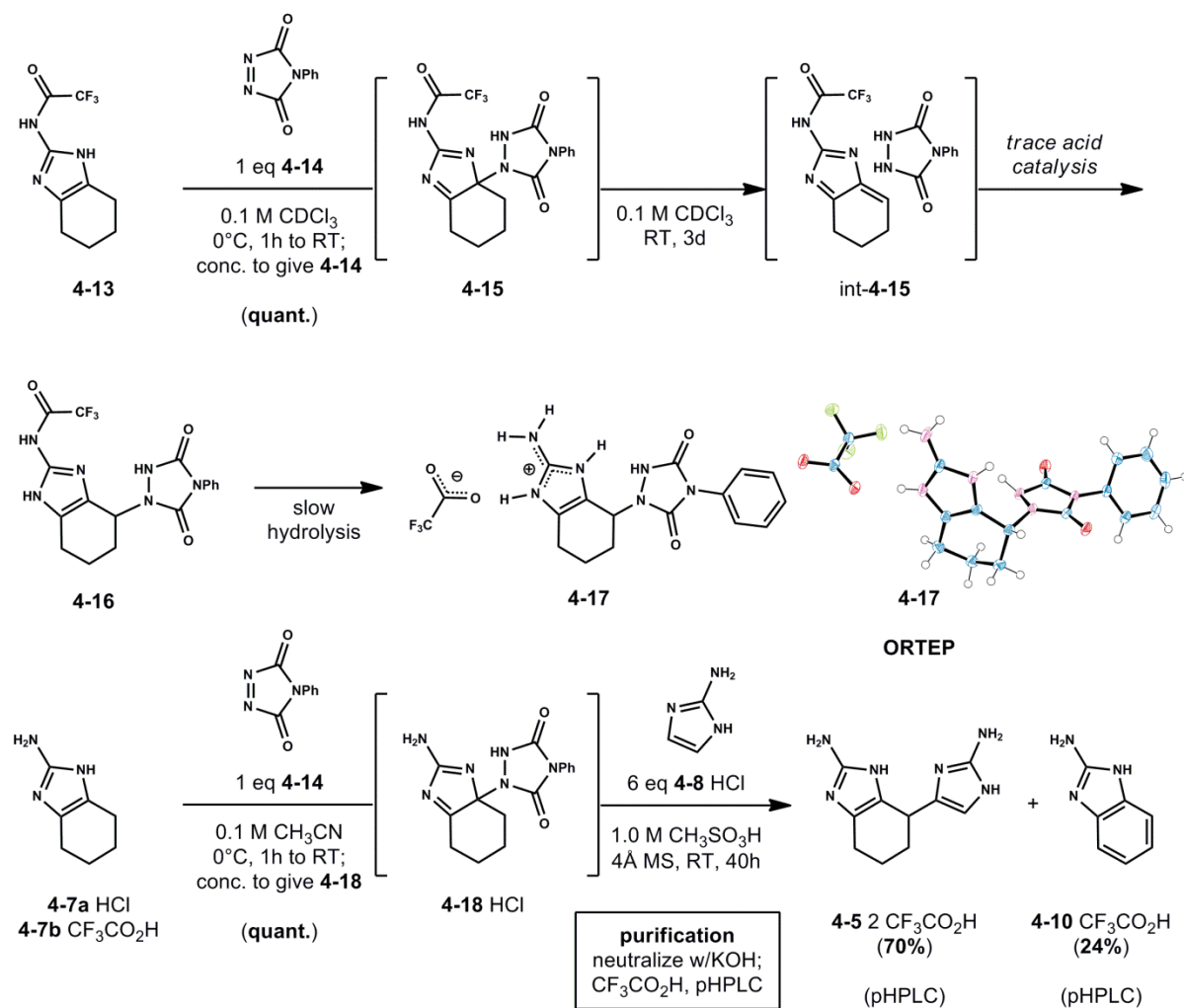


**Scheme 4.1.** Synthesis of bis-guanidine **4-5** via oxidative hetero-dimerization of 2-aminoimidazole (**4-7**) and (**4-8**)

Initially, we conducted experiments to explore the anticipated reactive nature of putative **int-4-7** (Scheme 4.1) and access desired bis-guanidine **4-5** quickly. Oxidative transformations of this type have been examined previously<sup>[12]</sup>, although the specific method (Br<sub>2</sub>, MeSO<sub>3</sub>H, RT) appears limited in substrate scope.<sup>[12a]</sup> Under identical conditions to those described by Horne and co-workers, the oxidation of 2-aminotetrahydrobenzimidazole hydrochloride **4-7** (condition 1) was capricious.<sup>[12a]</sup> It became apparent that over-oxidation of **4-7** to provide **4-10** and **4-11** was a process that out-competed substantial formation of desired bis-guanidine **4-5**. However,

the observation of **4-5** (LC/MS analysis) was promising. Ultimately, under similar conditions (CF<sub>3</sub>CO<sub>2</sub>H in place of MeSO<sub>3</sub>H, condition 2) the desired C-linked bis-guanidine **4-5** could be isolated alongside N-linked bis-guanidine **4-12** in moderate yield.<sup>[20]</sup> Other conditions examined included the use of N-bromosuccinimide (NBS), 2,3-Dichloro-5,6-dicyano-1,4-benzoquinone (DDQ), or iodine (I<sub>2</sub>) as alternative controlled oxidants were not more effective than molecular bromine (Br<sub>2</sub>). Also noteworthy, the use of trifluoroacetic acid was critical to the success of this transformation. Comparing condition (1) and (2) suggests that the initial oxidation of 2-aminoimidazole **4-7** in trifluoroacetic acid is controlled and further oxidation of **int-4-7** is minimized.

## 4.2.2 Reactivity of 2-aminoimidazoles with 1,2,4-Triazoline-3,5-diones and Singlet Oxygen.



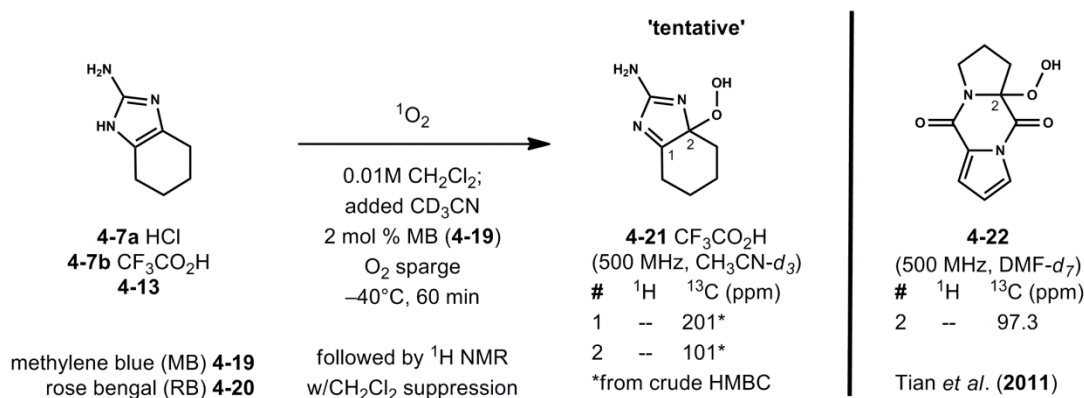
**Scheme 4.2.** Reactions of aminoimidazoles (**4-7**, **4-13**) with 4-phenyl-1,2,4-triazole-3,5-dione (PTAD) (**4-14**).

We were primarily interested in understanding the nature of oxidized intermediates (of type **int-4-7**). While exploring the reactivity of **4-7** with singlet oxygen (*vide infra*), we simultaneously examined the chemistry of 1,2,4-triazoline-3,5-diones (TADs). For solubility purposes, derivative **4-13** (Scheme 4.2) was prepared for reactions with PTAD **4-14**, initially monitored by <sup>1</sup>H NMR (500 MHz, CDCl<sub>3</sub>). To our delight, the first experiment with PTAD **4-14** was very informative.<sup>[21]</sup> Dissipation of the deep carmine color, attributed to **4-14**, was indicative of reactivity. Several structural elements of the putative PTAD adduct **4-15** were unclear in

regard to connectivity. Further spectroscopic analysis corroborated the structure of PTAD adduct **4-15**, and analogous experiments reported for indole containing systems are in agreement with such PTAD adduct connectivity.<sup>[10b]</sup> The same reaction solution of **4-15** (CDCl<sub>3</sub>, 48 h) left standing had undergone rearrangement to give isomeric product **4-16**. It was proposed that this rearrangement occurred under mild acidic conditions (CDCl<sub>3</sub>) via the putative intermediacy of **int-4-15**. Repeat experiments with excess trifluoroacetic acid or acetic acid facilitated this rearrangement and confirmed the initial hypothesis. Fortunately, these results were concluded with a crystal structure of derivative rearranged PTAD adduct **4-17** (CCDC 942602) presumably formed by the slow hydrolysis of **4-16** following purification by HPLC.<sup>[22]</sup> We immediately recognized the potential of this chemistry and quickly applied the method for the synthesis model bis-guanidine **4-5**.

Initial studies demonstrated that 2-aminoimidazoles **4-7** also formed PTAD adducts.<sup>[23]</sup> PTAD adduct **4-18** could be prepared on gram scale and was used without purification.<sup>[24]</sup> Under optimal conditions, the solid adduct **4-18** was combined with excess 2-aminoimidazole **4-8** (6 equiv) and reacted in neat methanesulfonic acid at RT for 40h to afford ageliferin core **4-5** in good yield with minimal over-oxidation products (such as **4-10**) observed.<sup>[25]</sup> One interpretation of this reaction can be described as a Michael-type addition of an enamine nucleophile (**4-7**, **4-13**) to an electron deficient species analogous to **4-14**.<sup>[26,27]</sup> Certainly, alternative pathways including Diels–Alder or ene-type reactivity are possible provided net olefin transposition and formation of a heteroatom-carbon bond.<sup>[11]</sup> Leach and Houk propose that ene reactions of 1,2,4-triazoline-3,5-diones occur in a stepwise fashion with diradical intermediates.<sup>[11]</sup> The research of Foote and co-workers suggest 4-methyl-1,2,4-triazoline-3,5-dione may undergo a net [4+2] addition with a guanosine derivative followed by rearrangement in a reaction pathway<sup>[7b]</sup>

analogous to the *endo*-peroxide formation observed when singlet oxygen is used to oxidize various substituted imidazoles.<sup>[28]</sup> Several reports have drawn parallel conclusions on the similarity of ene-type reactivity modes observed when using singlet oxygen and 4-substituted-1,2,4-triazoline-3,5-diones.<sup>[11]</sup>



**Scheme 4.3.** Aminoimidazole oxidations with singlet oxygen - reactivity parallels PTAD **4-14** oxidation chemistry.

The reactivity of 2-aminoimidazoles (**4-7**, **4-13**) singlet oxygen generated under photosensitized conditions with methylene blue (MB) **4-19** or rose bengal (RB) **4-20** (Scheme 4.3) was briefly examined. We anticipated experimental difficulty with regard to the solubility of highly polar salt forms (**4-7**) in organic solvents (CH<sub>2</sub>Cl<sub>2</sub>, CH<sub>3</sub>CN)<sup>[29]</sup> generally employed for photosensitized singlet oxygen generation. Reactions conducted under aqueous conditions analogous to those reported by Burrows were effective, although initial adduct intermediates (such as **4-21**) were not observed as major products.<sup>[8]</sup> Product analysis was complicated by hydrolysis and dimerization, which presumably arise from subsequent bimolecular reactions after formation of **4-21**. Fortunately, conditions to efficiently generate singlet oxygen were found wherein **4-7b**<sup>[29]</sup> suspended in dilute anhydrous CH<sub>2</sub>Cl<sub>2</sub> (0.01 M) with minimal added CD<sub>3</sub>CN (for solubility) formed tentatively assigned peroxy hemiaminal **4-21** as the major product.<sup>[30]</sup> Interestingly, the reactivity of singlet oxygen under these conditions parallels that of PTAD **4-14**, and data is in agreement with structure **4-21** as depicted (for comparative data see **4-22**).

Comparative key  $^1\text{H}$  and  $^{13}\text{C}$  NMR data for 4-21 and related adducts are tabulated in Figure 4.3. The figure aims to highlight similarity in  $^{13}\text{C}$  NMR resonances for imino-type (labeled C1,  $\delta$  (ppm) 198–202) and (hemi)-aminal-type (labeled C2,  $\delta$  (ppm) 84–101) functionality in oxidized adducts (**4-15**, **4-18**, and **4-21**). Additionally, key  $^{13}\text{C}$  NMR resonances support structural discernment between C-bound and N-linked adducts with regard to the benzylic position (labeled C3,  $\delta$  (ppm) 30–49) in adducts (**4-5**, **4-12**, and **4-16**).

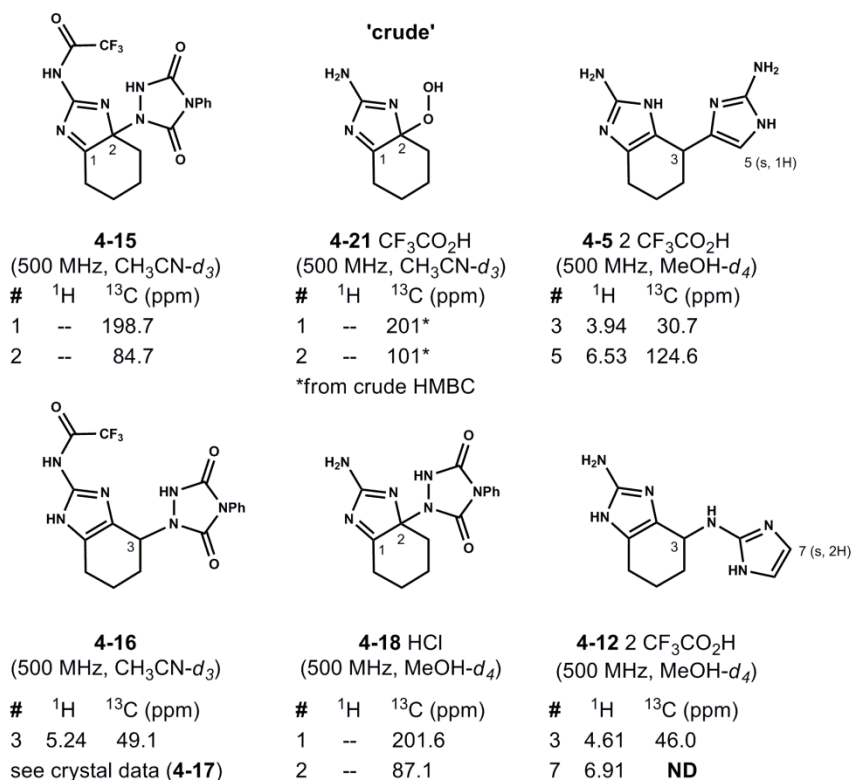


**Figure 4.3.** Key Characterization Data ( $^1\text{H}$ ,  $^{13}\text{C}$  NMR)

## Chapter 4 – Progress Toward the Total Synthesis of (-)-Ageliferin (Part II).

Andrew G. Roberts and Patrick G. Harran

### 4.3 Introduction.

#### 4.3.1 Proposed Synthesis of (-)-Ageliferin 4-1a.

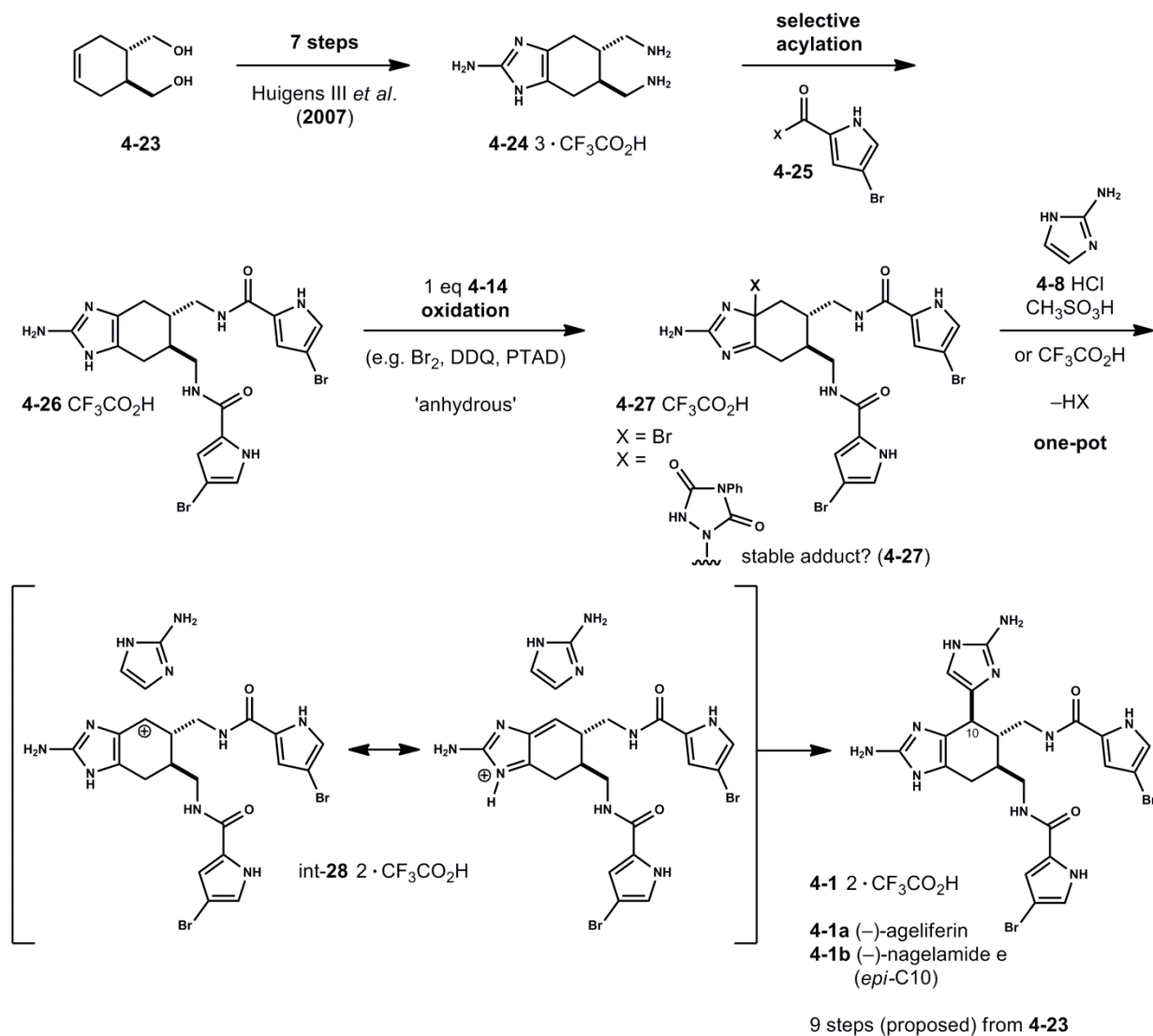


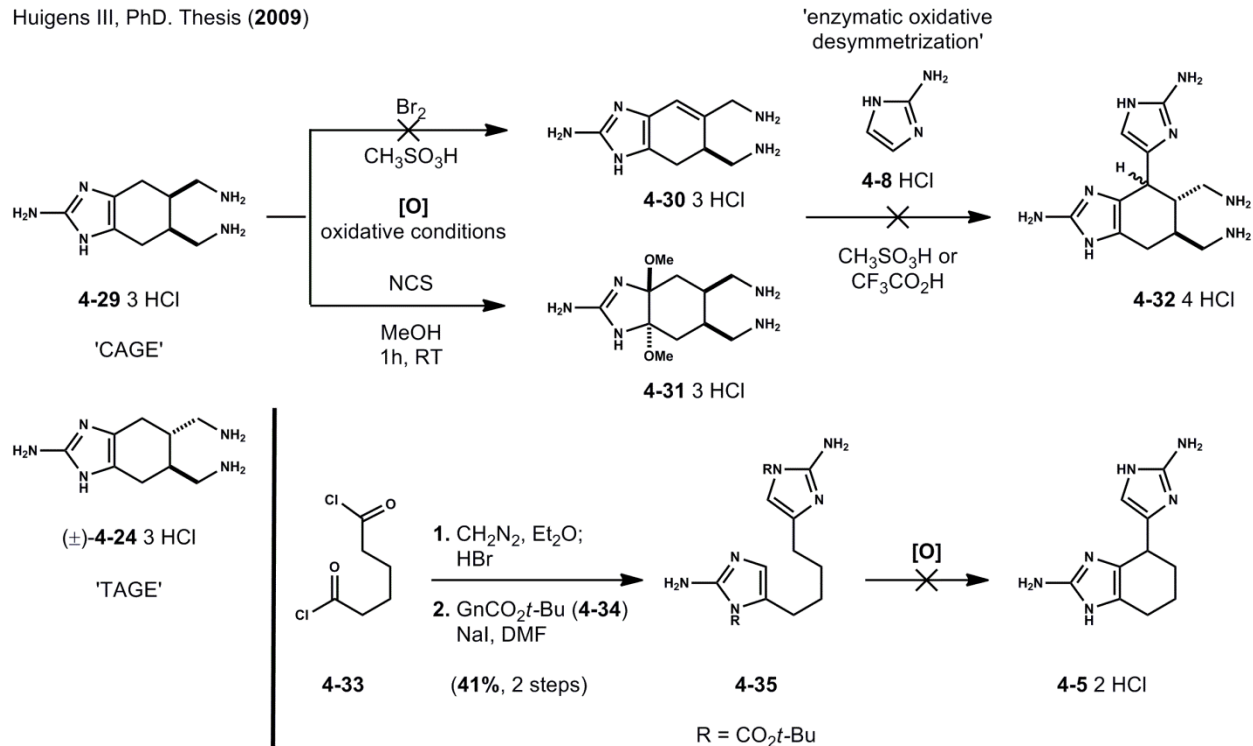
**Figure 4.4.** Proposed Synthesis of ageliferin (**4-1a**) and nagelamide e (**4-1b**) in 9 steps from chiral diol (**4-23a**). Application of novel 4-phenyl-1,2,4-triazoline-3,5-dione (PTAD) (**4-14**) oxidation method for the controlled alkylation of 2-aminoimidazole (**4-26**).



Inspired by the idea of converting ( $\pm$ )-ageliferin **4-1a** via an oxidative ring-contraction to ( $\pm$ )-axinellamine A (**4-4**) we developed the synthesis of ageliferin's bis-guanidine core **4-5**. With intent to further understand the ene-type reactivity modes of 1,2,4-triazoline-3,5-diones and 2-aminoimidazoles, a total synthesis of (-)-ageliferin **4-1a** was proposed (Figure 4.4) that would utilize this novel oxidative activation strategy. Although this proposal deviates from our longstanding goal of synthesizing complex pyrrole-imidazoles from diisocyanide dimers<sup>[1]</sup>, it would provide access to optically active materials (*e.g.* (-)-ageliferin **4-1a**, (-)-axinellamine A **4-4**) and the method appeared well established in model systems (**4-7**, **4-13**) (*vide supra*). Fortunately, desired intermediate **4-24** and its diacylated variant **4-26** were known compounds, albeit prepared in racemic form from  $C_2$ -symmetric diol **4-23**.<sup>[31]</sup> Our proposal entails the oxidative activation of **4-26** to provide PTAD adduct **4-27**, which would in turn undergo nucleophilic attack with 2-aminoimidazole **4-8** via the intermediacy of putative resonance stabilized electrophiles **int-4-28** to generate (-)-ageliferin **4-1a** directly. Although our proposed synthesis of (-)-ageliferin **4-1a** was inspired by this novel reactivity mode, we would be remiss not to mention the related work of Huigens and Melander.

### 4.3.2 Related Synthetic Approaches to (±)-Ageliferin (Huigens and Melander, 2009).

Huigens III, PhD. Thesis (2009)



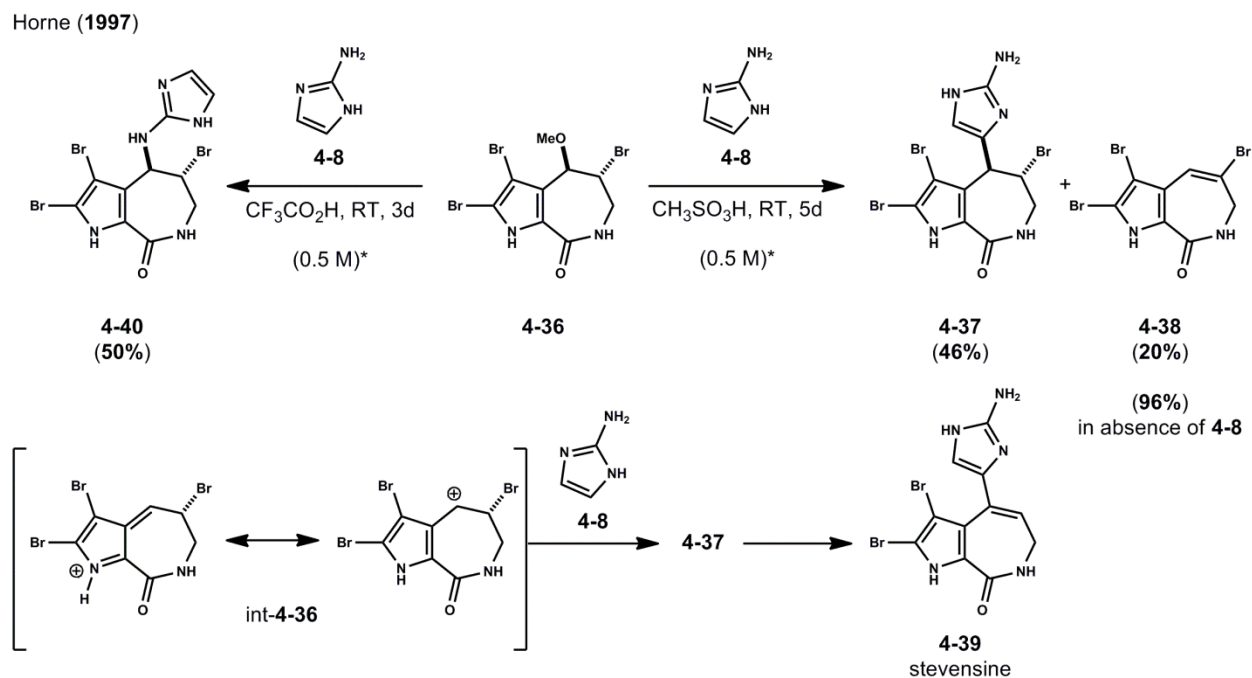
**Scheme 4.4.** Huigens *et al.* reported failed attempts to complete the total synthesis of (±)-ageliferin (**4-1a**) - Oxidative desymmetrization of 'CAGE' (**4-29**) is not productive.

Melander and co-workers hold general interest in novel compounds possessing anti-biofilm and anti-bacterial properties.<sup>[32]</sup> Along these research lines, and inspired by the reported anti-fouling activity of (–)-ageliferin **4-1a**, the group synthesized *cis*-bromoageliferin (CAGE) **4-29** and *trans*-bromoageliferin (TAGE) **4-24** analogues with demonstrated ability to inhibit the formation of *P. aeruginosa* biofilms (Scheme 4.4).<sup>[31a]</sup> Intuitively, Huigens proposed a synthesis of (±)-ageliferin **4-1a** from 'CAGE' **4-29**.<sup>[31b]</sup> Huigens and Melander postulated that the (–)-ageliferin core **4-32** may arise via an 'enzymatic oxidative desymmetrization'. In this event, *meso*-symmetric 'CAGE' **4-29** would undergo oxidation in a proposed chiral active site of an enzyme to provide **4-30**. It was further rationalized that upon extended protonation of **4-30** under thermodynamic conditions and subsequent nucleophilic attack with 2-aminoimidazole **4-8** would provide the (–)-ageliferin core **4-32**. Unfortunately, the total synthesis of (±)-ageliferin **4-1a** was

not realized via oxidative desymmetrization of ‘CAGE’ **4-29**, although valuable information can be gleaned from this unsuccessful approach. As reported by Huigens, and observed in our own research with model systems (**4-7**, **4-13**), oxidations with molecular bromine in substituted and non-substituted 2-aminotetrahydrobenzimidazoles are met with difficulty. Although few products were characterized from the efforts of Huigens, it is understood that substantial ‘*decomposition*’ describes the outcome of uncontrolled or over-oxidation when molecular bromine is employed. Lastly, in an alternative approach to (±)-ageliferin **4-1a**, Huigens reported the shortcomings of an intramolecular reaction that could have converted linear bis-guanidine **4-35** to ageliferin core **4-5** (*vide supra*) under oxidative conditions.

#### **4.3.3 Precedent in Related Systems, 2-aminoimidazole Oxidations.**

It should be noted that this proposal was formulated after the novel reactivity of 2-aminoimidazoles (**4-7**, **4-13**) with 4-phenyl-1,2,4-triazoline-3,5-dione **4-14** was discovered (Chapter 4, Part 1). We immediately recognized the potential of this activation–alkylation mode for the total synthesis of ageliferin **4-1a** and related dimeric pyrrole-aminoimidazole (PAI) alkaloids. Although analogous reactivity initiated with molecular bromine has been explored by Horne and co-workers<sup>[12]</sup>, the ability to isolate ‘activated’ adducts (**4-15**, **4-18**) prior to carbon-carbon bond formation between differentiated 2-aminoimidazole is a substantial improvement for the synthesis of non-symmetric bis-guanidines.

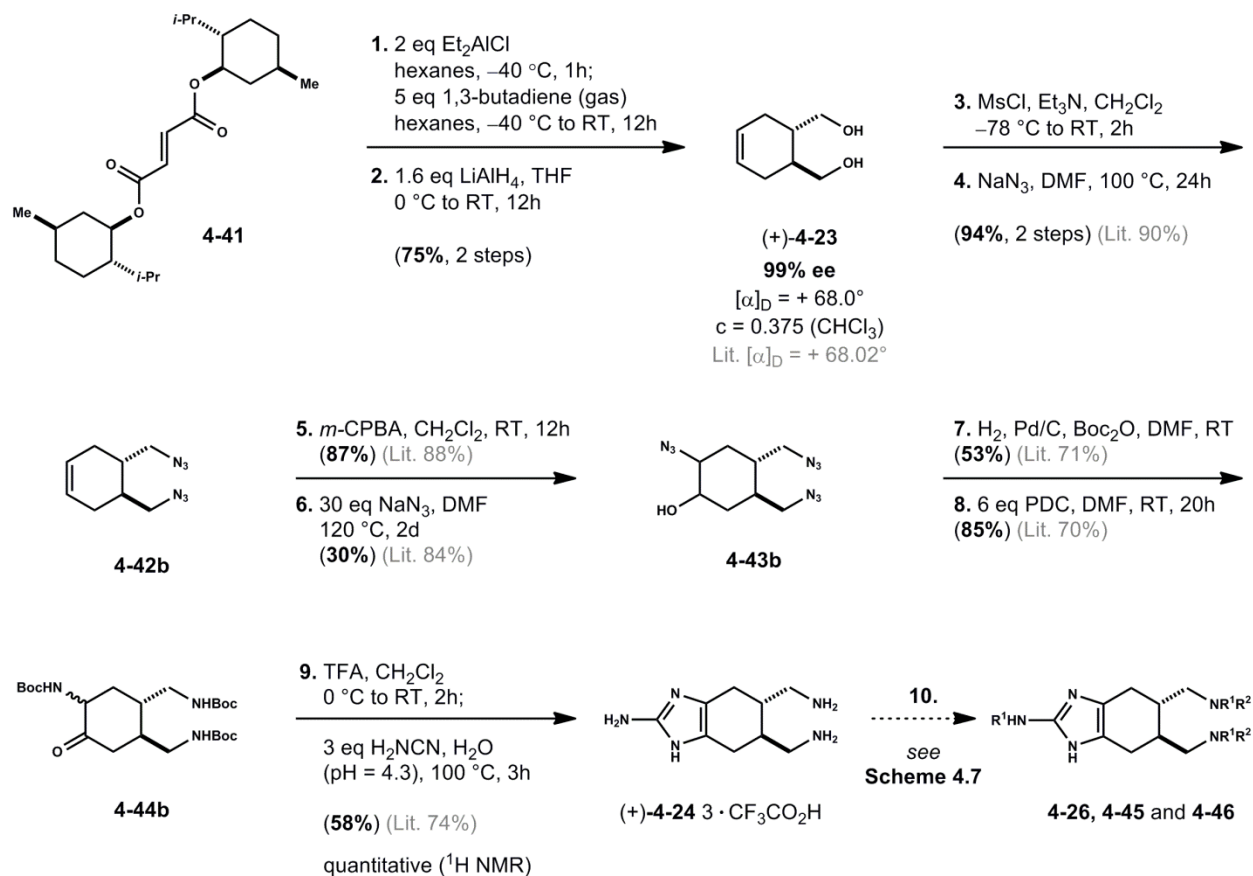


**Scheme 4.5.** Horne's 'biomimetic' synthesis of oroidin derived alkaloid stevensine **4-39**.

Horne and co-workers also realized the ability to 'trap' oxidized 2-aminoimidazoles in methanol as their corresponding bis-hemiaminal methyl ethers for subjection to subsequent reactions.<sup>[33]</sup> The seminal research of Horne demonstrated several reactivity modes in the oxidative transformation of 2-aminoimidazoles which culminated in the syntheses of related pyrrole-imidazole metabolites mauritiamine (not shown) and stevensine **4-39** (Scheme 4.5).<sup>[12]</sup> Stevensine **4-39** was ultimately accessed via the intermediacy of putative resonance stabilized carbocation **int-4-36** to provide 2-aminoimidazole **4-37** in methanesulfonic acid.<sup>[12b,34]</sup> The successful intermolecular alkylation in this strategy holds considerable promise for our analogous proposal. Equally noteworthy is the mention of N-linked isomer **4-40**, formed exclusively when trifluoroacetic acid is employed as solvent in place of methanesulfonic acid.<sup>[12b,20]</sup> With this precedent and our own model studies we were confident that (–)-ageliferin **4-1a** could be prepared similarly. Our attempts to apply a novel activation–alkylation mode for the total synthesis of (–)-ageliferin **4-1a** are described herein.

## 4.4 Results and Discussion.

### 4.4.1 Synthesis of *Trans*-substituted 2-aminoimidazole (4-24).

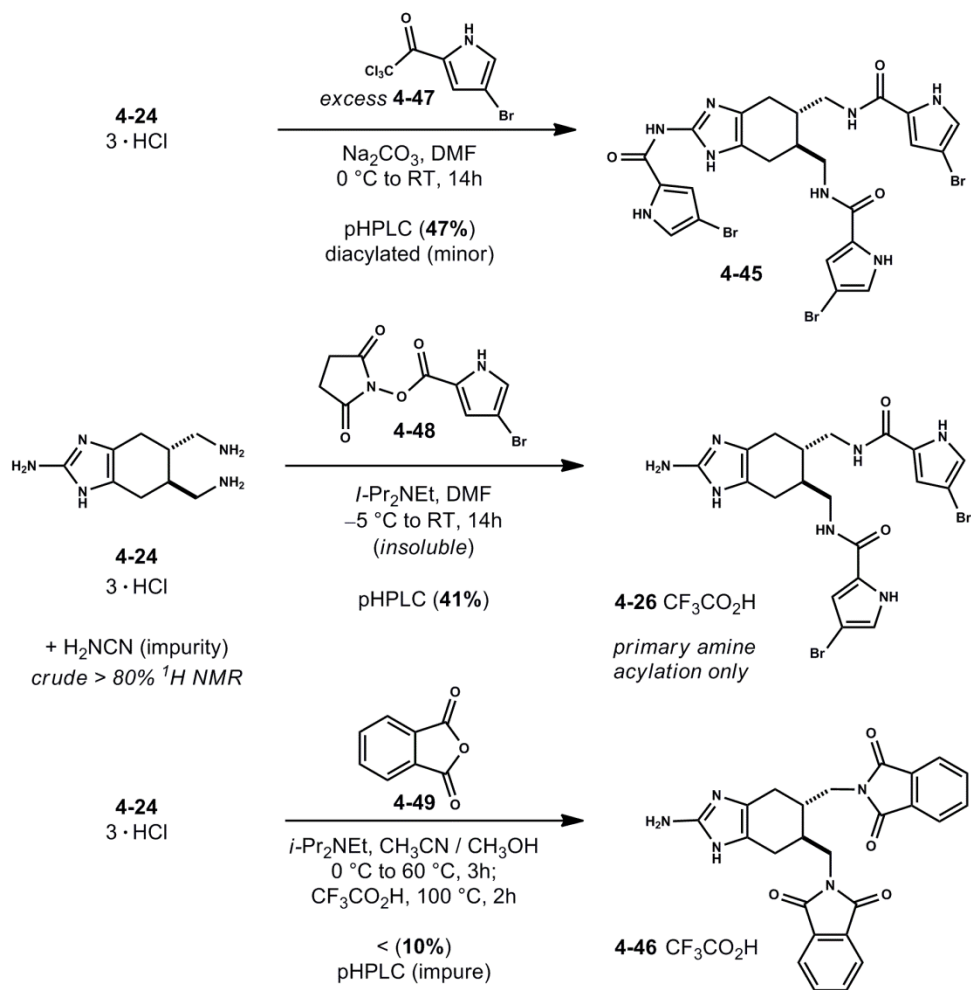


**Scheme 4.6.** Synthesis of substituted 2-aminoimidazole (**4-24**) in 9 steps from dimethylfumarate **4-41**. General strategy and conditions followed according to Huigens III, R. W. *et al. J. Am. Chem. Soc.*, **2007**, 129, 6966.

*Trans*-substituted 2-aminoimidazole **4-24** was prepared in 9 steps from (–)-dimethyl fumarate **4-41** (Scheme 4.6). The conversion of diol (+)-**4-23** to desired aminoimidazole **4-24** closely followed procedures developed by Huigens *et al.* for the synthesis of ‘TAGE’ (±)-**4-24**.<sup>[31]</sup> The chiral diol (+)-**4-23** was accessed via a previously reported Lewis acid promoted Diels–Alder cycloaddition utilizing excess 1,3-butadiene and dienophile (–)-dimethyl fumarate **4-41**.<sup>[35]</sup> The resultant cycloadduct diester (not shown) was reduced to yield C<sub>2</sub>-symmetric diol (+)-**4-23** in high enantiomeric excess (99% ee).<sup>[35c]</sup> Diol (+)-**4-23** was converted to diazide **4-42b** in two steps without purification. Elaboration of the diazide **4-42b** to triazido alcohol **4-43b**

proceeded without event, although the epoxide **4-43a** (not shown, d.r. 1:1) opening with excess sodium azide occurred with considerably lower yield than the reported protocol.<sup>[36]</sup> Triazido alcohol **4-43b** was reproducibly transformed into *trans*-substituted 2-aminoimidazole **4-24** by treatment with cyanamide under buffered aqueous conditions. With general access to **4-24**, several N-acylated derivatives were prepared (Step 10) to conduct a thorough study on the propensity of such compounds to undergo oxidation with PTAD **4-14**. Oxidations utilizing molecular bromine in methanesulfonic acid were not explored, in part due to the failures reported by Huigens, as well as our observations in model systems (**4-7**, **4-13**).<sup>[31b]</sup>

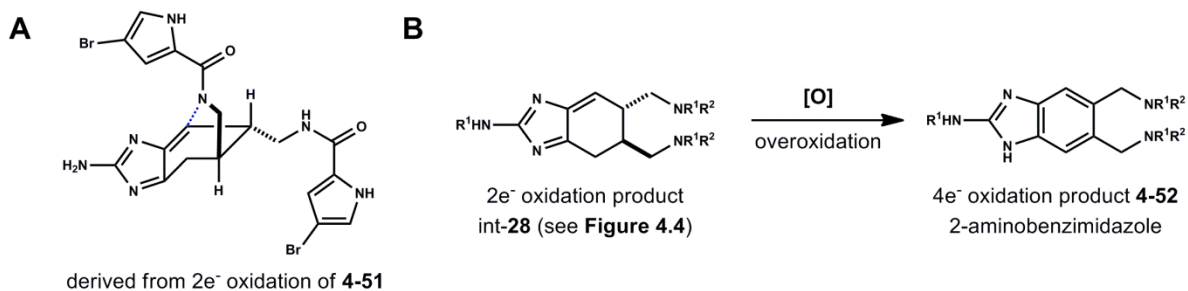
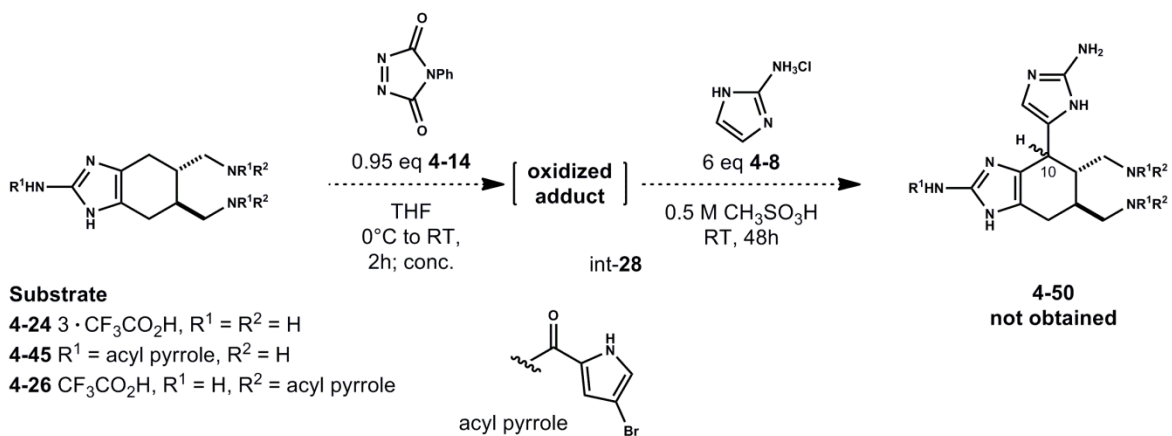
#### 4.4.2 Attempted Oxidative Activation–Alkylations to Access (–)-Ageliferin 4-1a.



**Scheme 4.7.** Derivatization of 2-aminotetrahydrobenzimidazole (**4-24**) for subsequent oxidation studies of aminoimidazoles (**4-26**, **4-45**, **4-46**).

In addition to *trans*-substituted 2-aminoimidazole **4-24**, three *N*-acylated derivatives (**4-45**, **4-26** and **4-46**) were prepared for subsequent oxidation studies with PTAD **4-14** and nucleophile 2-aminoimidazole **4-8** (Scheme 4.7). Reactions conducted on model systems indicated that both unprotected (**4-7**) in either salt form (HCl or CF<sub>3</sub>CO<sub>2</sub>H) and trifluoroacetylated variant **4-13** could undergo activation with PTAD **4-14**. Unfortunately, oxidation experiments with functionalized substrates **4-24**, **4-45** and **4-26** were capricious (Scheme 4.8) and prone to decomposition, ostensibly via overoxidation. In all cases, no PTAD adducts (**int-4-28**) could be

identified or isolated as previously observed in model systems (**4-15**, **4-18**). One similarity noted in the series (**4-24**, **4-26**, **4-45**) was the potential for intramolecular reactivity of a pendant nucleophilic amine or amide. Symmetry of the activated intermediate (**int-4-28**) could be disrupted by a cyclization event such as that depicted in **A** (**4-51**, Scheme 4.8). No evidence was obtained for an oxidized intermediate or product of this type, but the proposal served to explain the inability to observe (LCMS) or isolate any PTAD **4-14** adducts. Such was not the case in model systems (**4-7**, **4-13**) that lack aminomethyl side chains. Overoxidation depicted in **B** was commonly observed (LCMS) and resulted in complex reaction mixtures for the series. To overcome this propensity to overoxidize, experiments were conducted with bis-phthalimide derivative **4-46**. Unfortunately, this substrate was difficult to prepare and could not be isolated in high purity despite purification by preparative HPLC.<sup>[37]</sup>

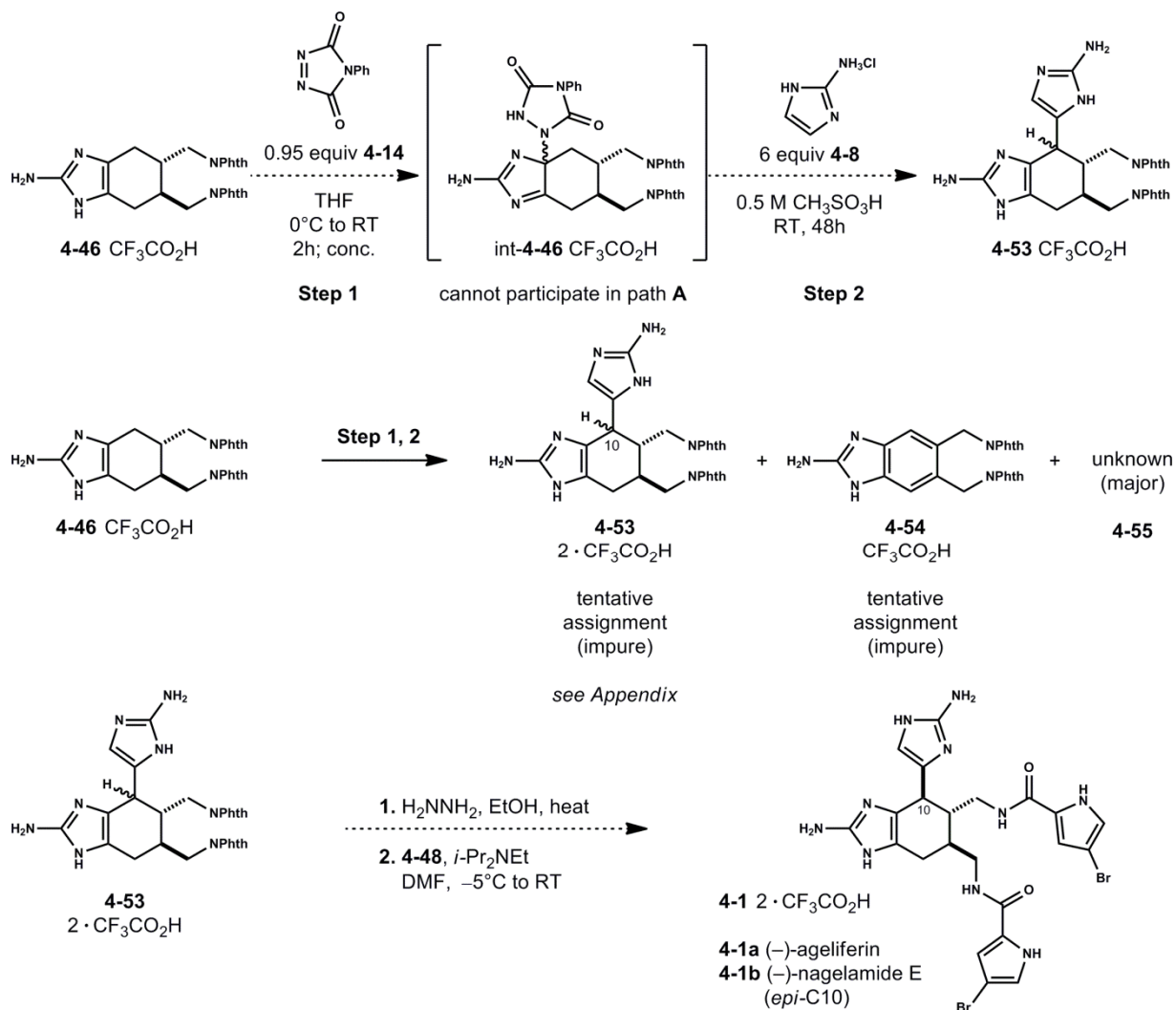


**Scheme 4.8.** Uncontrolled oxidation of ageliferin core substrates (**4-24**, **4-26**, **4-45**). Proposed side reactions (**A**) and (**B**) to explain observed overoxidized intermediates and inability to access general desired structures **4-50**.



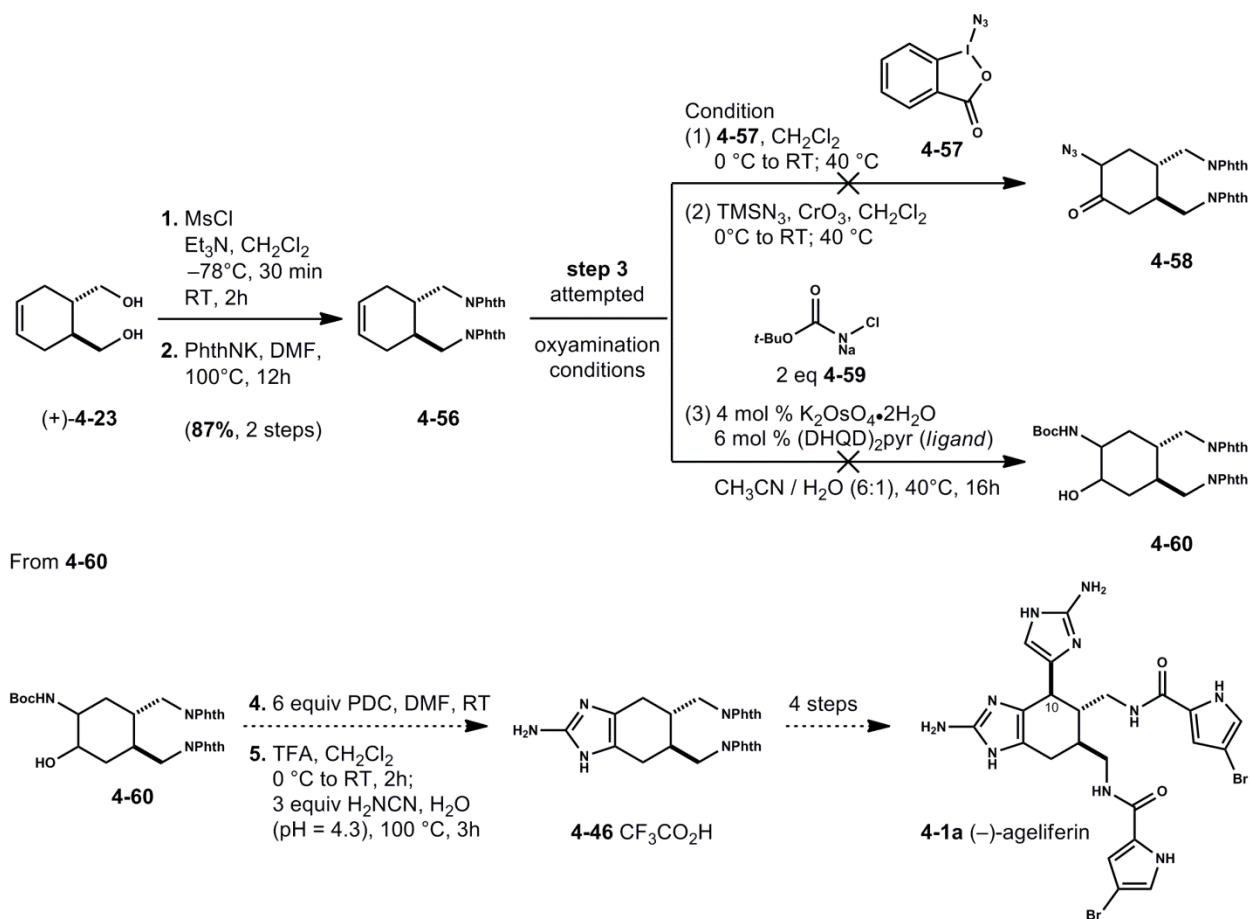
Although challenging to prepare, preliminary oxidation experiments were conducted with bis-phthalimide **4-46** (Scheme 4.9). Interestingly, when **4-46** is reacted with sub-stoichiometric quantities of PTAD **4-14** in THF the desired adduct **int-4-46** is readily observed by LC/MS analysis (LRMS-ESI ( $m/z$ ) calcd for  $[C_{33}H_{26}N_8O_6+H]^+$ : 631.2; found: 631.2) as a major component among further oxidized derivatives. Following concentration of this intermediate (**int-4-46**) and subjection to excess nucleophile **4-8** in methanesulfonic acid at RT, three presumed product species (**4-53**, **4-54** and **4-55**) were observed as monitored by LC/MS (see Appendix for details). The crude reaction was allowed to stir for 48h at RT following neutralization and direct purification by preparative HPLC. Unfortunately, the hydrolysis of phthalimide derivatives either during the reaction (step 2) or during purification made isolation of these intermediates difficult. However the direct observation of adduct **int-4-46** was promising and consistent with model studies. Furthermore, this observation supports the inability of this intermediate to directly participate in path **A** (Scheme 4.8). Purification of crude reaction mixtures provided tentatively assigned desired **4-53** (unassigned relative stereochemistry at C10, see Appendix) and tentatively assigned functionalized 2-aminotetrahydrobenzimidazole **4-54** (see Appendix) as a major side-product consistent with path **B** (Scheme 4.8). Additional product mixtures obtained were not further separated but are consistent with phthalimide hydrolysis (**4-55**, major) of several differentially oxidized and overoxidized intermediates. Although promising, the sequence was capricious (repeated twice with similar results) and suggests alternative N-protection strategies are required. If bis-guanidine **4-53** could be accessed efficiently, phthalimide removal by hydrazinolysis and selective diacylation with bromopyrrole carboxylic acid **4-48** would complete the total synthesis of (-)-ageliferin **4-1a** and/or nagelamide E **4-1b** (*epi*-C10).<sup>[38]</sup> Preliminary attempts to convert crude bis-guanidine **4-53** to ageliferin **4-1a**

were not successful. Currently, poor access to pure bis-phthalimide **4-46** hinders further useful experiments for the preparation of targeted bis-guanidine **4-53**. Preliminary experiments in this realm are encouraging. A scalable synthesis of **4-46** would allow refinement of this two-step sequence.



**Scheme 4.9.** Controlled oxidation of phthalimide protected 2-aminotetrahydrobenzimidazole (**4-46**) and alkylation with aminoimidazole (**4-8**).

#### 4.4.3 Alternative Synthesis of Bis-phthalimide Derivative (4-46).



**Scheme 4.10.** Proposed alternative synthesis of aminoimidazole (**4-46**) - general access to (-)-ageliferin (**4-1a**).

Lastly, an alternative synthesis of (-)-ageliferin **4-1a** is proposed from bis-phthalimide derivative **4-56** (Scheme 4.10). Although current access to functionalized 2-aminotetrahydrobenzimidazole **4-24** is reliable, the sequence is lengthy, and in our hands some transformations were low yielding.<sup>[31a]</sup> The proposed alternative route (Scheme 4.10) begins with an efficient synthesis of bis-phthalimide **4-56** that could be elaborated to oxyaminated compounds **4-58** or **4-60**. Attempts to convert olefin **4-56** to  $\alpha$ -azido ketone **4-58** using hypervalent iodosoazide **4-57** transfer chemistry<sup>[39]</sup> or the related azidotrimethylsilyl-chromium trioxide methods<sup>[40]</sup> were unsuccessful. Consequently, we diverted attention to Sharpless amino hydroxylation methods to access amino alcohol **4-60**. These attempts were also unsuccessful due

to the partial hydrolysis of phthalimide groups under the basic aqueous conditions.<sup>[41]</sup> Certainly, this method could be reexamined in continued efforts to complete the total synthesis of (-)-ageliferin **4-1a** in 9 steps, as proposed.

## 4.5 Conclusion.

The 2-aminoimidazole oxidation chemistry described in this chapter was inspired by the initial proposal to utilize ene-type reactivity of singlet oxygen and diazo electrophiles for the conversion of ( $\pm$ )-ageliferin **4-1a** to ( $\pm$ )-axinellamine A **4-4**. Several novel transformations were discovered, including 1) the oxidation of 2-aminoimidazoles (**4-7**, **4-13**) with PTAD **4-14** and singlet oxygen, 2) the subsequent rearrangement chemistry of PTAD adduct **4-15** and 3) the application of these methods to an efficient synthesis of ageliferin core **4-5**. The efficiency of these methods initiated interest in the total synthesis of (-)-ageliferin **4-1a** and the development of an asymmetric route to key  $C_2$ -symmetric intermediate bis-phthalimide **4-46**. The key oxidative transformation to desymmetrize and install the pendant 2-aminoimidazole (Scheme 4.9) would require further refinement to enable the proposed synthetic routes. The troublesome preparation of **4-46** hindered progress and ongoing efforts to access optically active dispacamide dimers via alternative means (Chapter 5) shifted our attention from this promising synthetic strategy.

## 4.6 References and Notes

- [1] (a) Ding, H.; Roberts, A. G.; Harran, P. G. *Chem. Sci.* **2013**, *4*, 303; (b) Ding, H.; Roberts, A. G.; Harran, P. G. *Angew. Chem. Int. Ed.* **2012**, *51*, 4340; (c) Li, Q.; Hurley, P.; Ding, H.; Roberts, A. G.; Akella, R.; Harran, P. G. *J. Org. Chem.* **2009**, *74*, 5909.
- [2] (a) Schenck, G. O. *Angew. Chem.* **1957**, *69*, 579; (b) For a review of the Schenck ene reaction: Prein, M.; Adam, W. *Angew. Chem. Int. Ed.* **1996**, *35*, 477.
- [3] Oxygen donor and oxygen acceptor substrates in Ti<sup>(IV)</sup>-catalyzed epoxidations: Adam, W.; Nestler, B. *J. Am. Chem. Soc.* **1993**, *115*, 7226.
- [4] Hoye, T. R.; Bottorff, K. J.; Caruso, A. J.; Dellaria, J. F. *J. Org. Chem.* **1980**, *45*, 4287.
- [5] (a) Khan, A. U.; Kasha, M. *Nature* **1964**, *204*, 241; (b) Foote, C. S.; Wexler, S. *J. Am. Chem. Soc.* **1964**, *86*, 3880-3881; (c) Corey, E. J.; Taylor, W. C. *J. Am. Chem. Soc.* **1964**, *86*, 3881; (d) For a comprehensive review of the physical and chemical properties of singlet oxygen: Kearns, D. R. *Chem. Rev.* **1971**, *71*, 395-427.
- [6] Singlet oxygen generated under aqueous conditions from sodium hypochlorite and hydrogen peroxide: Foote, C. A.; Wexler, S. *J. Am. Chem. Soc.* **1964**, *86*, 3879.
- [7] (a) Matsuura, T.; Saito, I. *Chem. Comm.* **1967**, 693; (b) For low temperature guanosine oxidations with singlet oxygen and MTAD: Sheu, C.; Kang, P.; Khan, S.; Foote, C. S. *J. Am. Chem. Soc.* **2002**, *124*, 3905.
- [8] For singlet oxygen generation with rose bengal in dilute buffered aqueous solutions: Ye, Y.; Muller, J. G.; Luo, W.; Mayne, C. L.; Shallop, A. J.; Jones, R. A.; Burrows, C. J. *J. Am. Chem. Soc.* **2003**, *125*, 13926.
- [9] (a) The first report of an ene reaction with 1,2,4-triazoline-3,5-diones: Pirkle, W. H.; Stickler, J. C. *Chem. Comm.* **1967**, 760; (b) Reactivity of 1,2,4-Triazoline-3,5-diones with electron-rich nitrogen heterocycles: Hall, J. H.; Kaler, L.; Herring, R. *J. Org. Chem.* **1984**, *49*, 2579.
- [10] (a) For the reactivity of PTAD with indole: Wilson, R. M.; Hengge, A. *Tetrahedron Lett.* **1985**, *26*, 3673; (b) Oxidations of the indole 2,3- $\pi$  bond with MTAD: Baran, P. S.; Guerrero, C. A.; Corey, E. J. *Org. Lett.* **2003**, *5*, 1999; (c) For an example of 4-methyl-1,2,4-triazoline-3,5-dione used in the total synthesis of Okaramine N: Baran, P. S.; Guerrero, C. A.; Corey, E. J. *J. Am. Chem. Soc.* **2003**, *125*, 5628.
- [11] For discussion of transition state and mechanism of triazolinediones in relation to singlet oxygen: Leach, A. G.; Houk, K. N. *Chem. Comm.* **2002**, 1243.
- [12] (a) Oxidative homo- and hetero-dimerization of alkyl substituted 2-aminoimidazoles: Xu, Y.; Yakushijin, K.; Horne, D. A. *J. Org. Chem.* **1996**, *61*, 9569; (b) Total synthesis of stevensine **4-39**: Xu, Y.; Yakushijin, K.; Horne, D. A. *J. Org. Chem.* **1997**, *62*, 456.

- [13] Kinnel, R. B.; Gehrken, H.-P.; Swali, R.; Skoropowski, G.; Scheuer, P. *J. Org. Chem.* **1998**, *63*, 3281.
- [14] (a) O'Malley, D. P.; Li, K.; Maue, M.; Zografos, A. L.; Baran, P. S. *J. Am. Chem. Soc.* **2007**, *129*, 4762. (b) Unfortunately, the des-chloro (C13) spirocyclopentane core obtained held incorrect relative stereochemistry and the group diverted to an alternative linear construction of this scaffold en route to the first total synthesis of the axinellamines (**4-4**).
- [15] O'Malley, D. P., Ph.D. Dissertation, The Scripps Research Institute, **2008**, UMI #3313886.
- [16] For general interest in the Diels–Alder type reactivity of 4- or 5-vinyl imidazoles see: Lovely, C. J., Du, H.; Dias, H. V. R. *Org. Lett.* **2001**, *3*, 1319; (b) For related Diels–Alder cycloadditions of vinyl imidazoles: (b) Walters, M. A.; Lee, M. D.; *Tetrahedron Lett.* **1994**, *35*, 8307. (c) Deghati, P. Y. F.; Wanner, M. J.; Koomen, G. J. *Tetrahedron Lett.* **1998**, *39*, 4561.
- [17] For a discussion of the oxidative ring-contraction method: (a) Wang, S.; Dilley, A. S.; Poullennec, K. G.; Romo, D. *Tetrahedron* **2006**, *62*, 7155; (b) Dransfield, P. J.; Wang, S.; Dilley, A.; Romo, D. *Org. Lett.* **2005**, *7*, 1679; (c) For access to a *trans*-azabicyclo[3.3.0]octane core: Zancanella, M. A.; Romo, D. *Org. Lett.* **2008**, *10*, 3685.
- [18] For a biomimetic synthesis of dibromophakellin see: Foley, L. H.; Büchi, G. *J. Am. Chem. Soc.* **1982**, *104*, 1776.
- [19] (a) Ma, Z.; Lu, J.; Wang, X.; Chen, C. *Chem. Comm.* **2011**, *47*, 427; (b) Another proposal has been put forth with regard to a similar ageliferin-palau'amine hybrid structure: Feldman, K. S.; Nuriye, A. Y.; Li, J. *J. Org. Chem.* **2011**, *76*, 5042.
- [20] This mixture of isomers (**4-5**, **4-12**) is likely dependent on solvent Brønsted acid strength and has been observed previously (see Ref. 12b).
- [21] Interestingly, even at elevated temperatures, no reaction was observed between **4-7b** and acyclic bis(2,2,2-trichloroethyl) azodicarboxylate or diethyl azodicarboxylate.
- [22] CCDC 942602 (Compound **4-17**) contains the supplementary crystallographic data for this chapter. These data can be obtained free of charge from The Cambridge Crystallographic Data Centre via [www.ccdc.cam.ac.uk/data\\_request/cif](http://www.ccdc.cam.ac.uk/data_request/cif).
- [23] It was *determined* that CH<sub>3</sub>CN was the optimal solvent for this transformation due to its ability to solubilize salt forms **4-7**.
- [24] PTAD adduct **4-8** was stable in several neutral solvents (including MeOH-*d*<sub>4</sub>) at RT and readily characterized as its hydrochloride salt.
- [25] No N-linked isomers **4-12** were observed when MeSO<sub>3</sub>H was employed as solvent (see Ref. 12b, 20).

[26] For the use of dimethyl azodicarboxylate as an oxidant in the synthesis of cephalosporin C: Woodward, R. B.; Heusler, K.; Gosteli, J.; Naegeli, P.; Oppolzer, W.; Ramage, R.; Ranganathan, S.; Vorbrüggen, H. *J. Am. Chem. Soc.* **1966**, *88*, 852.

[27] Diels–Alder reactions of PTAD: Cookson, R. C.; Gilani, S. S. H.; Stevens, I. D. R. *J. Chem. Soc.* **1967**, 1905.

[28] (a) Kang, P.; Foote, C. S. *J. Am. Chem. Soc.* **2002**, *124*, 9629; (b) For an earlier, comparable study: Sonnenberg, J.; White, D. M. *J. Am. Chem. Soc.* **1964**, *86*, 5685.

[29] The trifluoroacetate salt form (**4-7b**) is generally more soluble in aprotic organic solvents (CH<sub>2</sub>Cl<sub>2</sub>, CHCl<sub>3</sub>, CH<sub>3</sub>CN) than the corresponding hydrochloride (**4-7a**).

[30] The reaction was monitored by <sup>1</sup>H NMR (500 MHz, with CH<sub>2</sub>Cl<sub>2</sub> suppression). Aliquots (0.5-mL) could be concentrated with a stream of Ar for further characterization.

[31] (a) Huigens III, R. W.; Richards, J. J.; Parise, G.; Ballard, E.; Zeng, W.; Deora, R.; Melander, C. *J. Am. Chem. Soc.* **2007**, *129*, 6966; (b) Huigens III, R. W., Ph.D. Dissertation, North Carolina State University, **2009**.

[32] For a perspective, see: Worthington, R. J.; Richards, J. J.; Melander, C. *Org. Biomol. Chem.* **2012**, *10*, 7457-7474

[33] For use of this method in the synthesis of mauritiamine: Olofson, A.; Yakushijin, K.; Horne, D. A. *J. Org. Chem.* **1997**, *62*, 7918.

[34] Solvent, reaction concentration (0.5 M) and the use of excess nucleophile **4-8** were crucial to the success of these reactions. Interestingly, experiments suggest **4-38** is not a productive intermediate when reintroduced to reaction conditions with excess **4-8**. A similar logic can explain the non-productivity of **4-38** and proposed intermediate **4-30**.

[35] (a) For the Diels–Alder reaction see: (a) Heathcock, C. H.; Davis, B. R.; Hadley, C. R. *J. Med. Chem.* **1989**, *32*, 197. (b) Doherty, S.; Knight, J. G.; Bell, A. L.; Harrington, R. W.; Clegg, W. *Organometallics* **2007**, *26*, 2465; (c) For an explanation of diastereoselectivity in a similar Diels–Alder reaction: Furuta, K.; Iwanaga, K.; Yamamoto, H. *Tetrahedron Lett.* **1986**, *27*, 4507; (d) For the LiAlH<sub>4</sub> reduction see: Garcia, M.-E. J.; Frölich, U.; Koert, U. *Eur. J. Org. Chem.* **2007**, 1991.

[36] It should be noted that Huigens *et al.* (Ref. 31) developed alternative procedures for a similar transformation in the ‘CAGE’ **4-29** series (NaN<sub>3</sub>, H<sub>2</sub>SO<sub>4</sub>, MeOH/H<sub>2</sub>O (1:8), reflux) although these conditions were not examined.

[37] Selective acylation of the primary amines of **4-24** proved difficult when phthalic anhydride was used in excess with crude **4-24** (containing H<sub>2</sub>NCN). The addition of MeOH after the initial acylation step minimized guanidine acylation.



[38] In either outcome, the equilibration of **4-1** at C-10 has been established: O'Malley, D. P.; Li, K.; Zografos, A. L.; Baran *J. Am. Chem. Soc.* **2007**, 4762.

[39] For the preparation and use of reagent **4-57**: Zhdankin, V. V.; Kuehl, C. J.; Krasutsky, A. P.; Formanek, M. S.; Bols, J. T. *Tetrahedron Lett.* **1994**, 35, 9677.

[40] Azidotrimethylsilyl-chromium trioxide is readily generated from trimethylsilyl azide and chromium trioxide: Reddy, M. V. R.; Kumareswaran, R.; Vankar, Y. D. *Tetrahedron Lett.* **1995**, 36, 6751.

[41] (a) Herranz, E.; Biller, S. A.; Sharpless, K. B. *J. Am. Chem. Soc.* **1978**, 100, 3596; (b) Herranz, E.; Biller, S. A.; Sharpless, K. B. *J. Org. Chem.* **1980**, 45, 2710; (c) O'Brien, P.; Osborne, S. A.; Parker, D. D. *Tetrahedron Lett.* **1998**, 39, 4099.

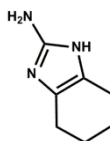
## 4.7 Experimental (Part I).

### 4.7.1 Materials and Methods.

Unless stated otherwise, reactions were performed under an argon (Ar) atmosphere in flame-dried glassware. Tetrahydrofuran (THF), chloroform ( $\text{CHCl}_3$ ), methylene chloride ( $\text{CH}_2\text{Cl}_2$ ), diethyl ether ( $\text{Et}_2\text{O}$ ), toluene ( $\text{PhCH}_3$ ), benzene ( $\text{PhH}$ ), dimethoxyethane (DME), dimethyl formamide (DMF) and acetonitrile ( $\text{CH}_3\text{CN}$ ) were dried and deoxygenated through activated alumina solvent drying systems or distilled prior to use. Column chromatography was performed on silica gel 60 (SiliCycle, 240-400 mesh). Thin layer chromatography (TLC) and preparative thin layer chromatography (pTLC) utilized pre-coated plates (silica gel 60 PF254, 0.25 mm or 0.5 mm). Purification of advanced intermediates employed an Agilent 1200 Preparative HPLC (pHPLC) system equipped with an Agilent Quadrupole 6130 ESI-MS detector and an automated fraction collector. Mobile phases (Mobile phase A:  $\text{H}_2\text{O}$ , Mobile Phase B:  $\text{CH}_3\text{CN}$ ) were prepared with 0.1% or 1% trifluoroacetic acid ( $\text{CF}_3\text{CO}_2\text{H}$ ) or 0.1% formic acid as indicated. Advanced intermediates isolated and characterized as trifluoroacetate salts are denoted as (2- $\text{CF}_3\text{CO}_2\text{H}$ ) in data tables. The trifluoroacetate salt may be omitted from structures in schemes for clarity. NMR spectra were recorded on Bruker Avance spectrometers (500 MHz or 600 MHz). Data for  $^1\text{H}$  NMR spectra are reported as follows: chemical shift ( $\delta$  ppm) (multiplicity, coupling constant (Hz), integration) at 298K, unless stated otherwise, and are referenced to a residual solvent peak. Data for  $^{13}\text{C}$  NMR spectra are reported in terms of chemical shift ( $\delta$  ppm) and are referenced to residual solvent peak.

## 4.7.2 Experimental Procedures and Characterization Data.

### Preparation of 4,5,6,7-tetrahydro-1H-benzo[d]imidazol-2-amine hydrochloride (**4-7a**).



**4-7a** HCl

2-aminocyclohexanone hydrochloride was prepared according to Baumgarten, H. E.; Peterson, J. M. *J. Am. Chem. Soc.* **1960**, *82*, 459-463 and Alt, G. H.; Knowles, W. S. *Org. Syn.* **1973**, *5*, 208; **1965**, *45*, 16.

A solution containing 2-aminocyclohexanone hydrochloride (1.00 g, 6.7 mmol, 1.0 equiv) and cyanamide (2.24 g, 53.5 mmol, 8.0 equiv) in H<sub>2</sub>O (133-mL) was adjusted from approx. pH = 2 to pH = 4.3 with 10 wt% NaOH and the resultant solution was heated to 100°C for 3h. Concentration in vacuo provides a quantitative yield of 4,5,6,7-tetrahydro-1H-benzo[d]imidazol-2-amine hydrochloride (**4-7a**) (<sup>1</sup>H NMR, 500 MHz, H<sub>2</sub>O-*d*<sub>2</sub>) as an off-white solid contaminated with excess cyanamide hydrochloride (<sup>13</sup>C NMR, 125 MHz, H<sub>2</sub>O-*d*<sub>2</sub>). This mixture was trifluoroacetylated by the addition of excess CF<sub>3</sub>CO<sub>2</sub>H (2.56-mL, 33.4 mmol, 5 equiv) and TFAA (4.75-mL, 33.4 mmol, 5 equiv) to a suspension of crude (**4-7a**) (6.7 mmol, 1.0 equiv) in CH<sub>2</sub>Cl<sub>2</sub> (17.6-mL) at RT for 1h. The mixture was diluted with CHCl<sub>3</sub> (80-mL) and carefully washed with H<sub>2</sub>O (10-mL), saturated aqueous NaHCO<sub>3</sub> (2 × 10-mL), dried over Na<sub>2</sub>SO<sub>4</sub>, filtered and concentrated in vacuo provide 2,2,2-trifluoro-N-(4,5,6,7-tetrahydro-1H-benzo[d]imidazol-2-yl)acetamide (**4-13**) (1.1 g, 71%) as an off-white solid.

4,5,6,7-tetrahydro-1H-benzo[d]imidazol-2-amine hydrochloride (**4-7a**) can be prepared quantitatively by the acidic hydrolysis of 2,2,2-trifluoro-N-(4,5,6,7-tetrahydro-1H-benzo[d]imidazol-2-yl)acetamide (**4-13**) as a suspension in 2 M aqueous HCl (0.2 M reaction concentration) heated to 60°C for 20 min followed by concentration in vacuo.

**Note:** Alternatively, crude 4,5,6,7-tetrahydro-1H-benzo[d]imidazol-2-amine (**4-7a**) can be purified as the free-base via flash column chromatography (SiO<sub>2</sub>, isocratic CH<sub>2</sub>Cl<sub>2</sub>/MeOH/conc. NH<sub>4</sub>OH (90:9:1)) with traces of cyanamide as a highly polar impurity.

**Note:** 4,5,6,7-Tetrahydro-1H-benzo[d]imidazol-2-amine has been previously prepared and characterized as the ethyl sulfate salt. (Little, T. L.; Webber, S. E. *J. Org. Chem.* **1994**, *59*, 7299.

#### **4,5,6,7-tetrahydro-1H-benzo[d]imidazol-2-amine (4-7) (freebase):**

<sup>1</sup>H NMR (500 MHz, MeOH-*d*<sub>4</sub>): δ (ppm) 2.45-2.40 (m, 4H), 1.84-1.78 (m, 4H); <sup>13</sup>C NMR (125 MHz, MeOH-*d*<sub>4</sub>): δ (ppm) 147.8, 121.9, 23.2, 21.1; LRMS-ESI (*m/z*) calcd for [C<sub>7</sub>H<sub>11</sub>N<sub>3</sub>+H]<sup>+</sup>: 138.10; found: 138.1

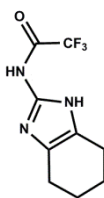
### Preparation of 4,5,6,7-tetrahydro-1H-benzo[d]imidazol-2-amine (4-7b).

4,5,6,7-tetrahydro-1H-benzo[d]imidazol-2-amine (**4-7b**) ( $\text{CF}_3\text{CO}_2\text{H}$ ) was prepared by dissolution of the free base 4,5,6,7-tetrahydro-1H-benzo[d]imidazol-2-amine (**4-7**) in MeOH (0.2 M) and addition of 1.2 equiv  $\text{CF}_3\text{CO}_2\text{H}$  followed by concentration in vacuo.

### 4,5,6,7-tetrahydro-1H-benzo[d]imidazol-2-amine (4-7b) ( $\text{CF}_3\text{CO}_2\text{H}$ ):

$^1\text{H NMR}$  (500 MHz, MeOH- $d_4$ ):  $\delta$  (ppm) 2.44-2.42 (m, 4H), 1.83-1.81 (m, 4H);  $^{13}\text{C NMR}$  (125 MHz, MeOH- $d_4$ ):  $\delta$  (ppm) 148.0, 121.9, 23.2, 21.1; **HRMS-ESI** ( $m/z$ ) calcd for  $[\text{C}_7\text{H}_{11}\text{N}_3+\text{H}]^+$ : 138.1031; found: 138.1044.

### Synthesis of 2,2,2-trifluoro-N-(4,5,6,7-tetrahydro-1H-benzo[d]imidazol-2-yl)acetamide (4-13).



4-13

See above procedure for the preparation of 4,5,6,7-tetrahydro-1H-benzo[d]imidazol-2-amine hydrochloride (**4-7a**) (71%, 2 steps from 2-aminocyclohexanone).

For the use of trifluoroacetyl as an orthogonal protecting group for guanidine synthesis: Bartoli, S.; Jensen, K. B.; Kilburn, J. D. *J. Org. Chem.* **2003**, 68, 9416.

### 2,2,2-trifluoro-N-(4,5,6,7-tetrahydro-1H-benzo[d]imidazol-2-yl)acetamide (4-13):

$^1\text{H NMR}$  (500 MHz, MeOH- $d_4$ ):  $\delta$  (ppm) 2.52 (s, 4H), 1.84 (s, 4H); **LRMS-ESI** ( $m/z$ ) calcd for  $[\text{C}_9\text{H}_{10}\text{F}_3\text{N}_3\text{O}+\text{H}]^+$ : 234.09; found: 234.1.

### Preparation of 1H-imidazol-2-amine hydrochloride (4-8).



4-8 HCl

Methylisothiourea hydrochloride was prepared according to Kurzer, F.; Lawson, A. *Org. Syn.* **1963**, 4, 645; **1954**, 34, 67.

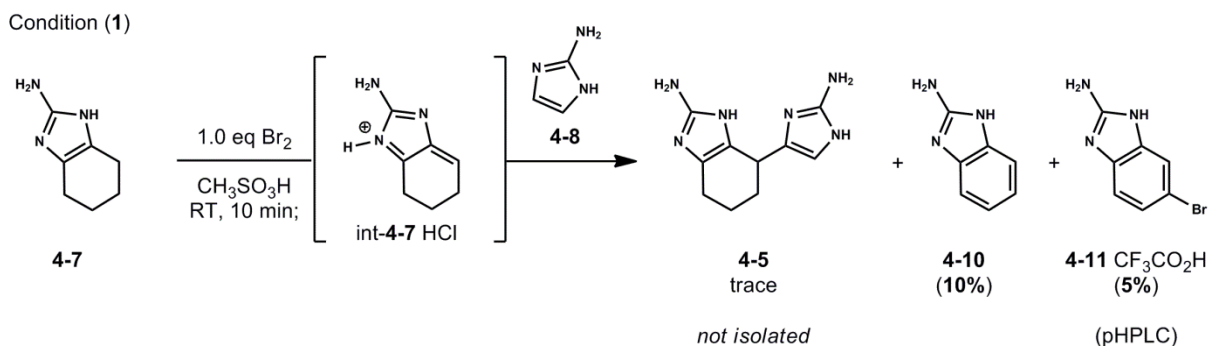
1H-imidazol-2-amine hydrochloride (**4-8**) was prepared according to Weinmann, H. Harre, M.; Koenig, K.; Merten, E.; Tilstam, U. *Tetrahedron Lett.* **2002**, 43, 593 with minor procedural changes (see below).

Methylisothiurea hydrochloride (8.00 g, 72.7 mmol, 1.0 equiv) was dissolved in degassed DI-H<sub>2</sub>O (20-mL) at RT followed by the addition of aminoacetaldehyde dimethyl acetal (8.71 g, 82.8 mmol, 1.14 equiv) via syringe in one portion. The reaction was heated to 50°C for 2h in an oil-bath to form intermediate 1-(2,2-dimethoxyethyl)guanidine quantitatively (observed by <sup>1</sup>H NMR of reaction aliquot, H<sub>2</sub>O-*d*<sub>2</sub>). The reaction was cooled to RT and 5.7-mL conc. HCl was added. The mixture became dark brown and was heated to 100°C for 45 min followed by concentration in vacuo (high-vacuum, 24h) to give 1H-imidazol-2-amine hydrochloride (**4-8**) (8.2 g, 94%, crude yield) as light brown hygroscopic solid that was used without further purification.

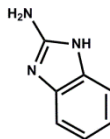
### 1H-imidazol-2-amine hydrochloride (**4-8**):

<sup>1</sup>H NMR (500 MHz, H<sub>2</sub>O-*d*<sub>2</sub>): δ (ppm) 6.73 (s, 2H); <sup>1</sup>H NMR (500 MHz, MeOH-*d*<sub>4</sub>): δ (ppm) 6.80 (s, 2H); <sup>13</sup>C NMR (125 MHz, MeOH-*d*<sub>4</sub>): δ (ppm) 148.7; 114.3.

### Attempted Synthesis (Condition 1) of Model Compound (**4-5**).



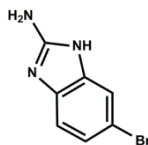
To a solution of free base 4,5,6,7-tetrahydro-1H-benzo[d]imidazol-2-amine (**4-7**) (300 mg, 2.17 mmol, 1.0 equiv) in neat CH<sub>3</sub>SO<sub>3</sub>H (2.2-mL) was added Br<sub>2</sub> (338 mg, 2.17 mmol, 1.0 equiv, by weight) at RT. The resultant dark mixture was allowed to stir at RT for 10 min followed by the addition of 1H-imidazol-2-amine hemi-sulfate (**4-8**) (574 mg, 2.17 mmol, 1 equiv) in one portion. The solution was allowed to stir at RT for 12h followed by neutralization with 3 M aqueous KOH (pH = 10). Concentration in vacuo provided a dark oil that was subjected to flash column chromatography eluting with EtOAc/acetone/H<sub>2</sub>O/formic acid (5:3:1:1) to afford free base (**4-10**) (29 mg, 10%) and impure (**4-11**) (est. yield ~5%, LRMS-ESI (*m/z*) calcd for [C<sub>7</sub>H<sub>6</sub>BrN<sub>3</sub>+H]<sup>+</sup>: 211.98; found: 212.0). A portion of impure free-base (**4-11**) was further purified by preparative HPLC for characterization purposes. LCMS analysis of the crude reaction mixture indicates that desired (**4-5**) (LRMS-ESI (*m/z*) calcd for [C<sub>10</sub>H<sub>14</sub>N<sub>6</sub>+H]<sup>+</sup>: 219.14; found: 219.2) is present although not in substantial quantity relative to (**4-10**) (LCMS, UV detection at 280-nm and MS analysis).



4-10

**1H-benzo[d]imidazol-2-amine (4-10):**

<sup>1</sup>H NMR (500 MHz, MeOH-*d*<sub>4</sub>): δ (ppm) 7.37-7.34 (m, 2H), 7.28-7.25 (m, 2H); <sup>13</sup>C NMR (125 MHz, MeOH-*d*<sub>4</sub>): δ (ppm) 147.8, 117.8, 23.2, 21.1; LRMS-ESI (*m/z*) calcd for [C<sub>7</sub>H<sub>7</sub>N<sub>3</sub>+H]<sup>+</sup>: 134.07; found: 134.1

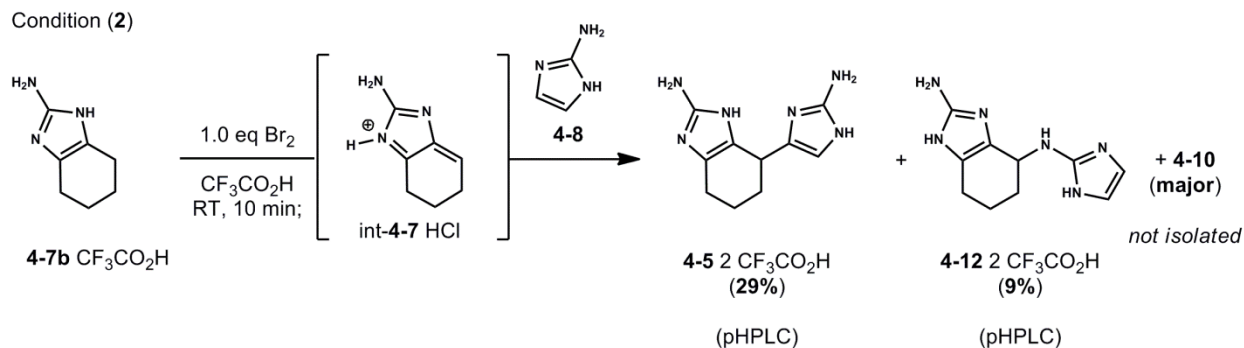


4-11 CF<sub>3</sub>CO<sub>2</sub>H

**6-bromo-1H-benzo[d]imidazol-2-aminium trifluoroacetate (4-11):**

<sup>1</sup>H NMR (500 MHz, H<sub>2</sub>O-*d*<sub>2</sub>): δ (ppm) 7.42 (s, 1H), 7.29 (d, *J* = 8.5 Hz, 1H), 7.13 (d, *J* = 8.5 Hz, 1H); LRMS-ESI (*m/z*) calcd for [C<sub>7</sub>H<sub>6</sub>BrN<sub>3</sub>+H]<sup>+</sup>: 211.98; found: 212.0.

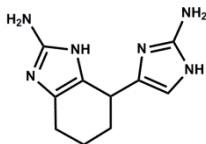
**Synthesis (Condition 2) of Model Compound (4-5) and *N*-bound Isomer (4-12).**



To a solution of 4,5,6,7-tetrahydro-1H-benzo[d]imidazol-2-amine (**4-7b**) (CF<sub>3</sub>CO<sub>2</sub>H) (100 mg, 0.40 mmol, 1.0 equiv) in neat CF<sub>3</sub>CO<sub>2</sub>H (794-μL, 0.5 M) was added Br<sub>2</sub> (62 mg, 0.40 mmol, 1.0 equiv, by weight) at RT. The resultant dark mixture was allowed to stir for 10 min followed by the addition of 1H-imidazol-2-amine hemi-sulfate (**4-8**) (316 mg, 2.4 mmol, 6 equiv) in one portion. The solution was allowed to stir at RT for 40h followed by concentration in vacuo. Purification of a portion of the crude mixture (approx. 1/10 total) by HPLC provided C-bound bis-guanidine (**4-5**) (5.0 mg, 29%) and N-bound bis-guanidine (**4-12**) (1.5 mg, 9%).

**Note:** These conditions were not further optimized and repeat experiments had variable yields. Horne and co-workers noted such variability and dependence on order of reagent addition and reaction times for the initial oxidation in analogous hetero-dimerization reactions. (Xu, Y.; Yakushijin, K.; Horne, D. A. *J. Org. Chem.* **1996**, *61*, 9569.)

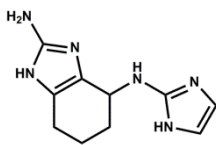
**HPLC conditions:** Waters Sunfire C18 column (19 × 250-mm) with UV detection at 254-nm; Solution A: H<sub>2</sub>O w/0.1% CF<sub>3</sub>CO<sub>2</sub>H and Solution B: CH<sub>3</sub>CN w/0.1% CF<sub>3</sub>CO<sub>2</sub>H; increase gradient of Solution B from 5% to 30%, 1-10 min; 30% to 100%, 10-12min; flow rate: 20-mL/min.



4-5 2 CF<sub>3</sub>CO<sub>2</sub>H

**7-(2-amino-1H-imidazol-4-yl)-4,5,6,7-tetrahydro-1H-benzo[d]imidazol-2-amine (4-5) (2 CF<sub>3</sub>CO<sub>2</sub>H):**

<sup>1</sup>H NMR (500 MHz, H<sub>2</sub>O-*d*<sub>2</sub>): δ (ppm) 6.45 (s, 1H), 3.93-3.90 (m, 1H), 2.44-2.41 (m, 2H), 2.05-2.01 (m, 1H), 1.81-1.74 (m, 3H); <sup>13</sup>C NMR (125 MHz, H<sub>2</sub>O-*d*<sub>2</sub>): δ (ppm) 146.9, 146.2, 127.7, 123.5, 118.5, 110.0, 28.9, 28.2, 19.2, 18.8; <sup>1</sup>H NMR (500 MHz, MeOH-*d*<sub>4</sub>): δ (ppm) 6.52 (s, 1H), 3.97-3.90 (m, 1H), 2.57-2.44 (m, 2H), 2.15-2.05 (m, 1H), 1.93-1.79 (m, 3H); <sup>13</sup>C NMR (125 MHz, MeOH-*d*<sub>4</sub>): δ (ppm) 149.3, 148.7, 129.2, 124.6, 120.2, 111.5, 30.7, 30.1, 20.9, 20.6; LRMS-ESI (*m/z*) calcd for [C<sub>10</sub>H<sub>14</sub>N<sub>6</sub>+H]<sup>+</sup>: 219.14; found: 219.2.



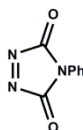
4-12 2 CF<sub>3</sub>CO<sub>2</sub>H

**N<sup>4</sup>-(1H-imidazol-2-yl)-4,5,6,7-tetrahydro-1H-benzo[d]imidazole-2,4-diamine (4-12) (2 CF<sub>3</sub>CO<sub>2</sub>H):**

<sup>1</sup>H NMR (500 MHz, MeOH-*d*<sub>4</sub>): δ (ppm) 6.91 (s, 2H), 4.64-4.60 (m, 1H, methine), 2.60-2.43 (m, 2H), 2.11-2.00 (m, 1H), 1.99-1.88 (m, 3H); LRMS-ESI (*m/z*) calcd for [C<sub>10</sub>H<sub>14</sub>N<sub>6</sub>+H]<sup>+</sup>: 219.14; found: 219.2.

**2-Aminoimidazole Oxidations with 4-Phenyl-1,2,4-triazoline-3,5-dione (PTAD) (4-14).**

**Synthesis of 4-Phenyl-1,2,4-triazoline-3,5-dione (PTAD) (4-14).**



4-14

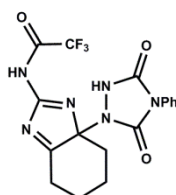
4-Phenyl-1,2,4-triazoline-3,5-dione (PTAD) (4-14) was prepared from 4-phenyl-1,2,4-triazolidine-3,5-dione via oxidation with *tert*-butyl hypochlorite following procedure developed

by Cookson, R. C.; Gupte, S. S.; Stevens, I. D. R.; Watts, C. T. *Org. Syn.* **1988**, 6, 936; **1971**, 51, 121.

### PTAD Oxidation of (4-13).

Purified (4-13) (10.1 mg, 0.04 mmol, 1.0 equiv) was dissolved in  $\text{CHCl}_3-d_1$  (0.45-mL) and cooled to  $0^\circ\text{C}$  with ice-water bath followed by the addition of PTAD (4-14) (9 mg, 0.05 mmol, 1.2 equiv) in a NMR tube. After stirring for 10 min at  $0^\circ\text{C}$  the carmine color dissipates to a light pink (indicative of reaction completion) and the solution was further stirred for 50 min at which point the reaction was judged complete by  $^1\text{H}$  NMR (500 MHz,  $\text{CHCl}_3-d_1$ , broadened signal but indicative of a non-symmetric structure) and LCMS analysis (UV detection at 254-nm and LRMS-ESI ( $m/z$ ) calcd for  $[\text{C}_{17}\text{H}_{15}\text{F}_3\text{N}_6\text{O}_3+\text{H}]^+$ : 409.12; found: 409.2). The  $^1\text{H}$  NMR analysis indicates quantitative conversion ( $>90\%$  purity) to PTAD adduct (4-15). The same reaction left to stand at RT for 48h had slowly converted to crude rearranged PTAD adduct (4-16). After purification by HPLC rearranged PTAD adduct (4-16) (10 mg, 60% from (4-13)) as a colorless film. Crystals suitable for x-ray diffraction of rearranged PTAD adduct (4-17) were grown by slow evaporation of (4-16) in  $\text{CH}_3\text{CN}-d_3$  (0.5-mL). Presumably slow hydrolysis occurs from purification by HPLC with aqueous eluent.

**HPLC conditions:** Waters Sunfire C18 column (19  $\times$  250-mm) with UV detection at 254-nm; Solution A:  $\text{H}_2\text{O}$  w/0.1%  $\text{CF}_3\text{CO}_2\text{H}$  and Solution B:  $\text{CH}_3\text{CN}$  w/0.1%  $\text{CF}_3\text{CO}_2\text{H}$ ; increase gradient of Solution B from 5% to 30%, 1-10 min; 30% to 100%, 10-12min; flow rate: 20-mL/min.

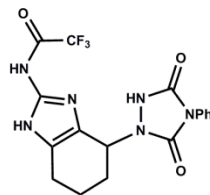


4-15

### PTAD Adduct (4-15):

$^1\text{H}$  NMR (600 MHz,  $\text{CH}_3\text{CN}-d_3$ ):  $\delta$  (ppm) 10.0 (bs, 1H), 8.43 (bs, 1H), 7.49-7.37 (m, 5H), 3.05-2.87 (m, 2H), 2.86 (td,  $J = 13.0, 6.5$  Hz, 1H), 2.37-2.31 (m, 1H), 1.84-1.78 (m, 2H), 1.69-1.57 (m, 2H);  $^1\text{H}$  NMR (500 MHz,  $\text{DMSO}-d_6$ ):  $\delta$  (ppm) 11.36 (s, 1H, -NH), 11.11 (bs, 1H, -NH), 7.51-7.38 (m, 5H), 3.01 (d,  $J = 13.5$  Hz, 1H), 2.94-2.91 (m, 1H), 2.86-2.80 (m, 1H), 2.28-2.21 (m, 1H), 1.78-1.66 (m, 2H), 1.64-1.48 (m, 2H);  $^{13}\text{C}$  NMR (125 MHz,  $\text{DMSO}-d_6$ ):  $\delta$  (ppm) 197.2, 169.6, 166.7, 166.4, 153.0, 130.9, 129.1, 128.4, 126.0, 116.3 (q,  $J_{\text{CF}} = 287$  Hz,  $-\text{CF}_3$ ) 83.7, 38.1, 29.8, 28.5, 20.4; LRMS-ESI ( $m/z$ ) calcd for  $[\text{C}_{17}\text{H}_{15}\text{F}_3\text{N}_6\text{O}_3+\text{H}]^+$ : 409.12; found: 409.2.

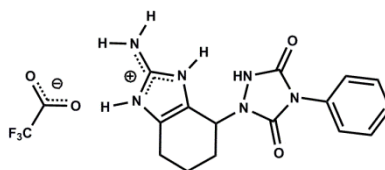




4-16

**Rearranged PTAD Adduct (4-16):** (apparent mixture (1:1) of **4-16** and **4-17**, unassigned)

$^1\text{H NMR}$  (500 MHz,  $\text{CH}_3\text{CN}-d_3$ ):  $\delta$  (ppm) 11.60 (bs, 1H), 11.21 (bs, 1H), 7.57-7.37 (m, 10H), 7.01 (bs, 2H), 5.33-5.28 (m, 1H), 5.22-5.17 (m, 1H), 2.71-2.40 (m, 5H), 2.13-1.98 (m, 7H);  $^{13}\text{C NMR}$  (125 MHz,  $\text{CH}_3\text{CN}-d_3$ ):  $\delta$  (ppm) 154.4, 154.3, 154.1, 154.0, 149.0, 146.4, 132.7, 129.98, 129.97, 129.2, 128.4, 127.3, 127.2, 49.09, 49.05, 27.6, 27.4; **LRMS-ESI** ( $m/z$ ) calcd for  $[\text{C}_{17}\text{H}_{15}\text{F}_3\text{N}_6\text{O}_3]^+$ : 409.12 ; found: 409.2



4-17

**Rearranged PTAD Adduct (4-17):**

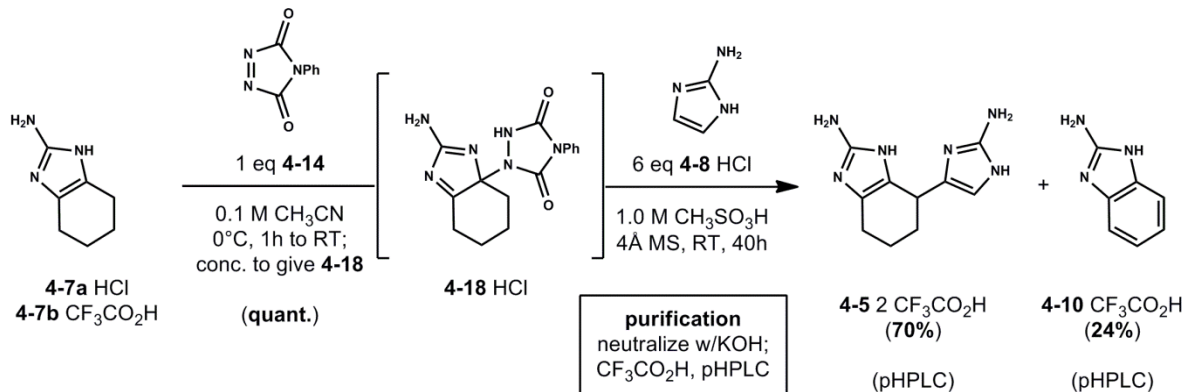
**LRMS-ESI** ( $m/z$ ) calcd for  $[\text{C}_{15}\text{H}_{16}\text{N}_6\text{O}_2+\text{H}]^+$ : 313.14; found: 313.2.

#### Acid catalyzed rearrangement to provide Rearranged PTAD Adduct (4-16)

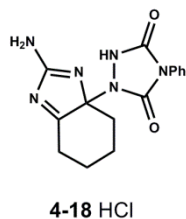
To a solution containing (**4-13**) (5 mg, 0.02 mmol, 1.0 equiv) in  $\text{CHCl}_3-d_1$  (214- $\mu\text{L}$ , 0.1 M) was added PTAD (**4-13**) (3.7 mg, 0.02 mmol, 1.0 equiv) at RT. The reaction was allowed to stir for 1h at which point oxidation was judged complete by LCMS analysis (**LRMS-ESI** ( $m/z$ ) calcd for  $[\text{C}_{17}\text{H}_{15}\text{F}_3\text{N}_6\text{O}_3]^+$ : 409.12 ; found: 409.2). The solution was split into equal portions (approx. 100- $\mu\text{L}$  each) and concentrated in separate 1 dram vials (Vial 1, 2). To Vial 1 was added  $\text{CH}_3\text{CN}-d_3$  (0.5-mL) and  $\text{CF}_3\text{CO}_2\text{H}$  (100- $\mu\text{L}$ ) at RT. To Vial 2 was added  $\text{CH}_3\text{CN}-d_3$  (0.5-mL) and glacial HOAc (100- $\mu\text{L}$ ) at RT. The contents of each vial were transferred to NMR tubes and monitored by  $^1\text{H NMR}$  (500 MHz,  $\text{CH}_3\text{CN}-d_3$ ) over 12h. Analysis with LCMS (UV detection at 254-nm and MS analysis) was indicative of the conversion of adduct (**4-15**) to rearranged adduct (**4-16**) as observed in the previous experiment conducted with  $\text{CHCl}_3$  alone. After 20h, each reaction was purified by HPLC to provide the corresponding rearranged adduct (**4-16**). As a relative observation the conversion of (**4-15**) to rearranged adduct (**4-16**) was accelerated in the  $\text{CF}_3\text{CO}_2\text{H}$  experiment.

**HPLC conditions:** Waters Sunfire C18 column (19  $\times$  250-mm) with UV detection at 254-nm; Solution A:  $\text{H}_2\text{O}$  w/0.1%  $\text{CF}_3\text{CO}_2\text{H}$  and Solution B:  $\text{CH}_3\text{CN}$  w/0.1%  $\text{CF}_3\text{CO}_2\text{H}$ ; increase gradient of Solution B from 5% to 30%, 1-10 min; 30% to 100%, 10-12min; flow rate: 20-mL/min.

## Synthesis of Model Compound (4-5) via oxidation with PTAD (4-14).



A suspension of (**4-7a**) (1.00 g, 5.75 mmol, 1.0 equiv) in CH<sub>3</sub>CN (57.5-L) was cooled to 0°C in an ice-water bath followed by the addition of PTAD (**4-14**) (1.01 g, 5.75 mmol, 1.0 equiv) in a single portion. The resultant heterogeneous light red mixture was stirred at 0°C for 10 min and then slowly allowed to reach RT. The reaction was stirred at RT for 1h followed by concentration in vacuo at approx. 30°C (water bath) to give crude (**4-18**) as a light red powder. Residual CH<sub>3</sub>CN was removed under prolonged high-vacuum (3h) to give crude (**4-18**) (2.0 g, quant., crude yield) that was used in the subsequent step without further purification.



### PTAD Adduct (**4-18**) (HCl):

<sup>1</sup>H NMR (500 MHz, MeOH-*d*<sub>4</sub>): δ (ppm) 7.52-7.39 (m, 5H), 3.09-2.94 (m, 3H), 2.46-2.38 (m, 1H), 1.96-1.60 (m, 4H); <sup>13</sup>C NMR (125 MHz, CH<sub>3</sub>CN-*d*<sub>3</sub>): δ (ppm) 201.6, 169.2, 156.0, 155.6, 132.1, 130.3, 129.9, 126.9, 87.1, 39.7, 31.7, 30.1, 21.6; LRMS-ESI (*m/z*) calcd for [C<sub>15</sub>H<sub>16</sub>N<sub>6</sub>O<sub>2</sub>+H]<sup>+</sup>: 313.14; found: 313.2

A portion of crude (**4-18**) (1.00 g, 2.87 mmol, 1.0 equiv) and 1H-imidazol-2-amine hydrochloride (**4-8**) (2.05 g, 17.2 mmol, 6.0 equiv) were dissolved in neat CH<sub>3</sub>SO<sub>3</sub>H (2.9-mL, 1.0 M) followed by the addition of 4 Å MS (approx. 200 mg). The dark viscous solution was stirred RT for 40h at which point two products were observed by LCMS analysis. The reaction mixture was cooled to 0°C with an ice-water bath and slowly neutralized with aqueous 10 M KOH (approx. 16-mL) to pH = 12. The light brown solution was allowed to reach RT followed by the addition of CF<sub>3</sub>CO<sub>2</sub>H (approx. 2-mL, pH = 3) in preparation for purification by HPLC. Purification provided C-bound bis-guanidine (**4-5**) (0.90 g, 70%) (retention time: 6.5 min) as a light brown solid and overoxidized 2-aminobenzimidazole (**4-10**) (0.17 g, 24%) (retention time: 8.5 min) as a light brown solid. Both compounds were isolated as their corresponding trifluoroacetate salts after lyophilization.

**HPLC conditions:** Waters Sunfire C18 column (19 × 250-mm) with UV detection at 254-nm; Solution A: H<sub>2</sub>O w/0.1% CF<sub>3</sub>CO<sub>2</sub>H and Solution B: CH<sub>3</sub>CN w/0.1% CF<sub>3</sub>CO<sub>2</sub>H; increase gradient of Solution B from 5% to 30%, 1-10 min; 30% to 100%, 10-12min; flow rate: 20-mL/min.

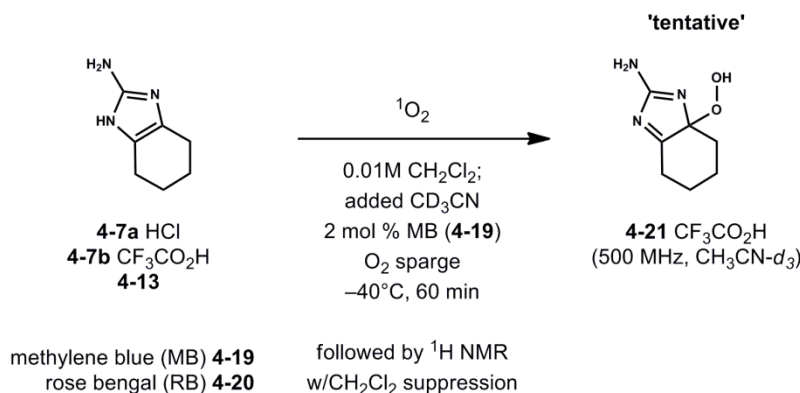
**7-(2-amino-1H-imidazol-4-yl)-4,5,6,7-tetrahydro-1H-benzo[d]imidazol-2-amine (4-5) (2 CF<sub>3</sub>CO<sub>2</sub>H):**

<sup>1</sup>H NMR (500 MHz, MeOH-*d*<sub>4</sub>): δ (ppm) 6.52 (s, 1H), 3.97-3.90 (m, 1H), 2.57-2.44 (m, 2H), 2.15-2.05 (m, 1H), 1.93-1.79 (m, 3H); <sup>13</sup>C NMR (125 MHz, MeOH-*d*<sub>4</sub>): δ (ppm) 149.3, 148.7, 129.2, 124.6, 120.2, 111.5, 30.7, 30.1, 20.9, 20.6; **LRMS-ESI** (*m/z*) calcd for [C<sub>10</sub>H<sub>14</sub>N<sub>6</sub>+H]<sup>+</sup>: 219.14; found: 219.2.

**1H-benzo[d]imidazol-2-amine (4-10):**

<sup>1</sup>H NMR (500 MHz, MeOH-*d*<sub>4</sub>): δ (ppm) 7.37-7.34 (m, 2H), 7.28-7.25 (m, 2H); <sup>13</sup>C NMR (125 MHz, MeOH-*d*<sub>4</sub>): δ (ppm) 147.8, 117.8, 23.2, 21.1; **LRMS-ESI** (*m/z*) calcd for [C<sub>7</sub>H<sub>7</sub>N<sub>3</sub>+H]<sup>+</sup>: 134.07; found: 134.1.

**2-aminoimidazole Oxidations with Singlet Oxygen**

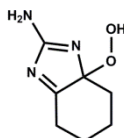


**Preparation of methylene blue (MB, 4-19) stock solution (SS):** Methylene blue (4-19) (15 mg, 0.05 mmol, MW 319.85) was dissolved in anhydrous CH<sub>2</sub>Cl<sub>2</sub> (50-mL) and degassed with Ar sparging for 15 min. (calcd 0.3 mg/mL, 0.94 mM)

Purified (4-7b) (CF<sub>3</sub>CO<sub>2</sub>H) (30 mg, 0.12 mmol, 1.0) was suspended in MB-SS (3.0-mL, calcd. 0.003 mmol of MB, 0.02 equiv) and further diluted with CH<sub>2</sub>Cl<sub>2</sub> (6.0-mL, total volume = 9-mL) in a borosilicate (Type I, Class A, 16 × 150 mm, 320-nm cut-off) test tube. The light blue solution was agitated by sonication to remove insoluble (4-7b) from side walls for 3 min. The solution was cooled to -40°C with a dry ice-CH<sub>3</sub>CN bath. The reaction was sparged continuously with dry O<sub>2</sub> (g) delivered via needle (20 gauge) from a balloon. The reaction was initiated by exposure to a 500-W sunlamp (approx. 8 cm from reaction) and stirred at -40°C. Aliquots taken for analysis at t = 30 min and t = 60 min indicated that no reaction was occurring (LCMS analysis, UV detection at 254-nm and MS). For increased solubility of (4-7b), CD<sub>3</sub>CN (1.0-mL) was added to the reaction and the temperature was maintained at -40°C. Further irradiation for 60 min (additional) provided complete oxidation of (4-7b) to tentatively assigned (4-21). An aliquot (0.5-mL) taken at t = 120 min (total time) was concentrated at RT with a

stream of Ar and analyzed by  $^1\text{H}$  NMR (500 MHz,  $\text{CD}_3\text{CN}-d_3$ , 0.5-mL). (**4-21**) was tentatively assigned by HMBC spectroscopy and showed diagnostic  $^{13}\text{C}$  NMR shifts in agreement with similar PTAD adduct compounds.

**Note:** Methylene blue (**4-19**) was found to be an efficient photosensitizer under the above conditions. The reaction was not further optimized.



**4-21**  $\text{CF}_3\text{CO}_2\text{H}$   
(500 MHz,  $\text{CH}_3\text{CN}-d_3$ )

**3a-hydroperoxy-4,5,6,7-tetrahydro-3aH-benzo[d]imidazol-2-amine (4-21) ( $\text{CF}_3\text{CO}_2\text{H}$ ):**  
LRMS-ESI ( $m/z$ ) calcd for  $[\text{C}_7\text{H}_{11}\text{N}_3\text{O}_2+\text{H}]^+$ : 170.09; found: 170.1; LRMS-ESI ( $m/z$ ) calcd for  $[\text{C}_7\text{H}_{13}\text{N}_3\text{O}_3+\text{H}]^+$ : 188.10; found: 188.1 (hydrate  $[\text{M}+\text{H}_2\text{O}+\text{H}]^+ = [\text{C}_7\text{H}_{11}\text{N}_3\text{O}_2+\text{H}_2\text{O}+\text{H}]^+$ )

### Key Characterization Data for Related Compounds

Key Characterization Data ( $^1\text{H}$ ,  $^{13}\text{C}$  NMR, MS)

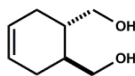
<p><b>4-15</b> (500 MHz, <math>\text{CH}_3\text{CN}-d_3</math>)</p> <table border="0"> <thead> <tr> <th>#</th> <th><math>^1\text{H}</math></th> <th><math>^{13}\text{C}</math> (ppm)</th> </tr> </thead> <tbody> <tr> <td>1</td> <td>--</td> <td>198.7</td> </tr> <tr> <td>2</td> <td>--</td> <td>84.7</td> </tr> </tbody> </table>	#	$^1\text{H}$	$^{13}\text{C}$ (ppm)	1	--	198.7	2	--	84.7	<p><b>'crude'</b> <b>4-21</b> <math>\text{CF}_3\text{CO}_2\text{H}</math> (500 MHz, <math>\text{CH}_3\text{CN}-d_3</math>)</p> <table border="0"> <thead> <tr> <th>#</th> <th><math>^1\text{H}</math></th> <th><math>^{13}\text{C}</math> (ppm)</th> </tr> </thead> <tbody> <tr> <td>1</td> <td>--</td> <td>201*</td> </tr> <tr> <td>2</td> <td>--</td> <td>101*</td> </tr> </tbody> </table> <p>*from crude HMBC</p>	#	$^1\text{H}$	$^{13}\text{C}$ (ppm)	1	--	201*	2	--	101*	<p><b>4-5</b> 2 <math>\text{CF}_3\text{CO}_2\text{H}</math> (500 MHz, <math>\text{MeOH}-d_4</math>)</p> <table border="0"> <thead> <tr> <th>#</th> <th><math>^1\text{H}</math></th> <th><math>^{13}\text{C}</math> (ppm)</th> </tr> </thead> <tbody> <tr> <td>3</td> <td>3.94</td> <td>30.7</td> </tr> <tr> <td>5</td> <td>6.53</td> <td>124.6</td> </tr> </tbody> </table> <p>5 (s, 1H)</p>	#	$^1\text{H}$	$^{13}\text{C}$ (ppm)	3	3.94	30.7	5	6.53	124.6
#	$^1\text{H}$	$^{13}\text{C}$ (ppm)																											
1	--	198.7																											
2	--	84.7																											
#	$^1\text{H}$	$^{13}\text{C}$ (ppm)																											
1	--	201*																											
2	--	101*																											
#	$^1\text{H}$	$^{13}\text{C}$ (ppm)																											
3	3.94	30.7																											
5	6.53	124.6																											
<p><b>4-16</b> (500 MHz, <math>\text{CH}_3\text{CN}-d_3</math>)</p> <table border="0"> <thead> <tr> <th>#</th> <th><math>^1\text{H}</math></th> <th><math>^{13}\text{C}</math> (ppm)</th> </tr> </thead> <tbody> <tr> <td>3</td> <td>5.24</td> <td>49.1</td> </tr> </tbody> </table> <p>see crystal data (<b>4-17</b>)</p>	#	$^1\text{H}$	$^{13}\text{C}$ (ppm)	3	5.24	49.1	<p><b>4-18</b> HCl (500 MHz, <math>\text{MeOH}-d_4</math>)</p> <table border="0"> <thead> <tr> <th>#</th> <th><math>^1\text{H}</math></th> <th><math>^{13}\text{C}</math> (ppm)</th> </tr> </thead> <tbody> <tr> <td>1</td> <td>--</td> <td>201.6</td> </tr> <tr> <td>2</td> <td>--</td> <td>87.1</td> </tr> </tbody> </table>	#	$^1\text{H}$	$^{13}\text{C}$ (ppm)	1	--	201.6	2	--	87.1	<p><b>4-12</b> 2 <math>\text{CF}_3\text{CO}_2\text{H}</math> (500 MHz, <math>\text{MeOH}-d_4</math>)</p> <table border="0"> <thead> <tr> <th>#</th> <th><math>^1\text{H}</math></th> <th><math>^{13}\text{C}</math> (ppm)</th> </tr> </thead> <tbody> <tr> <td>3</td> <td>4.61</td> <td>46.0</td> </tr> <tr> <td>7</td> <td>6.91</td> <td>ND</td> </tr> </tbody> </table> <p>7 (s, 2H)</p>	#	$^1\text{H}$	$^{13}\text{C}$ (ppm)	3	4.61	46.0	7	6.91	ND			
#	$^1\text{H}$	$^{13}\text{C}$ (ppm)																											
3	5.24	49.1																											
#	$^1\text{H}$	$^{13}\text{C}$ (ppm)																											
1	--	201.6																											
2	--	87.1																											
#	$^1\text{H}$	$^{13}\text{C}$ (ppm)																											
3	4.61	46.0																											
7	6.91	ND																											

## 4.7 Experimental (Part II).

### 4.7.2 Experimental Procedures and Characterization Data.

#### Synthesis of 2-aminoimidazole (4-24) en route to (-)-ageliferin (4-1a).

#### (1*S*,2*S*)-cyclohex-4-ene-1,2-diyldimethanol (4-23).



(+)-4-23

(1*S*,2*S*)-cyclohex-4-ene-1,2-diyldimethanol (**4-23**) was prepared in 2 steps (75%) from (-)-dimenthyl fumarate following literature procedures with minor modifications.<sup>[1,2]</sup>

(-)-dimenthyl fumarate (59.6 g, 0.15 mol, 1.0 equiv) was dissolved in anhydrous hexanes (1-L, 0.5 M) in a 3-L round bottom three-necked flask and cooled to  $-40^{\circ}\text{C}$  with a dry ice- $\text{CH}_3\text{CN}$  bath. A solution of  $\text{Et}_2\text{AlCl}$  (304-mL, 0.30 mol, 2.0 equiv, 1.0 M in hexanes) was added over 15 min via cannulation under Ar. The reaction slowly turns light yellow to light orange-red in color during complexation. The homogeneous mixture was stirred at  $-40^{\circ}\text{C}$  for 30 min followed by the addition of 1,3-butadiene (41.1 g, 0.76 mol, 5.0 equiv, calcd. by weight difference of gas canister). The reaction was stirred for 4h at  $-40^{\circ}\text{C}$  at which point the cold bath was removed and allowed to slowly reach RT. After stirring at RT for 12h, the reaction was cooled to  $0^{\circ}\text{C}$  and very slowly quenched with 0.2 M aqueous HCl (400-mL). The resultant yellow biphasic mixture was allowed to separate. The aqueous layer was extracted with  $\text{Et}_2\text{O}$  ( $3 \times 500\text{-mL}$ ) and combined organics (including hexanes layer) were washed with saturated aqueous  $\text{NaHCO}_3$ ,  $\text{H}_2\text{O}$ , brine, dried over  $\text{Na}_2\text{SO}_4$ , filtered and concentrated in vacuo to provide intermediate diester (59.0 g, 0.13 mol) as a crude oil that was used in the subsequent step without further purification.

A suspension of  $\text{LiAlH}_4$  (8.2 g, .22 mmol, 1.6 equiv) in THF (860-mL) was cooled under Ar to  $0^{\circ}\text{C}$ . Crude diester (59.0 g, 0.13 mol) was dissolved in THF (860-mL) and cannulated into the  $\text{LiAlH}_4$  over 20 min with vigorous evolution of  $\text{H}_{2(\text{g})}$  observed. **Note:** appropriate ventilation is required during cannulation. The reaction was stirred at  $0^{\circ}\text{C}$  for 1h and slowly allowed to reach RT and further stirred for 12h. The reaction was cooled again to  $0^{\circ}\text{C}$  and carefully quenched in succession with  $\text{H}_2\text{O}$  (80-mL) (**Caution! Initial quench solutions must be added dropwise.**) and 2 M aqueous NaOH (80-mL). The precipitous slurry was allowed to reach RT and was heated to reflux with a heating mantle for 90 min. After cooling to RT, the white precipitate was separated from organics via decantation. Additional fresh THF (500-mL),  $\text{H}_2\text{O}$  (100-mL) and 2 M aqueous NaOH (100-mL) were added to the precipitate and the resultant mixture was reflux for 90 min. After cooling to RT, the organic layer was decanted and combined organics were filtered through Celite and rinsed with THF ( $2 \times 200\text{-mL}$ ). The filtrate was allowed to separate in a separatory funnel and the organic layer was washed with brine, dried over  $\text{Na}_2\text{SO}_4$ , filtered and concentrated in vacuo to provide a clear oil. Purification by flash column chromatography ( $\text{CH}_2\text{Cl}_2/\text{MeOH}$  isocratic (99:1)) provides recovered (-)-menthol (41 g, 86%) ( $R_f = 0.9$ ,  $\text{CH}_2\text{Cl}_2/\text{MeOH}$  (95:5)) as

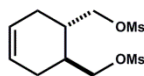
a colorless oil and (1*S*,2*S*)-cyclohex-4-ene-1,2-diyl dimethanol (**4-23**) (16.1 g, 75%) as a light yellow oil that crystallizes upon standing.

**(1*S*,2*S*)-cyclohex-4-ene-1,2-diyl dimethanol (**4-23**):**

$R_f = 0.2$ , CH<sub>2</sub>Cl<sub>2</sub>/MeOH (95:5); <sup>1</sup>H NMR (500 MHz, CHCl<sub>3</sub>-*d*<sub>1</sub>): δ (ppm) 5.66-5.65 (m, 1H), 3.75-3.73 (m, 1H), 3.61-3.59 (m, 1H), 2.70 (bs, 1H), 2.04-2.00 (m, 1H), 1.89-1.85 (m, 1H), 1.71-1.69 (m, 1H); <sup>13</sup>C NMR (125 MHz, CHCl<sub>3</sub>-*d*<sub>1</sub>): δ (ppm) 126.2, 66.3, 39.8, 28.6; LRMS-ESI (*m/z*) calcd for [C<sub>8</sub>H<sub>14</sub>O<sub>2</sub>+H]<sup>+</sup>: 143.1; found: 143.1; [α]<sub>D</sub> = + 68.0° (c = 0.375, CHCl<sub>3</sub>), 99% *ee*, (Lit. [α]<sub>D</sub> = + 68.02° (c = 0.375, CHCl<sub>3</sub>)).<sup>[2]</sup>

((5*S*,6*S*)-2-amino-4,5,6,7-tetrahydro-1*H*-benzo[*d*]imidazole-5,6-diyl)dimethanamine (**4-24**) was prepared in 7 steps from enantiopure (1*S*,2*S*)-cyclohex-4-ene-1,2-diyl dimethanol (**4-23**) closely following procedures developed by Huigens III, R. W.; Richards, J. J.; Parise, G.; Ballard, E.; Zeng, W.; Deora, R.; Melander, C. *J. Am. Chem. Soc.* **2007**, 129, 6966.

**Synthesis of (1*S*,2*S*)-cyclohex-4-ene-1,2-diylbis(methylene)dimethanesulfonate (**4-42a**).**



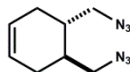
**4-42a**

Purified (1*S*,2*S*)-cyclohex-4-ene-1,2-diyl dimethanol (**4-23**) (6.00 g, 42 mmol, 1.0 equiv) was dissolved in CH<sub>2</sub>Cl<sub>2</sub> (70-mL) and cooled to -78°C with dry ice-acetone bath for 10 min followed by the addition of Et<sub>3</sub>N (20.2-mL, 145 mmol, 3.4 equiv) in one portion and the subsequent dropwise addition of methanesulfonyl chloride (11.3-mL, 145 mmol, 3.0 equiv) over 5 min. The reaction solution was removed from the -78°C bath and allowed to slowly warm to RT. The mixture becomes viscous and light yellow to orange over time which may require stirring rate adjustment for adequate mixing. After stirring at RT for 2h, the mixture was quenched by the addition of brine (50-mL) and the resultant layers were separated. The organic layer was washed with brine (5 × 10-mL), dried over Na<sub>2</sub>SO<sub>4</sub>, filtered and concentrated in vacuo to give crude bis-mesylate (**4-42a**) (overweight, assume 42 mmol) as light yellow oil that was used in the subsequent step without further purification.

**(1*S*,2*S*)-cyclohex-4-ene-1,2-diylbis(methylene)dimethanesulfonate (**4-42a**):** (crude)

<sup>1</sup>H NMR (500 MHz, CHCl<sub>3</sub>-*d*<sub>1</sub>): δ (ppm) 5.66-5.64 (m, 2H), 4.31-4.19 (m, 4H), 3.04 (s, 6H), 2.25-2.10 (m, 4H), 2.08-1.97 (m, 2H); <sup>13</sup>C NMR (125 MHz, CHCl<sub>3</sub>-*d*<sub>1</sub>): δ (ppm) 124.9, 70.9, 37.5, 33.7, 26.0; LRMS-ESI (*m/z*) calcd for [C<sub>10</sub>H<sub>18</sub>O<sub>6</sub>S<sub>2</sub>+H]<sup>+</sup>: 299.06; found: 299.1.

### Synthesis of (4*S*,5*S*)-4,5-bis(azidomethyl)cyclohex-1-ene (4-42b).



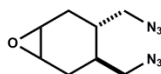
4-42b

Crude bis-mesylate (**4-42a**) (assume 42 mmol, 1.0 equiv) was dissolved in DMF (135-mL) at RT followed by the addition of NaN<sub>3</sub> (20.1 g, 309 mmol, 7.4 equiv) in one portion. The reaction was fitted with a reflux condenser and heated to 100°C in a pre-heated oil bath behind a blast-shield for 16h. The heterogeneous mixture was cooled to RT followed by the addition of brine (200-mL). The resultant mixture was diluted with EtOAc (1-L) and allowed to separate after mixing in a separatory funnel. The organic layer was washed with brine (6 × 50-mL), dried over Na<sub>2</sub>SO<sub>4</sub>, filtered and concentrated in vacuo to give bis-azide (**4-42b**) (7.6 g, 94%, 2 steps) as a brown oil that was used in the subsequent step without further purification.

### Synthesis of (4*S*,5*S*)-4,5-bis(azidomethyl)cyclohex-1-ene (4-42b):

<sup>1</sup>H NMR (500 MHz, CHCl<sub>3</sub>-*d*<sub>1</sub>): δ (ppm) 5.62-5.56 (m, 2H), 3.33 (d, *J* = 4.8 Hz, 4H), 2.15-2.05 (m, 2H), 1.95-1.82 (m, 4H); <sup>13</sup>C NMR (125 MHz, CHCl<sub>3</sub>-*d*<sub>1</sub>): δ (ppm) 125.1, 54.4, 34.8, 27.0; LRMS-ESI (*m/z*) calcd for [C<sub>8</sub>H<sub>12</sub>N<sub>6</sub>+H]<sup>+</sup>: 193.12; found: 193.1.

### Synthesis of (3*S*,4*S*)-3,4-bis(azidomethyl)-7-oxabicyclo[4.1.0]heptane (4-43a).



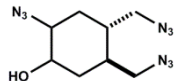
4-43a

Crude (**4-42b**) (7.6 g, 39.5 mmol, 1.0) was dissolved in CH<sub>2</sub>Cl<sub>2</sub> (232-mL) and the reaction was shielded from ambient light followed by the addition of *meta*-chloroperoxybenzoic acid (*m*-CPBA) (9.04 g, 40.3 mmol, 1.02 equiv, calcd at 77 wt % purity). The reaction mixture was allowed to stir at RT for 12h, quenched with saturated aqueous NaHCO<sub>3</sub> (50-mL) and transferred to a separatory funnel. The organic layer was separated, dried over Na<sub>2</sub>SO<sub>4</sub>, filtered and concentrated in vacuo to give crude epoxide (**4-43a**) as a colorless oil. Purification of the resultant oil by flash column chromatography (hexanes/EtOAc gradient, (9:1) to (3:1)) provided epoxide (**4-43a**) (7.15 g, 87%) as a mixture of inseparable, yet inconsequential diastereomers (d.r. 1:1).

### (3*S*,4*S*)-3,4-bis(azidomethyl)-7-oxabicyclo[4.1.0]heptane (4-43a):

<sup>1</sup>H NMR (500 MHz, CHCl<sub>3</sub>-*d*<sub>1</sub>): δ (ppm) 3.45-3.11 (m, 6H), 2.20-2.04 (m, 4H), 1.83-1.67 (m, 3H), 1.59-1.49 (m, 1H); <sup>13</sup>C NMR (125 MHz, CHCl<sub>3</sub>-*d*<sub>1</sub>): δ (ppm) 54.1, 54.0, 52.3, 51.2, 34.5, 32.1, 29.0, 27.8; LRMS-ESI (*m/z*) calcd for [C<sub>8</sub>H<sub>12</sub>N<sub>6</sub>O+H]<sup>+</sup>: 209.12; found: 209.1.

### Synthesis of (4*S*,5*S*)-2-azido-4,5-bis(azidomethyl)cyclohexanol (**4-43b**).



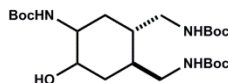
**4-43b**

Purified epoxide (**4-43a**) (3.96 g, 19 mmol, 1 equiv) was dissolved in DMF (240-mL) followed by the addition of NaN<sub>3</sub> (37.1 g, 570 mmol, 30 equiv). The reaction was fitted with a reflux condenser and heated to 120°C in a pre-heated oil bath behind a blast-shield for 48h. The heterogeneous mixture was cooled to RT followed by the addition of brine (100-mL). The resultant mixture was diluted with EtOAc (1-L) and allowed to separate after mixing in a separatory funnel. The organic layer was washed with brine (6 × 50-mL), dried over Na<sub>2</sub>SO<sub>4</sub>, filtered and concentrated in vacuo to give a crude light yellow oil. Purification of the resultant oil by flash column chromatography (hexanes/EtOAc gradient, (9:1) to (1:1)) provided tris-azido-alcohol (**4-43b**) (1.41 g, 30%) as a mixture of inseparable, yet inconsequential diastereomers (d.r. 1:1).

### Synthesis of (4*S*,5*S*)-2-azido-4,5-bis(azidomethyl)cyclohexanol (**4-43b**):

<sup>1</sup>H NMR (500 MHz, CHCl<sub>3</sub>-*d*<sub>1</sub>): δ (ppm) 3.91 (q, *J* = 3.9 Hz, 1H), 3.70 (dd, *J* = 4.4, 3.6 Hz, 1H), 3.48-3.21 (m, 8H), 2.27 (d, *J* = 2.8 Hz, 1H), 2.11-1.33 (m, 13H); <sup>13</sup>C NMR (125 MHz, CHCl<sub>3</sub>-*d*<sub>1</sub>): δ (ppm) 72.8, 67.9, 66.0, 61.4, 54.4, 54.2, 53.9, 53.7, 37.8, 37.3, 36.6, 34.1, 33.43, 33.38, 31.9, 28.4; LRMS-ESI (*m/z*) calcd for [C<sub>8</sub>H<sub>13</sub>N<sub>9</sub>O+H]<sup>+</sup>: 252.13; found: 252.1.

### Synthesis of (1*S*,2*S*) triamino-alcohol (**4-44a**).



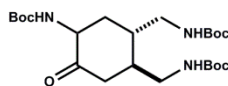
**4-44a**

Purified tris-azido-alcohol (**4-43b**) (1.20 g, 4.7 mmol, 1.0 equiv) and di-*tert*-butyl dicarbonate (3.49 g, 16 mmol, 3.4 equiv) were dissolved in DMF (10-mL) in a 50-mL round bottom flask flushed with Ar. This solution was transferred via syringe to a second flask containing 10 wt % Pd/C (246 mg) in DMF (15-mL) that was previously saturated with H<sub>2</sub> (g) (15 min sparge with 1 atm balloon). The resultant heterogeneous mixture was flushed with H<sub>2</sub> (g), fitted with a H<sub>2</sub> (g) balloon (1 atm) and allowed to stir at RT for 48h. The mixture was judged complete by TLC analysis and filtered through Celite. The Celite was rinsed with EtOAc and the combined filtrate was washed with brine, dried over Na<sub>2</sub>SO<sub>4</sub>, filtered and concentrated in vacuo to provide crude triamino-alcohol (**4-44a**). Purification of the resultant oil by flash column chromatography (hexanes/EtOAc gradient, (9:1) to (1:2)) provided triamino-alcohol (**4-44a**) (1.2 g, 53%) as a colorless oil. The <sup>1</sup>H NMR displayed significant line broadening as noted by Huigens III *et al.* (2007).



**(4-44a):**

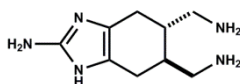
<sup>1</sup>H NMR (500 MHz, CHCl<sub>3</sub>-d<sub>1</sub>): δ (ppm) 5.21-4.87 (m, 3H), 3.69 (bs, 1H), 3.55 (bs, 1H), 3.31-2.95 (m, 4H), 2.47 (bs, 1H), 2.08-2.06 (m, 1H), 1.85-1.8 (m, 1H), 1.77-1.75 (m, 2H), 1.51-1.41 (m, 29H); **LRMS-ESI** (*m/z*) calcd for [C<sub>23</sub>H<sub>43</sub>N<sub>3</sub>O<sub>7</sub>+H]<sup>+</sup>: 474.32; found: 474.3; **LRMS-ESI** (*m/z*) calcd for [C<sub>18</sub>H<sub>35</sub>N<sub>3</sub>O<sub>5</sub>+H]<sup>+</sup>: 374.27; found: 374.3 (-CO<sub>2</sub>*t*-Bu)

**Synthesis of (1*S*,2*S*) triamino-ketone (4-44b).****4-44b**

To a solution of **(4-43a)** (550 mg, 1.16 mmol, 1.0 equiv) in anhydrous DMF (18-mL) was added pyridinium dichromate (PDC) (2.63 g, 6.98 mmol, 6.0 equiv) in a single portion. The resultant dark orange slurry was allowed to stir at RT for 20h at which point the oxidation was judged complete by TLC analysis. The reaction was diluted with brine (10-mL) and extracted with EtOAc (2x50-mL). The combined organics were washed with brine (3 × 20-mL), dried over Na<sub>2</sub>SO<sub>4</sub>, filtered and concentrated in vacuo to provide crude **(4-44b)** as a yellow oil. Purification by flash column chromatography (hexanes/EtOAc gradient, 100% to (2:3)) provided **(1*S*,2*S*)** triamino-ketone **(4-44b)** (470 mg, 85%) as a white foam. The <sup>1</sup>H NMR displayed significant line broadening as noted by Huigens III *et al.* (2007).

**(4-44b):**

<sup>1</sup>H NMR (500 MHz, CHCl<sub>3</sub>-d<sub>1</sub>): δ (ppm) 5.38 (bs, 1H), 5.01 (bs, 1H), 4.83 (bs, 1H), 4.25 (m, 1H), 3.57 (m, 1H), 3.45-3.12 (m, 2H), 2.94 (m, 1H), 2.73 (m, 1H), 2.31 (m, 2H), 1.93 (m, 1H), 1.73 (m, 1H), 1.42 (s, 27H); **LRMS-ESI** (*m/z*) calcd for [C<sub>23</sub>H<sub>41</sub>N<sub>3</sub>O<sub>7</sub>+H]<sup>+</sup>: 472.30; found: 472.3 **LRMS-ESI** (*m/z*) calcd for [C<sub>18</sub>H<sub>33</sub>N<sub>3</sub>O<sub>5</sub>+H]<sup>+</sup>: 372.25; found: 372.3 (-CO<sub>2</sub>*t*-Bu)

**Synthesis of ((5*S*,6*S*)-2-amino-4,5,6,7-tetrahydro-1*H*-benzo[d]imidazole-5,6-diyl)dimethanamine (4-24) (3·CF<sub>3</sub>CO<sub>2</sub>H).****(+)-4-24 3·CF<sub>3</sub>CO<sub>2</sub>H**

Purified **(1*S*,2*S*)** triamino-ketone **(4-44b)** (470 mg, 1.00 mmol, 1.0 equiv) was dissolved in CH<sub>2</sub>Cl<sub>2</sub> (8-mL, 0.18M) and cooled to 0°C with an ice-water bath followed by the dropwise addition of CF<sub>3</sub>CO<sub>2</sub>H (2.0-mL). The reaction was stirred at 0°C for 1h at which point the bath was removed and the solution was allowed to reach RT. The reaction was stirred at RT for 1h followed by concentration in vacuo to give a light yellow oil. The oil was redissolved in MeOH (10-mL) followed by the addition of HCl in 1,4-dioxane (30-mL, 4.0 M solution) and the acidic solution was concentrated in vacuo to provide an off-white powder that was used in the subsequent step without further purification (assume 1.00 mmol). The resultant white powder was dissolved in H<sub>2</sub>O (10-mL, 0.1 M) followed by the addition of cyanamide (319 mg, 7.78

mmol, 7.8 equiv). The solution was adjusted to pH = 4.3 with 10 % aqueous NaOH and heated to 100°C in a pre-heated oil bath for 3h. After cooling to RT, the reaction was diluted with EtOH (20-mL) and concentrated in vacuo to provide crude (**4-24**) (quant. conversion, <sup>1</sup>H NMR, 500 MHz, H<sub>2</sub>O-*d*<sub>2</sub>) contaminated with excess cyanamide. Purification of the incipient residue by flash column chromatography (12 g SiO<sub>2</sub>, 100% MeOH saturated with NH<sub>3</sub>) provided free base (**4-24**) (600 mg, overweight, still contains cyanamide and/or salts) as a light brown solid. Further purification of this material (approx. 500 mg of crude) by HPLC yielded pure (**4-24**) (**3 CF<sub>3</sub>CO<sub>2</sub>H**) (315.4 mg, 56% for 2 steps) (retention time: 2.1 min).

**Note:** The remaining column purified material free base (**4-24**) (100 mg, calcd at 60% purity) was used in subsequent derivatization reactions without further purification.

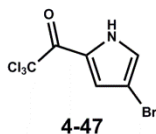
**HPLC conditions:** Waters Sunfire C18 column (19 × 250-mm) with UV detection at 254-nm; Solution A: H<sub>2</sub>O w/0.1% CF<sub>3</sub>CO<sub>2</sub>H and Solution B: CH<sub>3</sub>CN w/0.1% CF<sub>3</sub>CO<sub>2</sub>H; increase gradient of Solution B from 5% to 30%, 1-10 min; 30% to 100%, 10-12min; flow rate: 20-mL/min.

**(+)-(4-24) (3·CF<sub>3</sub>CO<sub>2</sub>H):**

<sup>1</sup>H NMR (500 MHz, H<sub>2</sub>O-*d*<sub>2</sub>): δ (ppm) 3.13-3.06 (m, 2H), 3.08 (dd, 2H), 2.71-2.69 (m, 2H), 2.52-2.46 (m, 2H), 2.42 (bs, 2H); <sup>1</sup>H NMR (500 MHz, MeOH-*d*<sub>4</sub>): δ (ppm) 3.08 (dd, 2H), 2.98 (dd, 2H), 2.76 (dd, 2H), 2.61-2.52 (m, 2H), 2.46 (bs, 2H); <sup>13</sup>C NMR (125 MHz, MeOH-*d*<sub>4</sub>): δ (ppm) 148.9, 118.4, 42.7, 34.5, 20.7; LRMS-ESI (*m/z*) calcd for [C<sub>9</sub>H<sub>17</sub>N<sub>5</sub>+H]<sup>+</sup>: 196.16; found: 196.2; [α]<sub>D</sub> = +2.0° (c = 0.15, EtOH / H<sub>2</sub>O (1:1))

**Derivatization of 2-aminoimidazole (4-24).**

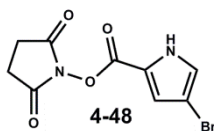
**Synthesis of 1-(4-bromo-1H-pyrrol-2-yl)-2,2,2-trichloroethanone (4-47).**



2,2,2-Trichloro-1-(1H-pyrrol-2-yl)ethanone (5.0 g, 23.6 mmol, 1.0 equiv) and NaOAc (2.13 g, 26 mmol, 1.1 equiv) were suspended in CHCl<sub>3</sub> (240-mL). The heterogeneous mixture was cooled to -15°C (dry ice-CH<sub>3</sub>CN bath) followed by the dropwise addition of Br<sub>2</sub> (1.29-mL, 26 mmol, 1.1 equiv). The reaction was stirred at -15°C for 1h and allowed to warm to RT over 30 min at which point TLC analysis indicated complete conversion to two new products. The mixture was quenched with saturated aqueous NaHCO<sub>3</sub> (50-mL) and the organic layer was separated and washed with saturated aqueous NaHCO<sub>3</sub> (2 × 20-mL), brine (30-mL), dried over Na<sub>2</sub>SO<sub>4</sub>, filtered and concentrated in vacuo to provide a crude solid. Analysis of the crude mixture indicated the products were the desired mono- and dibrominated derivatives (<sup>1</sup>H NMR, 500 MHz, CHCl<sub>3</sub>-*d*<sub>1</sub>, ~7:1 ratio). The crude solid was purified by flash column chromatography (hexanes/EtOAc gradient, 100% hexanes to (95:5)) to provide 1-(4,5-dibromo-1H-pyrrol-2-yl)-2,2,2-trichloroethanone (0.84g, 10%), enriched mixture (3.40 g, 50%, ~10:1) and desired 1-(4-bromo-1H-pyrrol-2-yl)-2,2,2-trichloroethanone (**4-47**) (1.95 g, 28%) as a light yellow solid.

**1-(4-bromo-1H-pyrrol-2-yl)-2,2,2-trichloroethanone (4-47):**

<sup>1</sup>H NMR (600 MHz, CHCl<sub>3</sub>-d<sub>1</sub>): δ (ppm) 9.51 (bs, 1H), 7.36 (d, *J* = 1.5 Hz, 1H), 7.16 (d, *J* = 1.5 Hz, 1H); LRMS-ESI (*m/z*) calcd for [C<sub>6</sub>H<sub>3</sub>BrCl<sub>3</sub>NO+H]<sup>+</sup>: 291.85; found: 291.9.

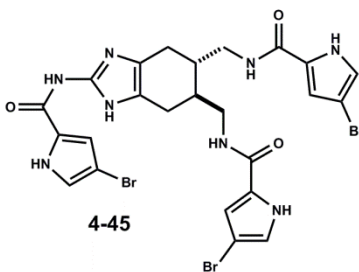
**Synthesis of 2,5-dioxopyrrolidin-1-yl 4-bromo-1H-pyrrole-2-carboxylate (4-48).**

4-bromo-1H-pyrrole-2-carboxylic acid was prepared from the basic hydrolysis of 1-(4-bromo-1H-pyrrol-2-yl)-2,2,2-trichloroethanone (**4-47**) in 1 M aqueous NaOH (0.4 M reaction concentration) at 0°C warm to RT for 1h.

To a solution containing 4-bromo-1H-pyrrole-2-carboxylic acid (502 mg, 2.64 mmol, 1.0 equiv) and 1-Ethyl-3-(3-dimethylaminopropyl)carbodiimide hydrochloride (EDC HCl) (516 mg, 2.69 mmol, 1.02 equiv) in DMF (13.2-mL) was added N-hydroxysuccinimide (NHS) (319 mg, 2.77 mmol, 1.05 equiv) and (*i*-Pr)<sub>2</sub>NEt (0.46-mL, 2.64 mmol, 2.0 equiv) via syringe at RT. The reaction was stirred for 12h at RT, diluted with EtOAc (40-mL) and washed with H<sub>2</sub>O, brine, dried over Na<sub>2</sub>SO<sub>4</sub>, filtered and concentrated in vacuo to provide a crude oil. The oil was purified by flash column chromatography (hexanes/EtOAc gradient, (9:1) to (1:1)) to provide (**4-48**) (550 mg, 73%) as a light yellow solid.

**2,5-dioxopyrrolidin-1-yl 4-bromo-1H-pyrrole-2-carboxylate (4-48):**

<sup>1</sup>H NMR (500 MHz, MeOH-*d*<sub>4</sub>): δ (ppm) 7.20 (d, *J* = 1.5 Hz, 1H), 7.11 (d, *J* = 1.5 Hz, 1H), 2.87 (s, 4H); <sup>13</sup>C NMR (125 MHz, MeOH-*d*<sub>4</sub>): δ (ppm) 172.0, 156.5, 127.8, 120.6, 118.7, 98.9, 26.5; LRMS-ESI (*m/z*) calcd for [C<sub>9</sub>H<sub>7</sub>BrN<sub>2</sub>O<sub>4</sub>+H]<sup>+</sup>: 286.97; found: 287.0.

**Synthesis of Triacylated Derivative (4-45).**

Crude column purified (**4-24**) (100 mg, 0.31 mmol, 1.0 equiv, calcd at 60% purity) was dissolved in DMF (1.5-mL) with solid Na<sub>2</sub>CO<sub>3</sub> (195 mg, 1.84 mmol, 6.0 equiv) at RT followed by the addition of 1-(4-bromo-1H-pyrrol-2-yl)-2,2,2-trichloroethanone (**4-47**) (350 mg, 1.22 mmol, 4.0 equiv). The resultant slurry was heated to 60°C for 16h. The mixture was cooled to RT and diluted with EtOAc (50-mL). The organics were washed with brine (5 × 10-mL), dried over Na<sub>2</sub>SO<sub>4</sub>, filtered and concentrated in vacuo to give crude (**4-45**) (103 mg, 47%, calcd from est.

0.31 mmol **4-24**) as a light purple solid. Further purification by HPLC provided (**4-45**) (38 mg, 17%) (retention time: 9.6 min) as a tan powder.

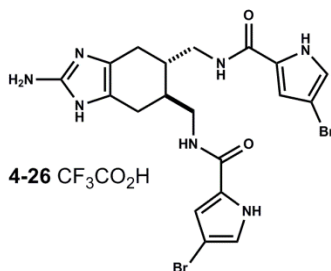
**HPLC conditions:** Waters Sunfire C18 column (19 × 250-mm) with UV detection at 254-nm; Solution A: H<sub>2</sub>O w/0.1% CF<sub>3</sub>CO<sub>2</sub>H and Solution B: CH<sub>3</sub>CN w/0.1% CF<sub>3</sub>CO<sub>2</sub>H; increase gradient of Solution B from 5% to 100%, 0.5-14 min; flow rate: 20-mL/min.

**(4-45):**

<sup>1</sup>H NMR (500 MHz, MeOH-*d*<sub>4</sub>): δ (ppm) 7.12 (s, 1H), 7.13 (s, 1H), 6.91 (d, *J* = 1.0 Hz, 2H), 6.80 (d, *J* = 1.0 Hz, 2H), 3.45-3.31 (m, 4H), 2.82 (dd, *J* = 15.5, 4.5 Hz, 2H), 2.53-2.49 (m, 2H), 2.33-2.31 (m, 2H); <sup>1</sup>H NMR (500 MHz, CH<sub>3</sub>CN-*d*<sub>3</sub>): δ (ppm) 13.41 (bs, 2H), 10.63 (s, 1H), 10.49 (s, 2H), 7.30 (s, 2H), 7.11 (s, 1H), 6.92 (s, 2H), 6.71 (s, 2H), 3.46 (bs, 2H), 3.22 (bs, 2H), 2.70-2.67 (m, 2H), 2.38-2.35 (m, 2H), 2.17 (bs, 2H); <sup>13</sup>C NMR (125 MHz, MeOH-*d*<sub>4</sub>): δ (ppm) 162.9, 162.8\*, 158.7, 139.9, 127.4, 127.3\*, 126.3, 125.2, 122.9, 121.9, 116.6, 113.3, 98.5, 97.5, 42.4, 42.3\*, 36.0, 21.4; <sup>13</sup>C NMR (125 MHz, CH<sub>3</sub>CN-*d*<sub>3</sub>): δ (ppm) 161.4, 158.8, 140.5, 127.4, 126.0, 125.1, 122.7, 121.4, 117.1, 112.7, 98.2, 97.0, 42.0, 35.6, 22.2; **LRMS-ESI** (*m/z*) calcd for [C<sub>24</sub>H<sub>23</sub>Br<sub>3</sub>N<sub>8</sub>O<sub>3</sub>+H]<sup>+</sup>: 710.95; found: 710.7.

\*duplicate peaks observed in MeOH-*d*<sub>4</sub> possibly due to non-symmetric rotamers (see tabulated data in CH<sub>3</sub>CN-*d*<sub>3</sub>)

**Synthesis of Diacylated Derivative (4-26).**

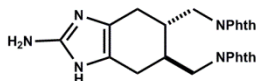


Purified (**4-24**) (**3** CF<sub>3</sub>CO<sub>2</sub>H) (44.2 mg, 0.08 mmol, 1.0 equiv) was suspended in DMF (1.6-mL) followed by the addition of (*i*-Pr)<sub>2</sub>NEt (50-μL, 0.29 mmol, 3.5 equiv) via syringe and the resultant heterogeneous mixture was agitated by sonication for 2 min. The reaction was cooled to 0°C with an ice-water bath followed by the addition of (**4-48**) (47.2 mg, 0.16 mmol, 2.0 equiv) in one portion. After stirring for 2h at 0°C the bath was removed and the reaction was allowed to reach RT. After stirring for 12h at RT the mixture was quenched by the addition of CF<sub>3</sub>CO<sub>2</sub>H (200-μL) and was purified by HPLC directly. Purification provided (**4-26**) (22 mg, 41%) (retention time: 9.9 min) as a tan powder after lyophilization.

**HPLC conditions:** Waters Sunfire C18 column (19 × 250-mm) with UV detection at 254-nm; Solution A: H<sub>2</sub>O w/0.1% CF<sub>3</sub>CO<sub>2</sub>H and Solution B: CH<sub>3</sub>CN w/0.1% CF<sub>3</sub>CO<sub>2</sub>H; increase gradient of Solution B from 5% to 70%, 0.5-13 min; 70% to 100%, 13-15 min; flow rate: 20-mL/min.

**(4-26):**

<sup>1</sup>H NMR (500 MHz, MeOH-*d*<sub>4</sub>): δ (ppm) 6.92 (d, *J* = 1.5 Hz, 2H), 6.78 (d, *J* = 1.5 Hz, 2H), 3.44-3.32 (m, 4H), 2.70 (dd, *J* = 15.0, 5.0 Hz, 2H), 2.38-2.24 (m, 4H); <sup>13</sup>C NMR (125 MHz, MeOH-*d*<sub>4</sub>): δ (ppm) 162.8, 148.5, 127.4, 122.9, 119.5, 113.3, 97.5, 42.4, 36.1, 21.2; LRMS-ESI (*m/z*) calcd for [C<sub>19</sub>H<sub>21</sub>Br<sub>2</sub>N<sub>7</sub>O<sub>2</sub>+H]<sup>+</sup>: 540.02; found: 539.9.

**Synthesis of Bis-Phthalimide Derivative (4-46).**

**4-46** CF<sub>3</sub>CO<sub>2</sub>H

Crude (**4-24**) (3 HCl) (60 mg, 0.20 mmol, 1.0 equiv, MW 304.65 g/mol) was suspended in CH<sub>3</sub>CN/CH<sub>3</sub>OH (5:1) (3.6-mL) followed by the addition of (*i*-Pr)<sub>2</sub>NEt (100-μL). To the resultant heterogeneous mixture was added phthalic anhydride (44 mg, 0.30 mmol, 1.5 equiv) and the reaction was heated to 60°C in a sealed vial for 3h. The solution was cooled to RT followed by the addition of CF<sub>3</sub>CO<sub>2</sub>H (250-μL), fitted with a reflux condenser and heated to 100°C for 3h. The solution was concentrated in vacuo and redissolved in CH<sub>3</sub>CN/DMSO (3:1) (2-mL) for direct purification by HPLC to provide (**4-46**) (CF<sub>3</sub>CO<sub>2</sub>H) (8.5 mg, 8% from **4-24**) as a white film (retention time: 13.9 min).

**Note:** The addition of CH<sub>3</sub>OH to the initial reaction was discovered experimentally and serves to minimize acylation events on guanidine. Low yields are attributed to the observation of substantial phthalimide hydrolysis during purification with aqueous acidic eluent. (LRMS-ESI (*m/z*) calcd for [C<sub>25</sub>H<sub>23</sub>N<sub>5</sub>O<sub>5</sub>+H]<sup>+</sup>: 474.18; found: 474.2.)

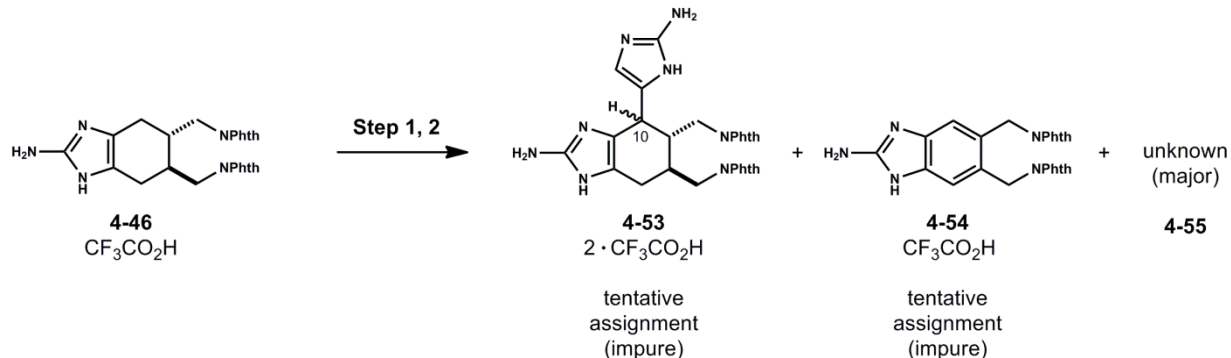
**HPLC conditions:** Waters Sunfire C18 column (19 × 250-mm) with UV detection at 254-nm; Solution A: H<sub>2</sub>O w/0.1% CF<sub>3</sub>CO<sub>2</sub>H and Solution B: CH<sub>3</sub>CN w/0.1% CF<sub>3</sub>CO<sub>2</sub>H; increase gradient of Solution B from 5% to 10%, 0.5-2 min; 10% to 60%, 2-18 min; flow rate: 20-mL/min.

**(4-46) (CF<sub>3</sub>CO<sub>2</sub>H):**

<sup>1</sup>H NMR (500 MHz, CH<sub>3</sub>CN-*d*<sub>3</sub>): δ (ppm) 12.01 (s, 2H), 7.84-7.58 (m, 8H), 7.35 (s, 2H), 3.67 - 3.57 (m, 4H), 2.74 (dd, *J* = 15.1, 5.2 Hz, 2H), 2.44-2.37 (m, 2H), 2.36-2.29 (m, 2H); <sup>13</sup>C NMR (125 MHz, CH<sub>3</sub>CN-*d*<sub>3</sub>): δ (ppm) 169.5, 149.3, 135.3, 133.1, 123.9, 118.9\* (coincident with CH<sub>3</sub>CN-*d*<sub>3</sub>), 41.2, 34.4, 20.8. LRMS-ESI (*m/z*) calcd for [C<sub>25</sub>H<sub>21</sub>N<sub>5</sub>O<sub>4</sub>+H]<sup>+</sup>: 456.17; found: 456.2.

\*obtained from HMBC data

### Attempted Synthesis of (4-53) from Bis-Phthalimide Derivative (4-46).



Step 1 – A stock solution of PTAD (4.6 mg) in THF (300- $\mu$ L) was prepared and cooled to  $-40^{\circ}\text{C}$ . To a solution of crude (**4-46**) (CF<sub>3</sub>CO<sub>2</sub>H) (est. 80% pure by <sup>1</sup>H NMR integration, major impurity - phthalic acid) (6.0 mg, 0.008 mmol, 1.0 equiv) in THF (0.58-mL) at  $-40^{\circ}\text{C}$  was added PTAD stock solution (188- $\mu$ L, calcd. 0.7 equiv). The reaction was shielded from light (wrapped in foil) and stirred at  $-40^{\circ}\text{C}$  for 30 min. The reaction was allowed to slowly reach RT and was stirred at RT for 1h. The presumed adduct **int-(4-46)** could be observed by LC-MS analysis of a reaction aliquot (LRMS-ESI ( $m/z$ ) calcd for [C<sub>33</sub>H<sub>26</sub>N<sub>8</sub>O<sub>6</sub>+H]<sup>+</sup>: 631.21; found: 631.2). The light red solution was concentrated with a stream of Ar and dried further on high vacuum for 12h. The light red solid was used directly without further purification.

**PTAD adduct int-(4-46):** (after Step 1)

**LRMS-ESI** ( $m/z$ ) calcd for [C<sub>33</sub>H<sub>26</sub>N<sub>8</sub>O<sub>6</sub>+H]<sup>+</sup>: 631.21; found: 631.2.

Step 2 – 1H-imidazol-2-amine hydrochloride (**4-8**) (20 mg, 0.16 mmol, 20 equiv) was evaporated from benzene (3  $\times$  1.0-mL) and added to the vial containing presumed PTAD adduct **int-(4-46)** (assume 0.008 mmol). To this solid mixture was added 3 Å MS followed by the addition of neat CH<sub>3</sub>SO<sub>3</sub>H (100- $\mu$ L). The CH<sub>3</sub>SO<sub>3</sub>H was previously degassed by sparging with Ar for 15 min. The light brown reaction was stirred for 40h at RT and was monitored by LC-MS. After 40h, the reaction was cooled to 0 $^{\circ}\text{C}$  and quenched by the slow addition of saturated aqueous NaHCO<sub>3</sub> (500- $\mu$ L). The dark brown mixture was diluted with CH<sub>3</sub>CN (1.0-mL) and acidified with neat CF<sub>3</sub>CO<sub>2</sub>H (300- $\mu$ L). The mixture was filtered and purified by HPLC.

**Reaction Analysis:** Three major products were observed by LC-MS analysis (tentatively assigned as **4-53**, **4-54** and **4-55**, see below). Purification by HPLC provided three impure fractions after lyophilization (tentatively assigned as **4-53**, **4-54** and **4-55**). A yield was not obtained.

**HPLC conditions:** Waters Sunfire C18 column (19  $\times$  250-mm) with UV detection at 254-nm; Solution A: H<sub>2</sub>O w/0.1% CF<sub>3</sub>CO<sub>2</sub>H and Solution B: CH<sub>3</sub>CN w/0.1% CF<sub>3</sub>CO<sub>2</sub>H; increase gradient of Solution B from 5% to 30%, 0.5-10 min; 30% to 100%, 10-14 min; flow rate: 20-mL/min.

**(4-53) (2·CF<sub>3</sub>CO<sub>2</sub>H)** (retention time: 10.7 min):

<sup>1</sup>H NMR (500 MHz, MeOH-*d*<sub>4</sub>): see annotated spectrum (tentative, impure); LRMS-ESI (*m/z*) calcd for [C<sub>28</sub>H<sub>24</sub>N<sub>8</sub>O<sub>4</sub>+H]<sup>+</sup>: 537.20; found: 537.1

**(4-54) (CF<sub>3</sub>CO<sub>2</sub>H)** (retention time: 12.5 min):

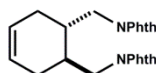
<sup>1</sup>H NMR (500 MHz, MeOH-*d*<sub>4</sub>): see annotated spectrum (tentative, impure); LRMS-ESI (*m/z*) calcd for [C<sub>25</sub>H<sub>17</sub>N<sub>5</sub>O<sub>4</sub>+H]<sup>+</sup>: 452.14; found: 452.0.

**(4-55)** (unknown mixture) (retention time: 12.1 min):

LRMS-ESI (*m/z*) observed: 285.0, 470.1, 569.1, 591.1

### Alternative Synthesis of Bis-Phthalimide Derivative (4-46).

Synthesis of 2,2'-((1*S*,2*S*)-cyclohex-4-ene-1,2-diylbis(methylene))bis(isoindoline-1,3-dione) (4-56).



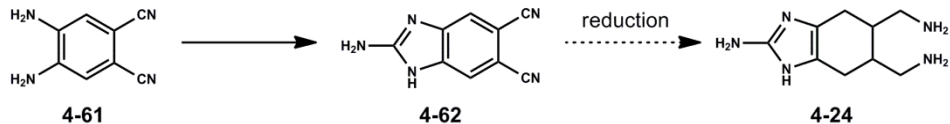
4-56

Crude bis-mesylate (**4-42a**) (2.3 g, 7.7 mmol, 1.0 equiv) was dissolved in DMF (250-mL) followed by the addition of potassium phthalimide (3.01 g, 16.2 mmol, 2.1 equiv). The reaction was fitted with a reflux condenser and heated to 115°C for 12h in an oil bath. The crude mixture was poured into ice-water (approx. 400-mL) and the white precipitate (**4-46**) was collected via filtration. Subsequent rinsing with H<sub>2</sub>O (2 × 5-mL) and drying in vacuo provided bis-phthalimide (**4-56**) (2.69 g, 87%) as a white solid.

**(4-56):**

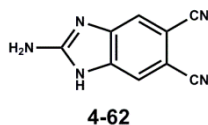
<sup>1</sup>H NMR (500 MHz, DMSO-*d*<sub>6</sub>): δ (ppm) 7.86-7.80 (m, 10H), 5.63 (s, 2H), 3.62-3.51 (m, 4H), 2.28-2.24 (m, 2H), 2.07-2.06 (m, 2H), 1.79-1.75 (m, 2H); <sup>13</sup>C NMR (125 MHz, DMSO-*d*<sub>6</sub>): δ (ppm) 168.2; 134.6, 131.5, 124.2, 123.1, 40.7, 32.0, 24.2; LRMS-ESI (*m/z*) calcd for [C<sub>24</sub>H<sub>20</sub>N<sub>2</sub>O<sub>4</sub>+H]<sup>+</sup>: 401.15; found: 401.1.

### Alternative Attempted Synthesis of 2-aminoimidazole (4-24).



4,5-diaminophthalonitrile (**4-61**) was prepared in 6 steps from benzene-1,2-diamine via an efficient route developed by Burmester, C.; Faust, R. *Synthesis* **2008**, 8, 1179.

### Synthesis of 2-amino-1H-benzo[d]imidazole-5,6-dicarbonitrile (4-62).



4,5-diaminophthalonitrile (**4-61**) (200 mg, 1.26 mmol, 1.0 equiv) was dissolved in CH<sub>3</sub>CN/H<sub>2</sub>O (5:1) (5.27-mL) followed by the addition of cyanogen bromide (135 mg, 1.26 mmol, 1.0 equiv) at RT. The mixture was heated to 80°C for 2h at which point conversion to (**4-62**) was approx. 15% (LCMS analysis, UV detection at 254-nm). The reaction was cooled to RT and an additional portion of cyanogen bromide (405 mg, 3.8 mmol, 3 equiv) was added and the reaction was heated to 100°C and stirred overnight. The resultant mixture was cooled to RT, quenched with conc. aqueous NH<sub>4</sub>OH (1-mL), saturated with solid NaCl, and extracted with CHCl<sub>3</sub>/MeOH (9:1) (3 × 10-mL). The combined organics were washed with brine, dried over Na<sub>2</sub>SO<sub>4</sub>, filtered and concentrated in vacuo to afford 2-amino-1H-benzo[d]imidazole-5,6-dicarbonitrile (**4-62**) (280 mg, 99%, overweight - may contain salts).

### 2-amino-1H-benzo[d]imidazole-5,6-dicarbonitrile (4-62):

<sup>1</sup>H NMR (500 MHz, MeOH-*d*<sub>4</sub>): δ (ppm) 7.60 (s, 2H); <sup>13</sup>C NMR (500 MHz, MeOH-*d*<sub>4</sub>): δ (ppm) 162.2, 144.0, 118.5, 117.5, 106.6; LRMS-ESI (*m/z*) calcd for [C<sub>9</sub>H<sub>5</sub>N<sub>5</sub>+H]<sup>+</sup>: 184.06; found: 184.1.



### 4.7.3 Experimental References.

[1] For the Diels–Alder reaction, see: (a) Heathcock, C. H.; Davis, B. R.; Hadley, C. R. *J. Med. Chem.* **1989**, 32, 197. (b) Doherty, S.; Knight, J. G.; Bell, A. L.; Harrington, R. W.; Clegg, W. *Organometallics* **2007**, 26, 2465.

[2] For the  $\text{LiAlH}_4$  reduction, see: Garcia, M.-E. J.; Frölich, U.; Koert, U. *Eur. J. Org. Chem.* **2007**, 1991.

## APPENDIX THREE

### Spectra Relevant to Chapter Four:

#### Chapter 4 – Regarding an Alternative Route to (±)-Axinellamine A from (±)-Ageliferin

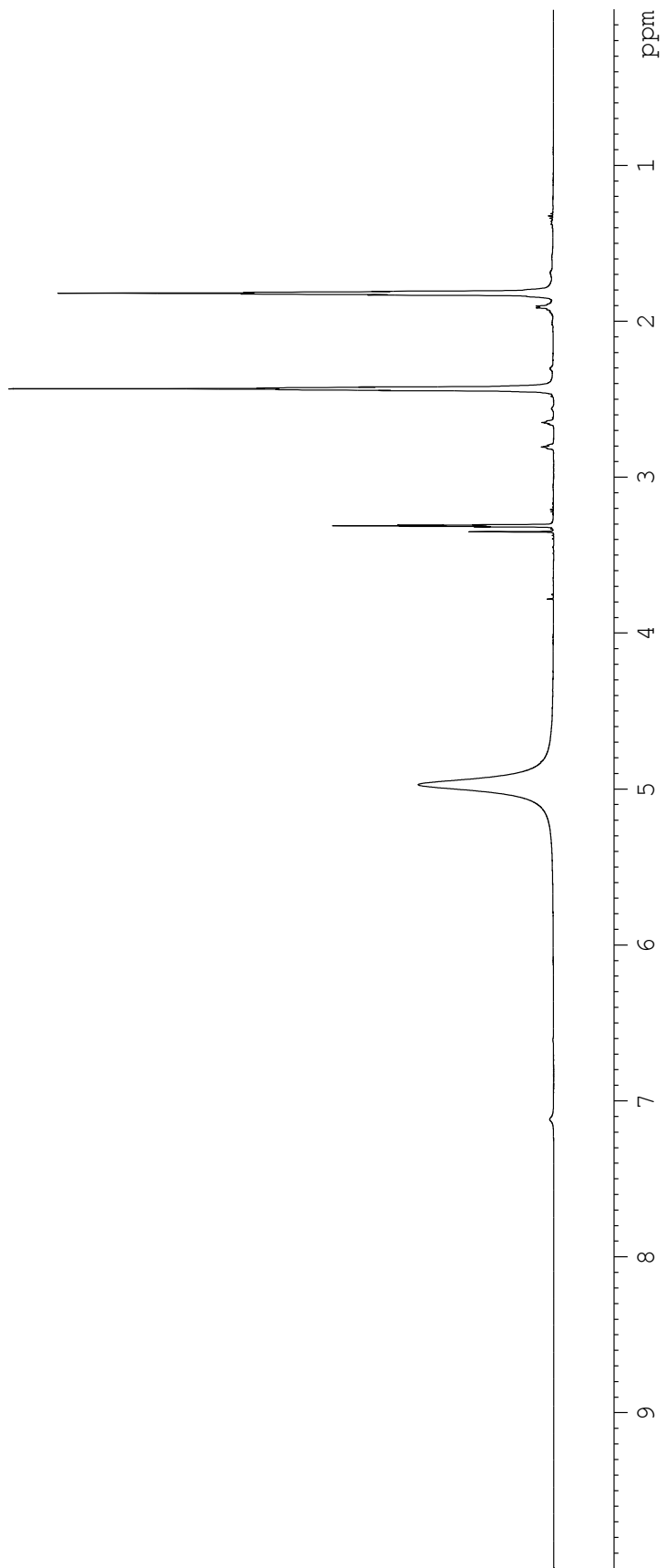
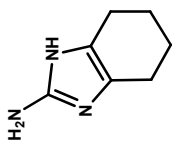
##### *Controlled, oxidative transformations of 2-aminoimidazoles (Part I)*

*Andrew G. Roberts, Hui Ding and Patrick G. Harran*

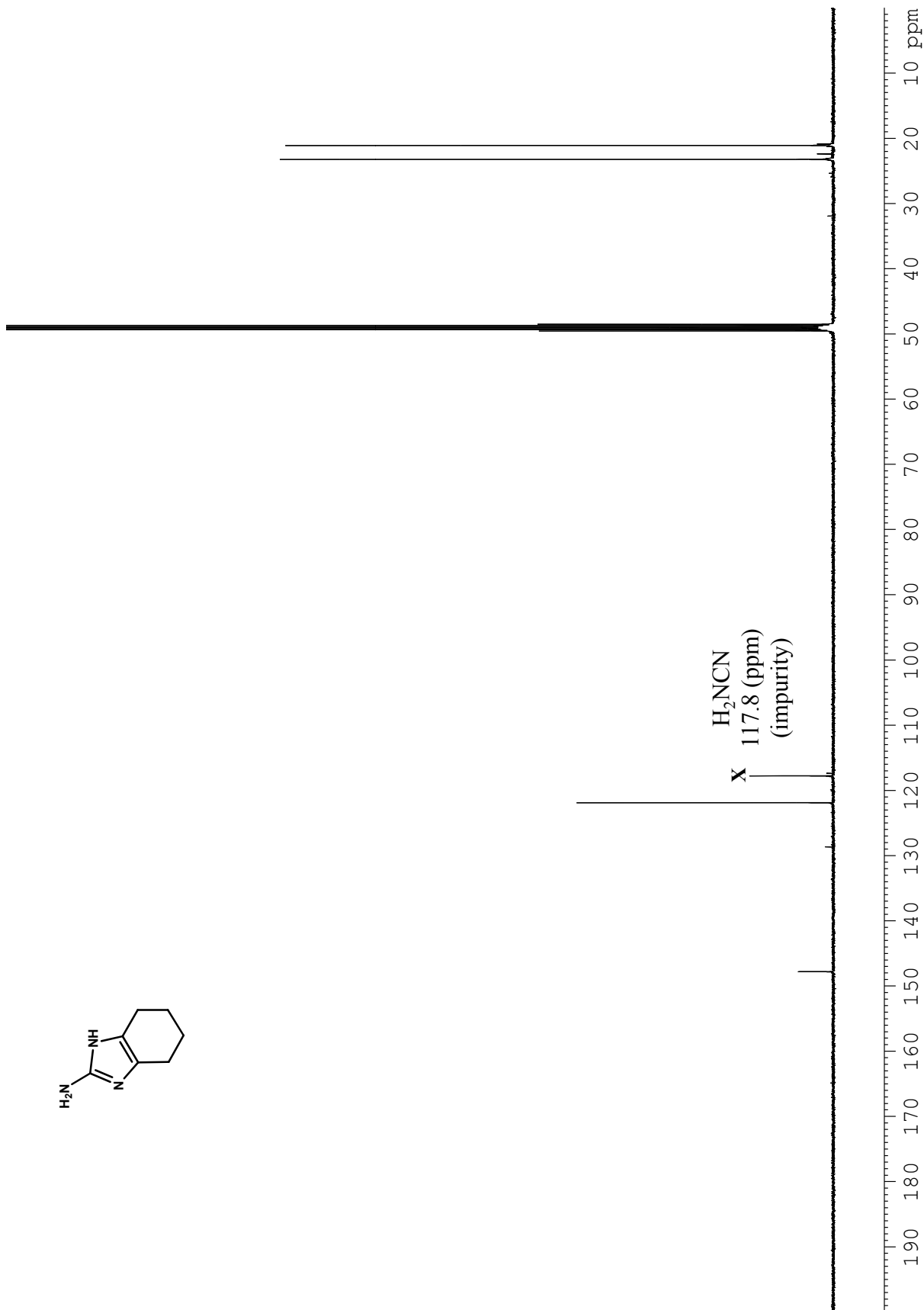
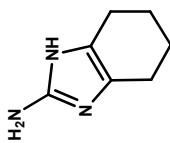
*and*

#### Chapter 4 – Progress Towards the Total Synthesis of (-)-Ageliferin (Part II).

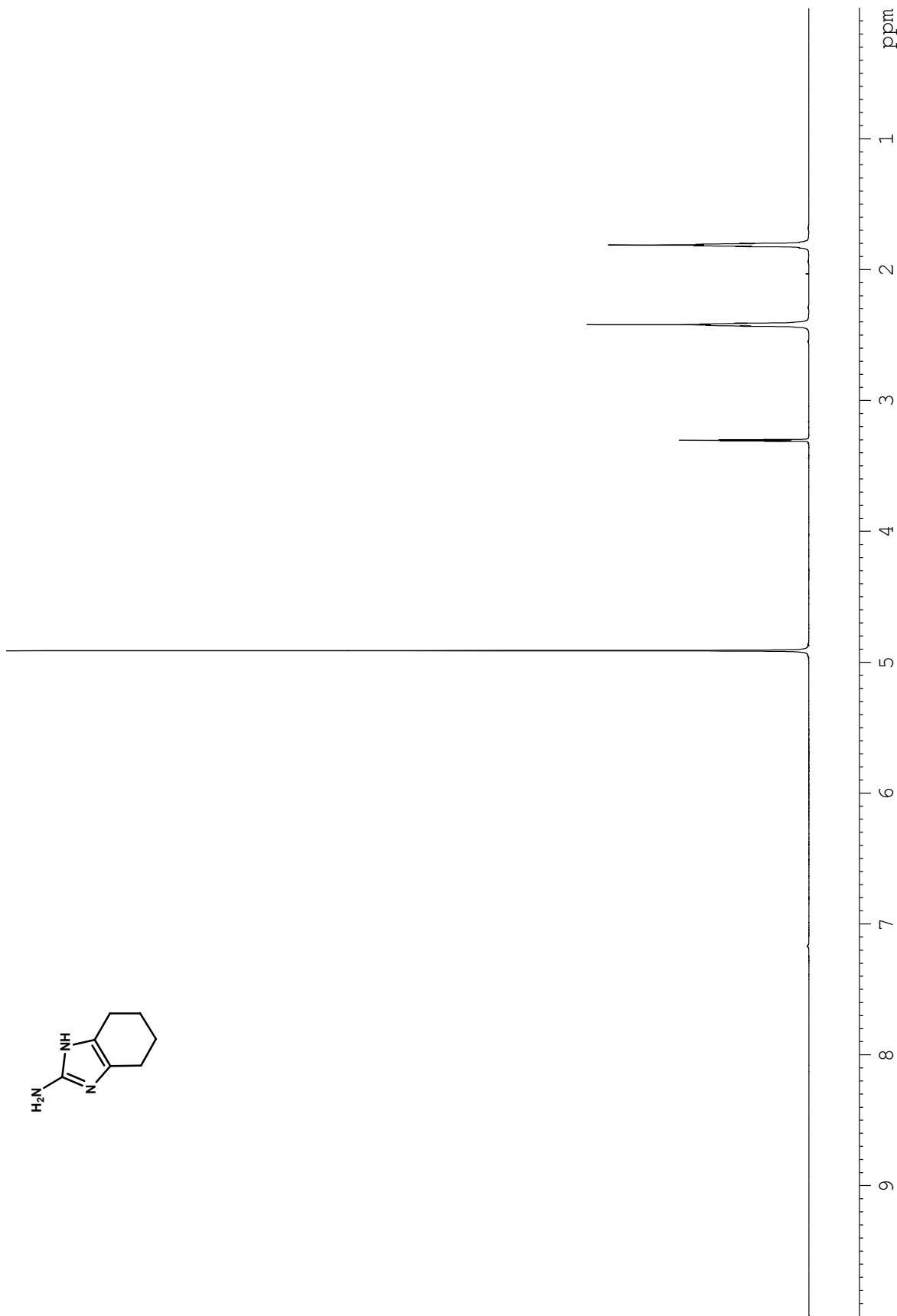
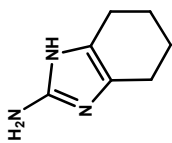
*Andrew G. Roberts and Patrick G. Harran*



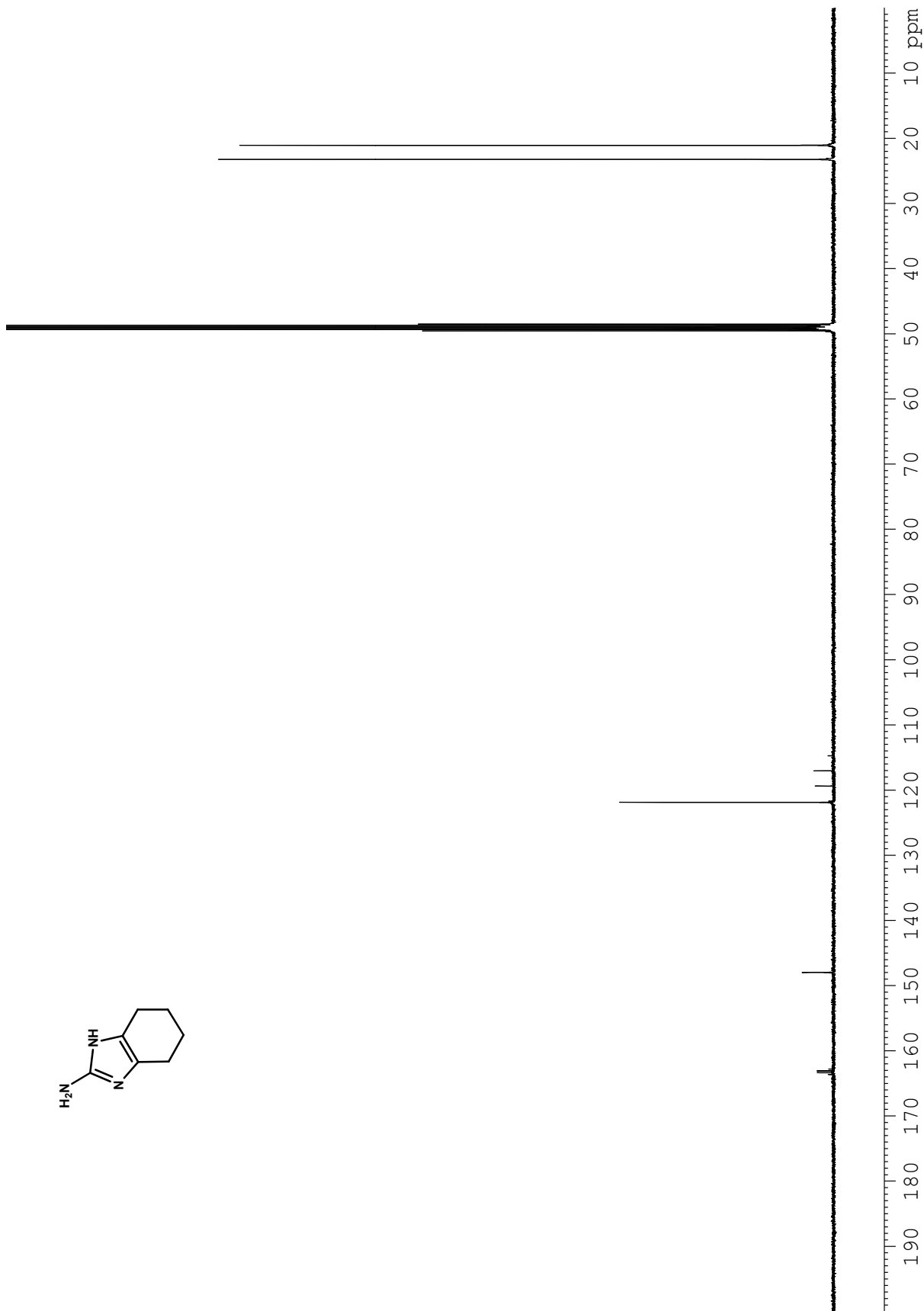
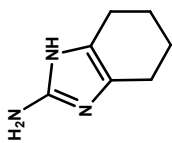
**Figure A3.1.** <sup>1</sup>H NMR (500 MHz, MeOH-*d*<sub>4</sub>) spectrum of compound 4-7 (freebase).



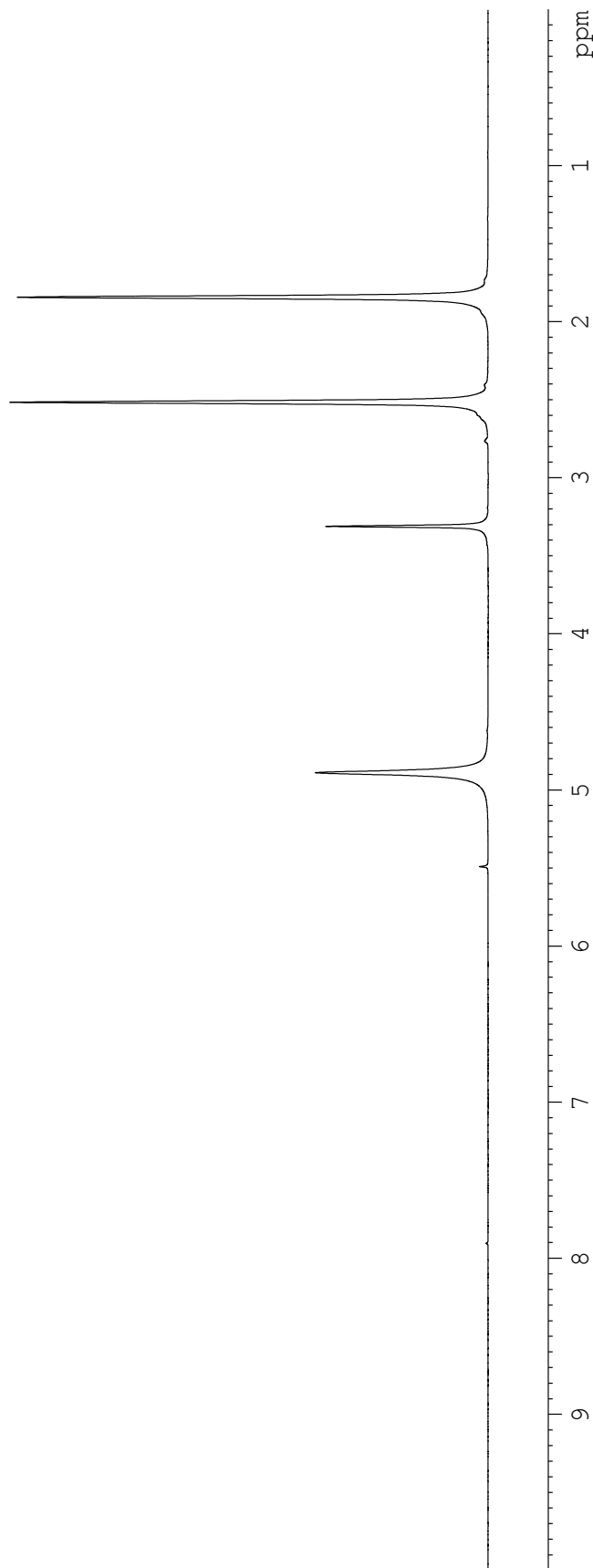
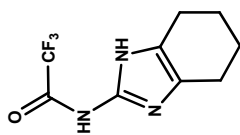
**Figure A3.2.**  $^{13}\text{C}$  NMR (125 MHz,  $\text{MeOH-}d_4$ ) of compound 4-7 (freebase).



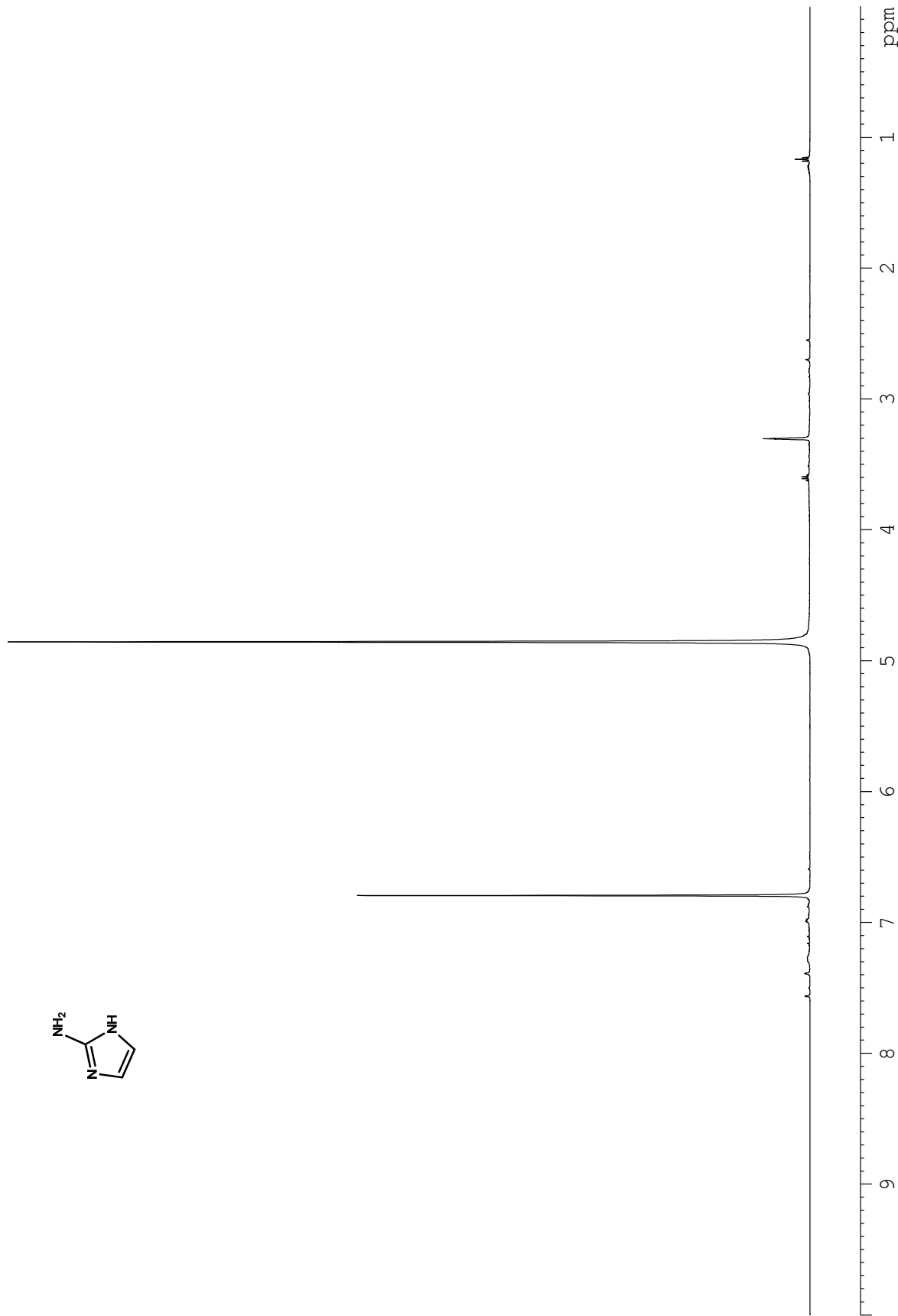
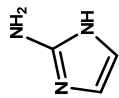
**Figure A3.3.**  $^1\text{H}$  NMR (500 MHz,  $\text{MeOH-}d_4$ ) spectrum of compound 4-7b ( $\text{CF}_3\text{CO}_2\text{H}$ ).



**Figure A3.4.**  $^{13}\text{C}$  NMR (125 MHz,  $\text{MeOH-}d_4$ ) spectrum of compound 4-7b ( $\text{CF}_3\text{CO}_2\text{H}$ ).

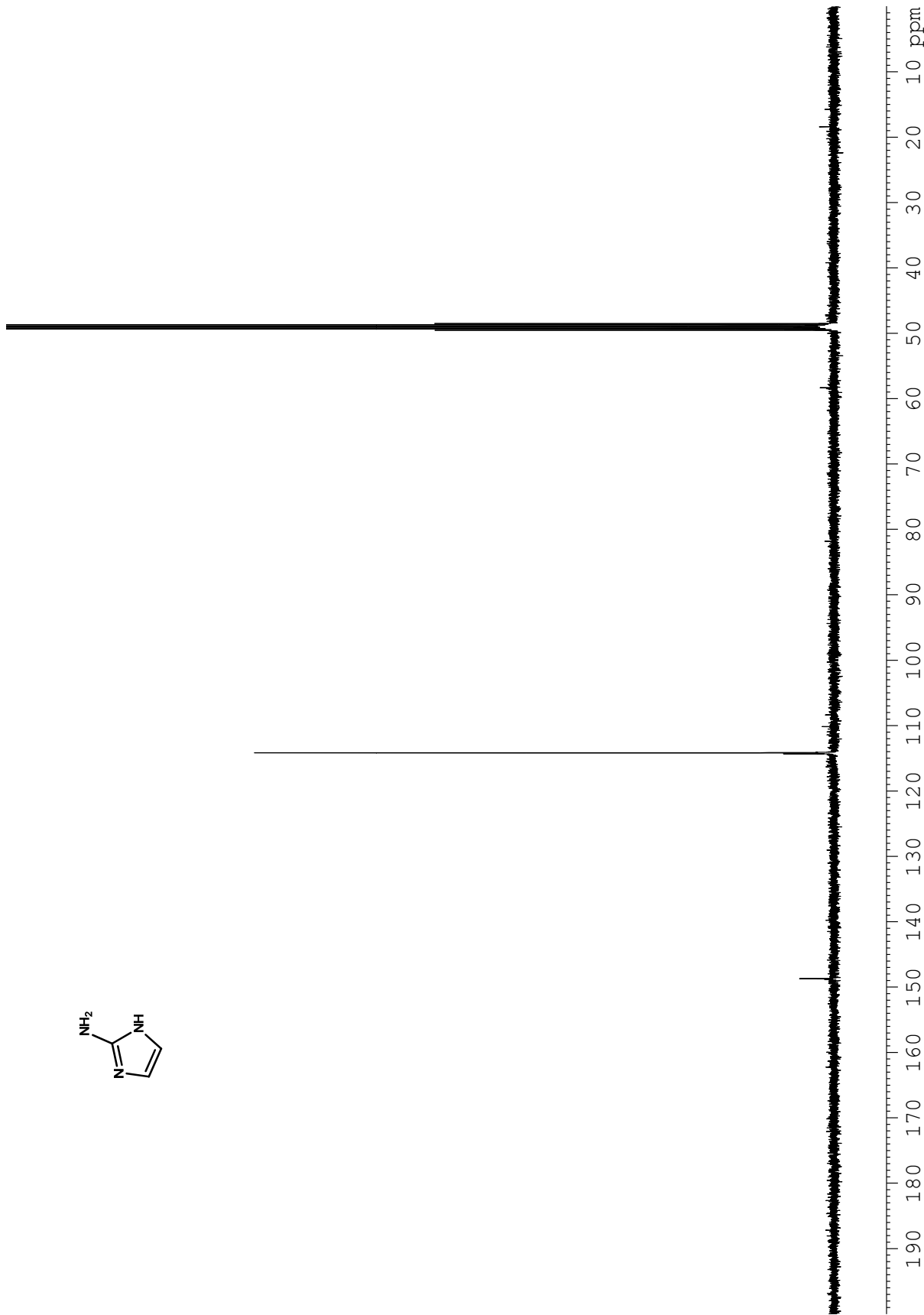
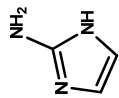


**Figure A3.5.**  $^1\text{H}$  NMR (500 MHz,  $\text{MeOH-}d_4$ ) spectrum of compound **4-13**.

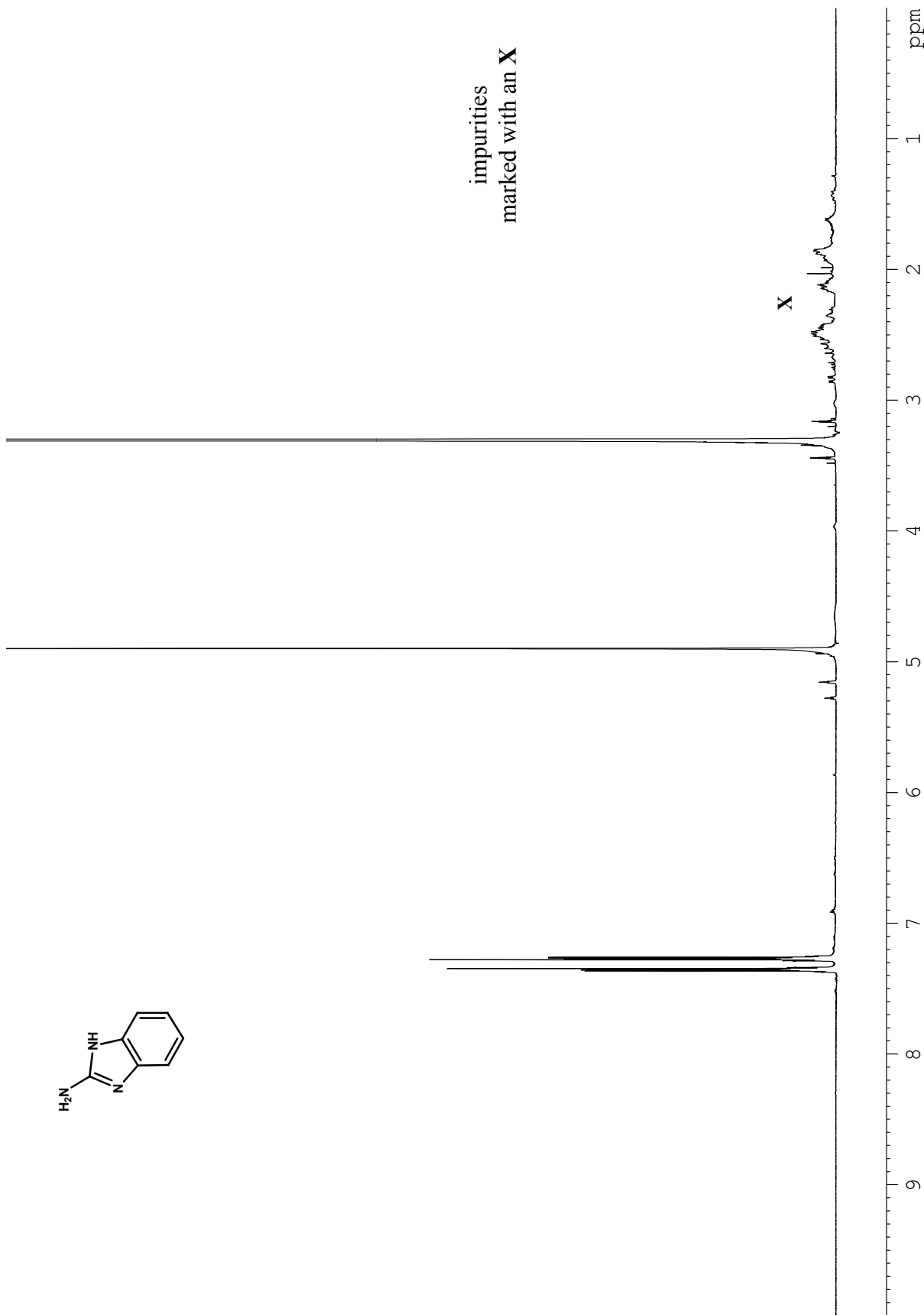
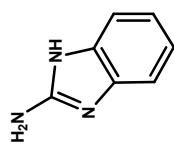


**Figure A3.6.**  $^1\text{H}$  NMR (500 MHz,  $\text{H}_2\text{O}-d_2$ ) spectrum of compound 4-8 (HCl).

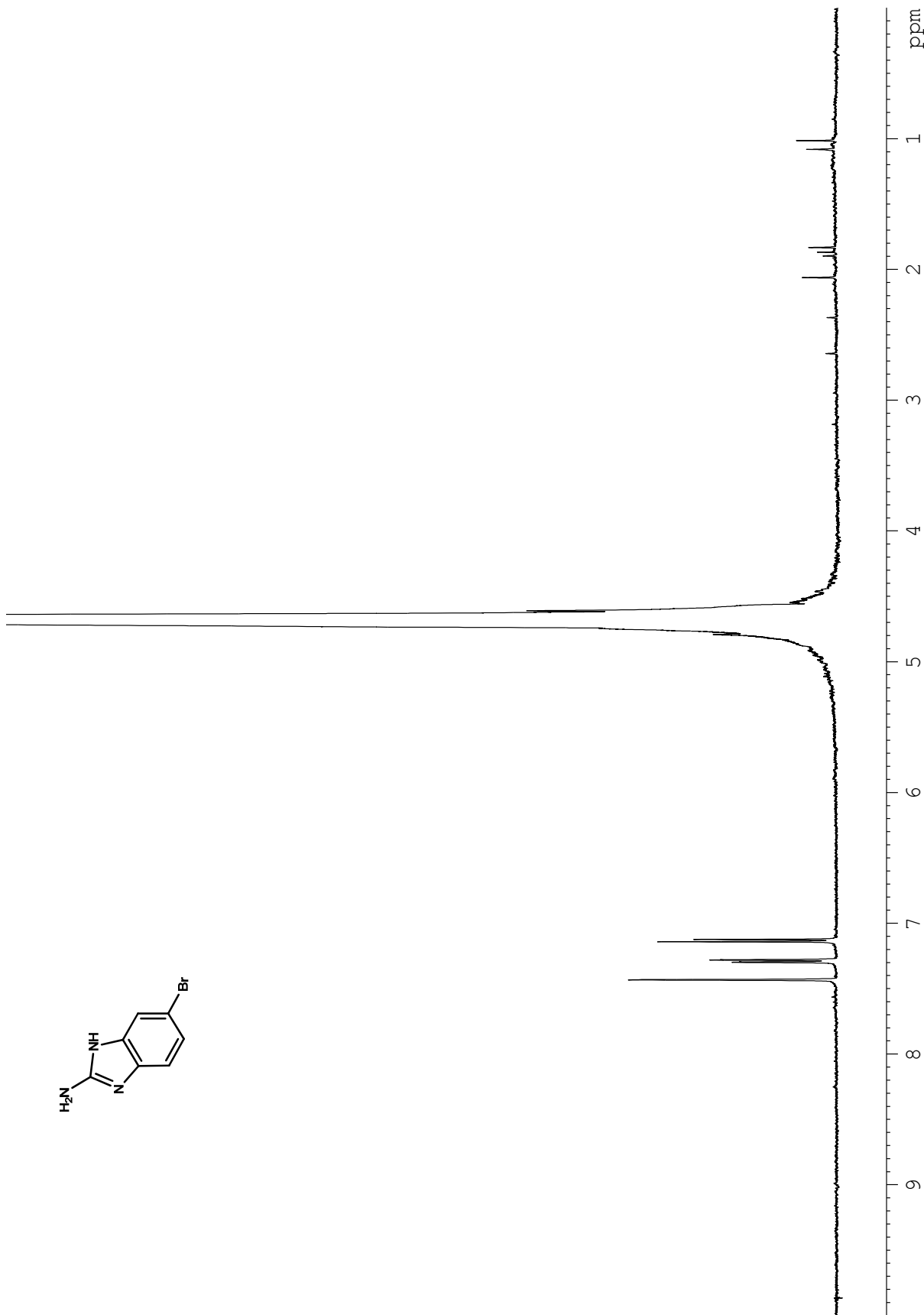
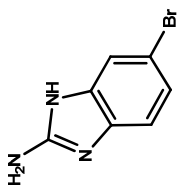




**Figure A3.7.** <sup>13</sup>C NMR (125 MHz, MeOH-*d*<sub>4</sub>) spectrum of compound 4-8 (HCl).

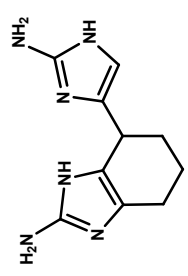
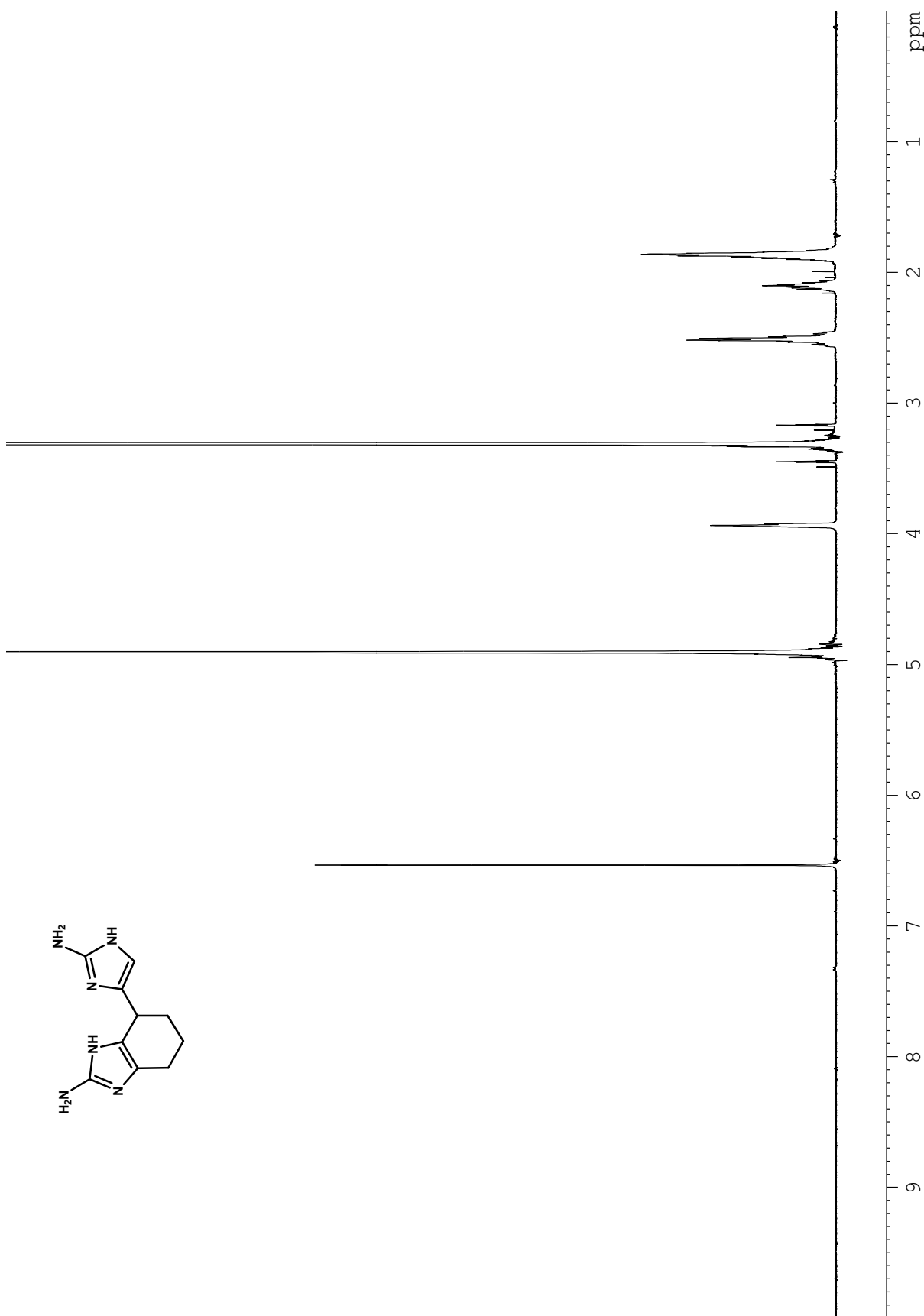


**Figure A3.8.**  $^1\text{H}$  NMR (500 MHz,  $\text{MeOH-}d_4$ ) spectrum of compound 4-10 (freebase).

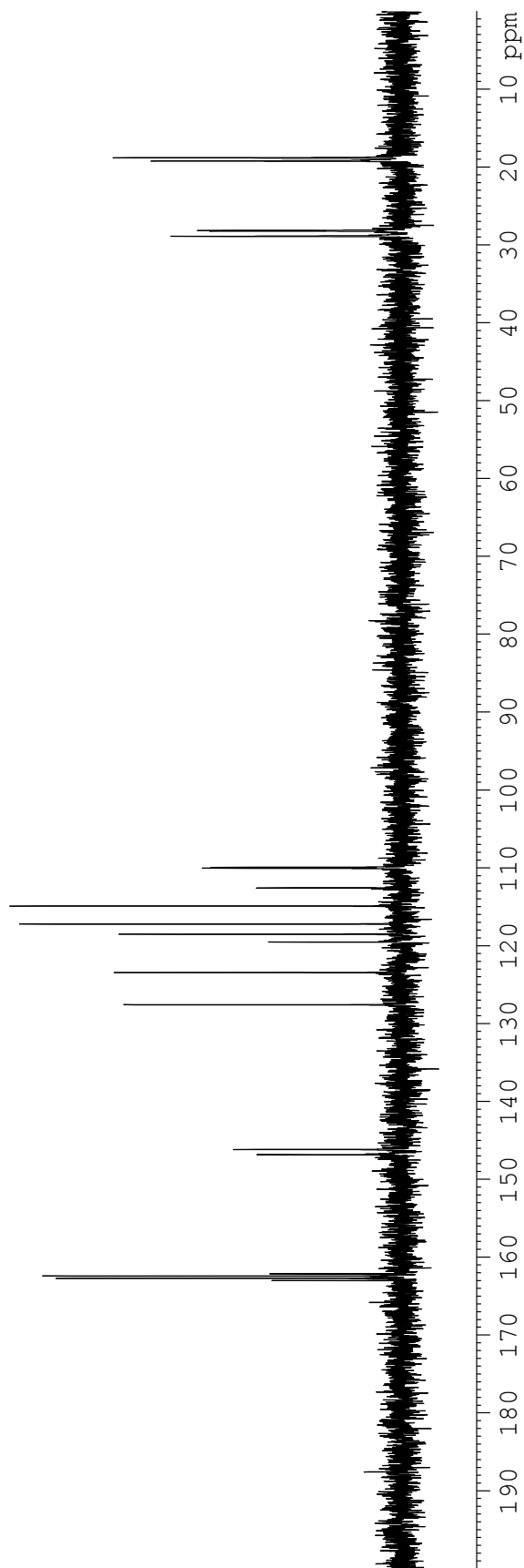
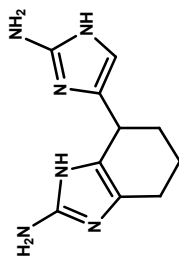


**Figure A3.9.** <sup>1</sup>H NMR (500 MHz, H<sub>2</sub>O-*d*<sub>2</sub>) spectrum of compound 4-11 (CF<sub>3</sub>CO<sub>2</sub>H).

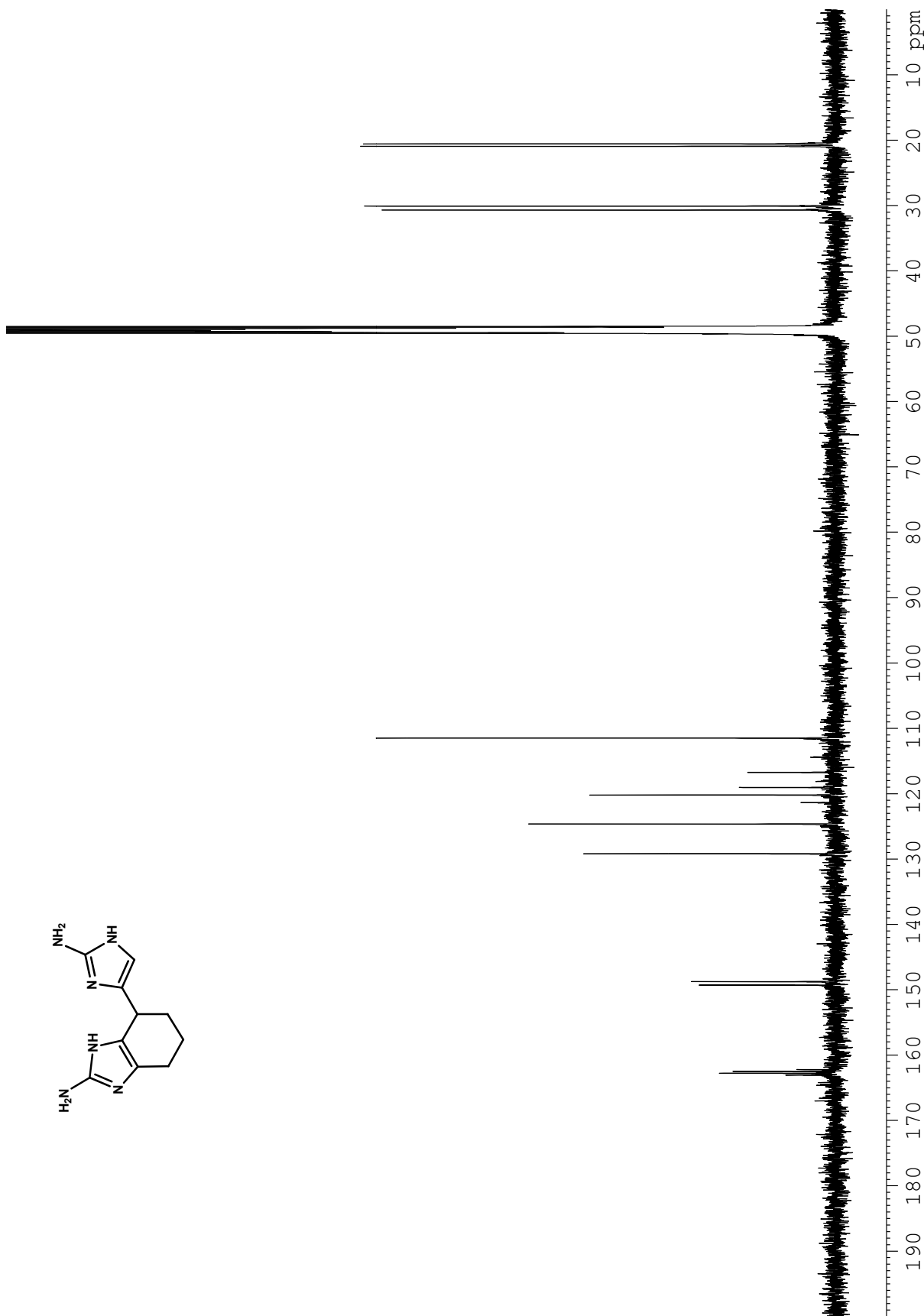
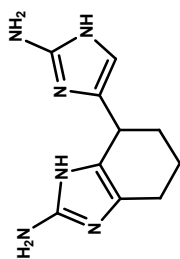




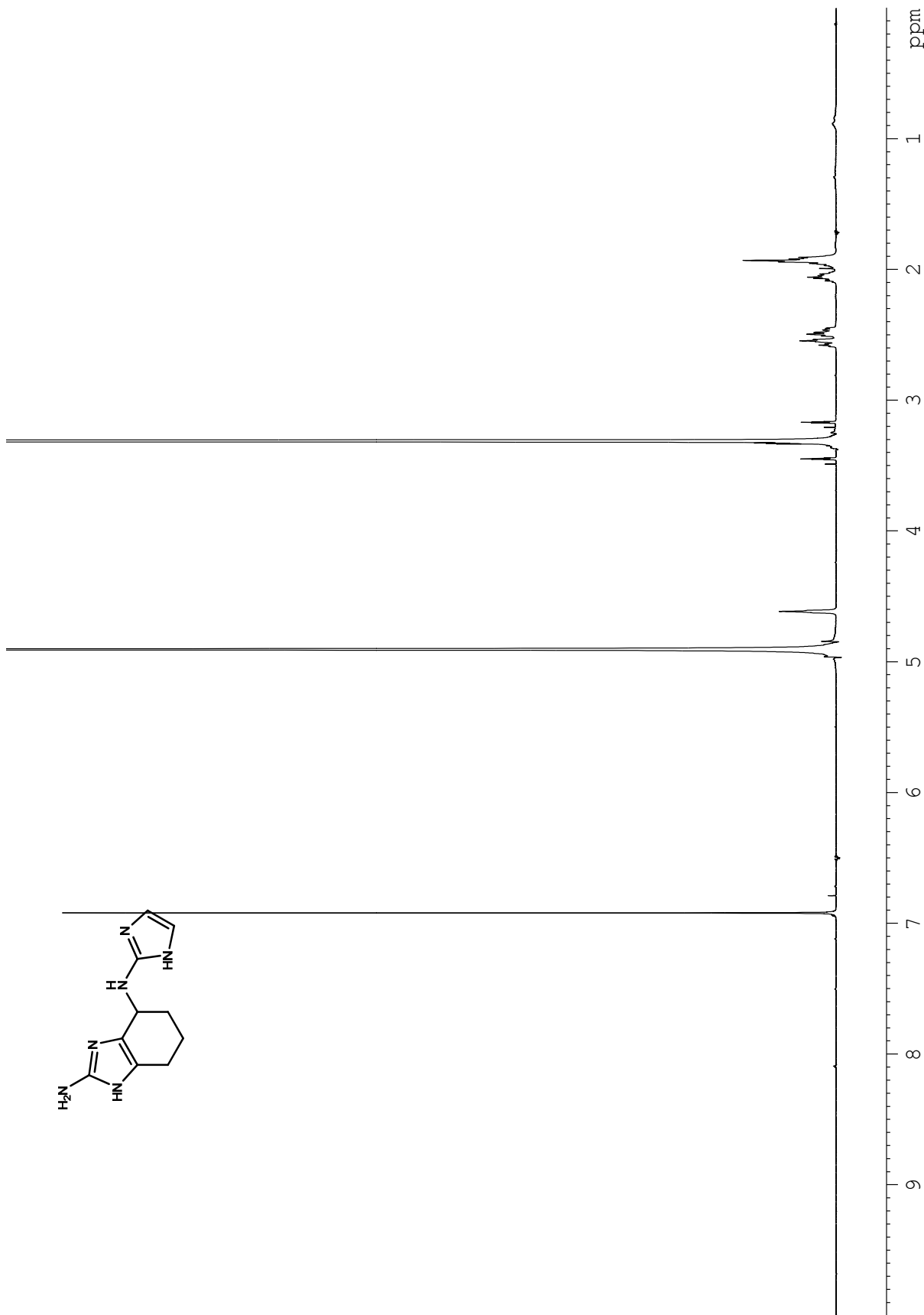
**Figure A3.11.** <sup>1</sup>H NMR (500 MHz, MeOH-*d*<sub>4</sub>) spectrum of compound 4-5 (2·CF<sub>3</sub>CO<sub>2</sub>H).



**Figure A3.12.** <sup>13</sup>C NMR (125 MHz, H<sub>2</sub>O-*d*<sub>2</sub>) spectrum of compound 4-5 (2-CF<sub>3</sub>CO<sub>2</sub>H).

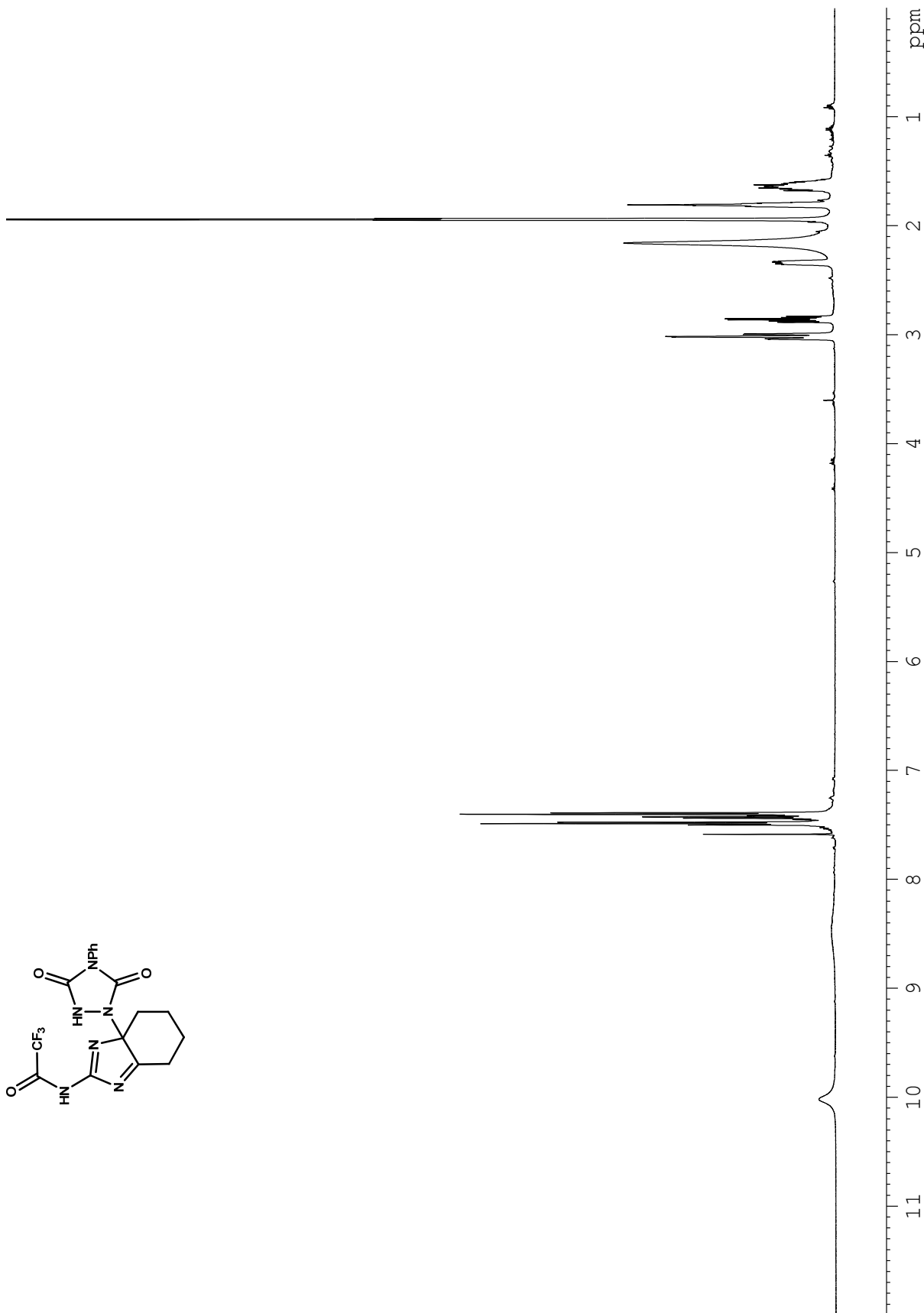
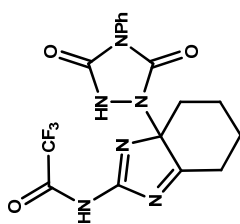


**Figure A3.13.**  $^{13}\text{C}$  NMR (125 MHz, MeOH-*d*<sub>4</sub>) spectrum of compound 4-5 (2-CF<sub>3</sub>CO<sub>2</sub>H).

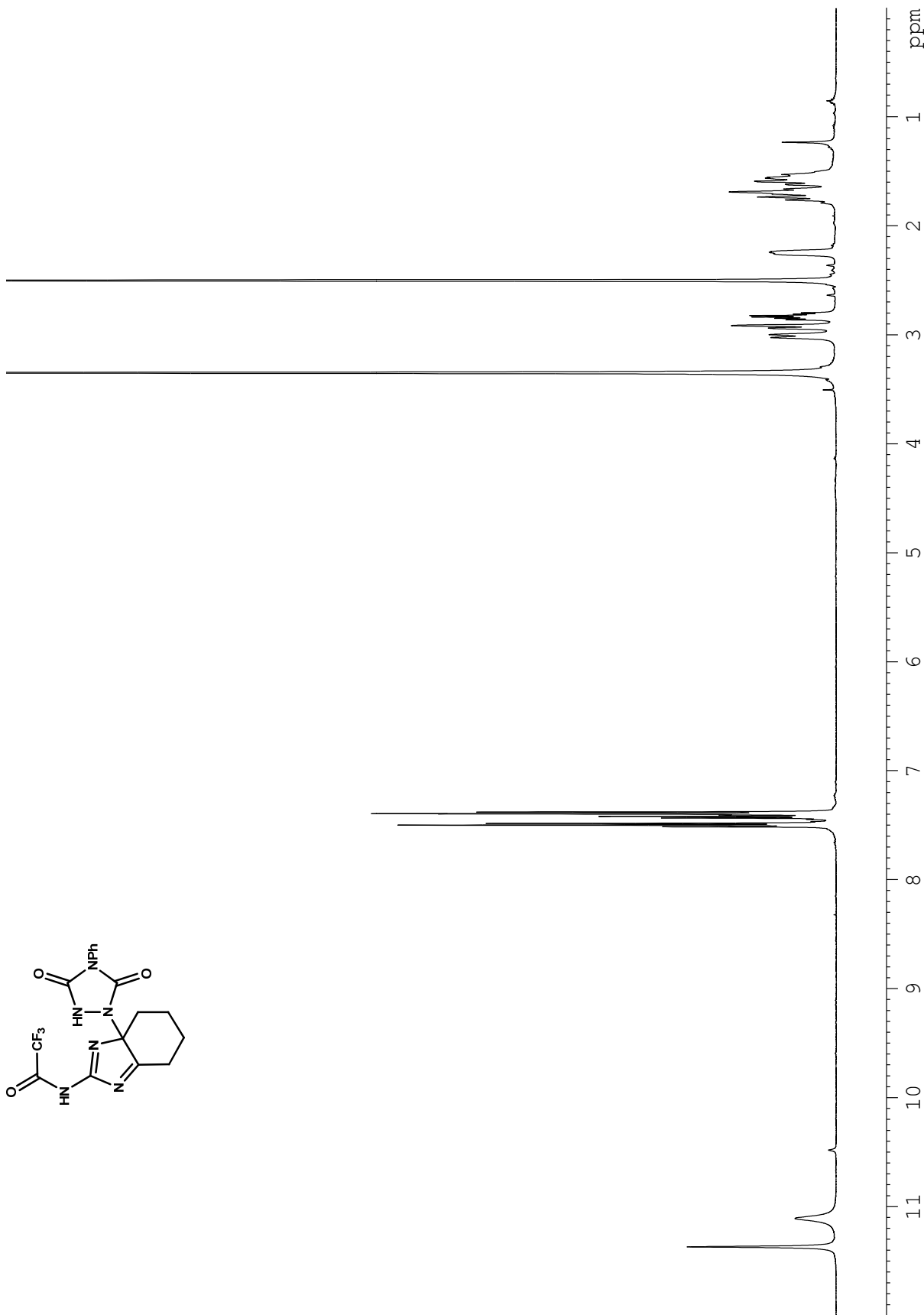
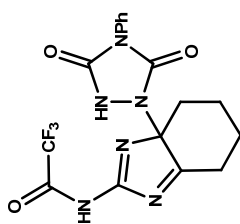


**Figure A3.14.** <sup>1</sup>H NMR (500 MHz, MeOH-*d*<sub>4</sub>) spectrum of compound 4-12 (2·CF<sub>3</sub>CO<sub>2</sub>H).

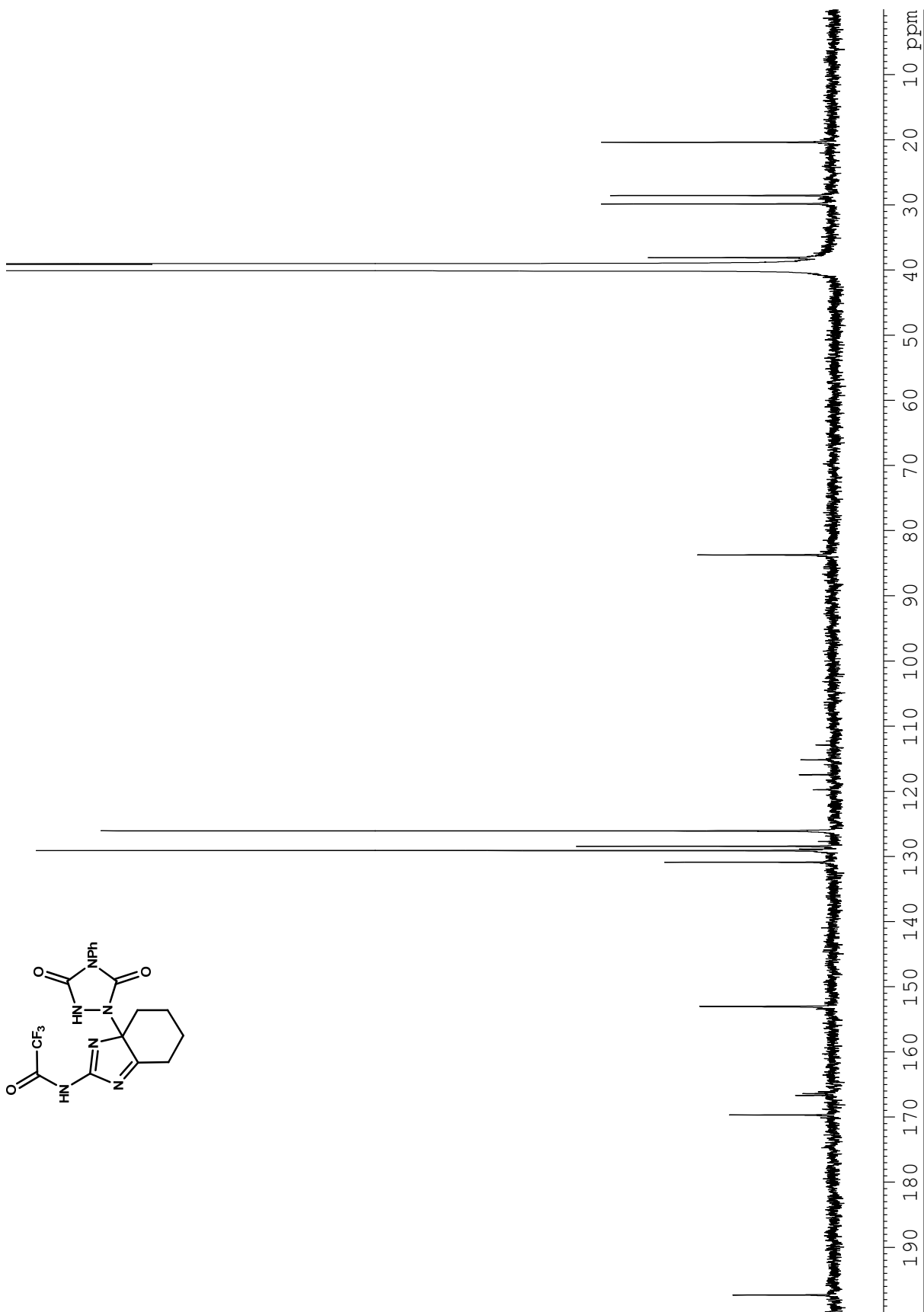
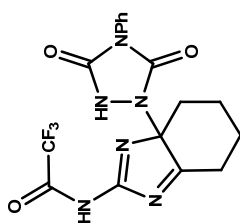




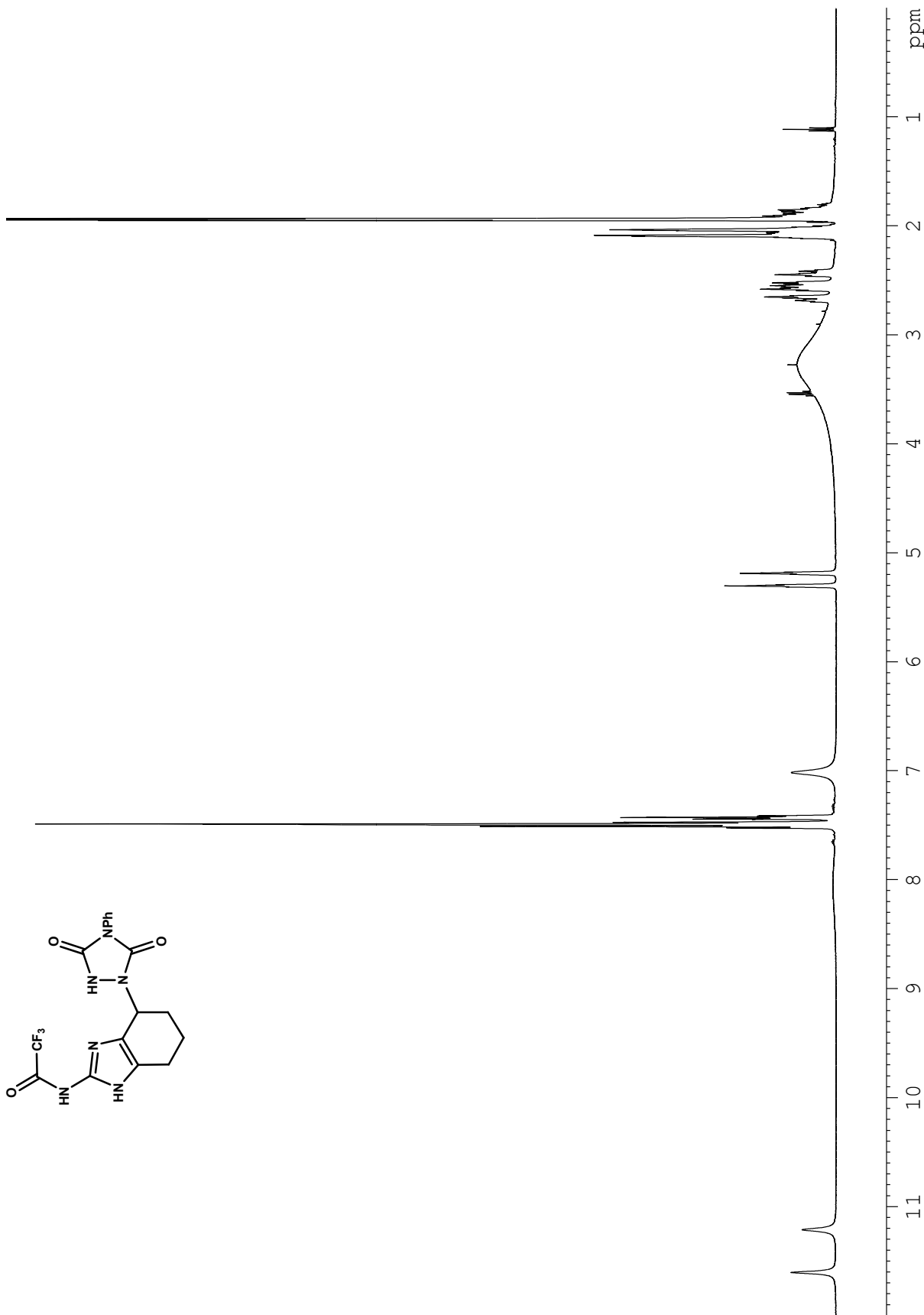
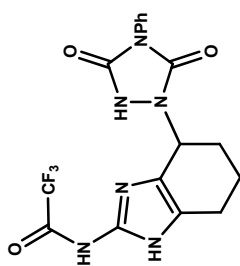
**Figure A3.15.**  $^1\text{H}$  NMR (500 MHz,  $\text{CH}_3\text{CN}-d_3$ ) spectrum of compound **4-15**.



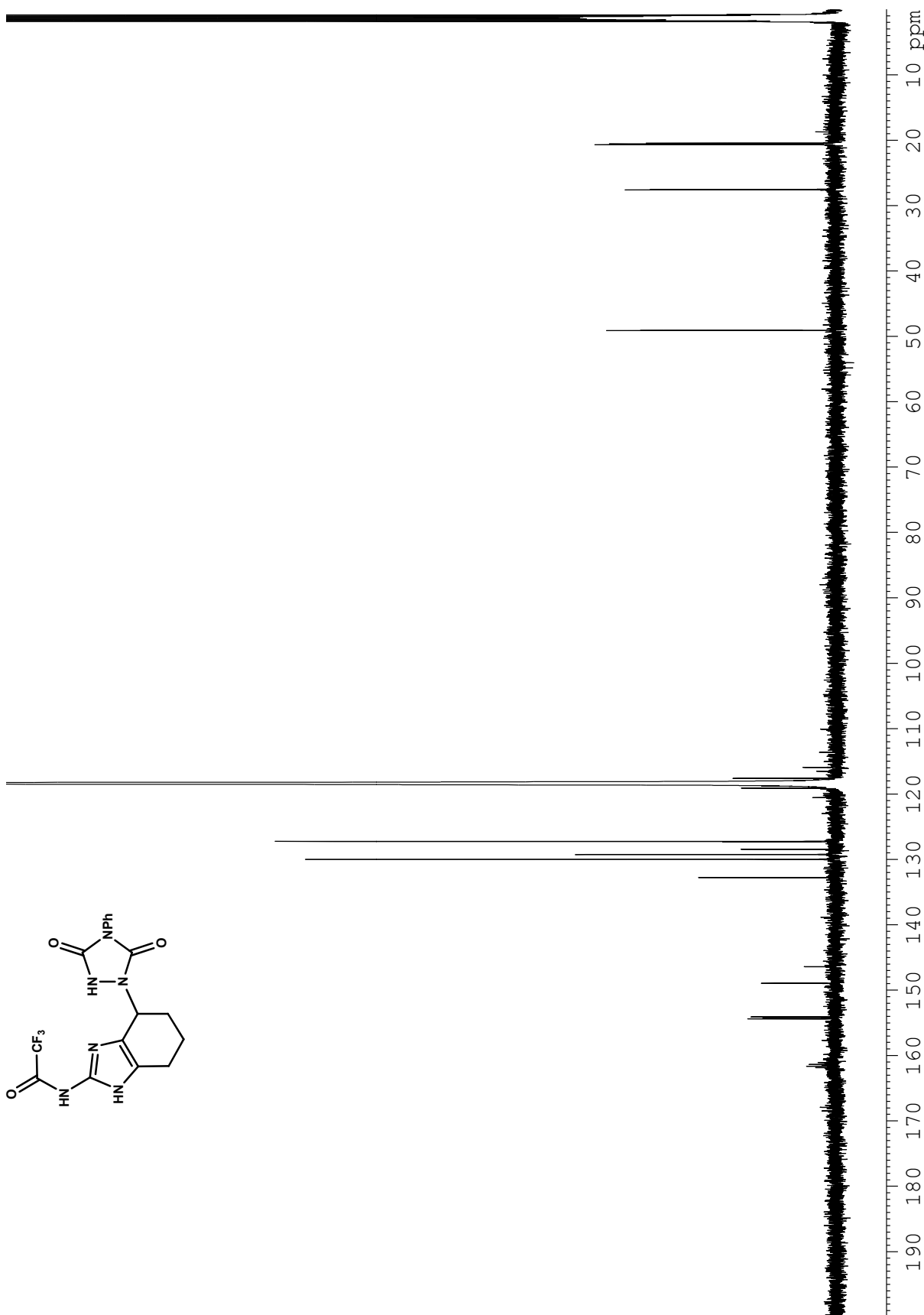
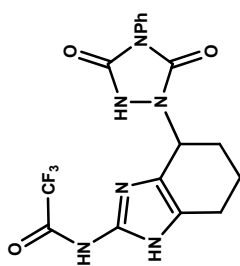
**Figure A3.16.**  $^1\text{H}$  NMR (500 MHz,  $\text{DMSO-}d_6$ ) spectrum of compound 4-15.



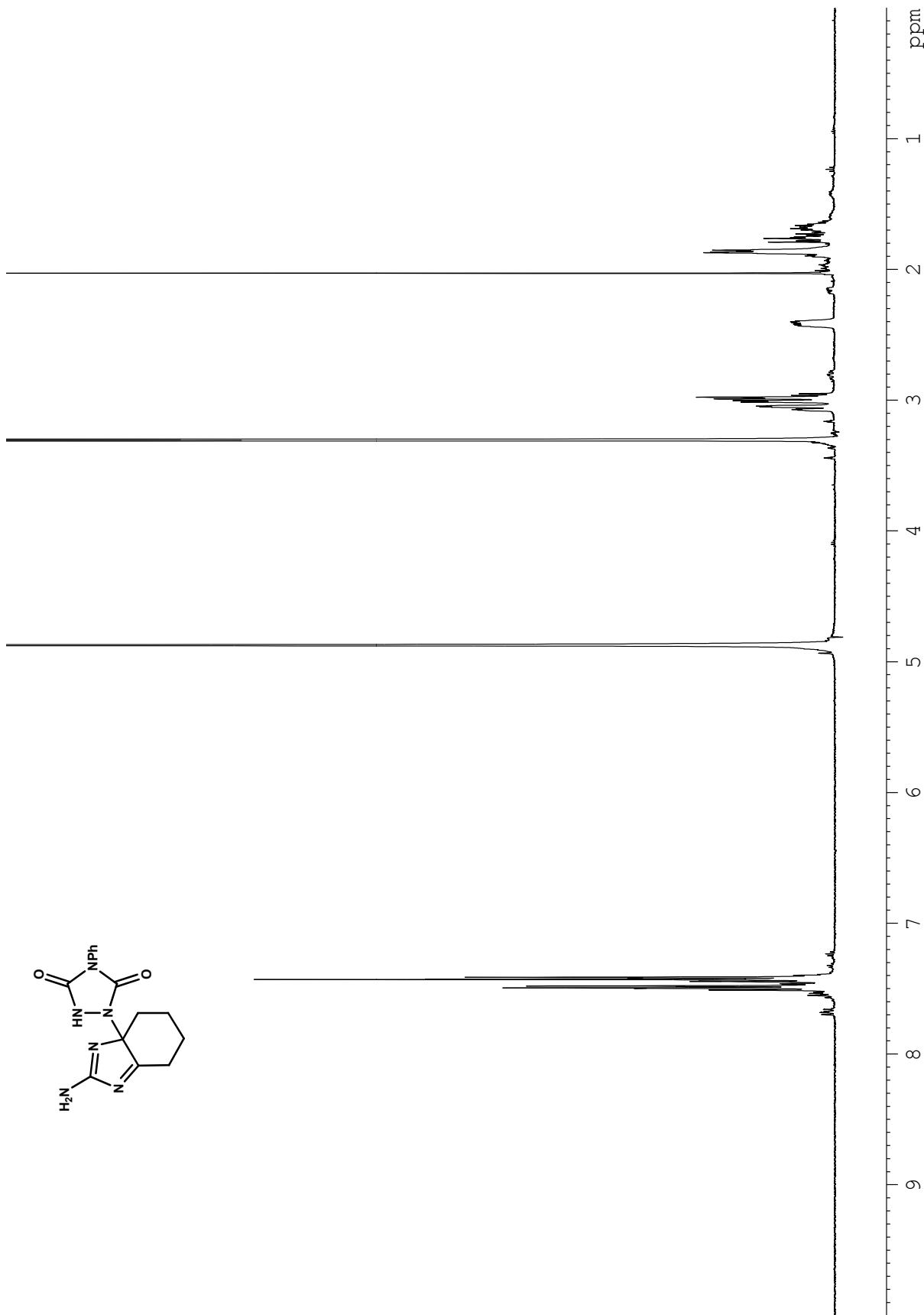
**Figure A3.17.**  $^{13}\text{C}$  NMR (125 MHz,  $\text{DMSO-}d_6$ ) spectrum of compound **4-15**.



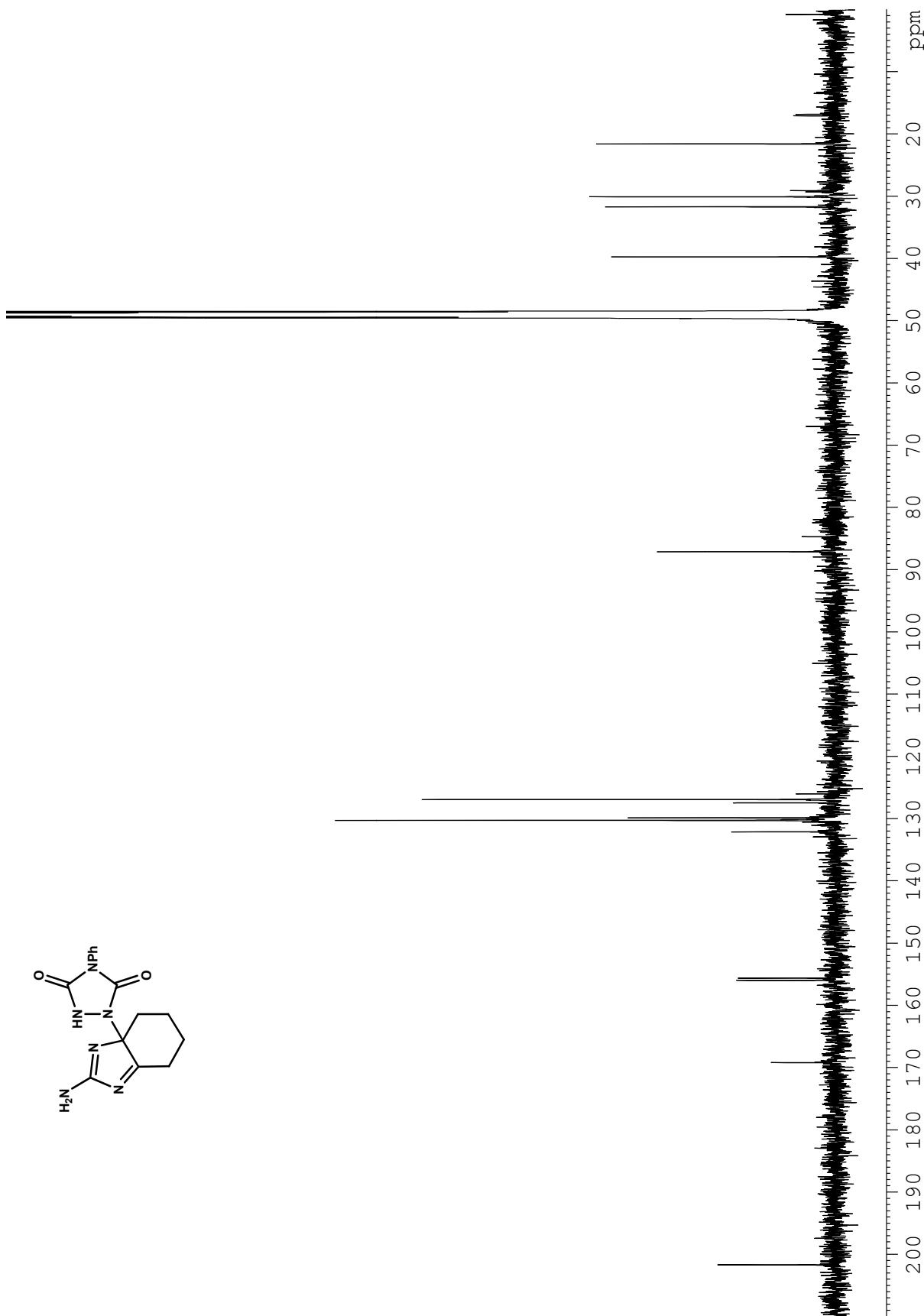
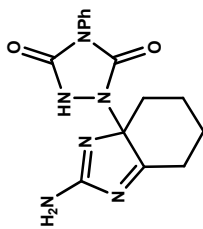
**Figure A3.18.** <sup>1</sup>H NMR (500 MHz, CH<sub>3</sub>CN-*d*<sub>3</sub>) spectrum of compound 4-16 (contains 4-17 (CF<sub>3</sub>CO<sub>2</sub>H)).



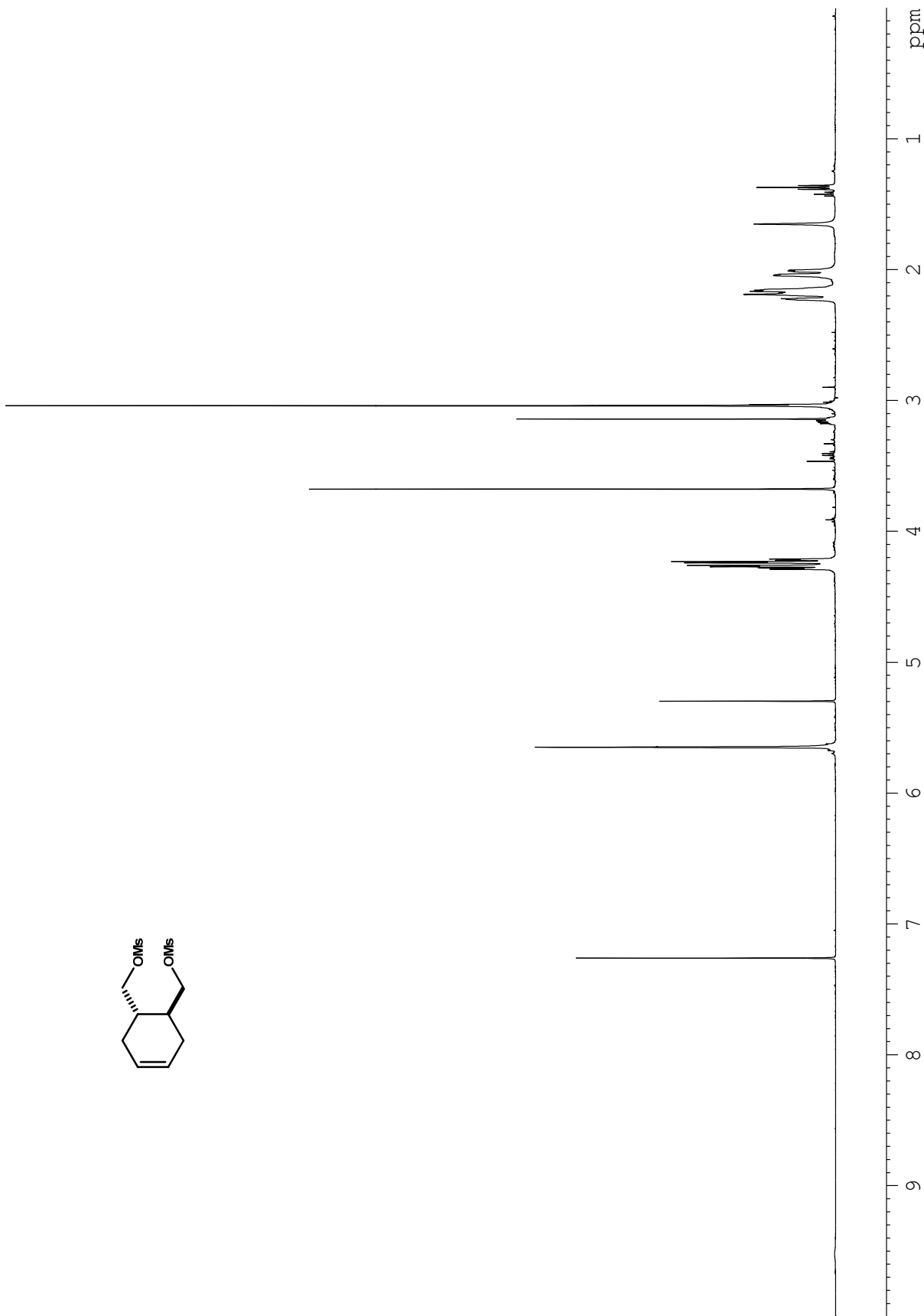
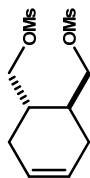
**Figure A3.19.**  $^{13}\text{C}$  NMR (125 MHz,  $\text{CH}_3\text{CN-}d_3$ ) spectrum of compound 4-16 (contains 4-17 ( $\text{CF}_3\text{CO}_2\text{H}$ )).



**Figure A3.20.** <sup>1</sup>H NMR (500 MHz, MeOH-*d*<sub>4</sub>) spectrum of compound 4-18 (HCl).

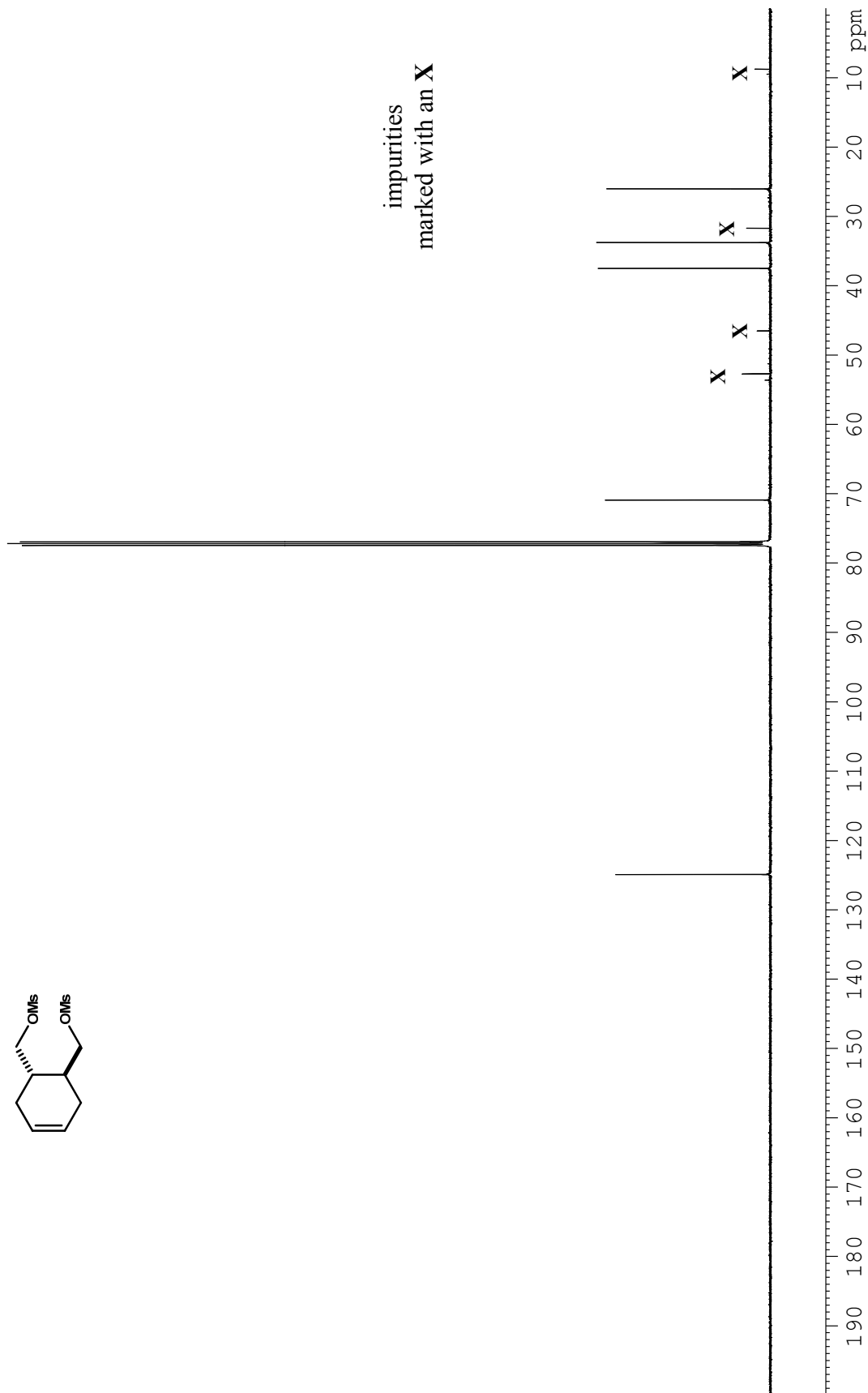
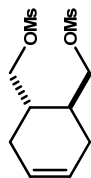


**Figure A3.21.**  $^{13}\text{C}$  NMR (125 MHz,  $\text{MeOH-}d_4$ ) spectrum of compound **4-18 (HCl)**

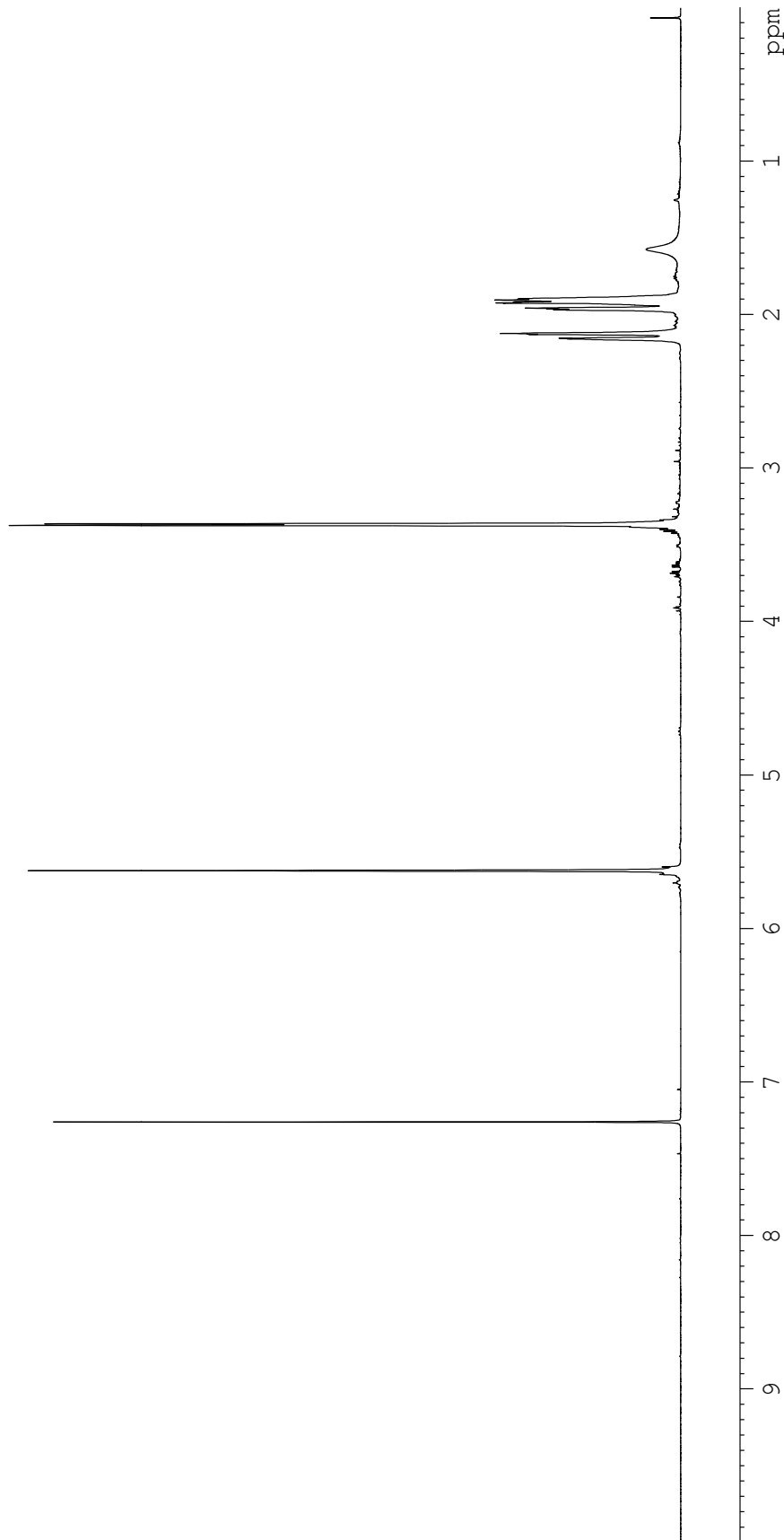
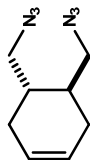


**Figure A3.22.**  $^1\text{H}$  NMR (500 MHz,  $\text{CHCl}_3-d_1$ ) spectrum of compound **4-42a**.

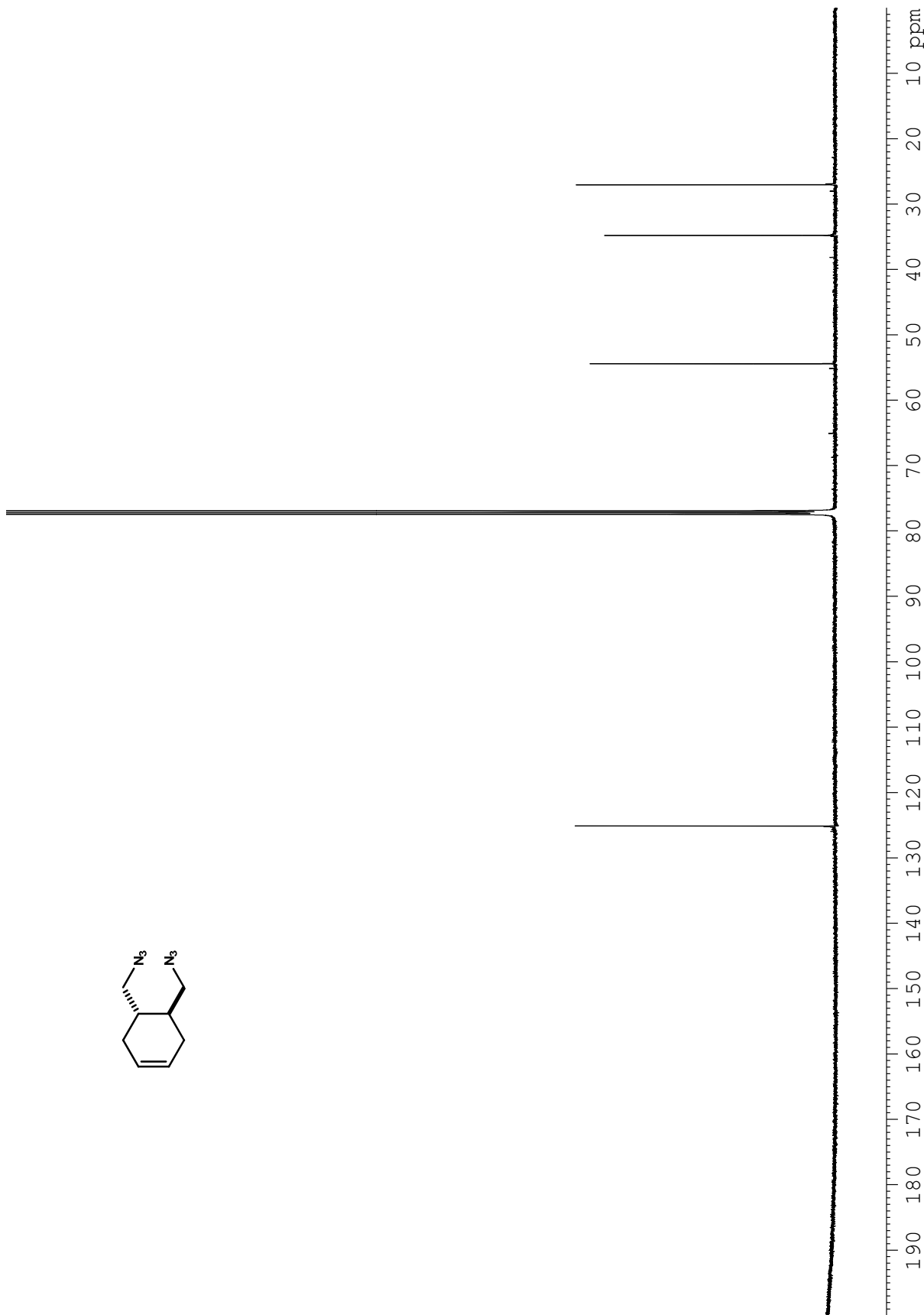
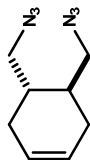




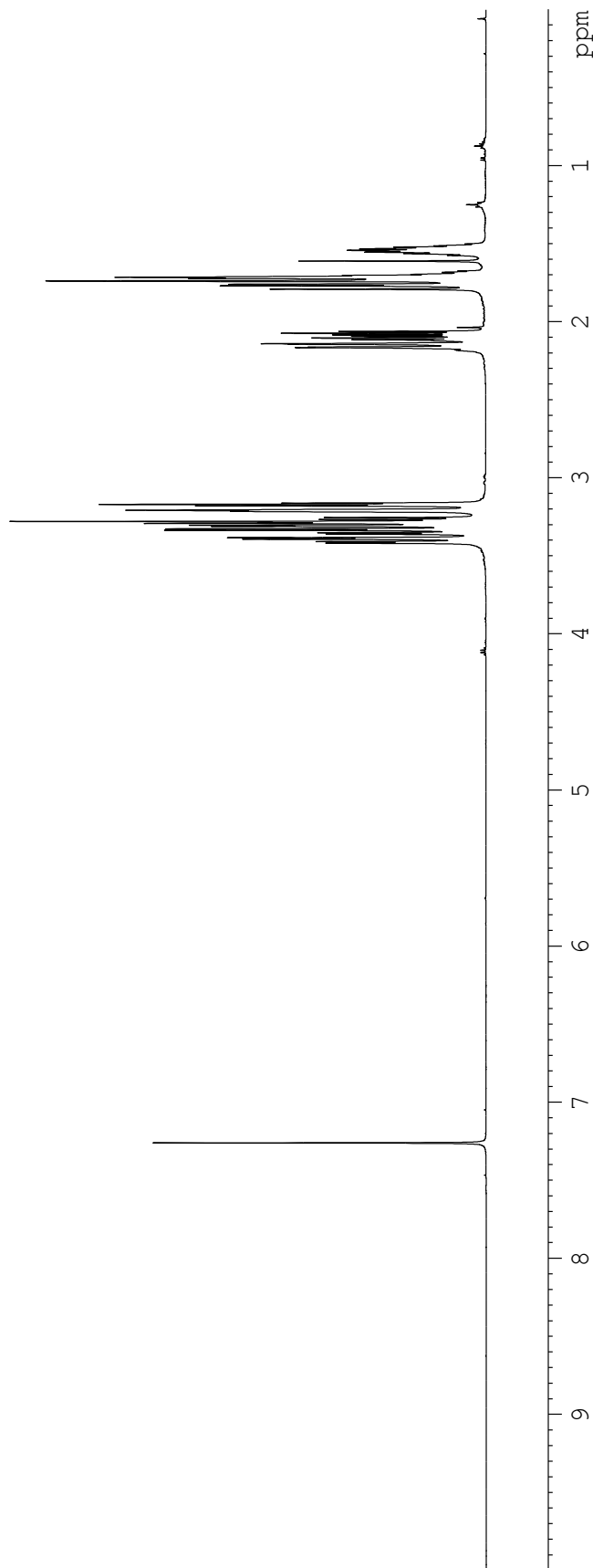
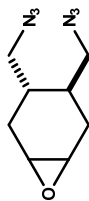
**Figure A3.23.**  $^{13}\text{C}$  NMR (125 MHz,  $\text{CHCl}_3-d_1$ ) spectrum of compound 4-42a.



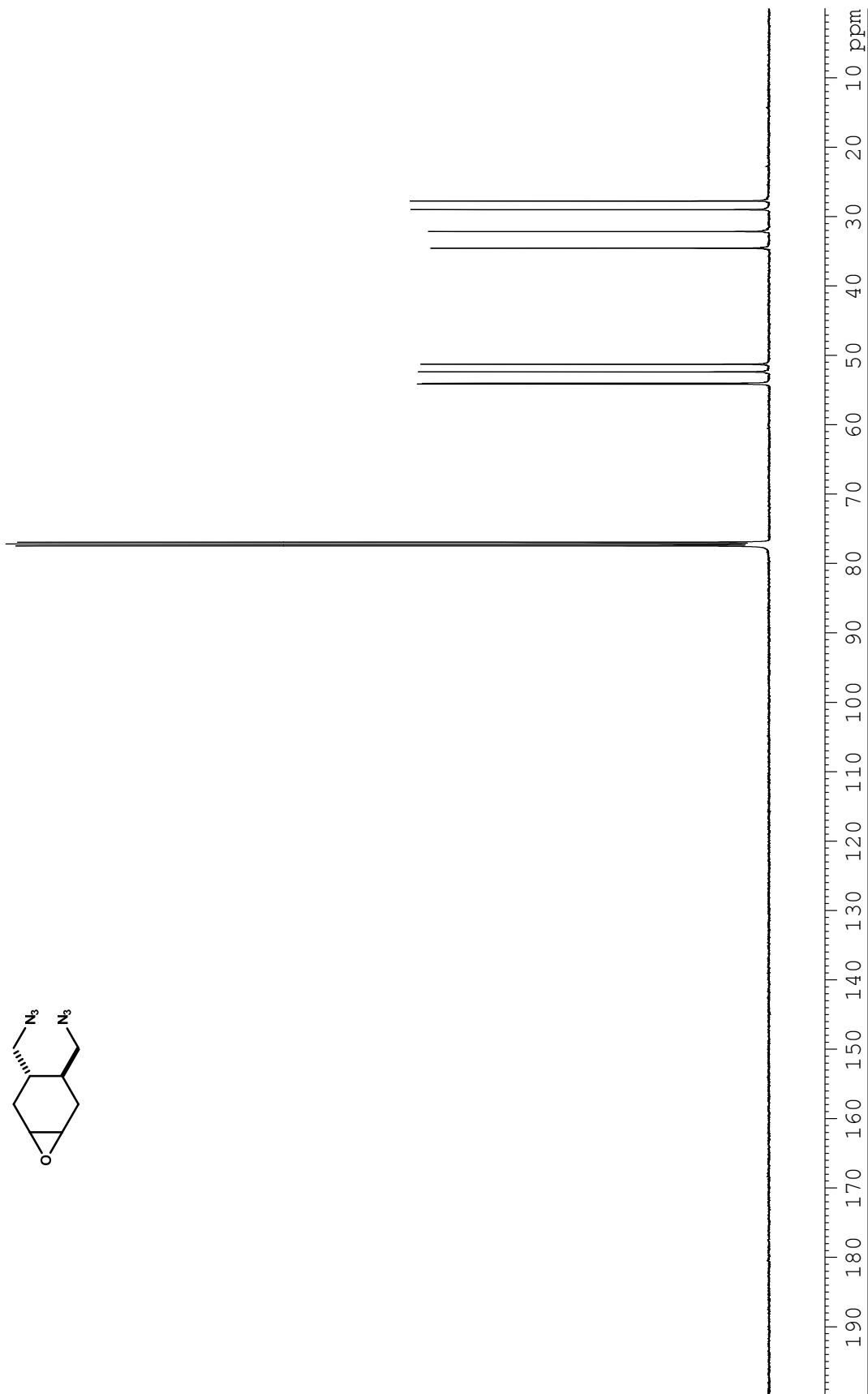
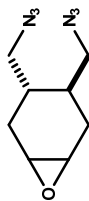
**Figure A3.24.**  $^1\text{H}$  NMR (500 MHz,  $\text{CHCl}_3$ - $d_1$ ) spectrum of compound **4-42b**.



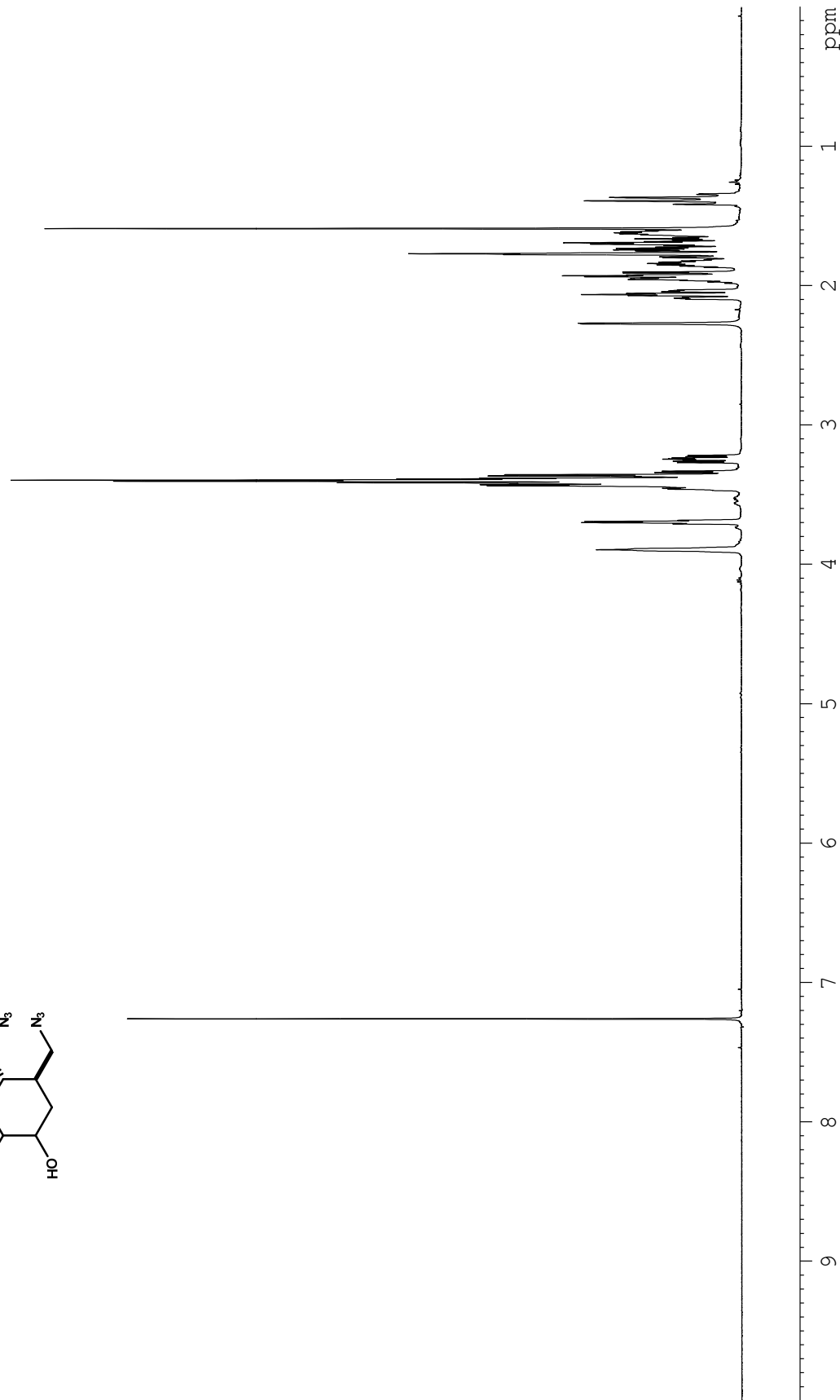
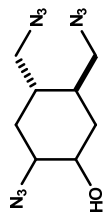
**Figure A3.25.**  $^{13}\text{C}$  NMR (125 MHz,  $\text{CHCl}_3$ - $d_1$ ) spectrum of compound 4-42b.



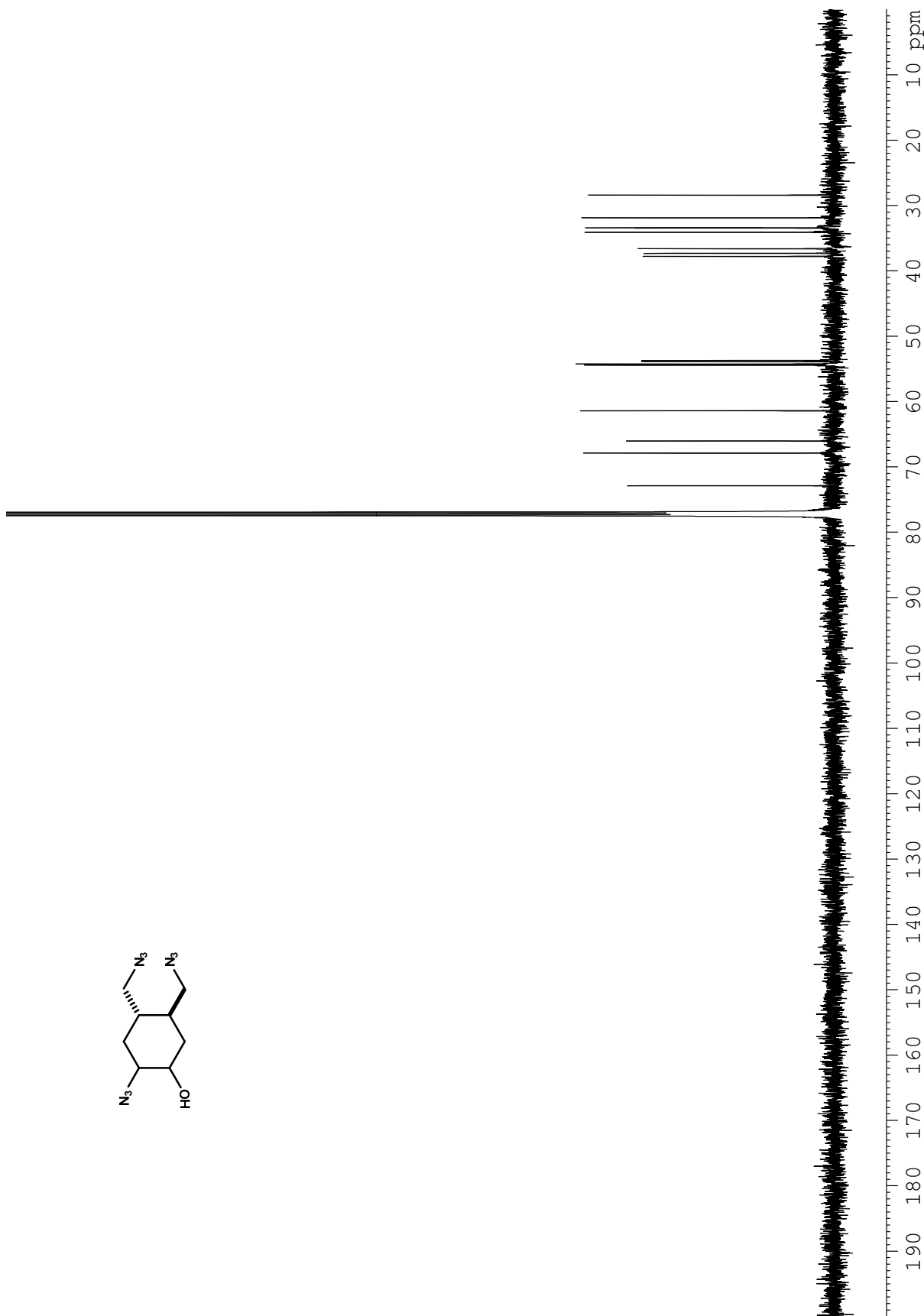
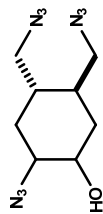
**Figure A3.26.** <sup>1</sup>H NMR (500 MHz, CHCl<sub>3</sub>-d<sub>1</sub>) spectrum of compound 4-43a.



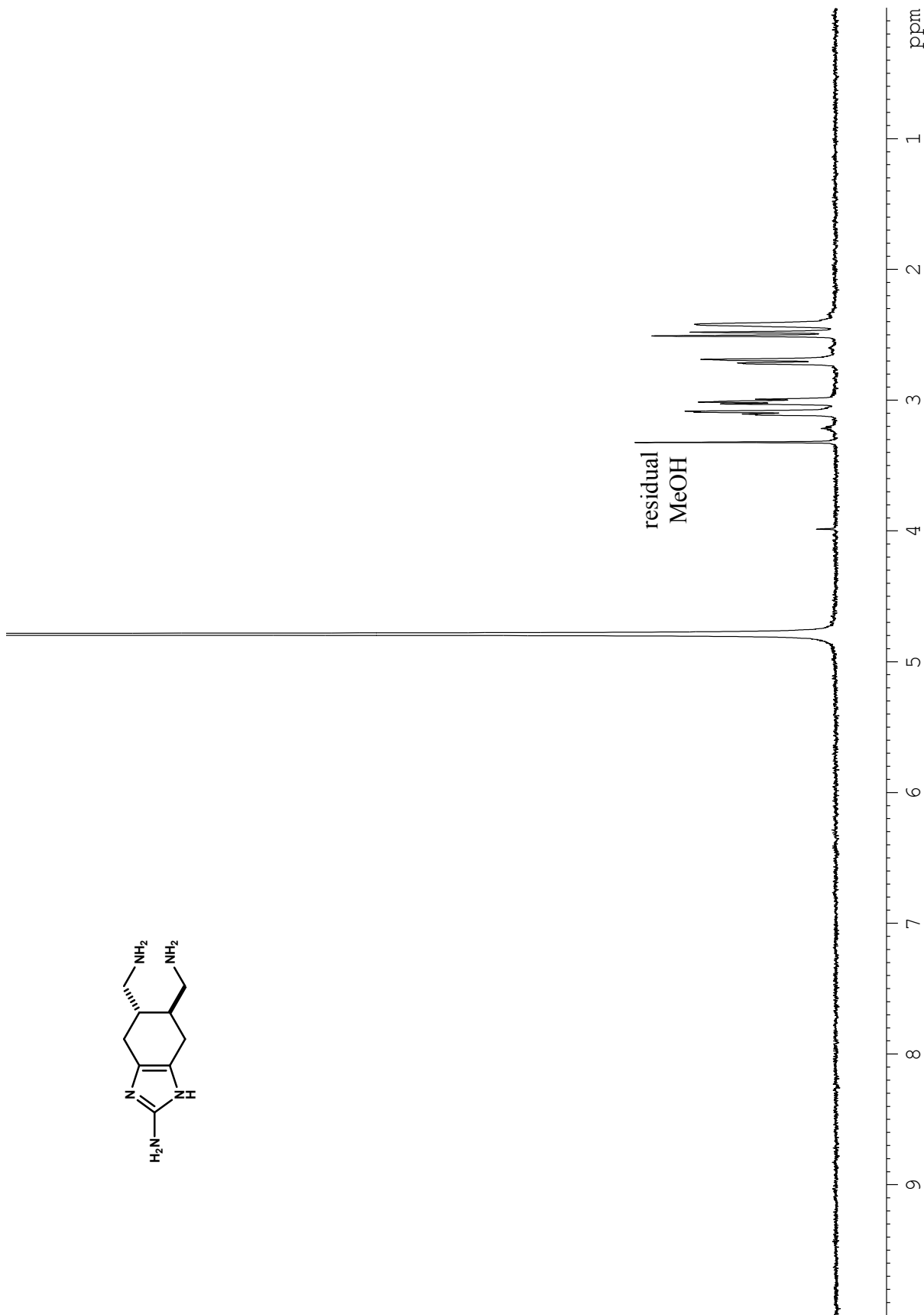
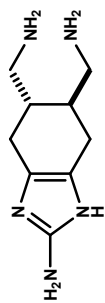
**Figure A3.27.**  $^{13}\text{C}$  NMR (125 MHz,  $\text{CHCl}_3$ - $d_1$ ) spectrum of compound 4-43a.



**Figure A3.28.** <sup>1</sup>H NMR (500 MHz, CHCl<sub>3</sub>-d<sub>1</sub>) spectrum of compound 4-43b.



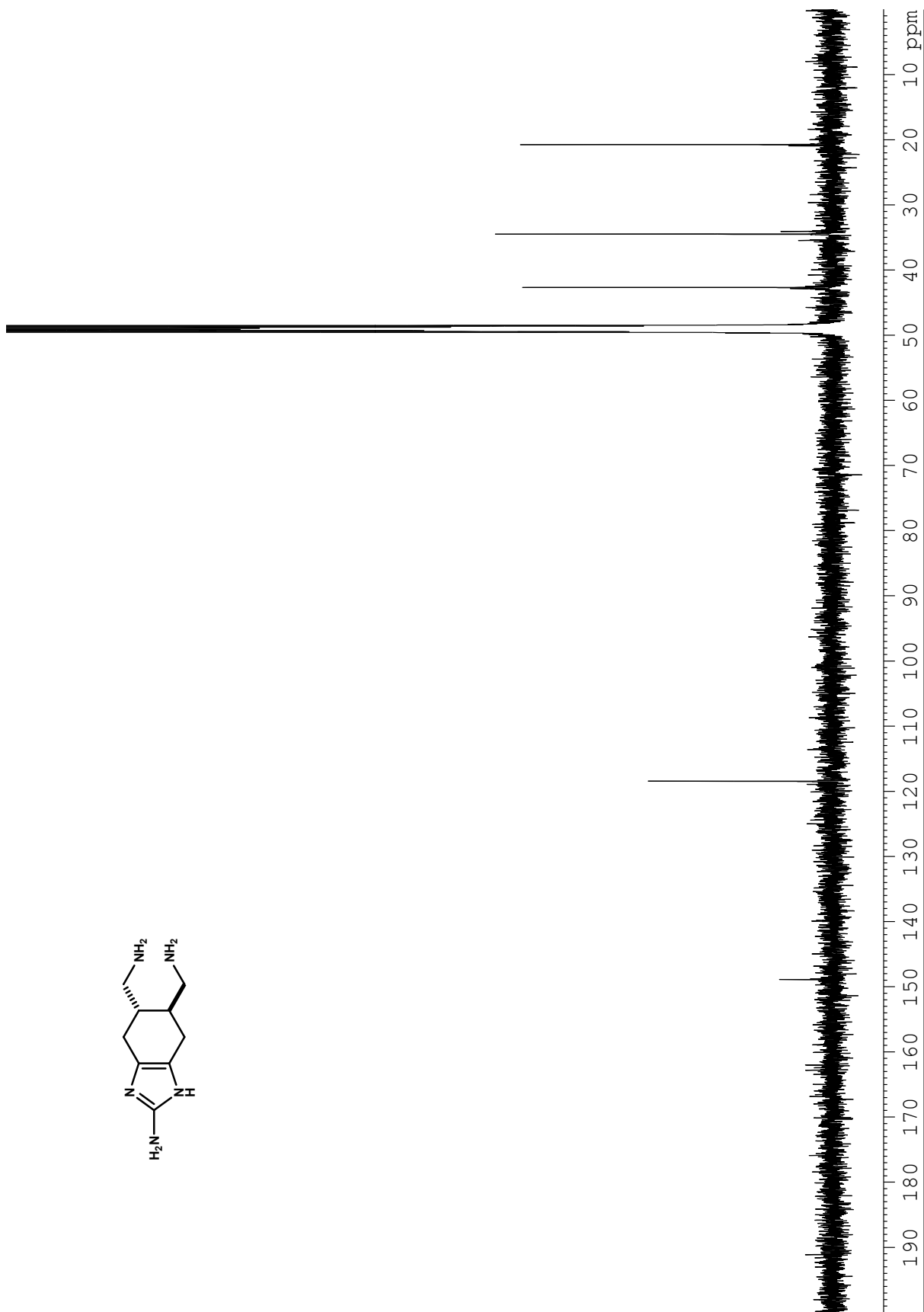
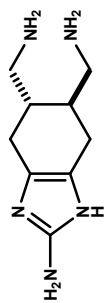
**Figure A3.29.** <sup>13</sup>C NMR (125 MHz, CHCl<sub>3</sub>-d<sub>1</sub>) spectrum of compound 4-43b.



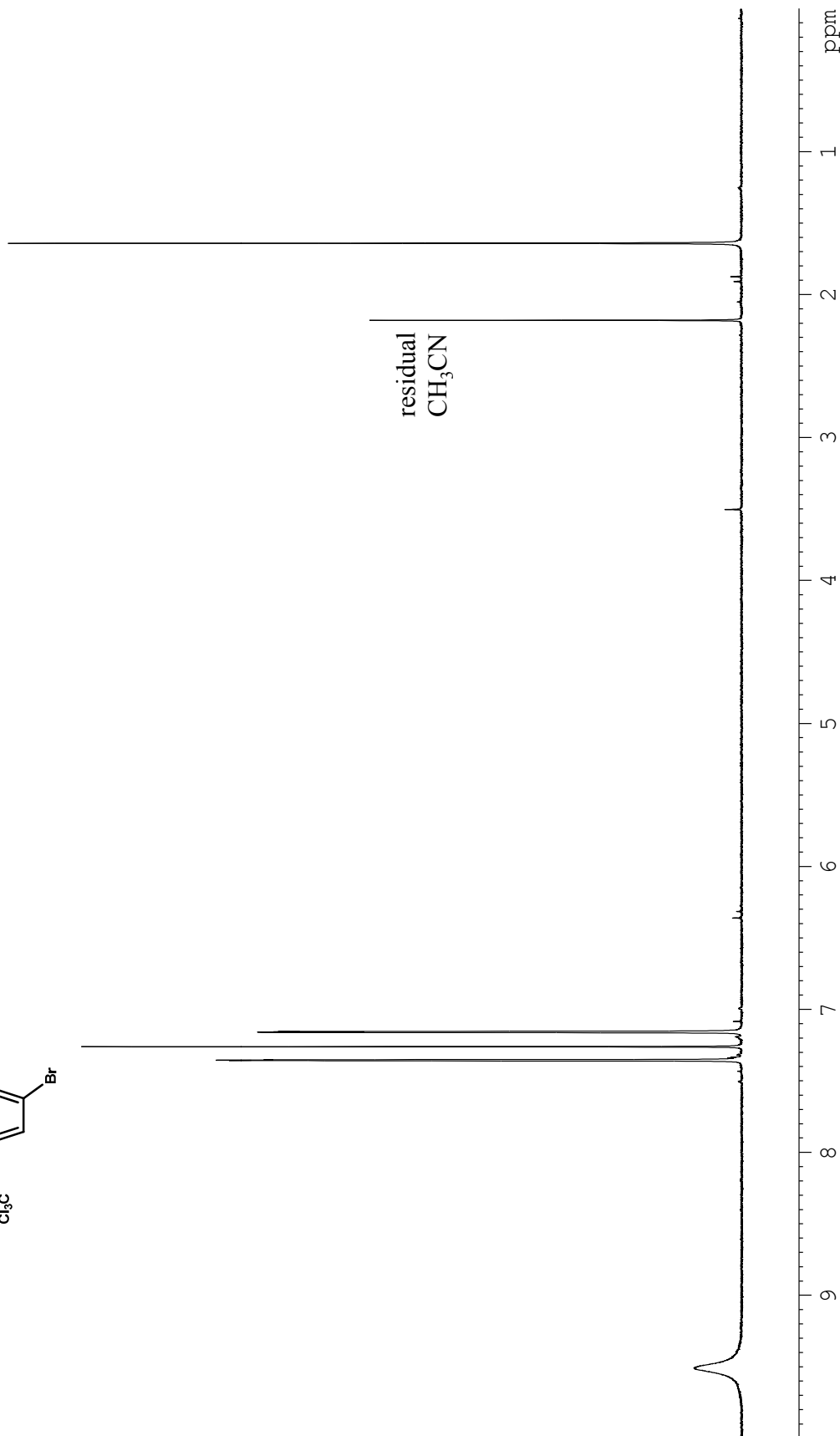
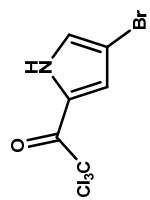
**Figure A3.30.** <sup>1</sup>H NMR (500 MHz, H<sub>2</sub>O-*d*<sub>2</sub>) spectrum of compound 4-24 (3·CF<sub>3</sub>CO<sub>2</sub>H).



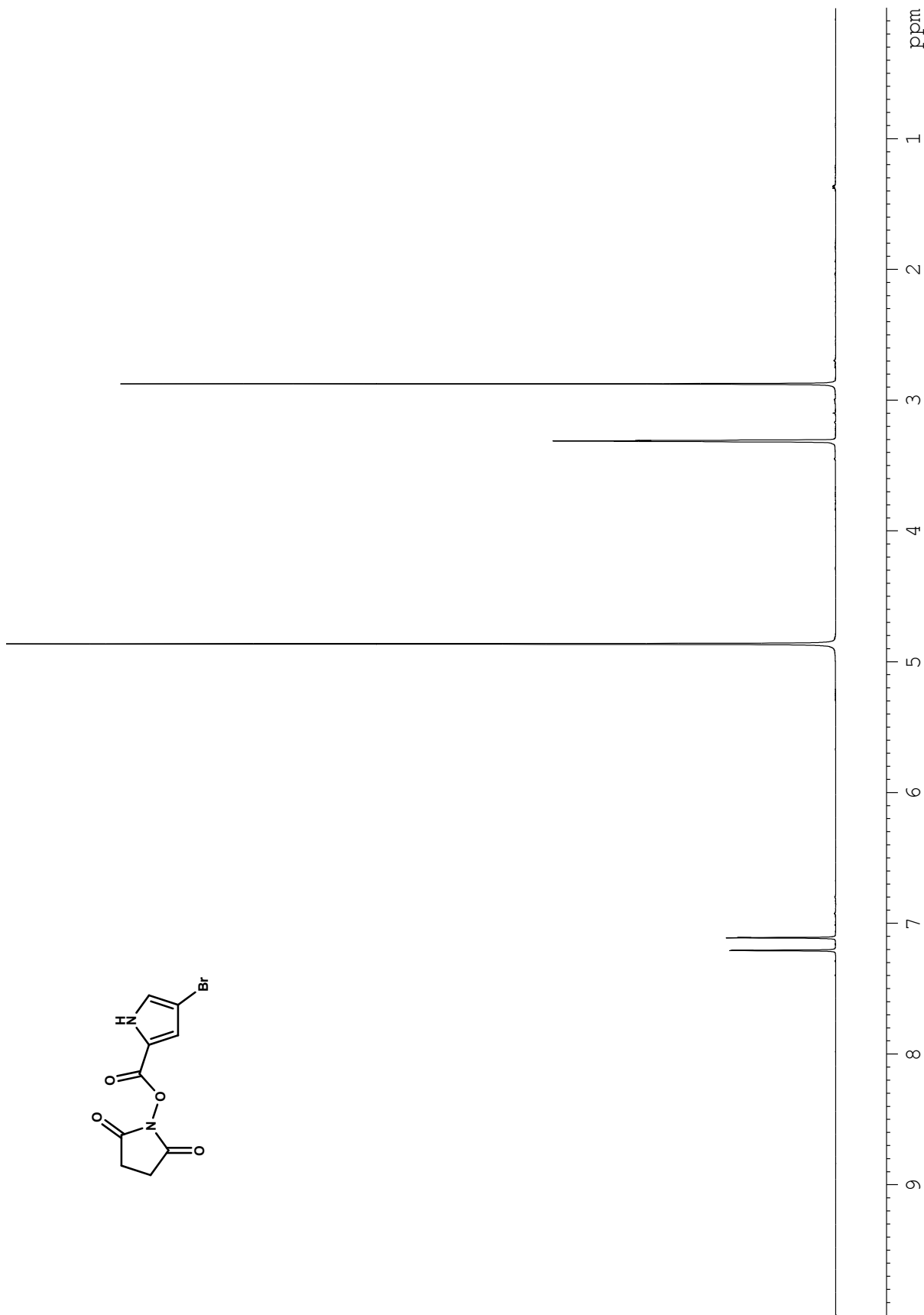
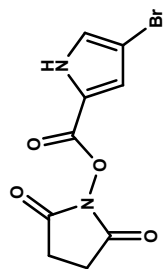




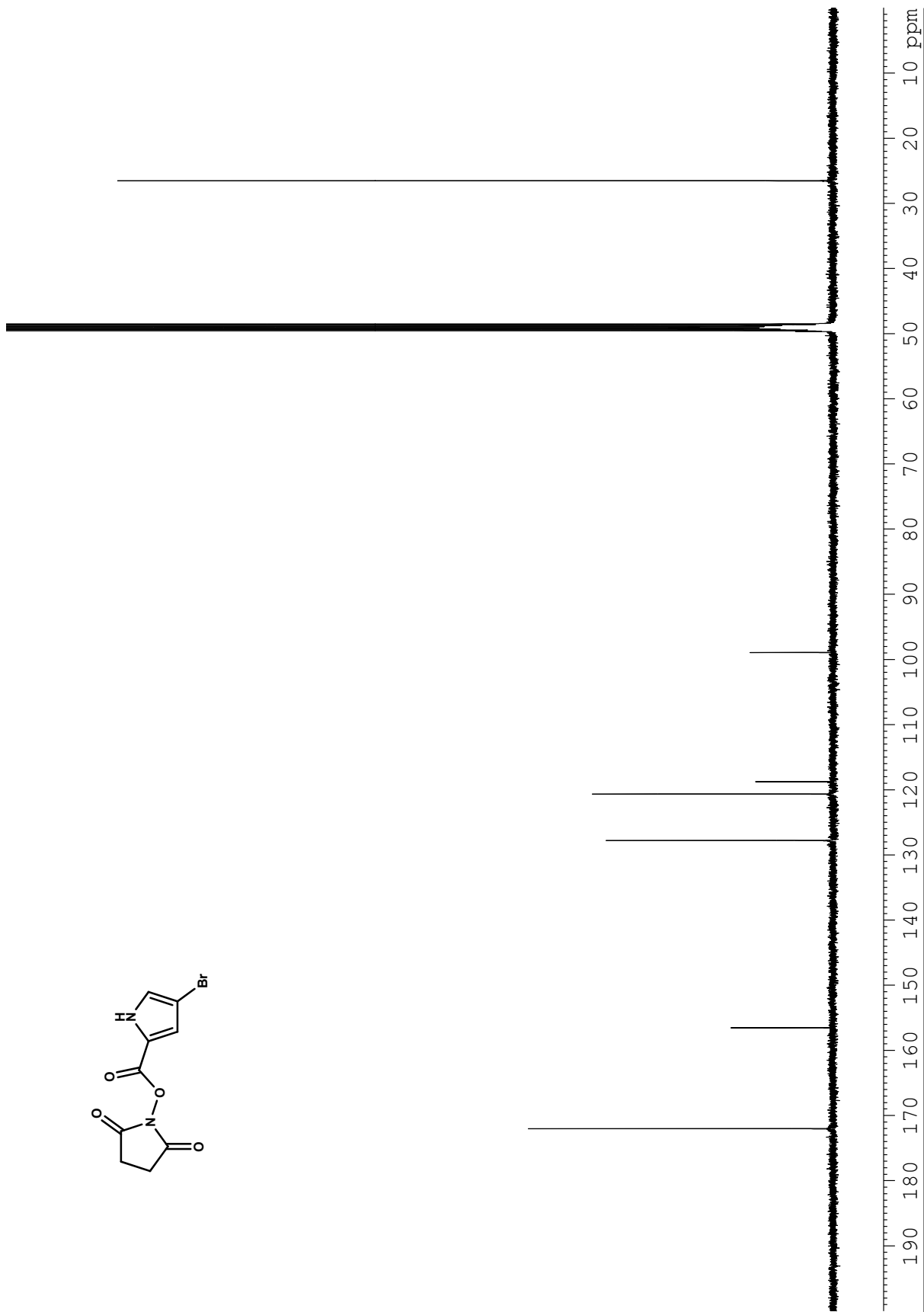
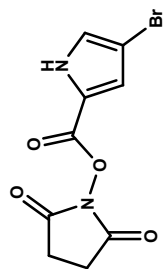
**Figure A3.32.**  $^{13}\text{C}$  NMR (125 MHz,  $\text{MeOH-}d_4$ ) spectrum of compound 4-24 ( $3 \cdot \text{CF}_3\text{CO}_2\text{H}$ ).



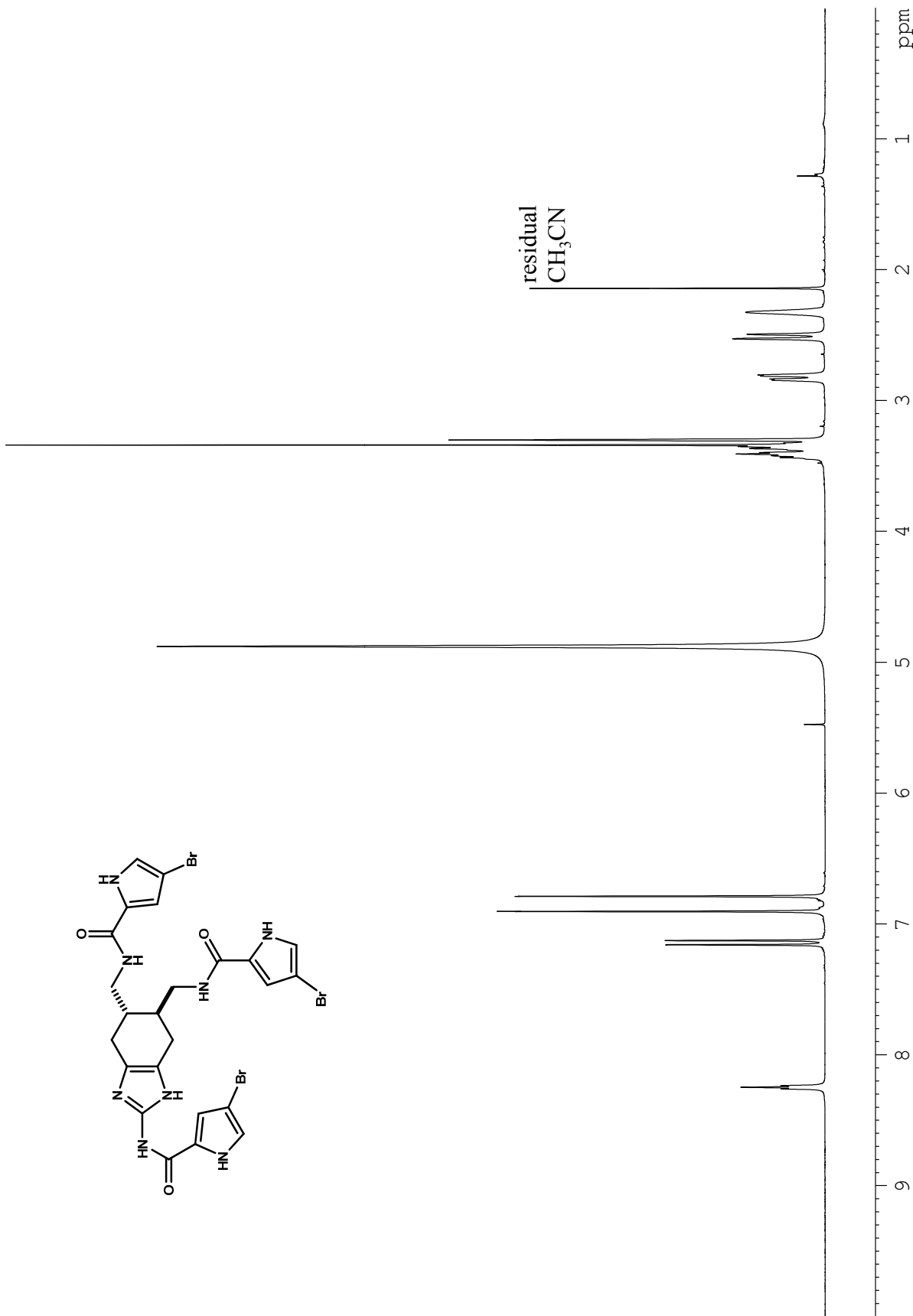
**Figure A3.33.**  $^1\text{H}$  NMR (500 MHz,  $\text{CHCl}_3$ ) spectrum of compound 4-47.



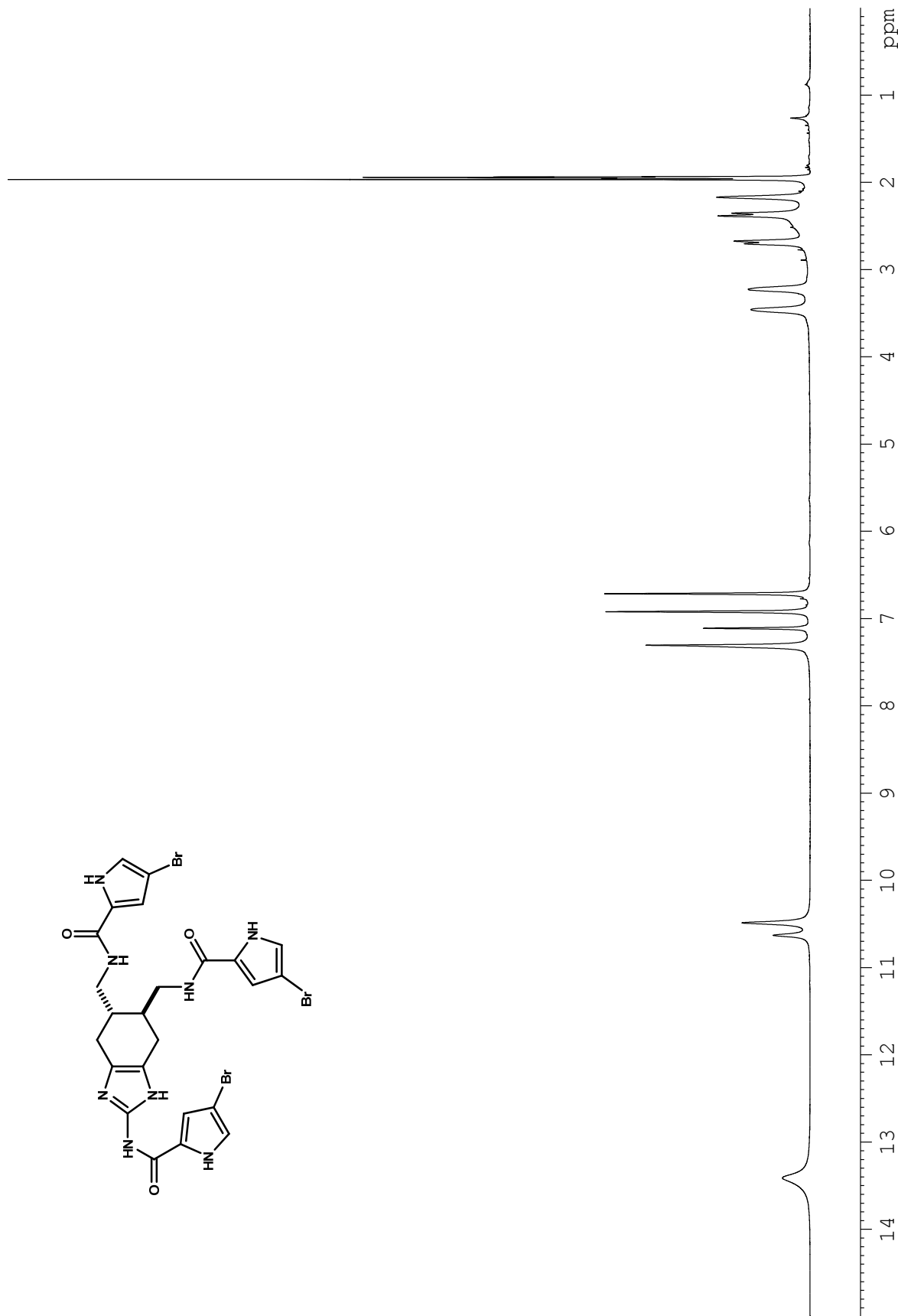
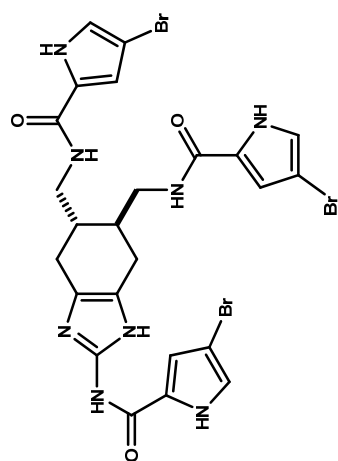
**Figure A3.34.** <sup>1</sup>H NMR (500 MHz, MeOH-*d*<sub>4</sub>) spectrum of compound 4-48.



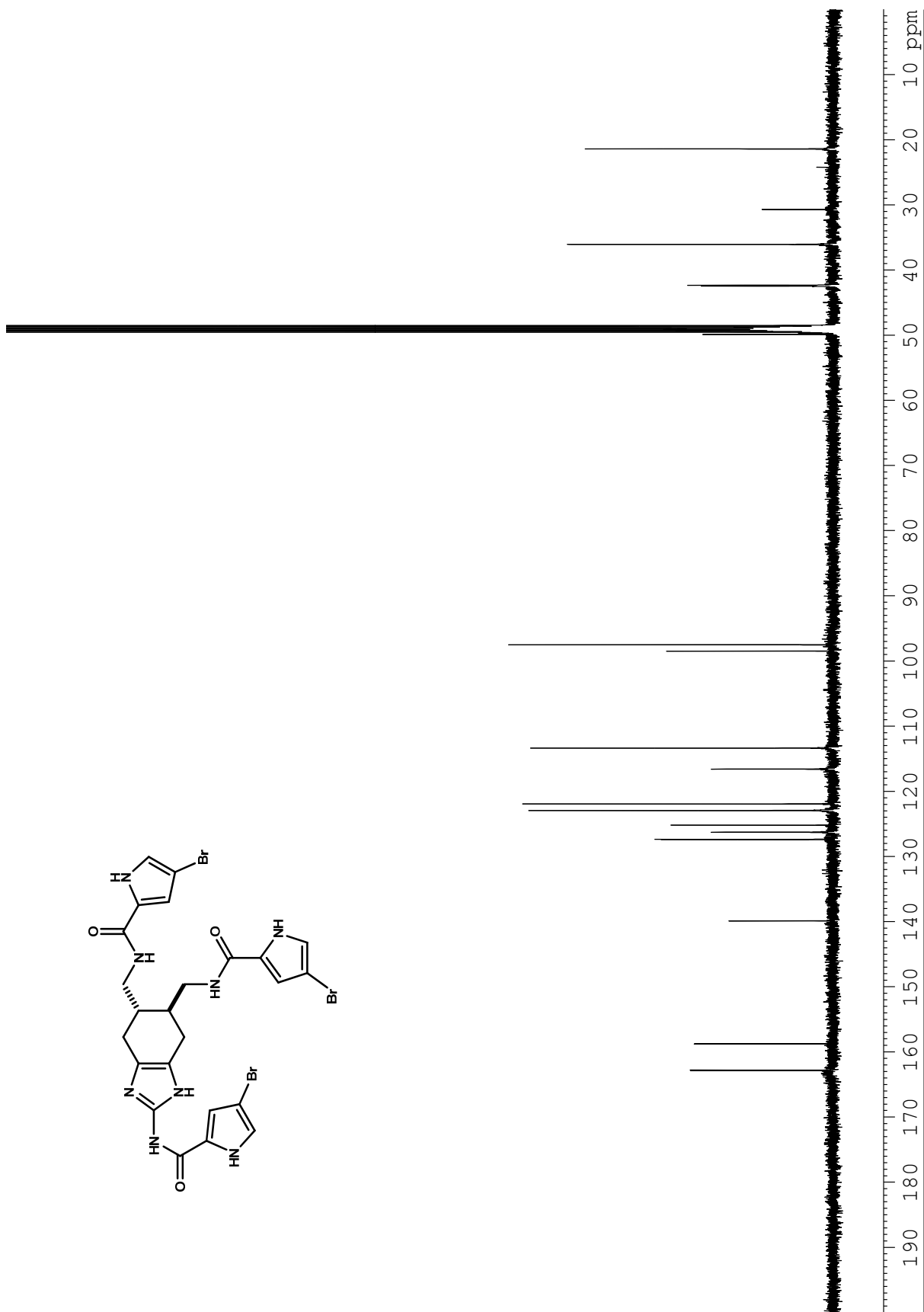
**Figure A3.35.**  $^{13}\text{C}$  NMR (125 MHz,  $\text{MeOH-}d_4$ ) spectrum of compound 4-48.



**Figure A3.36.** <sup>1</sup>H NMR (500 MHz, MeOH-*d*<sub>4</sub>) spectrum of compound 4-45.

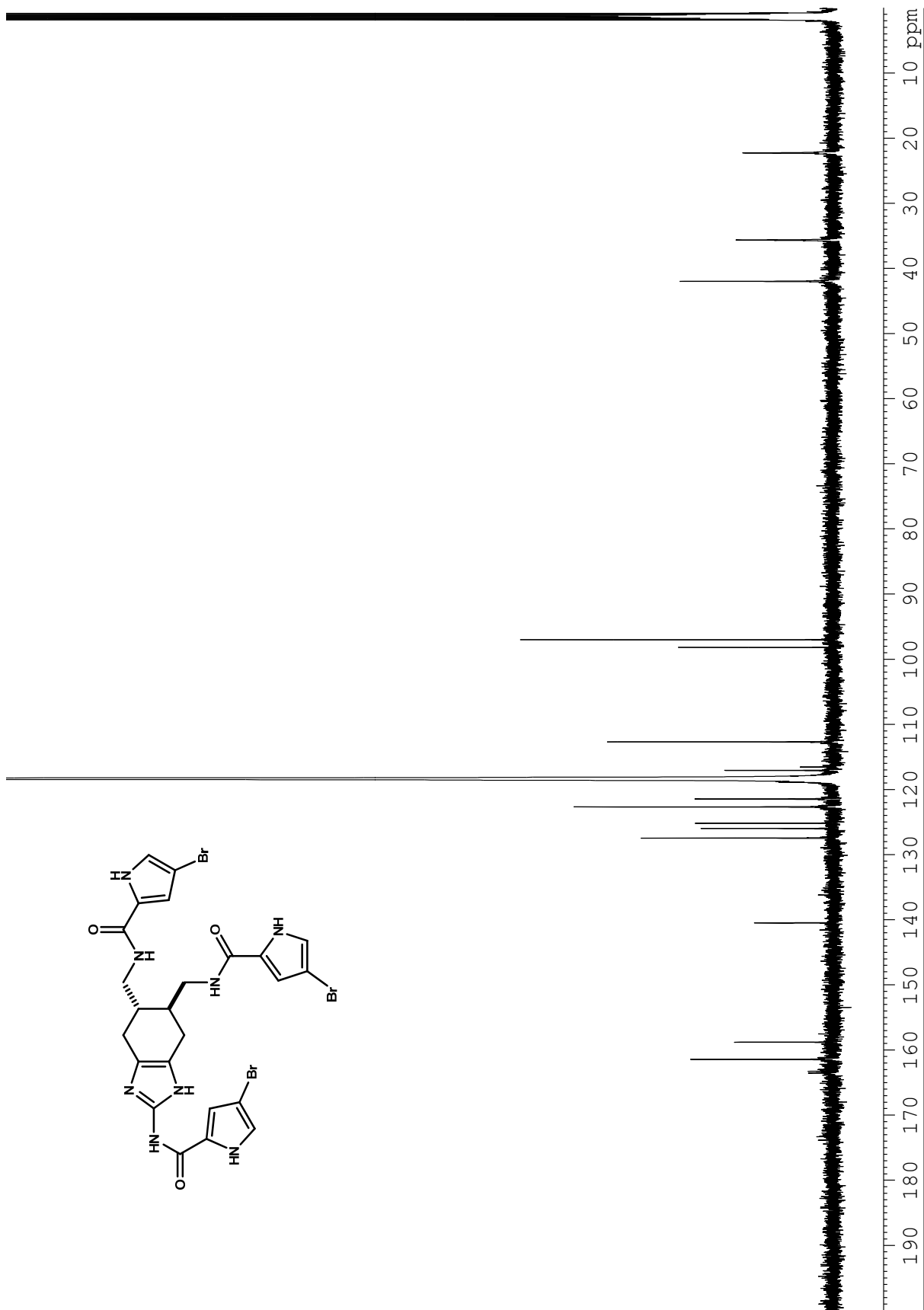


**Figure A3.37.** <sup>1</sup>H NMR (500 MHz, CH<sub>3</sub>CN-*d*<sub>3</sub>) spectrum of compound 4-45.

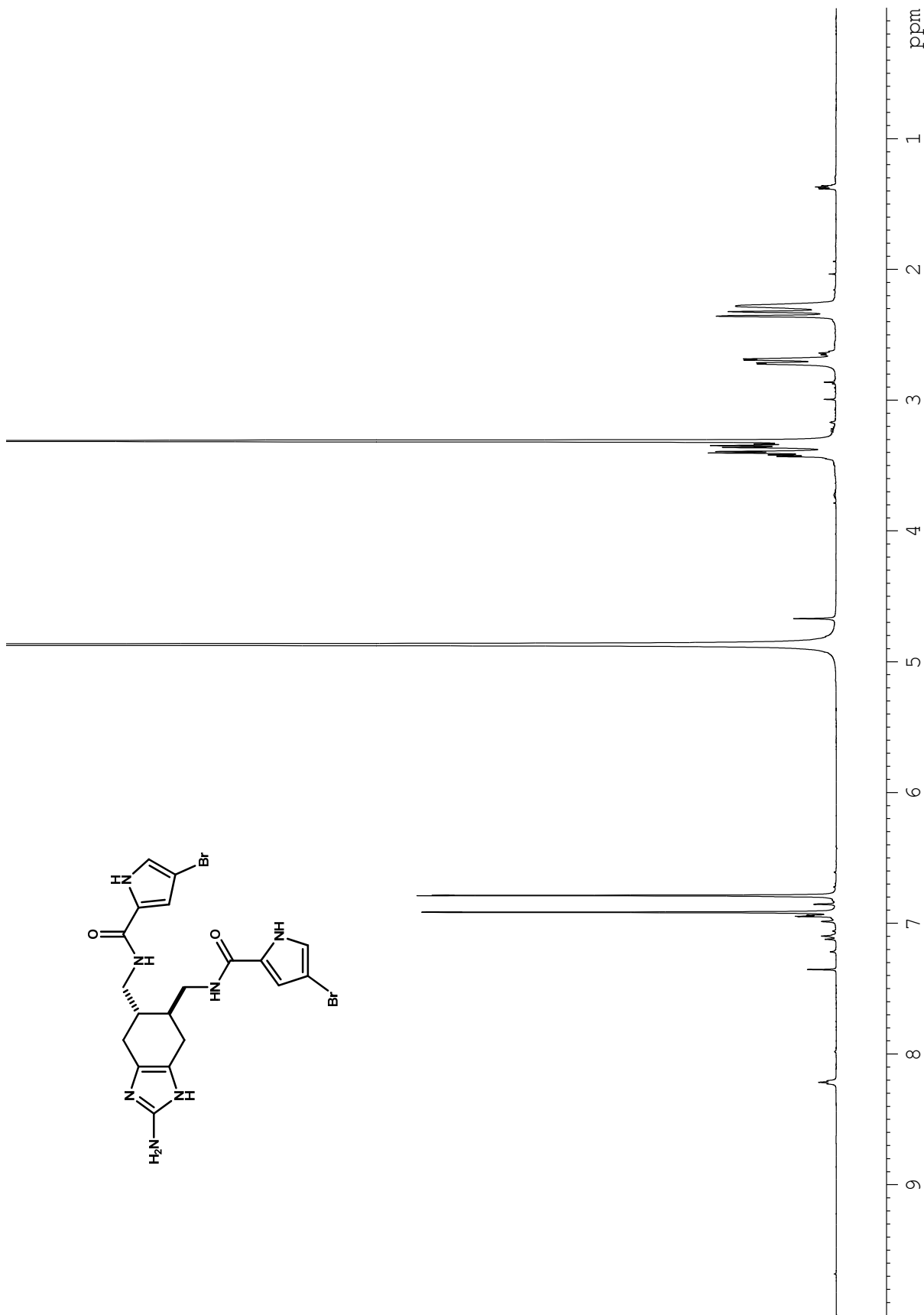


**Figure A3.38.**  $^{13}\text{C}$  NMR (125 MHz,  $\text{MeOH-}d_4$ ) spectrum of compound 4-45.

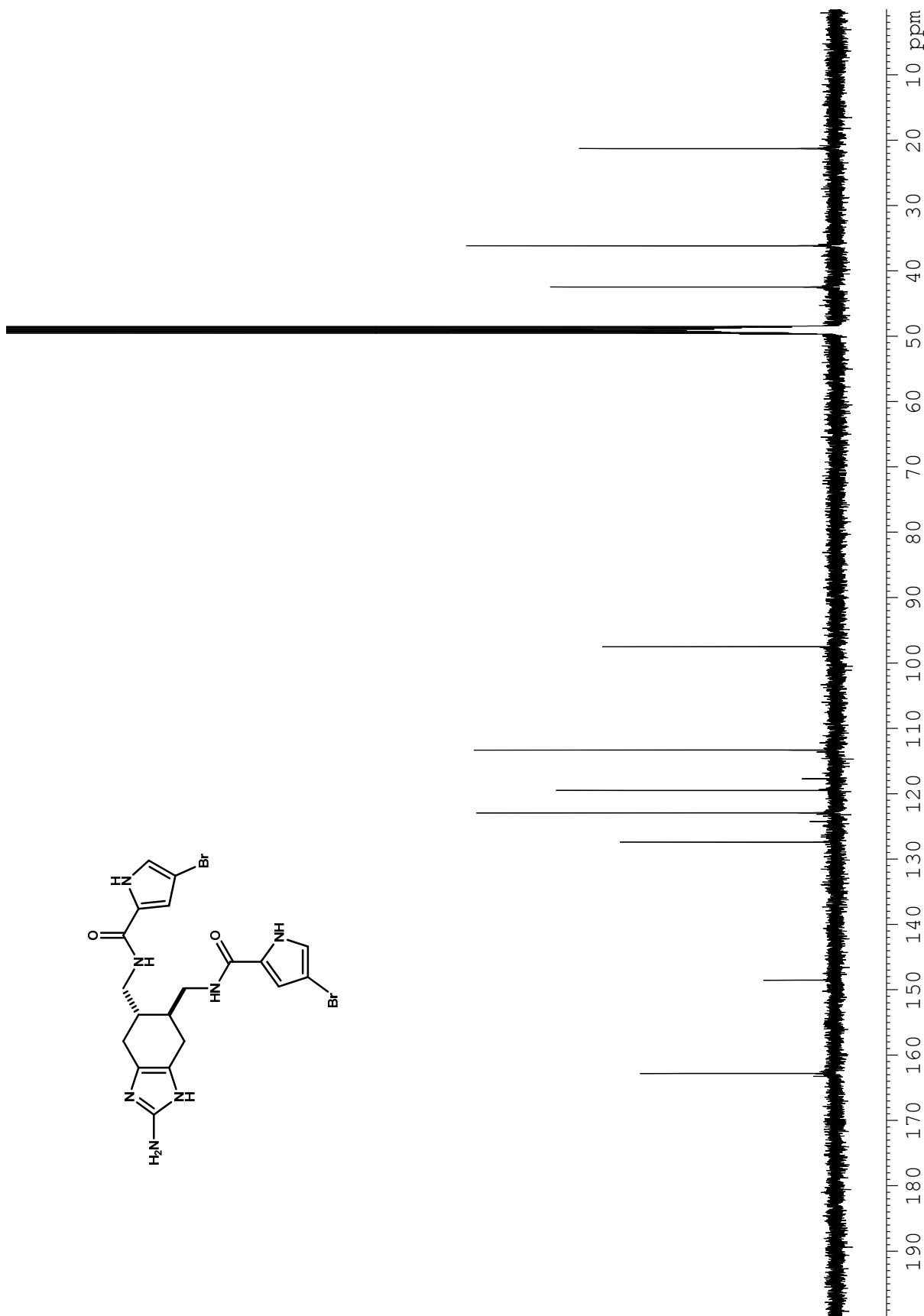




**Figure A3.39.**  $^{13}\text{C}$  NMR (125 MHz,  $\text{CH}_3\text{CN}-d_3$ ) spectrum of compound 4-45.



**Figure A3.40.** <sup>1</sup>H NMR (500 MHz, MeOH-*d*<sub>4</sub>) spectrum of compound 4-26 (CF<sub>3</sub>CO<sub>2</sub>H).



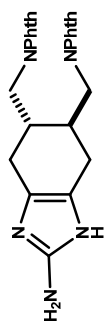


**Figure A3.42.** <sup>1</sup>H NMR (500 MHz, CH<sub>3</sub>CN-*d*<sub>3</sub>) spectrum of compound 4-46 (CF<sub>3</sub>CO<sub>2</sub>H).

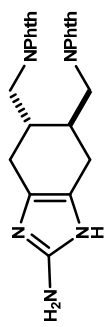


**Figure A3.43.**  $^{13}\text{C}$  NMR (125 MHz,  $\text{CH}_3\text{CN}-d_3$ ) spectrum of compound 4-46 ( $\text{CF}_3\text{CO}_2\text{H}$ ).

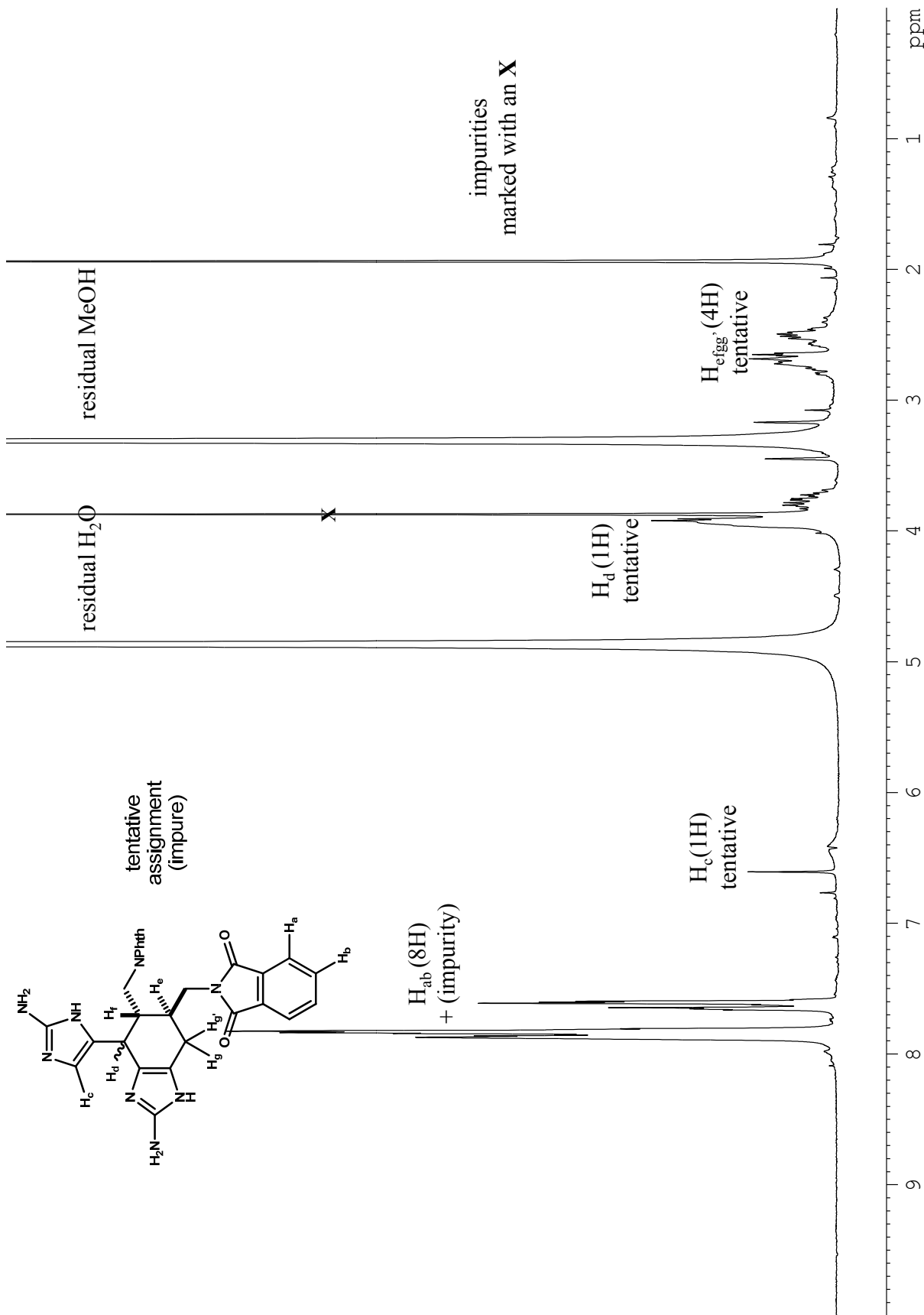


**Figure A3.44.** <sup>1</sup>H NMR (500 MHz, MeOH-*d*<sub>4</sub>) spectrum of compound 4-53 (2·CF<sub>3</sub>CO<sub>2</sub>H) (impure).

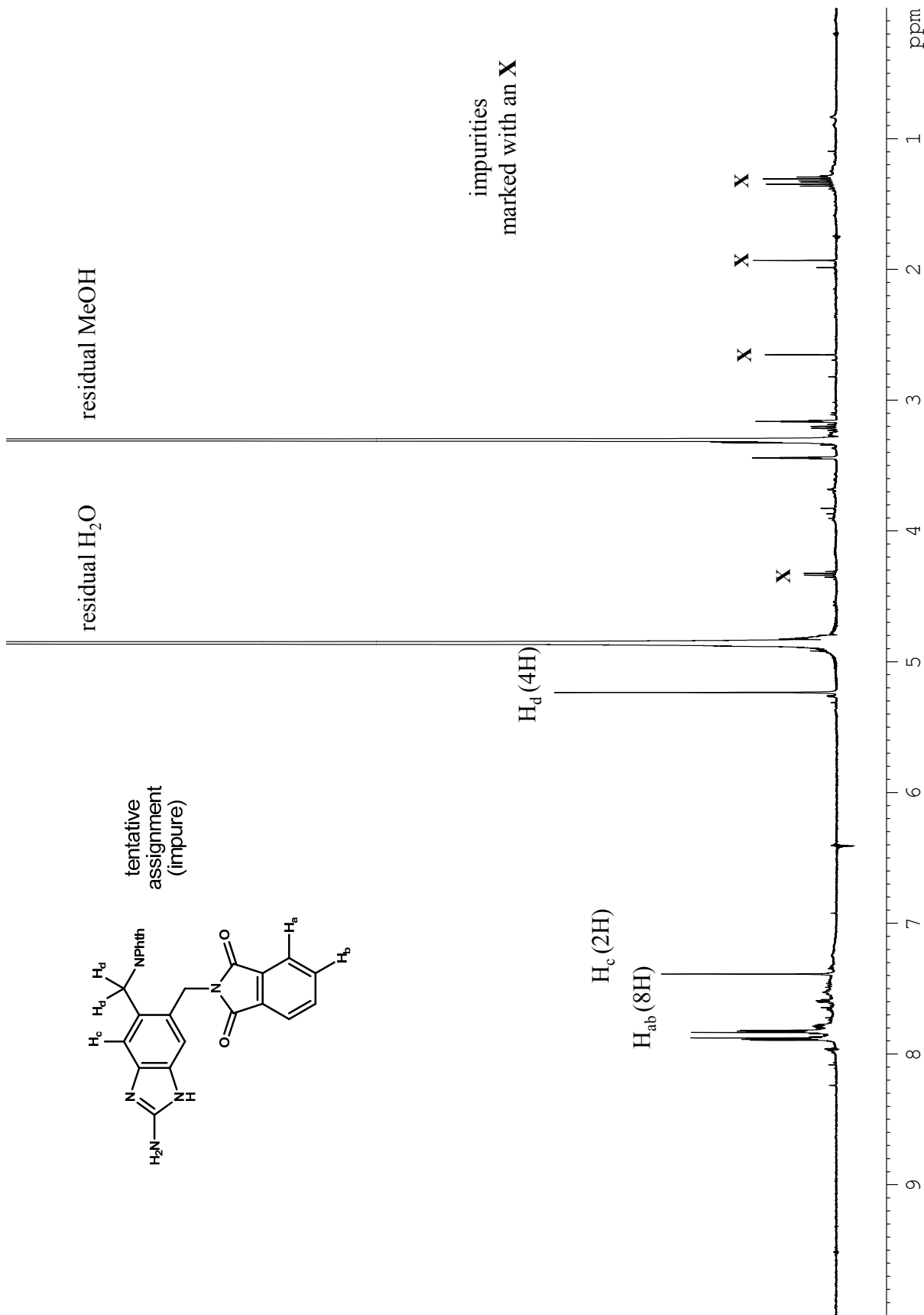


**Figure A3.45.** <sup>1</sup>H NMR (500 MHz, MeOH-*d*<sub>4</sub>) spectrum of compound 4-54 (CF<sub>3</sub>CO<sub>2</sub>H) (impure).

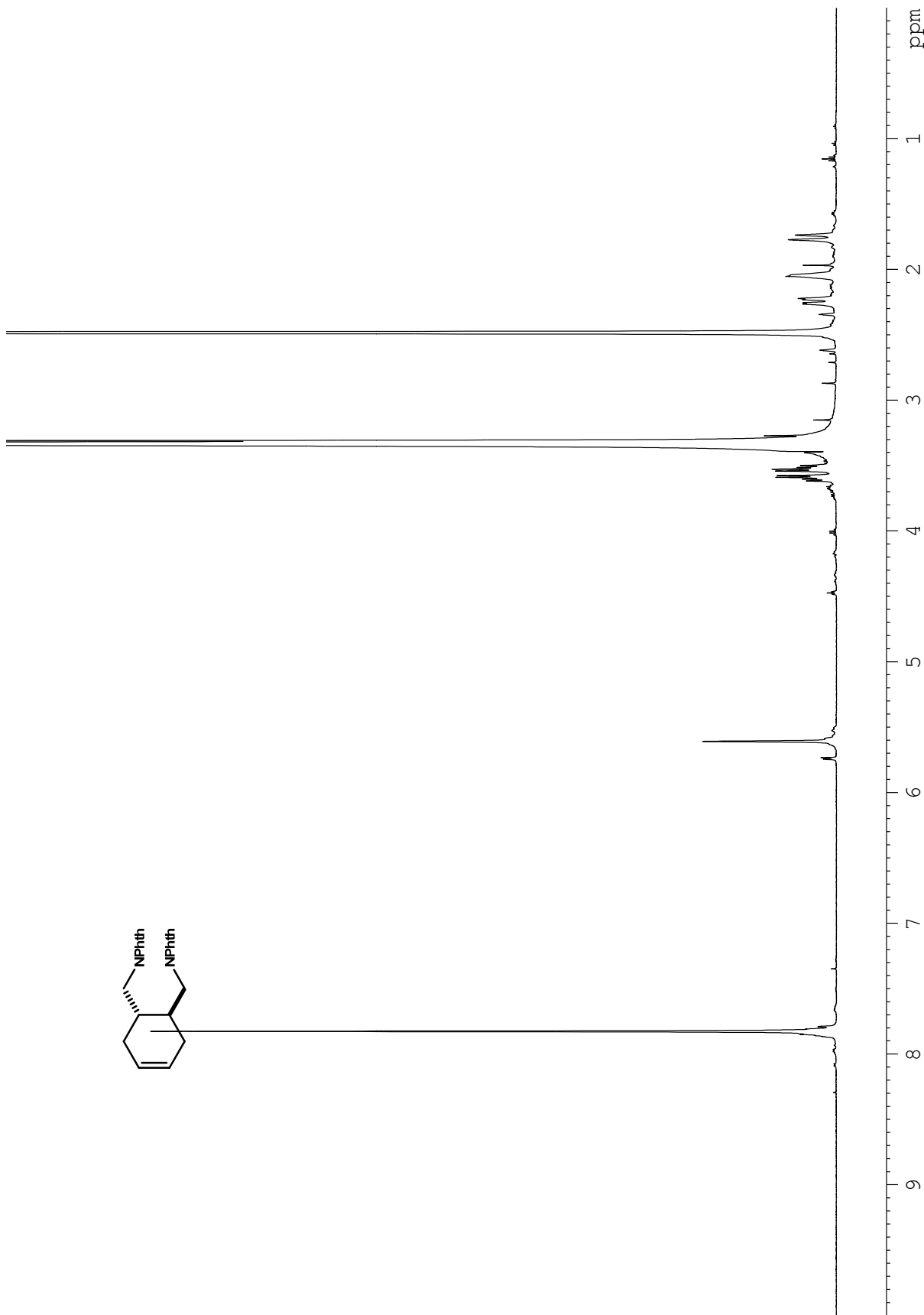


**Figure A3.46.** <sup>1</sup>H NMR (500 MHz, DMSO-*d*<sub>6</sub>) spectrum of compound 4-56.



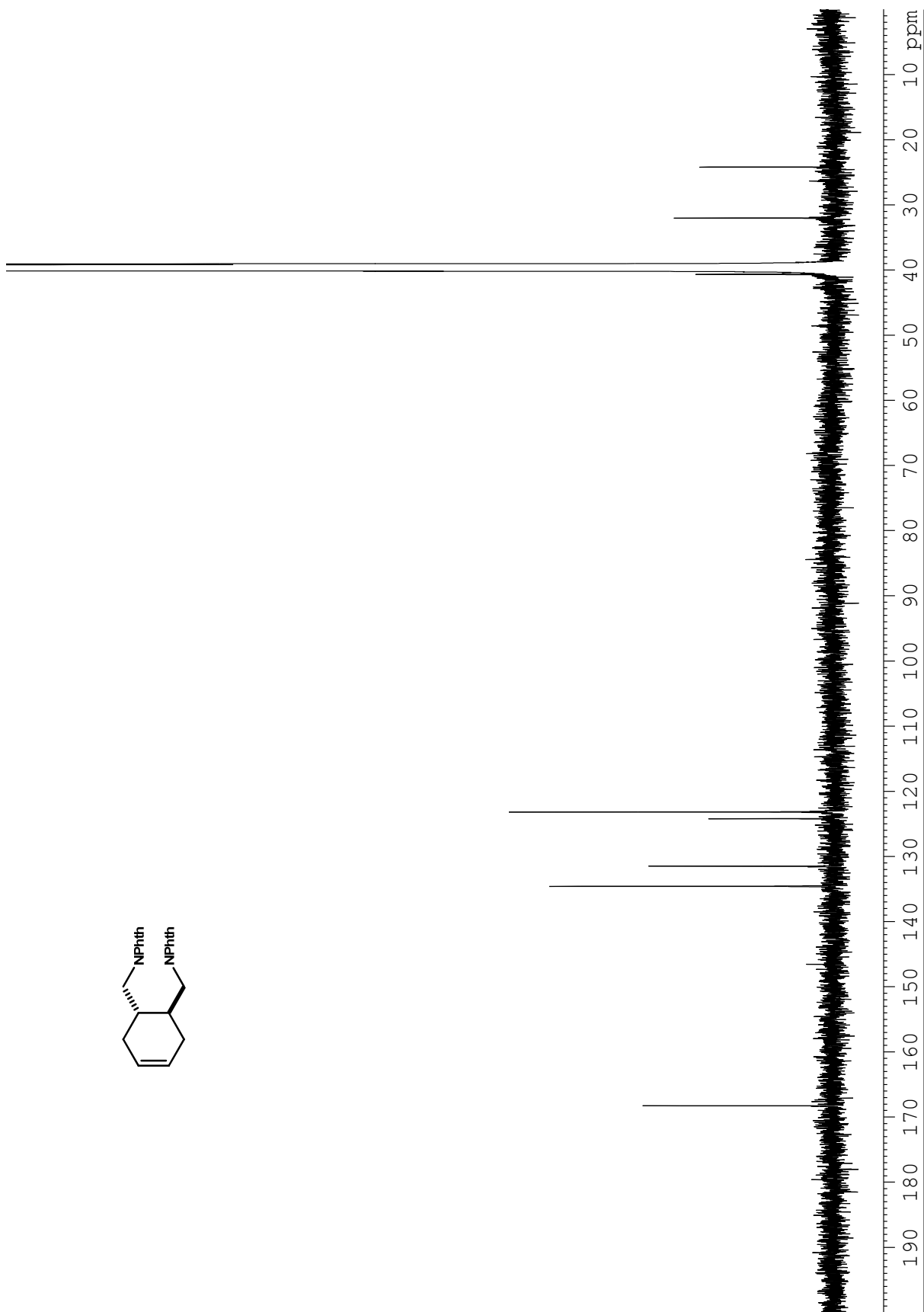
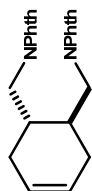


**Figure A3.47.**  $^{13}\text{C}$  NMR (125 MHz,  $\text{DMSO-}d_6$ ) spectrum of compound **4-56**.

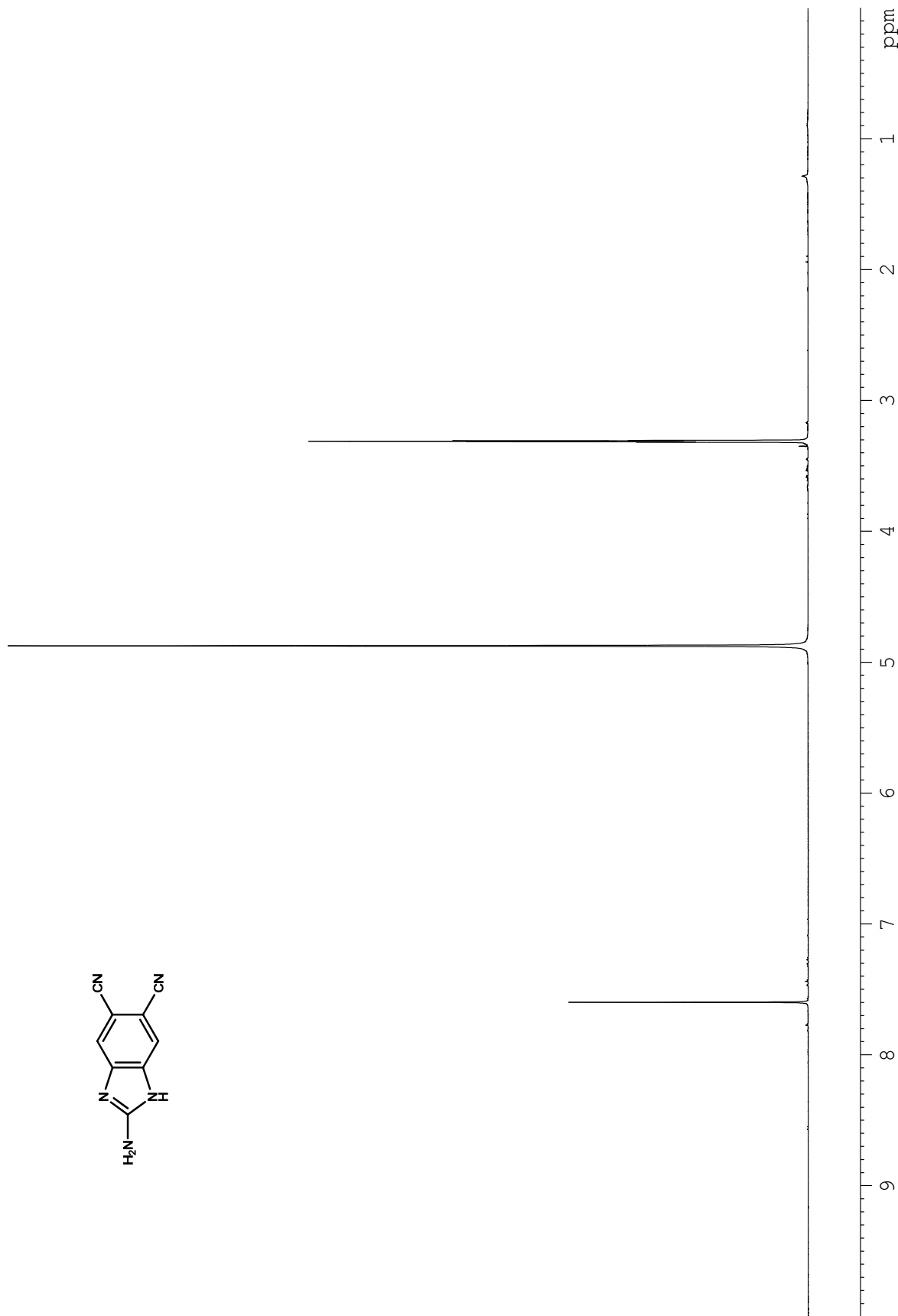
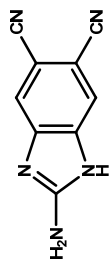


**Figure A3.48.** <sup>1</sup>H NMR (500 MHz, MeOH-*d*<sub>4</sub>) spectrum of compound 4-62.

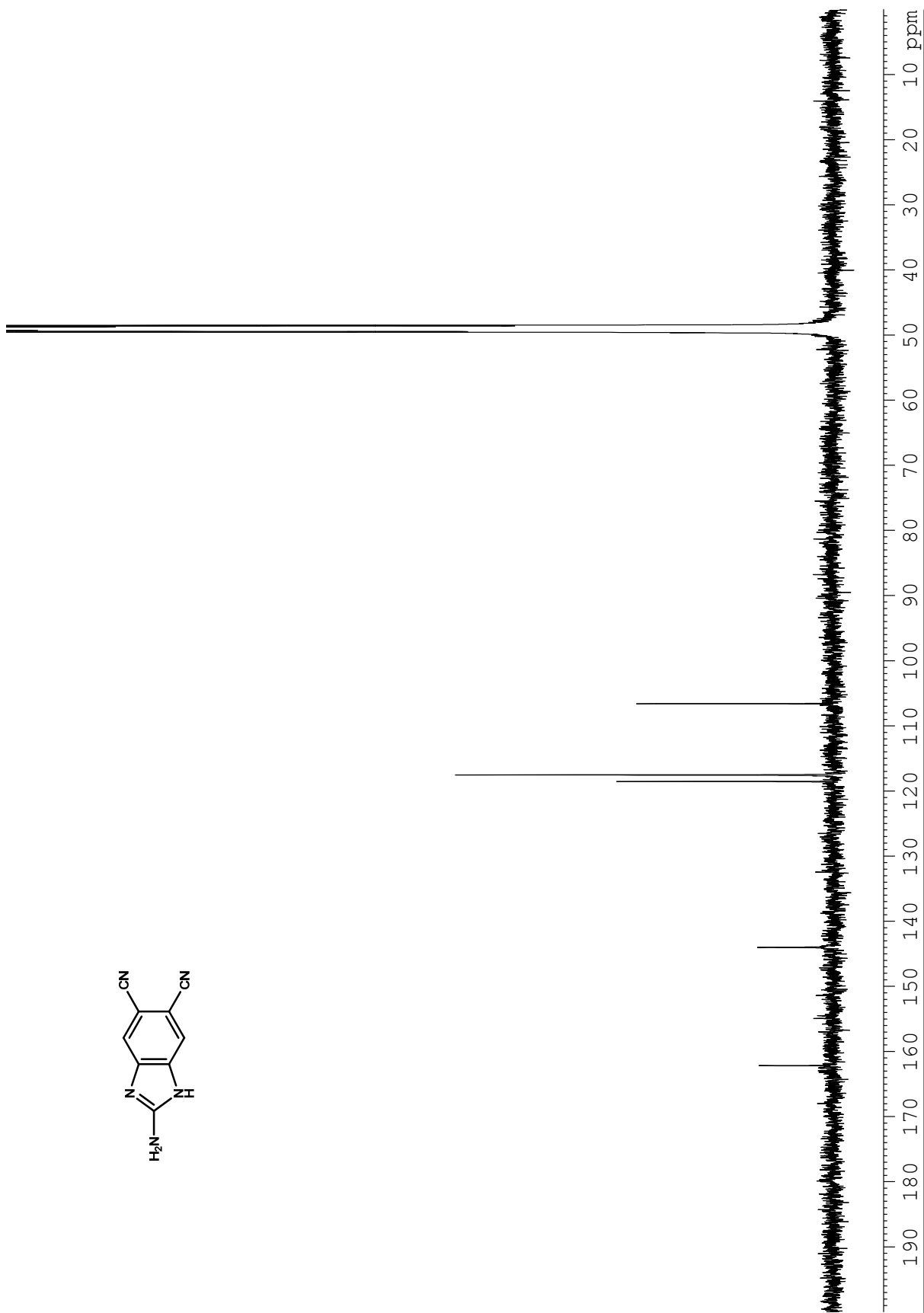
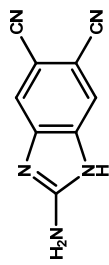


**Figure A3.49.** <sup>13</sup>C NMR (125 MHz, MeOH-*d*<sub>4</sub>) spectrum of compound 4-62.

## Chapter 5 – Alternative Access to Dispacamide Dimers:

*Auto-oxidation of 3,3'-bipyrrolidines for the synthesis of dimeric pyrrole–imidazole alkaloids*

*Andrew G. Roberts, Hui Ding and Patrick G. Harran*

### 5.1 Introduction.

#### 5.1.1 Introduction and General Strategy.

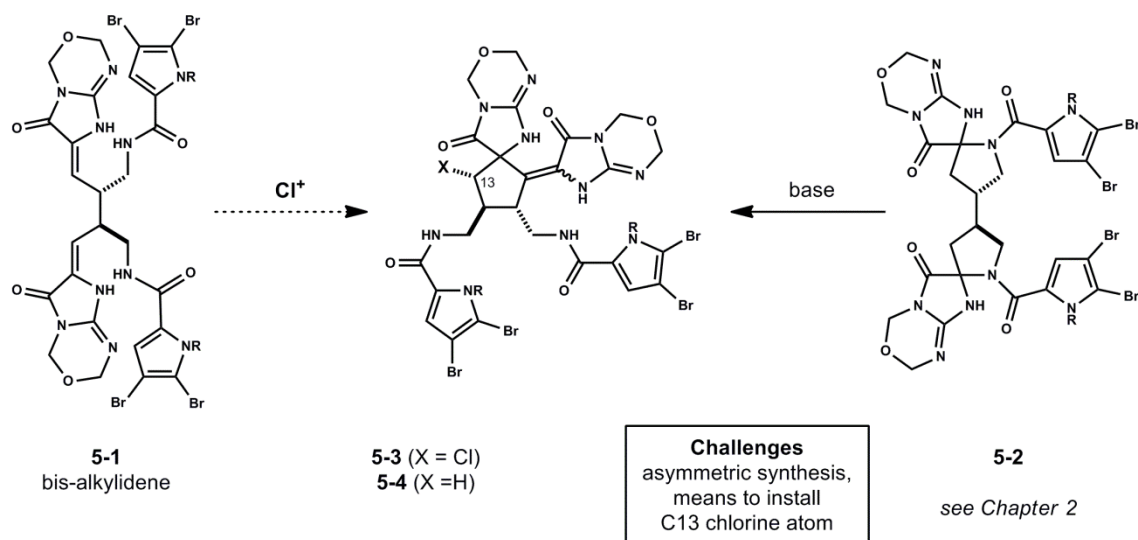


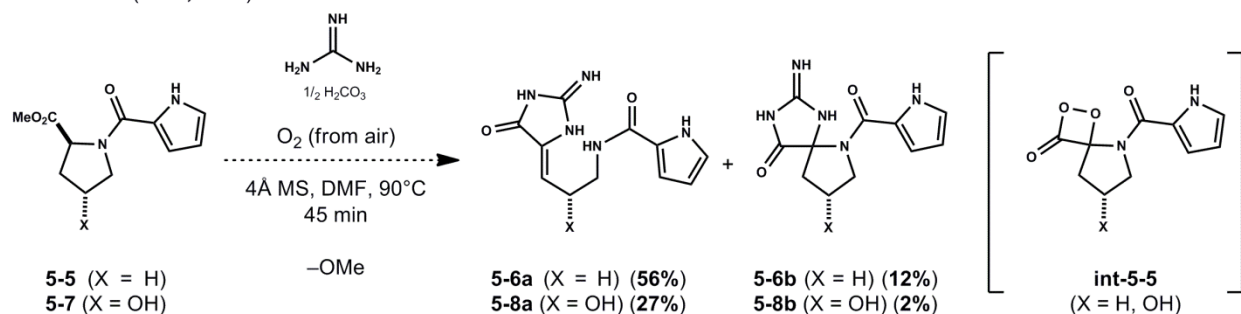
**Figure 5.1.** Prospect and current understanding of displacamide dimer equilibrium - Proposed oxidative spirocyclization of 'bis-alkylidene' **5-1** to access chlorinated spirocyclopentane **5-3** (X = Cl). Base promoted spirocycloisomerization of 'bis-spirocycles' **5-2** provides **5-2** (X = H).

We are interested in preparing a bis-alkylidene of type **5-1** as a reactive intermediate for direct access to chlorinated spirocyclopentane **5-3** via oxidative desymmetrization (Figure 5.1).<sup>[1]</sup> However, previously targeted bis-alkylidenes of type **5-1** exist as bis-spirocycles of type **5-2**. Therefore, we reported the impact of this structural equilibrium. Dimeric bis-spirocycles of type **5-2** spirocycloisomerize to spirocycloalkylidenes **5-4** (Chapter 2). Spirocycloalkylidene **5-4** was a useful intermediate en route to halogen-deficient axinellamines (Chapter 2) and ageliferin (Chapter 3).<sup>[1cd]</sup> Our interest in this unique equilibrium, as it pertains to the reactivity of displacamide dimers (*e.g.* **5-1** and **5-2**), has been renewed. We sought alternative methods to

prepare spirocycloalkylidenes **5-3** and **5-4**. An intriguing reaction reported in 2004 by Al-Mourabit and co-workers is the primary inspiration for these experiments.<sup>[2]</sup>

### 5.1.2 Auto-oxidative Incorporation of Guanidine into Partially Oxidized Proline Dimers.

Al-Mourabit (2004, 2007)



**Proposal:** Access to 'bis-alkylidenes' **5-10** or spirocycles (**5-11**, **5-12**) under auto-oxidation conditions

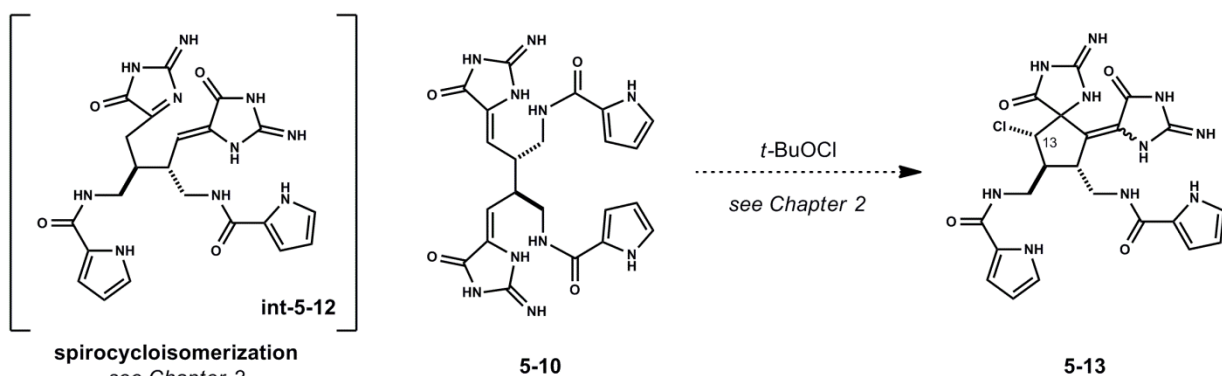
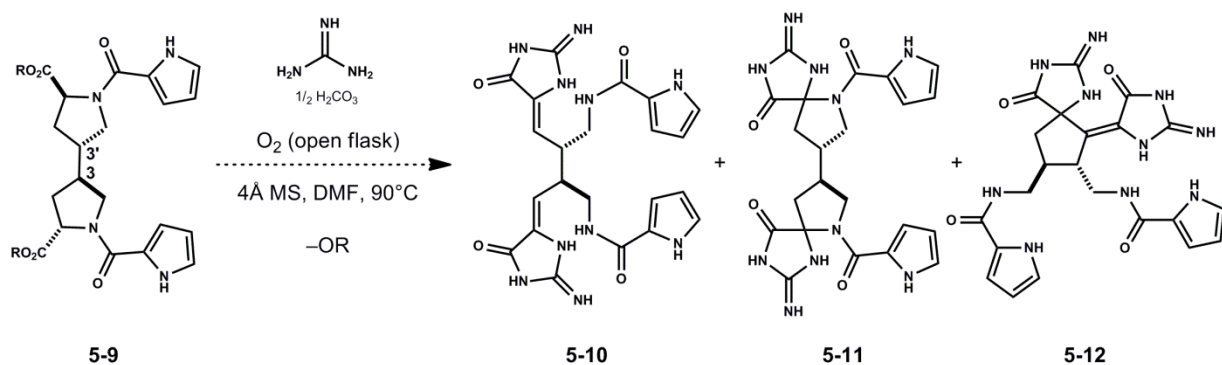


**Figure 5.2.** Alternative access to dispacamide dimers - Al-Mourabit's provocative biomimetic synthesis of non-halogenated dispacamides (**5-6**, **5-8**), synthesis of 'bis-alkylidene' **5-10** via the auto-oxidative guanidine incorporation of dimer **5-9**.

In order to study the equilibrium of dispacamide dimers (such as **5-1** and **5-2**, Figure 5.1), we sought succinct synthetic access to key intermediates. While impressed by the propensity of bis-

spirocycles **5-2** to undergo base-catalyzed spirocycloisomerization to desymmetrized spirocycloalkylidenes (**5-4**, X = H, C13) the system did not readily permit chlorine incorporation at C13 as initially intended (see Chapter 2).<sup>[1c]</sup> In previous systems, bis-alkylidenes of type **5-1** were not isolated or observed in situ, preventing access to chlorinated spirocycloalkylidenes (**5-3**, X = Cl) via oxidative desymmetrization. We aimed to address several challenging issues that limited our current synthetic strategy (see Chapter 2); notwithstanding, the key tenets of this project would be maintained. Specifically, we desired an asymmetric synthesis of dispacamide dimers with means to introduce the requisite C13 chlorine atom.

We targeted dimeric intermediate **5-9** (Figure 5.2). It was proposed that 3,3'-bipyrrolidine **5-9** could be readily prepared via homodimerization of a *L*-4-hydroxyproline derivative. In line with the results of Al-Mourabit, target homodimer **5-9** would serve as an efficient precursor to dispacamide dimers, namely bis-alkylidene **5-10** and/or bis-spirocycles **5-11** when reacted with guanidine under aerobic conditions. We also recognize the potential for reactive intermediates (**5-10**, **5-11**) to funnel towards isomeric spirocycloalkylidenes **5-12** as observed previously by us provided under basic conditions.<sup>[1ac]</sup> In a creative series of reports, the Al-Mourabit group demonstrated efficient auto-oxidation of *N*-acylated *L*-proline derived monomer (**5-5**, X = H) to generate non-brominated dispacamide (**5-6a**, X = H) and minor spirocyclic isomer (**5-6b**, X = H).<sup>[2a]</sup> The reaction requires oxygen to generate a reactive dioxetanone intermediate (**int-5-5**, X = H) that traps guanidine. Subsequent loss of hydrogen peroxide and cyclization yields **5-6a** and **5-6b**. This process is analogous to the formation of dioxetanone intermediates underlying firefly bioluminescence.<sup>[3]</sup> Recent studies demonstrate analogous transformations with intermediates derived from the *N*-acylation of *trans*-4-hydroxy-*L*-proline, wherein **5-7** provides isomers **5-8a** and **5-8b** albeit with diminished yield.<sup>[2c]</sup> With substantial precedent for the oxidative

incorporation of guanidine, the challenge was reduced to the efficient preparation of dispacamide dimer precursor **5-9**.

In line with previous efforts towards the synthesis of dispacamide dimers described in Chapter 2, we desired to maintain a symmetry-based approach. It was envisioned that a  $C_2$ -symmetric dimer of type **5-9** or its corresponding 3,3'-epimer (Figure 5.3) could be prepared via the homodimerization of an appropriately functionalized monomer (e.g. **5-14a**, **5-15a**, **5-15b**) derived from *trans*-4-hydroxy-L-proline. This symmetry-based strategy could expedite access to bis-alkylidene **5-10** or spirocycloalkylidenes **5-12**, primarily requiring an efficient preparation of homodimer **5-9** as a single diastereomer. We initially considered classical methods for the dimerization of carboxylic acid **5-14a** via Kolbe electrolysis<sup>[4]</sup> or radical homocoupling of the respective Barton thioester<sup>[5]</sup>. However, the preparation of its synthetic precursor **5-14b** (R = Me) was lengthy (5 steps from *trans*-4-hydroxy-L-proline)<sup>[6]</sup> and therefore not examined in detail. From 4-bromopyrrolidine monomers **5-15a** or **5-15b**, we envisioned efficient access to dimer **5-9** by classical Wurtz homocoupling<sup>[7]</sup> or reductive homodimerization via transition metal catalysis.<sup>[8]</sup> The later method was most attractive in light of recent developments in the area of nickel-catalyzed cross- and homocoupling of alkyl halides.<sup>[9]</sup> In addition, chiral ligand spheres could potentially permit stereocontrol in the proposed C–C bond formation event between two  $sp^3$  hybridized centers.

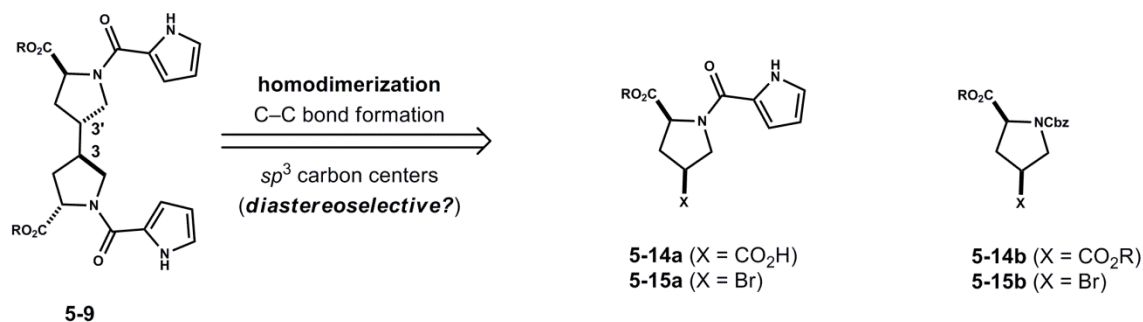


**Figure 5.3.** Targeted 3,3'-bipyrrrolidine homodimer **5-9** - methods for controlled dimerization (diastereoselective?).

### 5.1.3 Literature Precedent for the Reductive Dimerization of Unactivated Alkyl Halides.

With regard to Wurtz-type homocoupling methods, De Sá and co-workers have reported a useful comparison of reaction conditions for bi-phasic homo-coupling of alkyl and benzyl halides.<sup>[10]</sup> The thorough investigation notes a dependence on various additives (*e.g.* NH<sub>4</sub>Cl, K<sub>2</sub>HPO<sub>4</sub>) and pH in aqueous media. From this study, bi-phasic conditions with saturated aqueous K<sub>2</sub>HPO<sub>4</sub> and benzene conducted at room temperature are described as optimal conditions for the stoichiometric CuI / Zn promoted coupling of secondary iodides and bromides. We reasoned these methods could provide initial access to dimers **5-9**, however we anticipated poor diastereocontrol.<sup>[11]</sup> Several recent reports suggested ligand assisted nickel-catalysis could address this challenge.<sup>[9,12]</sup>

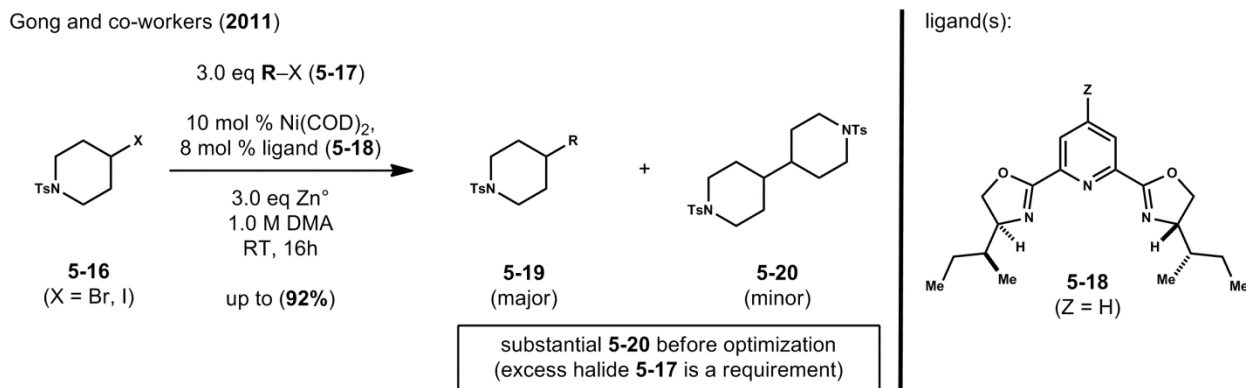


**Figure 5.4.** Nickel-catalyzed reductive cross-coupling of unactivated alkyl halides - minimization of homodimerization events.

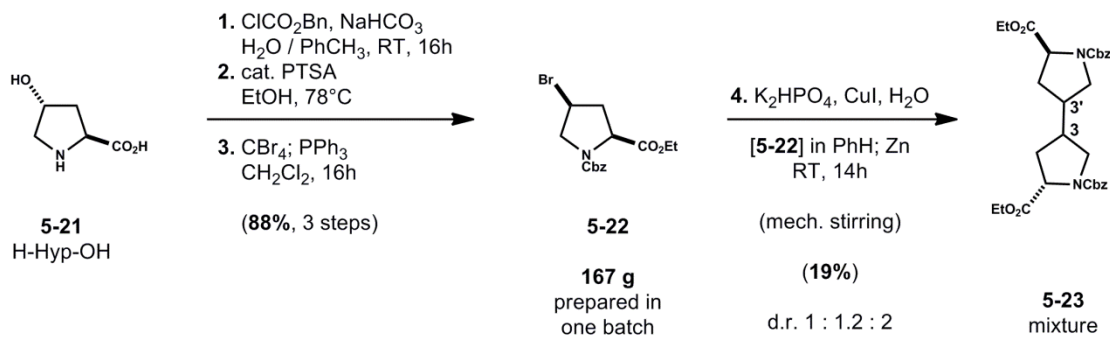
Several recent methods have emerged for the nickel-catalyzed sp<sup>3</sup>-sp<sup>3</sup> homocoupling<sup>[12bc]</sup> and cross-coupling<sup>[12a]</sup> of unactivated alkyl halides. We were particularly attracted the research of Gong and co-workers whose efforts to optimize reductive cross-coupling of differentiated alkyl halides addressed primary issues of substantial homocoupling.<sup>[12a]</sup> In addition, model substrate *N*-tosyl piperidine halides **5-16** (Figure 5.4, X = Br, I) were related to our target monomers **5-15** (Figure 5.3). Intriguingly, preliminary experiments with halide **5-16**, as thoroughly described in supplementary information, provided homocoupled by-product, 4,4'-bipiperidine **5-20** in



substantial quantities. This suggested that in the absence of excess cross-coupling partner **5-17** (3 equiv) one would obtain homodimer **5-20** as the major product. Notably, optimized conditions employ 10 mol % Ni(COD)<sub>2</sub>, 8 mol % ligand **5-18** (Z = H), 3 equiv Zn in DMA at room temperature.<sup>[11a]</sup> Other related homocoupling methods similarly employ 0.5-5 mol % NiCl<sub>2</sub>-glyme, ligand: 2,2':6',2''-terpyridine<sup>[12bc]</sup> or (*R,R*)-Ph-pybox<sup>[12c]</sup>, co-reductant: 1 equiv Mn<sup>[11b]</sup> or 1 equiv Zn<sup>[12c]</sup> in 1.0 M DMF<sup>[12bc]</sup> or THF-NMP<sup>[12c]</sup> at room temperature to 80°C. However, these methods do not adequately address diastereostereomeric outcomes in asymmetric reactions as expected for the dimerization of **5-15**. We anticipated the use of chiral pybox ligands (*e.g.* **5-18**, Z = H) could address this issue.

## 5.2 Results and Discussion.

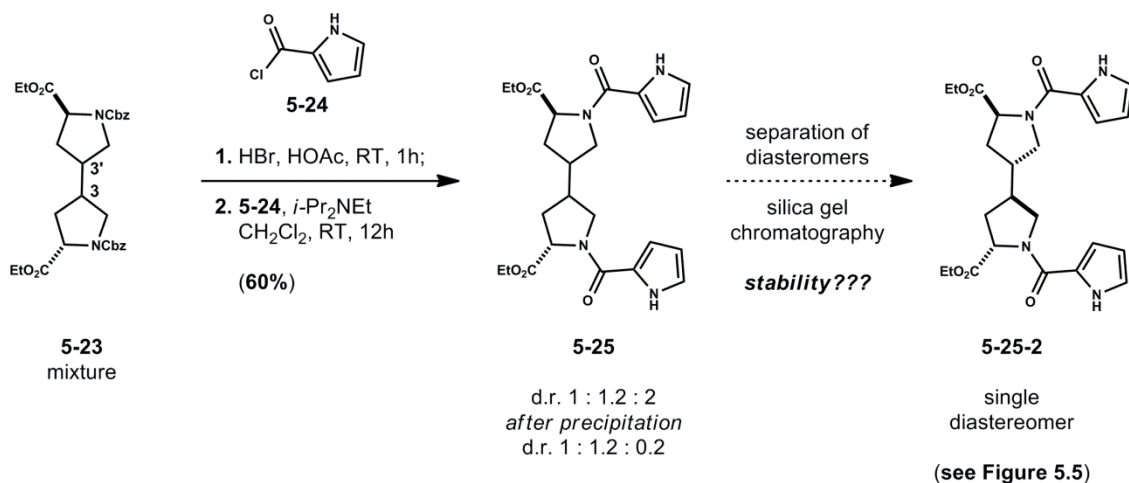
### 5.2.1 Initial Preparation of 4-Bromopyrrolidine Monomer 5-22, Dimerization and Characterization.



**Scheme 5.1.** Synthesis and dimerization of (2S,4S)-1-benzyl 2-ethyl 4-bromopyrrolidine-1,2-dicarboxylate (**5-22**) to access 3,3'-bipyrrrolidine homodimers **5-23** (initial preparation procedures).

4-bromopyrrolidine **5-22** was synthesized in three steps, with minor procedural modifications, from *trans*-4-hydroxy-L-proline **5-21** in high yield (Scheme 5.1).<sup>[13]</sup> Notably, bromide **5-22** was prepared on scale (167 g obtained in a single-batch, **88%**) and only required a single purification by column chromatography for the sequence. With access to monomer **5-22**, we initially examined Wurtz-type homocoupling methods to obtain 3,3'-bipyrrrolidine dimers **5-23**.<sup>[10]</sup> Using bi-phasic conditions, benzene and saturated aqueous  $\text{K}_2\text{HPO}_4$  reported by De Sá *et al.*, dimers **5-23** were obtained in low-yield, with reaction mass balance consisting primarily of reduced product Cbz-*L*-proline ethyl ester derived from monomer **5-22**. The reaction was not optimized, however it should be noted that the homocoupling could be conducted at room temperature or 0°C. Lower temperature required prolonged reaction times (+14h). Changing reaction solvent from benzene to acetone was tolerated but did not improve yield or diastereoselectivity (*vide infra*). Homodimers **5-23** were obtained as a mixture of 3,3'-bipyrrrolidine diastereomers as observed by  $^1\text{H}$  NMR analysis (500 MHz,  $\text{CHCl}_3-d_1$ ). Quantification was hampered by rotational isomerism observed in  $^1\text{H}$  NMR spectra. We were anxious to elaborate homodimers **5-23** to key

dimeric substrate **5-23** (Scheme 5.2) in hopes of separating and characterizing the mixture at a later point.



**Scheme 5.2.** Initial synthetic route to access acyl-pyrrole homodimers (**5-25**) from 3,3'-bipyrrolidines (**5-23**) (synthetic route is 3 steps from bromo-pyrrolidine monomer **5-22**).

The conversion of diastereomeric mixtures **5-23** to target dimer **5-25** was achieved by benzyloxycarbonyl deprotection with hydrobromic acid and subsequent *N*-acylation with **5-24** to provide a mixture of *N*-acylated 3,3'-bipyrrolidines in moderate yield (Scheme 5.2). Analysis of dimers **5-25** by HPLC (UV analysis 254-nm) indicated three separable diastereomers are formed (**5-25-1**:**5-25-2**:**5-25-3**, d.r. 1:1.2:2, UV integration) from the dimerization of monomer **5-22**. Initial purification by HPLC provided three individual diastereomers of dimers **5-25** denoted as **5-25-1**, **5-25-2**, and **5-25-3**. In addition, selective precipitation of one diastereomer **5-25-3**, was effected by dissolution of the crude mixture **5-25** (initial d.r. 1:1.2:2) in CHCl<sub>3</sub> to provide an enriched mother liquor (d.r. 1:1.2:0.2) after filtration. With these analytical standards in hand, flash chromatography conditions (SiO<sub>2</sub>, eluting with CHCl<sub>3</sub>/MeOH (97:3)) were developed to separate remaining isomers **5-25-1** and **5-25-2** on preparative scales (100 mg to several grams). Unfortunately, recovery of pure isolated diastereomers (**5-25-1** separated from **5-25-2**) after chromatography was poor. Repeated purification of enriched mixtures was not tractable. In

addition, poor mass balance and recovery after repeated SiO<sub>2</sub> chromatography suggested that dimers **5-25** were unstable, perhaps decomposing oxidatively. This sequence provided sufficient isolated dimers for characterization and initial auto-oxidation studies (*vide infra*, Scheme 5.3).

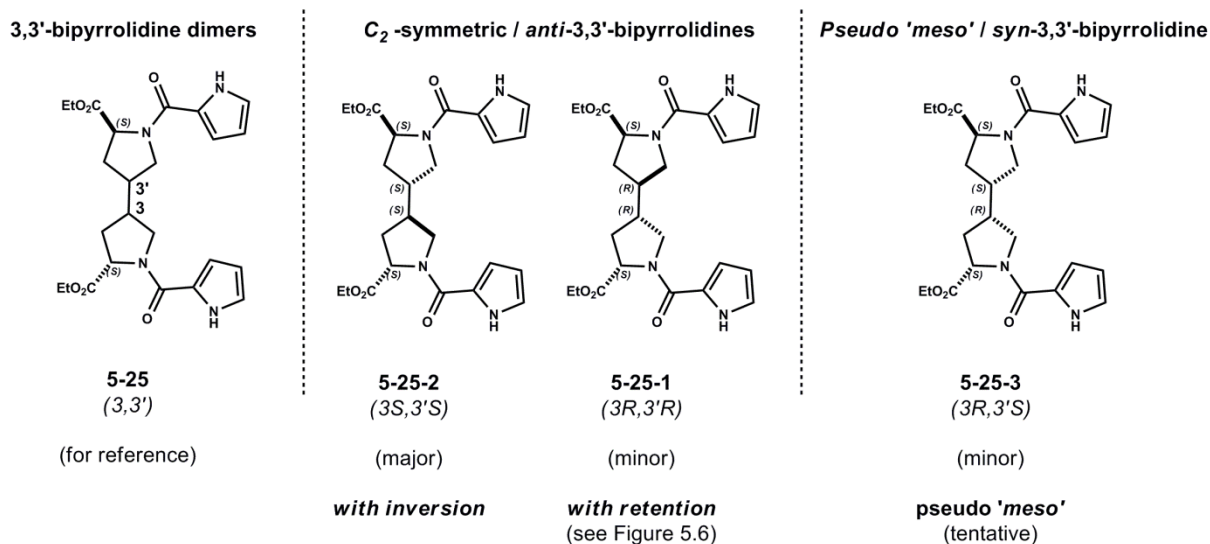


**Figure 5.5.** Analysis of diastereomers **5-25**, C<sub>2</sub>-symmetric (**5-25-1**, **5-25-2**) and pseudo 'meso' (**5-25-3**, **5-25-4**) 3,3'-bipyrrolidines.

It became apparent that a scalable and diastereoselective homodimerization method was necessary. We saw it prudent to completely characterize all diastereomers **5-25** obtained from the previous dimerization sequence. We were interested in the relative stereochemical outcome of dimers **5-25** resulting from C–C bond formation at positions denoted 3 and 3' (Figure 5.5). The dimers can be further distinguished by grouping *anti*-3,3'-bipyrrolidines (namely C<sub>2</sub>-symmetric dimers, **5-25-1** and **5-25-2**) and *syn*-3,3'-bipyrrolidine (namely pseudo 'meso'-symmetric dimer, **5-25-3**). Moreover, <sup>1</sup>H and <sup>13</sup>C NMR analyses (DMSO-*d*<sub>6</sub>) of individual diastereomers **5-25** corroborated their grouping. Spectra of C<sub>2</sub>-symmetric dimers **5-25-1** and **5-25-2** possess an apparent symmetry, revealed by their 12 discrete <sup>1</sup>H resonances and 12 discrete <sup>13</sup>C resonances. This contrasted the spectral data obtained for tentatively assigned pseudo 'meso'-symmetric dimer **5-25-3** which possessed 21 discrete <sup>13</sup>C resonances.<sup>[14]</sup>

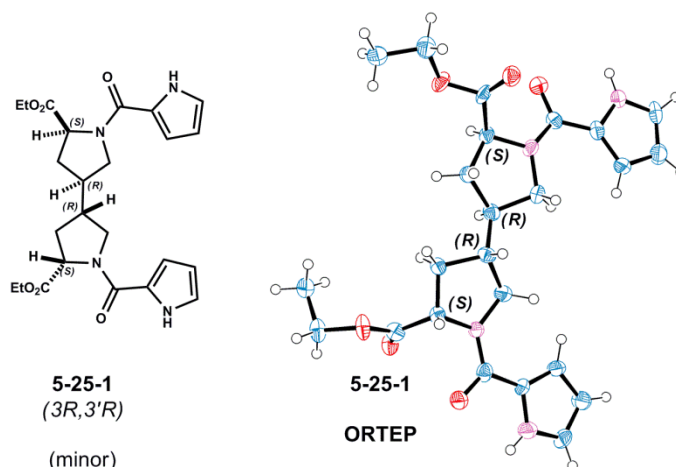


**Figure 5.6.** Characterization of minor  $C_2$ -symmetric diastereomer **5-25-1** ( $3R,3'R$ ) (X-ray structure - ORTEP)

Fortuitously, a crystal grown from a solution of  $DMSO-d_6$  suitable for X-ray diffraction was obtained for  $C_2$ -symmetric dimer **5-25-1** (CCDC 942604).<sup>[15]</sup> The structure of **5-25-1** (Figure 5.6, ORTEP representation) was insightful, as attempts to distinguish between **5-25-1** and **5-25-2** based on 2-D ROESY correlation experiments (500 MHz,  $DMSO-d_6$ ) were inconclusive. Absolute stereochemistry can be assigned to  $C_2$ -symmetric dimers directly as ( $3R,3'R,5S,5'S$ ) for **5-25-1** and ( $3S,3'S,5S,5'S$ ) for **5-25-2**. Moreover, diastereomer **5-25-1** can be described as the product of two reactive pyrrolidine monomers whose 3,3' C–C bond formed with retention of original configuration from bromide **5-22**. By analogy, diastereomer **5-25-2** arises from 3,3' C–C bond formation with net inversion of original bromide **5-22** configuration. This 1,3-diastereomeric relationship was important to our understanding of 3,3' C–C bond formation in dimerization events with subsequent nickel-catalyzed methods (*vide infra*).

### 5.2.2 Development of New Methods for the Homodimerization of **5-22**, Elaboration of Dimers (**5-23**) to Target *N*-acylated Dimers (**5-25-1** and **5-25-2**).

As previously mentioned, the CuI, Zn promoted homodimerization of **5-22** (Scheme 5.1) was not a suitable method for the selective preparation of either desired  $C_2$ -symmetric dimer **5-25-1** or **5-25-2**. We next examined a nickel-catalyzed reductive dimerization of **5-22** (Figure 5.7). Initial dimerization experiments with catalytic NiCl<sub>2</sub>·glyme (**A**) (Table 5.1, Entry 3<sup>[12a]</sup> and 4<sup>[12b]</sup>), tridentate pyridine ligands (**5-28**, **5-18**<sup>[16]</sup>), co-reductant Mn<sup>[12b]</sup> (2 equiv) in dimethylacetamide were promising. Notably, the use of NiCl<sub>2</sub>·glyme (**A**) in place of Ni(COD)<sub>2</sub> was procedurally convenient.<sup>[12bc]</sup> The failure of ligand **5-28** is a result that should be re-examined.<sup>[12b,17]</sup> However, we were intrigued by the potential for ligand-induced stereocontrol (Entry 4) and pursued the use of ligand **5-18**.

The results of extensive optimization are summarized in Figure 5.7 and Table 5.1. Entries 1 and 2 contrast the nickel-catalyzed results with Wurtz-type reductive dimerization of **5-22** using stoichiometric CuI and co-reductant Zn. An initial ligand screen indicated tridentate L-isoleucine derived pybox **5-18** (Entry 4) was superior to achiral tridentate ligand, tri-4-*tert*-butyl terpyridine **5-28** (Entry 3).<sup>[17]</sup> Control experiments with ligand **5-18** were conducted to optimize for reaction temperature, catalyst loading, and co-reductant Mn form (powder vs. granular) while maintaining diastereocontrol (Entry 5-9). Optimal conditions were found using 5 mol% NiCl<sub>2</sub>·glyme, 6.25 mol% **5-18**, and 2 equiv Mn (either granular or powdered form) in 1.0 M DMA at 0°C (Entry 12). An interesting result (Entry 10) was obtained when achiral tridentate pybox ligand **5-26** is employed. The experiment suggested that diastereocontrol may be substrate dependent, putatively through 1,3-diastereoiduction. However, direct comparison to chiral ligand **5-18** is not possible because the reaction requires heating for achiral ligand **5-26** to dissolve. The results

of Entry 11 with novel bidentate ligand **5-27** are tentative, with initial experiments indicating no productive reaction occurred.<sup>[18]</sup>

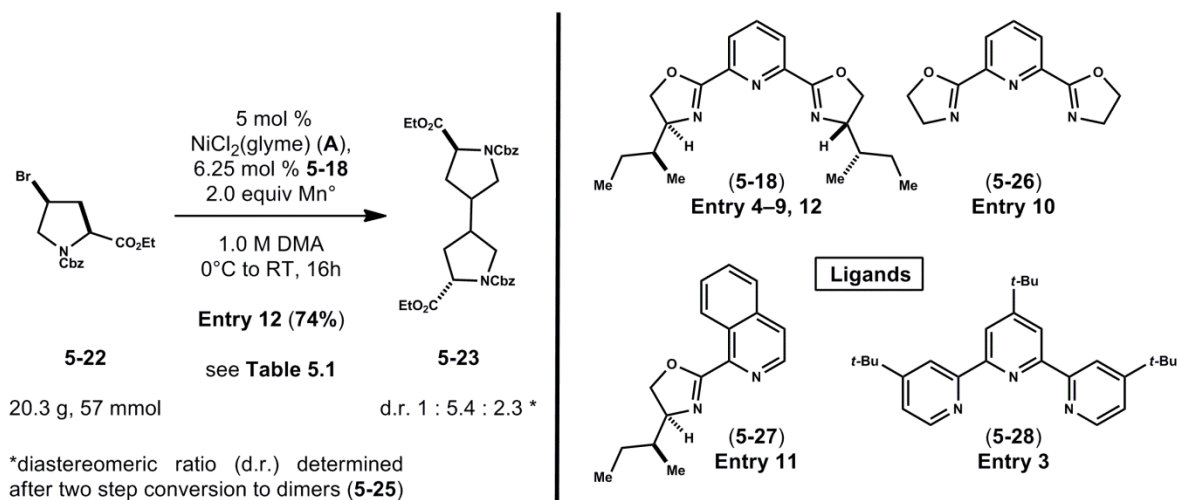


**Figure 5.7.** Nickel-catalyzed reductive homodimerization - Optimization of diastereoselectivity and yield (see Table 5.1).

**Table 5.1** Optimization of metal catalyzed reductive dimerization of bromide **5-22**.

Reactions were conducted with bromide **5-22**. Experiments employed metal-catalysis (CuI, Entry 1, 2 or NiCl<sub>2</sub>·glyme (**A**), Entry 3-12), ligand (**5-18**, **5-26**, **5-27**, **5-28**, Entry 3-12), and stoichiometric co-reductant (powdered Zn, Entry 1, 2 or Mn, Entry 3-12). With the exception of bi-phasic experiments (Entry 1, benzene / H<sub>2</sub>O and Entry 2 acetone / H<sub>2</sub>O), all were conducted in degassed polar aprotic solvent. Product diastereomeric ratio (d.r.) was inferred from d.r. observed (HPLC, UV analysis) after two-step conversion to dimers **5-25**.

<b>E</b>	<b>Catalyst / Ligand</b>	<b>Reductant</b>	<b>Solvent</b>	<b>Conc. / Temp. (°C)</b>	<b>Duration / Yield</b>	<b>d.r. 25-1:25-2:25-3</b>	<b>Notes</b>
<b>1</b>	1.0 eq CuI	2.0 eq Zn*	benzene	0.3 M RT, 0	16-20h <b>17-25%</b>	<b>1 : 1.2 : 2</b>	*reaction black with addition of Zn
<b>2</b>	1.0 eq CuI	2.0 eq Zn*	acetone	0.3 M RT, 0	16-20h <b>18-32%</b>	<b>1 : 1.4 : 2</b>	*reaction black with addition of Zn
<b>3</b>	2 mol % <b>A</b> 2 mol % <b>5-28</b>	2.0 eq Mn (granular)	DMA	1.0 M 40	ND (16h) <b>&lt;5%</b>	<b>NA</b>	product not isolated (LC/MS)
<b>4</b>	2 mol % <b>A</b> 2.5 mol % <b>5-18</b>	2.0 eq Mn (granular)	DMA	1.0 M 40	ND (16h) <b>32%*</b>	<b>1 : 3.4 : 3.8</b>	*approx. 40% conv. ( <b>5-22</b> major)
<b>5</b>	5 mol % <b>A</b> 6.25 mol % <b>5-18</b>	2.0 eq Mn (granular)	DMA	1.0 M 50	2.5h (12h) <b>59%</b>	<b>1 : 3.6 : 2</b>	--
<b>6</b>	10 mol % <b>A</b> 12.5 mol % <b>5-18</b>	2.0 eq Mn (powder)	DMA	1.0 M RT (23)	2.5h <b>65%*</b>	<b>1 : 4.4 : 2.9</b>	*yield calc. from ½ of crude
<b>7</b>	10 mol % <b>A</b> 12.5 mol % <b>5-18</b>	2.0 eq Mn (powder)	DMA	1.0 M 0	4.5h <b>71%</b>	<b>1 : 5.7 : 3.3</b>	set-up at 0°C, 2–4°C (fridge), see Entry 7
<b>8a</b>	10 mol % <b>A</b> 12.5 mol % <b>5-18</b>	2.0 eq Mn (granular)	DMA	1.0 M 0	4.5h* (10h) <b>75%</b>	<b>1 : 5.5 : 6.2</b>	*run overnight (est. complete at 4.5h) see Entry 7
<b>8b</b>	10 mol % <b>A</b> 12.5 mol % <b>5-18</b>	2.0 eq Mn (powder)	DMA	1.0 M 0	4.5h* (10h) <b>65%</b>	<b>1 : 5.1 : 2.5</b>	*run overnight (est. complete at 4.5h) see Entry 7
<b>9</b>	5 mol % <b>A</b> 6.25 mol % <b>5-18</b>	2.0 eq Mn (powder)	DMA	1.0 M 0	16h <b>43%</b>	<b>1 : 5.9 : 2.2</b>	*approx. 50% conv. ( <b>5-22</b> major), reaction slows at 0°C
<b>10</b>	5 mol % <b>A</b> 6.25 mol % <b>5-26</b>	2.0 eq Mn (powder)	DMA	1.0 M 0 to 50*	16h <b>65%</b>	<b>1 : 4.5 : 5.6</b>	*requires heating, <b>5-26</b> insoluble at lower temp.
<b>11</b>	5 mol % <b>A</b> 6.25 mol % <b>5-27</b>	2.0 eq Mn (powder)	DMA	1.0 M 0 to 50*	16h <b>&lt;5%</b>	<b>NA</b>	*no reaction, product not isolated (LC/MS)
<b>12</b>	5 mol % <b>A</b> 6.25 mol % <b>5-18</b>	2.0 eq Mn (powder)	DMA	1.0 M 0 to RT	16h <b>74%</b>	<b>1 : 5.4 : 2.3</b>	*90% conv., 20.3 g <b>5-22</b> scale

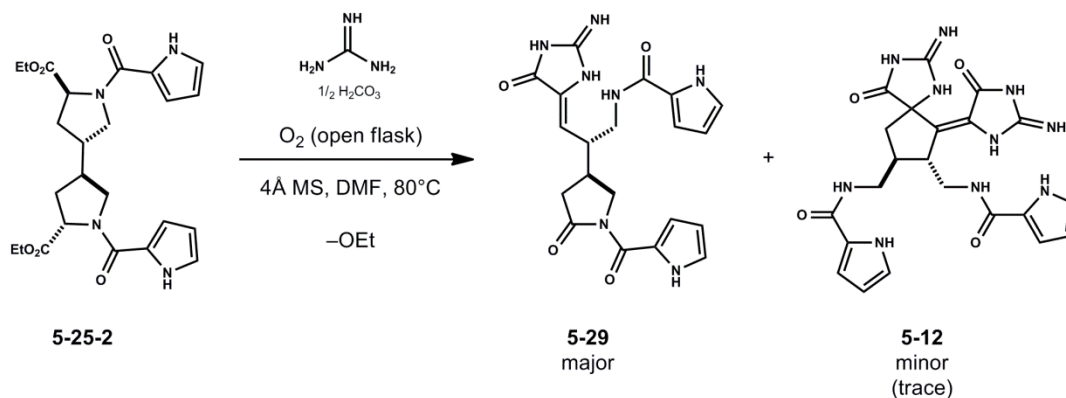


Optimized conditions (Entry 12) afforded elaborated dimers **5-25** with improved diastereoselectivity (d.r. 1:5.4:2.3) and high yield. Interestingly, the favored  $C_2$ -diastereomer in all dimerization experiments was **5-25-2** (Figure 5.5). This suggested an inherent selectivity for 3,3' C–C bond formation to occur with inversion of bromide **5-22** configuration. This selectivity is presumably due in part to 1,3-diastereoiduction, as well as ligand-assisted catalyst control. Further experiments with the (4*R*)-epimer of bromide **5-22** would be informative. Additionally, one could employ the enantiomer of ligand **5-18**, as derived from *D*-isoleucine, in analogous homodimerization experiments to determine whether observed diastereoselectivity is matched or mismatched with monomer substrate **5-22**.

### 5.2.3 Auto-oxidative Guanidine Incorporation of Precursor ‘dispacamide’ Dimer (5-25-2).

*The following research is a summary of preliminary results obtained for a series of reactions conducted with purified  $C_2$ -symmetric dimer 5-25-2. Similar results were obtained with its 3,3' epimer 5-25-1 to afford the same products albeit as optical antipodes. Currently, discovery research is being conducted with enriched mixtures of  $C_2$ -symmetric dimers 5-25-1 and 5-25-2 (~ d.r. 1:5.4). As characterized, the major  $C_2$ -symmetric dimer 5-25-2 would lead to natural antipodes of pyrrole–imidazole alkaloids (e.g. (–)-ageliferin).*

Following optimized procedures (*vide supra*), *N*-acylated 3,3'-bipyrrolidine dimers **5-25** can be routinely prepared in three steps from monomer **5-22** in good yield and diastereoselectivity. After precipitation of the pseudo-‘*meso*’-dimer **5-25-3** from  $\text{CHCl}_3$ , an enriched mixture of  $C_2$ -symmetric dimers **5-25-1** and **5-25-2** (d.r. 1 : 5.4) is obtained. Further purification by column chromatography affords either antipode for subsequent auto-oxidation studies. The major dimer **5-25-2** is depicted throughout the following schemes.

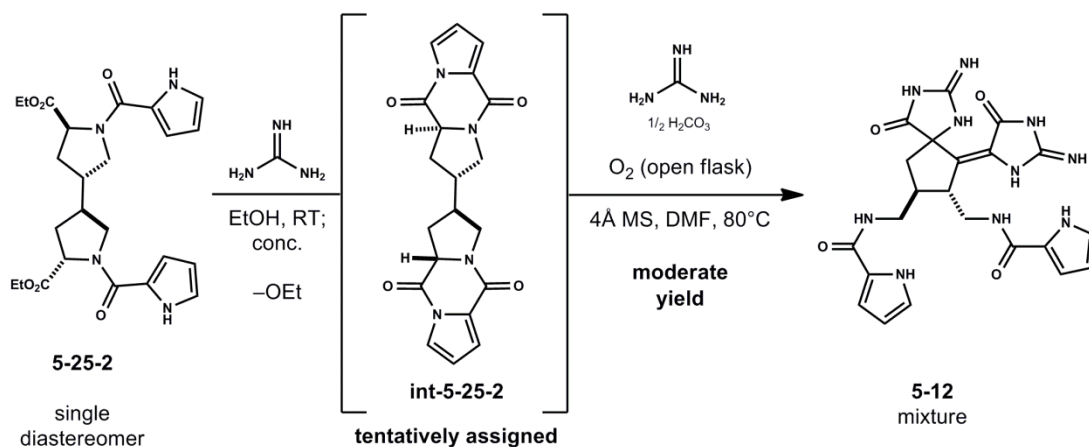


**Scheme 5.3.** Initial auto-oxidative guanidine incorporation attempts - initial method requires attention.

Preliminary experiments with dimer **5-25-2** showed promising results. When **5-25-2** (Scheme 5.3) was dissolved in anhydrous DMF and treated with guanidine carbonate under aerobic conditions with heating, several new products were observed. LC/MS analysis indicated that guanidine was incorporated into target dimeric products, though inefficiently. Interestingly, the major compound identified as **5-29** indicated oxidation had occurred at both  $\alpha$ -centers, and subsequently diverged to a desymmetrized product. Though mechanistic details are as of yet unclear, the mono-alkylidene glycohydrazide<sup>[19]</sup> **5-29** suggested reactivity observed by Al-Mourabit in monomeric systems<sup>[2ac]</sup> is directly translated in dimeric substrates. Compound **5-29** also contains a pyrrolidinone moiety, putatively arising from decarboxylation of an intermediate dioxetanone (see Figure 5.2, **5-5**). Pyrrolidinone by-products have also been observed by Al-Mourabit.<sup>[2a]</sup> We were nonetheless encouraged by the observation of trace products (LC/MS, MS analysis) with the correct mass for dual-oxidation and guanidine incorporation. It was apparent that this initial method would require refinement.

We proposed that compound **5-29** predominated due to inefficient guanidine addition into electrophilic  $\alpha$ -oxidized dimeric intermediates. A minor procedural change addressed this issue. When dimer **5-25-2** (Scheme 5.4) is initially treated with the free-base of guanidine in EtOH in the absence of air an uncharacterized intermediate **int-5-25-2** was formed. We posited that

guanidine could add to the ester functionality in **5-25-2** with loss of EtOH to form an *N*-acylated bis-guanidine intermediate (not shown).<sup>[20]</sup> This activated intermediate may undergo intramolecular displacement with loss of guanidine (2 equiv) to form bis-diketopiperazine **int-5-25-2** (Scheme 5.4) as an ideal substrate for subsequent auto-oxidation experiments.<sup>[21]</sup> *Characterization of intermediates along this pathway remains tentative, however this procedural modification proved advantageous.*

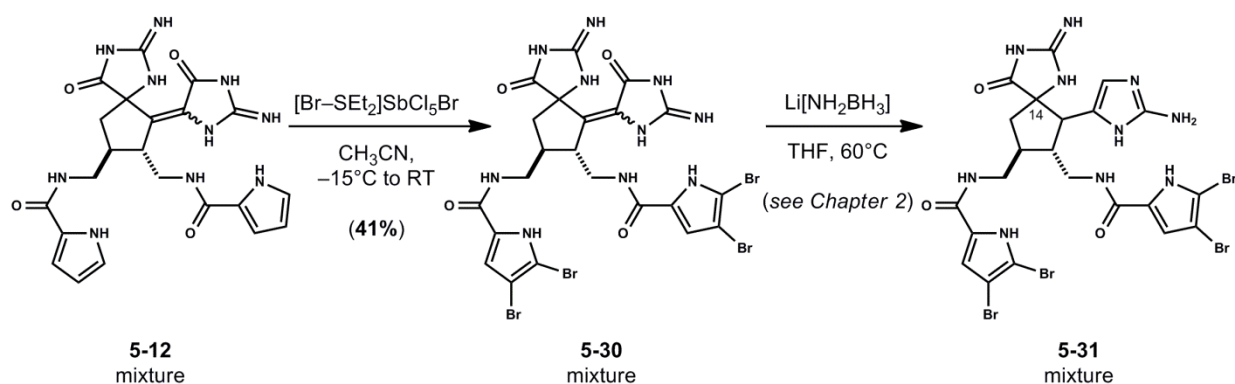


**Scheme 5.4.** Optimized conditions for the auto-oxidative incorporation of guanidine: reaction requires initial activation with guanidine followed by auto-oxidative incorporation of guanidine.

Following activation of diester **5-25-2** with guanidine, crude **int-5-25-2** was treated with guanidine carbonate under aerobic conditions to afford a mixture of diastereomeric spirocycloalkylidenes **5-12** (Scheme 5.4). The result is remarkable. Presumably, spirocycloalkylidenes **5-12** arise from a series of indeterminate events: dual  $\alpha$ -oxidation, dual incorporation of guanidine, and spirocyclization. The proposed 5-*exo*-trig spirocyclization event parallels reactivity previously observed in our research (see Chapter 2).<sup>[1c]</sup> In addition, we have not isolated any compounds suggestive of bis-alkylidene **5-10** composition (Figure 5.2). We believe that isomeric intermediates (*e.g.* bis-spirocycles **5-11**) proceed directly to products **5-12** under base catalysis. The reaction is involved and provides a mixture of several products. We have isolated and tentatively characterized individual isomers of **5-12** by analogy to previously

prepared pyrrole brominated spirocycloalkylidenes (*vide infra*, Scheme 5.5, and see Chapter 2). Efforts to optimize the oxidation reaction and purification to prepare **5-12** are ongoing.

Preliminary experiments suggested spirocycloalkylidene **5-12** mixtures could be converted to a corresponding mixture of tetrabrominated spirocycloalkylidenes **5-30** with Snyder's bromodiethylsulfonium bromopentachloroantimonate (BDSB) (Scheme 5.5).<sup>[22]</sup> Reactions with Br<sub>2</sub> or NBS in THF were inefficient and resulted in substantial overoxidation. Separation and complete characterization of diastereomeric brominated spirocycloalkylidenes **5-30** is ongoing. Access to **5-30** conveniently intercepts a previous synthetic intermediate described in Chapter 2 now accessible in presumed optically active form. Following previously developed conditions, the diastereomeric mixture **5-30** can be reduced with lithium amidotrihydroborate (LAB)<sup>[1c,23]</sup> to afford the corresponding mixture of aminoimidazoles **5-31**. Preliminary results indicated the desired diastereomer containing relative stereochemistry as shown in **5-31c** (Scheme 5.6) could be separated from the resultant mixture. Efforts to optimize this sequence (Scheme 5.5) are ongoing.

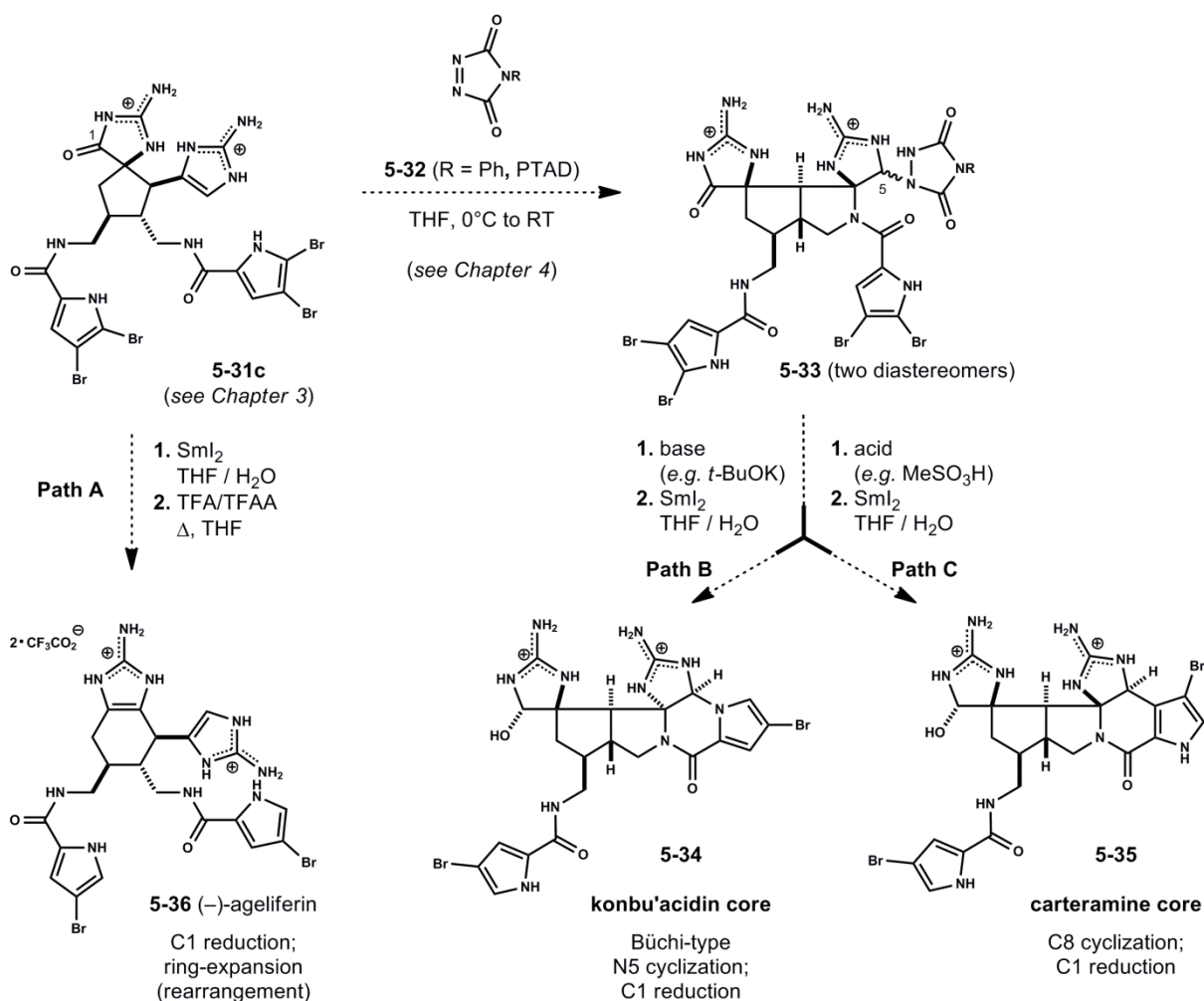


**Scheme 5.5.** Elaboration of spirocycloalkylidenes **5-12**: Controlled tetrabromination of **5-12** (mixture) with bromodiethylsulfonium bromopentachloroantimonate (BDSB); Glycocyamidine reduction of **5-30** (mixture) with lithium amidotrihydroborate (LAB).

This route provided rapid access to desired tetrabrominated spirocycloalkylidenes **5-12** in four steps from monomer **5-22**. The strategy combines compelling auto-oxidative reactivity as described by Al-Mourabit in monomeric systems<sup>[2]</sup> (Figure 5.2) followed by a remarkable

spirocyclization event in a dimeric systems to provide optically active spirocycloalkylidenes **5-12**. The mixture can be elaborated in two steps to aminoimidazole **5-31c** en route to (-)-ageliferin **5-36** and related dimeric pyrrole–imidazole alkaloids (Scheme 5.6).

### 5.2.4 Future Research: Endgame Strategies for the Synthesis of (-)-Ageliferin (**5-36**) and Intact Konbu'acidin (**5-34**) and Carteramine (**5-35**) Cores from a Common, Optically Active Intermediate (**5-31c**).



**Scheme 5.6.** Novel oxidative spirocyclization of **5-31c** utilizes 4-phenyl-1,2,4-triazole-3,5-dione (PTAD) **5-32** to access stable azabicyclo[3.3.0]octane adducts **5-33**. Various cyclization/rearrangement modes may enable syntheses of (-)-ageliferin **5-36** (Path A), konbu'acidin core **5-34** (Path B) and carteramine core **5-35** (Path C).

Preliminary experiments suggested aminoimidazole **5-31c** undergoes oxidation with phenyl-1,2,4-triazoline-3,5-dione (PTAD) **5-32** (Scheme 5.6) and related 1,2,4-triazoline-3,5-diones (see Chapter 4). This observed oxidation parallels ene-type reactivity of PTAD whereby a putative iminium ion intermediate generated from oxidation of the aminoimidazole moiety in **5-31c** is trapped by the pendant amide to form tentatively assigned azabicyclo[3.3.0]octane core **5-33** as a 1:1 mixture of C5 diastereomers in moderate yield. We envision divergent product outcomes from variable cyclization modes induced with strong base (Path B, Step 1, *e.g.* *t*-BuOK)<sup>[24]</sup> or strong acid (Path C, Step 1, *e.g.* MeSO<sub>3</sub>H)<sup>[25]</sup> and subsequent controlled reductions (Step 2, C1, C6' and C6'' reduction)<sup>[1cd,26]</sup> to form des-halo (C6', C6'', C13) konbu'acidin<sup>[27]</sup> **5-34** and des-halo (C6', C6'', C13) carteramine<sup>[28]</sup> **5-35**, respectively. In addition, we recognize the potential to access ageliferin **5-36** in optically active forms (derived from either *anti*-3,3'-bipyrrolidine dimer **5-25-1** or **5-25-2**), via initial glycoyamidine reduction (Step 1, C1 reduction)<sup>[1d]</sup> and subsequent ring expansion of an intermediate *N*-acyl amidinyliminium ion (Step 2, see Chapter 3).<sup>[1d]</sup>

### 5.3 Conclusion.

We have demonstrated the auto-oxidative incorporation of guanidine into *trans*-4-hydroxy-L-proline derived dimers **5-25-1** and **5-25-2**. This chemistry generates putative glycoamidines which confer the reactivity of proposed intermediates bis-alkylidene **5-10** and bis-spirocycles **5-11** (Figure 5.2) as fleeting intermediates that ultimately funnel to thermodynamically favored spirocyclic alkylidenes **5-12**. We propose a cascading process consistent with similar equilibria observed in dispacamide dimers previously studied by us (*see Chapter 2*). The requisite for 3,3'-bipyrrolidine precursors **5-25** (here termed dispacamide dimer precursors), led to the adaptation of procedures for the nickel-catalyzed reductive dimerization of *trans*-4-hydroxy-L-proline derivative **5-22** with moderate diastereocontrol. The homodimerization procedure marks an advance in the reductive dimerization of secondary alkyl halides with catalyst and substrate control of diastereoselectivity. These initial efforts provide access to optically active dispacamide dimer precursors **5-25**. The route conveniently intercepts a common intermediate aminoimidazole **5-31c** studied previously (*see Chapters 2 & 3*) by a considerably shortened synthetic sequence (6 steps from monomer **5-22**). Although preliminary findings are promising, the route requires procedural refinements and further investigation to complete proposed endgame strategies.

## 5.4 References and Notes.

[1] (a) Garrido-Hernandez, H.; Nakadai, M.; Vimolratana, M.; Li, Q.; Doundoulakis, T.; Harran, P. G. *Angew. Chem. Int. Ed.* **2005**, *44*, 765; (b) Li, Q.; Hurley, P.; Ding, H.; Roberts, A. G.; Akella, R.; Harran, P. G. *J. Org. Chem.* **2009**, *74*, 5909; (c) Ding, H.; Roberts, A. G.; Harran, P. G. *Angew. Chem. Int. Ed.* **2012**, *51*, 4416; (d) Ding, H.; Roberts, A. G.; Harran, P. G. *Chem. Sci.* **2013**, *4*, 303.

[2] (a) Travert, N.; Al-Mourabit, A. *J. Am. Chem. Soc.* **2004**, *126*, 10252; (b) Vergne, C.; Boury-Esnault, N.; Perez, T.; Martin, M.-T.; Adeline, M.-T.; Du, E. T. H.; Al-Mourabit, A. *Org. Lett.* **2006**, *8*, 2421; (c) Vergne, C.; Appenzeller, J.; Ratinaud, C.; Martin, M.-T.; Debitus, C.; Zaparucha, A.; Mourabit, A. *Org. Lett.* **2008**, *10*, 493.

[3] (a) The formation and decomposition of firefly dioxetanone: Min, C.; Ren, A.; Li, X.; Guo, J.; Zou, L.; Sun, Y.; Goddard, J. D.; Sun, C. *Chem. Phys. Lett.* **2011**, *506*, 269; (b) For a theoretical mechanistic study pertaining to firefly bioluminescence: Orlova, G.; Goddard, J. D.; Brovko, L. Y. *J. Am. Chem. Soc.* **2003**, *125*, 6962 and references cited therein.

[4] For Kolbe electrolysis dimerization methods of substrates comparable to **5-14a**: Hiebl, J.; Blanka, M.; Guttman, A.; Kollmann, H.; Leitner, K.; Mayrhofer, G.; Rovenszky, F.; Winkler, K. *Tetrahedron* **1998**, *54*, 2059.

[5] Barton, D. H.; Bridon, D.; Fernandez-Picot, I.; Zard, S. Z. *Tetrahedron* **1987**, *43*, 2733.

[6] For the preparation of **5-14b** (R = Me): Bridges, R. J.; Tanley, M. S.; Anderson, M. W.; Cotman, C. W.; Chamberlin, A. R. *J. Med. Chem.* **1991**, *34*, 717.

[7] (a) Wurtz, A. *Ann. Chim. Phys.* **1855**, *44*, 275; For selected methods see: (b) Coupling of alkyl and aryl halides in the presence of lithium metal and ultrasound: Lash, T. D.; Berry, D. J. *Chem. Educ.* **1985**, *62*, 85 and references cited therein; (c) Wurtz-type coupling with Manganese/Cupric Chloride in aqueous media: Ma, J.; Chan, T-H. *Tetrahedron Lett.* **1998**, *39*, 2499.

[8] We initially considered various transition-metal alternatives to nickel-catalysis. For selected methods, see: (a) Cobalt-catalyzed cross-coupling reactions: Cahiez, G.; Moyeux, A. *Chem. Rev.* **2010**, *110*, 1435; (b) For an example of reductive cobalt-catalysis in the synthesis of dimeric sesquiterpene lactones: Bagal, S. K.; Adlington, R. M.; Baldwin, J. E.; Marquez, R. *J. Org. Chem.* **2004**, *69*, 9100; (c) For CoCl(PPh<sub>3</sub>)<sub>3</sub> promoted dimerization of tertiary benzylic halides: Schmidt, M. A.; Movassaghi, M. *Angew. Chem. Int. Ed.* **2007**, *46*, 3725; (d) Copper catalyzed cross-coupling of non-activated secondary alkyl halides: Yang, C-T.; Zhang, Z-Q.; Liang, J.; Liu, J-H.; Lu, X-Y.; Chen, H-H.; Liu, L. *J. Am. Chem. Soc.* **2012**, *134*, 11124.

[9] For a comprehensive review on nickel-catalyzed cross-coupling of non-activated alkyl halides: Hu, X.; *Chem. Sci.* **2011**, *2*, 1867 and references cited therein.



[10] Reductive coupling of alkyl halides in aqueous media: De Sá, A. C. P. F.; Pontes, G. M. A.; dos Anjos, J. A. L.; Santana, S. A.; Bieber, L. W.; Malvestiti, I. *J. Braz. Chem. Soc.* **2003**, *14*, 429.

[11] Diastereocontrol was achieved in a similar C–C bond forming reaction. Using a comparable radical precursor, (2*S*,3*R*,4*R*)-1-benzyl 2-methyl 3-hydroxy-4-iodopyrrolidine-1,2-dicarboxylate, the 3-hydroxyl group was required to control facial selectivity during C–C bond formation at the 4-position. Ueda, M.; Ono, A.; Nakao, D.; Miyata, O.; Naito, T. *Tetrahedron Lett.* **2007**, *48*, 841.

[12] (a) Nickel-catalyzed reductive cross-coupling of unactivated alkyl halides: Yu, X.; Yang, T.; Wang, S.; Xu, H.; Gong, H. *Org. Lett.* **2011**, *13*, 2138; (b) Nickel-catalyzed reductive dimerization of alkyl halides: Prinsell, M. R.; Everson, D. A.; Weix, D. J. *Chem. Comm.* **2010**, *46*, 5743; (c) Ligand assisted nickel-catalyzed homocoupling of unactivated alkyl halides: Goldup, S. M.; Leigh, D. A.; McBurney, R. T.; McGonigal, P. R.; Plant, A. *Chem. Sci.* **2010**, *1*, 383.

[13] For the preparation of bromide **5-22** see experimental and Ref. 6. For the synthesis of the corresponding methyl ester **5-15b** (Figure 5.3, R = CH<sub>3</sub>) see: Wieland, T.; Schermer, D.; Rohr, G.; Faulstich, H. *Justus Liebigs Annalen der Chemie* **1977**, 806.

[14] The carbon spectrum (125 MHz, DMSO-*d*<sub>6</sub>) of **5-25-3** possessed 21 discrete <sup>13</sup>C resonances, of which 3 signals are coincident (presumed 2C per resonance) and account for 24C as confirmed by HSQC experiments (500 MHz, DMSO-*d*<sub>6</sub>).

[15] CCDC 942604 (Compound **5-25-2**) contain the supplementary crystallographic data for this chapter. These data can be obtained free of charge from The Cambridge Crystallographic Data Centre via [www.ccdc.cam.ac.uk/data\\_request/cif](http://www.ccdc.cam.ac.uk/data_request/cif).

[16] For the preparation of Pybox ligands **5-18** and **5-26**: Nishiyama, H.; Kondo, M.; Nakamura, T.; Itoh, K. *Organometallics* **1991**, *10*, 500.

[17] Ligand **5-28** was successful in comparable systems (see Ref. 12b and 12c) and could be operative under alternative conditions. For mechanistic studies involving terpyridine ligands (*e.g.* **5-28**): Jones, G. D.; Martin, J. L.; McFarland, C.; Allen, O. R.; Hall, R. E.; Haley, A. D.; Brandon, J.; Konovalova, T.; Desrochers, P. J.; Pulay, P.; Vicic, D. A. *J. Am. Chem. Soc.* **2006**, *128*, 13175.

[18] The use of novel ligand **5-27** was inspired by a recent method, see: Binder, J. T.; Cordier, C. J.; Fu, G. C. *J. Am. Chem. Soc.* **2012**, *134*, 17003.

[19] The term *glycocyamidine* refers to heterocyclic structures of type **2-1** which is often described as a 2-imino analog of the commonly known hydantoin heterocycle. The systematic name for glycocyamidine is 2-imino-4-imidazolidinone. For a review of glycocyamidine chemistry: Lempert, C. *Chem. Rev.* **1959**, *59*, 667.

- [20] Acylguanidines as activated intermediates for peptide synthesis: Hoffmann, E.; Diller, D. *Can. J. Chem.* **1965**, *43*, 3103.
- [21] Pyrrole-assisted oxidation of cyclic  $\alpha$ -amino acid derived diketopiperazines: Tian, H.; Ermolenko, L.; Gabant, M.; Vergne, C.; Moriou, C.; Retaillieu, P.; Al-Mourabit, A. *Adv. Synth. Catal.* **2011**, *353*, 1525.
- [22] Snyder, S. A.; Treitler, D. A.; Brucks, A. P. *J. Am. Chem. Soc.* **2010**, *132*, 14303.
- [23] Lithium amidotrihydroborate (LAB) reagent: Myers, A. G.; Yang, B. H.; Kopecky, D. J. *Tetrahedron Lett.* **1996**, *37*, 3623.
- [24] For a biomimetic synthesis of dibromophakellin see via a similar *N*-cyclization mode: Foley, L. H.; Büchi, G. *J. Am. Chem. Soc.* **1982**, *104*, 1776.
- [25] For C-bond formation under similar conditions using MeSO<sub>3</sub>H see: (a) Oxidative homo- and hetero-dimerization of alkyl substituted 2-aminoimidazoles: Xu, Y.; Yakushijin, K.; Horne, D. A. *J. Org. Chem.* **1996**, *61*, 9569; (b) Synthesis of stevensine: Xu, Y.; Yakushijin, K.; Horne, D. A. *J. Org. Chem.* **1997**, *62*, 456.
- [26] Dehalogenation with SmI<sub>2</sub> and related single-electron reductants: (a) For a selective monodebromination with concomitant deprotection using Zn, HOAc, MeOH, 40°C: Wang, S.; Romo, D. *Angew Chem. Int. Ed.* **2008**, *47*, 1284; (b) For a related monodebromination using SmI<sub>2</sub>, THF; MeOH: Jacquot, D. E. N.; Zollinger, M.; Lindel, T. *Angew. Chem. Int. Ed.* **2005**, *44*, 2295.
- [27] Konbu'acidin A isolation: Kobayashi, J.; Suzuki, M.; Tsuda, M. *Tetrahedron* **1997**, *53*, 15681.
- [28] Carteramine A isolation: Kobayashi, H.; Kitamura, K.; Nagai, K.; Nakao, Y.; Fusetani, N.; van Soest, R. W. M.; Matsunaga, S. *Tetrahedron Lett.* **2007**, *48*, 2127.

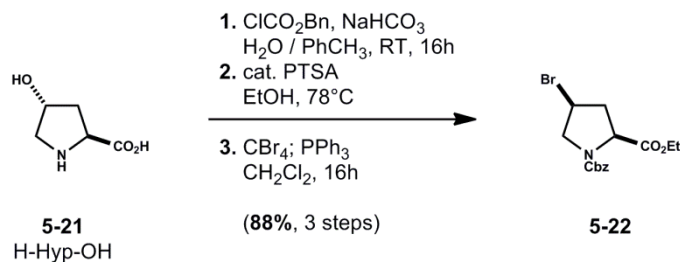
## 5.5 Experimental.

### 5.5.1 Materials and Methods.

Unless stated otherwise, reactions were performed under an argon (Ar) atmosphere in flame-dried glassware. Tetrahydrofuran (THF), chloroform (CHCl<sub>3</sub>), methylene chloride (CH<sub>2</sub>Cl<sub>2</sub>), diethyl ether (Et<sub>2</sub>O), toluene (PhCH<sub>3</sub>), benzene (PhH), dimethoxyethane (DME), *N,N*-dimethyl formamide (DMF), *N,N*-dimethylacetamide (DMA) and acetonitrile (CH<sub>3</sub>CN) were dried and deoxygenated through activated alumina solvent drying systems or distilled prior to use. NiCl<sub>2</sub>·glyme, powdered Zn, powdered Mn, and granular Mn were obtained from Sigma-Aldrich. Column chromatography was performed on silica gel 60 (SiliCycle, 240-400 mesh). Thin layer chromatography (TLC) and preparative thin layer chromatography (pTLC) utilized pre-coated plates (silica gel 60 PF254, 0.25 mm or 0.5 mm). Purification of advanced intermediates employed an Agilent 1200 Preparative HPLC (pHPLC) system equipped with an Agilent Quadrupole 6130 ESI-MS detector and an automated fraction collector. Mobile phases (Mobile phase A: H<sub>2</sub>O, Mobile Phase B: CH<sub>3</sub>CN) were prepared with 0.1% or 1% trifluoroacetic acid (CF<sub>3</sub>CO<sub>2</sub>H) or 0.1% formic acid as indicated. Advanced intermediates isolated and characterized as trifluoroacetate salts are denoted as (2·CF<sub>3</sub>CO<sub>2</sub>H) in data tables. The trifluoroacetate salt may be omitted from structures in schemes for clarity. NMR spectra were recorded on Bruker Avance spectrometers (500 MHz or 600 MHz). Data for <sup>1</sup>H NMR spectra are reported as follows: chemical shift (δ ppm) (multiplicity, coupling constant (Hz), integration) at 298K, unless stated otherwise, and are referenced to a residual solvent peak. Data for <sup>13</sup>C NMR spectra are reported in terms of chemical shift (δ ppm) and are referenced to residual solvent peak.

## 5.5.2 Experimental Procedures and Characterization Data.

### Synthesis of (2*S*,4*S*)-1-benzyl 2-ethyl 4-bromopyrrolidine-1,2-dicarboxylate (5-22).



(2*S*,4*R*)-1-benzyl 2-ethyl 4-hydroxypyrrolidine-1,2-dicarboxylate prepared from (2*S*,4*R*)-4-hydroxypyrrolidine-2-carboxylic acid (**5-21**) with minor modifications according to Bridges, R. J.; Tanley, M. S.; Anderson, M. W.; Cotman, C. W.; Chamberlin, A. R. *J. Med. Chem.* **1991**, *34*, 717.

(2*S*,4*R*)-4-hydroxypyrrolidine-2-carboxylic acid (**5-21**) (70.0 g, 0.53 mol, 1.0 equiv) and  $\text{NaHCO}_3$  (112.0 g, 1.33 mol, 2.5 equiv) were dissolved in  $\text{H}_2\text{O}$  (1000-mL) in a 2-L round bottom flask to give a viscous light yellow solution. A solution of benzyl chloroformate (88.7-mL, 0.63 mol, 1.2 equiv) in toluene (280-mL) was added to the reaction mixture dropwise via an addition funnel over 20 min at RT. The evolution of  $\text{CO}_2$  (g) was observed and the biphasic reaction was stirred vigorously at RT for 16h. The biphasic reaction mixture was separated and the aqueous layer was washed  $2 \times 300$ -mL with diethyl ether. The aqueous layer was carefully neutralized 6M  $\text{HCl}$  (aq) until an opaque solution was obtained (pH = 2). The acidic aqueous layer was extracted  $4 \times 500$ -mL with EtOAc. The combined organic layers were dried over  $\text{Na}_2\text{SO}_4$ , filtered and concentrated in vacuo to yield (2*S*,4*R*)-1-((benzyloxy)carbonyl)-4-hydroxypyrrolidine-2-carboxylic acid (146 g, crude weight) as a clear foam. The crude (2*S*,4*R*)-1-((benzyloxy)carbonyl)-4-hydroxypyrrolidine-2-carboxylic acid was dissolved in absolute EtOH (2.8-L) followed by the addition of *p*-toluenesulfonic acid (PTSA) (6.0 g, 31.5 mmol, 0.06 equiv) in a 5-L round bottom flask fitted with a 2-L solvent still head and reflux condenser. The clear solution was refluxed with a heating mantle for 16h at which point 2.4-L of EtOH was removed via distillation. The reaction was judged complete by TLC analysis and was cooled to RT. To the viscous solution was added solid  $\text{NaHCO}_3$  (20g) and the mixture was suspended in 500-mL EtOAc. The suspension was stirred for 1h and subsequently filtered through a mixture of Celite-solid  $\text{K}_2\text{CO}_3$ . The filter cake was washed  $3 \times 500$ -mL with EtOAc and the combined organics were concentrated in vacuo to yield (2*S*,4*R*)-1-benzyl 2-ethyl 4-hydroxypyrrolidine-1,2-dicarboxylate (152 g, 0.52 mol, 97%, crude yield) as a clear light yellow oil. The crude (2*S*,4*R*)-1-benzyl 2-ethyl 4-hydroxypyrrolidine-1,2-dicarboxylate (152 g, 0.52 mol, 1.0 equiv) and  $\text{CBr}_4$  (185 g, 0.57 mol, 1.1 equiv) were dissolved in  $\text{CH}_2\text{Cl}_2$  (1.7-L) in a 3-L round bottom flask fitted with a mechanical stirring apparatus. The solution was cooled to 0°C with an ice-water bath followed by the addition of  $\text{PPh}_3$  (164 g, 0.62 mol, 1.2 equiv) in four portions ( $4 \times 41$  g) added every 20 min to maintain RT. The reaction was stirred at RT for 16h until judged complete by TLC analysis. The crude reaction mixture was concentrated in vacuo to remove  $\text{CH}_2\text{Cl}_2$  (approx. 1-L) and precipitates (approx. 140 g) were removed *via* filtration. The filtrate was concentrated (approx. 500-mL total volume) to provide crude **5-22**. The crude filtrate was split into two equal

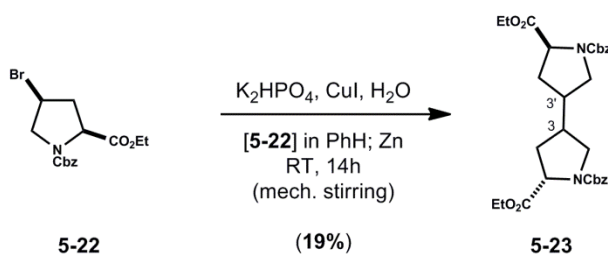
portions and purified by flash column chromatography (approx. 300 g SiO<sub>2</sub> / column). The column was eluted with hexanes (4-L) to remove PPh<sub>3</sub>, hexanes / EtOAc (4:1) (3-L), hexanes / EtOAc (7:3) (3-L) to provide fractions containing **5-22**. The desired fractions from both columns were combined and concentrated in vacuo to give (2*S*,4*S*)-1-benzyl 2-ethyl 4-bromopyrrolidine-1,2-dicarboxylate (**5-22**) (g, %) as a light yellow oil.

**(2*S*,4*S*)-1-benzyl 2-ethyl 4-bromopyrrolidine-1,2-dicarboxylate (**5-22**):**

<sup>1</sup>H NMR (500 MHz, CHCl<sub>3</sub>-*d*<sub>1</sub>): δ (ppm) 7.39-7.28 (m, 5H), 5.22-5.05 (m, 2H), 4.51-4.05 (m, 5H), 3.87-3.76 (m, 1H), 2.91-2.78 (m, 1H), 2.52-2.41 (m, 1H), 1.32-1.13 (m, 3H); <sup>13</sup>C NMR (125 MHz, CHCl<sub>3</sub>-*d*<sub>1</sub>): δ (ppm) 171.4, 171.1, 154.4, 154.0, 136.4, 136.3, 128.7, 128.6, 128.3, 128.25, 128.18, 128.1, 67.6, 67.5, 61.7, 58.6, 58.3, 56.0, 55.6, 42.1, 41.5, 41.1, 40.1, 14.2, 14.1; LRMS-ESI (*m/z*) calcd for [C<sub>15</sub>H<sub>18</sub>BrNO<sub>4</sub>+H]<sup>+</sup>: 356.1; found: 356.1; [α]<sub>D</sub> = -29.5° (c = 1.0, CHCl<sub>3</sub>)

**Synthesis of Dimers (**5-23**) (Method 1).**

**(5*S*,5'*S*)-1,1'-dibenzyl 5,5'-diethyl [3,3'-bipyrrolidine]-1,1',5,5'-tetracarboxylate (**5-23**).**



A solution of K<sub>2</sub>HPO<sub>4</sub> (228 g, 1.21 mol) dissolved in degassed H<sub>2</sub>O (280-mL, sparged for 15 min with Ar) was added to (2*S*,4*S*)-1-benzyl 2-ethyl 4-bromopyrrolidine-1,2-dicarboxylate (**5-22**) (54.7 g, 0.15 mol, 1.0 equiv) in a 500-mL round bottom flask that was stirred vigorously for 5 min to obtain an emulsion, followed by the addition of CuI (29.0 g, 0.15 mol, 1.0 equiv). The heterogeneous mixture was stirred for an additional 5 min and a blue-green color was observed. The reaction was initiated by the addition of degassed benzene (94-mL, sparged for 15 min with Ar) followed by Zn dust (19.7 g, 0.30 mol, 2.0 equiv) in four portions (4 × 4.9 g) added every 20 min until complete. Upon addition of Zn the heterogeneous reaction developed an iridescent and dark black color. The reaction was vigorously stirred at RT for 14h until judged complete by TLC analysis. The crude biphasic reaction was carefully quenched by the addition of 6M HCl (aqueous layer, pH = 3) and the dark precipitous mixture was filtered through Celite and the filter cake was washed 3 × 300-mL with CHCl<sub>3</sub>. The combined organics were washed with water (200-mL), brine (200-mL), dried over Na<sub>2</sub>SO<sub>4</sub>, filtered and concentrated in vacuo to provide a crude colorless oil. The oil was diluted with CHCl<sub>3</sub> (15-mL) and purified by flash column chromatography (approx. 300 g SiO<sub>2</sub>). The column was eluted with hexanes (2-L), hexanes / EtOAc (4:1) (2-L), hexanes / EtOAc (7:3) (2-L), hexanes / EtOAc (3:2) to provide fractions containing **5-23** as an inseparable mixture of three diastereomers (**5-23**, R<sub>f</sub> = 0.3, hexanes / EtOAc (3:2)). The desired fractions were concentrated in vacuo to give (5*S*,5'*S*)-1,1'-dibenzyl 5,5'-diethyl [3,3'-bipyrrolidine]-1,1',5,5'-tetracarboxylate (**5-23**) (7.6 g, 18%) as a colorless oil.

**Note 1:** The same experiment conducted at 0°C with prolonged reaction time is possible although no appreciable increase in yield is observed (range of yields obtained from multiple runs, 17–26%).

**Note 2:** The same experiment conducted at RT or 0°C with acetone used in place of benzene yields dimers (5-23) in comparable yield (range of yields obtained from multiple runs, 18–32%). Although acetone is used as the organic solvent, the reaction is still biphasic.

**(5*S,S'*)-1,1'-dibenzyl 5,5'-diethyl [3,3'-bipyrrolidine]-1,1',5,5'-tetracarboxylate (5-23) (mixture):**

<sup>1</sup>H NMR (500 MHz, CHCl<sub>3</sub>-*d*<sub>1</sub>): δ (ppm) 7.39-7.26 (m, 10H), 5.21-5.01 (m, 4H), 4.47-4.35 (m, 1H), 4.34-4.24 (m, 1H), 4.23-4.14 (m, 2H), 4.14-3.69 (m, 4H), 3.20-3.01 (m, 2H), 2.48-2.34 (m, 1H), 2.31-2.16 (m, 1H), 2.16-1.97 (m, 2H), 1.96-1.82 (m, 1H), 1.73-1.59 (m, 1H), 1.32-1.19 (m, 3H), 1.19-1.03 (m, 3H); LRMS-ESI (*m/z*) calcd for [C<sub>30</sub>H<sub>36</sub>N<sub>2</sub>O<sub>8</sub>+H]<sup>+</sup>: 553.3; found: 553.3.

**General Procedure for NiCl<sub>2</sub>(glyme) (A), Ligand, Mn Catalyzed Homocoupling of (5-22).**

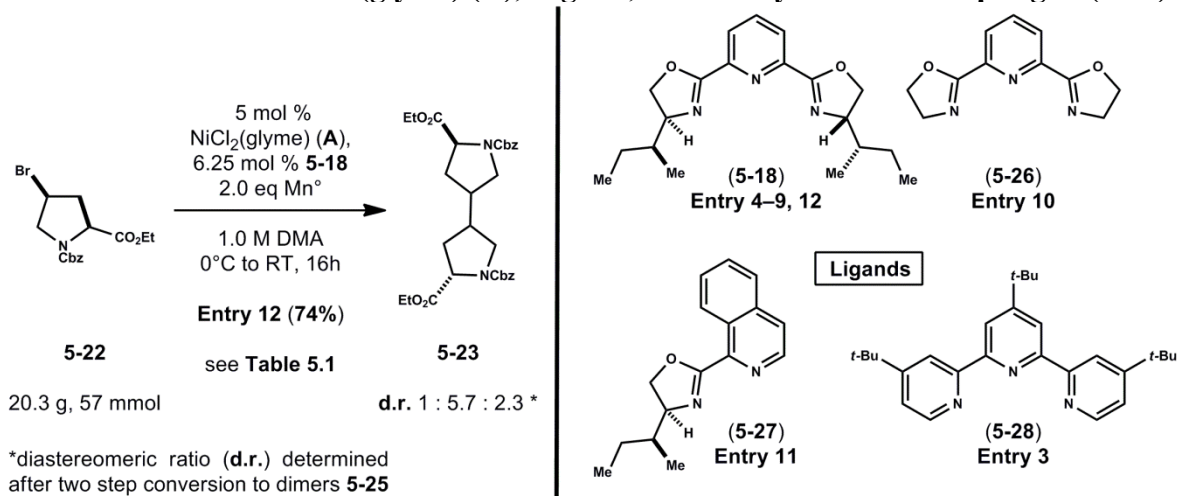


**Figure 5.6.** Nickel-catalyzed reductive homodimerization - Optimization of diastereoselectivity and yield. (see Table 5.1)

**Synthesis of (5*S,S'*)-1,1'-dibenzyl 5,5'-diethyl [3,3'-bipyrrolidine]-1,1',5,5'-tetracarboxylate (5-23).**

A solution of (2*S*,4*S*)-1-benzyl 2-ethyl 4-bromopyrrolidine-1,2-dicarboxylate (5-22) (1.0 equiv) in *N,N*-dimethylacetamide (DMA) (2.0 M) was degassed by sparging for 15 min with Ar (Vessel 1). In a second reaction vessel, NiCl<sub>2</sub>(glyme) (A) and the appropriate ligand (5-18, 5-26, 5-27, or 5-28) were dissolved in previously degassed *N,N*-dimethylacetamide (DMA) (equal volume as used in Vessel 1) and stirred at RT for 15 min. The solution in Vessel 1 was added to Vessel 2 *via* syringe or cannulation. If required, the mixture obtained was cooled below RT using an ice-water bath. The reaction was initiated by the addition of solid Mn<sup>0</sup> (2.0 equiv, powdered or granulated) in one portion and stirred at the given temperature. The reaction was judged complete by TLC or LCMS analysis. The dark reaction mixture is brought to RT and filtered through a short SiO<sub>2</sub> plug to remove inorganic materials and washed with EtOAc (3×). The combined organics were washed with 1M HCl (2×) (organic color changes from green to yellow/orange), water, brine, dried over Na<sub>2</sub>SO<sub>4</sub>, filtered and concentrated in vacuo to give a

crude yellow oil that was purified by flash column chromatography. (**5-23**,  $R_f = 0.3$ , hexanes / EtOAc (3:2))

### Specific Example: Entry 12.

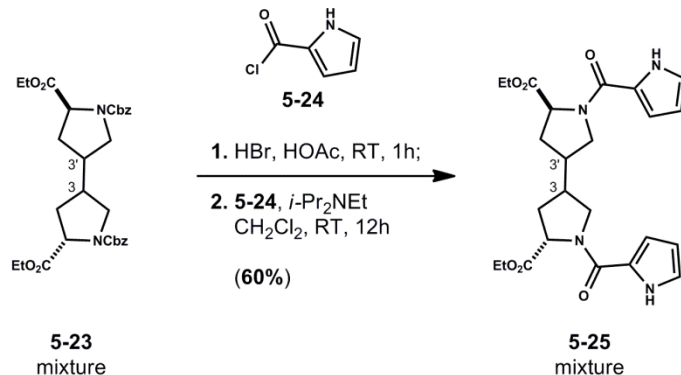
#### Synthesis of (5*S*,5'*S*)-1,1'-dibenzyl 5,5'-diethyl [3,3'-bipyrrolidine]-1,1',5,5'-tetracarboxylate (**5-23**).

A solution of (2*S*,4*S*)-1-benzyl 2-ethyl 4-bromopyrrolidine-1,2-dicarboxylate (**5-22**) (20.3 g, 57 mmol, 1.0 equiv) in *N,N*-dimethylacetamide (DMA) (28.5-mL, 2.0 M) was degassed by sparging for 15 min with Ar (Vessel 1). In a second reaction vessel, NiCl<sub>2</sub>(glyme) (A) (626 mg, 2.9 mmol, 0.05 equiv) and ligand (**5-18**) (1.18g, 3.6 mmol, 0.063 equiv) were dissolved in previously degassed *N,N*-dimethylacetamide (DMA) (28.5-mL) and stirred at RT for 15 min. The catalyst solution is initially deep green and becomes red-orange immediately. The solution in Vessel 1 was added to Vessel 2 *via* syringe and the mixture was cooled to 0°C with an ice-water bath. The reaction was initiated by the addition of solid Mn<sup>0</sup> (6.3 g, 114 mmol, 2.0 equiv, granular) in one portion and stirred at 0°C for 1h. The reaction was moved into a 2–4°C refrigerator and stirred for 16h, at which point conversion was determined to be approx. 80% by LCMS analysis. The reaction mixture was allowed to reach RT and stirred for an additional 3h followed by filtration through a short SiO<sub>2</sub> plug to remove inorganic materials and washed 3 × 200-mL with EtOAc. The combined organics were washed 2 × 100-mL with 1M HCl (organic color changes from green to yellow/orange), water, brine, dried over Na<sub>2</sub>SO<sub>4</sub>, filtered and concentrated in vacuo to give a crude yellow oil that was purified by flash column chromatography (approx. 200 g SiO<sub>2</sub>). (**5-23**,  $R_f = 0.3$ , hexanes / EtOAc (3:2)) The column was eluted with hexanes (2-L), hexanes / EtOAc (4:1) (2-L), hexanes / EtOAc (7:3) (2-L), hexanes / EtOAc (3:2) to provide fractions containing **5-23** as an inseparable mixture of three diastereomers (**5-23**,  $R_f = 0.3$ , hexanes / EtOAc (3:2)). The desired fractions were concentrated in vacuo to give (5*S*,5'*S*)-1,1'-dibenzyl 5,5'-diethyl [3,3'-bipyrrolidine]-1,1',5,5'-tetracarboxylate (**5-23**) (11.7 g, 74%) as a colorless oil.

#### (5*S*,5'*S*)-1,1'-dibenzyl 5,5'-diethyl [3,3'-bipyrrolidine]-1,1',5,5'-tetracarboxylate (**5-23**) (mixture):

<sup>1</sup>H NMR (500 MHz, CHCl<sub>3</sub>-*d*<sub>1</sub>): δ (ppm) 7.39-7.26 (m, 10H), 5.21-5.01 (m, 4H), 4.46-4.24 (m, 2H), 4.24-4.15 (m, 2H), 4.11-3.97 (m, 2H), 3.89-3.70 (m, 2H), 3.19-3.02 (m, 2H), 2.47-2.35 (m, 0.6H), 2.32-2.14 (m, 1.4 H), 2.14-1.97 (m, 2H), 1.97-1.82 (m, 1.4H), 1.72-1.58 (m, 0.6H), 1.31-1.21 (m, 3H), 1.20-1.07 (m, 3H); LRMS-ESI (*m/z*) calcd for [C<sub>30</sub>H<sub>36</sub>N<sub>2</sub>O<sub>8</sub>+H]<sup>+</sup>: 553.3; found: 553.3.

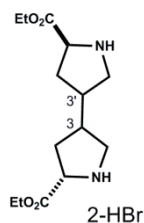
## Procedure for the Synthesis of Acylated Pyrrole Dimers (5-25).



### Specific Example: Entry 12.

#### Synthesis of (5*S*,5'*S*)-diethyl 1,1'-di(1*H*-pyrrole-2-carbonyl)-[3,3'-bipyrrolidine]-5,5'-dicarboxylate (5-25).

Purified (5*S*,5'*S*)-1,1'-dibenzyl 5,5'-diethyl [3,3'-bipyrrolidine]-1,1',5,5'-tetracarboxylate (5-23) (11.7 g, 21.3 mmol, 1.0 equiv, from Entry 12) was dissolved in conc. glacial acetic acid (15-mL) and cooled to 0°C with an ice-water bath followed by the addition of 33 wt% HBr in acetic acid (50-mL) in one portion. The light yellow-orange solution was allowed to warm to RT and the evolution of CO<sub>2</sub> gas was observed. The reaction was stirred at RT for 1h at which point a yellow precipitate began to form. The mixture was cooled again to 0°C for 15 min and further precipitation occurred. To the heterogeneous mixture was added 300-mL diethyl ether (previously cooled to -20°C) and further precipitation occurred during 1h storage in a -20°C freezer. The resultant slurry was separated cold by careful decantation to yield (5*S*,5'*S*)-diethyl [3,3'-bipyrrolidine]-5,5'-dicarboxylate 2-HBr (9.4 g, 99%, crude weight) as an off-white solid. This material was used crude without further purification.



#### 5,5'-diethyl-[3,3'-bipyrrolidine]-5,5'-dicarboxylate 2-HBr (crude mixture):

<sup>1</sup>H NMR (500 MHz, MeOH-*d*<sub>4</sub>): δ (ppm) 9.92-9.58 (bs, 2H), 9.24-8.93 (bs, 2H), 4.63-4.35 (m, 2H), 4.26-4.19 (m, 4H), 3.07-2.86 (m, 2H), 2.49-2.20 (m, 6H), 2.12-1.98 (m, 1.5 H), 1.78-1.64 (m, 0.5 H), 1.29-1.20 (m, 6H); <sup>13</sup>C NMR (125 MHz, MeOH-*d*<sub>4</sub>): δ (ppm) 168.7, 168.3, 62.24, 62.18, 58.7, 58.5, 58.4, 58.3, 48.70, 48.67, 48.5, 32.4, 32.1, 32.0, 13.9; LRMS-ESI (*m/z*) calcd for [C<sub>14</sub>H<sub>24</sub>N<sub>2</sub>O<sub>4</sub>+H]<sup>+</sup>: 285.2; found: 285.3.



## (5*S*,5'*S*)-diethyl 1,1'-di(1*H*-pyrrole-2-carbonyl)-[3,3'-bipyrrolidine]-5,5'-dicarboxylate (**5-25**) mixture.

Oxalyl chloride was added to a solution of 1*H*-pyrrole-2-carboxylic acid (5.9 g, 53.0, 2.5 equiv) in CH<sub>2</sub>Cl<sub>2</sub> (176-mL) at RT. Catalytic DMF (50- $\mu$ L) was added and the resultant solution was stirred at RT for 2h. Acid chloride formation was judged complete by TLC analysis of the resultant ester following aliquot quench with MeOH.

To a crude mixture of (5*S*,5'*S*)-diethyl [3,3'-bipyrrolidine]-5,5'-dicarboxylate 2-HBr (9.4 g, 21.3 mmol) suspended in CH<sub>2</sub>Cl<sub>2</sub> (212-mL, 0.1 M) with pyridine (20.5-mL) and DMAP (50 mg) was added the entire above solution of generated acid chloride (2.5 equiv). The resultant mixture was stirred at RT for 12h. The crude mixture was diluted with CHCl<sub>3</sub> (200-mL) and washed with H<sub>2</sub>O (2  $\times$  50-mL), saturated aqueous NaHCO<sub>3</sub>, brine, dried over Na<sub>2</sub>SO<sub>4</sub>, filtered and concentrated in vacuo to provide crude **5-25** (10.9 g, 109% yield) as an off-white tan solid. Crude analysis by LC-MS (UV-detection at 254-nm) indicates approximate dimer ratio **5-25-1:5-25-2:5-25-3** of 1:5.4:2.3. The crude mixture was dried under high-vacuum (3h) and suspended in anhydrous CHCl<sub>3</sub> (50-mL). The precipitous mixture was cooled to -20°C and stored overnight (12h). The precipitate was separated by vacuum filtration to give approximately 1.8 g of **5-25-3** (>90% purity) and an enriched filtrate containing **5-25-1:5-25-2:5-25-3** (1:5.3:0.5). Concentration and drying of this filtrate provided the enriched mixture as a tan foam (8.8 g). The enriched mixture **5-25-1:5-25-2:5-25-3** (1:5.3:0.5) could be used in subsequent steps without further purification. For analytical purposes, dimers **5-25-1:5-25-2:5-25-3** could be separated by preparative flash column chromatography eluting with CHCl<sub>3</sub>/MeOH (99:1) to CHCl<sub>3</sub>/MeOH (49:1) to provide first **5-25-2** followed by mixed fractions of **5-25-1:5-25-2**. Remaining fractions contain **5-25-1** co-eluting with residual **5-25-3**.

### Characterization of Dimers (**5-25**).

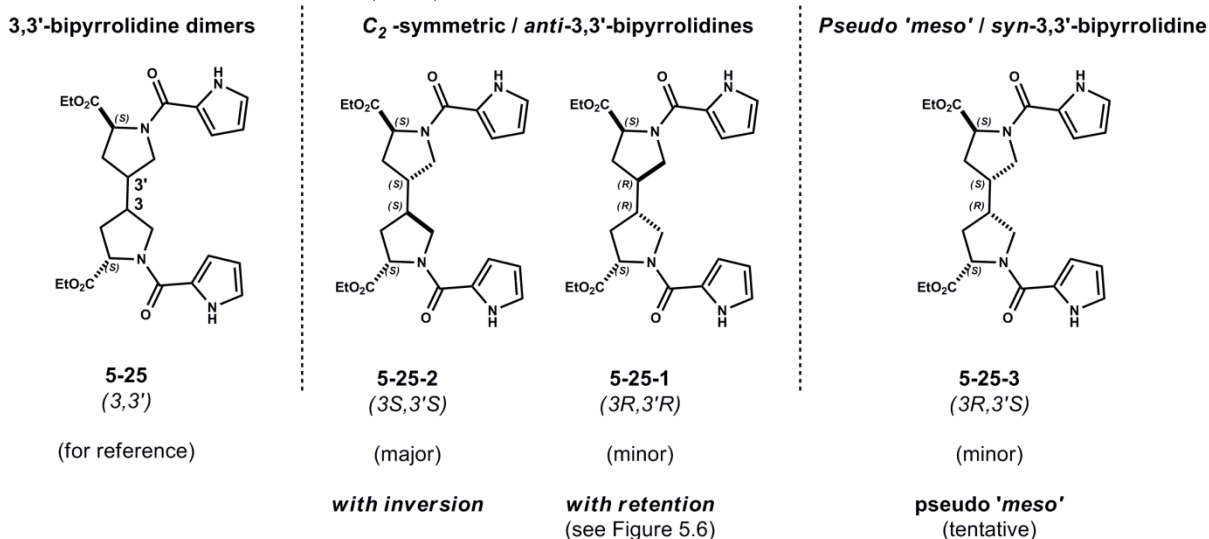


Figure 5.5. Analysis of diastereomers **5-25**, *C*<sub>2</sub>-symmetric (**5-25-1**, **5-25-2**) and *pseudo 'meso'* (**5-25-3**, **5-25-4**) 3,3'-bipyrrolidines.

Crystals suitable for x-ray diffraction of minor diastereomer (**5-25-1**) precipitated over 24h from a standing solution of **5-25-1** (~ 25 mg) in DMSO-*d*<sub>6</sub> (0.5-mL). For reference (CCDC 942604), and see Chapter 5, Section 5.2.2).

**HPLC Conditions:** Waters XSELECT Fluoro-Phenyl analytical column (5 μm, 4.6 × 250-mm) with UV detection at 254-nm; Solution A: H<sub>2</sub>O w/0.1% formic acid and Solution B: CH<sub>3</sub>CN w/0.1% formic acid; increase gradient of Solution B from 10% to 40%, 0.5-2 min; 40% to 60%, 2-23 min; 60% to 100%, 23-25 min. Flow rate: 1.0-mL/min.

**Order of Elution:** **5-25-1** (retention time: 12.0 min); **5-25-3** (retention time: 12.5 min), **5-25-2** (retention time: 12.9 min).

**(3*S*,3'*S*,5*S*,5'*S*)-diethyl 1,1'-di(1H-pyrrole-2-carbonyl)-[3,3'-bipyrrolidine]-5,5'-dicarboxylate (5-25-1):**

<sup>1</sup>H NMR (500 MHz, DMSO-*d*<sub>6</sub>): δ (ppm) 11.47 (bs, 2H), 6.93 (bs, 2H), 6.76 (bs, 2H), 6.18 (bs, 2H), 4.46-4.37 (m, 2H), 4.14-4.03 (m, 6H), 3.52-3.43 (m, 2H), 2.47-2.37 (m, 2H), 2.32-2.21 (m, 2H), 1.58-1.46 (m, 2H), 1.80 (t, *J* = 7.0 Hz, 6H); <sup>13</sup>C NMR (125 MHz, DMSO-*d*<sub>6</sub>): δ (ppm) 172.0, 159.9, 124.8, 122.0, 113.0, 109.0, 60.2, 59.8, 52.7, 42.0, 33.2, 14.1; LRMS-ESI (*m/z*) calcd for [C<sub>24</sub>H<sub>30</sub>N<sub>4</sub>O<sub>6</sub>+H]<sup>+</sup>: 471.2; found: 471.3.

**(3*R*,3'*R*,5*S*,5'*S*)-diethyl 1,1'-di(1H-pyrrole-2-carbonyl)-[3,3'-bipyrrolidine]-5,5'-dicarboxylate (5-25-2):**

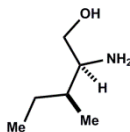
<sup>1</sup>H NMR (500 MHz, DMSO-*d*<sub>6</sub>): δ (ppm) 11.50 (bs, 2H), 6.93 (bs, 2H), 6.82 (bs, 2H), 6.18 (bs, 2H), 4.50 (d, *J* = 8.3 Hz, 2H), 4.16-4.04 (m, 6H), 3.57-3.49 (m, 2H), 2.41-2.32 (m, 2H), 2.06-1.94 (m, 4H), 1.20 (t, *J* = 7.1 Hz, 6H); <sup>13</sup>C NMR (125 MHz, DMSO-*d*<sub>6</sub>): δ (ppm) 172.1, 159.7, 124.8, 122.0, 113.0, 109.1, 60.3, 59.5, 51.9, 40.9, 32.3, 14.1; LRMS-ESI (*m/z*) calcd for [C<sub>24</sub>H<sub>30</sub>N<sub>4</sub>O<sub>6</sub>+H]<sup>+</sup>: 471.2; found: 471.3.

**(3*S*,3'*R*,5*S*,5'*S*)-diethyl 1,1'-di(1H-pyrrole-2-carbonyl)-[3,3'-bipyrrolidine]-5,5'-dicarboxylate (5-25-3):**

<sup>1</sup>H NMR (500 MHz, DMSO-*d*<sub>6</sub>): δ (ppm) 11.49 (bs, 1H), 11.46 (bs, 1H), 6.93 (bs, 2H), 6.77 (bs, 2H), 6.17 (bs, 2H), 4.52 (d, *J* = 9.1 Hz, 1H), 4.45-4.39 (m, 1H), 4.18-3.98 (m, 6H), 3.56-3.44 (m, 2H), 2.52-2.32 (m, 2H), 2.32-2.19 (m, 1H), 2.18-2.07 (m, 1H), 2.06-1.93 (m, 1H), 1.61-1.51 (m, 1H), 1.26-1.12 (m, 6H); <sup>13</sup>C NMR (125 MHz, DMSO-*d*<sub>6</sub>): δ (ppm); 172.1, 171.9, 159.9, 159.7, 124.8 (2C), 122.0 (2C), 113.1, 112.9, 109.1, 109.0, 60.3, 60.2, 60.0, 59.8, 52.5, 52.0, 42.2, 40.9, 33.3, 32.5, 14.1 (2C); LRMS-ESI (*m/z*) calcd for [C<sub>24</sub>H<sub>30</sub>N<sub>4</sub>O<sub>6</sub>+H]<sup>+</sup>: 471.2; found: 471.3.

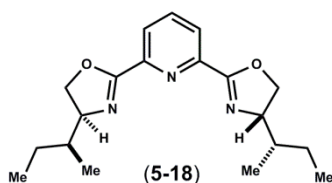
## Ligand Synthesis (5-18, 5-26, 5-27) for Homocoupling Experiments.

### Synthesis of (2*S*,3*S*)-2-amino-3-methylpentan-1-ol (isoleucinol).



Prepared in (84%) isolated yield from *L*-isoleucine according to: Meinzer, A.; Breckel, A.; Thaher, B. A.; Manicone, N.; Otto, H-H. *Hel. Chem. Acta.* **2004**, *87*, 90.

### Synthesis of 2,6-bis((*S*)-4-((*S*)-sec-butyl)-4,5-dihydrooxazol-2-yl)pyridine (5-18).

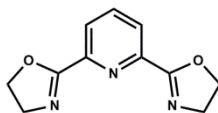


Prepared according to: Nishiyama, H.; Kondo, M.; Nakamura, T.; Itoh, K. *Organometallics* **1991**, *10*, 500.

#### 6-bis((*S*)-4-((*S*)-sec-butyl)-4,5-dihydrooxazol-2-yl)pyridine (5-18):

$^1\text{H NMR}$  (500 MHz, MeOH- $d_4$ ):  $\delta$  (ppm) 8.14-8.11 (m, 2H), 8.03 (dd,  $J = 8.5, 7.1$  Hz, 1H), 4.58-4.51 (m, 2H), 4.36-4.29 (m, 4H), 1.79-1.70 (m, 2H), 1.66-1.57 (m, 2H), 1.31-1.21 (m, 2H), 0.98 (t,  $J = 7.5$  Hz, 6H), 0.91 (d,  $J = 6.8$  Hz, 6H);  $^{13}\text{C NMR}$  (125 MHz, MeOH- $d_4$ ):  $\delta$  (ppm) 164.4, 148.0, 139.3, 127.1, 72.2, 71.4, 40.2, 26.9, 14.4, 11.9; **LRMS-ESI** ( $m/z$ ) calcd for  $[\text{C}_{19}\text{H}_{27}\text{N}_3\text{O}_2+\text{H}]^+$ : 330.2; found: 330.2

### Synthesis of 2,6-bis(4,5-dihydrooxazol-2-yl)pyridine (5-26).



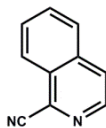
(5-26)

Prepared in a similar manner according to: Nishiyama, H.; Kondo, M.; Nakamura, T.; Itoh, K. *Organometallics* **1991**, *10*, 500.

#### 2,6-bis(4,5-dihydrooxazol-2-yl)pyridine (5-26):

$^1\text{H NMR}$  (500 MHz, MeOH- $d_4$ ):  $\delta$  (ppm) 8.11 (d,  $J = 7.0$  Hz, 2H), 8.04 (t,  $J = 7.8$  Hz, 1H), 4.57 (t,  $J = 6.0$  Hz, 4H), 4.09 (t,  $J = 10.0$  Hz, 4H);  $^{13}\text{C NMR}$  (125 MHz, MeOH- $d_4$ ):  $\delta$  (ppm) 165.5, 147.9, 139.4, 127.1, 69.8, 55.5; **LRMS-ESI** ( $m/z$ ) calcd for  $[\text{C}_{11}\text{H}_{11}\text{N}_3\text{O}_2+\text{H}]^+$ : 218.1; found: 218.2.

## Synthesis of isoquinoline-1-carbonitrile.

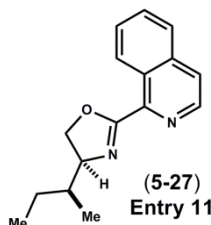


Prepared from isoquinoline in a similar manner according to: Boger, D. L.; Brotherton, J. S.; Panek, J. S.; Yohannes, D. *J. Org. Chem.* **1984**, *49*, 4050.

### isoquinoline-1-carbonitrile:

$^1\text{H NMR}$  (600 MHz,  $\text{CHCl}_3-d_1$ ):  $\delta$  (ppm) 8.66 (d,  $J = 5.5$  Hz, 1H), 8.36 (d,  $J = 8.0$  Hz, 1H), 7.95 (d,  $J = 7.8$  Hz, 1H), 7.91 (d,  $J = 5.5$  Hz, 1H), 7.83 (m, 2H); **LRMS-ESI** ( $m/z$ ) calcd for  $[\text{C}_{10}\text{H}_6\text{N}_2+\text{H}]^+$ : 155.1; found: 155.1.

## Synthesis of (*S*)-4-((*S*)-*sec*-butyl)-2-(isoquinolin-1-yl)-4,5-dihydrooxazole (**5-27**).



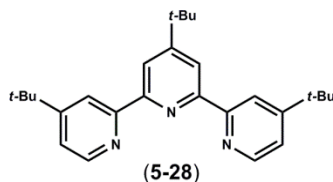
Prepared from isoquinoline-1-carbonitrile and (*2S,3S*)-2-amino-3-methylpentan-1-ol following reported similar conditions: Binder, J. T.; Cordier, C. J.; Fu, G. C. *J. Am. Chem. Soc.* **2012**, *134*, 17003.

To a flame-dried round bottom flask was added solid anhydrous  $\text{ZnCl}_2$  (90 mg, 0.65 mmol, 0.2 equiv) and the flask was shortly heated with a flame under high vacuum. After cooling to RT, the flask was purged with Ar followed by the addition of isoquinoline-1-carbonitrile (400 mg, 2.6 mmol, 1.0 equiv) and (*2S,3S*)-2-amino-3-methylpentan-1-ol (397 mg, 3.4 mmol, 1.3 equiv). The mixture was suspended in chlorobenzene (23-mL) and the light yellow heterogeneous reaction was heated behind a blast shield in a pre-heated oil bath at  $140^\circ\text{C}$  for 40h. TLC analysis indicates the reaction proceeds with full conversion of isoquinoline-1-carbonitrile. The reaction was cooled to RT and concentrated in vacuo at  $45^\circ\text{C}$  to give a crude orange oil. The crude oil was diluted with  $\text{CH}_2\text{Cl}_2$  (100-mL) and washed vigorously with  $\text{H}_2\text{O}$  ( $2 \times 25$ -mL). The aqueous layer was back extracted with  $\text{CH}_2\text{Cl}_2$  ( $3 \times 20$ -mL) and combined organics were washed with brine (20-mL), dried over  $\text{Na}_2\text{SO}_4$  and concentrated in vacuo. Purification by flash column chromatography (approx. 25 g  $\text{SiO}_2$ ) eluting with gradient hexane / EtOAc (9:1) to (3:7) provided pure fractions that were concentrated in vacuo to yield **5-27** (507 mg, 76%) as a light yellow solid. Recrystallization from hexane /  $\text{CH}_2\text{Cl}_2$  (9:1) provided **5-27** as light yellow powder used directly for catalysis (Entry 11).

**(S)-4-((S)-sec-butyl)-2-(isoquinolin-1-yl)-4,5-dihydrooxazole (5-27):**

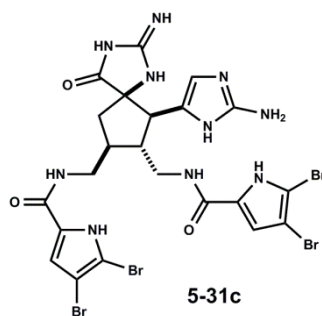
$^1\text{H NMR}$  (500 MHz,  $\text{CHCl}_3-d_1$ ):  $\delta$  (ppm) 9.25 (d,  $J = 8.5$  Hz, 1H), 8.64 (d,  $J = 5.6$  Hz, 1H), 7.90-7.86 (m, 1H), 7.81-7.77 (m, 1H), 7.76-7.22 (m, 2H), 4.62-4.52 (m, 1H), 4.51-4.43 (m, 1H), 4.33-4.24 (m, 1H), 1.92-1.83 (m, 1H), 1.78-1.68 (m, 1H), 1.41-1.32 (m, 1H), 1.04-0.96 (m, 6H);  $^{13}\text{C NMR}$  (125 MHz,  $\text{CHCl}_3-d_1$ ):  $\delta$  (ppm) 168.2, 140.9, 139.8, 138.9, 133.5, 131.3, 128.6, 128.1, 126.9, 126.5, 75.6, 66.8, 37.9, 26.1, 14.1, 11.4; **LRMS-ESI** ( $m/z$ ) calcd for  $[\text{C}_{16}\text{H}_{18}\text{N}_2\text{O}+\text{H}]^+$ : 255.2; found: 255.2;  $[\alpha]_{\text{D}} = -14.9^\circ$  ( $c = 0.09$ ,  $\text{CHCl}_3$ )

**Synthesis of 4,4',4''-tri-tert-butyl-2,2':6',2''-terpyridine (5-28).**



4,4',4''-tri-tert-butyl-2,2':6',2''-terpyridine was prepared from 4-tert-butylpyridine according to: Hadda, T. B.; Bozec, H. L. *Polyhedron* **1988**, 7, 575.

The spectroscopic data of compound **5-31c** (3 steps from **5-25-2**) is in agreement with previously synthesized ( $\pm$ )-aminoimidazole **2-51b** (Chapter 2, Section 2.5.2 Experimental, Compound **2-51b**).



**(5-31c) (2·CF<sub>3</sub>CO<sub>2</sub>H):**

$^1\text{H NMR}$  (600 MHz,  $\text{H}_2\text{O}-d_2$ ):  $\delta$  (ppm) 6.75 (s, 1H), 6.62 (s, 1H), 6.50 (s, 1H), 3.56-3.40 (m, 4H), 3.28 (d,  $J = 11.6$  Hz, 1H), 2.59 (dd,  $J = 14.6, 9.7$  Hz, 1H), 2.48-2.35 (m, 2H), 1.91 (dd,  $J = 14.6, 6.1$  Hz, 1H);  $^{13}\text{C NMR}$  (125 MHz,  $\text{H}_2\text{O}-d_2$ ):  $\delta$  (ppm) 178.0, 161.5, 160.9, 157.9, 146.9, 126.1, 125.8, 121.5, 113.6, 113.2, 111.8, 106.08, 106.02, 99.0, 98.9, 71.8, 49.6, 46.5, 42.4, 41.9, 40.6, 38.4. **HRMS-ESI** ( $m/z$ ) calcd for  $[\text{C}_{22}\text{H}_{22}\text{Br}_4\text{N}_{10}\text{O}_3+\text{H}]^+$ : 794.8649; found: 794.8697.

## APPENDIX FOUR

### Spectra Relevant to Chapter Five:

#### Chapter 5 – Alternative Access to Dispacamide Dimers:

*Auto-oxidation of 3,3'-bipyrrolidines for the synthesis of dimeric pyrrole–imidazole alkaloids*

*Andrew G. Roberts, Hui Ding and Patrick G. Harran*

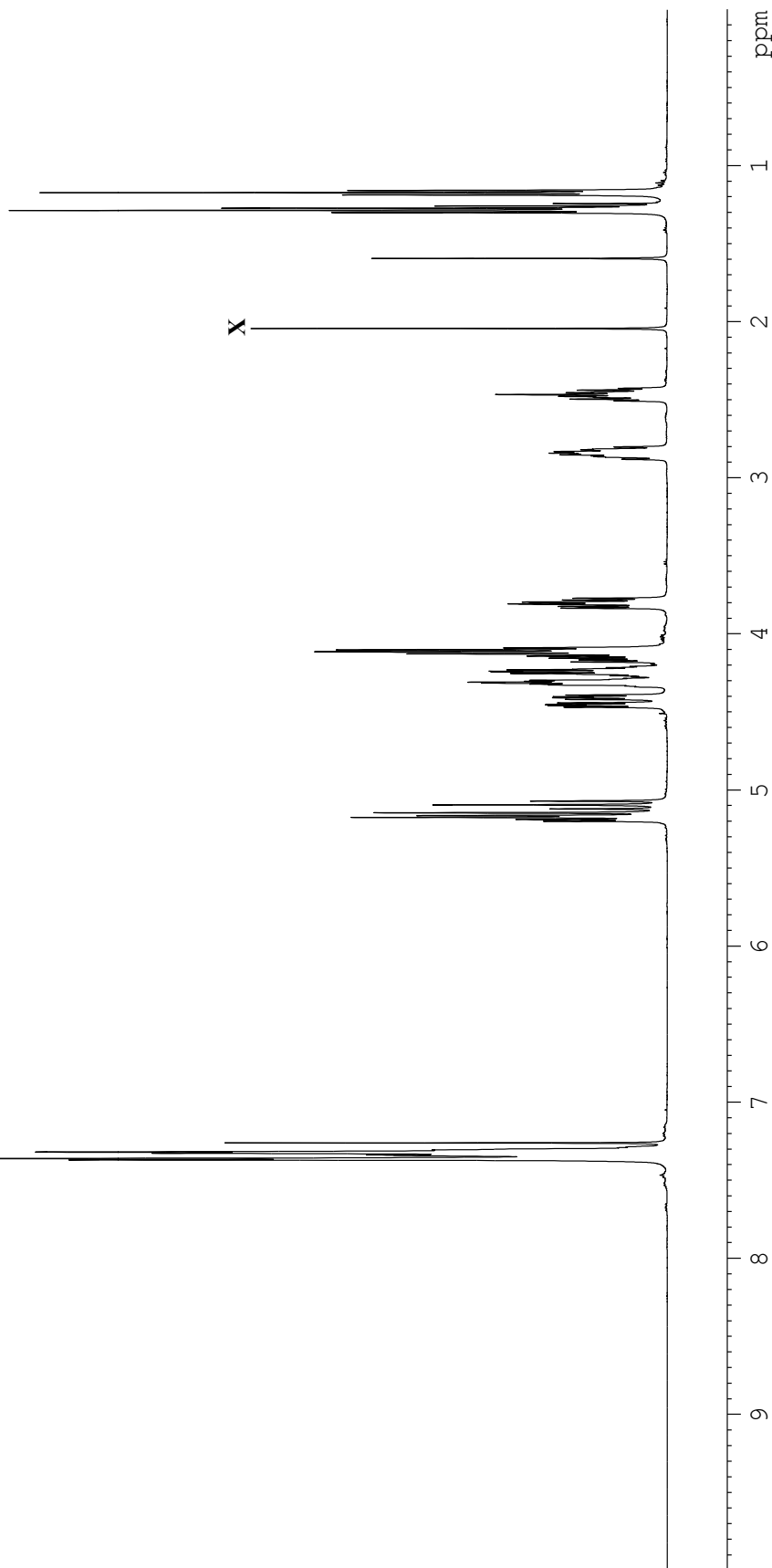
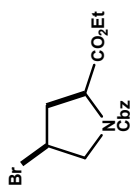


**Figure A4.1.** <sup>1</sup>H NMR (500 MHz, CHCl<sub>3</sub>-d<sub>1</sub>) spectrum of compound 5-22.

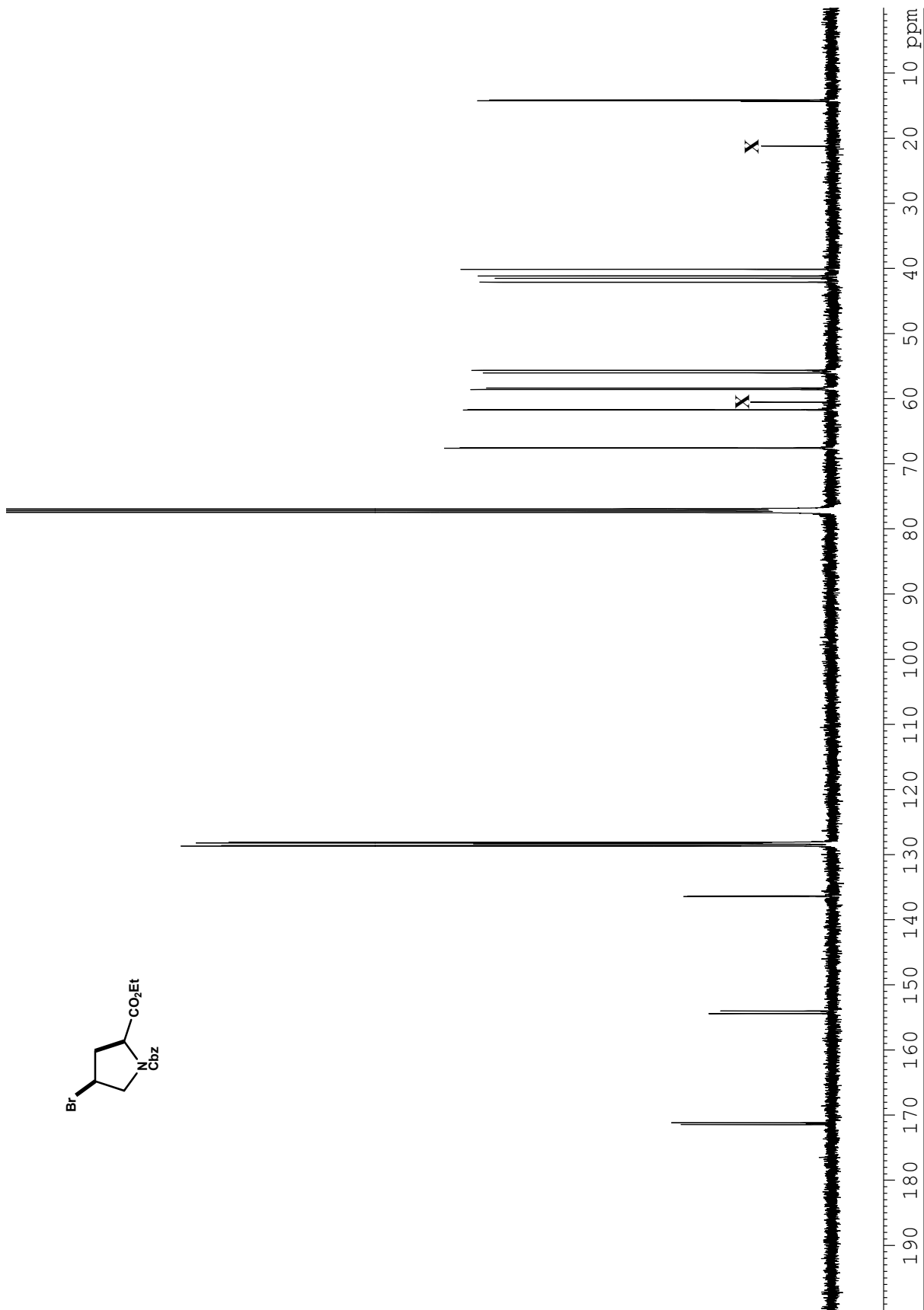
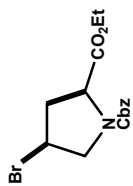


**Figure A4.2.** <sup>13</sup>C NMR (125 MHz, CHCl<sub>3</sub>-d<sub>1</sub>) spectrum of compound 5-22.



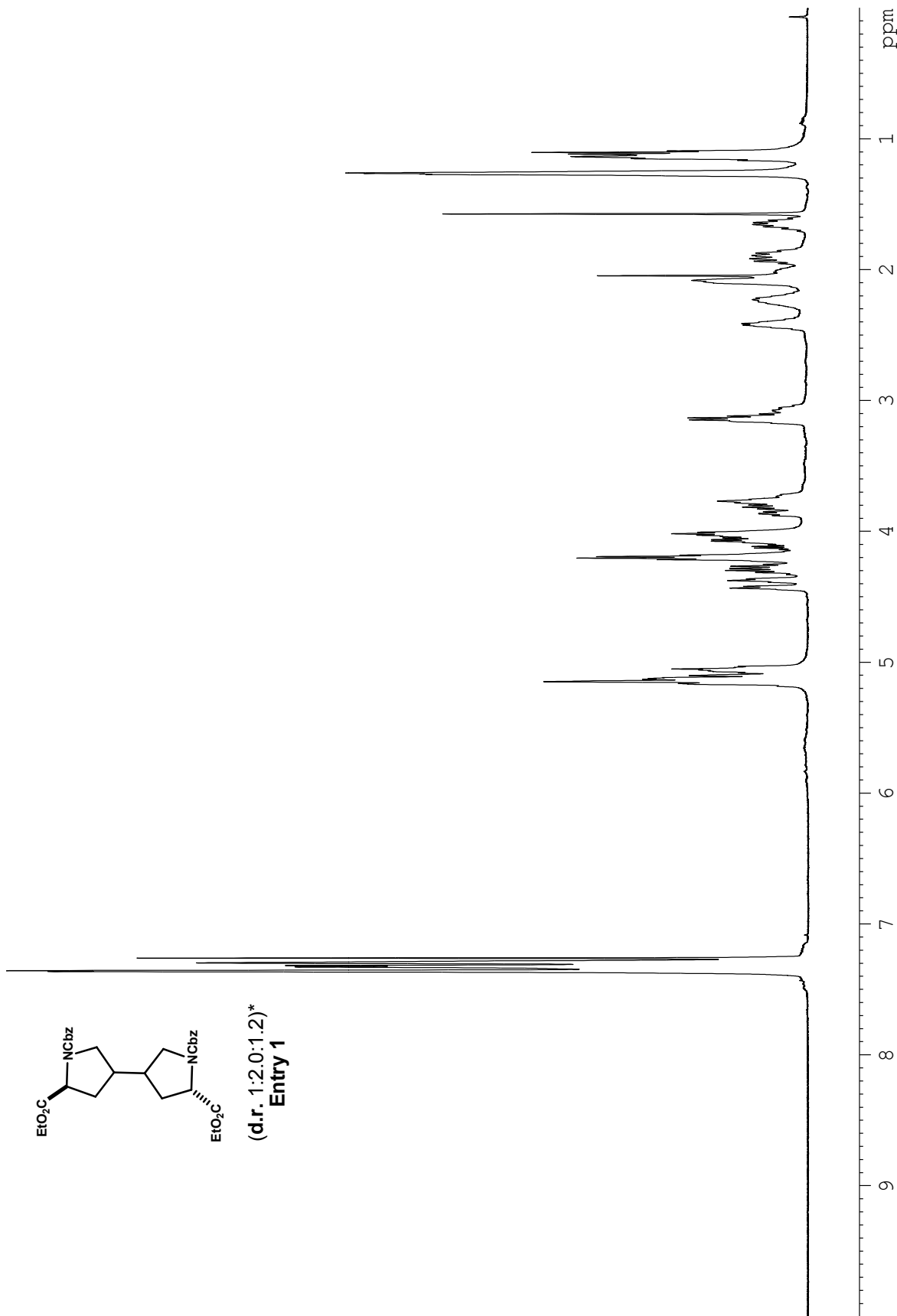
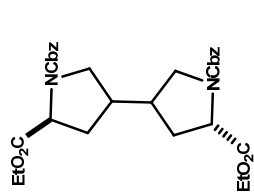


**Figure A4.3.** <sup>1</sup>H NMR (500 MHz, CHCl<sub>3</sub>-d<sub>1</sub>) spectrum of compound 5-23 (mixture) from Entry 1.



(d.r. 1:2.3:5.4)\*  
Entry 12

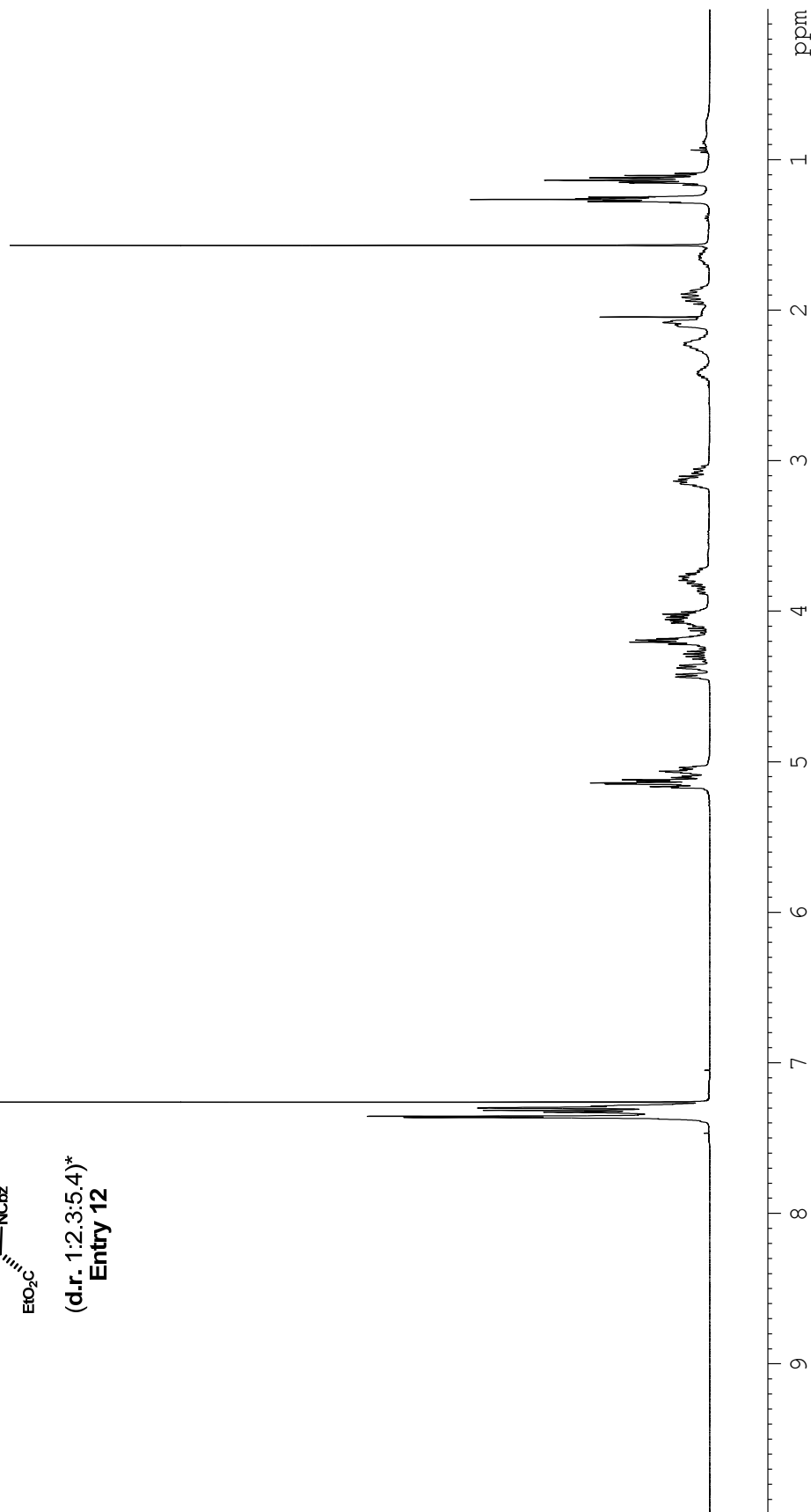
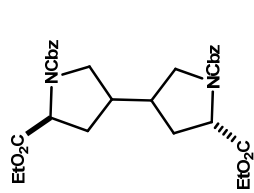


Figure A4.4. <sup>1</sup>H NMR (500 MHz, CHCl<sub>3</sub>-d<sub>1</sub>) spectrum of compound **5-23** (mixture) from Entry 12.



(d.r. 1:2.3:5.4)\*  
Entry 12

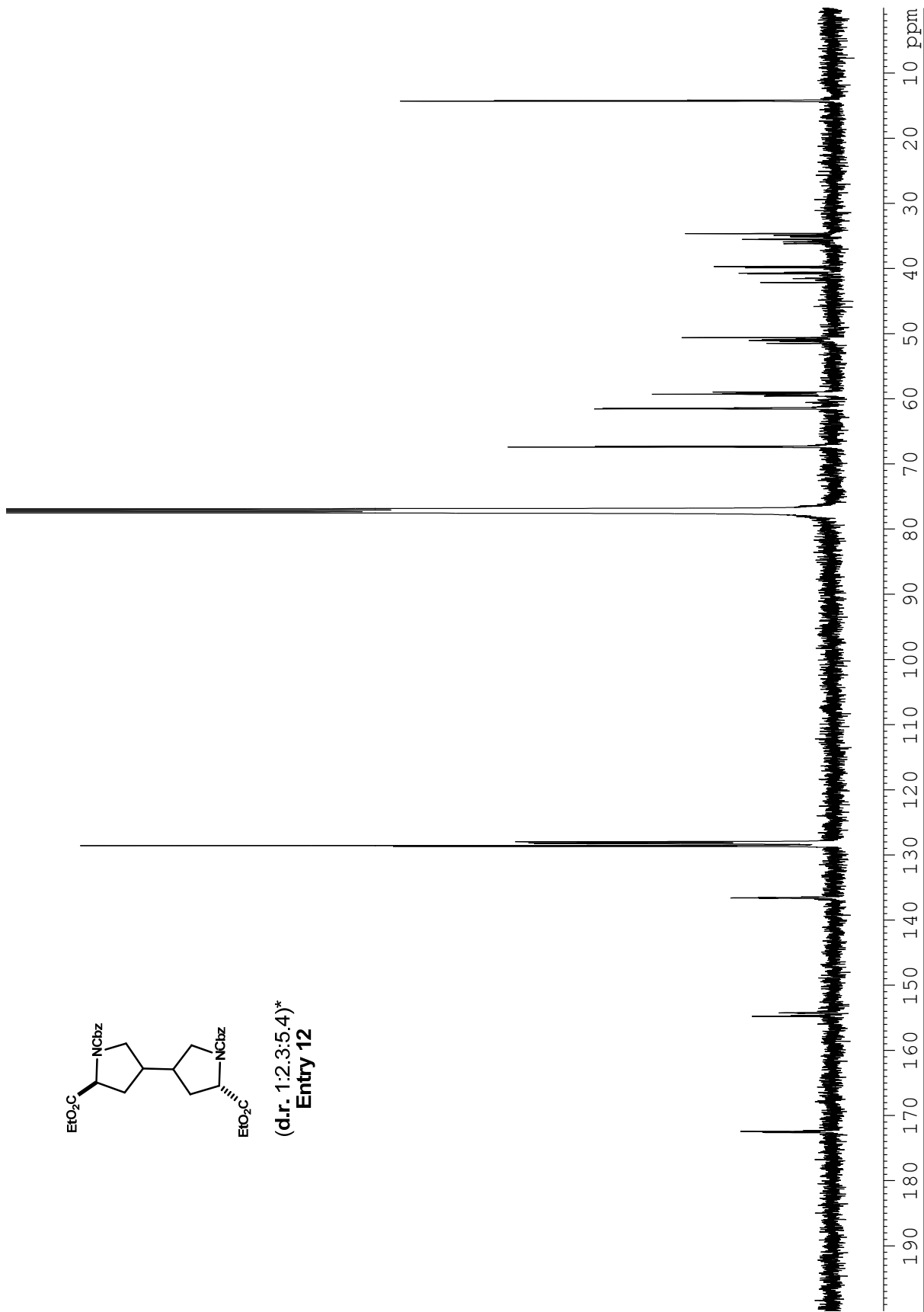
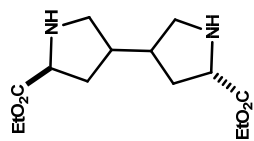


Figure A4.5.  $^{13}\text{C}$  NMR (125 MHz,  $\text{CHCl}_3$ - $d_1$ ) spectrum of compound 5-23 (mixture) from Entry 12.



2·HBr  
(crude)

(d.r. 1:2.3:5.4)\*

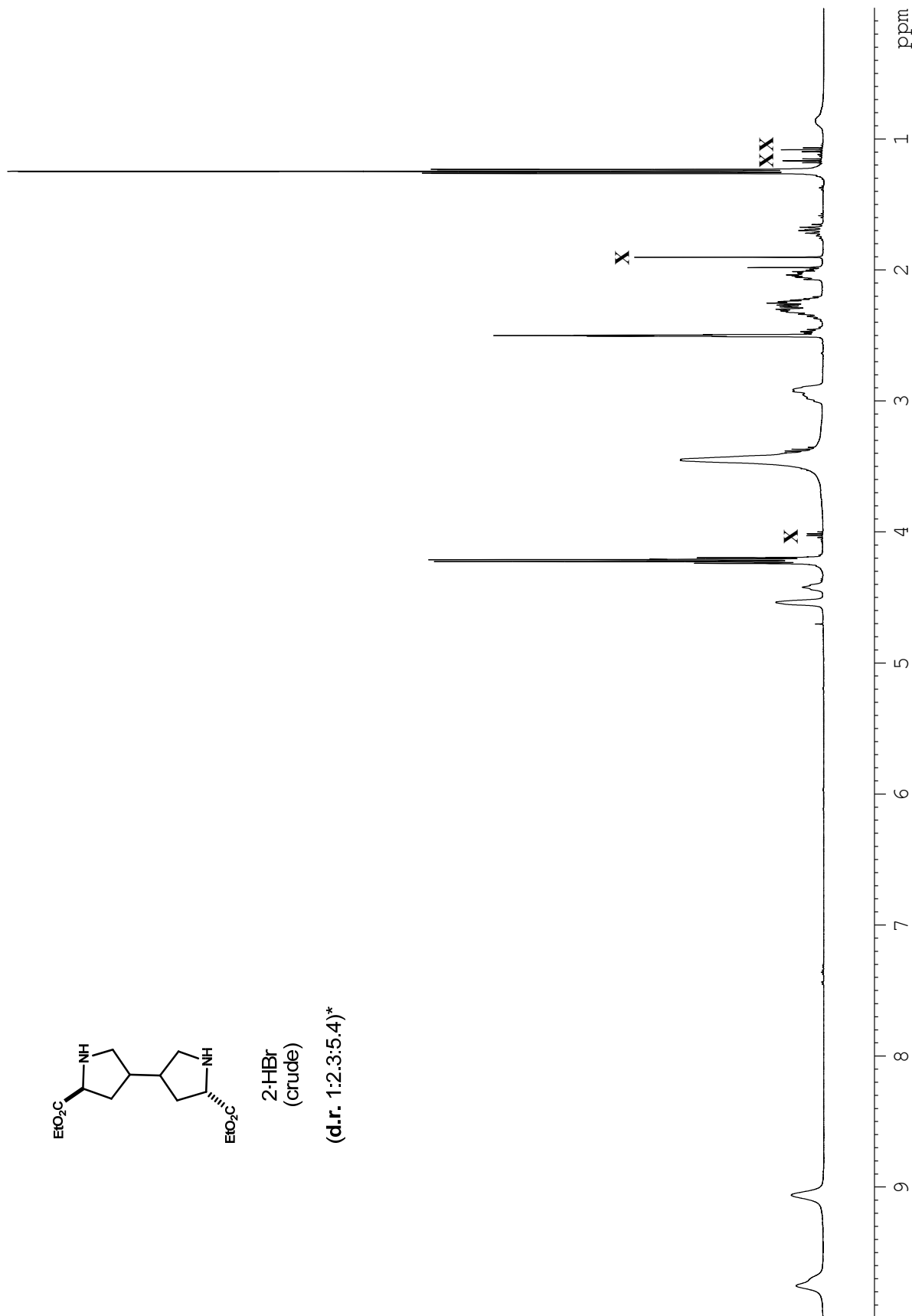
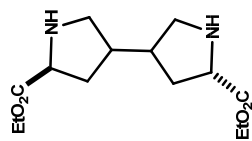
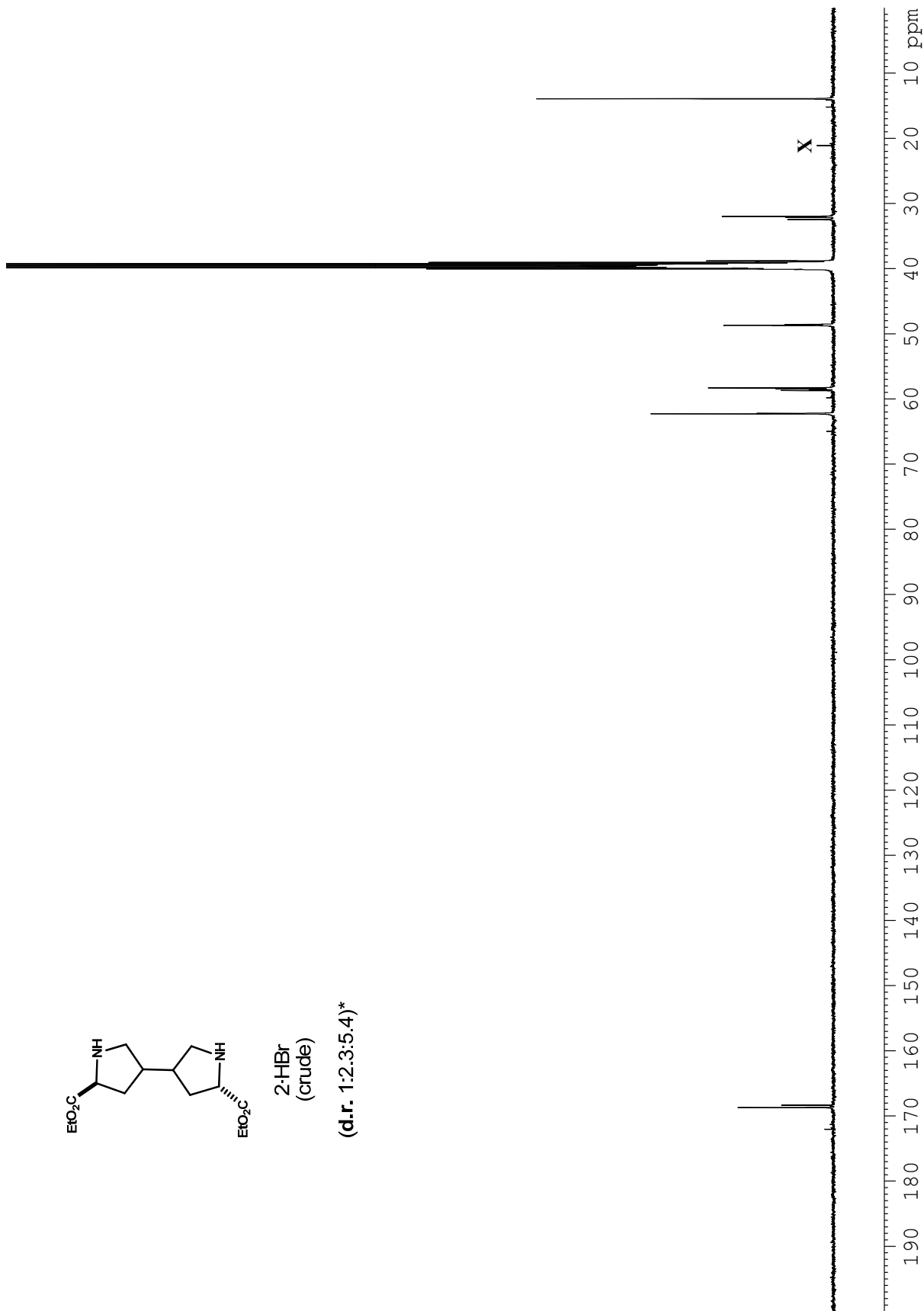


Figure A4.6. <sup>1</sup>H NMR (500 MHz, DMSO-*d*<sub>6</sub>) spectrum of diamine derived from **5-23** (mixture) from Entry 12.



2·HBr  
(crude)

(d.r. 1:2.3:5.4)\*



**Figure A4.7.** <sup>13</sup>C NMR (125 MHz, DMSO-*d*<sub>6</sub>) spectrum of diamine derived from **5-23** (mixture) from Entry 12.

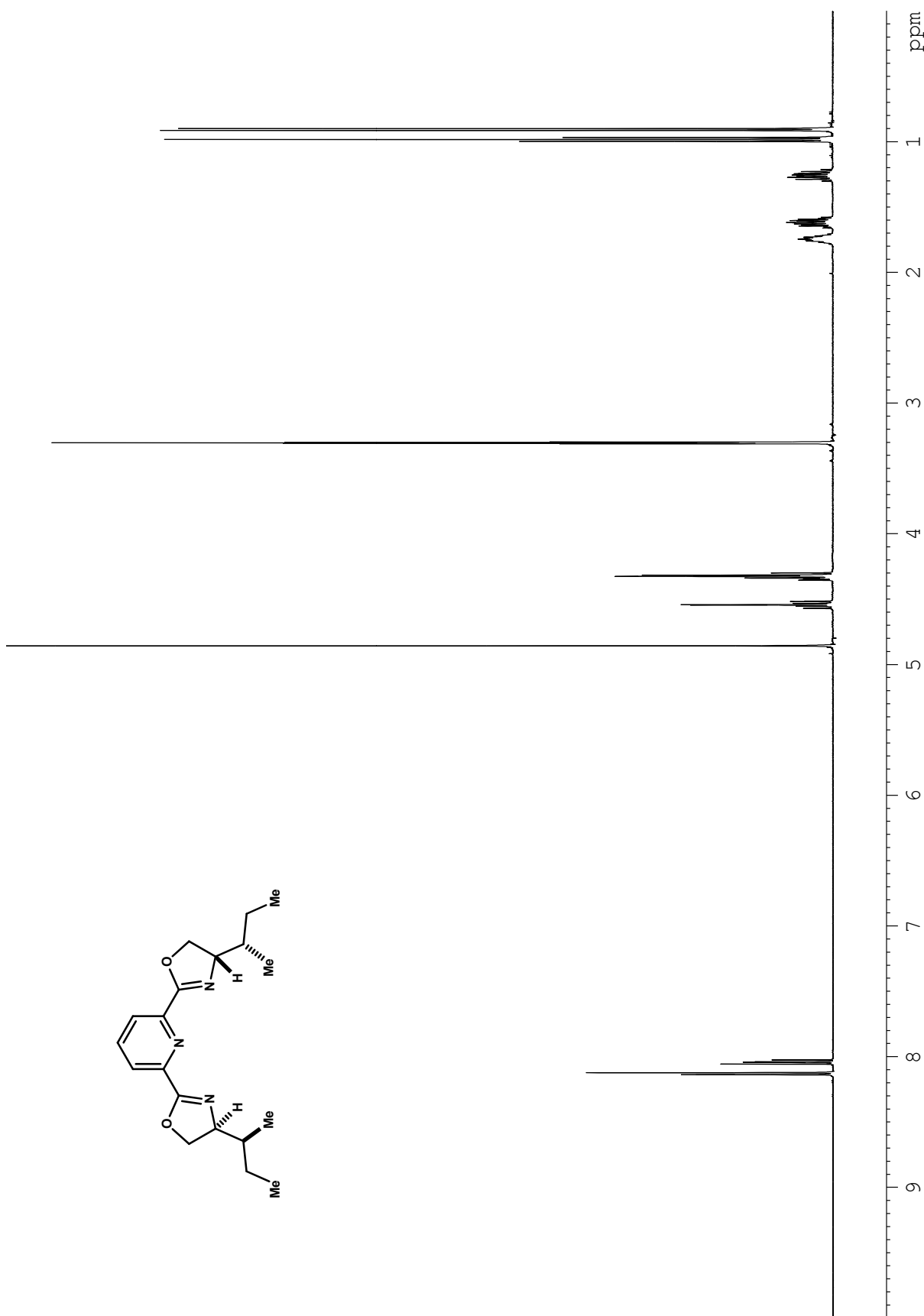


**Figure A4.8.** <sup>1</sup>H NMR (500 MHz, MeOH-*d*<sub>4</sub>) spectrum of compound **5-18**.

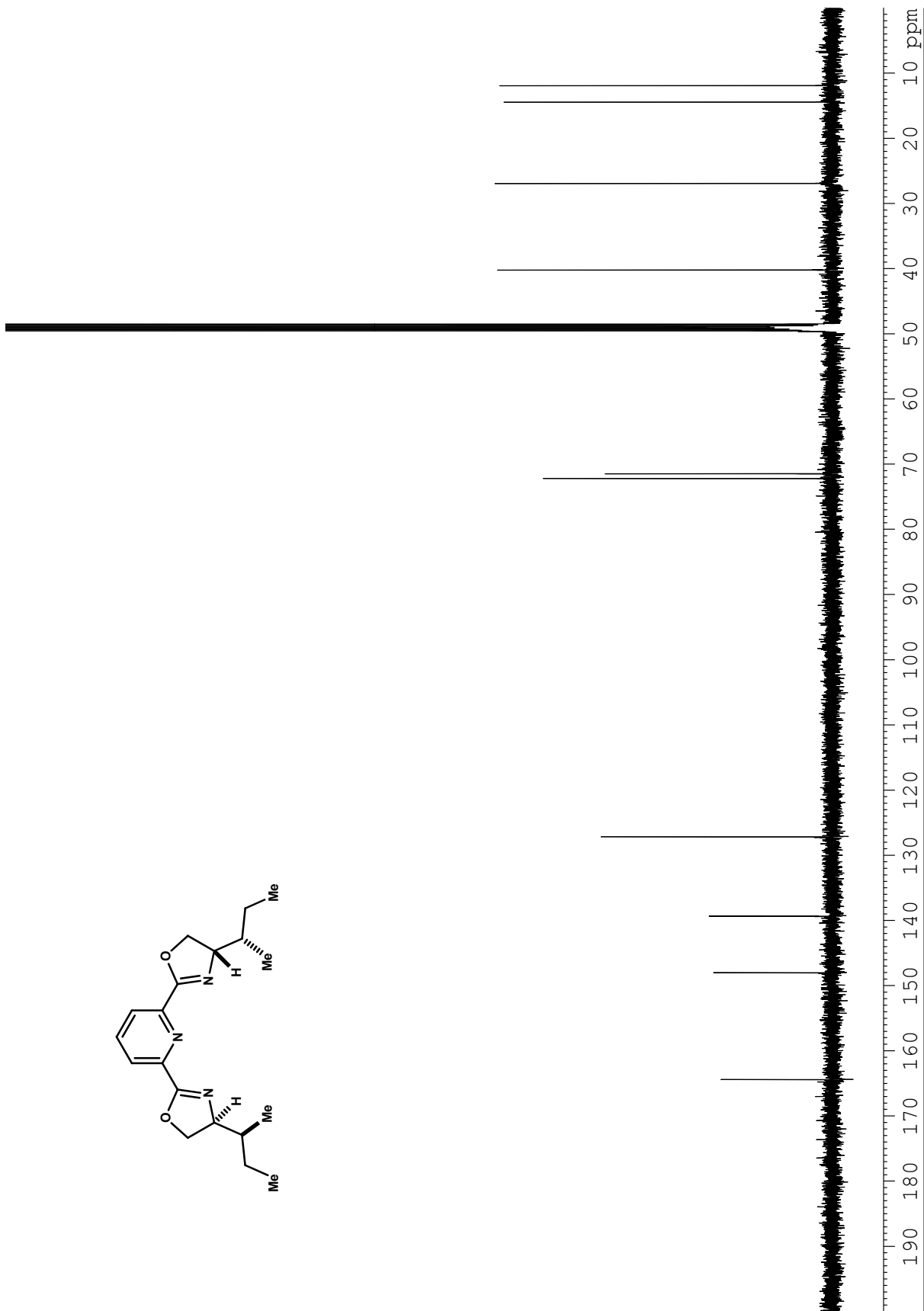
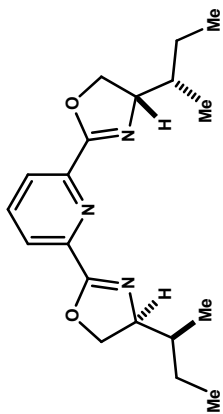


**Figure A4.9.**  $^{13}\text{C}$  NMR (125 MHz,  $\text{MeOH-}d_4$ ) spectrum of compound 5-18.

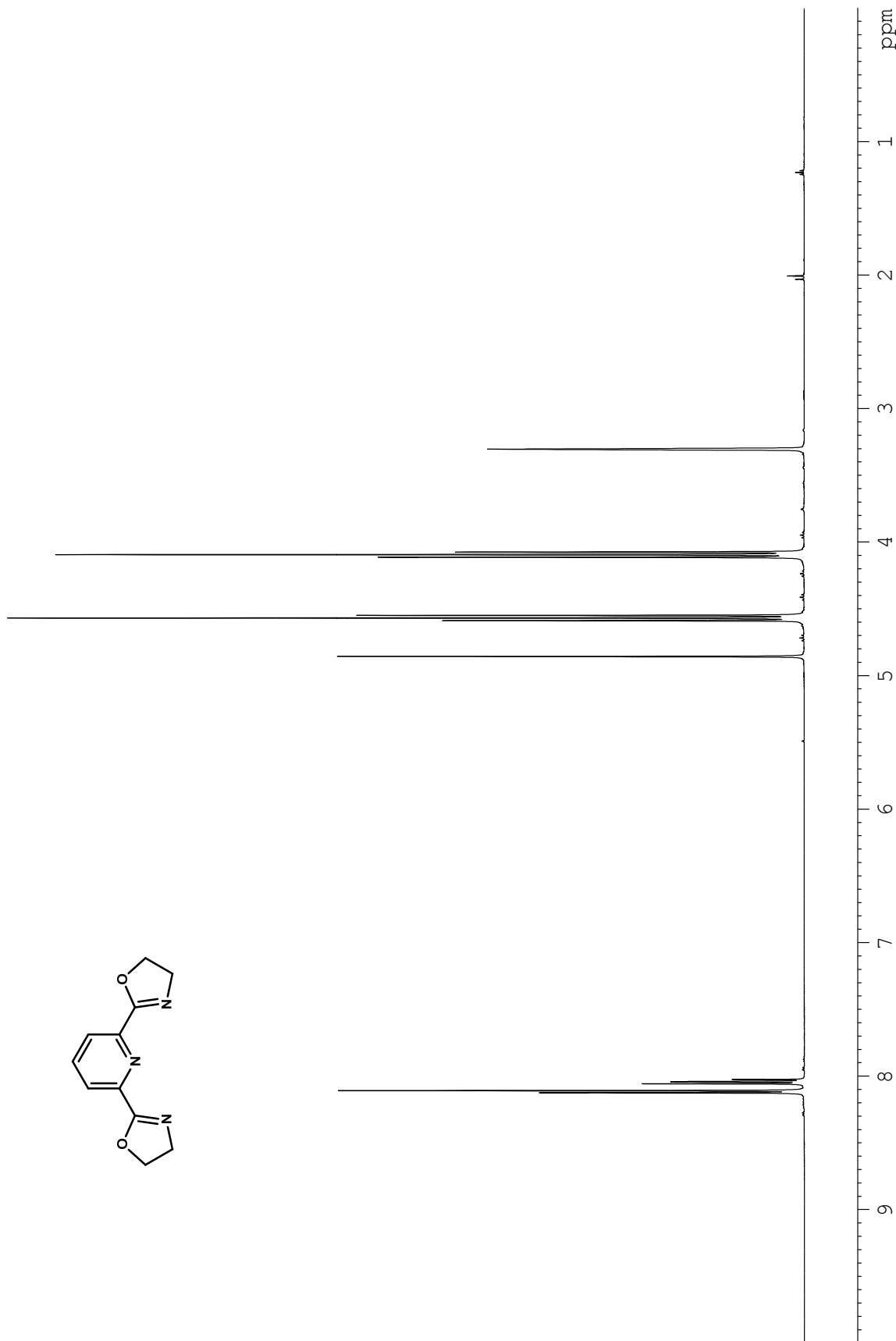
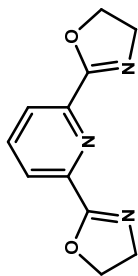


**Figure A4.10.** <sup>1</sup>H NMR (500 MHz, MeOH-*d*<sub>4</sub>) spectrum of compound 5-26.



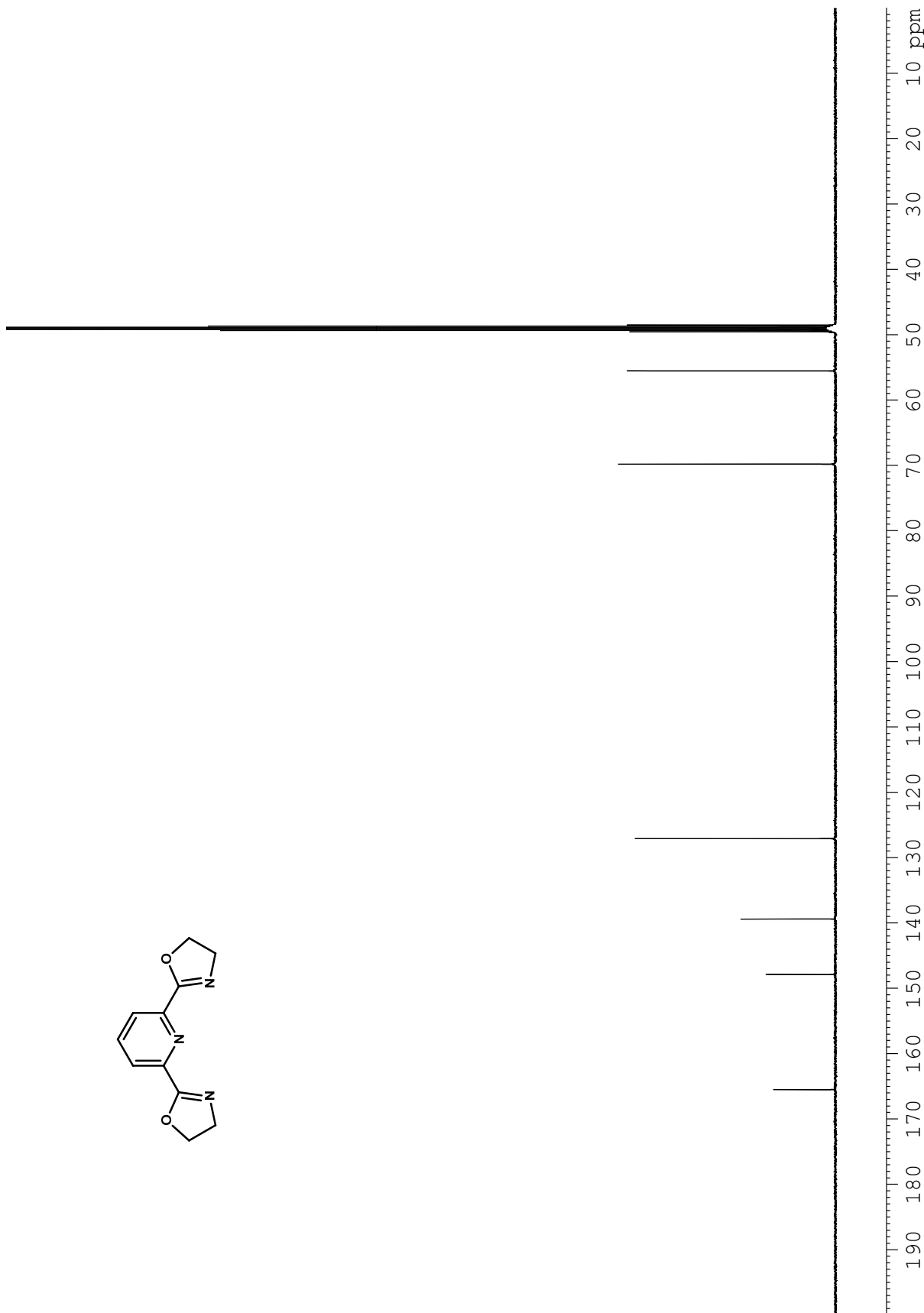
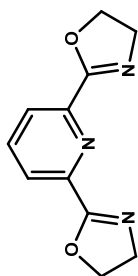


**Figure A4.11.**  $^{13}\text{C}$  NMR (125 MHz,  $\text{MeOH-}d_4$ ) spectrum of compound 5-26.

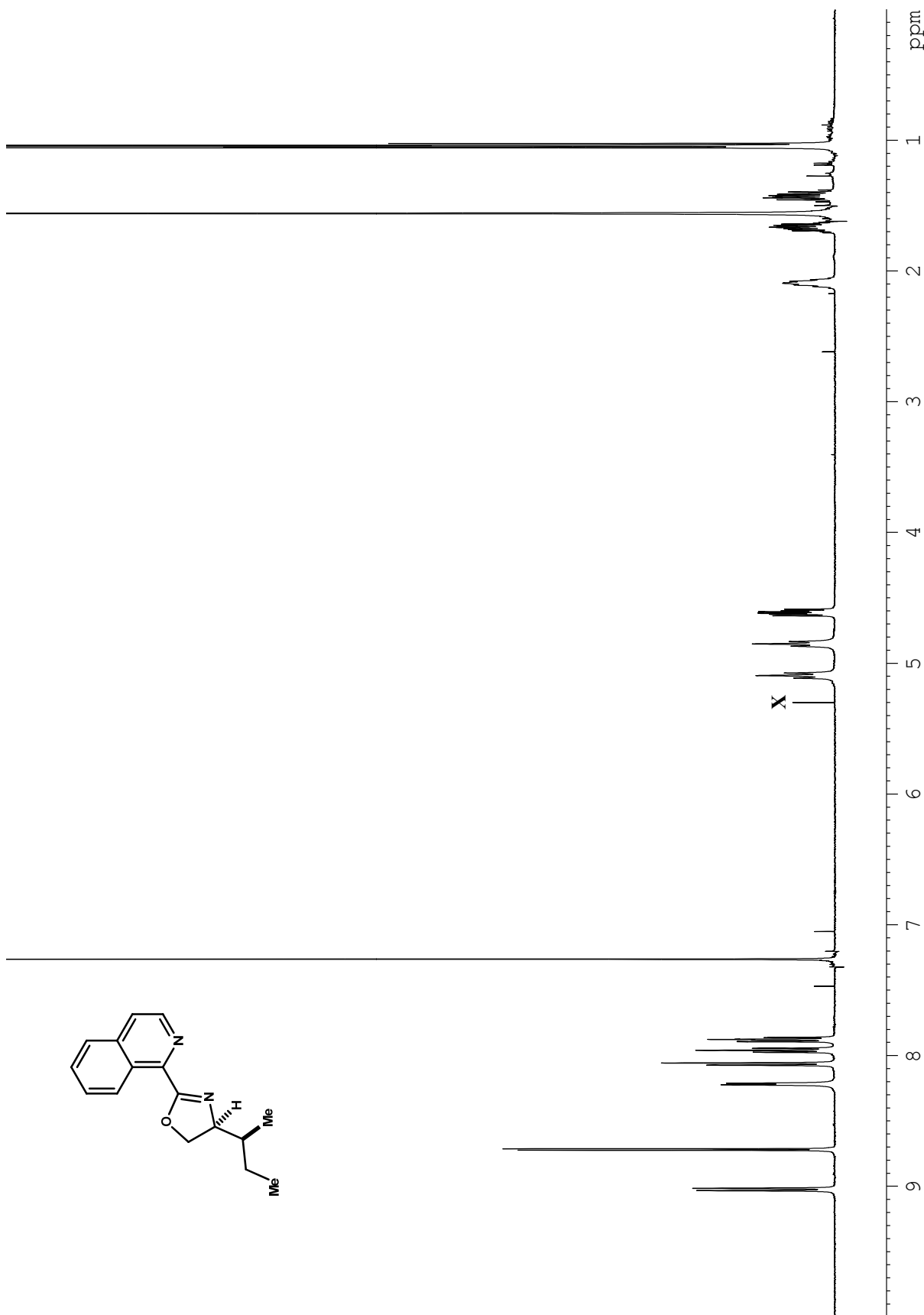
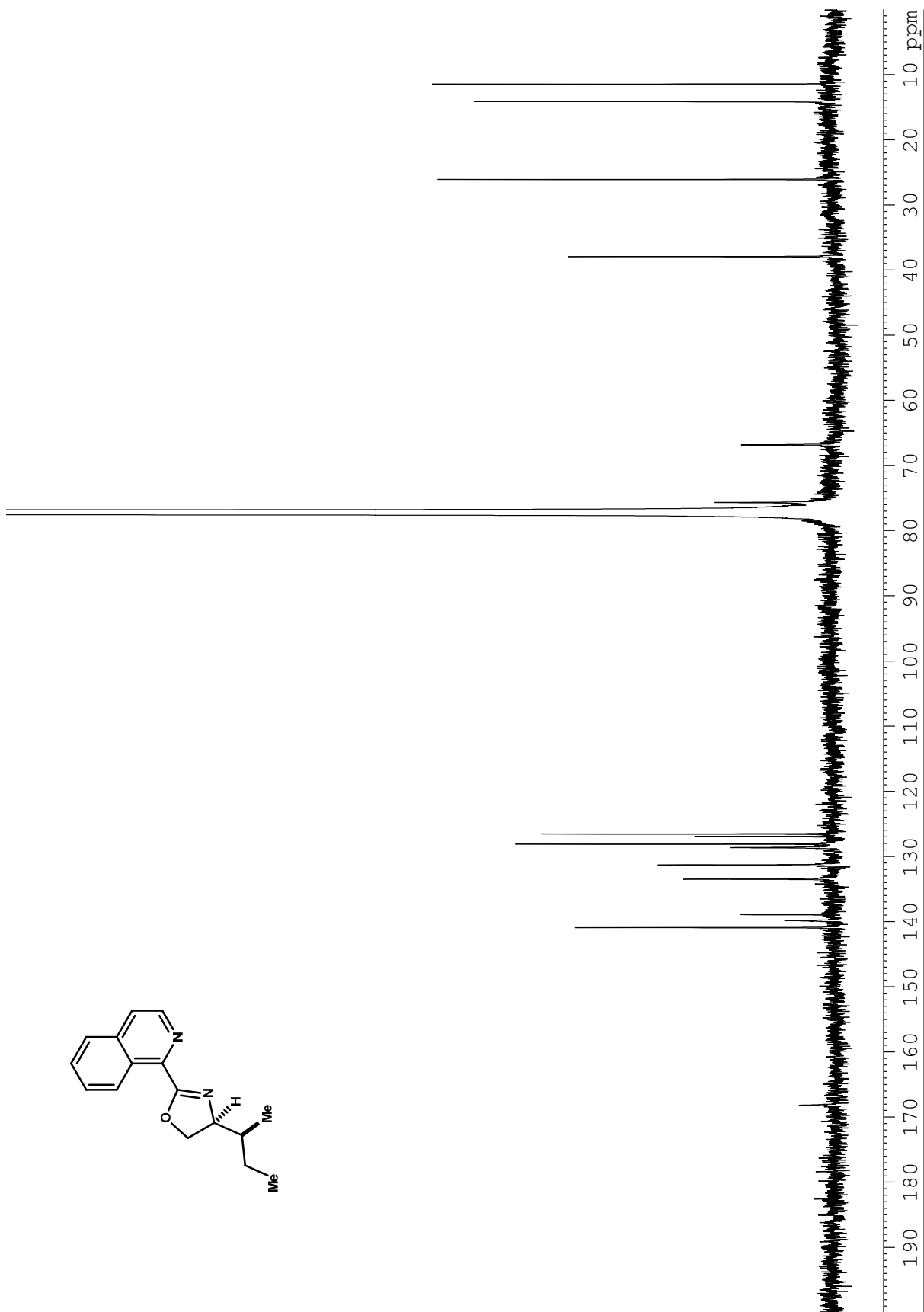
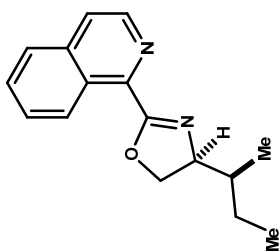
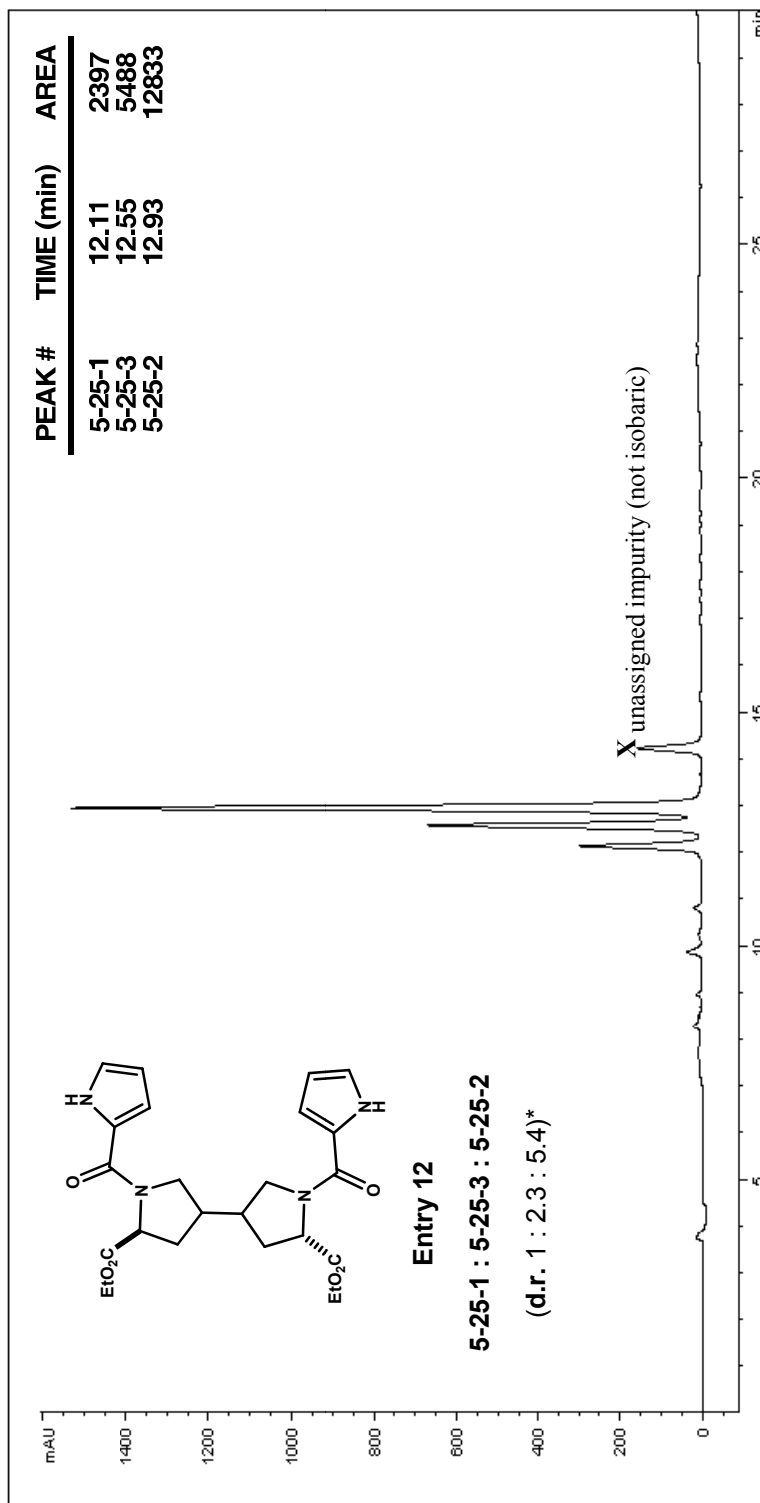


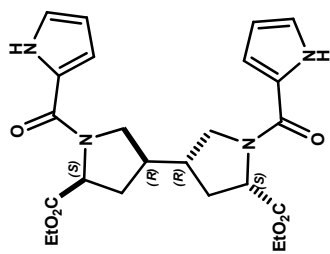
Figure A4.12. <sup>1</sup>H NMR (500 MHz, CHCl<sub>3</sub>-d<sub>1</sub>) spectrum of compound 5-27.



**Figure A4.13.** <sup>13</sup>C NMR (125 MHz, CHCl<sub>3</sub>-d<sub>1</sub>) spectrum of compound 5-27.



**Figure A4.14.** Analytical LC-MS UV trace (254-nm) of crude derivative mixture **5-25** from Entry 12.



**5-25-1**  
(3*R*, 3'*R*)  
(minor)

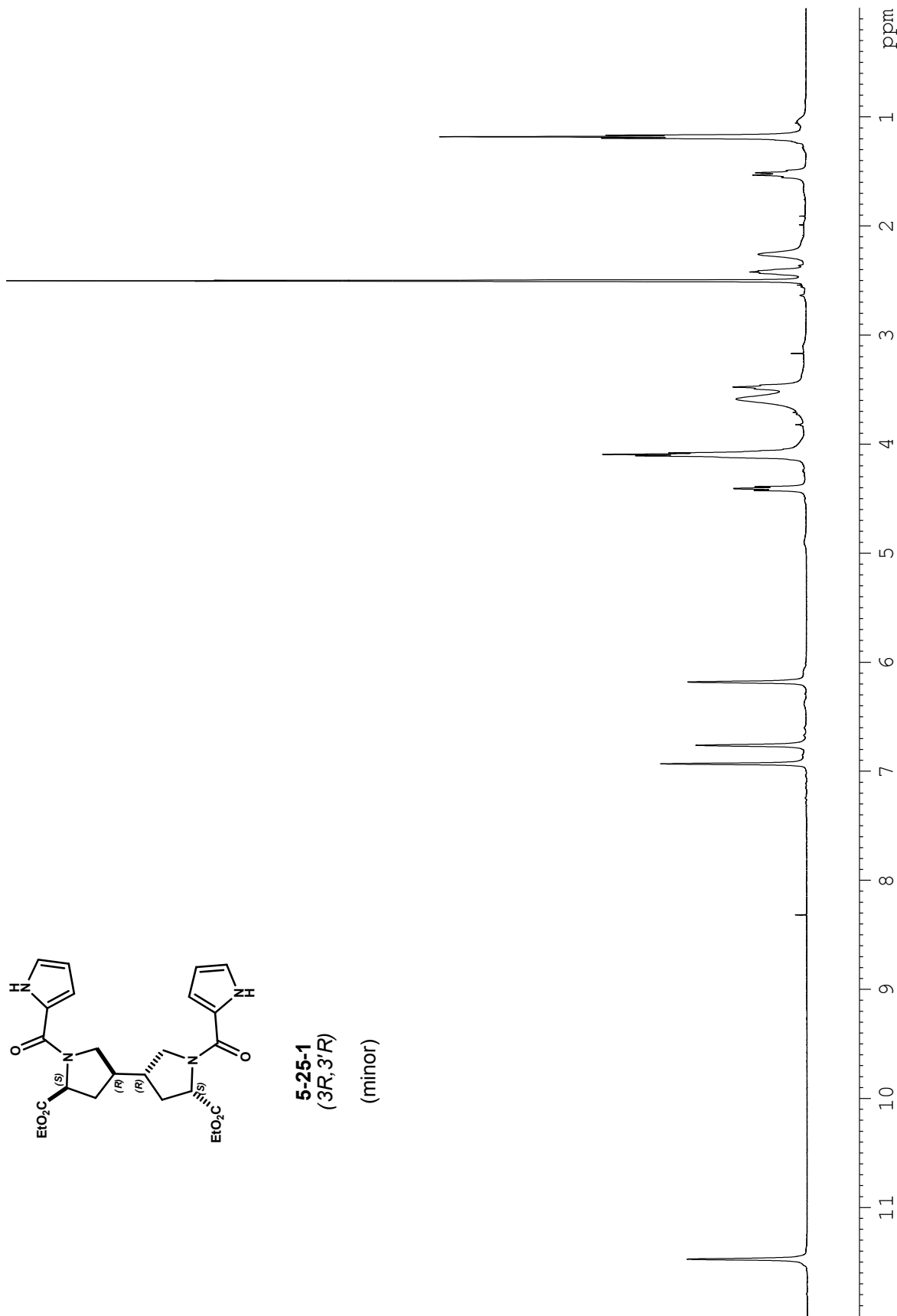
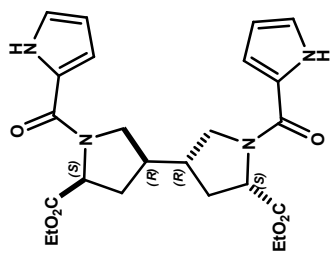
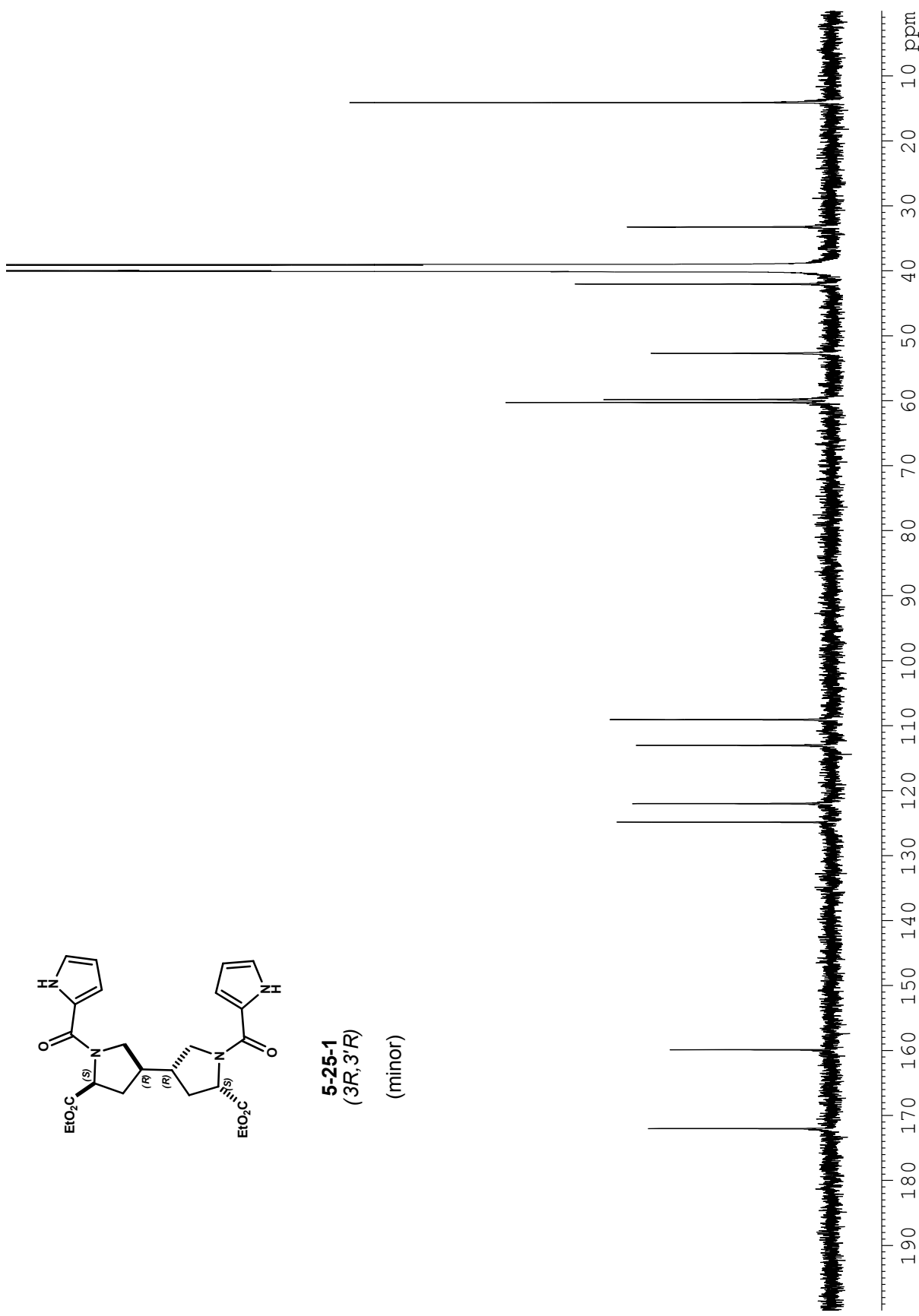
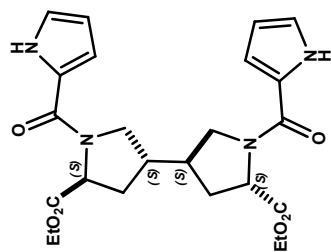


**Figure A4.15.** <sup>1</sup>H NMR (500 MHz, DMSO-*d*<sub>6</sub>) spectrum of compound **5-25-1**.



**5-25-1**  
(3*R*, 3'*R*)  
(minor)

**Figure A4.16.** <sup>13</sup>C NMR (125 MHz, DMSO-*d*<sub>6</sub>) spectrum of compound **5-25-1**.



**5-25-2**  
(3S,3'S)  
(major)

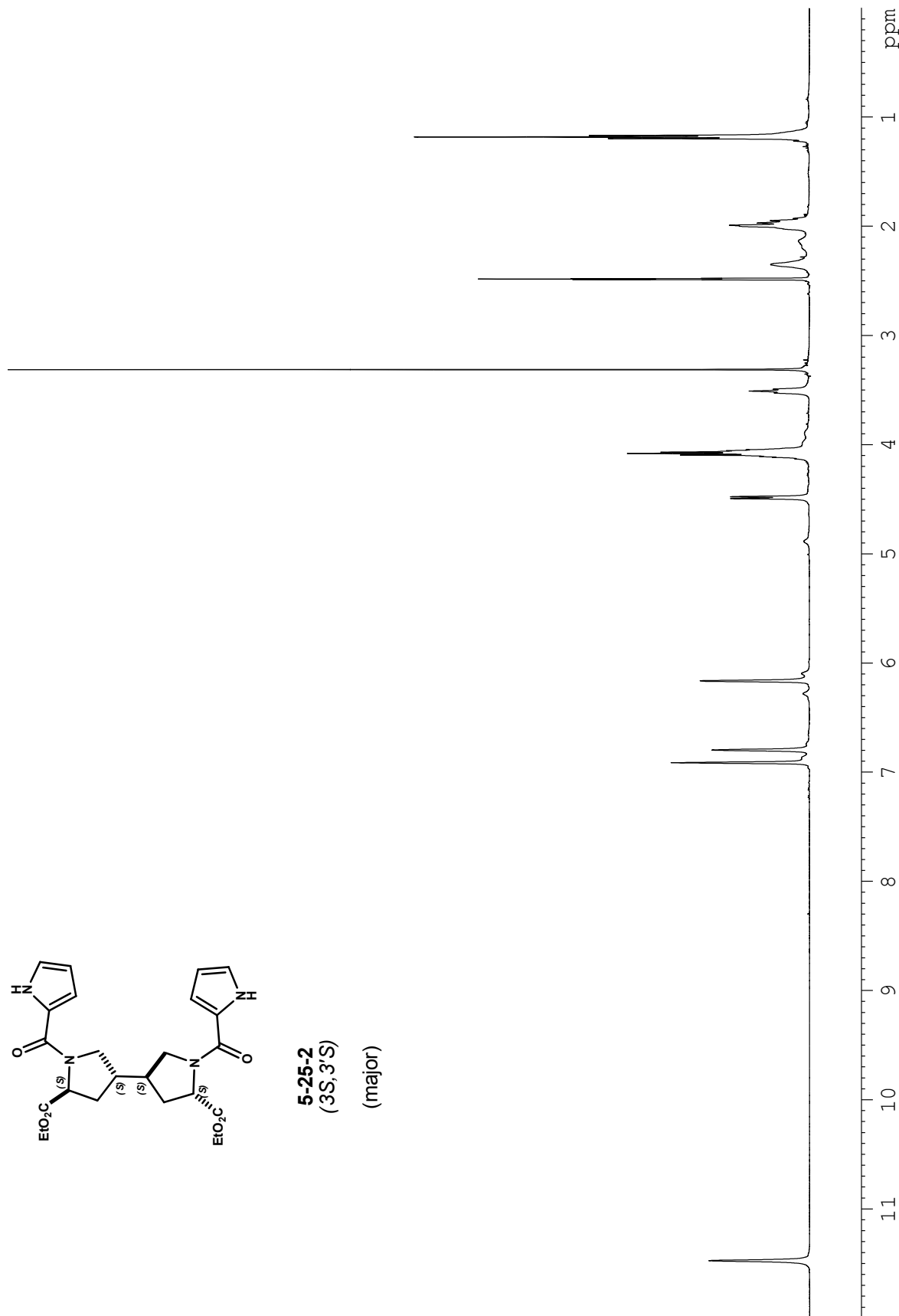
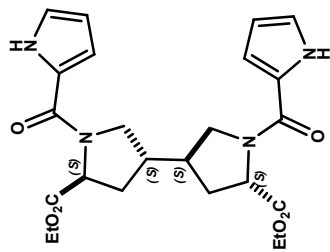


**Figure A4.17.** <sup>1</sup>H NMR (500 MHz, DMSO-*d*<sub>6</sub>) spectrum of compound **5-25-2**.



**5-25-2**  
(3S,3'S)  
(major)

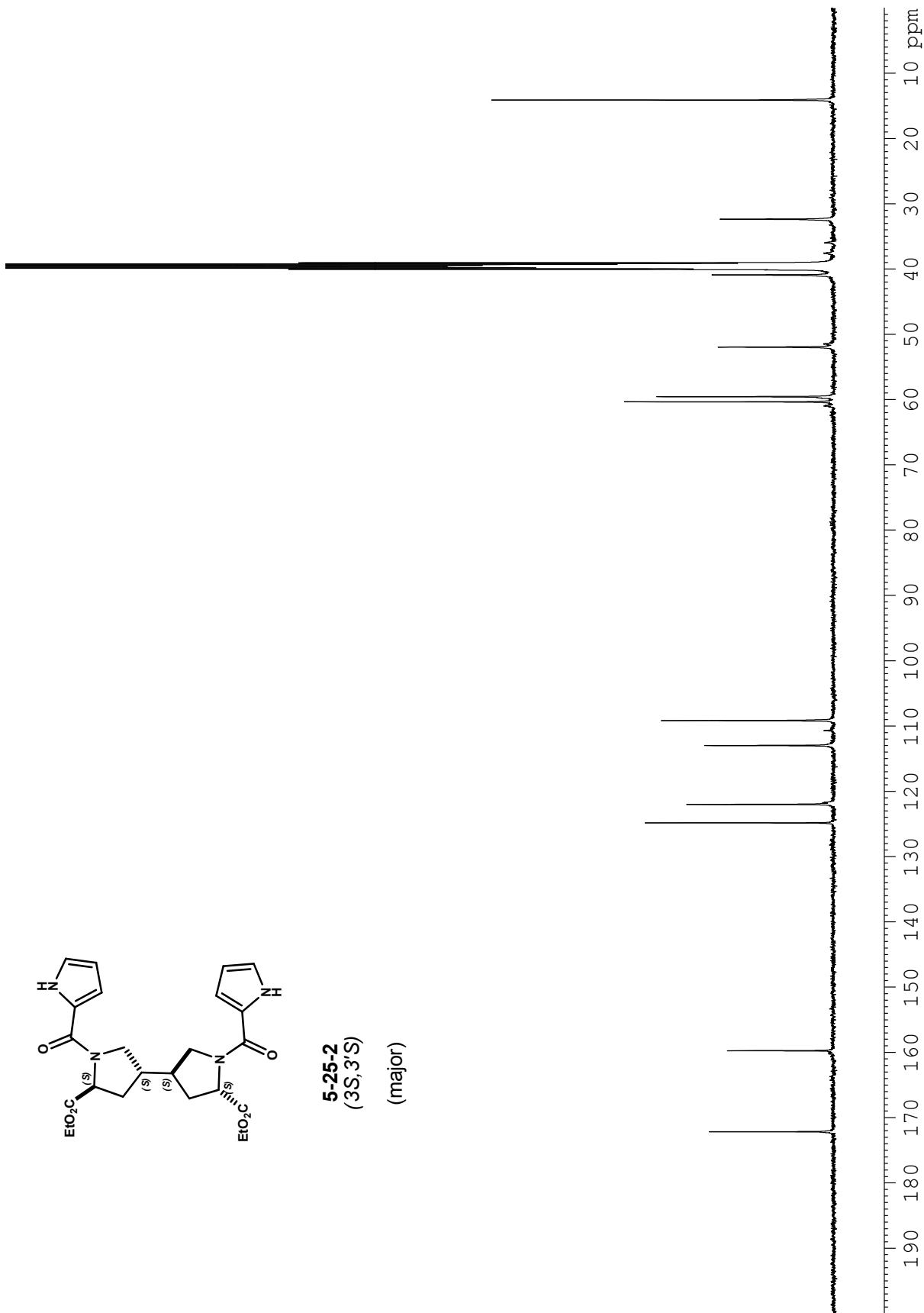
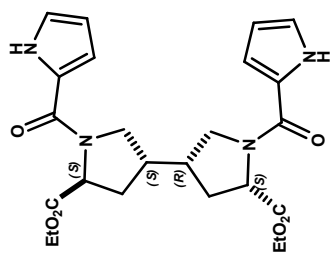
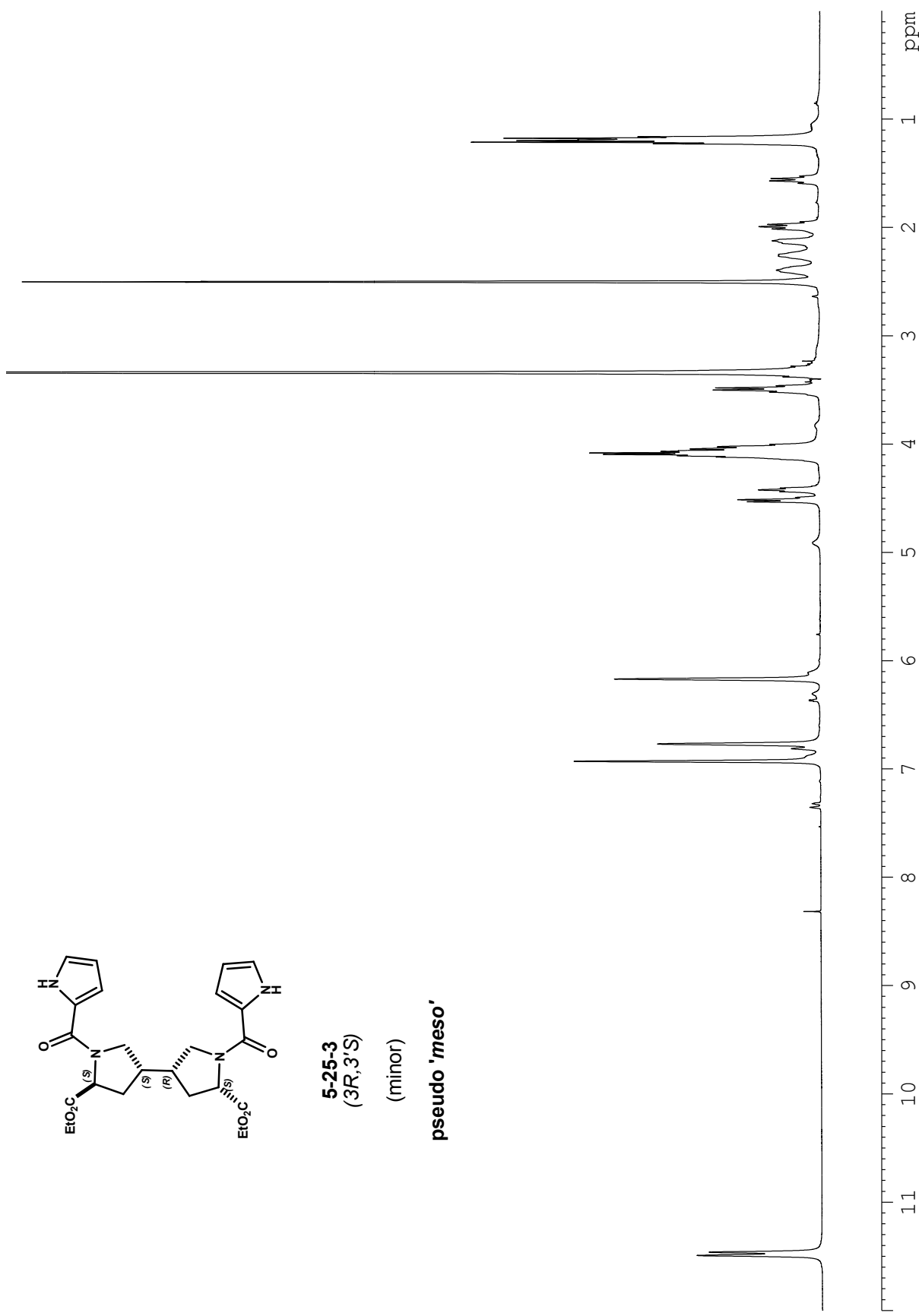


**Figure A4.18.**  $^{13}\text{C}$  NMR (125 MHz,  $\text{DMSO-}d_6$ ) spectrum of compound 5-25-2.



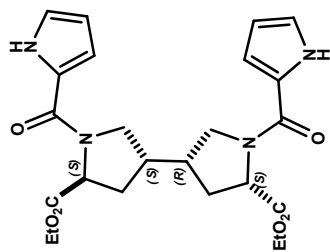


**5-25-3**  
(3*R*,3'*S*)

(minor)

pseudo 'meso'

**Figure A4.19.** <sup>1</sup>H NMR (500 MHz, DMSO-*d*<sub>6</sub>) spectrum of compound 5-25-3.



**5-25-3**  
(3R,3'S)

(minor)

pseudo 'meso'

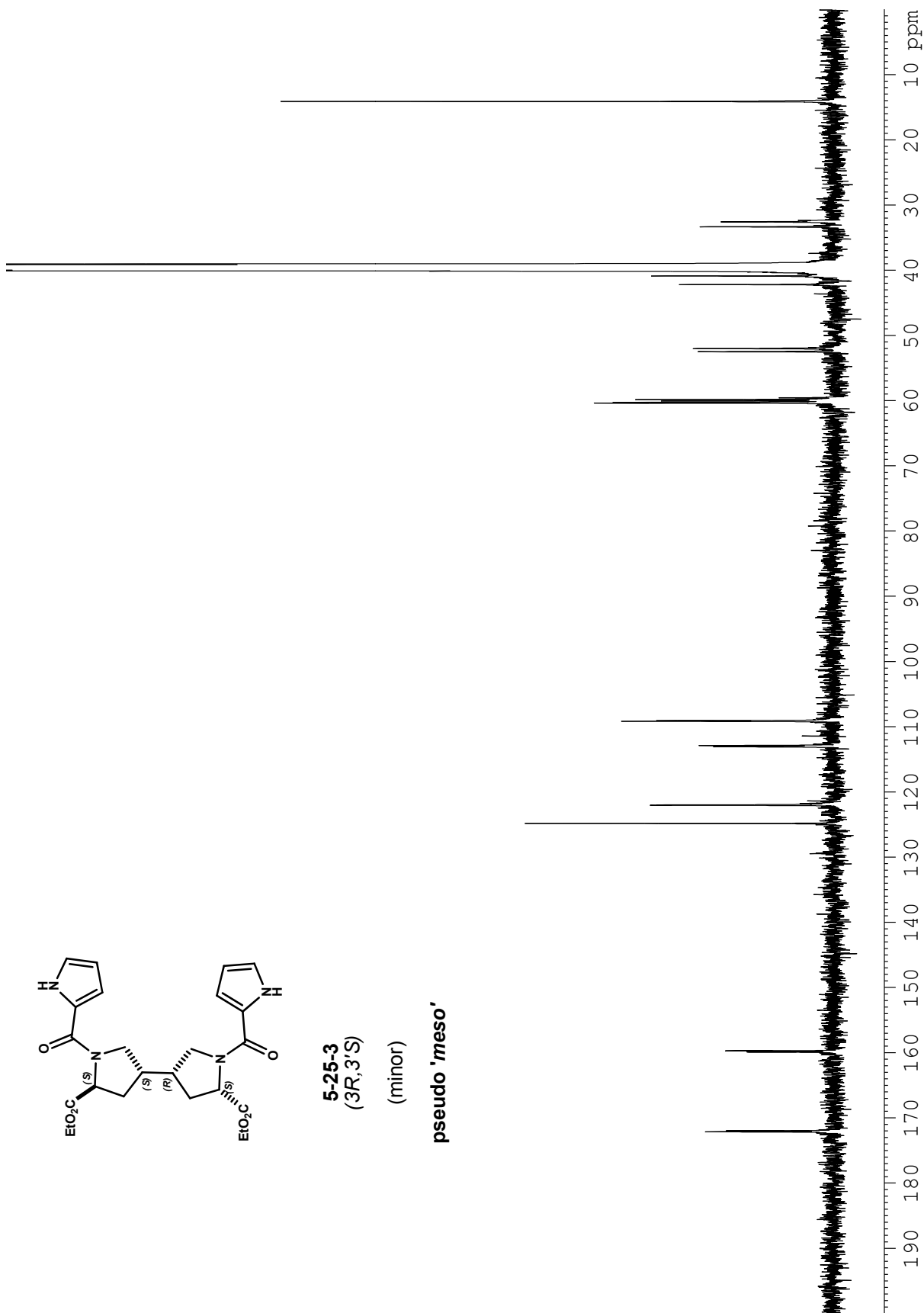


**Figure A4.20.** <sup>13</sup>C NMR (125 MHz, DMSO-*d*<sub>6</sub>) spectrum of compound **5-25-3**.